

DÉPARTEMENT DE GÉOSCIENCES – GÉOLOGIE ET PALÉONTOLOGIE  
UNIVERSITÉ DE FRIBOURG (SUISSE)

# **History of a Middle Berriasian transgression (Switzerland, France, and southern England)**

THÈSE

présentée à la Faculté des Sciences de l'Université de Fribourg (Suisse)  
pour l'obtention du grade de *Doctor rerum naturalium*

**Jonas TRESCH**

de Silenen, Suisse

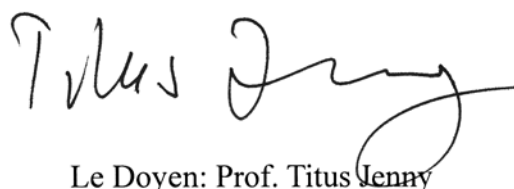
Thèse N° 1550

Multiprint SA, Fribourg, 2007

**Acceptée par la Faculté des Sciences de l'Université de Fribourg (Suisse)  
sur la proposition de:**

Prof. André STRASSER	Université de Fribourg (Suisse)	Directeur
Prof. Adrian IMMENHAUSER	Université de Bochum (Allemagne)	Expert
Dr. Hanspeter FUNK	ETH Zurich (Suisse)	Expert
Prof. Bernard GROBÉTY	Université de Fribourg (Suisse)	Président du jury

Fribourg, le 26 janvier 2007



Le Doyen: Prof. Titus Jenny



Directeur de thèse: Prof. André Strasser



*"However much you knock at nature's door, she will never answer you in comprehensible words."*  
**Ivan Sergeyevich Turgenev**



# TABLE OF CONTENTS

<b>ABSTRACT</b> .....	1	<b>3 - SEQUENCE ANALYSIS</b> .....	37
<b>ZUSAMMENFASSUNG</b> .....	3	3.1 INTRODUCTION.....	38
<b>RÉSUMÉ</b> .....	5	3.2 DEPOSITIONAL SEQUENCES.....	39
 <b>ACKNOWLEDGEMENTS</b> .....	7	3.2.1 Criteria for sequence identification and interpretation.....	39
 <b>1 - INTRODUCTION</b> .....	9	3.2.2 Terminology and applied sequence model.....	42
1.1 OBJECTIVES AND METHODS.....	9	3.2.3 Depositional sequences at different scales.....	44
1.2 GENERAL CONTEXT.....	11	3.2.4 Hierarchy and stacking of depositional sequences.....	47
1.2.1 Study area.....	11	3.2.5 Auto- versus allocyclicality.....	50
1.2.2 Stratigraphy.....	11	 <b>4 - SECTIONS OF THE SWISS AND FRENCH</b>	
1.2.3 Palaeogeography.....	13	<b>JURA PLATFORM</b> .....	53
1.2.4 Palaeoclimate and palaeoceanog- raphy.....	14	4.1 PREVIOUS WORK.....	54
 <b>2 - FACIES ANALYSIS AND INTERPRETATION</b> .....	17	4.2 GEOGRAPHIC SETTING.....	54
2.1 DEFINITIONS.....	17	4.3 PALAEOGEOGRAPHY.....	54
2.1.1 Microfacies.....	17	4.4 BIOSTRATIGRAPHY.....	55
2.2 APPROACH.....	17	4.5 LITHOSTRATIGRAPHY.....	58
2.3 CONSTITUENTS.....	18	4.6 DESCRIPTION AND INTERPRETATION OF THE SECTIONS.....	58
2.3.1 Allochems.....	18	4.6.1 Rusel.....	60
2.3.2 Fossil content.....	20	4.6.2 Cornaux.....	63
2.3.3 Other constituents.....	24	4.6.3 Marchairuz.....	68
2.4 SEDIMENTARY STRUCTURES.....	26	4.6.4 Crozet.....	72
2.4.1 Hydrodynamically formed structures.....	26	4.6.5 Chapeau de Gendarme.....	77
2.4.2 Biogenic structures.....	26	4.6.6 St. Claude.....	84
2.4.3 Structures indicating subaerial exposure.....	27	4.6.7 Lavans.....	88
2.5 EARLY DIAGENESIS.....	27	4.6.8 Thoirette.....	94
2.5.1 Compaction.....	27	4.6.9 Poizat.....	97
2.5.2 Cementation.....	28	4.6.10 Val de Fier.....	100
2.5.3 Alteration.....	28	4.6.11 Yenne.....	104
2.6 FACIES AND CONCEPTUAL FACIES MODELS.....	28	 <b>5 - SECTIONS OF THE DORSET REGION</b> .....	109
2.6.1 Criteria for a facies distinction.....	28	5.1 PREVIOUS WORK.....	109
2.6.2 Conceptual facies model for the Jura platform.....	29	5.2 GEOGRAPHIC SETTING.....	109
2.6.3 Conceptual facies model for the Dorset region.....	33	5.3 PALAEOGEOGRAPHY.....	110

5.4 BIOSTRATIGRAPHY.....	112	7.3 CYCLOSTRATIGRAPHY.....	176
5.5 MAGNETOSTRATIGRAPHY.....	115	7.3.1 Cyclostratigraphic framework.....	177
5.6 LITHOSTRATIGRAPHY.....	115	7.3.2 Completeness of sedimentary record.....	181
5.7 SPECIAL FEATURES.....	116	7.3.3 Precision of chronostratigraphic calibrations.....	182
5.8 DESCRIPTION AND INTERPRETATION OF THE SECTIONS.....	118	7.3.4 The long eccentricity cycle (400 ka): “A tuning fork”.....	183
5.8.1 Durlston Bay.....	118	7.3.5 Comparison with other Berriasian studies.....	183
5.8.2 Worbarrow Tout.....	132		
<b>6 - CORRELATIONS.....</b>	<b>141</b>	<b>8 - PALAEOCLIMATE AND ENVIRONMENTAL CHANGE.....</b>	<b>187</b>
6.1 METHODS OF CORRELATION.....	141	8.1 INTRODUCTION.....	187
6.1.1 Biostratigraphy.....	141	8.2 PALAEOCLIMATE DURING THE BERRIASIAN.....	188
6.1.2 Magnetostratigraphy.....	141	8.2.1 An overview.....	188
6.1.3 Lithofacies.....	142	8.3 EVIDENCES FROM THE STUDY AREAS.....	190
6.1.4 Depositional sequences and diagnostic intervals or surfaces.....	142	8.3.1 Clay minerals.....	190
6.2 CORRELATION OF THE JURA PLATFORM SECTIONS.....	143	8.3.2 Carbon and oxygen isotopes.....	194
6.2.1 Correlation of small-scale sequences.....	144	8.3.3 Other sedimentological indication...	196
6.2.2 Correlation of elementary sequences.....	147	8.4 LONG-TERM CHANGES.....	199
6.3 BASINAL SECTION (VOCONTIAN BASIN).....	152	8.4.1 Palaeotectonic evolution.....	199
6.3.1 The Vocontian basin.....	153	8.4.2 Palaeoceanographic evolution.....	200
6.3.2 Hemipelagic to pelagic depositional systems of the Vocontian basin .....	153	8.4.3 Palaeoclimatic evolution.....	203
6.3.3 Montclus section.....	154	8.5 SHORT-TERM PALAEOCLIMATE AND ENVIRONMENTAL CHANGES.....	204
6.3.4 Correlation of the Jura platform and the Vocontian basin sections.....	155	<b>9 - HISTORY OF A TRANSGRESSION.....</b>	<b>207</b>
6.4 CORRELATION OF THE DORSET SECTIONS.....	157	9.1 INTRODUCTION.....	207
6.4.1 Correlation of large-scale sequences (3 <sup>rd</sup> -order sequences).....	157	9.2 LONG-TERM EVOLUTION.....	207
6.4.2 Correlation of medium- and small-scale sequences.....	160	9.2.1 Long-term lowstand deposits.....	207
6.4.3 Correlation of elementary sequences.....	162	9.2.2 Initial transgression.....	208
6.5 CORRELATION OF ALL STUDIED SECTIONS.....	162	9.2.3 Long-term transgressive deposits.....	210
6.5.1 Biostratigraphy.....	162	9.2.4 Long-term maximum-flooding and highstand deposits.....	210
6.5.2 Magnetostratigraphy.....	165	9.3 SHORT-TERM EVOLUTION.....	211
6.5.3 Depositional sequences and diagnostic intervals (surfaces).....	165	9.3.1 High-resolution palaeogeographical evolution.....	211
6.5.4 Accommodation changes.....	169	9.3.2 Rates of palaeogeographic evolution.....	215
6.5.5 Comparison with other depositional regions.....	170	<b>10 – CONCLUSIONS AND OUTLOOK.....</b>	<b>217</b>
<b>7 - CYCLOSTRATIGRAPHY.....</b>	<b>173</b>	<b>REFERENCES.....</b>	<b>221</b>
7.1 INTRODUCTION.....	173	<b>PLATES.....</b>	<b>241</b>
7.1.1 Sea-level changes.....	173	<b>ANNEX.....</b>	<b>269</b>
7.2 ORBITAL FORCING.....	174	<b>CURRICULUM VITAE.....</b>	<b>271</b>
7.2.1 Effects of orbital forcing.....	174		

## ABSTRACT

---

The aim of this study is to correlate and interpret transgressive deposits of three different depositional regions with high resolution: the marginal-marine carbonates of the Jura platform (France and Switzerland) and the Dorset region (UK). Additionally, a hemipelagic section of the Vocontian basin (France) has been integrated into the high-resolution correlation scheme. The Middle Berriasian transgression has been chosen because, in combination with subsidence, transgressive intervals create accommodation space, which can be filled with sediments. The best chance to preserve sediments and to obtain a relatively complete sedimentary succession is during increasing accommodation space. The Middle Berriasian transgression lies between the 3<sup>rd</sup>-order sequence boundaries Be4 and Be5 according to the sequence and chronostratigraphic chart of HARDENBOL et al. (1998). The chosen sections are already well described and dated in the literature. In this study, all sections have been sampled on a decimetric scale in order to document their facies evolution in great detail. The observed facies zones have been integrated in two different facies models representing the palaeoenvironments of the Jura platform and the Dorset region. The facies and accommodation changes detected in each section are related to relative sea-level fluctuations and interpreted in terms of sequence stratigraphy (elementary, small-scale, and medium-scale sequences).

Most of the sections of the French and Swiss Jura platform have already been interpreted in terms of high-resolution sequence stratigraphy on the level of small-scale sequences (WAEHRY 1989, PASQUIER 1995, HILLGÄRTNER 1999). The lower part of the sections (Goldberg Formation and base of the Pierre Châtel Formation) has been dated by ammonites (CLAVEL et al. 1986) and with the help of charophyte-ostracode assemblages (MOJON 2002) and the upper part by benthic foraminifera (upper Pierre Châtel Formation

and Vions Formation; e.g., CLAVEL et al. 1986). A remarkable environmental change from inter- and supratidal (Goldberg Formation) to shallow marine deposits (Pierre Châtel Formation) on the Jura platform represents the Middle Berriasian transgression.

Both investigated sections of the Dorset region are described bed-by-bed in the literature (ENSOM 1985, CLEMENTS 1993). The upper part of the Lulworth Formation and the lower part of the Durlston Formation of the Durlston Bay and Worbarrow Tout sections have been re-logged on a decimetric scale and interpreted in terms of high-resolution sequence stratigraphy on the level of small-scale to elementary sequences. The rock succession implies a transgression from brackish-lagoonal to more marine environments. Marine conditions are indicated by the oyster banks of the Cinder Member, which corresponds to the Middle Berriasian transgression. The Durlston Bay section has been dated by magnetostratigraphy (OGG et al. 1991, 1994) and charophyte-ostracode assemblages (MOJON 2002). A high-resolution sequence-stratigraphical interpretation of the Dorset sections on the level of elementary and small-scale sequences is presented in this study for the first time.

The Montclus section of the Vocontian basin is well dated by ammonites and calpionellids and has been interpreted in terms of sequence- and cyclostratigraphy (PASQUIER 1995, HILLGÄRTNER 1999). The transgression in the basin is marked by a change from relatively thick, irregular limestone beds to thinner and more homogeneous limestone-marl alternations. A high-resolution sequence-stratigraphical correlation of the Montclus section with sections of the Jura platform has been published by STRASSER et al. (2004). The magnetostratigraphy established for the type-section of the Berriasian stage in Berrias (France) by GALBRUN (1985) and GALBRUN et al. (1986) can be correlated to the Montclus section due to the sequence-

stratigraphical interpretation of the Berrias section by STROHMENGER & STRASSER (1993).

A high-resolution correlation of several sections between the 3<sup>rd</sup>-order sequence boundaries has been worked out. This correlation framework fits well the bio- and magnetostratigraphical schemes published in the literature. The assumption that the base of the Pierre Châtel Formation on the Jura platform corresponds to the base of the Durlston Formation in Dorset (Cinder Member), discussed over decades in the literature, can be confirmed in this study.

According to HARDENBOL et al. (1998), the time span between the 3<sup>rd</sup>-order sequence boundaries Be4 and Be5 is about 1.7 million years. Eighteen to twenty small-scale sequences have been identified within this interval. Based on this time span and the investigated stacking pattern of the sections, it is assumed that the deposition of the small-scale sequences has been controlled by relative sea-level fluctuations in tune with 100-ka orbital eccentricity cycles.

For an even higher time resolution, eleven sections of the Jura platform and the two Dorset sections have been selected to examine the sedimentary record of the four small-scale sequences around the large-scale transgression. Several well-preserved small-scale sequences are composed of five elementary sequences. Therefore, it is assumed that elementary sequences represent orbital precession cycles (20 ka).

The interpretation of the subtle palaeoenvironmental changes within the small-scale sequences is more complex. Some elementary sequences can be correlated between the sections and are considered to be controlled by relative sea-level changes (extrinsic factors). Others, however, cannot (or only partly) be interpreted in terms of sequence stratigraphy because intrinsic (autocyclic) processes dominated their deposition. However, autocyclic intervals can at least be delimited at the base and top by sequence-

stratigraphical correlations.

Despite of the uncertainties in the correlation of elementary sequences, such high-resolution sequence-stratigraphical interpretations give the opportunity to reconstruct high-frequency palaeoenvironmental changes in different depositional realms with a time resolution of a few ten thousand years. The high-resolution sequence- and cyclostratigraphic correlation permits to monitor in detail the flooding of the Jura platform and the Dorset region. It can be shown that the transgression on the Jura platform is strongly diachronous mainly because of an important platform morphology and differential subsidence. Rapid facies changes occur in marginal-marine environments mainly due to threshold effects (e.g., flooding of morphological highs).

It is well known that a climate change from an arid, Mediterranean climate to more humid conditions took place during the Berriasian in NW and Central Europe (e.g., DECONINCK 1987, HALLAM et al. 1991, ALLEN 1998, ABBINK et al. 2001). The high-resolution sequence- and cyclostratigraphical interpretation of this study enables to analyze this climate change in more detail. It is assumed that oceanographic changes mainly related to the influence of cold Boreal and warm Tethyan surface waters were responsible for the climate change in these parts of Europe. A key role in the exchange of these water masses played the evolution of the Greenland-Norwegian Seaway during the Berriasian. Additional factors like the further widening of the proto-North Atlantic and the opening and closing of seaways between the epicontinental basins of Europe contributed to the climate change in the investigated regions. Climate changes on the Milankovitch-frequency band (orbital cycles) may have been controlled by variations in the extension of the atmospheric circulation cells and their palaeogeographic positions.

## ZUSAMMENFASSUNG

---

Das Ziel der vorliegenden Arbeit ist es, transgressive Sedimente verschiedener Ablagerungsräume in hoher Auflösung zu interpretieren und zu korrelieren: küstennahe Karbonate der Jura Plattform (Frankreich und Schweiz) und in Dorset (England). Zusätzlich ist eine hemipelagische Abfolge des Vocontischen Beckens (Frankreich) in die hochauflösende Korrelation integriert worden. Die Transgression im Mittleren Berriasium wird näher untersucht, weil in transgressiven Intervallen durch Zusammenspiel von Meeresspiegelanstieg und Subsidenz Akkommodationsraum geschaffen wird, der mit Sedimenten gefüllt werden kann. Die beste Möglichkeit, Sedimente zu konservieren und relativ komplette Abfolgen zu generieren, ist demzufolge während einer Zunahme von Akkommodation. Die Transgression im Mittleren Berriasium liegt zwischen den Sequenzgrenzen 3. Ordnung Be4 und Be5 gemäss der sequenz- und chronostratigraphischen Skala von HARDENBOL et al. (1998). In der Fachliteratur sind alle ausgewählten Profile gut beschrieben und datiert. Jedes Profil ist in der vorliegenden Arbeit nochmals in einem Dezimetermassstab beprobt worden, um die Faziesentwicklung im Detail zu studieren. Anhand der Faziesinterpretation jeder Probe sind mehrere Fazieszonen ausgeschieden worden, die in zwei Faziesmodellen (Jura Plattform und Dorset Region) integriert worden sind. Die Fazies- und Akkommodationsänderungen in den Profilen können relativen Meeresspiegelschwankungen zugeordnet und mit Hilfe der Sequenzstratigraphie interpretiert werden (Elementar-, "small-scale"- und "medium-scale"-Sequenzen).

Die meisten Profile der Jura Plattform sind bereits mit Hilfe der Sequenzstratigraphie in einer Auflösung von "small-scale"-Sequenzen analysiert worden (WAEHRY 1989, PASQUIER 1995, HILLGÄRTNER 1999). Der untere Abschnitt der Profile (Goldberg Formation

und Pierre Châtel Formation) ist mit Ammoniten (CLAVEL et al. 1986) und Charophyten-Ostrakoden-Vergesellschaftungen (MOJON 2002) datiert worden. Die Datierungen der oberen Abschnitte der Profile (Pierre Châtel Formation und Vions Formation) basieren auf benthischen Foraminiferen (z.B. CLAVEL et al. 1986). Die Transgression im Mittleren Berriasium der Jura Plattform ist durch einen bemerkenswerten Fazieswechsel von inter- bis supratidalen Sedimenten der Goldberg Formation zu flach-marinen Ablagerungen der Pierre Châtel Formation gekennzeichnet.

Die beiden Profile in Dorset sind in der Literatur detailliert beschrieben (ENSOM 1985, CLEMENTS 1993). Der obere Teil der Lulworth Formation und der untere Teil der Durlston Formation der Profile in Durlston Bay und in Worbarrow Tout sind nochmals aufgenommen (im Dezimetermassstab) und mit Hilfe der Sequenzstratigraphie mit einer Auflösung von "small-scale"- und Elementarsequenzen interpretiert worden. Die Gesteinsabfolgen der Dorset Profile spiegeln einen Fazieswechsel von brackisch-lagunären zu eher marinen Ablagerungen wieder. Die Austernbänke des Cinder Members weisen auf marine Verhältnisse hin, die der Transgression im Mittleren Berriasium entsprechen. Das Profil in Durlston Bay ist mit Magnetostratigraphie (OGG et al. 1991, 1994) und Charophyten-Ostracoden-Vergesellschaftungen (MOJON 2002) datiert worden. In der vorliegenden Arbeit wird erstmals eine hochauflösende Sequenzstratigraphie der Dorset Profile basierend auf Elementar- und "small-scale"-Sequenzen präsentiert.

Das Profil Montclus im Vocontischen Becken ist mit Ammoniten und Calpionellen datiert und mit Hilfe hochauflösender Sequenz- und Zyklusstratigraphie interpretiert worden (PASQUIER 1995, HILLGÄRTNER 1999). Die Transgression im Becken ist durch eine Änderung des Sedimentationsmusters von relativ dicken, unregelmässigen Kalkbänken zu dünneren

und homogenen Kalk-Mergel Wechsellagerungen gekennzeichnet. Eine hochauflösende sequenzstratigraphische Korrelation des Montclus Profils mit Profilen der Jura Plattform ist in STRASSER et al. (2004) publiziert worden. Die Magnetostratigraphie von GALBRUN (1985) und GALBRUN et al. (1986), die am Typusprofil des Berriasiums in Berrias (Frankreich) gemacht worden ist, kann dank der hochauflösenden Sequenzstratigraphie von STROHMENGER & STRASSER (1993) zum Montclus Profil korreliert werden.

Eine hochauflösende Korrelation von mehreren Profilen zwischen den Sequenzen 3. Ordnung ist in der vorliegenden Studie ausgearbeitet worden. Dieses Korrelationsgerüst passt gut in die publizierten bio- und magnetostratigraphischen Schemas. Die über Jahrzehnte in der Literatur diskutierte Annahme, dass die Basis der Pierre Châtel Formation der Jura Plattform der Basis der Durlston Bay Formation in Dorset (Cinder Member) entspricht, kann bestätigt werden.

Gemäss HARDENBOL et al. (1998) beträgt die Zeitspanne zwischen den Sequenzgrenzen 3. Ordnung Be4 und Be5 ungefähr 1.7 Millionen Jahre. In diesem Intervall sind achtzehn bis zwanzig „small-scale“-Sequenzen identifiziert worden. Basierend auf dieser Zeitspanne und der Ablagerungsmuster der Profile wird angenommen, dass die Ablagerung der „small-scale“-Sequenzen durch relative Meeresspiegelschwankungen im Takt mit orbitalen Exzentrizitätszyklen mit Perioden von 100000 Jahren (100 ka) kontrolliert worden sind.

Um eine höhere Zeitauflösung zu erreichen, sind die Sedimentabfolgen der vier „small-scale“-Sequenzen im Bereich der grossen Transgression von elf Profilen der Jura Plattform und von zwei Profilen der Dorset Region näher untersucht worden. Mehrere gut ausgebildete „small-scale“-Sequenzen bestehen aus fünf Elementarsequenzen, was auf eine Kontrolle orbitaler Präzessionszyklen mit Perioden von 20 ka hindeutet.

Die Interpretation von subtilen Änderungen in den Paläoablagerungsräumen innerhalb der „small-scale“-Sequenzen ist ziemlich komplex. Einige Elementarsequenzen können zwischen den Profilen korreliert werden. Es wird deshalb angenommen, dass diese Sequenzen hauptsächlich durch relative Meeresspiegelschwankungen hervorgerufen worden sind (extrinsische Faktoren). Andere Sedimentabfolgen innerhalb von „small-scale“-Sequenzen können nicht (oder nur teilweise) mit Hilfe von hochauflösender

Sequenzstratigraphie interpretiert werden. Diese Ablagerungen sind durch intrinsische (autozyklische) Prozesse kontrolliert worden. Autozyklische Sedimentabfolgen können jedoch zumindest durch sequenzstratigraphische Korrelationen an ihrer Basis und ihrem Top begrenzt werden.

Abgesehen von Korrelationsunsicherheiten der Elementarsequenzen, ermöglichen hochauflösende sequenzstratigraphische Interpretationen Rekonstruktionen der hochfrequenten Änderungen der Paläoablagerungsräumen verschiedener Sedimentationsmilieus mit einer zeitlichen Auflösung von einigen zehntausend Jahren. Die Überflutung der Jura Plattform und der Dorset Region kann dank der hochauflösenden sequenz- und zyklustratigraphischen Korrelation im Detail rekonstruiert werden. Die ausgeprägte Plattformmorphologie und differenzielle Subsidenz führen zu einer starken Diachronie der Transgression auf der Jura Plattform. Schwelleneffekte (z.B. Überflutung von morphologischen Hochzonen) führen zu abrupten Fazieswechsel in küstennahen Ablagerungsräumen.

Es ist bekannt, dass im Berriasium von Nordwest und Zentraleuropa ein Klimawechsel von ariden, mediterranen zu feuchteren Bedingungen stattfand (z.B. DECONINCK 1987, HALLAM et al. 1991, ALLEN 1998, ABBINK et al. 2001). Mit Hilfe der hochauflösenden sequenz- und zyklustratigraphischen Interpretation kann dieser Klimawechsel detailliert untersucht werden. Es wird angenommen, dass hauptsächlich ozeanographische Strömungsänderungen für diesen Klimawechsel in Nordwest und Zentraleuropa verantwortlich sind. Das Zurückdrängen von kalten borealen Oberflächenströmungen durch warme Wassermassen der Tethys hat wahrscheinlich zu diesem Klimawechsel im Mittleren Berriasium geführt. Eine Hauptrolle im Austausch von verschiedenen marinen Wassermassen im Berriasium hat die Entwicklung der Meeresenge zwischen Grönland und Norwegen gespielt. Zusätzliche Faktoren wie die fortschreitende Öffnung des Proto-Atlantiks sowie die Öffnung und Schliessung von Meerengen zwischen den epikontinentalen Becken in Europa haben zu dem Klimawechsel in den untersuchten Regionen beigetragen. Klimawechsel im Bereich von Milankovitch-Frequenzen (Orbitalzyklen) sind wahrscheinlich durch Änderungen in der Ausdehnung der atmosphärischen Zirkulationszellen und deren paläogeographischen Positionen hervorgerufen worden.



## RÉSUMÉ

---

Le but de cette étude est de corréler et d'interpréter les dépôts transgressifs de trois différentes zones de dépôt avec haute résolution: les carbonates marginaux de la plate-forme du Jura (Suisse et France) et de la région du Dorset (Angleterre). En plus, une coupe hémipélagique du bassin Vocontien (France) a été intégrée dans le schéma de corrélation haute résolution. La transgression du Berriasien moyen a été choisie parce que, en combinaison avec la subsidence, les intervalles transgressifs créent de l'espace d'accommodation, qui peut être rempli par des sédiments. La meilleure chance pour préserver les sédiments et obtenir une succession sédimentaire relativement complète est durant l'augmentation de l'espace d'accommodation. La transgression du Berriasien moyen est positionnée entre les limites de séquence de 3<sup>ème</sup> ordre Be4 et Be5 selon la charte chronostratigraphique et séquentielle de HARDENBOL et al. (1998). Les coupes étudiées sont déjà bien décrites et datées dans la littérature. Dans cette étude, les coupes ont été échantillonnées à une échelle décimétrique afin de documenter l'évolution des faciès en détail. Les zones de faciès observées ont été intégrées dans deux différents modèles de faciès représentant les paléoenvironnements de la plate-forme du Jura et de la région du Dorset. Les changements de faciès et d'accommodation détectés dans chaque coupe sont reliés aux fluctuations du niveau marin relatif et interprétés avec les outils de la stratigraphie séquentielle (séquences élémentaires, à court terme et à moyen terme).

La plupart des coupes de la plate-forme du Jura suisse et français ont déjà été interprétées par la stratigraphie séquentielle haute-résolution au niveau des séquences à court terme (WAEHRY 1989, PASQUIER 1995, HILLGÄRTNER 1999). La partie inférieure des coupes (Formation de Goldberg et base de la Formation de Pierre Châtel) a été datée par ammonites (CLAVEL et al. 1986) et avec l'aide des assemblages de charophytes

et d'ostracodes (MOJON 2002), tandis que la partie supérieure a été datée par les foraminifères benthiques (Formation de Pierre Châtel supérieure et Formation de Vions; p. ex., CLAVEL et al. 1986). Un remarquable changement environnemental de dépôts intertidaux et supratidaux (Formation de Goldberg) à des dépôts marins peu profonds (Formation de Pierre Châtel) sur la plate-forme du Jura représente la transgression du Berriasien moyen.

Les coupes dans la région du Dorset ont été décrites banc par banc dans la littérature (ENSOM 1985, CLEMENTS 1993). La partie supérieure de la Formation de Lulworth et la partie inférieure de la Formation de Durlston sur les coupes de Durlston Bay et de Worbarrow Tout ont été re-lechées à une échelle décimétrique et interprétées par la stratigraphie séquentielle haute-résolution au niveau des séquences à court terme et élémentaires. La succession sédimentaire implique une transgression d'environnements saumâtres-lagunaires à des environnements marins plus ouverts. Les conditions marines sont indiquées par des bancs d'huîtres caractérisant le Cinder Member, qui correspond à la transgression du Berriasien moyen. La coupe de Durlston Bay a été datée par magnétostratigraphie (OGG et al. 1991, 1994) et par les assemblages de charophytes et d'ostracodes (MOJON 2002). Une interprétation séquentielle à haute-résolution des coupes du Dorset au niveau des séquences élémentaires et à court terme est présentée dans cette étude pour la première fois.

La coupe de Montclus du Bassin Vocontien est bien datée par les ammonites et les calpionelles et a été interprétée en termes de stratigraphie séquentielle et cyclostratigraphie (PASQUIER 1995, HILLGÄRTNER 1999). Dans le bassin, la transgression est marquée par un changement de bancs calcaires irréguliers et relativement épais à des alternances marne-calcaire. Une étude de stratigraphie séquentielle haute résolution de la coupe de Montclus et des coupes de

la plate-forme du Jura a été publiée par STRASSER et al. (2004). La magnétostratigraphie établie pour la coupe-type de l'étage du Berriasien à Berrias (France) par GALBRUN (1985) et GALBRUN et al. (1986) peut être corrélée vers la coupe de Montclus grâce à l'interprétation séquentielle de la coupe de Berrias faite par STROHMENGER & STRASSER (1993).

Une corrélation haute-résolution des différentes coupes entre les limites de séquence de 3<sup>ème</sup> ordre a été accomplie. Ce cadre de corrélation s'accorde bien avec les schémas biostratigraphiques et magnétostratigraphiques publiés dans la littérature. L'hypothèse que la base de la Formation de Pierre Châtel sur la plate-forme du Jura corresponde à la base de la Formation de Durlston dans le Dorset (Cinder Member), discutée pendant des années dans la littérature, peut être confirmée dans cette étude.

Selon HARDENBOL et al. (1998), la durée entre les limites de séquence de 3<sup>ème</sup> ordre Be4 et Be5 est d'environ 1.7 millions d'années. Dix-huit à vingt séquences à court terme ont été identifiées dans cette intervalle. Basé sur cette durée et l'empilement hiérarchique des bancs, il est admis que le dépôt des séquences à court terme a été contrôlé par les fluctuations du niveau marin relatif en liaison avec les cycles orbitaux d'excentricité de 100 ka.

Pour une résolution de temps encore meilleure, onze coupes de la plate-forme du Jura et deux coupes du Dorset ont été sélectionnées pour examiner l'enregistrement sédimentaire de quatre séquences à court terme autour de la transgression à long terme. Plusieurs séquences à court terme bien préservées sont composées de 5 séquences élémentaires. Par conséquent, il est admis que les séquences élémentaires représentent des cycles orbitaux de précession de 20 ka.

L'interprétation des changements environnementaux subtiles à l'intérieur des séquences à court terme est complexe. Certaines séquences élémentaires peuvent être corrélées entre les coupes et sont considérées comme étant contrôlées par des changements du niveau marin relatif (facteurs extrinsèques). D'autres, cependant, ne peuvent pas (ou seulement partiellement) être interprétées en termes de stratigraphie séquentielle puisque que les processus intrinsèques (autocycliques)

dominaient durant le dépôt. Cependant, des intervalles autocycliques peuvent au moins être délimités à la base et au sommet par les corrélations par stratigraphie séquentielle.

Malgré certaines incertitudes dans la corrélation des séquences élémentaires, de telles interprétations séquentielles haute résolution donnent l'opportunité de reconstruire les changements environnementaux haute fréquence dans différents domaines de dépôt avec une résolution temporelle de quelques dizaines de milliers d'années. La corrélation séquentielle et cyclostratigraphique haute résolution permet d'examiner en détail l'inondation de la plate-forme du Jura et de la région du Dorset. Il peut être montré que la transgression est fortement diachrone sur la plate-forme du Jura principalement à cause de la morphologie de la plate-forme et de la subsidence différentielle. De rapides changements de faciès surviennent dans les environnements marins marginaux principalement dû à des effets de seuil (p. ex., inondation des hauts topographiques).

Il est bien connu qu'un changement climatique d'un climat aride méditerranéen vers des conditions plus humides prirent place durant le Berriasien dans l'Europe centrale et du nord-ouest (p. ex., DECONINCK 1987, HALLAM et al. 1991, ALLEN 1998, ABBINK et al. 2001). L'interprétation séquentielle et cyclostratigraphique haute résolution de cette étude permet d'analyser le changement climatique plus en détail. Il est suggéré que les changements océanographiques principalement reliés à l'influence des eaux de surface boréales froides et téthysiennes chaudes furent responsables du changement climatique dans ces parties de l'Europe. Un rôle-clé dans l'échange de ces masses d'eau joua dans l'évolution du détroit entre le Groenland et la Norvège durant le Berriasien. Des facteurs additionnelles comme l'ouverture persistante du proto-Atlantique Nord et l'ouverture et la fermeture des détroits entre les bassins épicontinentaux de l'Europe contribuèrent au changement climatique dans les zones étudiées. Les changements climatiques dans la bande de fréquence de Milankovitch peuvent avoir été contrôlés par des variations dans l'extension des cellules de circulation atmosphérique et dans leurs positions paléogéographiques.

## ACKNOWLEDGEMENTS

---

This work would not have been possible without the support of many colleagues, friends, and family to whom I am deeply thankful.

First, I would like to thank my “Doktorvater” André Strasser, who gave me the opportunity to leave the steep valleys of Central Switzerland (“Suisse primitive”), to cross the “Röschtigraß” (language limit between the German and the French parts of Switzerland) and to settle down in the medieval capital of Fribourg (“basse ville”). The four years in Fribourg passed quickly not only because of the extraordinary, but mainly because of the interesting sedimentological approach I applied in my PhD study. Going into the details of sedimentology fascinated me since the exploring activities as a child in the sandbox. André taught me how to look at rocks in detail, to extract the essential geological information and to relate them to a wider context. Moreover, I learned how to chase for indications of Quaternary sea-level highstands along different coasts. I am sure, that I will continue to hunt for sea-level highstands. Furthermore, I want to thank André for his constant interest in my work, his intellectual support, his enormous patience, and refreshing humour.

I further thank Adrian Immenhauser (University of Bochum) and Hanspeter Funk (ETH Zurich) that they agreed to be experts and jury members for my dissertation and that they gave time and effort for evaluating this PhD study.

Christian Caron, our institute’s director, cares for outstanding working conditions: a personal office with the newest technical equipments (computer, microscopes). He also showed me the preciseness and complexity of the French language. Moreover, he has an enormous confidence in his PhD students because he entrusted his private car to me on a field excursion

to the Jura Mountains a week after I past my driving test. Nearly, the car ...!

Big thanks go to Elias Samankassou, who helped me with his enormous knowledge in facies analysis under the microscope and in the field. Moreover, he took most of the excellent field pictures displayed in this study. Elias was always open for questions and gave good advices. Thank you very much!

Niels Rameil introduced me into the secrets of the institute. Besides his huge knowledge about carbonates and other things, he supported and advised me with his extraordinary computer knowledge. He is also a source for outstanding music I did not know before. Moreover, he was one of the organizers of the film evenings (Geocinema) at the institute. Thanks Niels!

I was engaged in good technical negotiations (e.g., about strange things in thin sections, graphical problems) with my office neighbour Stéphanie Védrine. She also had endless patience when I tried to explain something in my Swiss “primitive” French. Her critical advices helped me much to improve my ideas. Moreover, she translated my abstract into the French Résumé. Thank you very much!

Big thanks go to all other members of the sedimentology group in Fribourg. Richi Waite shares my view on the town of Fribourg to a large extent (e.g., on the tower of the Saint Nicolas cathedral). Take care on your legs! Noémie Stienne supported me during the snorkeling lessons for Elie in the Red Sea. Dani Marty gave me literature on dinosaur tracks and tried to determine the dinosaur footprints (cf. Pl. 12/3).

I thank Jean-François Deconinck and his team for their friendly welcome at the University of Dijon (France) and the measurements, determinations, and interpretations of the clay minerals. I also would like to thank László Kocsis and Torsten Vennemann for the measurements of the stable isotopes at the University

of Lausanne (Switzerland).

During the first year in Fribourg I shared the office with Cécile Bonnet in the sphere of action of the dynamic tectonic group of Jon Mosar. They taught me important French words and expressions. Jon always insisted on the importance of tectonics for sedimentological processes and bombarded me with the corresponding literature on palaeotectonics and plate dynamics.

The exercise lessons in geology (“tépé”) were always a pleasure thanks to the excellent ambiance and the curious first year students. The excellent teaching skills of Jon Mosar and Christian Caron and the good team of assistants (Luc Braillard, Corinne Saudan and others) contributed to this good learning atmosphere. I profited from the teaching team and from the partly tough but interesting questions of the students.

Many thanks go to Jean-Pierre Berger, who gave me important literature on charophytes and ostracodes. He also gave me some ideas about the “ostracodites”. His excellent teaching skills in lectures and on excursions widened my poor knowledge in paleontology.

Silvia Spezzaferri organized and managed the successful excursion to the Red Sea. She always stressed the importance of micropalaeontology for geosciences, especially foraminifera, with a lot of dedication. Viva i foraminiferi!

Michèle Caron’s famous cakes and the continuous supply of “Coeurs de France” sweetened many hard working days at the institute (and allayed many peckish stomachs). Her helpfulness and cordiality contributed much to the good atmosphere at the institute. Thank you!

Bernard Grobéty and Vincent Serneels always cared for good contacts between the lower (geology) and the upper half (petrography) of the institute building. They are both interesting interlocutors with an enormous knowledge on many topics. Their instructive excursions to Cyprus and Sardinia remain unforgettable! Thank you very much!

All other PhD students contribute(d) to the good atmosphere at the institute. Big thanks go to: Andrea, Claire, Giacomo, Giordana, Kuno, Maëlle, Mikaël, Martin, Peter, Pierre, Thibault, Sabina, Sébastien, and Stephan. All the students in geology, which have been formed or are still in education at the institute are acknowledged as well. I wish you all the best for your master or PhD theses!

A great service has been done by the technical and administrative staff. Patrick Dietsché prepared

the excellent thin sections of this study and Daniel Cuennet had always the right tools for solving any technical problems. I would also like to thank Christoph Neururer, who was always interested in our work as geologists and asked many critical questions. Administrative concerns have efficiently been done by the secretaries Nicole Bruegger and Françoise Mauroux. They also hunted down many important publications.

I would equally like to thank Mister Caretti, the owner of the Val de Fier quarry (S.A.R.L. Caretti S.A.), who gave me the permission to work in the quarry and kindly informed me about the danger of rockfalls in his quarry.

Big thanks go to Katja von Allmen, who always has good ideas for activities outside the institute building. Her enthusiasm for the Swiss national football team (mainly Barnetta!) during the World Championships in summer 2006 inspired me and gave me a good reason to finish working on the PhD study.

Many thanks go to Claudius Pirkenseer and his wife Andrea for their hospitality. They invited me several times for dinner and gave me the unique opportunity to taste onion-rich Bavarian delicacies and true Bavarian beer. Moreover, Claudius provided me with hardrock music and introduced me to the secrets of electric guitars. His wide field of interests from gales to tubercles of ostracodes fascinated me much.

There were many friends who made sure that I crossed the Rötshgräben and went back to the German part of Switzerland. In particular, I would like to thank the ex-fellow students Alex & Gabi, Beat & Regula, Nicolas & Géraldine, and Lorenzi & Eveline.

Big thanks go to the Zuger connection Urs and Roli, on whom I can absolutely rely. They accompanied me on many unforgettable trips in Switzerland and abroad.

I thank my family for their material and immaterial support during all my studies and their interest in my work. In particular, I thank my mother, my father, and my uncle Hans, who enjoyed helping me in the field. Especially, Hans was well equipped to fight indefatigably against the hard carbonate rocks of the Pierre Châtel Formation. He left behind unambiguous geological tracks at many locations in the Jura Mountains.

The research presented in this GeoFocus volume was financed by the University of Fribourg and the Swiss National Science Foundation (project no. 2000-067736.02).

# 1 - INTRODUCTION

The aim of present study is to investigate a transgression within a narrow time interval (Middle Berriasian). A remarkable Middle Berriasian transgression has been described from sections on the Jura platform in France and Switzerland and from sections in the Dorset region of southern England since the late 19<sup>th</sup> century. Coastal sediments are very sensitive to sea-level changes and, therefore, excellent archives for the reconstruction of sea-level fluctuations in the past. HANCOCK & SKINNER (2000) wrote that “to geologists shorelines have a particular importance because they are relatively easy to identify in rock successions: they coincide not only with changes from strata with dominantly marine biota to strata with freshwater biota, or none, but also with many unconformities, and their migration demonstrates the clearest evidence of sea-level changes” (p. 887). The present study deals with high-frequency sea-level fluctuations and other controlling factors and attempts to evaluate their importance and expressions in the sedimentary record.

The dating of the Middle Berriasian transgression and its correlation between the Jura platform, southern England, and other European regions is a problem and has been discussed controversially in the literature over decades (e.g., CASEY 1973, WIMBLEDON & HUNT 1983, DÉTRAZ & MOJON 1989, ALLEN & WIMBLEDON 1991). The dating remains a challenge because on the Jura platform and in the Dorset region continental to shallow lagoonal sediments have been deposited in Late Tithonian to Middle Berriasian times (around the Jurassic/Cretaceous boundary). Open-marine organisms like ammonites and calpionellids, which are commonly used for dating Berriasian deposits, are rare or absent in these marginal-marine environments. However, charophyte-ostracodes assemblages have been applied successfully (MOJON 2002). Another problem is non-deposition and erosion in these marginal-marine environments. Especially during falling relative sea level (regressions), the sedimentary

record is incomplete. These problems can be addressed by a careful analysis of detailed sections, by sequence-stratigraphical correlations between platform and well-dated basinal sections, and by evaluation of the time involved in omission surfaces by a cyclostratigraphical interpretation.

In the last 10 years, the Fribourg research group investigated the Jura platform and other regions with high-resolution sequence- and cyclostratigraphy. Rocks representing a time interval of about 20 million years from the Oxfordian to the Valanginian have been investigated by several PhD studies (PASQUIER 1995, PITTET 1996, HILLGÄRTNER 1999, DUPRAZ 1999, COLOMBIÉ 2002, HUG 2003, RAMEIL 2005). In particular, Berriasian sections have been interpreted (STRASSER 1988, WAEHRY 1989, STRASSER 1994, PASQUIER 1995, PASQUIER & STRASSER 1997, STRASSER & HILLGÄRTNER 1997, HILLGÄRTNER 1998, HILLGÄRTNER 1999, HILLGÄRTNER & STRASSER 2003, STRASSER et al. 2004, RAMEIL 2005; cf. Fig. 1.1).

The present study takes advantage of this well-established biostratigraphical and sequence-stratigraphical framework. According to the sequence-stratigraphical interpretation of PASQUIER & STRASSER (1997) and HILLGÄRTNER (1999), the large-scale transgression lies between two major sequence-boundary intervals, which correspond to the 3<sup>rd</sup>-order sequence boundaries Be4 and Be5 in the sequence- and chronostratigraphic chart of HARDENBOL et al. (1998; cf. Fig. 1.2). The present study goes a step further in the resolution of time and space by focusing on an interval of only a few 100 thousand years.

## 1.1 Objectives and methods

The main objective of this study is to investigate the evolution of the Middle Berriasian transgression in the marginal-marine environments of the Jura

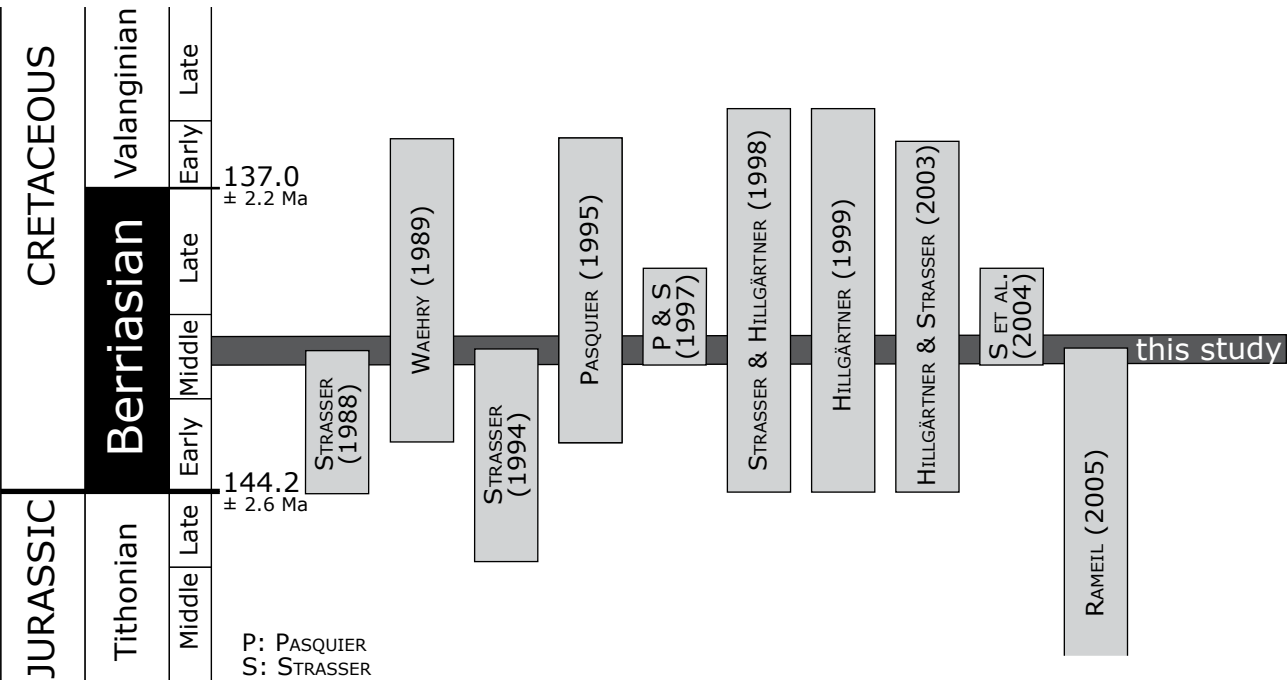


**Fig. 1.1** - Stratigraphic ranges of previous studies dealing with high-resolution sequence-stratigraphical interpretations of sections on the Jura platform around the Middle Berriasian transgression. All these investigations serve as a basis for the present study. Numerical ages are taken from the chronostratigraphy of GRADSTEIN et al. (1995).

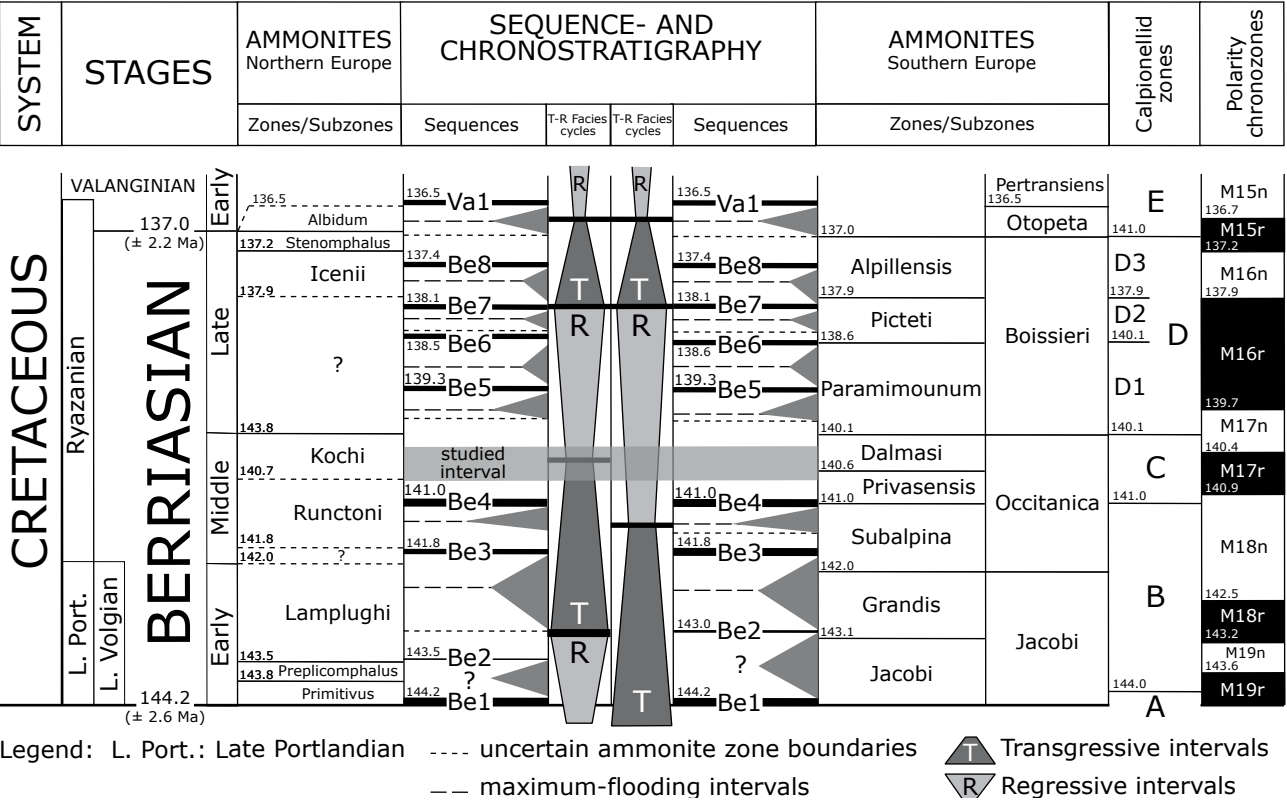


**Fig. 1.2** - Sequence- and chronostratigraphic chart of HARDENBOL et al. (1998). The studied interval around the Middle Berriasian transgression is shaded gray.

platform and the Dorset regions in space and time with high resolution. In order to achieve this aim, the study follows the following steps:

- logging the field outcrops in detail, interpreting them in terms of depositional environments and developing a facies model for each of the investigated regions (Jura platform and Dorset region; cf. Chap. 2)
- interpreting the facies evolution of each section in terms of high-resolution sequence stratigraphy (cf. Chap. 4 and 5)
- correlating the sections between the different palaeoenvironments based on the sequence-stratigraphical interpretation and the bio-, and magnetostratigraphic framework (cf. Chap. 6)
- evaluating the driving factors for the high-frequency sea-level changes and establishing a time frame through cyclostratigraphy (cf. Chap. 6 and 7)
- using the obtained sequence- and cyclostratigraphic framework in order to improve the understanding of the palaeoenvironmental dynamics during the Berriasian (with focus on Middle Berriasian times) in Central and NW Europe and estimating the importance of the different driving factors (e.g., climate, sea-level changes, tectonics, oceanic current pattern; cf. Chap. 8 and 9)

## 1.2 General context

### 1.2.1 Study areas

#### *Jura Mountains*

The studied sections are located in the central to southern Jura Mountains along the border of northwestern Switzerland and eastern France (cf. Fig. 1.3). The Jura mountain chain has been formed during a late Alpine phase (Miocene and Pliocene) in relation with the orogenesis of the Alps (cf. Chap. 4).

#### *Dorset region*

The Dorset sections are located in the south

and southeast of the Isle of Purbeck at the coast of the English Channel in southern England (cf. Fig. 1.3). Today's geometry of the Dorset outcrops is the result of Cenozoic contractional reactivations of the Mesozoic Purbeck Fault system (structural inversion; e.g., UNDERHILL & PATTERSON 1998, UNDERHILL 2002). Since 2001, the beautiful landscape of the Dorset coast is protected by the UNESCO as a World Heritage Site (see picture on the front page).

#### *Vocontian basin*

The deposits of the Vocontian basin are located in southeastern France in the French Subalpine Range (cf. Fig. 1.3). They have been incorporated into the Alpine orogenesis of the Western Alps during the Tertiary.

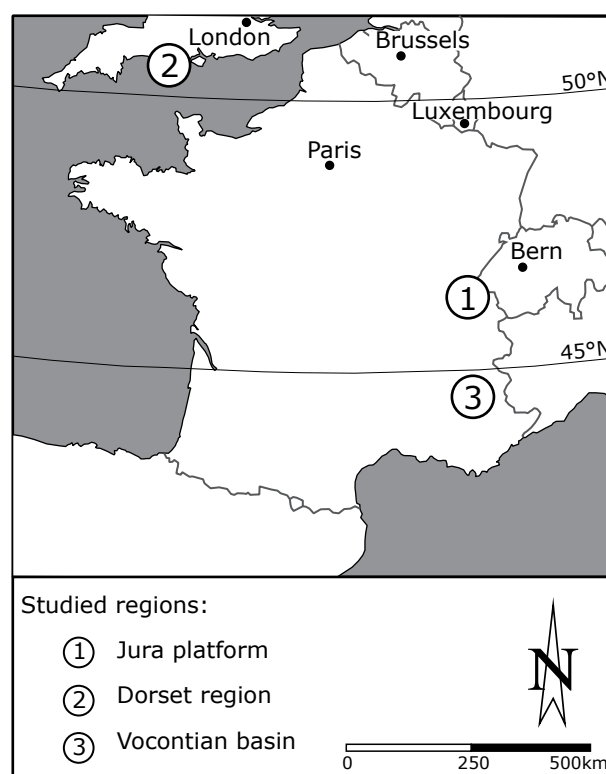


**Fig. 1.3** - Geographic locations of studied regions.

### 1.2.2 Stratigraphy

#### *Sequence- and chronostratigraphy*

According the sequence-stratigraphical correlations of PASQUIER (1995), PASQUIER & STRASSER (1997), HILLGÄRTNER (1999), and STRASSER et al.



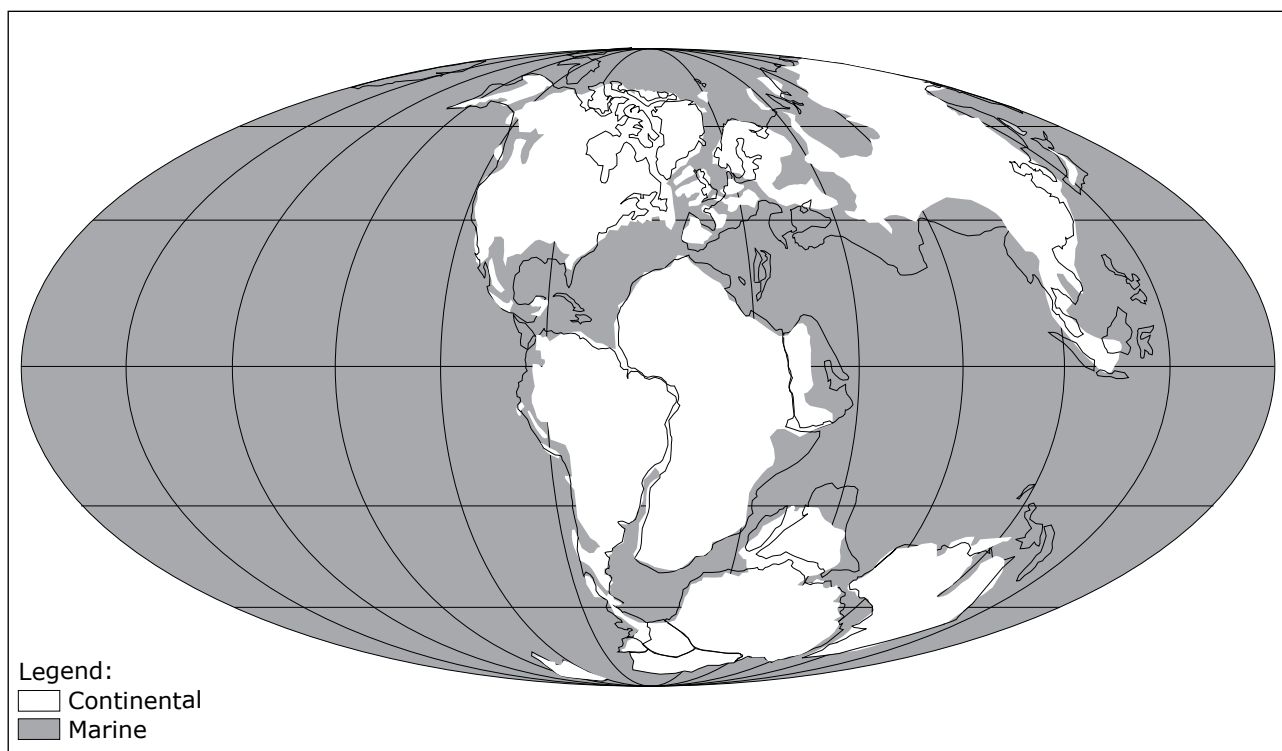


**Fig. 1.4** - Global palaeogeographic map of the Berriasian-Valanginian (modified from SMITH et al. 1994).

(2004), the investigated intervals of the sections on the Jura platform and the Montclus section lie between the 3<sup>rd</sup>-order sequence boundaries Be4 and Be5 in the sequence- and chronostratigraphic chart of HARDENBOL et al. (1998; cf. Fig. 1.2). According to this chart, the interval between these two large-scale sequence boundaries corresponds to the Middle (141.0 Ma) to Late Berriasian (139.3 Ma). The ages of the two large-scale sequence boundaries have been interpolated between two radiometrically dated tie-points: the Tithonian-Berriasian boundary ( $144.2 \pm 2.6$  Ma; corresponds to 3<sup>rd</sup>-order sequence boundary Be1) and the Berriasian-Valanginian stage boundary ( $137.0 \pm 2.2$ ; corresponds to 3<sup>rd</sup>-order sequence boundary Val1; HARDENBOL et al. 1998). The ages of the tie-points are based on the chronostratigraphy of GRADSTEIN et al. (1995). The stage boundary between the Berriasian and the Valanginian is mainly based on the study of BRALOWER et al. (1990), in which a U/Pb date of  $137.1 \pm 0.6$  Ma has been measured in volcanic horizons of the Grindstone Creek section in northern California. GRADSTEIN et al. (1995) calibrated biostratigraphical zonations of the Berriasian to Early Valanginian interval with magnetostratigraphical investigations derived from several studies (e.g., GALBRUN 1985, OGG & LOWRIE 1986, OGG et al. 1988, 1991, CHANNELL & GRANDESSO 1987, CHANNELL et al. 1987, 1995). A revised chronostratigraphic chart has

been published by GRADSTEIN et al. (2004). The timing of the tie-points for the Berriasian stage, however, has not been changed in this new chart. All other ages in the Berriasian stage (e.g., biostratigraphical zones, polarity chrons, and 3<sup>rd</sup>-order sequences) in the chart of HARDENBOL et al. (1998) are interpolated between these two radiometrically dated anchor points.

### **Biostratigraphy**

The base of the Middle Berriasian transgression on the Jura platform has been dated by some rare ammonites (CLAVEL et al. 1986, WAEHRY 1989; cf. Chap. 4). Moreover, a high-resolution biostratigraphy based on charophyte-ostracode assemblages has been established for the Berriasian by MOJON & STRASSER (1987), DÉTRAZ & MOJON (1989), and MOJON (2002). The top of the large-scale intervals (around the 3<sup>rd</sup>-order sequence boundary Be5) has been dated by the benthic foraminifera *Pseudotextulariella courtionensis* and *Pavlovecina allobroensis* (PASQUIER 1995, HILLGÄRTNER 1999; cf. Fig. 6.2). These two species have a limited biostratigraphical range and have commonly been used to date Late Berriasian deposits of the Jura platform (e.g., STEINHAUSER & LOMBARD 1969, STEINHAUSER & CHAROLLAIS 1971, DARSAC 1983, SALVINI-BONNARD et al. 1984, ADATTE & RUMLEY 1984,



CLAVEL et al. 1986, BLANC 1996).

For the marginal-marine sections of the Dorset region, detailed lithological logs have been published by ENSOM (1985) and CLEMENTS (1993). The corresponding interval in the Dorset sections (between the 3<sup>rd</sup>-order sequence boundary intervals Be4 and Be5) has been logged and interpreted in terms of high-resolution sequence stratigraphy in the present study (cf. Chap. 5). The investigated Durlston Bay section has been dated by ostracodes (e.g., ANDERSON & BAZLEY 1971, ANDERSON 1985), by ostracode-charophyte assemblages (MOJON 2002), and by magnetostratigraphy (OGG et al. 1991, 1994).

The Montclus section in the Vocontian basin is well dated by ammonites (Subalpina to Paramimounum subzones; LE HÉGARAT 1973) and by calpionellids (zones B to D1; JAN DU CHÊNE 1993, PASQUIER 1995, HILLGÄRTNER 1999; cf. Chap. 6). The ammonite zonation used in this study follows the sequence- and chronostratigraphic chart of HARDENBOL et al. (1998). Compared to the chronostratigraphic chart of GRADSTEIN et al. (2004), slight lithostratigraphic mismatches occur only in the Boreal ammonite zonations between the 3<sup>rd</sup>-order sequence boundaries Be4 and Be5 (cf. Chap. 6).

### Lithostratigraphy

The investigated lithostratigraphic interval covers the transition of the Goldberg Formation to the Pierre Châtel Formation in the sections of the Jura platform (cf. Chap. 4). In Dorset, the investigated intervals lie at the transition of the Lulworth Formation to the Durlston Formation (cf. Chap. 5). For the Berriasian deposits of the Montclus section (Vocontian basin) no lithostratigraphical subdivisions are given (PASQUIER 1995, HILLGÄRTNER 1999; cf. Chap. 6).

## 1.2.3 Palaeogeography

Several global palaeogeographic maps have been published, which cover the interval from latest Jurassic to earliest Cretaceous times (Tithonian to Valanginian; e.g., BARRON et al. 1981, FUNNELL 1990). The global map of palaeo-coastlines during Berriasian to Valanginian times published by SMITH et al. (1994) is displayed in Fig. 1.4. It illustrates the land-ocean distribution and the positions of the continents on the globe. Both factors are important for palaeoclimatic and palaeoceanographic reconstructions.

The break-up of Gondwana along the future South Atlantic started in the south and continued to the north

in Late Jurassic times. During the Berriasian, however, the Afro-Brazilian depression (a large, shallow basin in northeast Brazil) was still in the pre-rift stage (DA ROSA & GARCIA 2000). The Central Atlantic was already open and Iberia began to separate from North America during Middle Jurassic times (e.g., SCHETTINO & SCOTSE 2002). During the Tithonian, the opening of the Bay of Biscay may have started (e.g., OLIVET et al. 1996, GUILLOCHEAU 2000, CAVAZZA et al. 2004). The fact that continents were arranged close the palaeo-south pole (Antarctica, Australia) may have enabled

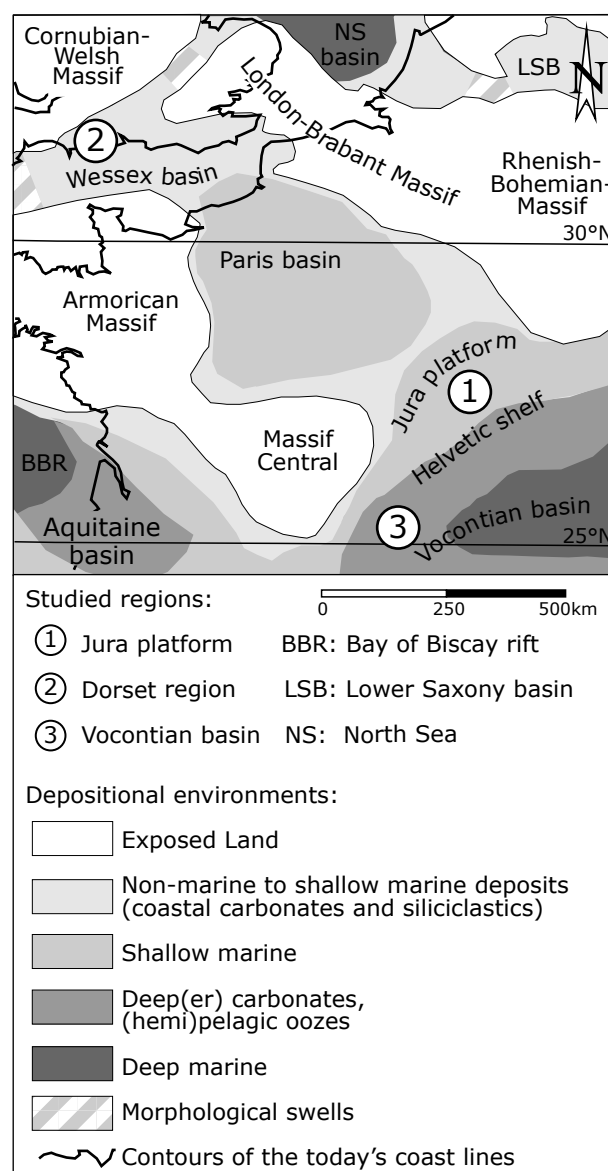


**Fig. 1.5** - Palaeogeographic situation of the studied regions. The palaeogeographic map is based on THIERRY & BARRIER (2000; modified for the Berriasian after ALLEN 1963, RAWSON & RILEY 1982, CURNELLE & DUBOIS 1986, KARNER 1987, ZIEGLER 1988, ARNAUD 1988, MUTTERLOSE 1992, STRAUSS et al. 1993, GUILLOCHEAU et al. 2000).

the growth of ephemeral ice sheets in Tithonian to Valanginian times (e.g., PRICE 1999, ALLEY & FRANKS 2003, MILLER et al. 2005).

Epicontinental shallow-marine seas and relatively small land masses covered the European continent during the Berriasian (European archipelago; cf. Fig. 1.5). The Vocontian basin was a branch of the western Tethys. The Jura platform was part of the northern continental margin of the western Tethys Ocean. Today's Dorset region was situated to the north of the Channel sub-basin during the Berriasian, which was a part of the epicontinental Wessex basin (e.g., RUFFELL 1995).

The palaeolatitude of the Jura platform was approximately 25 to 30° N according to palaeogeographic reconstructions (e.g., ZIEGLER 1988, THIERRY & BARRIER 2000, CAVAZZA et al. 2004). According to these reconstructions, the Vocontian basin was located about 2 to 3° further to the south. The Dorset region was in a palaeolatitudinal range of 30 to 35° N during the Berriasian. OGG et al. (1994) calculated a palaeolatitude of about 34° N based on palaeomagnetic measurements on sections of the Dorset region.

## 1.2.4 Palaeoclimate and palaeoceanography

### *Palaeoclimate*

During the Middle Berriasian, a long-term change from an arid, Mediterranean climate to more humid conditions has been postulated for Central and NW Europe mainly based on clay-mineralogical investigations (e.g., DECONINCK 1987, HALLAM et al. 1991, RUFFELL & RAWSON 1994, ALLEN 1998, SCHNYDER 2003, SCHNYDER et al. 2005a, 2006; cf. Chap. 8). This long-term climate change may be related to changes of surface water currents on the European archipelago and to the opening of the proto-North Atlantic. Climate fluctuations triggered by insolation changes on the Milankovitch-frequency band have been superimposed on this long-term climate change by influencing the extensions and positions of the atmospheric circulation cells (cf. Chap. 8).

### *Palaeoceanography*

During the Early Cretaceous, exchange of oceanic water masses and heat-transport was probably restricted to the Tethyan Pacific Ocean and some shallow marine

seaways (e.g., COVEY & BARRON 1988; cf. Chap. 8). During the Berriasian, a marine connection between the Central Atlantic and the western Tethys may have existed (ADATTE et al. 1996; cf. Fig. 1.4). Moreover, a marine connection between the Central Atlantic and the Tethyan Pacific via the Panama Seaway has been postulated (e.g., WINTERER 1991, BORNEMANN et al. 2003; cf. Fig. 1.4).

In Europe, marine water-mass exchanges probably occurred through shallow seaways between the epicontinental seas and the Tethyan Ocean. However, morphological swells, which opened and closed in tune with relative sea-level changes, controlled the water-mass exchanges and may strongly have influenced the palaeoclimate of Central and NW Europe during the Berriasian (e.g., SCHUDACK 1999, ABBINK et al. 2001, MICHALÍK 2002; cf. Chap. 8). A central role in the exchange of cold Boreal and warm Tethyan water-masses on the European archipelago played the widening of the proto-North Atlantic and the evolution of the Greenland-Norway Seaway in these times (e.g., HALLAM 1994, ALLEN 1998, MUTTERLOSE et al. 2003).

### *Eustatic sea-level changes*

The latest Jurassic and earliest Cretaceous is characterized by a long-term regressive trend at least in Europe. It has been postulated that this regression was of tectono-eustatic origin (2<sup>nd</sup>-order sequences or T-R facies cycles; e.g., RAWSON & RILEY 1982, HAQ et al. 1987, HARDENBOL et al. 1998, JACQUIN et al. 1998, HALLAM 2001, AURELL et al. 2003; cf. Fig. 1.2). For the Berriasian, several regional long-term sea-level curves have been presented (e.g., FLEXER et al. 1986, SURLYK 1991, SAHAGIAN et al. 1996; cf. Fig. 1.6). A long-term eustatic sea-level curve for the Cretaceous has been published by HAQ et al. (1987). A Middle Berriasian transgression is expressed in the sea-level curves of SURLYK (1991) and SAHAGIAN et al. (1996). In the other two sea-level curves, there are no indications of a transgression in Middle Berriasian times. These deviations may be explained by regionally different tectonic movements, by differences in dating, and/or by the applied backstripping models.

High-frequency eustatic sea-level fluctuations with low amplitudes were superimposed on this long-term sea-level trend. They are related to insolation changes on the Milankovitch-frequency band (cf. Chap. 7). However, eustatic sea-level signals are in many cases disturbed or obliterated by tectonic movements and other factors as discussed in Chap. 6 and 7.

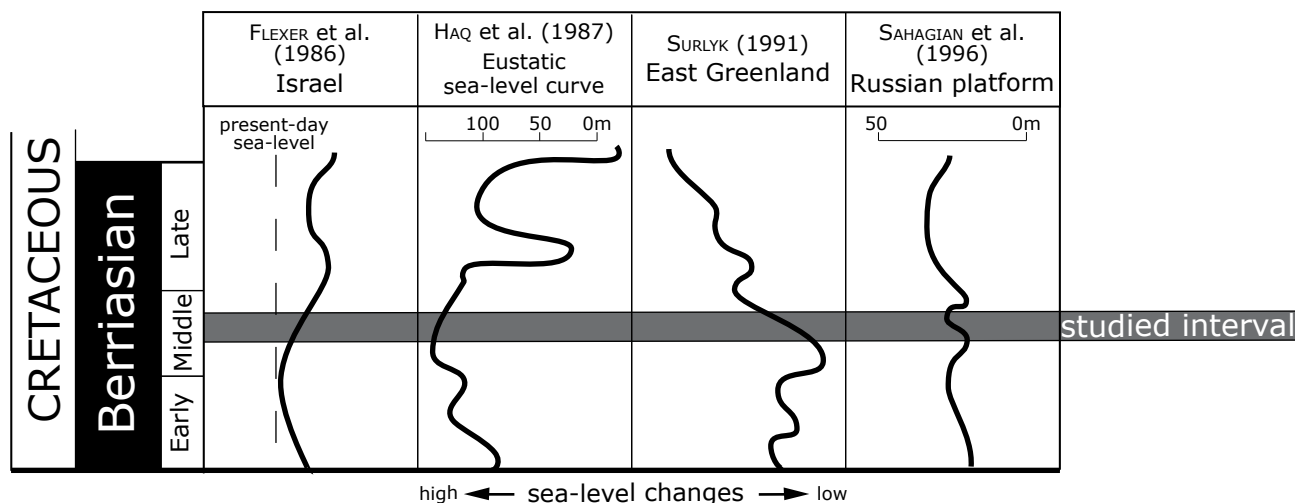


Fig. 1.6 - Comparison of several long-term sea-level curves of the Berriasian. Studied interval is shaded gray.

### Palaeobiogeography

During the Berriasian in the northern Hemisphere, marine floras and faunas show a clear differentiation into the Tethyan and the Boreal realm. The Boreal realm includes Russia, northern Europe, Greenland, and Alaska; the Tethyan realm comprises the areas farther south. This palaeogeographic differentiation is reflected in the use of two different stage names for the interval covering the Jurassic/Cretaceous boundary: in the Tethyan realm the stage names Tithonian and Berriasian are used, while in the Boreal realm

the terms Volgian and Ryazanian are employed (e.g., RUFFELL 1991, MUTTERLOSE et al. 2003; cf. Fig. 1.2). This provincialism of the marine biota has been related to the pronounced eustatic sea-level lowstand at the Jurassic/Cretaceous boundary, which makes the correlation of the Tethyan and Boreal realms difficult (e.g., CASEY 1973, SACHS et al. 1975, ZEISS 1983, WIMBLEDON & HUNT 1983, REMANE 1991, 1998, ALLEN & WIMBLEDON 1991, MUTTERLOSE 1992, HOEDEMAEKER & LEERFELD 1995, BARABOSKIN 1999, 2002, HOEDEMAEKER 2002, BORNEMANN et al. 2003, ZAKHAROV & ROGOV 2003; cf. Chap. 8).

\*\*\*\*\*



## 2 - FACIES ANALYSIS AND INTERPRETATION

### 2.1 Definitions

#### 2.1.1 Microfacies

In order to describe limestones in detail, collected field samples are prepared for investigation with optical microscopes (thin section analysis by plain and/or polarized light) and binocular microscopes (polished or etched slabs and acetate peels; e.g., FLÜGEL 2004). Magnification enables a better identification of the (micro-) fossils and allochems, texture, small-scale sedimentary structures and diagenetic features. Therefore, the term microfacies comprehends the sum of all palaeontological and sediment-petrographic criteria that can be obtained mainly by light-optical microscope investigations.

#### *Facies*

The term facies corresponds to the entity of all organic and inorganic characteristics of a sedimentary rock (Fig. 2.1). The identification of facies includes field observations (e.g., composition, colour, textures and sedimentary structures) and microfacies analysis (TUCKER & WRIGHT 1990, FLÜGEL 2004).

#### *Facies zone*

The term facies zone describes a depositional environment that is composed of one to several related types of facies. In contrast to the more or less linear geometry of “facies belts” (e.g., WILSON 1975, FLÜGEL 1982), facies zones are considered as the product of complex depositional processes creating rather facies mosaics than “facies belts” (WRIGHT & BURGESS 2005;

cf. Figs. 2.2 and 2.3).

### 2.2 Approach

The detailed interpretation of the carbonate rocks in terms of microfacies and facies is the base of this study. The challenge of sedimentological interpretations is to obtain the essential information from a sample by field observations and microfacies analysis and to define its facies. In this study, the facies represents the smallest lithological unit.

A total of 169 section meters has been logged and studied bed by bed. Thin section analyses of 666 samples were carried out by light-optical microscope investigations in order to determine depositional facies of the Jura platform and the Dorset realm. Etched slabs have been used to analyze larger constituents (e.g., oncoids and corals) and sedimentary structures in some rock samples. Additionally, 75 samples of marls were washed and sieved. The obtained fractions have been picked and analyzed under the binocular. On average, five samples per meter have been investigated for Jura platform sections. For the sections of the Dorset region, less samples have been analyzed (average: two samples per meter; cf. Annex 1).

Lateral transitions between facies at a certain time are common in shallow carbonate depositional systems. Hence, the description of a facies has to incorporate lateral variations over meters to several tens of meters. The goal is to integrate the different facies into representative depositional environments (facies zones).

The scientific approach to strictly separate description and interpretation is not used in this chapter in order to avoid repetition. The descriptions of the sedimentological features (constituents and sedimentary

structures) and their interpretation are based on the rich literature of carbonate sedimentology cited in the corresponding paragraphs. This chapter presents the major sedimentological features identified in the sections of the Jura platform and in the Dorset realm. Each constituent is interpreted within the context of the facies, in which it occurs. Special features found in the sections of the Dorset realm are discussed in Chapter 5. The aim of this chapter is to elaborate facies zones and to integrate them into conceptual facies models.

## 2.3 Constituents

This study deals with carbonate rocks, which are produced within the depositional system itself. Either they originate from fossils (skeletal grains) or they precipitate as allochems (non-skeletal grains) commonly with the help of biological mediation processes. Generally, the producing organisms reflect the ecological conditions of their depositional environment (e.g., water temperature, nutrients, salinity, turbidity, bathymetry, and currents).

### 2.3.1 Allochems

The term allochems is used as synonym for non-skeletal grains. Some allochems (e.g., oncoids, peloids, and ooids) are also controlled by biotic processes (FLÜGEL 2004).

#### *Peloids* (Pl. 1/1; 5/4)

Peloids are rounded, spherical to elliptical grains formed by crypto- or microcrystalline material without an internal structure (FLÜGEL 2004). Generally, peloids are smaller than ooids and oncoids (<1mm). The term peloid is non-genetic because the origin of these grains and the pathways of their formation are not fully understood. Peloids occur in all facies described in this study. Partly, they have a rock-building abundance forming peloid limestones (Pl. 1/1).

In some thin sections of Dorset the genesis of different peloids has been documented (SAMANKASSOU et al. 2005). The focus is set on peloids, which resulted from the more or less in-place breakdown of previously micritized bivalve shells.

Particular peloids are “fecal pellets” (Pl. 5/4). These rounded, usually fine-grained components derive from organisms that eat mud, digest organic

matter from the mud and then excrete the non-digested lime-mud (FLÜGEL 2004). Fecal pellets are rare in the investigated deposits.

#### *Ooids* (Pl. 1/2-3)

Ooids are spherical and egg-shaped carbonate or non-carbonate coated grains exhibiting a nucleus that can be of variable composition. The nucleus is surrounded by an external cortex, which is concentrically laminated (laminae). Many ooids have diameters in the range of 0.5 to 1 mm; most of them are smaller than 2 mm (FLÜGEL 2004). Based on their various microfabrics and primary mineralogies, ooids can often be attributed to different environments (marine, lacustrine, fluvial and continental; e.g., DAVIES et al. 1978, RICHTER 1983).

The exact nature of ooid formation is still discussed. It is generally accepted that ooid formation needs regularly agitated shallow waters over a certain time period. Such hydrodynamic conditions prevail in environments influenced by wave and/or current activities.

Modern carbonate ooid formation mainly takes place in tropical to subtropical waters with a supersaturation of  $\text{CaCO}_3$  and a minimal temperature in the range of 18-20 °C. Additionally, the water depth lies in the range of 1-5 meters (maximum 15 meters). It is important to consider transport processes when interpreting ooid-rich deposits.

The ooids found in this study are exclusively carbonate coated grains supposed to be of marine origin because of their co-occurrence with marine organisms. Ooids are present in the Goldberg and the Pierre Châtel Formation (cf. Chap. 4). STRASSER (1986) examined ooids in the Goldberg Formation and established a classification of six different ooid types and related them to specific palaeoenvironments. HILLGÄRTNER (1999) distinguished two main ooid types (radial and micritic) for the Early Cretaceous deposits of the French Jura. In this study, the following three different types of ooids are distinguished: micritic, superficial, and radial.

Micritic ooids are rather delicate to identify because their laminae are obliterated. This is probably due to a pervasive micritization of the cortex. They can easily be confused with rounded mud pebbles and/or fine-laminated, micritic oncoids. They occur in tidal flat to internal-lagoonal deposits together with other ooid types.

Superficial ooids (Pl. 1/3) have a thin cortex with one to two laminae. These ooids have been identified

in tidal flat to internal-lagoonal deposits in the Jura sections. Some superficial ooids have also been found in the Marly Freshwater Member of the Worbarrow Tout section (cf. Chap. 5).

Radial ooids (Pl. 1/2a-b) are characterized by several laminae composed of radial-fibrous crystals (FLÜGEL 2004). STRASSER (1986) divided the radial ooids of the Goldberg Formation into different types (3 to 5). Generally, the deposits of this study exhibit a mixture of different types of radial ooids, which complicates the interpretation of their origin. Radial ooids occur in tidal flat to open-lagoonal deposits of the Goldberg and Pierre Châtel Formation. They are probably produced in high-energy deposits (grainstones) and transported to low-energy environments by different hydrodynamic processes like currents, storms and washovers. HUSINEC & READ (2006) describe relatively large radial ooids from a flat-topped carbonate platform, which are similar to those displayed in Pl. 1/2a. They suggest that these ooids developed along low-energy shorelines, in intertidal ponds and/or lagoons on previously emergent hypersaline tidal flats. During transgression, these deposits migrated landwards forming extensive sheets. This interpretation may explain ooid-rich intervals, which are not characterized by cross-bedding structures (shoal deposits). However, unambiguous indications for beach deposits like keystone vugs and low-angle cross-bedding have not been detected in the investigated parts of the sections. Keystone vugs have been described in stratigraphically overlying sedimentary rocks (PASQUIER 1995, HILLGÄRTNER 1999; cf. Fig. 6.2).

Frequent transitions from one ooid type to another, coexistence of several types in the same facies, and superposition of various cortical laminae reflect gradual or abrupt changes in hydrodynamic regimes and environmental conditions (STRASSER 1986).

#### **Oncoids** (Pl. 1/4-6)

Oncoids are irregularly formed calcareous grains with non-concentric, micritic laminae around a nucleus. These laminae are mainly mediated by cyanobacteria and other encrusting organisms. Different types of oncoids have been described and classified in the literature (e.g., DAHANAYAKE 1977, 1983, HUG 2002, VÉDRINE et al. 2007). Oncoids mainly occur in the Pierre Châtel Formation (cf. Chap. 4). In this study, two types of oncoids are discerned.

Oncoids, which have a maximum diameter of 10 mm are called “small oncoids” (Pl 1/5). They are essentially formed of alternating micritic laminae

around a nucleus. Partly, the micritic laminae are not well-expressed, so that it is sometimes difficult to distinguish them from micritic ooids. This type of oncoid corresponds the type I oncoids of DAHANAYAKE (1977) or to type-3 oncoids of COLOMBIÉ (2002). The well-rounded to elliptical forms point to a continuous agitation in the environment of their origin. This type is abundant in the lagoonal facies of the examined sediments. The frequent co-occurrence with radial ooids in pack- to grainstones indicates moderate- to high-energy environments. In lower energy depositional settings, the co-occurrence with dasyclad algae indicates internal-lagoonal deposits.

Oncoids with a relatively thick, spherical to irregularly-formed cortex and a diameter in the range of a few millimeters to 3 cm (typically 1 cm) are called “*Bacinella*-oncoids” (Pl 1/6a-b). This denomination derives from the cyanobacteria *Bacinella irregularis* (see below), which plays an important role by creating the micritic or peloidal laminae of this type of oncoid. The *Bacinella*-oncoids are composed of discontinuous and/or continuous laminae (DAHANAYAKE 1977). This type of oncoid matches with the type II oncoids of DAHANAYAKE (1977) or the type-1 oncoids of COLOMBIÉ (2002). They are supposed to have formed in relatively calm hydrodynamic conditions with a low sediment supply.

Generally, the size and the shape (irregularity) of an oncoid are thought to represent the degree of water turbulence during its formation. Big and irregular oncoids formed in waters with low turbulence (DAHANAYAKE 1977). The *Bacinella*-oncoids are the main constituents of the frame- and rudstones deposited in open-lagoonal environments of the Pierre Châtel Formation (cf. Chap. 4).

Some oncoids display transitions from ooids (nucleus) to small oncoids. They are termed “oo-oncoids” (Pl 1/4) in this study. These grains can be found in lagoonal, high-energy deposits together with radial ooids and small oncoids.

#### **Intraclasts**

An intraclast is a carbonate fragment of lithified or partly lithified sediments, derived from erosion of nearby penecontemporaneous deposits. Generally, the place of origin lies within the depositional basin (FLÜGEL 2004). They have a size range of a few millimeters to several centimeters. Commonly, intraclasts contain allochems and/or fossils and have shapes from slightly rounded to elongate angular (“mud chips”, “flat-pebbles”; e.g., DEMICCO & HARDIE 1994).

They are formed on tidal flat as well as in lagoonal environments. Commonly, high-energy conditions are involved in their formation such as tidal currents, wave activity and/or storm events. In the sections, they are abundant in tidal channels and shoal deposits. Moreover, intraclasts are characteristic components of reworked sediments, which are good indicators for transgressive deposits in sequence-stratigraphical interpretations (cf. Chap. 3).

**Mud pebbles** are slightly rounded, micritic intraclasts without any internal structure. They can easily be confounded with micritic ooids. These intraclasts are mainly found in tidal deposits (tidal channels).

**Black pebbles** are a particular type of intraclasts. The characteristic feature is the intensive black staining on the micro- and macroscopic scale. Intervals containing black pebbles mainly occur in the Goldberg Formation (e.g., HÄFELI 1966, STRASSER & DAVAUD 1983, MOJON 2002). Black pebbles are thought to be indicators of nearby terrestrial environments (STRASSER 1984).

### 2.3.2 Fossil content

This term comprehends all carbonate grains, which can be identified as relics of animals or plants on a micro- and macroscopic scale. It includes fragmented as well as completely preserved fossils. Skeletal grains and bioclasts can be considered as synonyms for the term fossil content.

#### *Benthic foraminifera* (Pl. 2/1-10)

A variety of benthic foraminifera have been described from the Jura platform (e.g., SALVINI-BONNARD et al. 1984, CLAVEL et al. 1986, WAERHY 1989, PASQUIER 1995, BLANC 1996, HILLGÄRTNER 1999, MOJON 2002). Benthic foraminifera occur abundantly in most lagoonal environments of the Pierre Châtel Formation. The identification of the benthic foraminifera is based on comparisons with published illustrations (e.g., SEPTFONTAINE 1981, ARNAUD-VANNEAU & DARSAC 1984, EBELI & SCHLAGINTWEIT 1998, BUCUR et al. 2004, SCHLAGINTWEIT et al. 2005). Generally, the determinations are carried out on the genus-level. Miliolid foraminifera, small cyclamminids, and big cyclamminids have not been further determined. According to the systematic of SCHLAGINTWEIT et al. (2005), the most abundant and important benthic foraminifera identified in this study are:

- miliolid foraminifera (in general) (Pl 2/1a-c)
- small cyclamminids (in general; size in longitudinal section < 1 mm) (Pl 2/2a-b)
- *Andersenolina* sp. (ex *Trocholina* sp.) (Pl 2/3a-c)
- *Lenticulina* sp. (Pl 2/4a-b)
- *Nautiloculina* sp. (Pl 2/5a-b)
- *Redmondoides* sp. (ex *Valvulina* sp.) (Pl 2/6a-b)
- big cyclamminids (in general; size in axial section > 1 mm) (Pl 2/8-10)

Additionally, rare *Mohlerina* sp. (ex *Conicospirillina* sp.) (Pl 2/7) have been identified. The term “big cyclamminids” comprehends the genera of cyclamminid foraminifera, which generally have a size of more than 1 mm (longitudinal section). Different associations of benthic foraminifera can be attributed to the facies zones of the Jura sections (cf. Fig. 2.1).

**Tidal flat:** The abundance and diversity of foraminifera is strongly reduced. They were probably washed on the tidal flat by tidal currents and storm events from nearby lagoonal environments. This association comprehends small miliolids, small cyclamminids, lenticulins, and *Redmondoides* sp.

**Internal lagoon (restricted conditions):** The strongly reduced diversity of foraminifera characterizes this environment. The association of foraminifera is dominated by small cyclamminids, small miliolids, lenticulins, and *Redmondoides* sp. as in the tidal flat environments. Yet, the abundance of foraminifera is elevated in this depositional environment compared to the tidal flat. It is assumed that these foraminifera lived in such restricted, internal lagoons.

**Internal and open lagoon (normal-marine conditions):** A remarkable increase of abundance and diversity of foraminifera is displayed within this environment. Moreover, the size of the foraminifera increases as well. The association is dominated by larger miliolid foraminifera, big cyclamminids, *Andersenolina* sp., *Nautiloculina* sp., *Redmondoides* sp., and *Lenticulina* sp. As a convention, the terminology for the different genera of foraminifera is treated more universally in this study. As an example, the individuals of the genus *Lenticulina* are called “lenticulins”.

#### *Green algae* (Pl. 3/1-7)

**Dasyclad green algae** of Berriasian deposits are common and well-documented in the literature (e.g., DARGA & SCHLAGINTWEIT 1993, GRANIER & DELOFFRE 1993, SCHINDLER & CONRAD 1994, DIENI & RADOIČIĆ 1999, HUSINEC & SOKAČ 2006). It seems that the



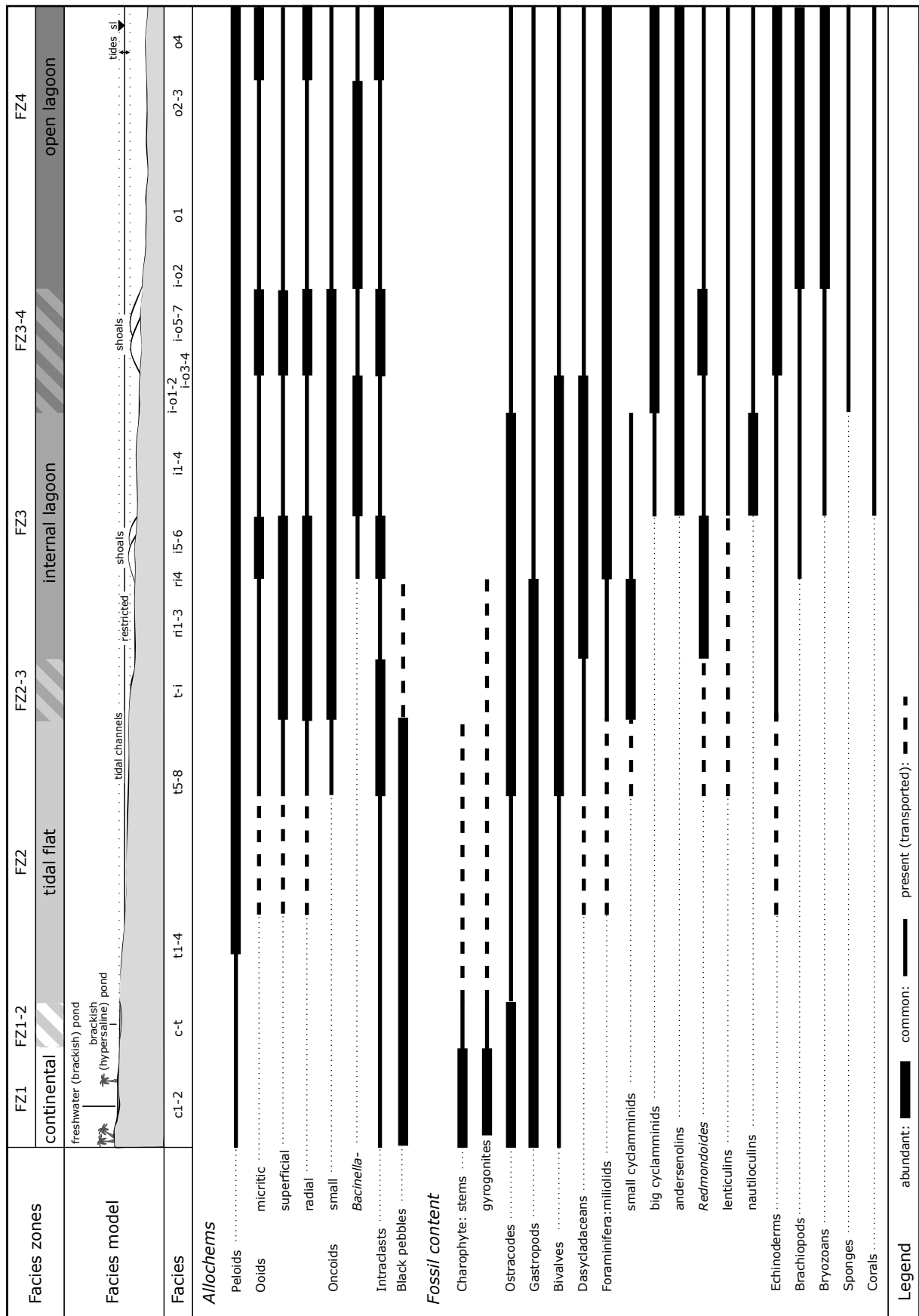


Fig. 2.1 - Distribution of important allochems and fossils in relation to the facies zones (sl: sea level).

Berriasian was an exceptional time for the preservation of dasycladaceans due to their spartic bodies (thallus) (MASSE et al. 1999).

These calcifying, photosynthetic algae occur mainly in shallow, lagoonal environments (FLÜGEL 2004). Mainly in the Pierre Châtel Formation, a rich occurrence of dasycladaceans has been documented (e.g., WAEHRY 1989, PASQUIER 1995). The identification of the dasyclad green algae is based on comparisons with published illustrations (e.g., BUCUR & SĂSĂRAN 2005, SCHLAGINTWEIT et al. 2005). Mainly the species *Clypeina sulcata* (ex *Clypeina jurassica*) (Pl. 3/1a-c) is well-documented in the Pierre Châtel Formation. Other genera of dasyclad green algae have been identified, but they are of minor quantitative importance (Pl. 3/2-6). Monospecific occurrence of *Clypeina sulcata* (Pl. 3/7) together with ostracodes probably points to somewhat brackish and/or hypersaline conditions due to restriction of a shallow lagoonal environment.

**Charophytes** (Pl. 4/1-2) are considered as a separate group of macrophytic green algae. In modern environments, they live submerged in shallow oligotrophic freshwater lakes, rivers and brackish waters of marginal seas. Additionally, they are usually regarded as indicators of healthy clear-water ecosystems in modern aquatic environments (COOPS 2002).

A regular succession of nodes with whorls of small branches, and internodes divides the erect and branched stem (thallus). Fossil charophytes are recorded by internode parts of the stem (Pl. 4/1a-c) and by the female oogonia (gametangia). The oogonium is formed of spiral cells maintained as calcified fructifications. Only the fructifications of the oogonium, called gyrogonite, are preserved in sediments (FLÜGEL 2004; Pl. 4/2a-h).

Charophyte stems (internode parts) and gyrogonites can be identified in the Jura and the Dorset sections. Generally, it is assumed that deposits containing stems as well as gyrogonites point to shallow freshwater ponds in continental settings (MOJON & STRASSER 1987, PLATT 1989) (Pl. 4/2d, f). Intraclasts containing charophyte stems have been found in tidal flat and lagoonal deposits. Gyrogonites are easily transported to tidal flat and lagoonal environments.

Charophytes have been used for the dating of Berriasian continental deposits (e.g., SCHUDACK 1991, FEIST et al. 1995, RIVELINE et al. 1996, COLIN et al. 2004). A biostratigraphical zonation of charophyte-ostracode assemblages has been established for the Jura sections (MOJON & STRASSER 1987, DÉTRAZ & MOJON 1989, MOJON 2002; cf. Chap. 4). MOJON (2002) applied the same assemblage zonation to the Durlston Bay section (cf. Chap. 5).

### **Ostracodes** (Pl. 4/3; 10/3-6)

Ostracode valves are present in all palaeo-environments of the Jura (Pl. 4/3) and the Dorset sections (Pl. 10/3-6). A striking phenomenon is the mass concentrations of ostracode valves, which occur in deposits of the Dorset sections (Pl. 10/6). Several explanations for this have been proposed (e.g., CARBONEL et al. 1988). Such mass-concentrations of ostracode valves probably point to extreme environmental stress factors (e.g., salinity fluctuations) or seasonally changing water bodies with ideal conditions for ostracode populations prevailing in shallow ponds of marginal-marine environments. EL ALBANI et al. (2004) describe monospecific populations of the ostracode *Fabanella bouloniensis* in Berriasian deposits and called them “ostracodites”. Similar observations have been made by HORNE (2002) who relates them to undisturbed deposits in calm waters. Ostracodes have been used as palaeoecological indicators for palaeosalinity reconstructions of shallow coastal waters in the Berriasian (e.g., CARBONEL et al. 1988, KEEN 1993). Distributions of ostracode species in the Purbeck Beds of Dorset are used to group them into faunicycles (e.g., ANDERSON & BAZLEY 1971, ANDERSON 1985; cf. Chap. 5). The interpretation of these faunicycles, however, remains controversial (e.g., KEEN 1993, HORNE, 1995; cf. Chap. 5).

Comparisons of some Berriasian genera of ostracodes with living relatives and their palaeoecological interpretations are given in HORNE (2002). Their palaeoecological interpretations are based on salinity, alkalinity, and persistence of the water bodies derived from analogy studies of modern ostracodes (Tab. 2.1).

Besides their palaeoecological importance, ostracodes are used to establish biostratigraphic zonations of continental realms (e.g., OERTLI 1963, COLIN & LETHIERS 1988, ELSTNER & MUTTERLOSE 1996, HORNE 1995, ANDREU et al. 1996, COLIN et al. 2004). The Dorset sections have been dated by ostracode biozonations (e.g., ANDERSON & BAZLEY 1971, ANDERSON 1985, HORNE 1995; cf. Chap. 5). Zonations based on charophyte-ostracode assemblages are used for the Berriasian of the Jura and the Dorset sections (cf. Chap. 4 and 5)

### **Gastropods** (Pl. 4/4)

They occur in all facies zones of the Jura (Pl. 4/4a-c) and Dorset sections. Gastropods are able to easily adapt to changes of environmental stress factors (e.g., rapid salinity changes, changing sedimentation rates

Berriasian genus	modern genus	salinity	alkalinity	persistence of water bodies
<i>Darwinula</i>	<i>Darwinula</i>	freshwater or slightly saline	high	permanent
<i>Cypridea</i>	<i>Bennelongia</i>	freshwater (saline lakes)	low	temporary (permanent)
<i>Fabanella</i>	<i>Cyprideis</i>	brackish, hypersaline and freshwater	?	temporary (permanent)
<i>Mantelliana</i>	<i>Diacypis</i>	hypersaline (salt lakes)	?	permanent and temporary

**Tab. 2.1** - Comparison of Berriasian genera of ostracodes with modern species. Their palaeoecological interpretations are based on ecological investigations of the corresponding living relatives (HORNE 2002).

and/or elevated water turbidity). The genera *Viviparus* and *Hydrobia* have been described in the Jura as well as in the Dorset sediments (e.g., CLEMENTS 1993, MOJON 2002). According to HUDSON et al. (1995) and RADLEY (2002), the genus *Viviparus* is considered as gastropod, which lives in fluctuating freshwater to brackish waters. The genus *Hydrobia* is assumed to be more related to “closed” periodically hypersaline waters, but also tolerates freshwater conditions.

#### **Bivalves** (Pl. 8/3; 10/1-2; 13/1-2)

They are omnipresent in all facies zones. Neomiodontids have been observed in the Jura and the Dorset sections (e.g., CLEMENTS 1993, MOJON 2002). They are common in fresh to brackish lagoons. In Dorset, bivalves are locally represented as dense, monogeneric shell concentrations. The shells have probably been washed shorewards from shallow lagoons to form “shell beaches” (EL-SHAHAT & WEST 1983; Pl. 10/1a-b; 13/1a-b). FLESSA (1998) reported balanced proportions of landward and seaward displacements of bivalve shells marginal-marine environment during the Holocene transgression. He stated that “shells can move landward only when they are within reach of waves – usually in depths of < 12m” (p. 189).

Generally, neomiodontids are considered as salinity-tolerant opportunists (HUDSON et al. 1995, RADLEY 2002). Monospecific assemblages of *Neomiodon angulata* of Berriasian-Valanginian deposits in Denmark have been related to toxic dinoflagellate blooms in shallow marginal lagoons (NOE-NYGARRD et al. 1987). Near-monotypic *Neomiodon* faunas have also been reported from brackish environments of Middle Jurassic deposits of Scotland (HUDSON et al. 1995).

Oysters have been identified in the Jura and Dorset section. They are mainly present in muddy, low-energy lagoonal deposits of the Jura sections. Some discontinuities interpreted as hardgrounds have been

encrusted by oysters (Pl. 8/3; cf. Chap. 4). In Dorset, the mass concentrations of oyster shells over several meters in height build up the famous Cinder Member (e.g., KELLY 1983, MORTER 1984; Pl. 13/2a-b; cf. Chap 5). They mainly contain the oyster *Praeexogyra distorta* (Pl 10/2). The Cinder Member represents large oyster banks, which grew in coastal bays or lagoons (RADLEY 2002; cf. Fig. 2.3). FÜRSICH (1993) relates Mesozoic low-diversity oyster associations to mesohaline conditions. He states that “in particular, one epifaunal group, the oysters successfully invaded these environments (mesohaline regime) at the latest by Mid-Jurassic time and formed banks and small patch reefs, often in fine-grained lagoonal muds” (p. 341).

#### **Brachiopods**

Brachiopods are stenohaline, sessile organisms preferring a firm substrate. They occur in internal- to open-lagoonal deposits of the Pierre Châtel Formation (platform settings with well agitated waters).

#### **Echinoderms**

Two groups can be distinguished: crinoids and echinoids. Most of the echinoderm fragments are represented by spines and plates of echinoids in the Pierre Châtel Formation. Echinoderms are strictly stenohaline organisms living in internal- to open lagoonal settings (e.g. DUPRAZ 1999). However, some echinoderms have also been found in intertidal and restricted lagoonal sediments. They can easily be transported and displaced by currents due to their porous skeletal structures. The echinoid *Hemicidaris purbeckensis* has been found in the Cinder Member in Dorset. It is the only known species of the English Purbeck (Berriasian sensu lato) according to RADLEY (2002).

### ***Bryozoans***

Bryozoans are suspension feeding organisms living in stenohaline environments. Encrusting forms (Pl. 5/1a) and fragments (Pl. 5/1b) are present in internal- and open-lagoonal sediments of the Pierre Châtel Formation.

### ***Sponges and Corals***

These types of organisms are very rare in the investigated part of the Pierre Châtel Formation. No bioconstructions of corals or sponges have been observed in the Jura sections. Corals and calcareous sponges only occur as reworked clasts in open-lagoonal deposits (Pl. 5/2-3). They probably derive from small patch reefs.

### ***Serpulids***

Serpulids are suspension feeding worms, which construct calcareous tubes. They live in very different environments on hard and firm sea bottoms (FLÜGEL 2004). Serpulids have been identified in tidal flat and lagoonal deposits of the Jura sections (Pl. 5/5a-c). Serpulids are common in the Berriasian “Serpulit Member” of Northwest Germany where they partly create buildups (e.g., WIESNER 1983).

### ***Microbes and associated binding and encrusting organisms***

Bacteria are important organisms for sediment binding and encrusting. In intertidal and lagoonal environments binding and encrusting are essential for sediment stabilization processes and the formation of oncoids. Additionally, bacteria are significant producers of carbonate mud by inducing carbonate precipitation (e.g., CHAFETZ 1986, CASTANIER et al. 1999, FOLK & CHAFETZ 2000, CASTANIER et al. 2000).

Their photo- and heterotrophic metabolisms enable bacteria to inhabit a wide range of environments. Besides bacteria, a variety of other organisms contribute to the binding, encrusting, and mud production in marginal-marine environments. The identification of cyanobacteria is based on comparison with published illustrations (e.g., FLÜGEL 2004, SCHLAGINTWEIT et al. 2005). Cyanobacteria have solely been identified in internal- to open-lagoonal deposits of the Pierre Châtel Formation.

*Bacinella irregularis* is related to a group of cyanobacteria (SCHMID & LEINFELDER 1996). It is an essential constituent of the *Bacinella*-oncoids (Pl. 1/6a-b). The importance of initial stabilization and cementation of carbonate sand by filaments of *Bacinella irregularis* and the formation of subtidal hardgrounds have been documented by HILLGÄRTNER et al. (2001). Commonly, it is associated with the microproblematicum *Lithocodium aggregatum* (Pl. 6/1a-b). The genus *Garwoodia* sp. is defined by its characteristic juxtaposed, round tubes (SCHLAGINTWEIT et al. 2005; Pl. 6/3).

### ***Plant debris***

In Dorset, some intervals contain microscopic plant debris. They are elongated, angular constituents delivered from nearby vegetation.

### ***Bone fragments***

Some small millimetric bone fragments have been identified in the Jura and the Dorset sections. They are amber to brownish in thin section under ordinary light. An open-network structure combined with a more compact outer texture is characteristic for bone fragments (FLÜGEL 2004). Especially the Dorset sections are well known for their rich vertebrate remains (cf. Chap. 5).

### ***Microproblematica***

This term is used to account for organisms found in thin sections, which are enigmatic with respect to their systematic position (FLÜGEL 2004). Additionally, some unidentified structures, which are worth to be documented have been depicted (Pl. 6/2, 5).

## **2.3.3 Other constituents**

### ***Siliciclastics***

In contrast to carbonate rocks, terrigenous clastic sediments are generally formed by the desintegration of parent rocks and mainly transported by rivers to coastal depositional environments. There, they can be picked up by ocean currents and redistributed on the platform and exported to the basin. They are important

constituents for the reconstruction of palaeoclimatic and palaeohydrological conditions of the source area (hinterland *sensu lato*; cf. Chap. 8).

The size of **quartz** grains is in the range of 0.05 to 0.2 mm with a mean of 0.1 mm in the Jura sections (HILLGÄRTNER 1999). Normally, quartz grains are angular to subrounded implying rather short transport distances. A high amount of quartz has been observed in some intervals of the Rusel and Cornaux sections (cf. Chap. 4).

Generally, the quartz content is higher in the Dorset sections compared to the Jura sections. A remarkable increase of the quartz abundance is displayed in the Scallop and Corbula Members (cf. Chap. 5).

A general increase of quartz grains have been reported from Late Berriasian to Early Valanginian deposits of NW and Central Europe (e.g., SLADEN & BATTEN 1984, PASQUIER 1995, HILLGÄRTNER 1999; cf. Chap. 8).

The **clay mineral** content is relatively reduced in the massive limestones of the Jura and Dorset sections. They are mainly concentrated in the marl intervals found in all depositional realms described in this study. The thickness of the marl layers varies between millimetric seams to metric intervals. They comprise illite, chlorite, kaolinite, and mixed-layers minerals as main constituents (cf. Chap. 8). Greenish-gray marls are abundant in the Goldberg Formation of Jura sections (DECONINCK & STRASSER 1987). The dark brownish to black marls have a relatively high amount of organic matter and pyrite. The TOC content of these marls in the Jura sections vary from 0.1 to 0.3% (DECONINCK & STRASSER 1987). Clay mineral analyses are used for palaeoclimate reconstructions (cf. Chap. 8).

### **Organic matter**

Dark marly limestones and marls contain small fragments of organic matter. Some laminated bituminous intervals have been observed in the Dorset sections (and smelled in the field). They are characterized by alternations of dark and light-coloured, fine laminae in clayey limestones. Commonly, they are rich in ostracodes and contain some charophyte stems (Pl 11/1a-b). It is assumed that they represent freshwater to slightly brackish, quiet-water ponds with anoxic bottom waters (cf. Chap. 5). Similar deposits have been described from the Berriasian of NW Germany (WIESNER 1983). According to this author, the dark laminated sediments can be related to high primary production of the green algae *Botryococcus* in

lacustrine environments. HUDSON et al. (1995) stated that “the distribution of *Botryococcus* is of particular interest as it appears to be an excellent index of low salinity” (p. 402).

### **Pyrite**

The formation of pyrite is usually linked to bacterial degradation of organic matter (sulphate reduction). Pyrite is commonly present as framboids or cubic crystals. This mineral has been observed in all investigated sections.

### **Glauconite/Chamosite**

Small, sub-millimetric green grains are interpreted as glauconite or chamosite minerals. The term glauconite is used as a general appellation because no geochemical analyses have been carried out in this study. They occur mainly in restricted lagoonal deposits of the Pierre Châtel Formation. Generally, glauconite is related to more open-marine settings with reduced sediment accumulation rates (condensation intervals) whereas chamosite occurs in shallow-marine, lagoonal deposits (e.g., VAN HOUTEN & PURUCKER 1984). Yet, glauconite minerals have also been found in shallow, coastal environments (EL ALBANI et al. 2005)

### **Evaporite pseudomorphs**

Some intervals of the Goldberg Formation are characterized by evaporite pseudomorphs after gypsum (Pl 8/1a-b). They are commonly associated with charophyte stems and gyrogonites as well as ostracodes. These intervals are interpreted as deposits of shallow freshwater to brackish ponds in continental domains, which become hypersaline during dry periods. This can be related to a seasonally semi-arid climate, which prevailed during the deposition of the Goldberg Formation (e.g., MOJON & STRASSER 1987). Evaporite pseudomorphs after gypsum have also been found in tidal flat deposits (Pl. 8/1c).

Evaporite pseudomorphs have also been detected in some intervals of the Worbarrow section. There, they are interpreted as halite cubes (ENSOM 1985; pers. observations). Some of these intervals are associated with charophyte stems and chert nodules. BURNE et al. (1980) interpreted such associations as the result of seasonally varying salinity within coastal ponds of semi-arid, Mediterranean-type climate zones.

***Dolomite***

In the Yenne section, the Pierre Châtel Formation contains dolomite, which has been replaced by calcite. This calcitization process is referred to as dedolomitization. There are several models explaining the formation of dolomites in shallow carbonate environments (e.g., WARREN 2000, RAMEIL 2005). In this study, no geochemical analyses have been made to constrain the formation of dolomites in the Yenne section.

***Lime mud***

The term “lime mud” is generally used as a synonym for “micrite”. The origin of lime mud is still discussed in the scientific community (a compilation is given in FLÜGEL 2004). Mud-supported sediments make up the majority of the rocks described in this study. They are considered to reflect low-energy settings. Detailed geochemical investigations of lime mud have not been undertaken in this study.

## 2.4 Sedimentary structures

The analysis of sedimentary structures and bedding surfaces is essential for the interpretation of ancient depositional environments. They reflect physical, chemical and/or biological conditions during and/or after the depositional processes. Some large-scale sedimentary structures can only be observed in the field (e.g., cross-stratifications, channels, erosion surfaces). Partly, they can be followed laterally over longer distances depending on the outcrop extension.

### 2.4.1 Hydrodynamically formed structures

***Lamination*** (Pl. 7/5; 10/1; 11/1-2)

Laminated sediments are formed by diverse processes in different environmental conditions (e.g. DEMICCO & HARDIE 1994). Commonly, lamination occurs in deposits where a homogenization by burrowing organisms is reduced or absent. It can be expressed by a change in granulometry and/or colour (Pl. 5/7; 11/2). Lamination in a water body is mainly associated with changing current and wave activity and/or with changing sediment supply. In the Dorset

sections, oriented shell accumulations of bivalves and ostracodes create massive laminated beds (EL-SHAHAT & WEST 1983; Pl. 10/1a-b). Well-preserved lamination has also been observed in bituminous intervals interpreted as shallow, freshwater pond deposits in the Dorset sections (Pl. 11/1a-b).

***Lenticular, wavy and flaser bedding*** (Pl. 11/3)

These terms are used following the classification of REINECK & WUNDERLICH (1968). The origin of these bedding types is related to alternating current and wave actions in shallow waters of inter- and subtidal environments (e.g., DEMICCO 1983). They reflect the tidal rhythms: tidal current and tidal slack waters.

***Wave ripples***

These sedimentary structures are produced by wave action in very shallow lagoonal and intertidal settings. Commonly, ripple height is in the range of a few centimeters.

***Cross bedding and shoals*** (Pl. 9/1-3)

In this study, large-scale cross bedding has been observed as decimetric bedforms in outcrops of the Pierre Châtel Formation (cf. Chap 4) (Pl. 9/1-3). These structures are composed of foreset-beds with a low-angle tabular geometry (e.g., SWINCHATT 1967, COLLINSON & THOMPSON 1982). A precise description of these bedforms cannot be made because of the two-dimensional view in the outcrops. Partly, reactivation surfaces are displayed within the foreset-beds (Pl. 9/2). The cross-bedded bedforms are interpreted as migrating shoals (sand waves) in tidally-influenced lagoonal settings. Shoals form large scale sandbody fields (shoal fields) on shallow carbonate platforms (e.g., BURCHETTE et al. 1990).

### 2.4.2 Biogenic structures

***Bioturbation***

Bioturbation is a common sedimentary structure in the studied intervals. It can be distinguished from the matrix due to their difference in colour and texture in thin sections. Bioturbation features have not been

studied and discriminated in detail because of the lack of well exposed bedding planes in the field. Nodular textures in subtidal settings have commonly been interpreted as bioturbated intervals. Such intervals may represent low sedimentation rates or omission phases (e.g., HILLGÄRTNER 1999).

### *Microbial mats*

In the intertidal to supratidal domains, dark, micritic lamination, which is commonly associated with birdseyes and desiccation cracks has been interpreted as remnants of fossil microbial mats (e.g., PRATT & JAMES 1992; Pl. 8/2a-b).

### *Encrustations and microborings*

Encrustation of shells and other bioclasts by organisms such as foraminifera, serpulids and sponges are common in shallow marine environments. Additionally, bioclasts are attacked by microborers including cyanobacteria, algae, and fungi causing micritization of the peripheral layers (micritic envelopes; e.g., FLÜGEL 2004, SAMANKASSOU et al. 2005). In some shells well-defined micrite-filled borings can be observed (Pl. 6/4).

## **2.4.3 Structures indicating subaerial exposure**

### *Desiccation cracks*

Desiccation cracks occur generally in inter- to supratidal environments. Such fissures are created by contraction of a muddy matrix due to evaporation and drying of the sediments. In thin sections, they display millimeter-scale fissures cutting through mud- to wackestones, which are filled by blocky cement and/or crystal silt (Pl 7/2a-b).

**Circumgranular cracks** are fine fissures around solid constituents (Pl 7/1). Generally, they are related to longer periods of subaerial exposure and the beginning of soil formation (ESTEBAN & KLAPPA 1983).

### *Birdseyes*

Birdseyes are millimeter-scale cavities in carbonate mud deposits (Pl. 7/3a-b; 8/2a-b). They are interpreted

as the product of active algal/microbial growth and/or trapping of gases deriving from the decomposition of organic matter. Birdseyes are characteristic features for inter- to supratidal deposits (SHINN 1983). Sheet cracks (Pl. 8/2a) are common in microbial mats of intertidal to supratidal domains. They are not discerned from birdseyes in the section descriptions.

### *Microkarst structures*

In the field, micro-reliefs have been interpreted as microkarst surfaces mainly formed by dissolution processes of CO<sub>2</sub>-enriched meteoric waters and/or plant activity (e.g., LOHMANN 1988). They indicate subaerial exposure of carbonate rocks during a certain time period. Some of these surfaces of the Pierre Châtel Formation resemble small cylindrical karst pits (a few centimeter in height) described by (VANSTONE 1998) (Pl 8/4a-b). Generally, karstification is related to seasonal, humid climates, in which extensive dissolution and cementation processes of carbonate take place (e.g., WRIGHT 1994; cf. Chap. 8). Besides their palaeoclimatic significance, karst surfaces represent important discontinuities for sequence-stratigraphical interpretations (e.g., HILLGÄRTNER 1998).

Additionally, small elongated cavities displaying a geopetal structure of vadose crystal silt and blocky cements have been found in some intervals of the Goldberg Formation (Pl 7/4a-b). The probably point to initial karstification processes (PLATT 1989).

## **2.5 Early Diagenesis**

The term early diagenesis describes processes, which affect sediments shortly after deposition. It includes compaction (geometric rearrangement of constituents and pressure solution), cementation, and alteration (mineral transformation, dissolution). These processes are controlled by the depositional environment and external factors. Complex interactions of chemical, physical, and biological mechanisms must be taken into account for post-depositional interpretations of carbonate rocks (e.g., TUCKER 1993). In this study, early diagenetic features (mainly cements) have been investigated by thin-section analysis.

### **2.5.1 Compaction**

During burial of unconsolidated sediments of just

one meter, dewatering and changes in packing density leads to initial compaction. Plastic deformation and crushing of constituents occur at greater burial depth (around 100 m; FLÜGEL 2004). Pressure solution at grain contacts forming stylolites is a common process leading to overpacking. Hence, it is important to account for modifications of the texture due to compaction in the sample classification.

### 2.5.2 Cementation

Cementation is the initial processes leading to sediment lithification. It is mainly caused by carbonate precipitation from fluids circulating in the pore space (TUCKER & WRIGHT 1990, FLÜGEL 2004). A few meters below the sediment surface, the rate of pore-fluid migration is drastically reduced. As a consequence, little cementation can take place (TUCKER 1993). The analysis of cement types gives information on the one hand about the composition of the pore fluids (e.g., freshwater, marine and/or mixture of them) and on the other hand about the depositional environment (e.g., vadose or phreatic cementation). Commonly, several cement types occur in pore spaces displaying different generations of cements.

Subaerial exposure and the influence of meteoric waters can lead to rapid cementation of carbonates (e.g., DRAVIS 1996, FRIEDMAN 1998). Early cementation in marine-phreatic environments is generally associated with omission processes or phases of reduced accumulation rates. Such syn-sedimentary cementation can lead to the formation of firm- and hardgrounds (e.g., FÜRSICH 1979, HILLGÄRTNER 1999).

### 2.5.3 Alteration

Recrystallization and dissolution are the main processes of early diagenetic alteration changing primarily lithified carbonates. Metastable minerals (depending on their chemical composition) can be transformed, dissolved and/or replaced by circulating pore fluids (e.g., aragonite, evaporite minerals).

The Pierre Châtel Formation of the Yenne section has partly been modified by dedolomitization processes (cf. Chap. 4). Sparitic sucrosic crystals with no traces of rhomb-shaped forms destroyed the primary texture of these sediments. RAMEIL (2005) classified this alteration as type-2 dedolomite and relates it to soil-influenced meteoric diagenesis associated with large-scale sequence boundaries.

## 2.6 Facies and conceptual facies models

In order to classify the samples, they are grouped into different facies. This section illustrates the criteria, which have been used to attribute the different facies to facies zones, on which the conceptual facies models are built.

### 2.6.1 Criteria for a facies distinction

#### *Ecology and abundance of constituents*

The facies classification takes into account the relative abundance of all the allochems and the fossil content within a sample. The relative abundance of a constituent in combination with its palaeoecological significance is considered as the main criteria for the attribution of a sample to a certain facies. Because of the strong inhomogeneity of the studied rocks, a quantitative analysis would simulate a precision that is not realistic. Therefore, the abundance is estimated qualitatively on the basis of thin sections.

A microscope magnification of 50x is used for the evaluation of the relative abundance of components. Estimations of their abundance are made with the help of frequency diagrams (BACELLE & BOSELLINI; in FLÜGEL 2004). The abundance of constituents is divided in three categories; their approximate percentage is indicated in brackets:

- **present:** A specific component is easily found in the field of observation (0.01-2.5%);
- **common:** Components are well-represented in the field of observation (2.5-20%);
- **abundant:** Components are frequent in the field of observation (20-100%; 100% is rarely the case).

#### *Texture*

The limestone texture is defined according to the descriptive classifications of DUNHAM (1962) and EMBRY & KLOVAN (1971) (both in FLÜGEL 2004). These classifications can be considered as a first approximation for the interpretation of energy conditions in the depositional environments (FLÜGEL 2004). Generally, samples, which contain a high amount of lime mud are



considered to represent low-energy conditions.

### ***Sedimentary structures***

Sedimentary structures are essential elements of a facies interpretation. They are incorporated in the facies classification according to their environmental significance.

## **2.6.2 Conceptual facies model for the Jura platform**

Tab. 2.2 shows the facies types identified in the sections of the Jura platform (cf. Chap. 4). They are grouped into different facies zones. The criteria for the division of these facies zones are mainly based on the studies of PASQUIER (1995), HILLGÄRTNER (1999), and STRASSER et al. (1999). The facies types within a facies zone are listed according to their texture ("depositional energy conditions").

Four facies zones (FZ) have been differentiated for the studied interval of the Middle Berriasian Jura platform. They are numbered from proximal to distal positions on the platform.

### ***FZ1 – continental domain***

This facies zone is mainly characterized by the co-occurrence of charophyte stems and gyrogonite. It is assumed that charophyte stems are good indicators for freshwater pond deposits. Commonly they are associated with ostracodes and gastropods. Partly, evaporite pseudomorphs are present and interpreted as evidence for seasonally ephemeral water bodies and changes from humid to arid conditions.

### ***FZ2 - tidal flat***

The samples attributed to the tidal flat zone are well-defined by their sedimentary structures. All of them contain at least one of the following sedimentary structures: Birdseyes, lamination, desiccation cracks and/or circumgranular cracks. Moreover, they faunal diversity in this facies zone is strongly reduced, or fauna is absent ("stressed environment"; e.g., PRATT & JAMES 1992). Ostracodes are common and partly abundant. They are associated with some gastropods, bivalves, and charophytes (gyrogonites and/or stems).

### ***FZ3 - internal lagoon***

Coastal lagoons are generally considered as "ephemeral features on a geological time scale as they form, evolve and infill within a short timespan" (COOPER 1994; p. 220). As morphodynamic systems, lagoons have been defined as "coastal water bodies, which are physically separated, to a greater or lesser extent, from the ocean by a strip of land" (WARD & ASHLEY 1989; p. 181).

In this study, the shallow lagoonal settings have been divided in internal- and open-lagoonal environments. The term "internal lagoon" describes a shallow marine basin, which is partly separated by a morphological "barrier" (e.g., shoal field) from the open lagoon. In other words, the internal lagoon is a morphologically separated part of the lagoonal system. It is assumed that internal lagoons represent more protected, low-energy settings than open-lagoonal basins.

An internal lagoon becomes restricted as soon as the water exchange with the open lagoon is reduced. The salinity either increases due to evaporation or decreases due to freshwater input. As a consequence, a reduced diversity of the fauna and flora can be observed in restricted lagoons. The occurrence of monospecific dasyclad algae in combination with a euryhaline faunal association (e.g. bivalves, gastropods, and ostracodes) points to restricted conditions in an internal-lagoonal environment.

Normal marine conditions are indicated by a diverse fauna and flora. All of the foraminifera genera (except the small cyclamminids) are common in normal lagoonal settings. Euryhaline organisms (e.g.; gastropods, bivalves, and ostracodes) occur together with an increasing amount of stenohaline ones (e.g., echinoderms, brachiopods, and bryozoans). In internal lagoonal deposits, the number of dasyclad green algae and small oncoids is elevated compared to the open-lagoonal sediments. Generally, peloids are abundant in lagoonal setting, whereas ooids (mainly radial and superficial) are concentrated in tidally influenced high-energy settings.

### ***FZ4 – open lagoon***

Additionally to the organisms of the internal lagoon, some coral debris, sponges, and red algae contribute to a further increase of the faunal and floral diversity. As a first approximation, it is assumed that the open-lagoonal setting is characterized by an increase of stenohaline organisms relative to the amount of euryhaline ones.

Facies	Dunham	Sedimentary structures	Allochems	Fossil content	Foraminifera	Depositional environments (energy conditions)
<b>Facies zone: FZ1 Continental domain (c)</b>						
c1	m-M			<u>charophytes</u> (stems, gyrogonites), ostracodes, gastropods, bivalves		freshwater pond (low-energy deposits)
c2	M (-W)	(birdseyes, desiccation cracks, circumgranular cracks)	intraclasts, peloids, (evaporite pseudomorphs)	<u>charophytes</u> (stems, gyrogonites), <u>ostracodes</u> , bivalves, gastropods		freshwater (brackish) pond (low-energy deposits, seasonally hypersaline)
<b>Facies zone: FZ1-2 Transition from continental domain to tidal flat (c-t)</b>						
c-t	M (-P)	birdseyes, (desiccation cracks, circumgranular cracks)	peloids, intraclasts, (pyrite)	<u>ostracodes</u> , <u>charophytes</u> (stems, gyrogonites), gastropods, bivalves		tidal flat pond (low-energy deposits)
<b>Facies zone: FZ2 Tidal flat (t)</b>						
t1	m-M		ooids	ostracodes, charophytes (gyrogonites, stems) gastropods, (dasycladaceans, echinoderms)	(foraminifera)	tidal flat (low-energy deposits)
t2	M	birdseyes, desiccation cracks, circumgranular cracks	<u>peloids</u> , intraclasts, (black pebbles, pyrite)	<u>ostracodes</u> , bivalves, (charophyte gyrogonites, gastropods)		tidal flat (low-energy deposits)
t3	M	birdseyes, desiccation cracks, (circumgranular cracks, lamination, microbial mats)	(peloids, mud pebbles, intraclasts, pyrite, evaporite pseudomorphs)	(ostracodes, gastropods)		tidal flat (low-energy deposits)
t4	M	birdseyes, (desiccation cracks, lamination)	<u>peloids</u> , mud pebbles, intraclasts, (ooids, pyrite)	<u>ostracodes</u> , charophyte (gyrogonites, stems), bivalves, gastropods, (serpulids)	(foraminifera)	tidal flat (low-energy deposits)
t5	M-W (-P)	birdseyes, lamination; (desiccation cracks, circumgranular cracks)	<u>peloids</u> , intraclasts, black pebbles (small oncoids)	<u>ostracodes</u> , charophyte (gyrogonites, stems), gastropods, bivalves, (echinoderms, serpulids)	(miliolids, small cyclam., <i>Redmondoides</i> )	tidal flat (low-energy deposits, storm layers?)
t6	M-P	birdseyes, lamination, (desiccation cracks, circumgranular cracks)	<u>peloids</u> , ooids (superficial, radial, micritic), intraclasts, mud pebbles, (black pebbles, small oncoids, pyrite)	<u>ostracodes</u> , bivalves, dasycladaceans, charophytes (gyrogonites, stems, bone fragments),	(small cyclam., lenticulins)	tidal flat (changing energy conditions, tidal channels?)
t7	M-P	lamination, birdseyes, desiccation cracks, microbial mats	<u>peloids</u> , ooids (superficial, radial, micritic), intraclasts, (organic matter, pyrite)	bivalves, gastropods, (serpulids)		tidal flat (low- to moderate energy deposits)
t8	W (-P)	birdseyes, desiccation cracks	intraclasts, mud pebbles	<u>ostracodes</u> , gastropods, bivalves	(small cyclam.)	tidal flat (low- to moderate energy deposits)

**Tab. 2.2** - Principal facies occurring in the Jura platform sections. The relative abundance of the constituents and the sedimentary structures for each facies type is indicated: abundant (underlined), common, and present (in brackets). Bioturbation and quartz content are not indicated. The abbreviations small cyclam., and big cyclam. label small and big cyclamminids, respectively.

Facies	Dunham	Sedimentary structures	Allochems	Fossil content	Foraminifera	Depositional environments (energy conditions)
Fazies zone: FZ2-3 <i>Transition from tidal flat to internal lagoon (t-i)</i>						
t-i	M-W (-P)	birdseyes, (lamination, flaser bedding, desiccation cracks)	peloids, oncoids (small), intraclasts, ooids (superficial, radial, micritic), (pyrite, glauconite?)	ostracodes, dasycladaceans, echinoderms, gastropods, bivalves, (charophyte gyrogonites, oysters)	miliolids, andersenolins, small cyclam., lenticulins, <i>Redmondoides</i>	tidal flat to internal-lagoon (low-energy deposits, restricted conditions?)
Fazies zone: FZ3 <i>Internal lagoon</i>						
restricted conditions (ri)						
ri1	m-M		ooids, (oncoids)	ostracodes, gastropods, bivalves, (dasycladaceans, echinoderms, bone fragments)	(foraminifera)	internal lagoon (low-energy deposits)
ri2	M-W	(lamination)	peloids, ooids (radial, micritic), oncoids (small), (black pebbles, intraclasts, organic matter, pyrite)	ostracodes, (echinoderms, dasycladaceans)	<i>Redmondoides</i> , small cyclam.	internal lagoon (low-energy deposits)
ri3	W-P (-G)	(lamination)	peloids, ooids (radial, superficial, micritic), oncoids (small), (black pebbles, pyrite, glauconite?)	dasycladaceans, ostracodes, gastropods, bivalves, (charophyte gyrogonites, echinoderms)	<i>Redmondoides</i> , small cyclam.	internal lagoon (moderate-energy deposits, tidally influenced)
ri4	P-G	(lamination, reactivation surfaces)	ooids (radial, micritic, superficial), peloids, intraclasts, oncoids (small)	ostracodes, echinoderms, bivalves	<i>Redmondoides</i> , small cyclam., miliolids	internal lagoon (high-energy deposits, shoals?)
normal conditions (i)						
i1	m-M		ooids, oncoids	gastropods, bivalves, dasycladaceans, ostracodes, echinoderms	foraminifera	internal lagoon (low-energy deposits)
i2	M-W		peloids, oncoids (small), ooids (radial, superficial), intraclasts, (black pebbles, organic matter, pyrite)	dasycladaceans, bivalves, ostracodes, echinoderms, (oysters, cyanobacteria)	miliolids, lenticulins, <i>Redmondoides</i> , andersenolins, small cyclam.	internal lagoon (low-energy deposits, restricted conditions?)
i3	W-P		peloids, oncoids (small), intraclasts, (pyrite)	dasycladaceans, ostracodes, gastropods, echinoderms, (bivalves, cyanobacteria)	miliolids, andersenolins, nautiloculins, lenticulins, small cyclam., big cyclam., <i>Redmondoides</i>	internal lagoon (moderate-energy deposits)
i4	(W-) P	(reactivation surfaces, low-angle tabular cross-bedding, lamination)	oncoids (small, <i>Bacinnella</i> ), peloids, ooids (radial, superficial, composite), intraclasts, (pyrite)	dasycladaceans, echinoderms, gastropods, bivalves, (brachiopods, bryozoans, cyanobacteria, ostracodes)	miliolids, andersenolins, lenticulins, nautiloculins, big cyclam., <i>Redmondoides</i>	internal lagoon (moderate-energy deposits, partly shoals)
i5	P-G	(low-angle tabular cross-bedding, lamination)	peloids, oncoids (small, <i>Bacinnella</i> ), intraclasts, ooids (radial), (pyrite)	dasycladaceans, echinoderms, gastropods, bivalves, (brachiopods, bryozoans, cyanobacteria, ostracodes)	lenticulins, miliolids, andersenolins, nautiloculins, big cyclam., <i>Redmondoides</i>	internal lagoon (high-energy deposits, partly shoals)
i6	P-G	(low-angle tabular cross-bedding, reactivation surfaces)	oncoids (small, <i>Bacinnella</i> ), peloids, intraclasts, ooids (micritic, radial), (black pebbles)	dasycladaceans, echinoderms, gastropods, bivalves, (brachiopods, bryozoans, cyanobacteria, ostracodes)	andersenolins, miliolids, big cyclam.,	internal lagoon (high-energy deposits, shoals)

Tab. 2.2 (continued)

Facies	Dunham	Sedimentary structures	Allochems	Fossil content	Foraminifera	Depositional environments (energy conditions)
Fazies zone: FZ3-4 <i>Transition from internal to open lagoon (i-o)</i>						
i-o1	m-M		oncoids	echinoderms, dasycladaceans, gastropods, (ostracodes)	foraminifera	internal to open lagoon (low-energy deposits)
i-o2	(W-) F		<u>oncoids</u> ( <i>Bacinella</i> , small) <u>peloids</u> , intraclasts, (pyrite)	dasycladaceans, echinoderms, gastropods, (brachiopods, bryozoans, sponges, cyanobacteria, bivalves, ostracodes)	miliolids, <i>Redmondoides</i>	internal to open lagoon (low-energy deposits)
i-o3	W-P		<u>peloids</u> , <u>oncoids</u> (small, <i>Bacinella</i> ) intraclasts, oids (superficial)	dasycladaceans, echinoderms, gastropods, bivalves, (brachiopods, bryozoans, ostracodes, cyanobacteria, sponges, "Thaumatoporella-ladders", oysters)	miliolids, big cyclam., <i>Redmondoides</i> , nautiloculins, andersenolins, lenticulins	internal to open lagoon (moderate-energy deposits)
i-o4	P (-G)		<u>peloids</u> , <u>oncoids</u> (small, <i>Bacinella</i> ), intraclasts	dasycladaceans, echinoderms, gastropods, bivalves, (brachiopods, bryozoans, cyanobacteria, sponges, ostracodes "Thaumatoporella-ladders")	big cyclam., miliolids, <i>Redmondoides</i> , andersenolins, lenticulins, nautiloculins,	internal to open lagoon (high-energy deposits)
i-o5	P (-G)	(low-angle tabular cross-bedding)	<u>oncoids</u> (small, <i>Bacinella</i> ) <u>peloids</u> , intraclasts	echinoderms, dasycladaceans, gastropods, bivalves, (brachiopods, bryozoans, cyanobacteria, sponges, ostracodes, "Thaumatoporella-ladders")	miliolids, andersenolins, big cyclam., nautiloculins, <i>Redmondoides</i> , (lenticulins)	internal to open lagoon (high-energy deposits, partly shoals)
i-o6	P-G	(reactivation surfaces, low-angle tabular cross-bedding)	<u>peloids</u> , <u>oids</u> (radial), oncoids (small, <i>Bacinella</i> ), intraclasts	echinoderms, dasycladaceans, (brachiopods, bryozoans, sponges, "Thaumatoporella-ladders", ostracodes, gastropods, bivalves)	andersenolins, miliolids, big cyclam., lenticulins, nautiloculins, ( <i>Redmondoides</i> )	internal to open lagoon (high-energy deposits, partly shoals)
i-o7	P-G (-R)	(low-angle tabular cross-bedding)	<u>peloids</u> , oncoids (small, <i>Bacinella</i> ), intraclasts	echinoderms, dasycladaceans, gastropods, bivalves, (brachiopods, sponges, ostracodes, "Thaumatoporella-ladders")	big cyclam., miliolids, <i>Redmondoides</i> , andersenolins, lenticulins, nautiloculins	internal to open lagoon (high-energy deposits, partly shoals)

Fazies zone: FZ4 <i>Open lagoon (o)</i>						
o1	F		<u>oncoids</u> ( <i>Bacinella</i> ), <u>peloids</u> , oids (radial), (pyrite)	echinoderms, gastropods, bivalves, brachiopods, dasycladaceans, (bryozoans, corals, sponges)	miliolids, andersenolins, lenticulins, big cyclam., <i>Redmondoides</i> nautiloculins	open lagoon (low-energy deposits)
o2	W-P		<u>peloids</u> , oncoids ( <i>Bacinella</i> , small), (pyrite)	echinoderms, brachiopods, gastropods, bivalves, dasycladaceans, (bryozoans, sponges, cyanobacteria, ostracodes "Thaumatoporella-ladders",)	miliolids, andersenolins, lenticulins, big cyclam., nautiloculins, <i>Redmondoides</i>	open lagoon (moderate-energy deposits)
o3	P (-G)		<u>peloids</u> , oncoids ( <i>Bacinella</i> , small), (pyrite)	echinoderms, brachiopods, gastropods, bivalves, dasycladaceans, (bryozoans, corals, sponges, cyanobacteria, serpulids)	miliolids, andersenolins, lenticulins, big cyclam., nautiloculins, <i>Redmondoides</i>	open lagoon (high-energy deposits)
o4	(G-) R		<u>oncoids</u> ( <i>Bacinella</i> ), <u>peloids</u>	echinoderms, gastropods, bivalves, (brachiopods, dasycladaceans, corals, sponges, cyanobacteria)	miliolids, andersenolins, lenticulins, big cyclam., nautiloculins, <i>Redmondoides</i>	open lagoon (high-energy deposits, shoals?)

Tab. 2.2 (continued)

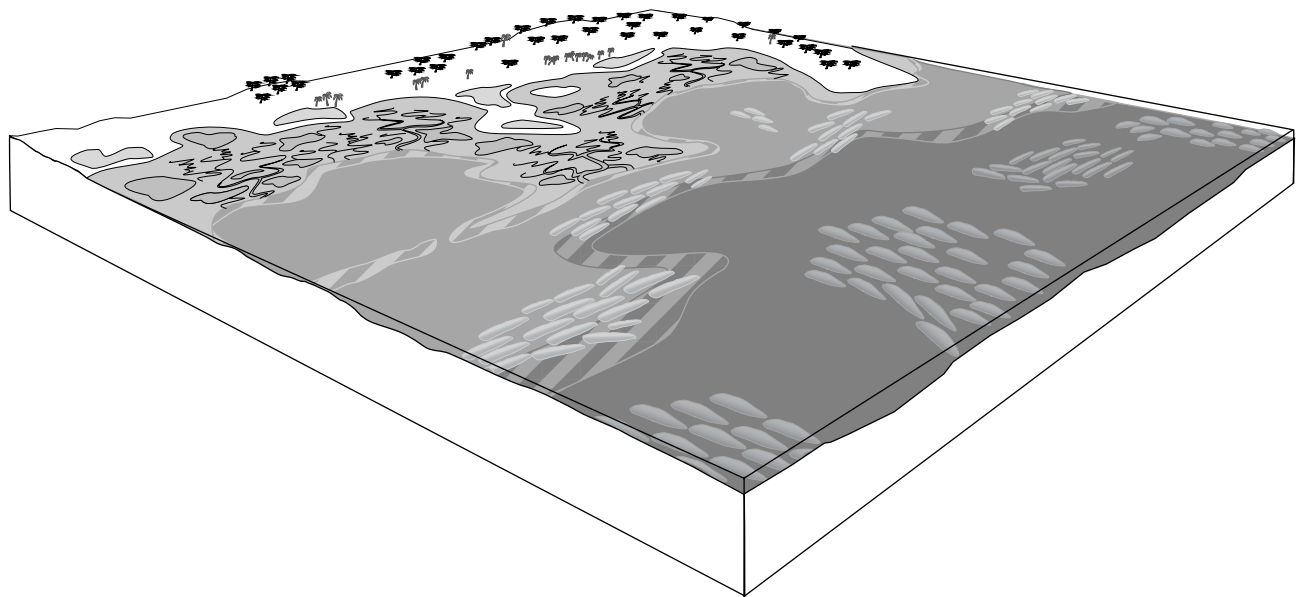
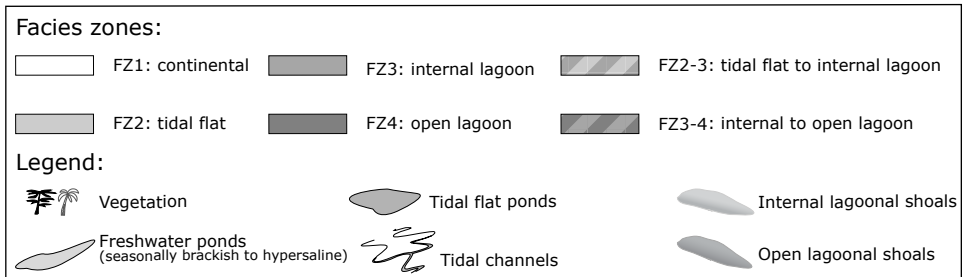


**Fig. 2.2** - Block diagram showing the interpretation of the spatial relations between the different facies zones of the Jura platform (not to scale).



Large *Bacinella*-oncooids forming float- and rudstones dominate in open-lagoonal deposits.

#### *Transitions between facies zones*

It has to be kept in mind that in nature transitions between facies zones are rather gradual. Especially in lagoonal settings where characteristic sedimentary structures are missing the definition of facies zones remains delicate. That is why transitional facies zones have been added in order to account for these problems. Hence, transitions between facies zones incorporate characteristics of both neighboring facies zones.

#### *Facies model*

The construction of an universal depositional model for natural systems is generally not possible because of the highly dynamic behavior in time and space of such systems. However, in the literature different facies models for shallow carbonate platforms have been published (e.g., WILSON 1975, TUCKER & WRIGHT

1990, FLÜGEL 2004). Such facies models are based on comparison with modern sedimentary systems of shallow carbonate platforms in a uniformitarian approach.

Based on the likely spatial distribution of the facies zones described above, a conceptual facies model is constructed. The three-dimensional block diagram (Fig. 2.2) illustrates a static, time-independent shallow carbonate platform and the lateral arrangement of its facies zones. Additionally, a two-dimensional cut through this carbonate platform (Fig. 2.1) displays the distribution and relative amount of the most important constituents found in the studied Jura sections.

### **2.6.3 Conceptual facies model for the Dorset region**

Less facies types have been distinguished in the Dorset realm than on the Jura platform. Because characteristic sedimentary structures are rare in the Dorset sections, the faunal constituents are important for the palaeoenvironmental interpretations of these deposits. Therefore, the sedimentological interpretation

Facies	Dunham	Sedimentary structures	Allochems	Fossil content	Depositional environments (energy conditions)
<b>Facies zone: FZ1 <i>Continental domain (c)</i></b>					
Dc1	m-M			charophytes (stems, gyrogonites), ostracodes, gastropods, bivalves	freshwater pond
<b>Facies zone: FZ1-2 <i>Transition from continental domain to tidal flat (c-t)</i></b>					
Dc-t1	M (-P)	(lamination)	peloids, intraclasts, (pyrite, chert nodules)	ostracodes, charophytes (stems, gyrogonites), bivalves, gastropods	tidal flat pond
Dc-t2	M-W	lamination	organic matter, (pyrite)	ostracodes, (charophyte stems, bone fragments)	bituminous freshwater (brackish) pond (restricted, dysoxic conditions)
<b>Facies zone: FZ2 <i>Tidal flat (t)</i></b>					
Dt1	m-M			ostracodes, charophytes (gyrogonite, stems), gastropods,	tidal flat (low-energy deposits)
Dt2	M	(birdseyes)	peloids, (mud pebbles, intraclasts, pyrite)	ostracodes, (gastropods, bivalves, plant debris)	tidal flat (low-energy deposits)
Dt3	M-P	lamination, (birdseyes)	peloids, intraclasts, (mud pebbles, superficial ooids)	(plant debris)	tidal flat (low-energy deposits, tidal channel?)
Dt4	(M-) W-P	(lamination, birdseyes)	peloids, intraclasts, (organic matter)	ostracodes, bivalves, gastropods	pond on tidal flat (low-to moderate-energy deposits)
<b>Facies zone: FZ2-3 <i>Transition from tidal flat to internal lagoon (t-i)</i></b>					
Dt-i	(M-P)	lamination, (birdseyes)	peloids, intraclasts, mud pebbles, (black pebbles, pyrite)	bivalves, ostracodes, gastropods, (charophytes stems, gyrogonites)	"shell beaches" (low-to moderate-energy deposits)
<b>Facies zone: FZ3 <i>Internal lagoon (i)</i></b>					
Di1	m-M	(black)		ostracodes, gastropods, bivalves, (bone fragments)	internal lagoon (low-energy deposits, restricted conditions)
Di2	M-W	(lamination)	peloids, (pyrite)	bivalves, oysters (Cinder Member), (echinoderms)	internal lagoon (low-energy deposits, restricted conditions)

**Tab. 2.3** - Principal facies occurring in the Dorset sections. The relative abundance of the constituents and the sedimentary structures for each facies type is indicated as follows: abundant (underlined>, common, and present (in brackets). Bioturbation and quartz content are not shown.

is mainly based on palaeocological data from the literature (e.g., EL SHAHAT & WEST 1983, ENSOM 1985, CLEMENTS 1993, HORNE 2002, RADLEY 2002). The facies zones and their corresponding facies types are shown in Tab. 2.3.

#### ***FZ1 – continental domain***

The characteristic features of this facies zone

correspond to the ones of the continental domain described for the Jura platform.

#### ***FZ2 - tidal flat***

Generally, the same criteria are valid as for the tidal flats of the Jura platform. Laminated beds are common whereas sedimentary structures like birdseyes and desiccation cracks are less abundant.

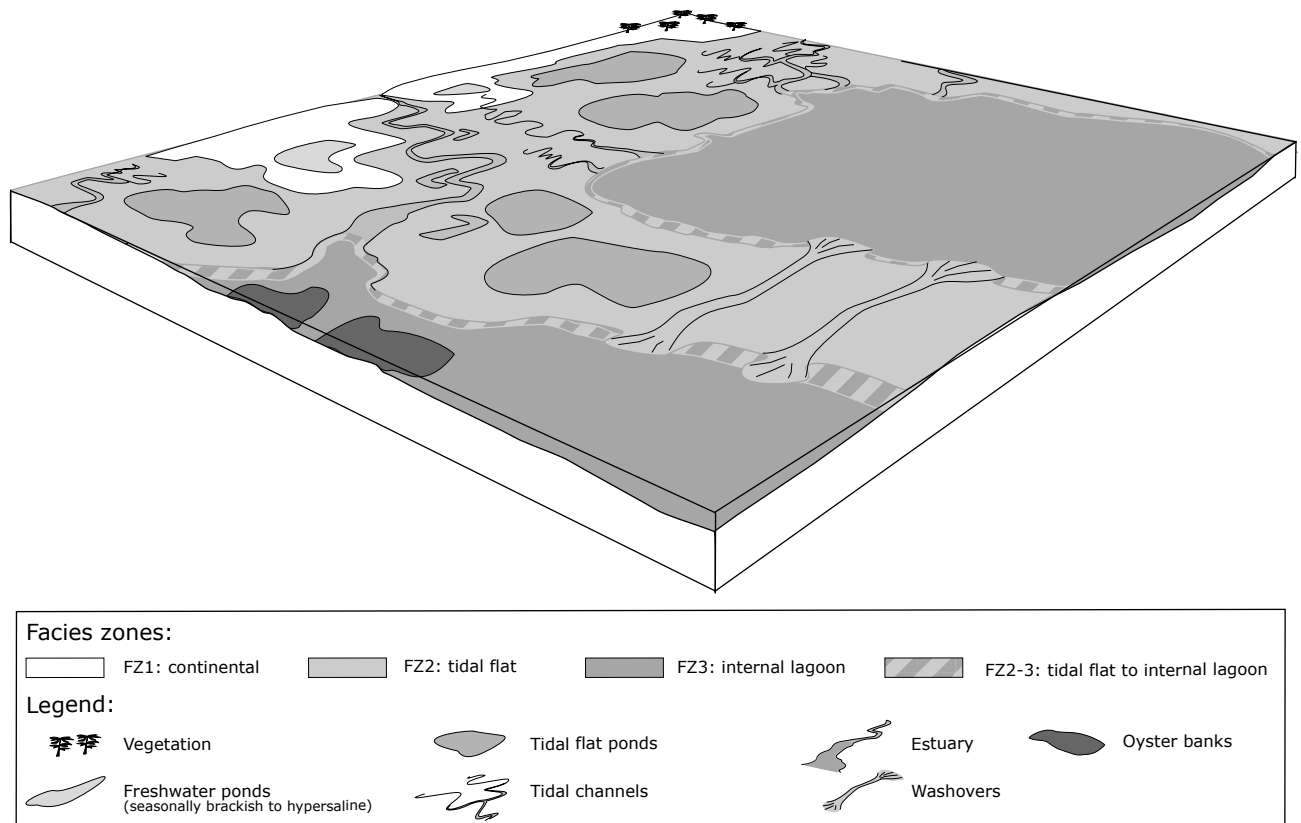


**Fig. 2.3** - Block diagram showing the interpretation of the spatial relations between the different facies zones of the Dorset realm (not to scale).

The fauna is dominated by ostracodes and bivalves displaying a strongly reduced diversity. Gastropods and some charophytes (gyrogonites and/or stems) are also present.

### ***FZ3 - internal lagoon***

Internal lagoonal settings are represented by the oyster banks of the Cinder Member. Additionally, the sediments of the Scallop Member have also been deposited in shallow, marginal lagoons (cf. Chap 5).

### ***Transitions between facies zones***

Transitions between the facies zones are defined according to the arguments mentioned for the Jura

platform. The thinly-laminated bituminous intervals are considered as freshwater to slightly brackish deposits at the transition from continental to tidally-influenced shallow ponds. The bivalve shell beds are considered to represent “shell beaches” at the transition from shallow lagoons to tidal flat environments.

### ***Facies model***

For the Dorset realm, no facies model has been found in the literature. A Dorset facies model is proposed mainly based on the studies of EL SHAHAT & WEST (1983), ENSOM (1985), and CLEMENTS (1993). The three-dimensional block diagram (Fig. 2.3) shows a conceptual facies model of a low-relief, coastal environment and the likely, time-independent, lateral arrangement of its facies zones.

\*\*\*\*\*





### 3 - SEQUENCE ANALYSIS

Until the 1950s, the interpretation of rock successions consisted primarily of a lithostratigraphic approach. This means that sediments have been mapped, correlated, and named by defining division (groups, formations, and members) according to their lithological similarity and their fossil content (MIALL & MIALL 2001; cf. Fig. 3.1a).

In the 1960s, the sedimentologists described rock successions in a process-oriented view based on facies analysis. The stratigraphic complexity has been interpreted in terms of facies successions, which are founded on process-response models (facies models; cf. Chap. 2; cf. Fig. 3.1b).

Sequence concepts have first been developed by SLOSS et al. (1949; in MIALL & MIALL 2001) and SLOSS (1963). A new methodology for documenting and interpreting the stratigraphic record has been introduced by the sequence-stratigraphical approach (cf. Fig. 3.1c). The breakthrough of these concepts was in the mid 1970s by a research group of EXXON. The development of high-quality reflexion-seismic techniques by petroleum geophysicists and geologists enabled the interpretation of the large-scale, three-dimensional architecture of sedimentary bodies by investigating stratigraphic surfaces and terminations.

In the course of the last 20 years, therefore, the philosophy of looking at and interpreting sediments changed strongly. MIALL & MIALL (2001) stated that “the rocks did not change, but the ‘objective’ facts that geologists extracted from them did” (p. 323). A

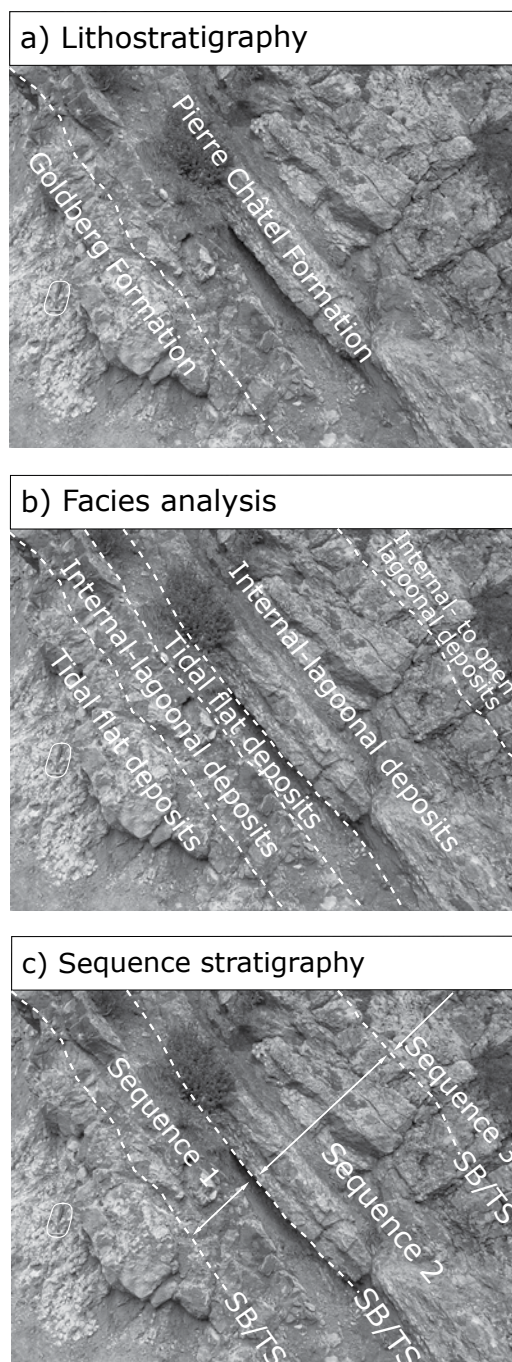


**Fig. 3.1** - (right side) Outcrop pictures of the lower part of the St. Claude section illustrating three methods of stratigraphic interpretations. a) Lithostratigraphical interpretation based on lithological divisions (e.g., formations). b) Interpretation based on a facies analysis (cf. Chap. 2). c) Sequence-stratigraphical interpretation showing several small-scale sequences. (SB: sequence boundary, TS: transgressive surface; hammer for scale).

combination of all three methods (lithostratigraphy, facies analysis, and sequence stratigraphy) is used for interpreting the sections presented in Chap. 4 and 5.

### 3.1 Introduction

The sequence-stratigraphical concept introduced by VAIL et al. (1977) of the EXXON research group is nowadays widely accepted in the scientific community. Based on reflexion-seismic interpretations, they developed a model that explains the observed stratigraphic patterns and the evolution of sedimentary basins as being influenced mainly by large-scale eustatic sea-level changes and subsidence. This sequence model was a tool to analyze and predict the lateral geometry of sediment bodies in order to search for petroleum reservoirs. The model then has been extensively discussed and modified by the scientific community (e.g., POSAMENTIER et al. 1988, POSAMENTIER & JAMES 1993, HUNT & TUCKER 1992, 1995, KOLLA et al. 1995). These subsequent models are mainly based on siliciclastic-dominated depositional system of passive margins.

Another use of sequence stratigraphy was the development of “global cycle charts” by HAQ et al. (1987; cf. Fig. 1.6). This approach is based on the assumption that the depositional sequences detected in different basins are caused by effects of global eustatic sea-level changes. However, these charts have been questioned by other researchers (e.g., MIALL 1986, 1991, HUBBARD 1988, CARTER 1998). Other factors than eustatic sea-level fluctuations including tectonics and/or sediment supply have to be considered by interpreting depositional sequences (e.g. CLOETINGH 1988, 1991, SCHLAGER 1991, 1993, 2005).

Due to the advancing seismic techniques and the combination with detailed borehole and field studies, high-resolution interpretations of lithological variations are obtained. These resulted in continuous modification and refinement of the principles and terms of sequence stratigraphy. Applications to individual case studies led to different definitions and views on the interpretation of sequences. Over the years, different schools of thought and models, depending on how sequences are identified and subdivided, and depending on the processes, which are involved, made their particular definitions. The concept of sequence stratigraphy has also been applied to smaller-scale systems (MITCHUM & VAN WAGONER 1991), and has been considered to be independent of scale (e.g., POSAMENTIER & JAMES 1993).

### *Siliciclastic versus carbonate depositional systems*

Originally, the sequence-stratigraphic approach has been developed to describe and analyze siliciclastic depositional systems. BOSENCE & WILSON (2003) stated that “it is not possible to transfer an understanding of siliciclastic sequence stratigraphy directly to the interpretation of carbonate successions” (p. 209). There are two main differences between the depositional mechanisms of these two sediment families. First, carbonate sediments are produced in-situ, or close to where they are deposited, as organic skeletons of calcium carbonate, as microbially-mediated sediments, or as sedimentary grains precipitated from seawater (cf. Chap. 2). Secondly, carbonate sediments are susceptible to dissolution and/or cementation depending on the chemistry of the circulating water (e.g., salinity, alkalinity, pH, and temperatures). A compilation of the differences between carbonate and siliciclastic depositional systems in respect to sequence analyses is given in BOSENCE & WILSON (2003). WRIGHT & BURGESS (2005) specify that “the concept differentiates carbonate sedimentary systems from siliciclastic ones in a quite fundamental manner whereby sediment is produced, at high rates, in localized areas, not necessarily requiring long distance, physically complex delivery systems from source to final depositional site” (p. 17). Carbonate production has been thought to be controlled significantly by light-dependent organisms, which are the main sediment producers in shallow-marine depositional system. This implies that the carbonate factory is related to water depth (photic zone). However, “the carbonate factory is spatially and temporally highly variable and is not simply a uniform production line” (WRIGHT & BURGESS, 2005; p. 17). Besides the carbonate production rate, also sediment transport and dissolution have to be considered when analyzing shallow-marine carbonates succession at high-resolution. The carbonate factory is, therefore, a spatially and temporally dynamic system, occurring at different water depths, depending on the environmental factors and the nature of the carbonate-producing biota (e.g., SCHLAGER 2005).

Under ideal conditions, carbonate-producing communities are able to fill or even overfill newly created accommodation space. Accordingly, shallow-marine carbonate depositional systems react to environmental changes (e.g., sea-level changes, turbidity, nutrient supply, water chemistry) resulting facies changes are used to interpret the sedimentary record in a section. By comparing characteristic facies patterns in several time-equivalent sections, it is possible to reconstruct depositional systems in detail over long distances.

## 3.2 Depositional sequences

### *Definition*

A depositional sequence is a succession of genetically related sediments. Commonly, inversions in the trend of an environmental change are marked by well-expressed facies changes (discontinuities) delimiting a depositional sequence. Through time, depositional sequences are repeated and vertically stacked. Accordingly, they are the stratigraphical expression of recurring environmental changes independent of scale and time. In the literature, the terms “cycle” and “cyclic” have been used to describe depositional sequences, although recurrences in natural systems are at the most quasi-periodic. In this study, these terms are reserved for sequences, which can be related to time-dependent relative sea-level fluctuations (cyclostratigraphy; cf. Chap. 7). The term “sequence” is used synonymously with “depositional sequence” in this study. Therefore, it complies partly with the original definition of VAIL et al. (1977).

### 3.2.1 Criteria for sequence identification and interpretation

Over the years, sedimentologists have used different criteria to identify and interpret depositional sequences. Sedimentological investigations make use of various parameters to wrest information from sediments. Among others, these are deepening-up and shallowing-up trends in general facies evolution, variations in ecological indicators, beds and discontinuities, and vertical variations in bed thickness (“stacking pattern”). Diagenetic features, stable isotope signatures, composition of clay minerals, and palynofacies can yield additional evidence. Some of the parameters used in this study are briefly presented below.

### *Facies evolution*

The study of lateral facies variations and vertical facies evolution is the principle tool in sequence analysis. In this study, the investigation of lateral facies variations is limited by the extension of the field outcrops. It is important for sequence-stratigraphical interpretation to look for lateral variations in bed thickness and geometry at outcrop scale. Such intervals may be related to sedimentary bodies such

as tidal channel and shoal deposits (cf. Pl. 9/1-3). Vertical facies evolution expressed as deepening-up and shallowing-up trends is commonly linked with the bathymetric evolution on shallow platforms. However, also sediment accumulation rate has to be considered: for example, if accumulation outpaces sea-level rise, a shallowing-up facies trend is created (e.g., HILLGÄRTNER 1998, STRASSER et al. 1999).

### *Discontinuity surfaces*

Discontinuity surfaces on shallow-marine carbonate platforms are characterized by a wide variety of elements (e.g., CLARI et al. 1995, IMMENHAUSER et al. 2000, SATTTLER et al. 2005). An excellent study on discontinuity surfaces has been published by HILLGÄRTNER (1998). Generally, all surfaces in a bed succession (excluded are “false discontinuities” of pure late-diagenetic and tectonic origin) indicate reactions of the sedimentary system to rapid environmental changes. Detailed analyses of each discontinuity surface, however, have to be made in order to extract information, on which environmental change caused its formation. In this study, such investigations are commonly limited by the extension and accessibility (thin intervals) of the surfaces. The formation of discontinuities can be related to processes such as erosion (subaqueous and subaerial), sub-aqueous omission, and facies changes, which are mainly controlled by fluctuations of the hydrodynamic condition of relative sea level and/or of sediment accumulation rate. The identification and interpretation of discontinuity surfaces is essential for interpreting and delimiting depositional sequences (HILLGÄRTNER 1998, SATTTLER et al. 2005).

### *Bioturbation*

Bioturbation is closely related to specific environmental conditions. The degree of bioturbation is mainly controlled by the sediment accumulation rate, oxygenation, substrate type, and nutrient availability. In platform environments, oxygenation levels and nutrient supply are rarely the decisive factors for bioturbation (HILLGÄRTNER 1999). Terrigenous input, however, is able to significantly raise nutrient levels. Consequently, overturns of benthic communities can be the result of increased nutrient levels leading to drops in carbonate productivity and accumulation rate (e.g., HALLOCK & SCHLAGER 1986, DUPRAZ & STRASSER 1999).

Nodular intervals in lagoonal and tidal flat en-

vironments of different substrate types are commonly related to bioturbation. Bioturbation associated with firm- and hardgrounds implies that sediment accumulation rate was the most important controlling factor in these environments (HILLGÄRTNER 1999).

Variations in sediment accumulation rates can be caused by relative sea-level fluctuations. During a rapid initial rise (initial flooding), the carbonate production usually starts up after a lag time (KENDALL & SCHLAGER 1981, STRASSER 1991). The fastest rise in relative sea level and consequently, the deepest water induce changes in the benthic community, which may lead to a drop in carbonate production rate and sediment starvation (maximum flooding). Other parameters such as variations of the hydrodynamic regime (e.g., sediment by-pass situation in high-energy conditions) and of the water quality (e.g., turbidity, salinity) additionally influence carbonate accumulation rate.

### ***Taphofacies***

Bioclastic concentrations (e.g., shellbeds) can be used for the identification of depositional sequences (e.g., KIDWELL 1993, KONDO et al. 1998). They generally indicate low sediment accumulation rates (condensation), caused by either sediment starvation during rising relative sea level, or erosion, reworking, and condensation during sea-level fall and lowstand. FÜRSICH & PANDEY (2003) relate shell concentrations containing shells with convex-up orientation as transgressive lag deposits due to reworking and transportation during intermittently high-energy conditions (cf. Chap. 5). Yet, they underline that other criteria (like fragility of shells, diversity of the fauna, size sorting of the shells, and percentage of disarticulated shells) have to be taken into account by interpreted shell concentrations in terms of sequence stratigraphy.

Bioclastic accumulations are rare on the Jura platform but abundant in the Dorset sections (cf. Chap. 5). They are considered to represent “shell beaches” (EL-SHAHAT & WEST 1983; cf. Chap. 2). It is assumed that they have been deposited during relative sea-level rise.

### ***Bedding and stacking pattern***

Single beds are always delimited by discontinuity surfaces of various types (HILLGÄRTNER 1999). Accordingly, the causes of bedding are complex and may originate from different processes. One bed may represent an entire depositional sequence, but a

depositional sequence may also comprehend several beds. The stacking pattern and thickness variations of depositional sequences (including beds) reflect environmental changes through time that caused variations in accommodation and/or accumulation rate. Stratification of sediments is usually due to the much more rapid changes of either sedimentation rates or sediment composition, than the more slowly migrations of facies zones (SCHWARZACHER 2000).

### ***Clay content***

In outcrops of carbonate platforms, clay-rich intervals normally weather back compared to massive limestone beds. This accentuates apparent bedding and indicates, as a first approximation, bedding rhythms and depositional sequences. Intervals covered with vegetation are often assumed to be entirely marly. In this study, however, marl intervals have been excavated, bringing out surprises: massive beds have been discovered within these marls (cf. Chap. 4). Such unexpected discoveries can, of course, completely change the sequence-stratigraphical interpretation.

Most clay minerals in marl intervals are of detrital origin and derive from erosion of crystalline bedrock and/or palaeosols. They are generally transported by rivers to the coastal plain and to marine depositional settings. There, they may be reworked by currents and waves (cf. Chap. 8). Clay minerals and carbonate mud (marls) commonly accumulate in low-energy conditions in supratidal to subtidal environments. In marine settings, they are deposited in shallow protected lagoons and in deeper, open-marine environments below the action of waves.

The proportion of clay minerals in carbonates can be related to two main phenomena (EINSELE & RICKEN 1991a): 1) decrease/increase of terrigenous input to the depositional environment with a constant rate of carbonate production (dilution cycle); 2) decrease/increase in carbonate production in the depositional environment with constant terrigenous influx (productivity cycle). Both phenomena are closely connected on shallow platforms (HILLGÄRTNER 1999). The occurrence and distribution of clay minerals on shallow carbonate platforms can be related to environmental changes caused by relative sea-level fluctuations and climate changes (STRASSER & HILLGÄRTNER 1998; cf. Fig. 3.2):

a) A fall of relative sea level enlarges the area of emersion in near-coastal settings (especially platforms with low relief). Therefore, an increase of clay input to shallow-marine environments caused by erosion can

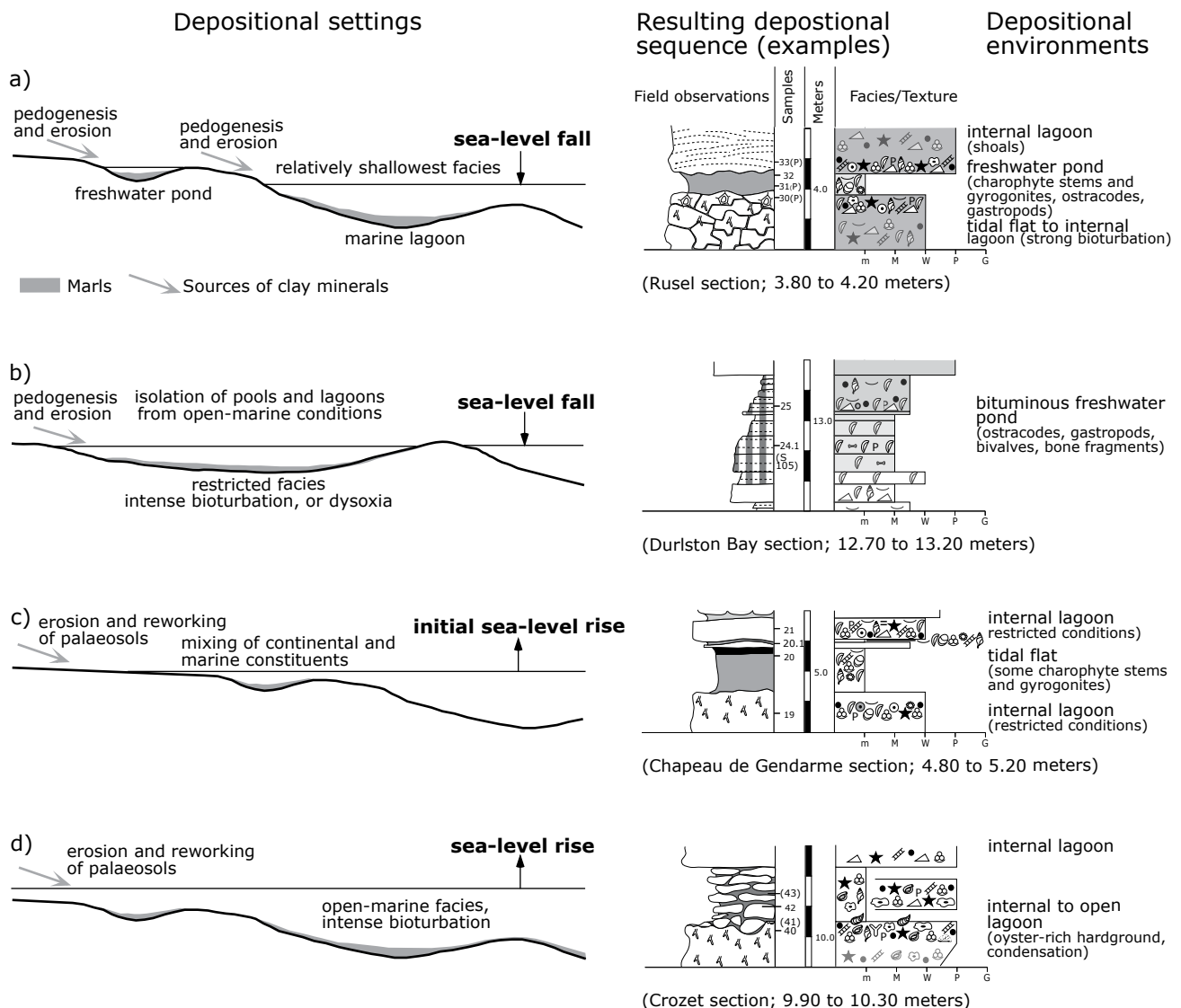


**Fig. 3.2** - Different models for clay occurrence in marginal-marine environments modified from STRASSER & HILLGÄRTNER (1998). Examples of the depositional sequences are taken from the studied sections. For legend of symbols see Figs. 4.6. and 5.7.

be postulated. Accordingly, the clays are associated with the shallowest facies. Sediments containing charophyte stems and oögonia (cf. Chap. 2) point to the formation of freshwater ponds on the partly emergent platform.

b) Low sea level can lead to isolation of pools and shallow lagoons reducing and/or cutting off open marine influence. Such an environmental isolation may reduce water-energy, enabling the settling out of clay minerals. In this case, the marl intervals are characterized by relatively restricted fauna, increased bioturbation (lowered accumulation rates) or dysoxic facies (e.g., bituminous intervals) due to reduced water circulation.

c) In some investigated marls, a mixture of continental and marine constituents has been collected.

Their interpretation in terms of high-resolution sequence stratigraphy is not straightforward. Such a mixture either points to a transitional environment between continental and marine areas (tidal flat), and/or to mixing processes during initial flooding of continental areas (transgressive deposits) by storms and spring tides (STRASSER, 1994), or to transport of continental constituents into marine environments during falling relative sea level. A quantification of the constituents and/or lateral correlation aids in solving this problem. Hence, for the interpretation of marl intervals and depositional sequences, it is important that their constituents are analyzed (washing and picking).

d) Rising sea level and maximum flooding can also provoke low-energy conditions by rising wave



base. Marls deposited under such conditions are characterized by open-marine constituents indicating a relatively deep facies. Such intervals are commonly intensively bioturbated. They probably reflect a reduction in carbonate production with constant clay input (productivity cycle). A rise in sea level can also lead to an additional input of clay minerals by the reworking and erosion of previously exposed palaeosols during transgression.

Furthermore, an elevation of rainfall in the hinterland increases the surficial runoff and may elevate the clay input into the marine depositional system. Clay minerals in marginal-marine environments, therefore, can be interpreted as a climate signal depending mainly on palaeolatitude and on atmospheric circulation patterns (e.g., PERLMUTTER & MATTHEWS 1989, 1992, KINDLER et al. 1997, ALLEN 1998).

### **Other criteria**

Trends in stable isotopes ( $\delta^{13}\text{C}$ ,  $\delta^{18}\text{O}$ ) have been used to interpret depositional and diagenetic histories of shallow carbonate limestones (e.g., ALLEN & MATTHEWS 1982, JOACHIMSKI 1991, 1994; cf. Chap. 8). However, the interactions of sedimentological and early diagenetic factors must be considered when using stable isotopes for the interpretation of depositional sequences in shallow marine carbonates (JOACHIMSKI 1991, 1994).

Palynofacies analyses investigate particulate organic matter in order to determine the ratio of terrestrial and marine influences. Such ratios then have been used to interpret depositional sequences in different environments (e.g., STEFFEN & GORIN 1993, PITTET & GORIN 1997, RAMEIL et al. 2000, SCHNYDER 2003, SCHNYDER et al. 2005a).

Geochemical analyses of trace elements (Sr, Mg, Na, Fe, and Mn) have been used to investigate environmental conditions and to relate changes in the composition of trace elements to depositional sequences (e.g., COLOMBIÉ 2002).

### **3.2.2 Terminology and applied sequence model**

The methodology for the interpretation of depositional sequences of shallow-water carbonates employed in this study is summarized in STRASSER et al. (1999). This study explains the ideas and techniques for analyzing depositional sequences with high-resolution based on field investigations of Late Oxfordian and Berriasian outcrops in the Jura Mountains. Over

more than a decade, the approach for interpreting successions of carbonate rock in outcrops have been improved and refined by the Fribourg working group (e.g., STRASSER 1994, PASQUIER 1995, PITTET 1996, PITTET & STRASSER 1998b, STRASSER & HILLGÄRTNER 1998, HILLGÄRTNER 1999, COLOMBIÉ 2002, HUG 2003, COLOMBIÉ & STRASSER 2005). The terminology is partly based on VAIL et al. (1991). However, the depositional sequences are not attributed to different “orders” that have a predefined connotation of time (STRASSER et al. 1999). Accordingly, the applied nomenclature has the advantage of being purely descriptive without implying any duration of a depositional sequence.

The term “systems tract”, which has been used to describe large-scale geometries mainly based on seismic investigations (e.g., VAIL et al. 1991) is not applied in this study because of the limited outcrop extensions. Accordingly, instead of lowstand, transgressive, and highstand systems tracts, the terms lowstand, transgressive, and highstand deposits have been used in the present study.

### **Accommodation space and sedimentary record**

KENDALL & SCHLAGER (1981) stated that “stratigraphic sequences of shallow-water deposits and their facies patterns are primarily controlled by the rates and types of sedimentation, local crustal movements, and eustatic sea level. These three controls act in consort with one another, though locally, one control may be more important than another. The facies anatomy of carbonate shelves and platforms reflects the combined effects of these three parameters” (p. 182).

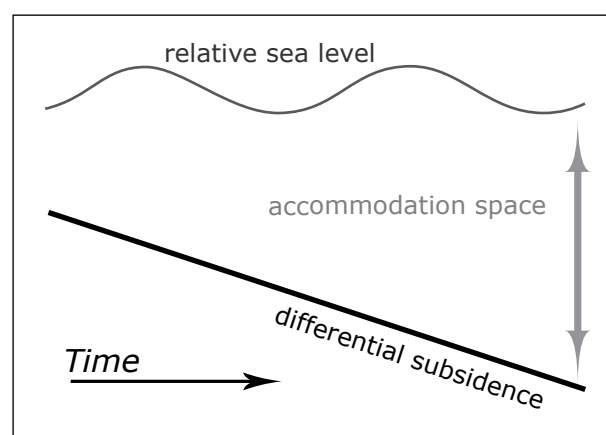


**Fig. 3.3** - Accommodation space represents the volume, which can be filled with sediments in a depositional basin. Changes in accommodation space over time is controlled by the combination of sea-level fluctuations and tectonic movements of the substrate (subsidence and/or uplift).

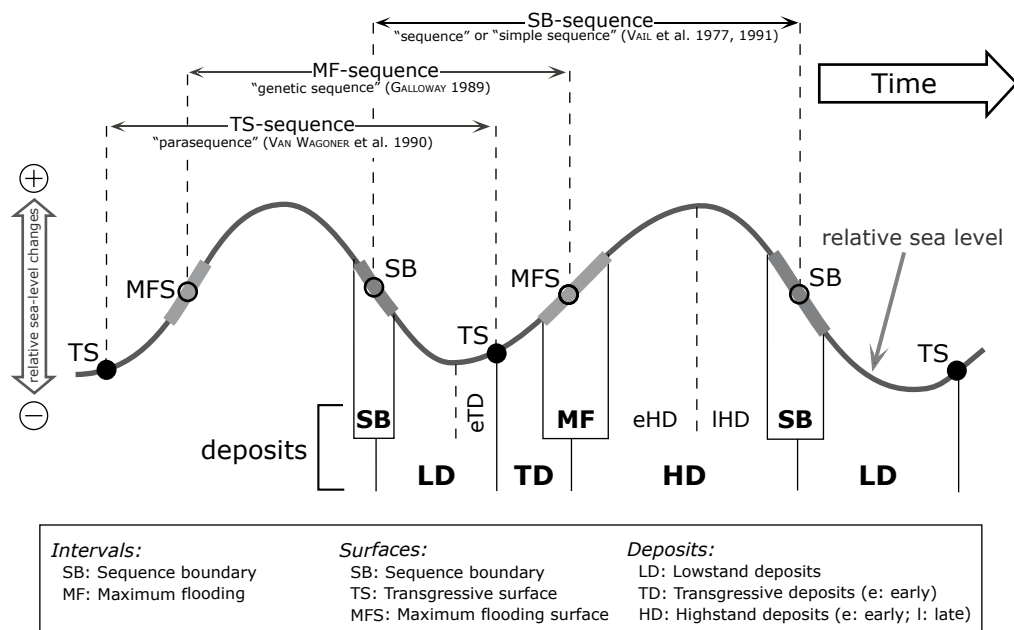


**Fig. 3.4** - Theoretical sequence model. The position of characteristic deposits and diagnostic surfaces (discontinuities) is independent of time and amplitude of relative sea-level fluctuations. If a distinct surface is not developed during fastest sea-level fall or rise, one may speak of a sequence-boundary or maximum-flooding interval, respectively. For more details on the used terms and concepts refer to text (modified from HILLGÄRTNER 1999, HUG 2003, and RAMEIL 2005).

The combination of changing sea level with local, vertical crustal movements (subsidence and/or uplift) creates accommodation space, which can be filled with sediments over the time (Fig. 3.3). Accommodation is, therefore, “the space made available for potential sediment accumulation, [which] is a function of both sea-level fluctuations and subsidence” (JERVEY 1988; in POSAMENTIER et al. 1988, p. 110)

The term “eustasy” describes a global sea level with reference to a fixed datum (e.g., center of the Earth; POSAMENTIER et al. 1988). The causes of world-wide sea-level changes are manifold (e.g., DONOVAN & JONES 1979, HSÜ & WINTERER 1980, DEWEY & PITMAN 1998; cf. Chap. 7). Because it is generally not clear whether investigated sedimentary records have primarily been controlled by eustatic sea-level changes, by tectonic movements and/or by sedimentary processes, the term “relative sea level” has been introduced. Relative sea level includes “local subsidence and/or uplift by referring to the position of a datum (e.g., basement) at or near the sea floor” (POSAMENTIER et al. 1988, p. 110).

Vertical crustal movements are commonly of basin-wide extension. Different processes have been proposed to explain long-term, interbasinal, tectonic movements (e.g., intraplate stresses; CLOETINGH 1988, 1991). The sections of the Jura platform and the Dorset region are located on subsiding passive margins, in

which differential subsidence has to be considered (references in Chap. 4 and 5). Hence, it cannot be excluded that periods of halt or even uplift affected the sedimentation in these regions during the time interval of consideration.

### *Sequence model for shallow carbonate platforms*

On the basis of observed depositional sequences, a sequence model has been developed. It illustrates the theoretical position of characteristic deposits and diagnostic surfaces (discontinuity surfaces) on a relative sea-level curve (Fig. 3.4). This model does not depend on the scale of the relative sea-level variation.

The diagnostic surface or interval, which corresponds to the time of fastest relative sea-level fall is called “sequence boundary” (SB). It marks a time of destruction of accommodation space when the possibility to create subaerial exposure is highest (cf. Fig. 3.6a). As a convention, a depositional sequence is defined between two sequence boundaries (VAIL et al. 1991; cf. Chap 4 and 5).

The interval corresponding to low relative sea level (lowstand deposits, LD), which follows the sequence boundary is usually very thin, not developed at all, and/or reworked in the transgressive sediments on shallow platforms. Additionally, it may be difficult to

distinguish lowstand deposits from sediments, which are formed during the initial phase of the subsequent transgression. Such deposits are called “early transgressive deposits” (eTD). Normally, it takes time for the carbonate production (carbonate factory) to start up after a subaerial emersion. KENDALL & SCHLAGER (1981) stated that “a rapid rise of the sea may thus ‘take a reef or platform by surprise’ and initiate a start-up period during which the system runs below its full growth potential, lagging behind the rise of the sea” (p. 195). Such a “start up” phase corresponds to the “lag time” of STRASSER (1991) and TIPPER (1997).

The diagnostic surface depicting an initial flooding is termed “transgressive surface” (TS). Commonly, this surface is well-expressed by an abrupt facies change from relatively restricted to more open-marine sediments. Transgressive lag deposits containing re-worked clasts (intraclasts), an abrupt increase of mean grain diameter, and minor erosion are other diagnostic features for transgressive surfaces. In very shallow environments where accommodation is low, lowstand deposits are missing so that the sequence boundary is directly overlain by the transgressive surface.

With increasing water depth and the recovery of the carbonate factory, ideal conditions prevail for the carbonate production to fill up the previously created accommodation space. Normally, this phase is characterized by relatively thick beds (STRASSER et al. 1999). On a larger scale, a thickening-up stacking pattern (beds become thicker stratigraphically upward) point to increasing accommodation space. The fastest rise in relative sea level leads to “maximum flooding” (MF) or to a “maximum-flooding surface” (MFS) if a distinct surface can be identified. These diagnostic intervals or surfaces are indicated by the relatively deepest and/or most open-marine facies. Intensely bioturbated intervals or distinct omission surfaces are good candidates for maximum floodings and/or maximum-flooding surfaces. At all scales, deposits, which point to a relative deepening and/or opening of the depositional system are termed “transgressive deposits” (TD). Transgressive deposits depict sediments between the transgressive surface and the maximum flooding.

After the maximum flooding, a shallowing up trend can commonly be identified within a depositional sequence. On a larger scale, a thinning-up stacking pattern is displayed (beds become thinner stratigraphically upwards). Such a trend reflects a slow-down in relative sea-level rise and an initial fall leading to a loss of accommodation. The corresponding sediments are named “highstand deposits” (HD). They are positioned between the maximum flooding and the sequence boundary. If the production of

carbonate matches the creation of accommodation space, the platform will grow preferentially vertically (aggradation). When identifiable in a section, such deposits are called “early highstand deposits” (eHD). A progradation takes place when the carbonate production is higher than the creation of accommodation space and the platform builds towards deeper and more open depositional settings. Sediments, which have been deposited during progradation are called “late highstand deposits” (lHD). However, these distinctions can only be made on large-scale investigations where the spatial geometry of the platform is identifiable.

### 3.2.3 Depositional sequences at different scales

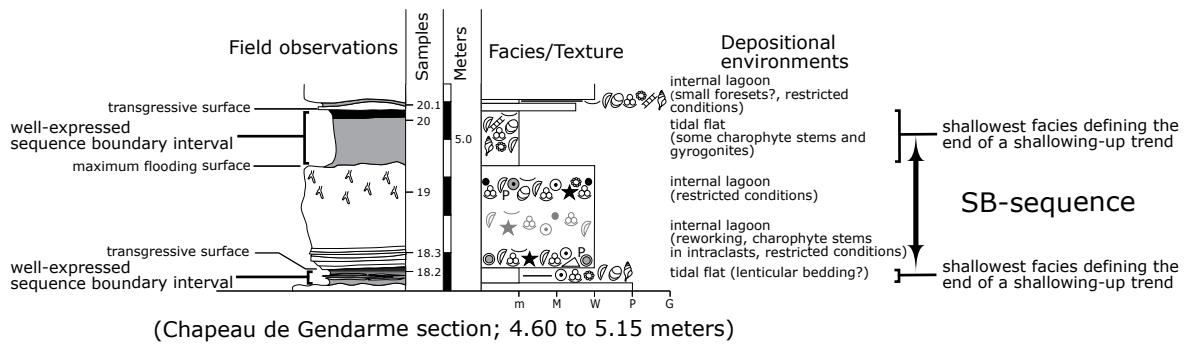
Four different descriptive types of depositional sequences in the shallow-marine sections of the Jura platform and the Dorset region can be distinguished (Fig. 3.5). The diagnostic signs enclose their characteristic facies evolution, which can be related to bathymetric changes, and their bounding surfaces and intervals. Besides shallowing or deepening trends, facies evolution may also indicate changes from more open-marine to more restricted conditions and vice versa. Basinal settings are characterized by only one type of depositional sequence (e.g., HILLGÄRTNER 1999, RAMEIL 2005).

#### *Deepening-shallowing sequences defined by sequence boundaries (SB-sequences)*

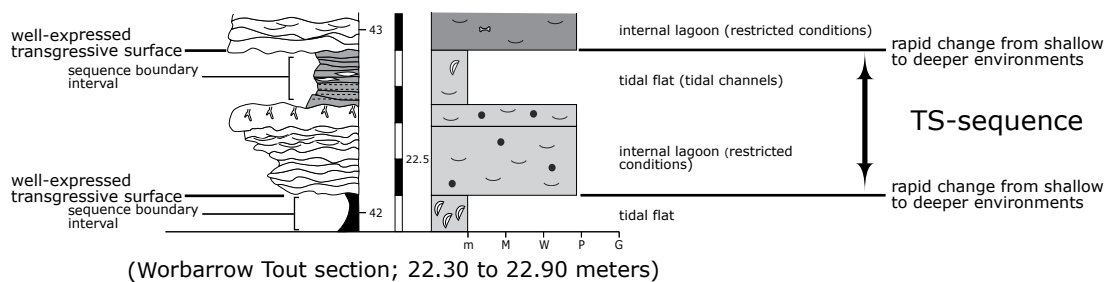
Facies analysis through time indicates that water depth first increased, then decreased. In shallow-water carbonate-dominated systems, many depositional sequences are asymmetric displaying a thin deepening-up and a thick shallowing-up part (e.g., JONES & DESCROCHERS 1992, PRATT & JAMES 1992). The shallowing-up trend is due to the high carbonate production and accumulation, which generally easily outpaces a relative sea-level rise as long as the environmental conditions are favorable (SCHLAGER 1981). The shallowing can be enhanced during decelerating rise and falling relative sea level. The sequence boundaries of such depositional sequences can be subtidal, intertidal or supratidal surfaces and/or intervals exhibiting the relatively shallowest facies of a sequence (STRASSER et al. 1999). If sea level drops below the depositional surface and non-consolidated deposits are eroded, an erosion surface marks the sequence boundary of the depositional sequence. Long-lasting sea-level falls below the carbonate seafloor



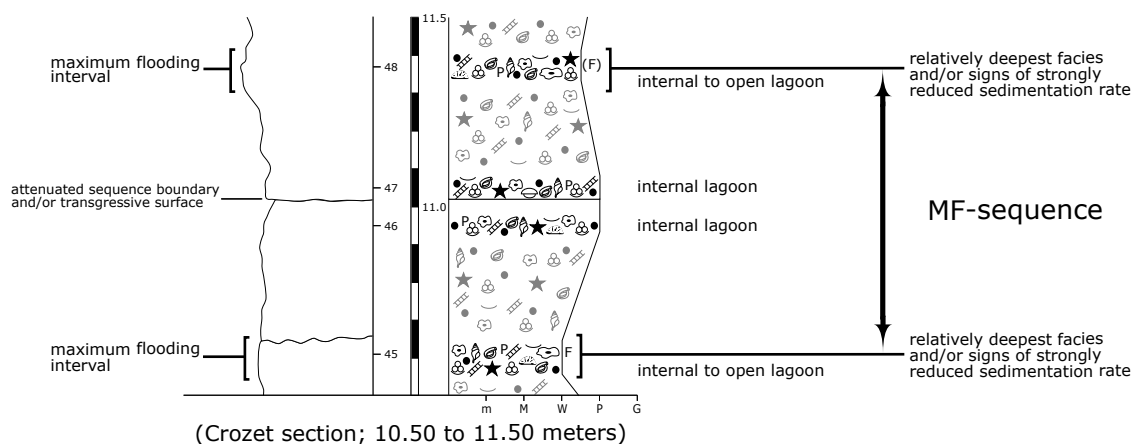
### Example for a SB-sequence



### Example for a TS-sequence



### Example for a MF-sequence



### Example for an aggrading sequence

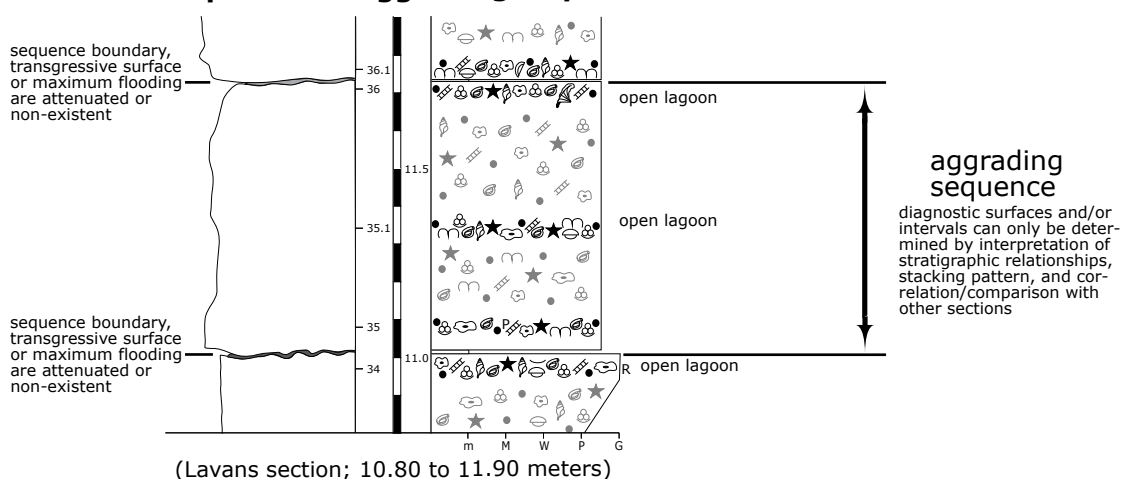


**Fig. 3.5** - Examples of SB-, TS-, MF-, and aggrading sequences (see text for discussion). The examples are all taken from the sections investigated in this study (cf. Chap. 4 and 5; for legend refer to Figs. 4.6 and 5.7).

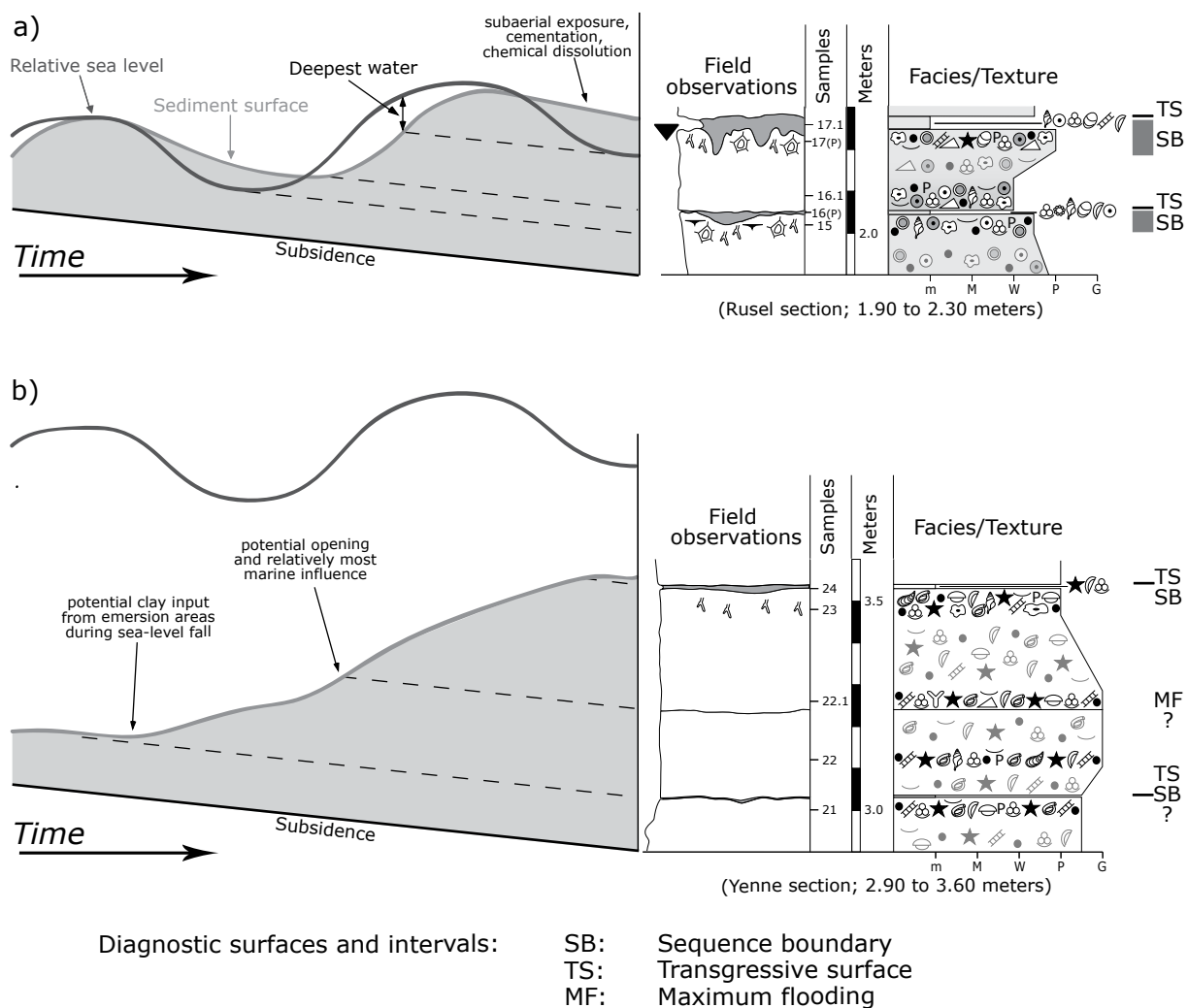


**Fig. 3.6** - Formation of a depositional sequence during an interval of a sea-level change. The model illustrates the evolution through time of one point of the shallow platform. After emersion and a certain lag time, high sediment production fills up the accommodation space created by the combination of relative sea-level rise and subsidence. a) An asymmetric sequence consisting of transgressive deposits. The highstand deposits are reduced, eroded, and/or dissolved during the following sea-level drop. b) In deeper waters, a depositional sequence may be marked indirectly through input of clays during sea-level fall, and through subtle facies changes. Generally, the identification of diagnostic surfaces and intervals is not straightforward because of missing threshold effects in deeper water. The examples are all taken from the sections investigated in this study (cf. Chap. 4 and 5; for legend refer to Figs. 4.6 and 5.7). Models modified from STRASSER et al. (1999).

may lead to freshwater cementation and/or chemical dissolution of carbonate and karstification (in humid climates; cf. Fig. 3.6a). This type of depositional sequence corresponds to the definitions of the classical sequence-stratigraphical model where sequence boundaries are formed during relative sea-level falls (called “sequence” or “simple sequence”; VAIL et al. 1977, 1991; cf. Fig. 3.4). Deepening-shallowing sequences that never reach intertidal or supratidal conditions have been termed “subtidal cycles” by OSLEGER (1991). The expression of diagnostic surfaces or intervals

in subtidal sediments may be weak due to missing threshold effects (Fig. 3.6b). Commonly, sequence boundaries in such environments are implied by thin marls supplied by erosion of the hinterland during sea-level fall.

#### ***Deepening-shallowing sequences defined by transgressive surfaces (TS-sequences)***

These depositional sequences are characterized

by sharp transgressive surfaces, implying rapid facies changes from relatively shallowest (or most restricted) to deeper (or more marine) (STRASSER et al. 1999). Facies changes related to sea-level fall or maximum flooding may be identifiable but are commonly too subtle to be developed as well-expressed diagnostic surface or interval. Sequences, which are bounded by marine flooding surfaces (transgressive surfaces) have been entitled “parasequences” by VAN WAGONER et al. (1990) (cf. Fig. 3.4). In the studied sections, most of the sequences can be attributed to this type of depositional sequences.

#### ***Shallowing-deepening sequences defined by maximum-flooding surfaces or intervals (MF-sequences)***

In this type of depositional sequence, the maximum-flooding surfaces and/or intervals are best marked in the sedimentary succession. They are, therefore, characterized by an inverse trend of facies evolution. The surfaces commonly are of the omission type underlined by intense bioturbation, fossil or mineral encrustations, and/or clays. A strongly reduced sedimentation rate and condensation can be suggested to be concentrated in such surfaces and intervals (HILLGÄRTNER 1999). This type of depositional sequence can be compared to the “genetic sequences” defined by GALLOWAY (1989) (cf. Fig. 3.4).

#### ***Aggrading sequences***

Facies changes in small sequences or thin beds are in many cases too subtle to be expressed as shallowing- or deepening-upward trend. This can be related to the absence of threshold effects in the depositional environment (cf. Fig. 3.6b). Accordingly, the identification of diagnostic features is not easy. Here, only the analysis of clay minerals, stable isotopes, palynofacies, or the overall context with lateral correlations can help. STRASSER et al. (1999) concluded that “nevertheless, the fact that such sequences are recognizable as beds or bedsets indicates that at least some clays have been washed into the system from an area that was more sensitive to environmental changes” (p. 207).

#### ***Basinal sequences***

These sequences cannot be compared with the

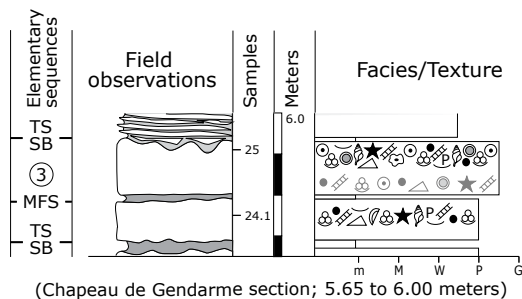
ones described from shallow-marine environments (HILLGÄRTNER 1999). Such depositional sequences consist of marl-limestone alternations where both lithologies show subtle internal variation. Marl-limestone alternations in basins have been discussed controversially in the literature. These alternations may be related to climatically induced changes in planctonic carbonate productivity at the top of the water column in open-marine basins and the detritic supply of clay minerals (e.g., EINSELE & RICKEN 1991a). Moreover, phases of carbonate-mud export from the carbonate platform to the basin may also be responsible for marl-limestone alternations (e.g., PASQUIER & STRASSER 1997, PITTET & STRASSER 1998a, PITTET et al. 2000, COLOMBIÉ & STRASSER 2003). These concepts concentrate on depositional mechanisms, which are controlled by external forces. Other researchers explain marl-limestone alternations on the basis of post-depositional processes like differential diagenesis during burial (e.g., RICKEN & EDER 1991, WESTPHAL et al. 2004a, b). In some, but especially in large-scale depositional sequences, lowstand deposits comprehend relatively thick intervals of resedimented carbonates (e.g., STROHMENGER & STRASSER 1993). Maximum floodings in large-scale basinal sequences are mainly expressed by sediment starvation (intervals or surfaces of iron/manganese crusts, concentration of fossils, and bioturbation). A basinal section (Montclus) is presented in Chap. 6. Its sequence-stratigraphical interpretation is based on the studies of PASQUIER (1995), PASQUIER & STRASSER (1997), HILLGÄRTNER (1999), and STRASSER et al. (2004).

### **3.2.4 Hierarchy and stacking of depositional sequences**

Depositional sequences of shallow marine settings are commonly stacked in a hierarchical pattern (bundling; e.g., GOLDHAMMER et al. 1990, OSLEGER & READ 1991, LEHMANN et al. 1998, LEHRMANN & GOLDHAMMER 1999, RASPINI 2001). The high-resolution investigation presented in this study concentrates mainly on the identification of the smallest depositional sequences (elementary and small-scale sequences). Larger sequences (medium- and large-scale sequences) have been studied in the Dorset region (cf. Chap. 5). Good explications on large-scale sequences of shallow-marine and hemipelagic depositional settings are given in HILLGÄRTNER (1999) and RAMEIL (2005). Large-scale sequences measure several tens of meters. They correspond to 3<sup>rd</sup>-order sequences of the traditional sequence-stratigraphical models (e.g., VAIL

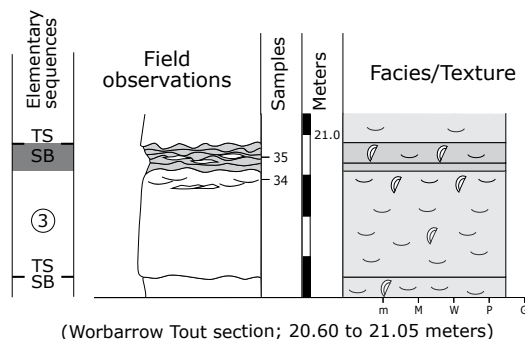
## Jura platform

## a) Elementary sequences



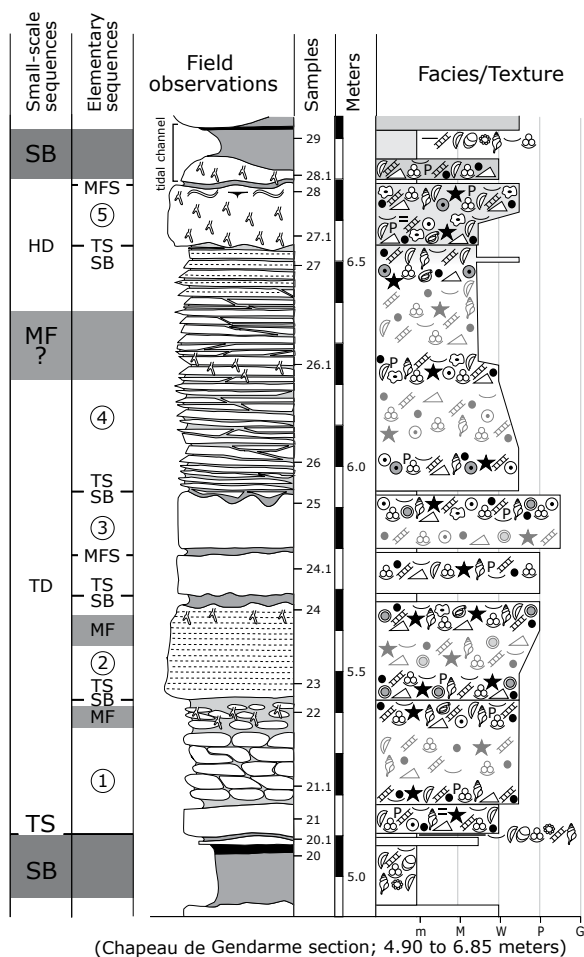
(Chapeau de Gendarme section; 5.65 to 6.00 meters)

## Dorset region

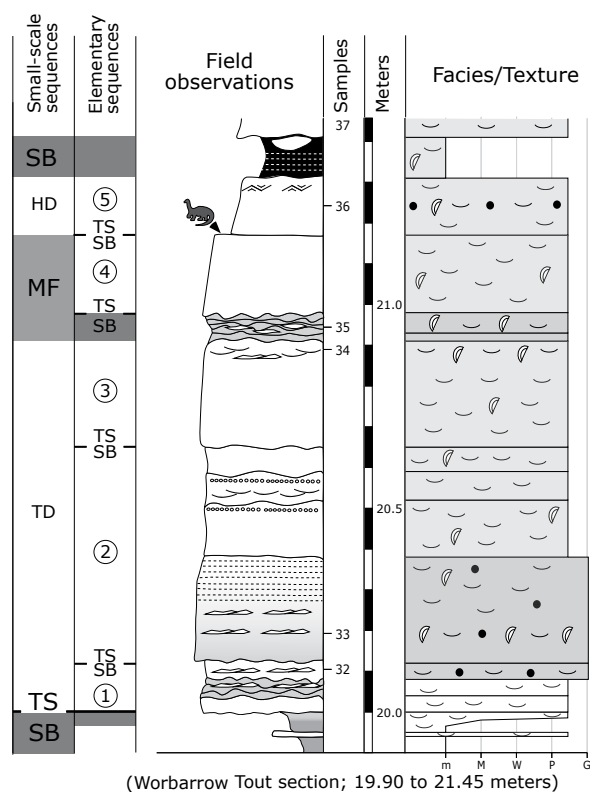


(Worbarrow Tout section; 20.60 to 21.05 meters)

## b) Small-scale sequences



(Chapeau de Gendarme section; 4.90 to 6.85 meters)



(Worbarrow Tout section; 19.90 to 21.45 meters)

**Fig. 3.7** - Hierarchy of depositional sequences of the Jura platform (Chapeau de Gendarme; on the left side) and Dorset region (Worbarrow Tout; on the right side). a) One elementary sequence of each of the two depositional regions is displayed as an example. They illustrate the third elementary sequence of the small-scale sequences shown below. b) One (composite) small-scale sequence of the same sections. Each consists of five well-expressed elementary sequences. For the depositional and sequence-stratigraphical interpretation refer to Chap. 4 and 5 (for legend refer to Figs. 4.6 and 5.7).

et al. 1991). An overview of the lateral relationship of these different depositional sequences is given in Chap. 6.

### *Elementary sequences*

These sequences are the smallest units detectable in outcrops. STRASSER et al. (1999) described them as “sequences that show a facies evolution corresponding to the shortest recognizable cycle of environmental change (including sea-level change)” (p. 207). In this context, a cycle describes the process, which leads to the formation of a depositional sequence. Elementary sequences consist of one to several beds, which display either a deepening-shallowing or a shallowing-deepening trend of facies evolution (Fig. 3.7a). Yet, many beds consist of a rather homogeneous facies evolution, which complicates their interpretation as an elementary sequence.

In the basin, one well-defined limestone-marl alternation is commonly interpreted to correspond to an elementary sequence (HILLGÄRTNER 1999). However, in some cases, one environmental cycle can also produce two alternations (PITTET & STRASSER 1998a). In the studied sections, elementary sequences of the shallow-marine environments and the basin range in thickness from a few centimeters to 10s of centimeters.

### *Small-scale (composite) sequences*

Small-scale sequences are composed of 2 to 6 elementary sequences (Fig. 3.7b). They commonly display a well-defined deepening-shallowing facies evolution, which is bounded by important discontinuities (SB- or TS-sequences). Shallowing-deepening trends (MF-sequences) are rare in the investigated sections. An asymmetric architecture in the facies evolution (shallowing vs. deepening) of small-scale sequences is frequently observed (STRASSER 1991). In a small-scale deepening-shallowing sequence, elementary deepening-shallowing sequences dominate. In such small-scale sequences, the shallowing-up trend is generally well developed towards the top of the sequence. The inverse pattern is true for shallowing-deepening sequences.

Small-scale sequences in basinal settings commonly are defined by thickening-up or thinning-up trends composed of a set of 4 to 6 limestone beds, and/or by a bundling of 4 to 6 limestone beds between relatively thick marly intervals (HILLGÄRTNER 1999). The sequence boundaries of the basinal small-scale

sequences are placed at the base of the relatively thickest limestone beds. It is thought that these beds have been formed during lowstand conditions when planktonic productivity was concentrated above the hemi- to pelagic depositional setting while the platforms were at least partly exposed. With rising sea level, carbonate productivity increases also on the platform, less nanoplankton is produced and deposited in the open ocean, and potentially more marl-rich intervals are formed (STRASSER et al. 2004). Small-scale sequences in the shallow-marine environments and in the basin measure from a few to several meters in the studied sections.

### *Medium-scale (composite) sequences*

Medium-scale sequences generally comprehend 3 to 4 small-scale sequences. Their facies evolutions are similar to those of the small-scale sequences. They are delimited by well-expressed discontinuity surfaces or intervals due to erosion and/or non-deposition (SB- and/or TS-sequences). Commonly, they are characterized by a rather symmetric deepening-shallowing facies evolution and by a well-developed maximum-flooding interval. Thickening-up of beds and small-scale sequences may occur in the lower part, thinning-up in the upper part of a medium-scale sequence.

In the basin, medium-scale sequences can only be identified by abrupt changes in the stacking pattern of small-scale sequences (HILLGÄRTNER 1999). This is indicated by a change in the thickness of limestone beds and/or marl intervals. These variations of thickness are related to changes in sedimentation rates and the ratio of lime versus clay sedimentation. Medium-scale sequences in the shallow-marine environments and in the basin are in the range of few meters to tens of meters.

### *Superposition of relative sea-level changes*

The sedimentary record of shallow-marine deposits cannot be explained by a simple, theoretical sinus-curve sequence model. It reflects rather a complex stacking pattern reflected with changes in the thicknesses of sequences and beds, facies evolution (deepening/shallowing trends), and the enhanced or attenuated expression of diagnostic surfaces and intervals (RAMEIL 2005). Such stacking patterns have been interpreted as the expression of several superimposed relative sea-level fluctuations creating an intricate, composite sea-

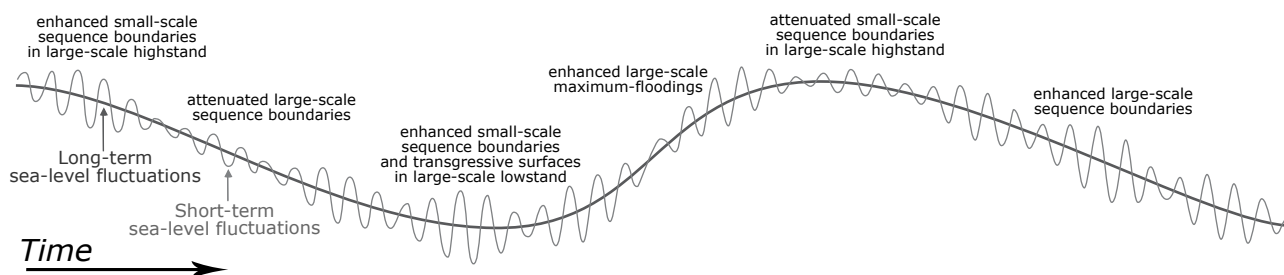


**Fig. 3.8** - Hypothetical short-term sea-level changes with varying amplitudes superimposed on a long-term sea-level fluctuation. Such a superposition can be used to explain enhanced or attenuated diagnostic surfaces in the sedimentary record. STRASSER et al. (1999) used the variations of the caloric equator calculated from fluctuations of orbital parameters during the Quaternary by BERGER (1978) to construct the high-frequency curve. The sketch is based on the assumption that orbital insolation changes are directly translated into sea-level changes (modified from STRASSER et al. 1999).

level curve (e.g., GOLDHAMMER et al. 1990, MITCHUM & VAN WAGONER 1991, OSLEGER & READ 1991, EINSELE & RICKEN 1991b, STRASSER 1994, LEHRMANN & GOLDHAMMER 1999; cf. Fig. 3.8). Such a composite sea-level curve, therefore, comprehends different amplitudes and frequencies depending on the scales of the superimposed relative sea-level variations.

The expression (enhancement and/or weakening) of diagnostic surfaces and intervals and the facies evolution within a sequence (types of sequences) depends on the relative position of smaller sequences on a larger sea-level trend (cf. Fig. 3.8). The analyses of these characteristics in the sedimentary record, therefore, may help to reconstruct a sea-level trend. When a small-scale sequence is superimposed on a larger-scale sea-level rise, its maximum flooding will be enhanced, whereas the sequence boundaries will be attenuated. As a consequence, the maximum-flooding surfaces and/or intervals will be better expressed than the sequence boundaries (MF-sequences). Sequence boundaries, in contrast, will be accentuated by a falling trend (SB-sequences). Transgressive surfaces will be underlined when different orders of initial floodings are superimposed on a long-term trend (TS-sequences) (e.g., PASQUIER 1995, HILLGÄRTNER 1999).

Superimposition of different amplitudes and frequencies of relative sea-level fluctuations commonly leads to a multiplication of diagnostic surfaces and intervals on a larger sea-level trend (e.g., MONTAÑEZ & OSLEGER 1993, PASQUIER & STRASSER 1997). Such clusters of diagnostic surfaces and/or intervals have been called “maximum-flooding zone” (MFZ), “sequence-boundary zone” (SBZ), and “transgressive-surface zone” (TSZ).

High-frequency fluctuations of high amplitude superimposed on a falling long-term sea-level trend can only be recorded in short time intervals during the high-frequency sea-level rises. Accordingly, the preservation potential of such sequences is rather low,

leading to an incomplete sedimentary record (“missed beats” sensu GOLDHAMMER et al. 1990; cf. Fig. 3.9).

#### *Why investigating transgressive deposits?*

During a long-term transgressive trend, accommodation increases so that the preservation potential of depositional sequences is commonly highest (cf. Fig. 3.9). Consequently, the record of depositional sequences is thought to be best developed in transgressive deposits. Additionally, it can be assumed that the completeness of the sedimentary record is highest during increasing accommodation space.

### **3.2.5 Auto- versus allocyclic**

In this chapter, it has been assumed that the sedimentary record was always controlled by relative sea-level fluctuations. Processes like subsidence/uplift, eustasy, or climate controlling clay input are overregional. Such external processes (extrinsic) have been termed “allocyclic” (EINSELE & RICKEN 1991b). In shallow-marine carbonate systems, however, processes like carbonate production and carbonate accumulation are strongly controlled by local, “autocyclic” factors (intrinsic).

#### *Autocyclic*

Different random-based autocyclic models have been developed to explain the stacking pattern and/or the facies evolution of shallow-marine sedimentary successions. Shallowing-up sequences in intertidal carbonate systems have been explained by the combination of vertical aggradation and lateral progradation of tidal flats during a stable relative sea

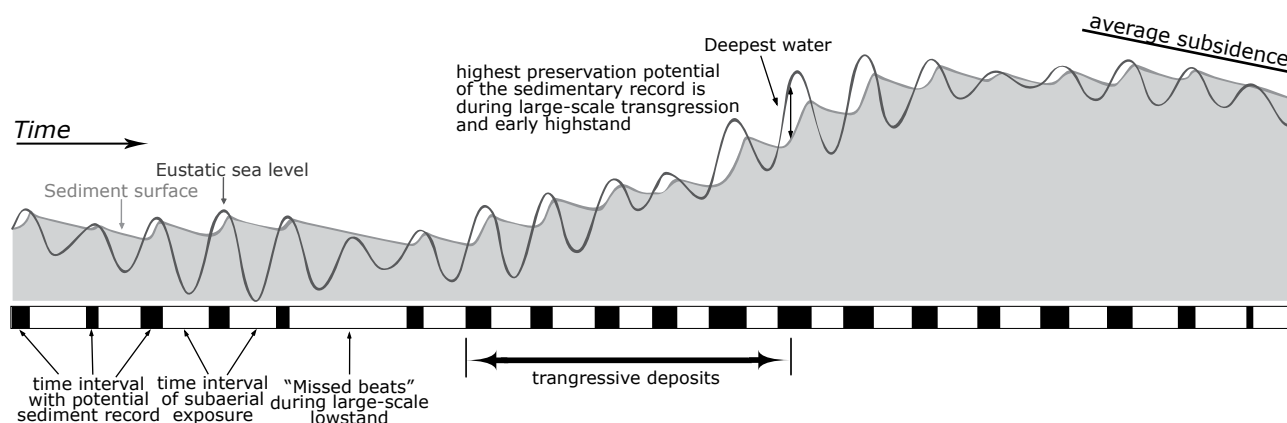


**Fig. 3.9** - Sedimentary record of high-frequency sea-level changes with varying amplitudes, superimposed on a longer-term trend. This model describes the evolution through time of one point in a shallow marine environment. It is based on the study of Early Berriasian sections of the French Jura Mountains (STRASSER 1994; amplitude of sea-level change: 1-8 m; average subsidence rate: 5 m/100 ka). Much of the shallow platform deposits are not recorded because of erosion during subaerial exposure (white intervals; modified from STRASSER et al. 1999).

level (“tidal-flat model” according to GINSBURG 1971; in LEHRMANN & GOLDHAMMER 1999). CLOYD et al. (1990) presented a model for discontinuous fining-up carbonate sequences involving migration of tidal channels and channel levees. Other models related the deposition of laterally discontinuous sequences to the migration of complex patterns of tidal islands and coexistent subtidal areas and channels (“tidal flat-island model”; PRATT & JAMES 1986, SATTERLEY 1996). PRATT & JAMES (1992) stated that “(...) this tidal flat-island model severely limits the architectural predictability of ancient platforms, as the constituent facies, particularly the supratidal caps, are of inherently limited regional extent” (p. 315). Other researchers used statistical methods to proof the randomness of sedimentary successions (e.g., DRUMMOND & WILKINSON 1993a, b, WILKINSON et al. 1996, 1997).

These models, however, convince only for laterally discontinuous shallowing-up sequences (SCHLAGER 2005). They do not explain subtidal sequences and/or sequences characterized by vadose diagenetic overprints (e.g., KENDALL & SCHLAGER 1981, OSLEGER 1991, OSLEGER & READ 1991, STRASSER 1991). On the other hand, intervals of shoal and tidal channel deposits are strongly controlled by autocyclic processes (cf. Chap. 6). Hence, they are of limited lateral extension, displaying rather a local depositional geometry.

### *Allocyclicity*

Allocyclic forcing of sedimentary systems can be imposed by different environmental changes. However, relative sea-level fluctuations have the

most direct influence in shallow-marine depositional settings (e.g., GOODWIN & ANDERSON 1985, ANDERSON & GOODWIN 1990). Normally, such processes affect the sedimentary record on a larger lateral scale than autocyclic processes (HILLGÄRTNER 1999). Therefore, it is thought that depositional sequences, which can be correlated between widely-spaced sections have mainly been controlled by allocyclic processes. Different studies made by the Fribourg working group showed that small- and medium-scale sequences can be traced between measured sections for distances of up to 100 km (e.g., PASQUIER 1995, PASQUIER & STRASSER 1997, PITTET & STRASSER 1998b, HILLGÄRTNER 1999, COLOMBIÉ 2002, COLOMBIÉ & STRASSER 2003, RAMEIL 2005). Therefore, it is possible to establish a sequence-stratigraphical framework at least on the level of small- and medium-scale sequences. The interpretation and correlation of elementary sequences remains a challenge. An attempt to push the limits of high-resolution sequence-stratigraphical interpretations by correlating elementary sequences over long distances is presented in this study (cf. Chap. 6).

Commonly, it is not straightforward to distinguish whether extrinsic and/or intrinsic processes have been involved in the deposition of the observed sedimentary succession in shallow-marine systems (GOODWIN & ANDERSON 1985, STRASSER 1991). These processes are intimately connected, strongly depending on the scale of consideration. Facies mosaics describe facies arrangements at a relatively small spatial scale and are, therefore, sensitive to local, autocyclic processes (WRIGHT & BURGESS 2005; cf. Chap. 2). At a larger scale of investigation, modern shallow-marine carbonate depositional systems display gradational



and linear trends in facies distributions (e.g., GISCHLER & LOMANDO 1999, WRIGHT & BURGESS 2005, SCHLAGER 2005). In high-resolution investigations of outcrops at the scale of elementary sequences, auto- and allocyclic processes have to be considered by interpreting the sedimentary record. RANKEY (2004) concludes that “(...) if we are to interpret the intrinsic and extrinsic processes responsible for the accumulation of the stratigraphic record, it is imperative to recall that the real world is a multivariate system, and one, in which spatial and temporal context is important” (p. 6). The high-resolution sequence-stratigraphical approach presented in this chapter is, therefore, an instrument to analyze depositional sequences in detail and to relate them to extrinsic and/or intrinsic processes. POSAMENTIER & JAMES (1993) stressed that “most

importantly, however, sequence stratigraphy must be viewed as a tool or approach rather than a rigid template” (p. 3). Such an investigation cannot be based on one section alone because of the highly dynamic nature of shallow-marine depositional systems. Hence, it is essential to use and correlate several sections over long-distances from platform to basin and from one sedimentary basin to another in order to filter out local and effects like platform morphology and differential subsidence (STRASSER et al. 1999, cf. Chap. 6).

The advantage of sequence stratigraphy is that this method does not only allow to correlate lithological units laterally. Instead, it investigates environmental changes in lithological units and relates them in a process-oriented approach to extrinsic and/or intrinsic depositional forces.

\*\*\*\*\*



## 4 - SECTIONS OF THE SWISS AND FRENCH JURA PLATFORM

Eleven sections of the Jura platform have been logged in detail and interpreted with high resolution (elementary sequence scale). This high-resolution interpretation is based on a well-established sequence-stratigraphical framework (small- and medium-scale sequences) published in the literature (e.g., WAEHRY 1989, PASQUIER 1995, HILLGÄRTNER 1999, STRASSER et al. 2004; cf. Chap. 6). This study focuses on the first three to four small-scale sequences at the base of

the Pierre Châtel Formation. In order to enable such detailed interpretations, the sections have been chosen according to the following criteria:

- continuous outcrops
- well dated and/or interpreted in terms of sequence-stratigraphy based on previous work
- absence of major tectonic disturbance
- good access to the section

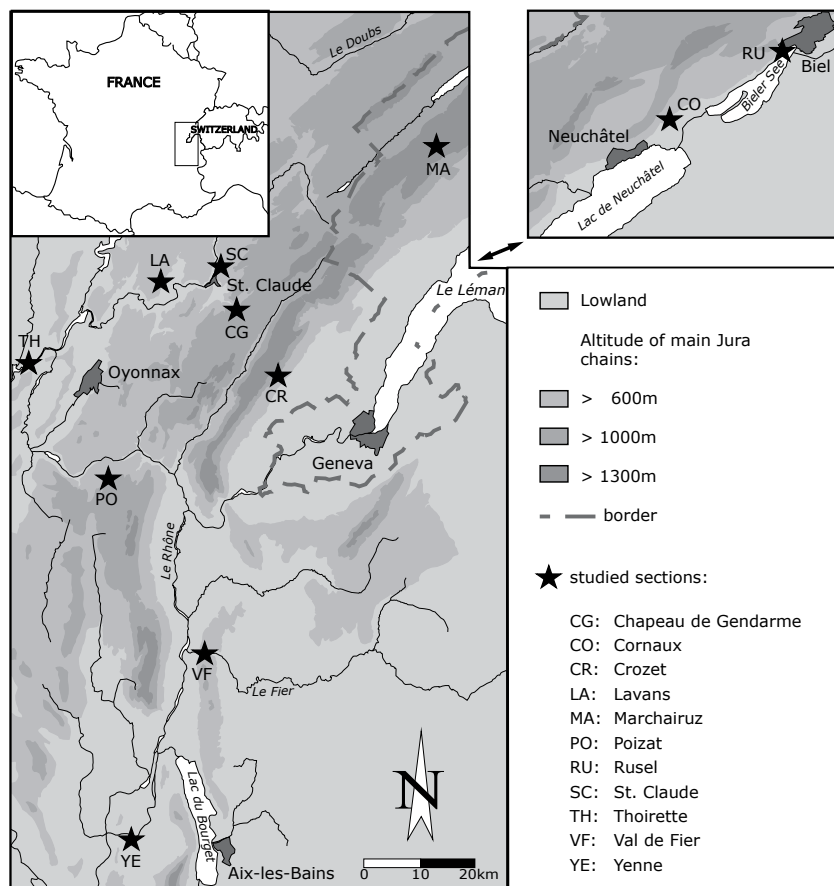


**Fig. 4.1** - Location of studied sections in the central and southern Jura Mountains (Switzerland and France).

## 4.1 Previous work

The most important studies concerning the Berriasian of the Jura platform are given in the description of the sections. A good compilation of “historic milestones” on the Berriasian of the Jura platform is given in PASQUIER (1995) and HILLGÄRTNER (1999).

## 4.2 Geographic setting

The studied sections are all located in the central and southern Jura Mountains of Switzerland and France (Fig. 4.1). The Jura is a relatively young mountain chain formed during a late Alpine phase (Miocene and Pliocene). It mainly consists of Mesozoic sedimentary rocks, which have been detached from their substratum along incompetent members of Triassic formations (TRÜMPY 1980). The studied sections are located in the “Folded Jura”, which is characterized by a succession of anti- and synclines with more or less NE-SW-oriented axes. Two main strike-slip fault zones (Vuache and Pontarlier) cut through these anti- and synclines, delimiting large tectonic compartments (WILDI et al. 1989; Fig. 4.2). The Mesozoic sediment cover continues under the Tertiary Molasse basin in the south and east of the Jura chain.

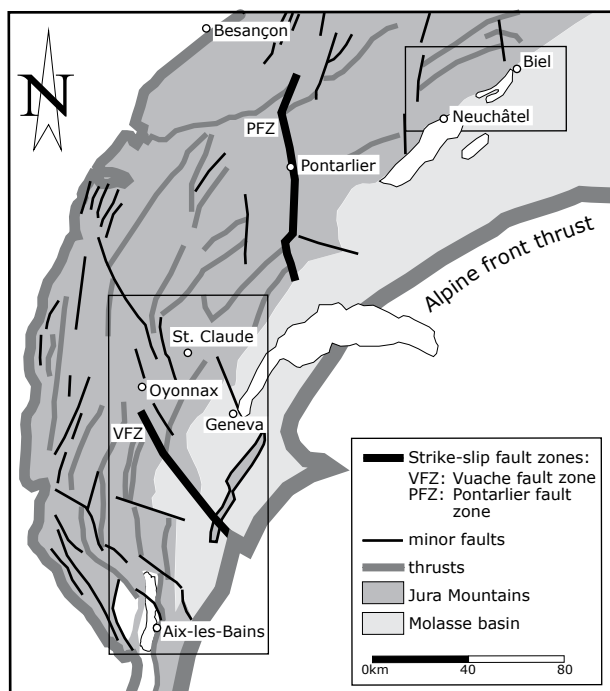


**Fig. 4.2** - Geological map of the central and southern Jura Mountains (modified from CHANTRAINE et al. 1996 in DERCOURT 1997). The boxes indicate the position of the maps displayed in Fig 4.1.

Early Cretaceous deposits are only present in the central and southern part of the Swiss and French Jura mountains, approximately south of an E-W line between Biel and Besançon (TRÜMPY 1980).

Most of the sections presented in this chapter are located on the first anticline along the Jura chain from Biel to Yenne (Rusel, Cornaux, Marchairuz, Crozet, Val de Fier, and Yenne sections; cf. Fig. 4.1). Three sections are close to the French town of St. Claude (Chapeau de Gendarme, St. Claude, and Lavans sections). The Thoirrette section is in the region of Oyonnax in the valley of the river Ain. The Poizat section outcrops in the region of Nantua in France.

## 4.3 Palaeogeography

The Jura platform mainly consists of shallow-marine sediments, which have been deposited on a passive continental margin. During the Berriasian, this platform was never far from exposure with maximum water depths of a few tens of meters (HILLGÄRTNER 1999). The Jura platform is located at the northern margin of the oceanic Ligurian Tethys and makes up the central part of the North-Tethys platform (Fig. 4.3). It corresponds to the continuation of the southeastern part of the Paris basin (ARNAUD 1988). During the Berriasian, the Jura platform was surrounded by continental areas to the north by the Renish-Bohemian Massif and to the west by the Armorican and the Central Massifs (e.g., ZIEGLER 1988, DÉTRAZ & MOJON 1989, THIERRY & BARRIER 2000, GUILLOCHEAU et al. 2000). Siliciclastics found on the Jura platform mainly derive from these land areas. The Paris basin was separated from the Jura platform and the Ligurian Tethys by a morphological barrier in the region of the French town Dijon (Burgundy High; e.g., RUSCIADELLI 1999, GUILLOCHEAU et al. 2000). However, during the Early Cretaceous, marine connections through this barrier by a narrow NW to SE-oriented depression have been proposed (CURNELLE & DUBOIS 1986).

The Helvetic shelf represents the western and southern continuation of the North-Tethys platform, including the southwestern part of the Helvetic shelf (Delphino-Helvetic shelf according to DÉTRAZ & MOJON 1989). This realm consists of carbonates and siliciclastics derived from the northern continental areas. The subsidence rate of the North-Tethyan margin generally increases from the north (Jura platform) to the south (Helvetic shelf) (WILDI et al. 1989, LOUP 1992). The southern Jura platform is separated from the Vocontian basin (or Dauphinois basin) by the Liassic palaeofaults Cévennes and Isère (southeastern France) (ARNAUD 1988, DERCOURT 1997).

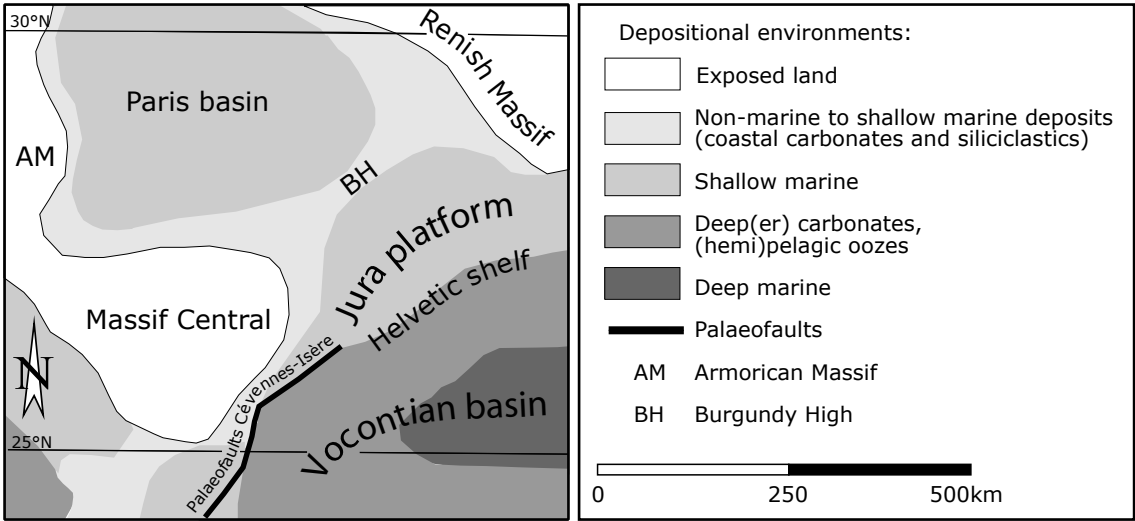


Fig. 4.3 - Palaeogeographic situation of the western Ligurian Tethys based on the map of THIERRY & BARRIER (2000; modified for the Berriasian from CURNELLE & DUBOIS 1986, ZIEGLER 1988, ARNAUD 1988, GUILLOCHEAU et al. 2000).

4.4 Biostratigraphy

The studied interval has been dated by some ammonites and by charophyte-ostracode assemblage zones. The chronostratigraphy combined with bio- and lithostratigraphy of the Jura sections is illustrated in Fig. 4.4.

Ammonites

Some ammonites have been found on the southern Jura platform by CLAVEL et al. (1986). They can be attributed to the ammonite subzones displayed in Tab. 4.1. Moreover, a fragment of an ammonite has been collected from the base of the Pierre Châtel Formation of the Crozet section (WAEHRY 1989). It is attributed to the Privasensis ammonite subzone (determined by Le Hégarat in WAEHRY 1989). However, this ammonite fragment probably has been transported from the shelf to the shallow Jura platform during the transgression of the Pierre Châtel Formation (WAEHRY 1989, MOJON 2002).

Charophytes

Several biostratigraphical schemes based on charophytes have been published for marginal-marine environments of the Berriasian (e.g., SCHUDACK 1993, 1996, MARTÍN-CLOSAS & SERRA-KIEL 1991). A European charophyte biozonation for the Berriasian has been published by RIVELINE et al. (1996). This charophyte biozonation has been used for the European chronostratigraphic framework published

Chronostratigraphic framework						Southern to central Jura platform			This study
Stage	Sequences	1	2	3	4	5			
	Be5 139.3	Late	BOISSIERI	Paramimounum	Formations	Biozones	Assemblage zones	Formations	
				Subzones					
				Biozones					
							</		

1 Chronostratigraphic framework (HARDENBOL et al. 1998)  
2 European charophyte biozonation (RIVELINE et al. 1996)  
3 Formations (CLAVEL et al. 1986)  
4 Charophyte biozonation, assemblage zones and formations (MOJON 2002)  
5 Formations of this study based on PASQUIER (1995), HILLGÄRTNER (1999), and STRASSER et al. (2004)  
Priv.: Privasensis G.: Globator  
Jac.: Jacobi H.: Hemiglobator  
H. proto.: Hemiglobator protoincrassatus

Fig. 4.4 - Comparison of the chronostratigraphic framework (HARDENBOL et al. 1998) with bio- and lithostratigraphic schemes (formations) published for the Jura platform of the studied interval.

Informal sub-stages (HARDENBOL et al. 1998)	Ammonite subzones (HARDENBOL et al. 1998)	studied formations of the Jura platform (CLAVEL et al. 1986)
Late Berriasian	<i>Paramimounum</i>	Vions Formation
Middle Berriasian	<i>Subalpina-Dalmasi</i>	top Purbeck to Pierre Châtel Formation
Early Berriasian	<i>Jacobi- Grandis</i>	upper part of the Purbeck (Goldberg Formation)

**Tab. 4.1** - Comparison of the studied formations based on ammonites found on the Jura platform (CLAVEL et al. 1986) with the ammonite subzones of the European chronostratigraphic framework of HARDENBOL et al. (1998).

by HARDENBOL et al. (1998). It is defined by the first appearance or total ranges of species or subspecies of Clavatoraceae, according to the systematics for the Berriasian of MARTÍN-CLOSAS (1989, 1996) and SCHUDACK (1993) (in RIVELINE et al. 1996) (Tab. 4.2).

The taxonomy of charophytes is traditionally based on characteristics of the gyrogonites (cf. Chap. 2). Therefore, it can be taken as a “species-organ” classification (RIVELINE et al. 1996). Charophytes are

biozonation published by MOJON (2002).

Moreover, MOJON (2002) combined the charophyte biozonation with an ostracode zonation based on the genus “*Cypridae*”. The combination of the charophyte biozonation with ostracodes enables a further division of the biozones into “continental cenozones”. These represent “zones of mixed associations of several taxa” (MOJON 2002; p. 187). They are chronologically numbered and labeled with “M” (according to the

Informal sub-stages (HARDENBOL et al. 1998)	Ammonite subzones (HARDENBOL et al. 1998)	Charophyte biozonation (RIVELINE et al. 1996)
early and middle Late Berriasian	<i>Paramimounum- Picteti</i>	<i>Globator maillardi nurrensis</i>
late Middle Berriasian	<i>Privasensis- Dalmasi</i>	<i>Globator maillardi incrassatus</i>
latest Late Tithonian to early Middle Berriasian	<i>Jacobi- Subalpina</i>	<i>Globator maillardi maillardi</i>

**Tab. 4.2** - Comparison of the charophyte biozonations of RIVELINE et al. (1996) with the European chronostratigraphic framework of HARDENBOL et al. (1998).

considered to be sensitive to geological events and evolved with high rates during the Mesozoic. This is why they constitute a good biostratigraphical tool for continental areas. Moreover, thanks to their abundance, their wide geographical distribution, and their occurrence in coastal areas, “they provide valuable possibilities for correlations between the marine and the terrestrial realms” (RIVELINE et al. 1996; p. 455)

A charophyte biozonation for the Berriasian has been published by MOJON & STRASSER (1987) and MOJON (2002). It is considered as “zones of total distribution of taxa” based on the phylogenetic lineages of the charophytes *Hemiglobator-Globator* (the prefix “*Hemi-*” characterizes precursor forms of the genus *Globator*; MOJON 2002). This biozonation is mainly based on charophytes deriving from the Jura platform. Compared to the charophyte biozonation of RIVELINE et al. (1996), most of the charophyte zones of MOJON (2002) are shifted (cf. Fig. 4.4). This can be explained by the regional character of the charophyte

author’s last name). In this study, the “continental cenozones” are called charophyte-ostracode assemblages (abbreviated assemblage zones; Tab. 4.3).

Difficulties arise when charophytes are used as a biostratigraphical dating tool. Polymorphism of charophyte gyrogonites due to palaeoecological changes must be considered when defining new taxa (MOJON 1989, 2002). MARTÍN-CLOSAS & SERRA-KIEL (1991) related evolutionary patterns of charophytes during the Late Jurassic and Early Cretaceous to changes in ecosystems (e.g., climate, palaeotectonics, sea-level fluctuations). Contrarily, stable ecological conditions and the installation of freshwater environments during the Berriasian in the Mesogean Basin (Spain) enabled charophytes to evolve by anagenesis (MARTÍN-CLOSAS & SERRA-KIEL 1991). MOJON (2002) related the morphological adaptations of the genus *Hemiglobator* to palaeoecological changes during the sea-level rise in the Early to Middle Berriasian. He concludes that sea-level changes control the characteristic mutations of

Ammonite subzones (HARDENBOL et al. 1998)	Charophyte biozonation (MOJON 2002)	Assemblage zones (MOJON 2002)	studied formations of the Jura platform (MOJON 2002)
<i>Paramimounum</i>	<i>Hemiglobator nurrensis</i>	M5	Vions Formation
<i>(Subalpina-) Privasensis- Dalmasi</i>	<i>Hemiglobator neocomensis</i>	M4	transition Purbeck (Goldberg Formation) to Pierre Châtel Formation
<i>Grandis- Subalpina</i>	<i>Hemiglobator maillardi</i>	M3	Purbeck (Goldberg Formation)
<i>Grandis</i>	<i>Hemiglobator protoincrassatus</i>	M2?	
<i>Jacobi- Grandis</i>	<i>Hemiglobator praecursor</i>	M1a-M1b	

**Tab. 4.3** - Comparison of the charophyte biozonation, the assemblage zones and the formations of the Jura platform according to MOJON (2002) with the European chronostratigraphic framework of HARDENBOL et al. (1998). The assemblage zones M2 and M3 are mainly present on the Central Jura platform. In the southern part of the Jura platform, the assemblage zone M2 is strongly condensed and M3 is absent (MOJON 2002).

the phylogenetic lineage of this genus.

Similar observations have been made by SCHUDACK (1991) in different West-European regions of the Berriasian. This author states that direct correlations of charophyte biozonation with short term eustatic sea-level changes are not evident mainly because of the insufficient precision of charophyte biozonations. SCHUDACK (1991) adds that during supraregional

regressions, the evolutionary speed of charophyte evolution is increased.

The studied sections have been dated by MOJON (2002) and lie in the charophyte-ostracode assemblage zones M1b to M4 (except the Marchairuz section; see below). The zonation by ostracodes will be further discussed in relation to the sections of the Dorset region in chapter 5.

CLAVEL et al. (1986)				southern Jura		central Jura	region of Biel	this study
				STEINHAUSER & LOMBARD (1969)	MOUTY (1966)	STEINHAUSER & CHAROLLAIS (1971)	HÄFELI (1966)	
Stages	Ammonites			Formations	Formations	Formations	Formations	Formations
BERRIASIAN	Middle	OCCITANICA		Pierre Châtel	Calcaire de Thoiry	Unité moyenne calcaire massive	Marbre bâtard	Mergel- und Kalkzone
		Privasensis	Dalmasi					
		Subalpina				Purbeckian	Purbeckian	
	Early	JACOBI	Grandis	Purbeckian	Goldberg			

Pierre Châtel	studied interval
Goldberg	

**Fig. 4.5** - Overview of nomenclatures of formations and ammonite biostratigraphy (CLAVEL et al. 1986). Formation boundaries are commonly not well defined in the literature. Formations (names) used in this study are indicated on the right side (modified from PASQUIER 1995).

## 4.5 Lithostratigraphy

The lithological variations along the Jura platform led to many different stratigraphic subdivisions. Figure 4.5 summarizes the most important lithostratigraphical schemes proposed in the literature for the Berriasian from the eastern part (region of Biel) throughout the Jura chain towards the southern part of the studied Jura platform (cf. Fig. 4.1). The nomenclature used in this study is based on the formal lithostratigraphical subdivisions of HÄFELI (1966) and STEINHAUSER & LOMBARD (1969).

The lower part of the studied sections has commonly been termed “Purbeckian” (French: “Purbeckien”). This appellation refers to the characteristic succession of peritidal deposits resembling the “Purbeck Beds” *sensu anglico* (e.g., CAROZZI 1948, HÄFELI 1966, AINARDI 1977, STRASSER 1988; cf. Chap. 5). In order to avoid any confusion, this formation is referred to as Goldberg Formation in this study according to the lithostratigraphical definition of HÄFELI (1966) based on the Goldberg section close to the town of Biel (cf. Fig. 4.1). This formation is commonly covered by vegetation because of its incompetent lithology (marls and mudstones).

A succession of massive beds with lagoonal facies marks a major marine transgression at the top of the Goldberg Formation. These characteristic beds can be easily recognized in the field because of their resistance to weathering. They have been used to define a new lithostratigraphical unit in the literature (e.g., MOUTY 1966, HÄFELI 1966, STEINHAUSER & CHAROLLAIS 1971; cf. Fig. 4.5). In this study, this formation is referred to as Pierre Châtel Formation according to the definition of STEINHAUSER & LOMBARD (1969). The name derives from the valley Pierre Châtel, in which the Yenne section is located (cf. Fig. 4.29).

## 4.6 Description and interpretation of the sections

The sections have been investigated and sampled in greater detail than in any of the previous studies. A sedimentological description and interpretation is given as a graphical log for each section. The sections are illustrated using a scale of 1 : 20. In parts of a section where sedimentological data are not sufficient to propose an unequivocal sequence-stratigraphical interpretation, a best-fit solution is used. This best-fit

solution is based on comparison and correlation of the section with other sections. For methods and procedure of correlation refer to chapter 6.

The sections are presented in the following way (Fig. 4.6a):

- **Column ①** indicates lithostratigraphic units.
- **Column ②** outlines the charophyte-ostracode assemblage zones according to MOJON (2002). Brackets indicate reworked species of an earlier assemblage zones (according to MOJON 2002)
- **Column ③** displays the sequence-stratigraphical interpretation. Small-scale and elementary sequences are numbered in anticipation according to lateral correlations (cf. Chap 6). They are counted from SB/TS to SB/TS, even when they are not well delimited. The “3<sup>rd</sup>-order” sequence-stratigraphic framework on the left side of this column is already displayed in this chapter to avoid repetitions. It is in agreement with the sequence-stratigraphic nomenclature of HARDENBOL et al. (1998).
- **Column ④** shows the logged section with the field observations (weathering profile) and sedimentary structures (left side), and the constituents and texture (right side) according to DUNHAM (1962) and EMBRY & KLOVAN (1971) (both in FLÜGEL 2004). The relative abundance of each constituent in a sample is indicated by the amount of symbols (cf. Fig. 4.6b; Chap. 2):
  - one symbol: present
  - two symbols: common
  - three symbols: abundant
- **Column ⑤** gives the interpretation of the depositional environments. On the right side, the facies of each sample is indicated (cf. Tab. 2.2). Additionally, the relative bathymetric trend between supratidal and shallow subtidal is illustrated on the right side.

The position of each section is indicated on a map and by coordinates. A legend for these maps is provided in Fig. 4.7. The sections are presented more or less from NE to SW (following the approximate orientation of the today’s extension of the Jura Mountains; cf. Fig. 4.1).

The Rusel and Chapeau de Gendarme sections

①	②	③	④	⑤	a
<div style="border: 1px solid black; padding: 2px; margin-bottom: 2px;">Formations</div> <div style="border: 1px solid black; padding: 2px;">Assemblage zones</div>	<div style="border: 1px solid black; padding: 2px;">Sequence stratigraphy</div> <div style="display: flex; justify-content: space-between; font-size: 0.8em;"> <div style="border: 1px solid black; padding: 2px;">"3rd-order" sequences</div> <div style="border: 1px solid black; padding: 2px;">Small-scale sequences</div> <div style="border: 1px solid black; padding: 2px;">Elementary sequences</div> </div>		<div style="border: 1px solid black; padding: 2px; margin-bottom: 2px;">Section name</div> <div style="display: flex; justify-content: space-between; font-size: 0.8em;"> <div style="border: 1px solid black; padding: 2px;">Field observations</div> <div style="border: 1px solid black; padding: 2px;">Samples Meters</div> <div style="border: 1px solid black; padding: 2px;">Facies/Texture</div> </div>	<div style="border: 1px solid black; padding: 2px;">Sedimentological interpretation</div> <div style="display: flex; justify-content: space-between; font-size: 0.8em;"> <div style="border: 1px solid black; padding: 2px;">Facies zone</div> <div style="border: 1px solid black; padding: 2px;">Depositional environment (comments)</div> <div style="border: 1px solid black; padding: 2px;">supratidal intertidal shallow subtidal</div> </div>	

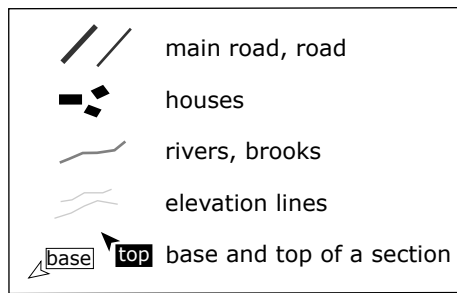
  

<p><b>Field observations</b></p> <p>Sedimentary structures</p> <ul style="list-style-type: none"> <li> Karstification</li> <li> Desiccation cracks</li> <li> Birdseyes</li> <li> Circumgranular cracks</li> <li> Bioturbation</li> <li> Wave ripples</li> <li> Current ripples</li> <li> Firm- and hardgrounds</li> <li> Lamination</li> <li> Reactivation surfaces</li> <li> Low-angle cross-stratification</li> <li> Flaser bedding</li> <li> Lenticular bedding</li> <li> Wavy bedding</li> <li> Microbial mats</li> </ul> <p>Lithology</p> <table style="width: 100%; border-collapse: collapse;"> <tr><td style="width: 20px; height: 10px; background-color: white; border: 1px solid black;"></td><td>Limestone</td></tr> <tr><td style="width: 20px; height: 10px; background-color: lightgray; border: 1px solid black;"></td><td>Marly Limestone</td></tr> <tr><td style="width: 20px; height: 10px; background-color: gray; border: 1px solid black;"></td><td>Gray marls</td></tr> <tr><td style="width: 20px; height: 10px; background-color: darkgray; border: 1px solid black;"></td><td>Dark-grey marls</td></tr> <tr><td style="width: 20px; height: 10px; background-color: brown; border: 1px solid black;"></td><td>Brown-reddish marls</td></tr> <tr><td style="width: 20px; height: 10px; background-color: black; border: 1px solid black;"></td><td>Black marls</td></tr> </table> <p>Other features</p> <p>p. o. □ Pinch out</p> <p> Joints</p> <p> Faults with direction of displacement</p>		Limestone		Marly Limestone		Gray marls		Dark-grey marls		Brown-reddish marls		Black marls	<p><b>Facies/Texture</b></p> <p>Facies (descriptive elements / components)</p> <table style="width: 100%; border-collapse: collapse;"> <tr> <td style="width: 50%; vertical-align: top;"> <ul style="list-style-type: none"> <li> Peloids</li> <li> Ooids radial</li> <li> micritic</li> <li> superficial</li> <li> Small oncoids</li> <li> Big oncoids</li> <li> Intraclasts</li> <li> Mud pebbles</li> <li> Black pebbles</li> <li> Organic matter</li> <li> Bone fragments</li> <li> Bivalves</li> <li> Gastropods</li> <li> Oysters</li> </ul> </td> <td style="width: 50%; vertical-align: top;"> <ul style="list-style-type: none"> <li> Brachiopods</li> <li> Bryozoans</li> <li> Echinoderms</li> <li> Foraminifera (benthic)</li> <li> Miliolids</li> <li> Coral debris</li> <li> Serpulids</li> <li> Ostracodes</li> <li> Charophyte oogonia</li> <li> stems</li> <li> Green algae</li> <li> Bacinella</li> <li> Lithocodium</li> <li> Sponges</li> </ul> </td> </tr> </table> <table style="width: 100%; border-collapse: collapse;"> <tr> <td style="width: 50%; vertical-align: top;"> <p>Non-calcareous components</p> <ul style="list-style-type: none"> <li> P Pyrite</li> <li> Evaporite pseudomorphs</li> <li> Siliciclastics (present)</li> <li> Siliciclastics (common)</li> </ul> </td> <td style="width: 50%; vertical-align: top;"> <p>Texture</p> <table style="width: 100%; border-collapse: collapse;"> <tr><td style="width: 20px;">m:</td><td>Marls</td></tr> <tr><td>M:</td><td>Mudstones</td></tr> <tr><td>W:</td><td>Wackestones</td></tr> <tr><td>P:</td><td>Packstones</td></tr> <tr><td>G:</td><td>Grainstone</td></tr> <tr><td>F/R:</td><td>Float- / Rudstones</td></tr> </table> </td> </tr> </table> <p>Abundance of constituents in a sample</p> <p>present (one symbol): </p> <p>common (two symbols): </p> <p>abundant (three symbols): </p> <p>Black symbols: observed in thin section Gray symbols: observed by hand lens on outcrop or interpreted between samples</p>	<ul style="list-style-type: none"> <li> Peloids</li> <li> Ooids radial</li> <li> micritic</li> <li> superficial</li> <li> Small oncoids</li> <li> Big oncoids</li> <li> Intraclasts</li> <li> Mud pebbles</li> <li> Black pebbles</li> <li> Organic matter</li> <li> Bone fragments</li> <li> Bivalves</li> <li> Gastropods</li> <li> Oysters</li> </ul>	<ul style="list-style-type: none"> <li> Brachiopods</li> <li> Bryozoans</li> <li> Echinoderms</li> <li> Foraminifera (benthic)</li> <li> Miliolids</li> <li> Coral debris</li> <li> Serpulids</li> <li> Ostracodes</li> <li> Charophyte oogonia</li> <li> stems</li> <li> Green algae</li> <li> Bacinella</li> <li> Lithocodium</li> <li> Sponges</li> </ul>	<p>Non-calcareous components</p> <ul style="list-style-type: none"> <li> P Pyrite</li> <li> Evaporite pseudomorphs</li> <li> Siliciclastics (present)</li> <li> Siliciclastics (common)</li> </ul>	<p>Texture</p> <table style="width: 100%; border-collapse: collapse;"> <tr><td style="width: 20px;">m:</td><td>Marls</td></tr> <tr><td>M:</td><td>Mudstones</td></tr> <tr><td>W:</td><td>Wackestones</td></tr> <tr><td>P:</td><td>Packstones</td></tr> <tr><td>G:</td><td>Grainstone</td></tr> <tr><td>F/R:</td><td>Float- / Rudstones</td></tr> </table>	m:	Marls	M:	Mudstones	W:	Wackestones	P:	Packstones	G:	Grainstone	F/R:	Float- / Rudstones
	Limestone																												
	Marly Limestone																												
	Gray marls																												
	Dark-grey marls																												
	Brown-reddish marls																												
	Black marls																												
<ul style="list-style-type: none"> <li> Peloids</li> <li> Ooids radial</li> <li> micritic</li> <li> superficial</li> <li> Small oncoids</li> <li> Big oncoids</li> <li> Intraclasts</li> <li> Mud pebbles</li> <li> Black pebbles</li> <li> Organic matter</li> <li> Bone fragments</li> <li> Bivalves</li> <li> Gastropods</li> <li> Oysters</li> </ul>	<ul style="list-style-type: none"> <li> Brachiopods</li> <li> Bryozoans</li> <li> Echinoderms</li> <li> Foraminifera (benthic)</li> <li> Miliolids</li> <li> Coral debris</li> <li> Serpulids</li> <li> Ostracodes</li> <li> Charophyte oogonia</li> <li> stems</li> <li> Green algae</li> <li> Bacinella</li> <li> Lithocodium</li> <li> Sponges</li> </ul>																												
<p>Non-calcareous components</p> <ul style="list-style-type: none"> <li> P Pyrite</li> <li> Evaporite pseudomorphs</li> <li> Siliciclastics (present)</li> <li> Siliciclastics (common)</li> </ul>	<p>Texture</p> <table style="width: 100%; border-collapse: collapse;"> <tr><td style="width: 20px;">m:</td><td>Marls</td></tr> <tr><td>M:</td><td>Mudstones</td></tr> <tr><td>W:</td><td>Wackestones</td></tr> <tr><td>P:</td><td>Packstones</td></tr> <tr><td>G:</td><td>Grainstone</td></tr> <tr><td>F/R:</td><td>Float- / Rudstones</td></tr> </table>	m:	Marls	M:	Mudstones	W:	Wackestones	P:	Packstones	G:	Grainstone	F/R:	Float- / Rudstones																
m:	Marls																												
M:	Mudstones																												
W:	Wackestones																												
P:	Packstones																												
G:	Grainstone																												
F/R:	Float- / Rudstones																												

<p><b>Sequence stratigraphy</b></p> <ul style="list-style-type: none"> <li>— SB — Sequence boundary</li> <li>— TS — Transgressive surface</li> <li>— MFS — Maximum-flooding surface</li> </ul>	<table style="width: 100%; border-collapse: collapse;"> <tr> <td style="width: 20px; height: 10px; background-color: gray; border: 1px solid black;"></td> <td>Sequence-boundary interval</td> </tr> <tr> <td style="width: 20px; height: 10px; background-color: lightgray; border: 1px solid black;"></td> <td>Maximum-flooding interval</td> </tr> </table>		Sequence-boundary interval		Maximum-flooding interval
	Sequence-boundary interval				
	Maximum-flooding interval				

Fig. 4.6 - Legend for Jura sections.



**Fig 4.7** - Legend for all maps describing geographical positions of the measured sections

have been chosen to present sedimentological and sequence-stratigraphical interpretations in higher detail compared to the other sections. This was done in order to provide examples of how the environmental and sequence-stratigraphical interpretations are extracted from the sedimentary record.

#### 4.6.1 Rusel

The Rusel section was first described by HÄFELI (1966). His study concentrates on a lithological and palaeontological description of the Rusel section. PASQUIER (1995) established a sequence-stratigraphical interpretation of the Goldberg, Pierre Châtel, and Vions Formations, which serves as a base for the sequence-stratigraphical interpretation of the part of the Rusel section presented in this study.

#### *Geographic and stratigraphic setting*

The Rusel section is situated in a small abandoned quarry above the lake of Biel (cf. Fig. 4.8). It lies on

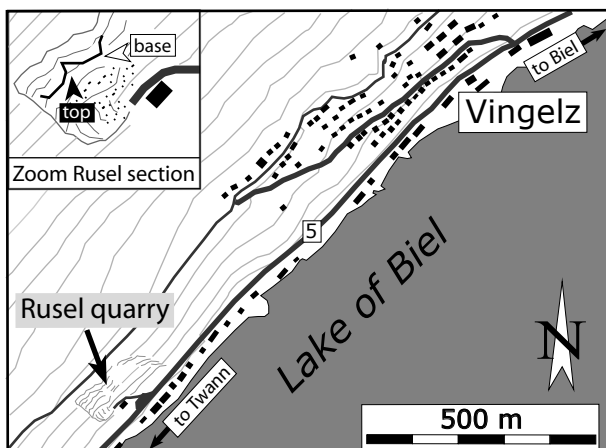


**Fig. 4.8** - Location of the Rusel section.

the southern limb of the first Jura Mountain anticline called the “Seekette Antiklinale”. The outcrop can be found close to the state highway (No. 5) between Biel and Tüscherz (coordinates 582.620/219.320, Swiss National Topographic map, 1/25000, 1125 Chasseral). The section is logged from the eastern to the western corner of the quarry along the massive beds of the Pierre Châtel Formation (cf. Zoom of Fig. 4.8). The section is dated by charophyte-ostracode assemblages and ranges from zone M1b to M4 (Mojon in PASQUIER 1995).

#### *Sedimentological interpretation* (Fig. 4.9a-b)

The thin ooid-rich layers (grainstones) in the massive packstone at the base of the section mainly contain radial and superficial ooids, intraclasts, black pebbles and rare charophyte stems. This sediment composition (continental and marine components) reflects a mixing and/or reworking during high-energy conditions. They are interpreted as tidal channel and/or storm layer deposits. The overlying part of the Goldberg Formation consists of a nodular, marly succession (about 1.50 meters). The nodules are commonly surrounded by gray-greenish marls. At the base of this nodular interval, charophytes (stems and gyrogonites) point to continental, freshwater pond deposits (from 0.35 to 0.70 meters). Evaporites (now preserved as pseudomorphs) have probably formed in seasonally hypersaline conditions (dry season) in these continental ponds. A change to fossil-poor mudstones with birdseyes and some ostracodes is interpreted as tidal flat environment. Emersion features (circumgranular and desiccation cracks) point to exposure of the tidal flat towards the top of the Goldberg Formation. A marl bed between thin mudstone layers at the top of the Goldberg Formation is rich in charophytes and ostracodes. These marls are interpreted as freshwater pond deposits. According to Mojon (in PASQUIER 1995), they lie in the assemblage zone M1b.

Massive ooid-rich wacke- to packstone beds (internal-lagoonal deposits) mark the base of the Pierre Châtel Formation. The thickness of the first bed changes laterally by several decimeters. This is probably due to the development of an important palaeomorphology during the emersion of the Goldberg Formation. HÄFELI (1966) interprets the local occurrence of conglomerates (called “Basiskonglomerat”) at the transition from the Goldberg to the Pierre Châtel Formation as lag deposits of a major transgression.

At the top of the first bed, birdseyes and desiccation cracks indicate tidal flat to internal-lagoonal deposits.



The combination of charophytes (stems and gyrogonites) with marine constituents (foraminifera) in the following thin marl layer is considered to represent tidal flat deposits. A massive ooid-rich bed overlies the thin tidal flat interval (from 2.05 to 2.25 meters).

At 2.25 meters, a karst surface caps this massive bed (cf. Pl. 8/4). The karst is characterized by an irregular surface (up to 8 cm relief). It is covered by tidal to internal-lagoonal deposits (lenticular and flaser beddings). An opening of the depositional system is displayed by the deposition of laminated, ooid-rich internal-lagoonal sediments. The change to low-energy conditions (wackestones) is interpreted as a slight deepening and/or protection of the depositional environment. High-energy conditions are reflected by the deposition of two massive ooid-rich pack- to grainstone beds (from 2.40 to 2.75 meters). The first bed is characterized by reactivation surfaces, which might have been created by changing water currents (tidal currents). Moreover, this bed pinches out laterally indicating a limited extension of this bed. Accordingly, it is interpreted as a high-energy shoal body, which has been deposited in a restricted, internal-lagoonal setting. It is assumed that this shoal body is a part of larger shoal field. A thin marl layer separates the two massive beds. It is considered to represent condensed, low-energy sediments, which have been deposited during a deepening of the system. The second massive bed is characterized by lamination. This is related to an increase of tidal influence during a shallowing of the depositional environment. A decrease of depositional energy is displayed by the following wackestone bed (from 2.75 to 2.90 meters). A deepening of the depositional environment and/or local protection from currents behind shoals may lead to this drop in the water-energy. Lamination at the top to the following massive bed (from 2.90 to 3.10 meters) indicates stronger tidal influence during falling relative sea level. It is capped by a thin marl layer considered to represent tidal flat deposits (at 3.10 meters). The following thick, ooid-rich wacke- to packstone is interpreted as an interval of restricted internal-lagoonal deposits (from 3.10 to 3.50 meters). At its base (at 3.15 meters), a grainstone interval containing intraclasts points to an increase of the energy regime. It reflects an increase of tidal activity and/or deposits of a storm event. The deposition of charophyte gyrogonites at the top of this bed is considered as a gradually shoaling of the depositional environment (from 3.40 to 3.50 meters). The following beige-brownish marls probably point to reduced water circulation in a restricted, lagoonal environment.

A gradual increase of siliciclastics characterizes the nodular interval (from 3.55 to 4.00 meters). At the top

of this bed, circumgranular cracks and the analysis of stable isotopes measured by PASQUIER (1995) indicate emersion (from 3.95 to 4.05 meters). The deposition of freshwater pond sediments (charophyte- and ostracode-rich marls) points to a remarkable emersion interval. This marl interval belongs to the assemblage zone M4 (according to Mojon in PASQUIER 1995).

During an opening of the system, massive shoal beds with reactivation surfaces have been deposited. They consist of high-energy, internal-lagoonal deposits. A reddish karst surface at the top of this shoal interval (at 4.90 meters) points to an important loss of accommodation space resulting in emersion (PASQUIER 1995). The following marl interval displays low-energy conditions probably due to protection behind a shoal field. The top of the section shows the beginning of a further opening of the depositional system. Steep cliffs of massive, thick intervals characterize the following bed succession of the Rusel section (PASQUIER 1995).

The Rusel section contains the highest amount of siliciclastics of all the measured Jura sections described in this study (up to about 30% in the interval from 3.65 to 4.10 meters). This may indicate a relatively proximal position of the Rusel section on the Jura carbonate platform.

#### *Sequence-stratigraphical interpretation* (Fig. 4.9a-b)

The upper part of the Goldberg Formation (nodular succession) is interpreted as a condensed interval. The dating by charophyte-ostracode assemblages points to deposits between sequence boundaries Be2 to Be4 (according to HARDENBOL et al. 1998).

Three small-scale sequences have been identified in the lower part of the Pierre Châtel Formation. They are all delimited by well-expressed emersion features interpreted as small-scale sequence boundaries. Comparing the facies evolution and the stacking pattern of this section with the other sections, it is assumed that at Rusel one small-scale sequence is missing at the base of the Pierre Châtel Formation. Moreover, it is suggested that the first and the second elementary sequences of small-scale sequence 2 are also absent (cf. Chap. 6). Hence, the first bed of the Pierre Châtel Formation represents the third elementary sequence of small-scale sequence 2. This small-scale sequence is limited by the 3<sup>rd</sup>-order sequence boundary at the base and a karst surface at the top. It comprises two elementary sequences.

Small-scale sequence 3 consists of five elementary sequences. The transgressive deposits of this small-scale sequence comprehend four elementary sequences. The first elementary sequence is composed of

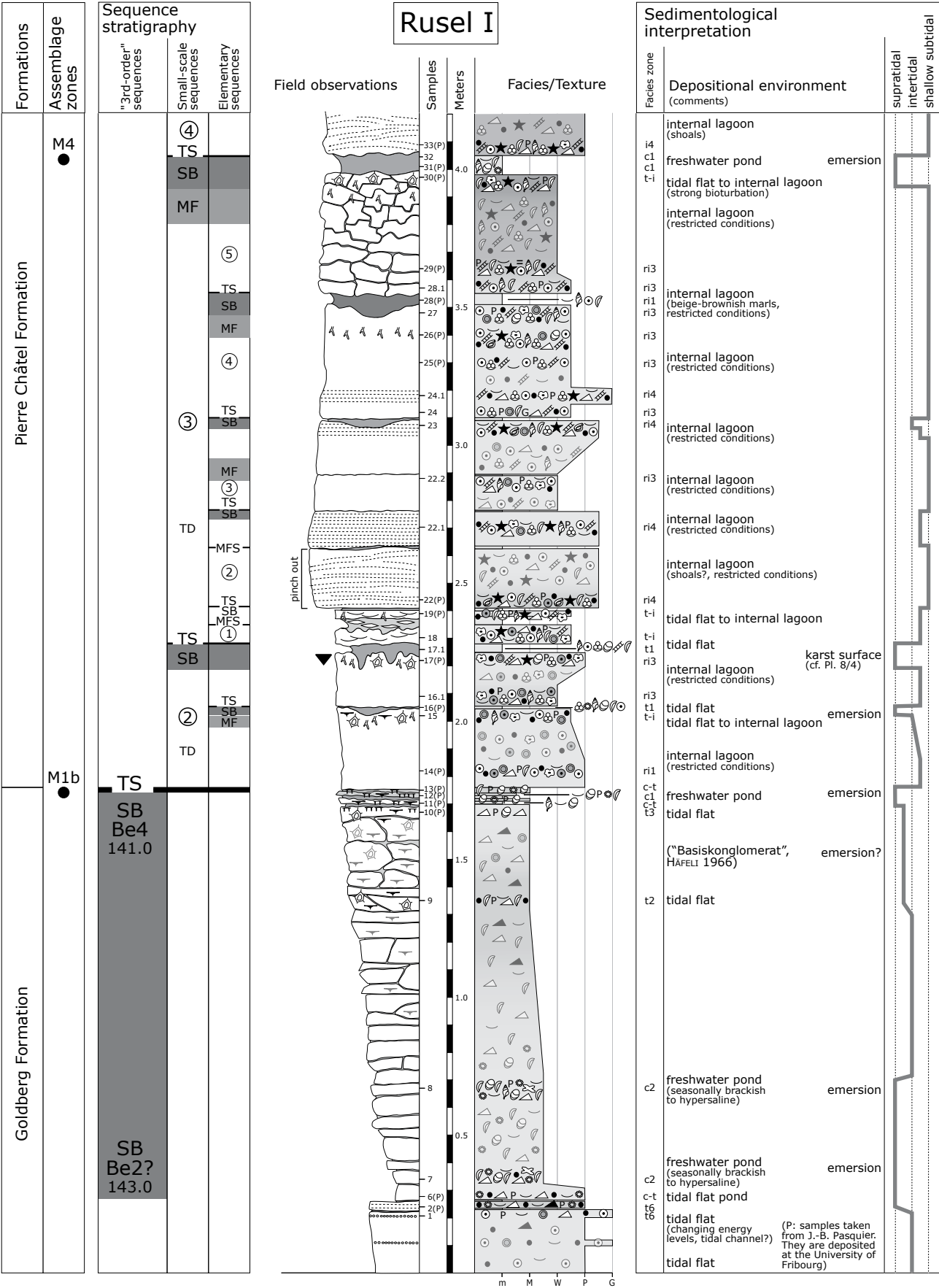


Fig. 4.9a - Rusel section (part I).

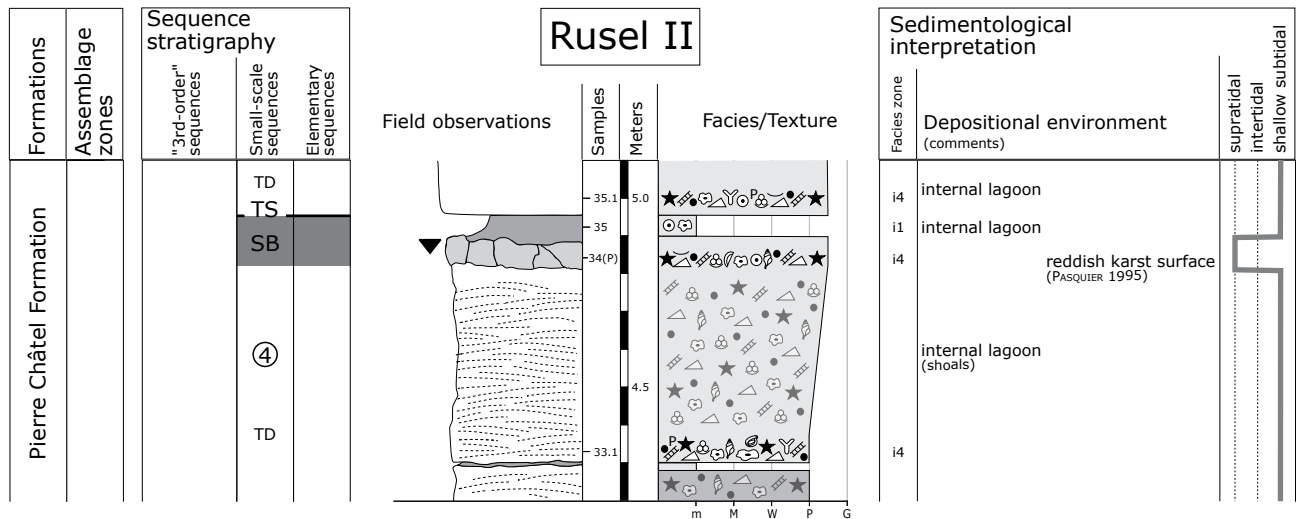


Fig. 4.9b - Rusel section (part II)

tidal flat to internal-lagoon deposits and displays a strongly reduced thickness. The base of the following high-energy bed represents the transgressive surface of the second elementary sequence. The surface at the top of this bed reflects an environmental change from shallow, high-energy (shoal bed) to relatively deeper, low-energy deposits (thin marl layer). This layer is considered to represent the maximum flooding of the second elementary sequence. The third elementary sequence consists of two beds consisting of restricted, internal-lagoon deposits. Its maximum flooding is assumed to be located around the thin marly joint, which separates these two beds (maximum-flooding interval). The thin marl layer (tidal flat deposits) at the top of the second bed indicates the sequence boundary of the fourth elementary sequence. This sequence encompasses the following massive bed. The bioturbated interval at its top is considered as maximum flooding. The following beige-brownish marl interval, which is composed of restricted internal-lagoon deposits, is thought to represent the sequence boundary of the fifth elementary sequence. The amount of siliciclastics increases gradually during the deposition of the fifth elementary sequence. This may indicate progressively forced exposure and erosion of siliciclastics in the nearby hinterland during decreasing relative sea level. Bioturbation at the top of the following nodular bed is interpreted as the maximum-flooding interval of the fifth elementary sequence as well as of small-scale sequence 3.

The maximum-flooding interval is immediately overlain by the sequence boundary of small-scale sequence 4. Circumgranular cracks superimposed on the bioturbated sediments suggest a relative sea-level fall (STRASSER 1991). Highstand deposits are missing.

The strongly asymmetry of small-scale sequence 3 can be explained by the superposition of several orders of sequences. The superposition of a drastic relative sea-level fall on small-scale sequence and the elementary sequence scale leads to emersion (deposition of freshwater pond deposits). The comparison of this interval (small-scale sequence 3) with other sections of the Jura platform shows that such a well-expressed sequence boundary occurs solely in the Rusel section. This implies that the platform morphology in Rusel and the position of the Rusel section on the platform are important local factors.

The transgressive deposits of small-scale sequence 4 consist of high-energy shoal deposits. A sequence-stratigraphical interpretation is not straightforward because these deposits have probably been controlled by autocyclic processes. The sequence boundary of this small-scale sequence at the top of the shoal deposits is well-marked by the reddish karst surface. This karst surface reflects an important sea-level drop.

#### 4.6.2 Cornaux

A section in the Cornaux quarry was first described by STEINHAUSER & CHAROLLAIS (1971). They presented a detailed bed-by-bed description and correlated it with other sections of the Jura platform.

#### Geographic and stratigraphic setting

The section is located in the quarry exploited for cement production by the company Juracime S.A. (Fig. 4.10). It lies on the first anticline of the Jura

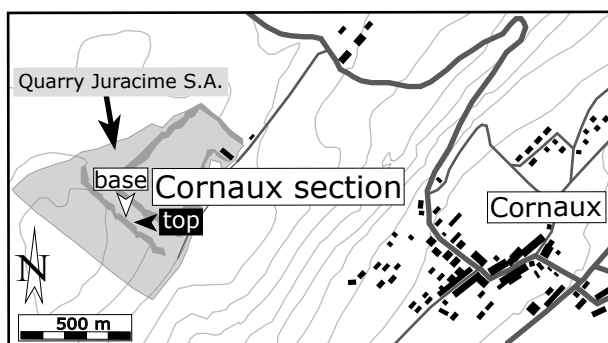


Fig. 4.10 - Location of the Cornaux section.

Mountains about 200 meters above the small village of Cornaux (coordinates 567.250/209.860, Swiss National Topographic map, 1/25000, 1144 Val de Ruz).

The section has been dated by MOJON (2002) and ranges from the charophyte-ostracode assemblage zones M1b to M4. Due to the ongoing quarrying, the weathering profile is rather fresh and not well accentuated. The section is partly cut by faults.

#### ***Sedimentological interpretation*** (Fig. 4.11a-d)

The Goldberg Formation consists of marls and mudstones (massive to nodular). They are interpreted as tidal flat deposits. Hypersaline conditions prevailed during the deposition of the beds containing evaporite pseudomorphs and microbial mats (from 1.30 to 1.55 meters). A nodular marl interval marks the top of the Goldberg Formation (at 2.30 meters). The upper part of the Goldberg Formation was dated by MOJON (2002). It is in the range of the assemblage zones M1b to M2.

The base of an ooid-rich bed is considered as the boundary between the Goldberg and the Pierre Châtel Formation (at 2.35 meters). This bed marks the beginning of increasing accommodation space indicated by the deposition of several massive ooid-rich wacke- to grainstones. They are interpreted as internal-lagoonal deposits. Several intervals of tidal flat deposits intercalate the succession of internal-lagoonal sediments. They reflect periods of decreasing accommodation space. The black marls (at 3.95 meters) have been dated by MOJON (2002). They lie in the assemblage zone M4.

The stratigraphically overlying bed succession consists of restricted, internal-lagoonal deposits. This succession is interrupted by two intervals of normal-marine, internal-lagoonal sediments, which point to a slight opening of the depositional system (from 5.70 to 5.90 meters and from 6.30 to 6.80 meters). Black marls interpreted as tidal flat pond deposits cap a succession

of restricted, internal lagoon beds (at 7.00 meters). These marls lie in the assemblage zone M4 (according to MOJON 2002).

The deposition of restricted, internal-lagoonal sediments reflects an opening of the depositional environment. During a deepening trend, normal-marine, internal-lagoonal facies have been deposited (from 8.45 to 9.45 meters). This trend culminates in an interval of nodular, bioturbated marls interpreted as condensation in an internal-lagoonal setting (at 8.80 meters). A decrease of accommodation space is marked by the deposition of restricted, internal-lagoonal deposits (from 9.25 to 9.55 meters).

The deposition of normal-marine, internal-lagoonal sediments points to a slight deepening of the system. A thick interval characterized by low-angle foresets is interpreted as internal-lagoonal shoal deposits. The deepening trend keeps up to the top of the section culminating in an open-lagoonal environment. This opening is indicated by float- and rudstone deposits (at 12.20 to 13.10 meters). These intervals are dominated by large oncoids with *Bacinella* (floatstones and rudstones; EMBRY & KLOVAN 1971; in FLÜGEL 2004). The change to restricted internal-lagoonal deposits marks a decrease of accommodation space at the top of the section.

#### ***Sequence-stratigraphical interpretation*** (Fig. 4.11a-d)

Condensation, emersion and reworking intervals characterize the top of the Goldberg Formation. The dating by charophyte-ostracode assemblages indicates a 3<sup>rd</sup>-order sequence boundary zone covering the range from Be2 to Be4 at the top of the Goldberg Formation (according to HARDENBOL et al. 1998).

Small-scale sequence 1 consists of four to five elementary sequences. Two to three elementary sequences constitute the transgressive part of this small-scale sequence. Its maximum flooding is not well-expressed. Probably it lies in the massive bed of the third elementary sequence. This interpretation is based on lateral correlation (cf. Chap. 6). The highstand deposits of small-scale sequence 1 consist of two elementary sequences (fourth and fifth ones). Both of them are composed of massive beds capped by black marls indicating a drop of relative sea level.

Small-scale sequence 2 is composed of at least five elementary sequences. The transgressive deposits comprise at least three elementary sequences. The slight increase of relative sea level causes an environmental change to normal-marine, internal-lagoonal deposits in the fourth elementary sequence. The facies change is interpreted as maximum flooding

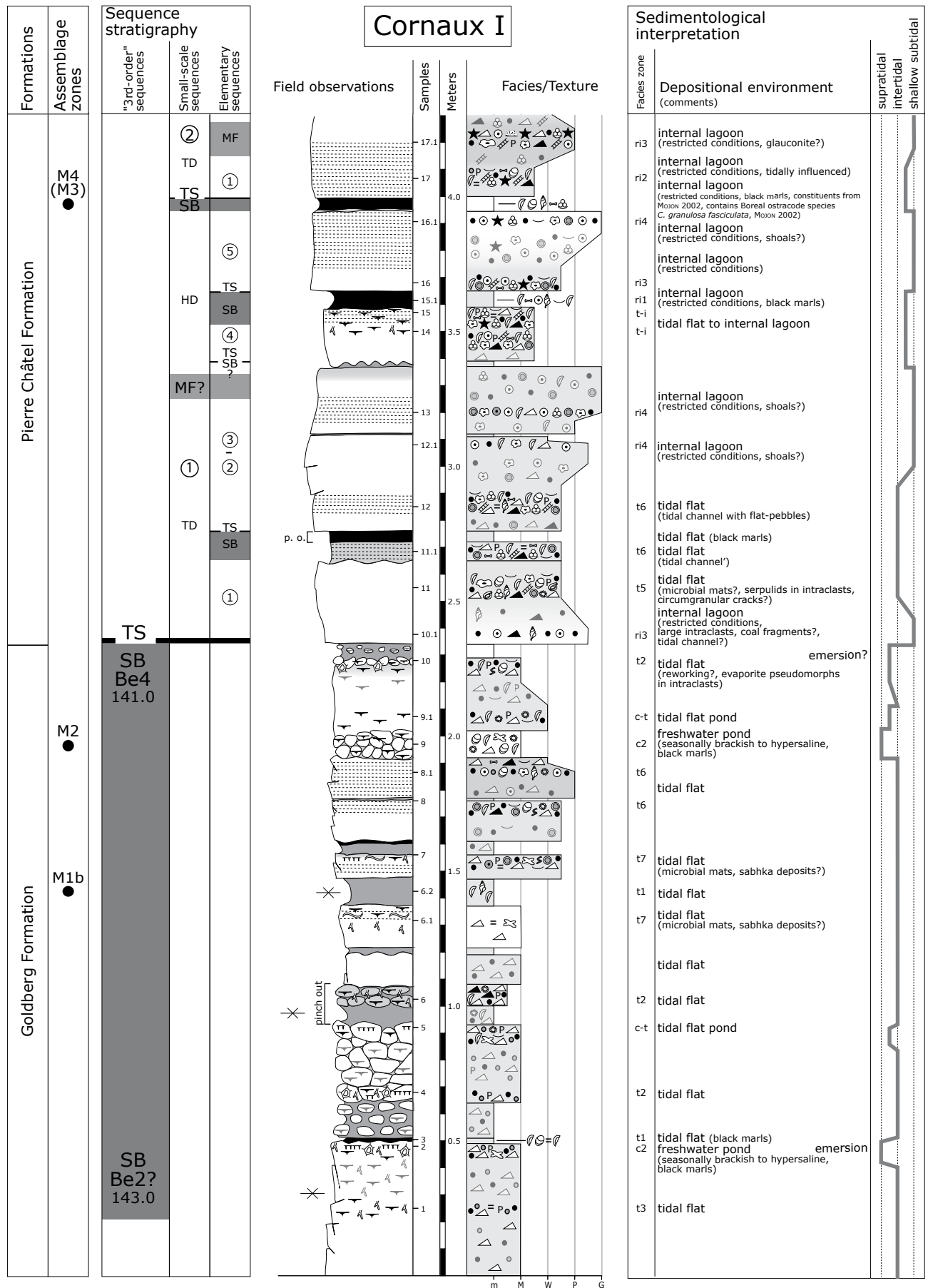
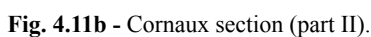


Fig. 4.11a - Cornaux section (part I).





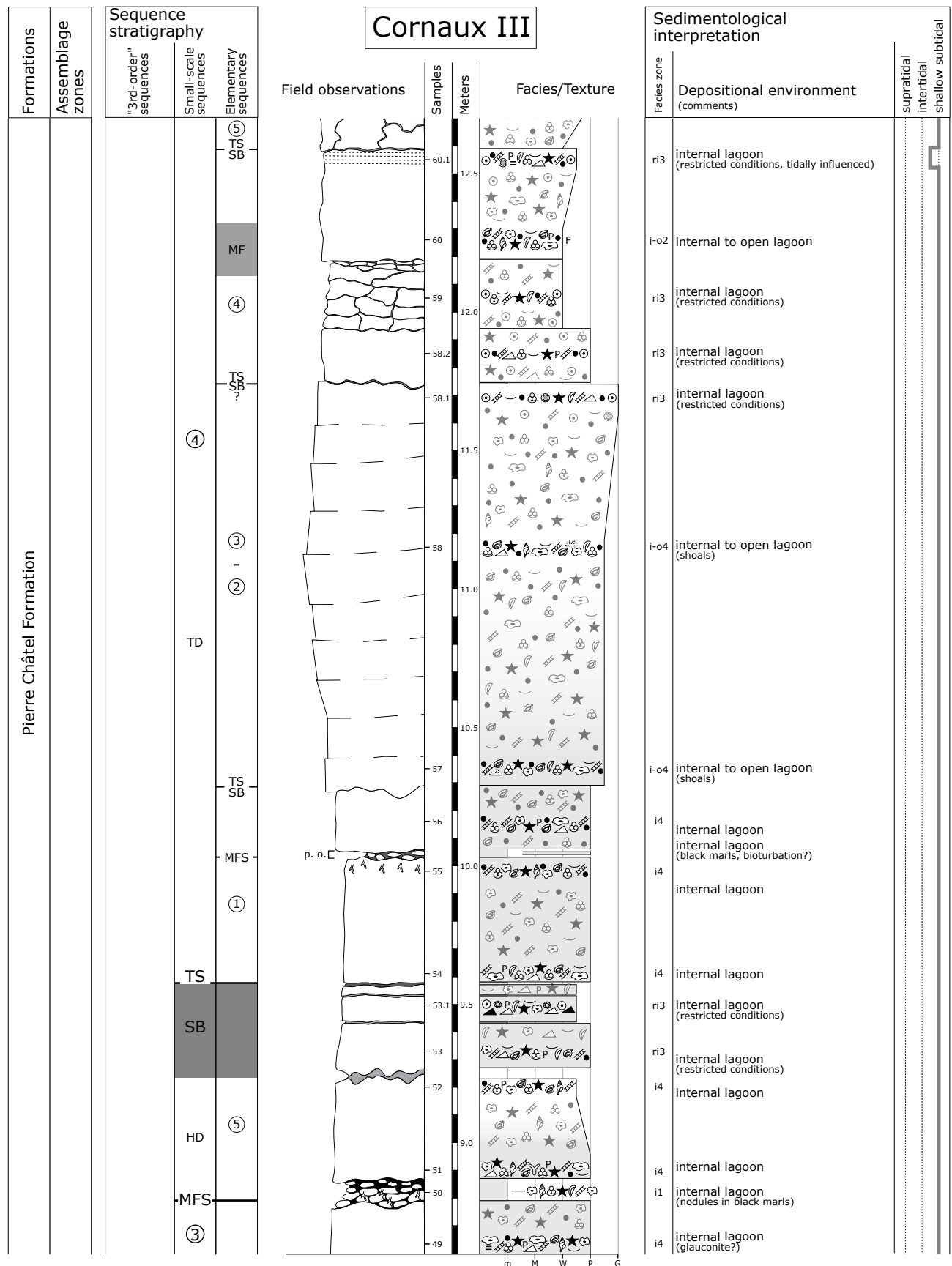


Fig. 4.11c - Cornaux section (part III).

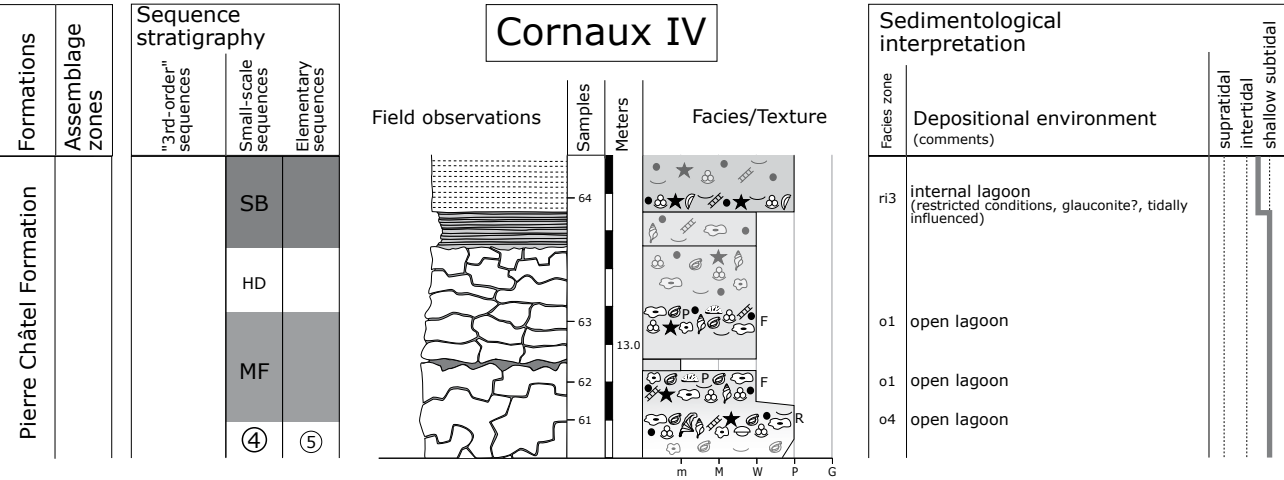


Fig. 4.11d - Cornaux section (part IV).

of this small-scale sequence. The upper part of the forth and the fifth elementary sequence represents the highstand deposits.

Tidal flat pond deposits (black marls) mark a drop of relative sea level interpreted as sequence boundary at the base of small-scale sequence 3. It comprehends at least four elementary sequences. The transgressive deposits are composed of three to four elementary sequences. The base of the nodular, bioturbated interval is considered as maximum-flooding surface of this small-scale sequence. The highstand deposits comprise the upper part of the fifth elementary sequence.

The change to an interval of restricted, internal-lagoonal deposits reflects a decrease of relative sea level interpreted as small-scale sequence boundary. The shoal interval within small-scale sequence 4 makes the interpretation of elementary sequences difficult (autocyclic processes). However, using lateral correlation, it is assumed that three to four elementary sequences are present in the transgressive part of small-scale sequence 4. Open-lagoonal conditions in the fifth elementary sequence mark the maximum flooding of this small-scale sequence. The highstand deposits are reduced and comprehend the upper part of the fifth elementary sequence. The restricted, internal-lagoonal deposits are considered as sequence boundary at the base of the following small-scale sequence.

4.6.3 Marchairuz

The Marchairuz section was first described by FALCONNIER (1931) (in BLANC 1996). A detailed bed-by-bed description was published by MOUTY (1966). PASQUIER (1995) described the entire Berriasian interval of the Marchairuz section and interpreted it in terms

of sequence stratigraphy. Moreover, PASQUIER (1995) presented a regional correlation of the Marchairuz section with other sections of the Jura platform and other depositional realms.

Geographic and stratigraphic setting

The section is situated close to the Marchairuz pass, which is on top of the first anticline of the Jura Mountains (Fig. 4.12). The section outcrops along the pass road on the northern limb of the anticline about 500 m from the pass. A small forest track on the right side when bounding for Le Brassus cuts the base of the section (coordinates 508.870/156.460, Swiss National Topographic map, 1/25000, 1241 Marchairuz).

The base of the Marchairuz section (Goldberg Formation) is covered by the forest track and

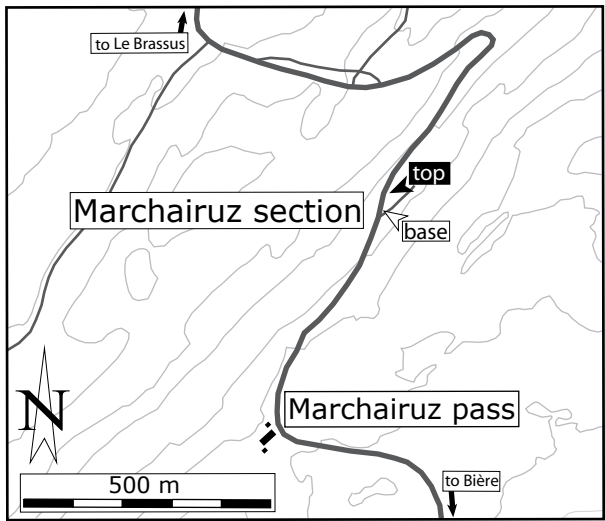


Fig. 4.12 - Location of the Marchairuz section.



vegetation. This section has not been dated by charophyte-ostracode assemblages. Indirect dating is based on the foraminifera *Pavlovecina allobroensis* and *Pseudotextulariella courtionensis* at the base of the Vions Formation (PASQUIER 1995). This assemblage of foraminifera is characteristic for the *Paramimounum* ammonite zone (CLAVEL et al. 1986). The sequence-stratigraphical framework established by PASQUIER (1995) serves as a basis for the sequence-stratigraphical interpretation presented in this study.

#### ***Sedimentological interpretation*** (Fig. 4.13a-c)

The base of the Marchairuz section has been excavated (from 0 to 2.25 meters). It consists of massive internal-lagoonal deposits of the Pierre Châtel Formation. Facies typical of the Goldberg Formation occur on the other side of the forest track but have not been reached by the excavation. Open-lagoonal sediments point to a slight increase of accommodation space (from 1.85 to 1.95 meters). The following marl interval is dominated by constituents (ooids, ostracodes, gastropods, dasycladaceans, foraminifera, and echinoderms), which point to an internal-lagoonal depositional environment.

A pronounced opening of the depositional system is indicated by the deposition of internal-lagoonal grainstones (from 2.25 to 2.75 meters). They are capped by a nodular marl interval, which probably reflect a shallowing. Massive, high-energy deposits with reactivation surfaces represent an interval of shoals (from 2.80 to 5.05 meters; cf. Pl. 9/2). The thin marl layers between the massive shoal deposits probably point to intervals of reduced water energy (reduced wave and/or tidal current activity) resulting in accumulation of clay minerals. This can be related to a reduced hydrodynamic level behind the shoal field and/or a deepening of the depositional environment. A deepening of the lagoonal setting is indicated by the marl interval at the top of this shoal succession (from 5.05 to 5.15 meters). The layer within this marl interval displays an internal-lagoonal composition (small and big oncoids, foraminifera, dasycladaceans, echinoderms, some brachiopods, and bryozoans).

An opening of the depositional environment is indicated by a massive shoal bed (from 5.15 to 5.55 meters). Internal- to open-lagoonal sediments point to a further opening of the depositional system (from 5.55 to 7.95 meters). Several intervals of internal-lagoonal deposits reflect slight decreases of accommodation space within this bed succession. The nodular marl interval at the top of this bed succession pinches out

laterally. It may point to a slight deepening and/or protection of the depositional system, which enabled the accumulation of clay minerals in low-energy conditions. The surface at the base of this marl interval is covered by nodules and considered as a hard-ground. Accordingly, it is thought that this hardground represents a strongly condensed interval.

Internal- to open-lagoonal sediments have been deposited at the top of the section (from 8.10 to 10.50 meters). A partly nodular floatstone interval containing big oncoids reflects change to lower energy conditions caused by a slight deepening of the depositional system (from 8.65 to 8.75 meters). The nodules probably indicate bioturbation. A block of "beach-rock" described by PASQUIER (1995) could not be identified in this study (at 9.90 meters).

#### ***Sequence-stratigraphical interpretation*** (Fig. 4.13a-c)

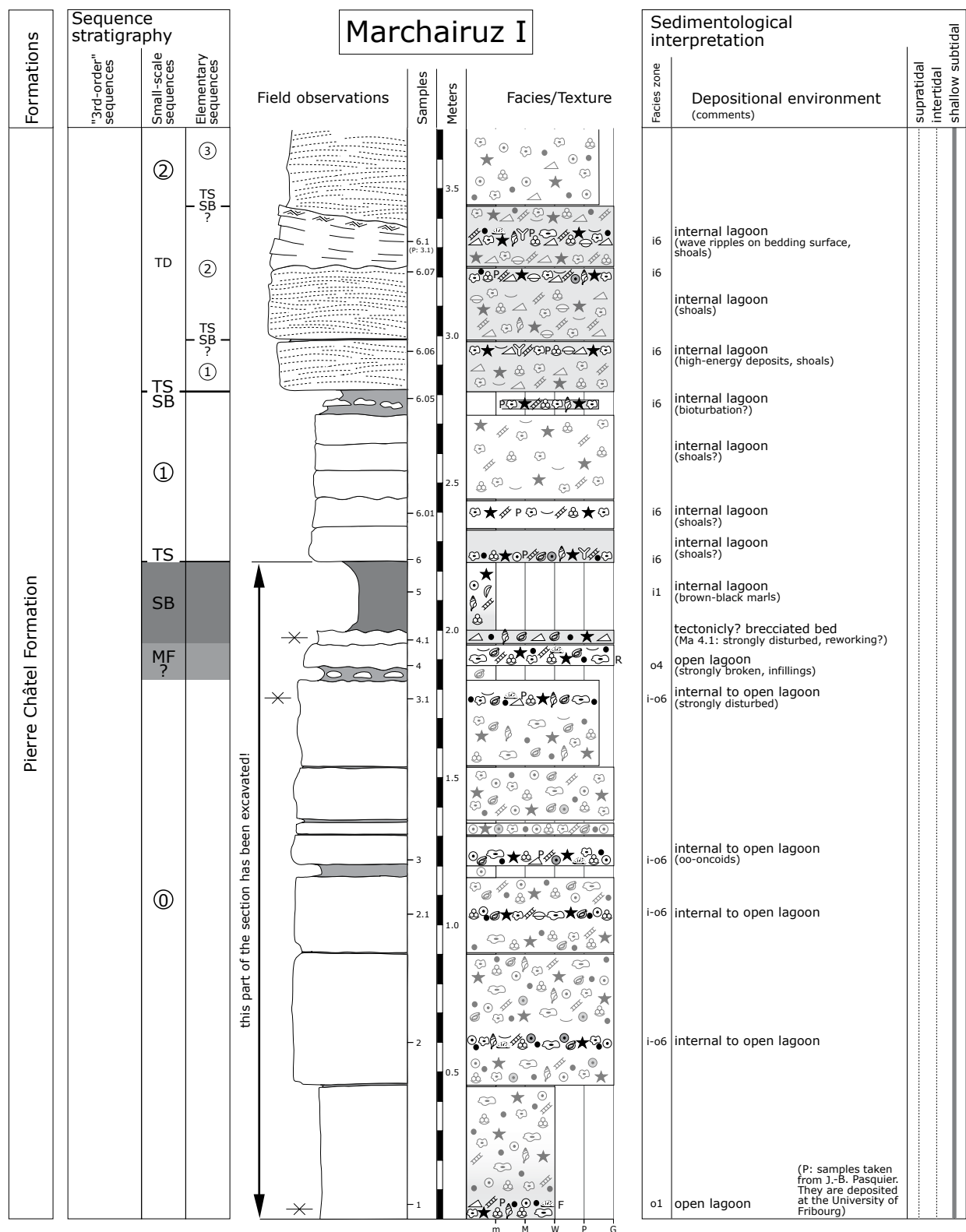
The sequence-stratigraphical interpretation of this section is based on the sequence-stratigraphical framework given in PASQUIER (1995). Only parts of the excavated beds at the base of this section, however, have been described by PASQUIER (1995). The sequence-stratigraphical interpretation of this section is mainly based on lateral correlation with other sections.

It is assumed that the excavated beds represent at least one small-scale sequence (small-scale sequence 0). This would imply that, in the area of Marchairuz section, the transgression superposing Pierre Châtel facies on top of Goldberg facies occurred at least one small-scale sequence below the transgression in the other sections.

Small-scale sequence 1 can only be interpreted through correlation (cf. Chap. 6). There are no unambiguous facies changes allowing a satisfying sequence-stratigraphical interpretation.

The sequence-stratigraphical interpretation of the elementary sequences within small-scale sequence 2 is not straightforward because of the dominance of autocyclic processes during the deposition of the shoal interval. Interpreting the thin marl layers between the shoal beds as elementary sequence boundaries, this small-scale sequence consists of at least four elementary sequences.

The base of the following massive shoal bed indicates a sequence boundary and the transgressive surface of small-scale sequence 3. The transgressive deposits of this small-scale sequence comprehend at least four elementary sequences. The nodular surface at the base of the marl interval is interpreted as maximum-flooding surface of this small-scale sequence. The



The transition from the Goldberg to the Pierre Châtel Formation is covered by the forest track. An outcrop of the Goldberg Formation is situated about 3m below the base of this section.

**Fig. 4.13a** - Marchairuz section (part I).

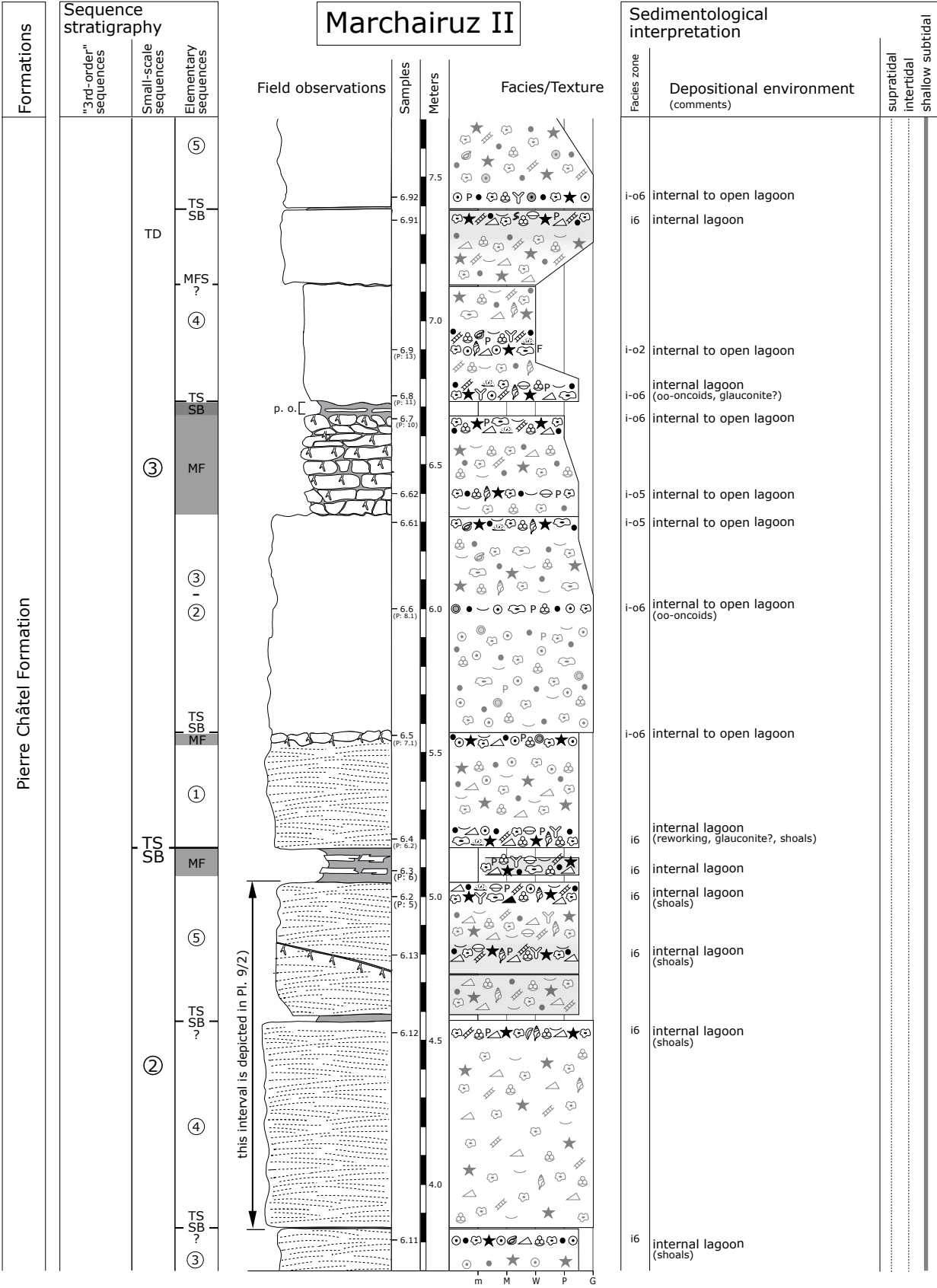


Fig. 4.13b - Marchairuz section (part II).

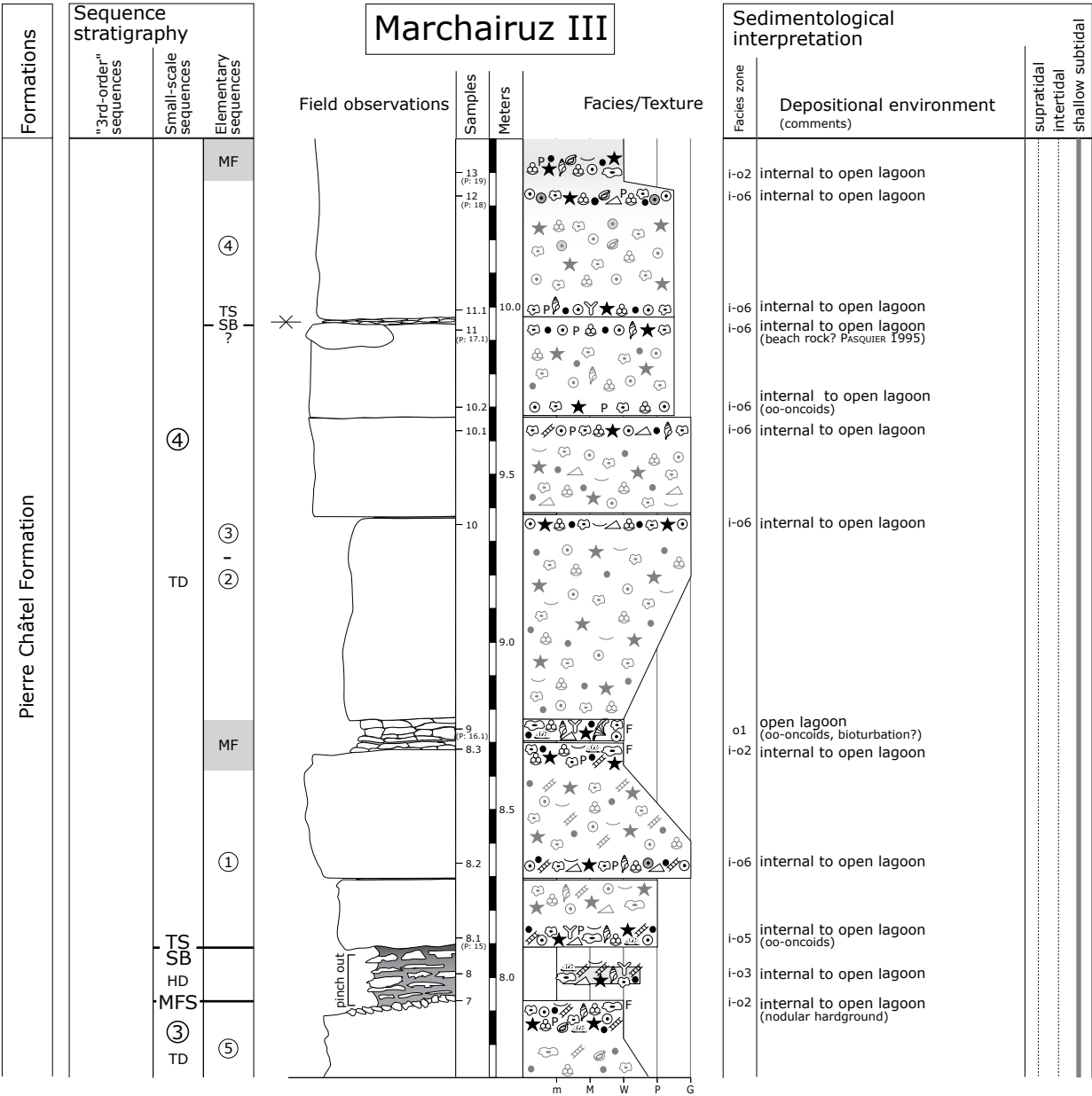


Fig. 4.13c - Marchairuz section (part III).

highstand deposits are strongly reduced. The lateral pinch out may be related to syndimentary tectonics.

The base of the following massive bed is considered as transgressive surface of small-scale sequence 4. The top of the measured section probably comprehends at least three elementary sequences of this small-scale sequence (transgressive deposits). The sequence boundaries of the elementary sequences are not well-expressed. The floatstone interval is considered as a maximum flooding of the first elementary sequence of this small-scale sequence.

The sequence-stratigraphical interpretation of this section is not without difficulties. This is mainly due

to the lack of biostratigraphical markers and the thick intervals of deposits, which have been controlled by autocyclic processes (shoals). Moreover, all the sediments have been deposited in subtidal environments where relative sea-level changes commonly produce only subtle facies contrasts due to the absence of threshold effects (cf. Chap. 3).

4.6.4 Crozet

The Crozet section was first described by MOUTY (1966). He labelled the section ‘Coupe de Thoiry’ and

designated the Pierre Châtel Formation as 'Calcaire de Thoiry' (cf. Fig. 4.5).

STRASSER (1988) interpreted the deposits of the Goldberg Formation of this section as peritidal shallowing-upward sequences, which have been controlled by auto- and allocyclic processes. Moreover, he elaborated a lateral correlation framework of the Goldberg Formation of this section with other Jura platform sections. A first sequence-stratigraphical interpretation of this section was established by WAEHRY (1989).

#### **Geographic and stratigraphic setting**

The section is situated on the first (southern-most) anticline of the Jura Mountains (Fig. 4.14). It outcrops along a forest road on the southwestern limb of the anticline and is situated above the villages Villeneuve and Crozet at about 860 m.a.s. (coordinates 487.750/125.660, Swiss National Topographic map, 1/25000, 1280 Chasseral).

The section has been dated by MOJON (2002). The top of the Goldberg Formation lies in the charophyte-ostracode assemblage zone M4. At the base of the Pierre Châtel Formation, an ammonite fragment was

found and determined as *Berriasella* cf. *privasensis* (WAEHRY 1989). The ammonite species is attributed to the Middle Berriasian (Privasensis subzone in Occitanica ammonite zone). Probably, the ammonite fragment was transported during the Middle Berriasian transgression from the shelf onto the shallow Jura platform.

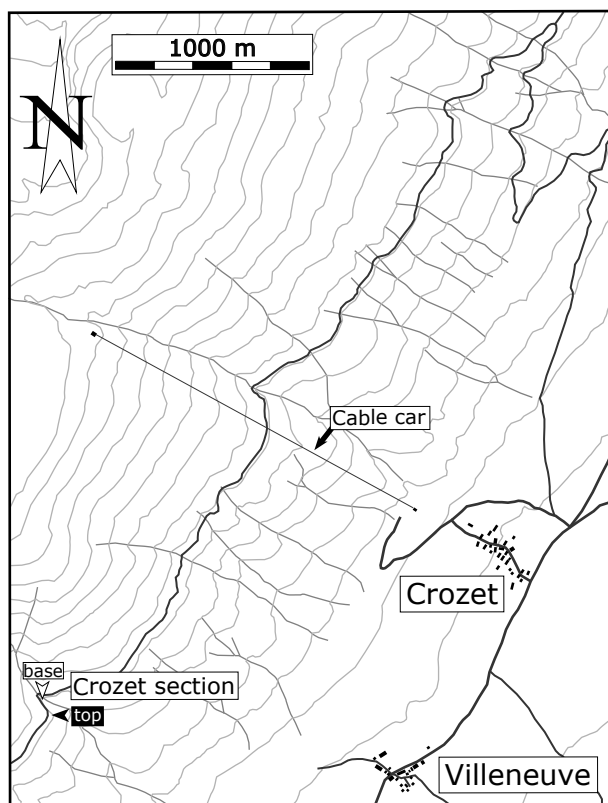
#### **Sedimentological interpretation** (Fig. 4.15a-c)

The first massive bed at the base of the Goldberg Formation consists of freshwater pond deposits. The following succession of massive beds marks a deepening to a tidal flat and/or an internal-lagoonal environment. Tidal flat deposits at the top of this succession point to a slight decrease of accommodation space (from 1.80 to 2.25 meters). The top of the Goldberg Formation is dominated by marls interpreted as continental deposits (freshwater ponds with seasonally brackish to hypersaline conditions). These marls lie in the assemblage zone M4 (with reworked fauna of the assemblage zone M3; MOJON 2002).

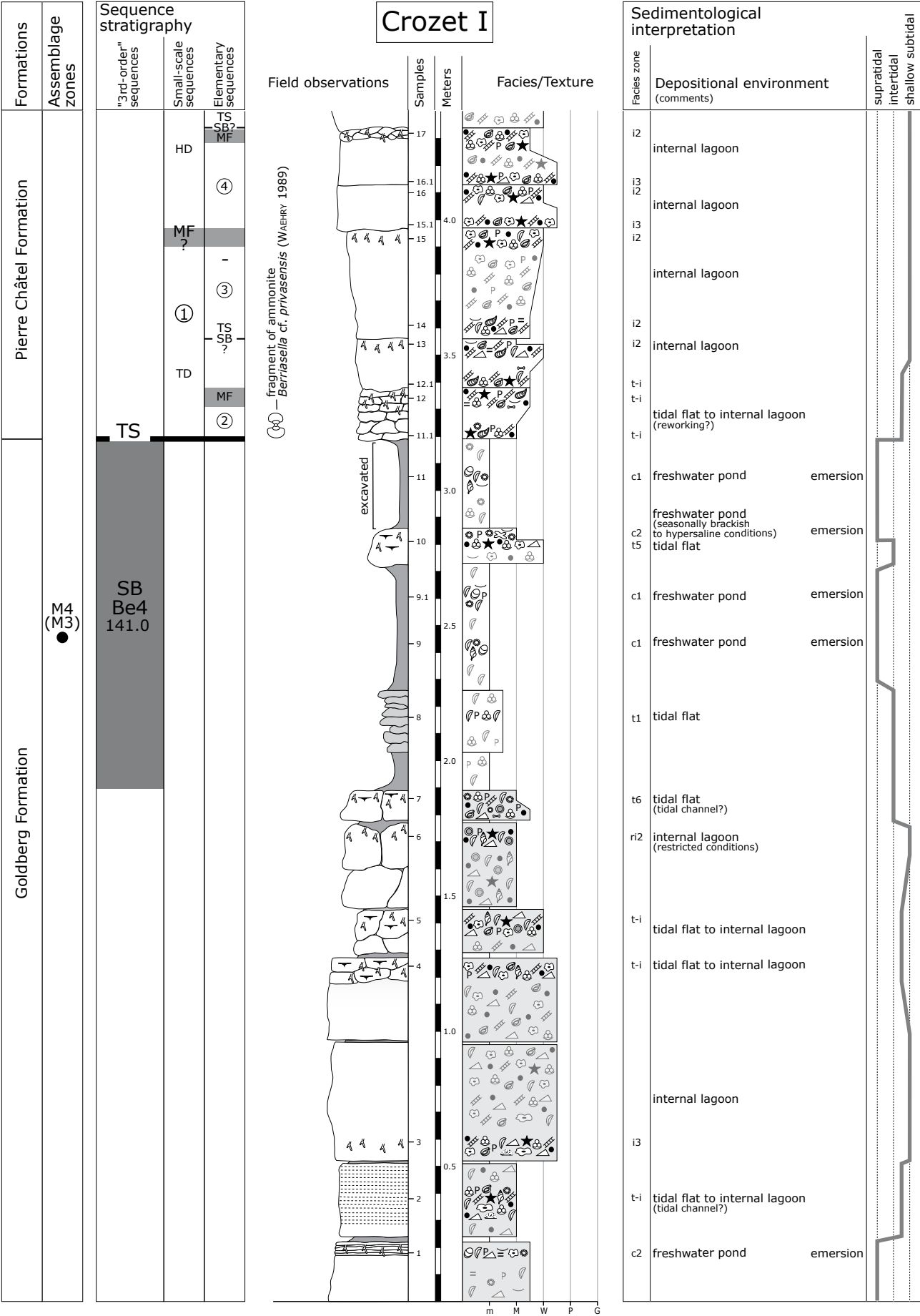
The onset of lagoonal conditions at the base of the Pierre Châtel Formation marks a marine transgression and an increase of accommodation space. Mud- to wackestones of an internal-lagoonal setting characterize the base of the Pierre Châtel Formation. Bioturbated, oncoid-rich sediments are interpreted as a slight deepening of the lagoon (from 4.25 to 4.50 meters). A gradual change from a lagoonal to a tidal flat environment is observed at about 4.50 meters.

The following brownish marl to mudstone interval is interpreted as tidal flat deposit (at 4.70 meters). An initial opening of the system is marked by a bed of internal-lagoonal deposits, which is rich in reworked intraclasts at its base. A floatstone interval dominated by big oncoids indicates a further opening of the depositional environment from internal-lagoonal to more open-lagoonal conditions (from 5.25 to 5.50 meters). At 5.50 meters, a reverse fault cuts the section. The throw of this fault is about 1 meter (WAEHRY, 1989 and pers. observation). Restricted, internal-lagoonal conditions prevail up to a rapid shallowing marked by tidal flat deposits (microbial mats and birdseyes; from 6.45 to 6.60 meters).

A succession of massive pack- to grainstones covers the tidal flat deposits. These beds are deposited in an internal- to open-lagoonal setting during a deepening of the depositional system. Partly, high-energy sediments have been deposited within this succession (reworked intraclasts at 6.65 meters and a rudstone interval at 7.00 meters). A further opening of



**Fig. 4.14** - Location of the Crozet section.



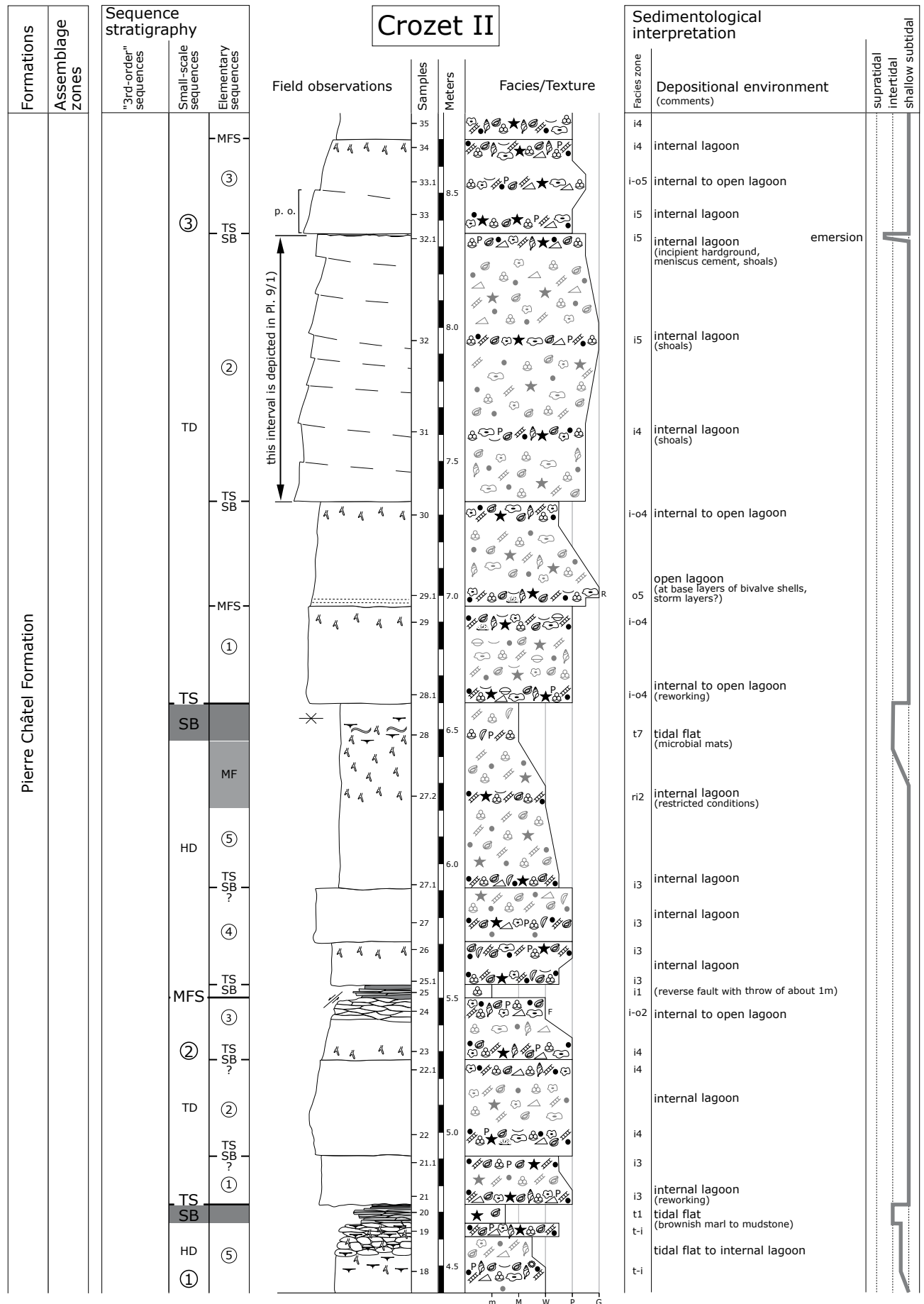


Fig. 4.15b - Crozet section (part II).

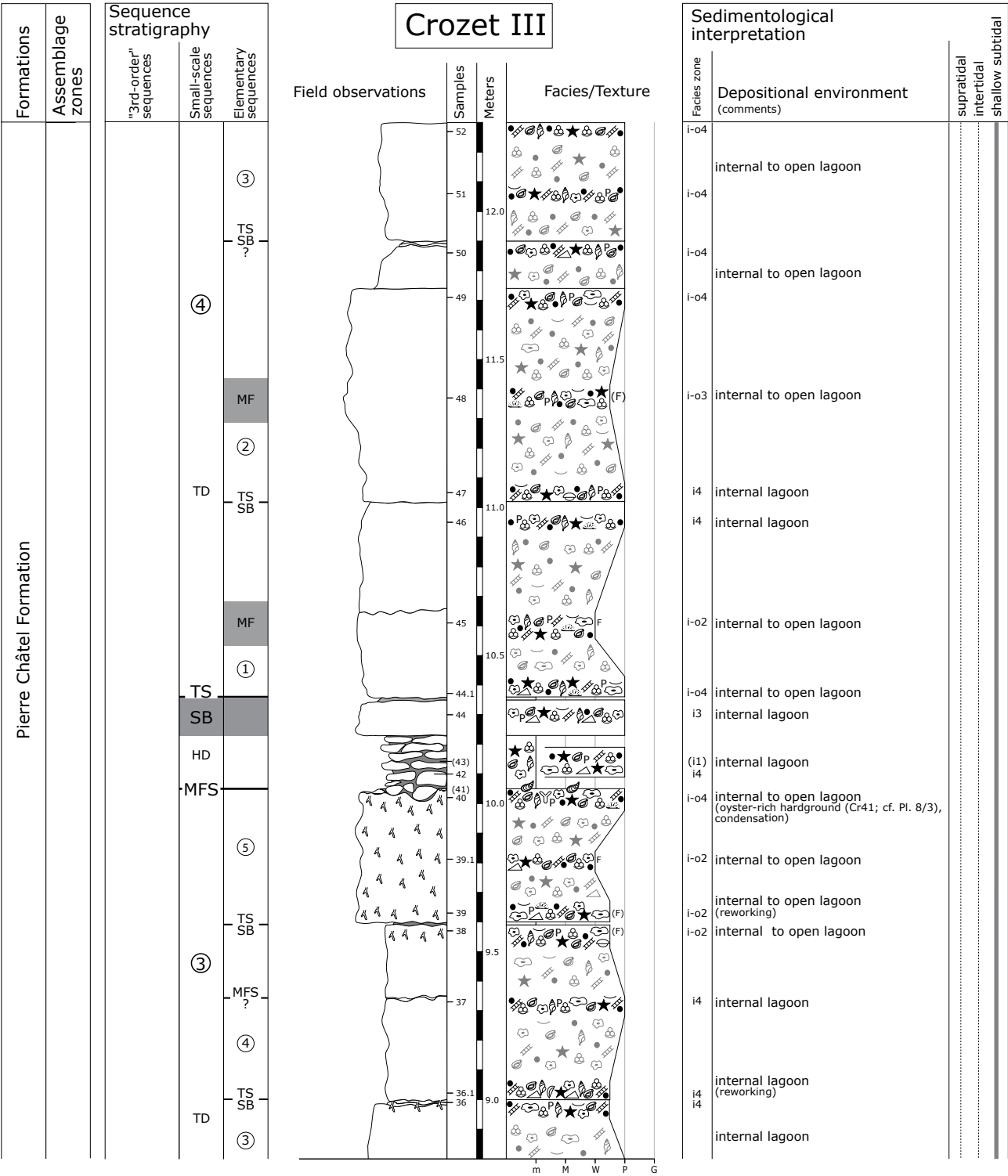


Fig. 4.15c - Crozet section (part III).

the system is marked by thick shoal interval indicated by low-angle foresets in an internal-lagoonal setting (from 7.35 to 8.35 meters; cf. Pl. 9/1). At the top of the shoal interval meniscus cements indicate the development of incipient hardgrounds and emersion during decreasing accommodation space (at 8.35

meters). Internal- to open-lagoonal conditions prevail up to 9.50 meters. The following strongly bioturbated sediments are interpreted as an interval of reduced sedimentation in an internal-lagoonal environment (from 9.50 to 10.05 meters). Condensation culminates in development of a hardground surface overgrown



by oysters (cf. Pl. 8/3). A nodular, marly interval of internal-lagoonal deposits covers this hardground.

A slight increase of accommodation space is marked by the transition to massive, oncoid- and intraclast-rich beds (from 10.25 to 10.35 meters). The top of the Crozet section is dominated by a succession of massive, internal- to open-lagoonal beds. This succession is partly interrupted by floatstone intervals, which contain big oncoids. They are considered to reflect relatively low-energy conditions during slight deepening of the depositional environment. The following bed succession is covered by vegetation and partly tectonically disturbed. This is why a further logging of the Crozet section has not been carried out.

#### ***Sequence-stratigraphical interpretation*** (Fig. 4.15a-c)

The massive beds at the base of the section are considered to belong to a sequence below the 3<sup>rd</sup>-order sequence boundary Be4. Emersion at the top of the Goldberg Formation leads to strong condensation during the deposition of the continental marl intervals. The dating by charophyte-ostracode assemblages indicates that this interval corresponds to the 3<sup>rd</sup>-order sequence boundary Be4 (according to HARDENBOL et al. 1998).

In small-scale sequence 1, the sequence boundaries of the elementary sequences are not well expressed. It is assumed that at least four elementary sequences are recorded. The first two elementary sequences have been deposited during a rise in relative sea level. They represent the transgressive deposits of small-scale sequence 1. The bioturbated, oncoid-rich interval is considered as maximum flooding of small-scale sequence 1. The highstand of this small-scale sequence is well expressed by the change from lagoonal to tidal flat deposits (falling relative sea level) and comprises the fourth and the fifth elementary sequences.

The brownish marl to mudstone interval is interpreted as sequence boundary between small-scale sequences 1 and 2. The interpretation of elementary sequences is equivocal within small-scale sequence 2. It is supposed that it consists of at least four elementary sequences. The transgressive deposits comprehend at least two elementary sequences. The discontinuity at the top of the floatstone interval is taken as maximum-flooding surface of small-scale sequence 2. Falling relative sea level leads to the change from restricted, internal-lagoonal to tidal flat sediments interpreted as highstand deposits (fourth and fifth elementary sequences).

Tidal flat deposits mark the sequence boundary of small-scale sequence 3. This sequence is composed of five well-defined elementary sequences. A rise of relative sea level creates accommodation space for the deposition of the following succession of the relatively thick, massive internal- to open-lagoonal beds. They represent the transgressive deposits of this small-scale sequence (first to fifth elementary sequence). The oyster-rich hardground is considered as maximum-flooding surface of small-scale sequence 3. It is supposed that strong condensation prevailed during the deposition of the nodular, marly internal-lagoonal interval (highstand deposits).

The massive, internal-lagoonal bed represents the sequence-boundary zone between small-scale sequences 3 and 4. A rise in relative sea level leads to the deposition of the internal- to open-lagoonal sediments at the base of this small-scale sequence (transgressive deposits). The top of the Crozet section probably consists of at least two elementary sequences, but their sequence boundaries are badly expressed. Yet, the floatstone intervals can be considered as maximum floodings on the elementary sequence scale.

### **4.6.5 Chapeau de Gendarme**

The Chapeau de Gendarme section was first described bed-by-bed by MOUTY (1966). A first sequence-stratigraphical interpretation was carried out by WAEHRY (1989). He used the Chapeau de Gendarme section as a basis for a synthetic lithological and biostratigraphical log. Sequence-stratigraphical correlations of this section with other sections (Jura platform and Vocontian basin) were established by WAEHRY (1989) and HILLGÄRTNER (1999).

A high-resolution sequence-stratigraphical interpretation of the Chapeau de Gendarme section (on an elementary sequence scale) was published by STRASSER et al. (2004).

#### ***Geographic and stratigraphic setting***

The section follows the department road (D436) between the town of St. Claude and the village of Septmoncel (coordinates 874.550/2157.075, IGN map, 1/25000, 3327ET Morez - Les Rousses; cf. Fig. 4.16). It outcrops on the same road side as the famous landmark “Chapeau de Gendarme”, which describes the hinge of a small fold (HILLGÄRTNER 1999). The distance between the small road bridge below the “Chapeau de Gendarme” to the base of the section

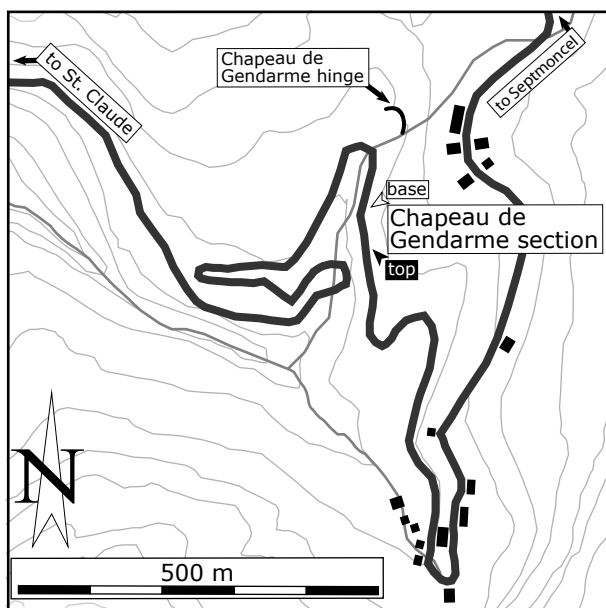


Fig. 4.16 - Location of the Chapeau de Gendarme section.

is about 50 meters (in direction to Septmoncel). The section has been dated by MOJON (2002) and ranges from the charophyte-ostracode assemblage zones M2 to M4. It is well accessible and not disturbed tectonically.

#### ***Sedimentological interpretation*** (Fig. 4.17a-d)

The top of the Goldberg Formation consists of marls and mudstones. The base of the section starts with fossil-poor marls and mudstones (from 0.00 to 2.80 meters). They are interpreted as tidal flat deposits. Partly, they contain desiccation and circumgranular cracks indicating emersion. A marl interval, which is partly covered by vegetation, is rich in ostracodes and charophytes (stems and gyrogonites; from 2.80 to 3.15 meters). It is interpreted as freshwater pond deposits. MOJON (2002) attributes this interval to the assemblage zone M3. The following nodular interval consists of tidal flat deposits. A mudstone interval, which is rich in ostracodes and charophytes (stems and gyrogonites), is considered to represent freshwater pond sediments (from 3.50 to 3.65 meters). It also contains some reworked foraminifera from nearby tidal flat and/or lagoonal environments. The top of the Goldberg Formation is characterized by a thin wacke- to packstone bed, which is rich in charophyte stems and gyrogonites indicating continental freshwater conditions (from 3.65 to 3.75 meters).

Reworking at the base of the thinly-bedded wacke- to packstone interval has been interpreted as

boundary between the Goldberg and the Pierre Châtel Formations. At the top of the following massive wacke- to packstone bed (from 3.75 to 4.15 meters), birdseyes indicate a decrease of accommodation space and the change to tidally influenced internal-lagoonal deposits. The surface at the top of this bed is slightly undular and covered by a marl interval with flat pebbles (at 4.15 meters). It probably reflects a tidal channel interval. An opening of the system is indicated by three ooid-rich internal-lagoonal beds (from 4.25 to 4.60 meters). The following bed contains a mixture of marine and freshwater components. It is interpreted as tidal flat sediments deposited during decreasing accommodation space. Reworking and a change to a restricted, internal-lagoonal environment point to an opening of the system during the deposition of the following massive bed (from 4.60 to 4.95 meters).

A decrease of accommodation space led to the deposition of the following marl interval. It contains a mixture of marine and freshwater constituents, which is characteristic for tidal flat sediments. This marly interval is capped by a small, black marl layer (thickness of about 2 centimeters) suggesting restricted, oxygen-poor depositional conditions. According to MOJON (2002), the ostracodes and charophytes of this marl interval are reworked from assemblage zone M3. An opening of the depositional system is marked by the change to an internal-lagoonal depositional setting. The following nodular interval is bioturbated at the top, which is considered as pronounced condensation (from 5.20 to 5.45 meters). A laminated, massive bed follows the nodular interval. It consists of internal-lagoonal deposits. The massive, ooid-dominated pack- to grainstone has been deposited in an internal-lagoonal environment (from 5.80 to 5.95 meters). Restricted, internal-lagoonal conditions prevailed during the deposition of the following thinly-bedded interval, which reflects a slight decrease of accommodation space. Bioturbation points to condensation within the thinly-bedded interval (at 6.25 meters). Increasing tidal influence (changing energy conditions) at the top of the thinly-bedded interval is postulated because of lamination (partly microbial mats) and the deposition of thin ostracode layers. Restricted conditions prevail during the deposition of the following massive, bioturbated internal-lagoonal bed. Birdseyes at the top of this bed indicate a pronounced tidal influence during a decrease of accommodation space (at 6.70 meters). An undulating surface is assumed to mark the bottom of a tidal channel (at 6.75 meters). The tidal channel is filled by marls (from 6.75 to 6.85 meters). This marl interval contains ostracodes and some charophytes (stems and gyrogonites) belonging to assemblage zone

M4 (according to MOJON 2002).

The following massive bed is characterized by alternations of microbial mats and layers of high-energy deposits indicating tidal influence in a restricted internal-lagoonal environment. The massive bed is capped by internal-lagoonal marls. Flat nodules with intraclasts point to reworking processes at the base of the following massive bed (at 7.00 meters). Lamination and ostracode layers indicate changing energy conditions within a partly bioturbated, internal-lagoonal environment. Reworked lithoclasts point to high-energy conditions in the internal-lagoonal environment during the deposition of the following two packstone beds (from 7.25 to 7.45 meters). They are capped by a grainstone bed indicating high-energy conditions in the internal lagoon (from 7.45 to 7.50 meters). Such an increase of the hydrodynamic energy can be related to more tidally-influenced conditions during a shallowing of the depositional environment (from subtidal to more intertidal conditions). A deepening of the system is displayed by an interval of internal- to open-lagoonal sediments (from 7.50 to 8.20 meters). The nodular, bioturbated, pack- to grainstone interval is interpreted as high-energy sediments, which are partly rummaged through by organisms during decreasing energy conditions (from 7.75 to 7.85 meters). At the top of this interval, lamination probably indicates tidal influence during decreasing accommodation space. The following beds are dominated by internal-lagoonal sediments up to a bed characterized by birdseyes (at 8.85 meters). A floatstone interval has been deposited during a slight deepening of the depositional system (from 8.50 to 8.60 meters). The protected, low-energy conditions subsist up to a reddish, tidal-influenced interval containing birdseyes (from 8.85 to 9.60 meters). Internal-lagoonal deposits, which are strongly bioturbated (from 9.10 to 9.20 meters), dominate the bed succession up to the reddish tidal flat interval. This facies change indicates a remarkable decrease of accommodation space.

A slight opening of the depositional system is indicated by the deposition of the following tidal flat to internal-lagoonal sediments. A nodular, strongly bioturbated internal- to open-lagoonal interval (floatstone) marks a further opening of the system (at 10.00 meters). The nodular interval is overlain by a massive bed composed of internal-lagoonal deposits. Increased energy conditions are displayed by massive pack- to grainstones (from 10.25 to 10.50 meters). The following bioturbated, nodular packstone represents a condensation interval within an internal- to open-lagoonal environment (at 10.70 meters). A thickening-up trend of the following bed succession

points to increasing accommodation space (from 10.70 to 11.70 meters). This succession is composed of two resembling intervals. Each of these intervals is characterized by a massive internal-lagoonal bed at the base capped by nodular, bioturbated internal- to open-lagoonal deposits. These nodular, bioturbated beds are interpreted as condensation intervals during periods of slight deepening of the depositional system. The following massive beds display a wacke- to packstone texture (from 11.70 to 13.10 meters). An interval of strong bioturbation reflects condensation in an internal- to open-lagoonal setting during a deepening of the depositional system (from 12.40 to 12.70 meters). The following marl interval is interpreted as deposits of an internal-lagoonal environment. It indicates a decrease of accommodation space at the top of the section.

#### *Sequence-stratigraphical interpretation* (Fig. 4.17a-d)

The top of the Goldberg Formation lying in the charophyte-ostracode assemblage zone M3 (MOJON 2002) is thought to correspond to the 3<sup>rd</sup>-order sequence boundary interval Be3 to Be4 (according to HARDENBOL et al. 1998). Small-scale sequences identified by WAEHRY (1989) and HILLGÄRTNER (1999) at the base of this section are in accordance with the sequence-stratigraphical interpretation made in this study.

The facies change from lacustrine to marine conditions at the base of the first massive bed is considered as transgressive surface of small-scale sequence 1. This environmental change marks the boundary between the Goldberg and the Pierre Châtel Formation. Based on the correlation with the other sections (Chap. 6) it is assumed that the second elementary sequence is represented by the massive, internal-lagoonal deposits within the first massive bed. This implies that the first elementary sequence is missing. The tidal channel interval is considered as sequence boundary of the following elementary sequence. The sequence-stratigraphical interpretation of the following three ooid-rich beds is not straightforward. They have probably been controlled by autocyclic processes. By means of lateral correlation, it is assumed that they represent two elementary sequences (third and fourth elementary sequences). The maximum flooding of this small-scale sequence cannot be determined. It is supposed that it is located in the third and/or fourth elementary sequence. A fall of the relative sea level caused a shift to tidal flat deposits representing the sequence boundary of the fifth elementary sequence. It comprehends the massive bed of restricted, internal

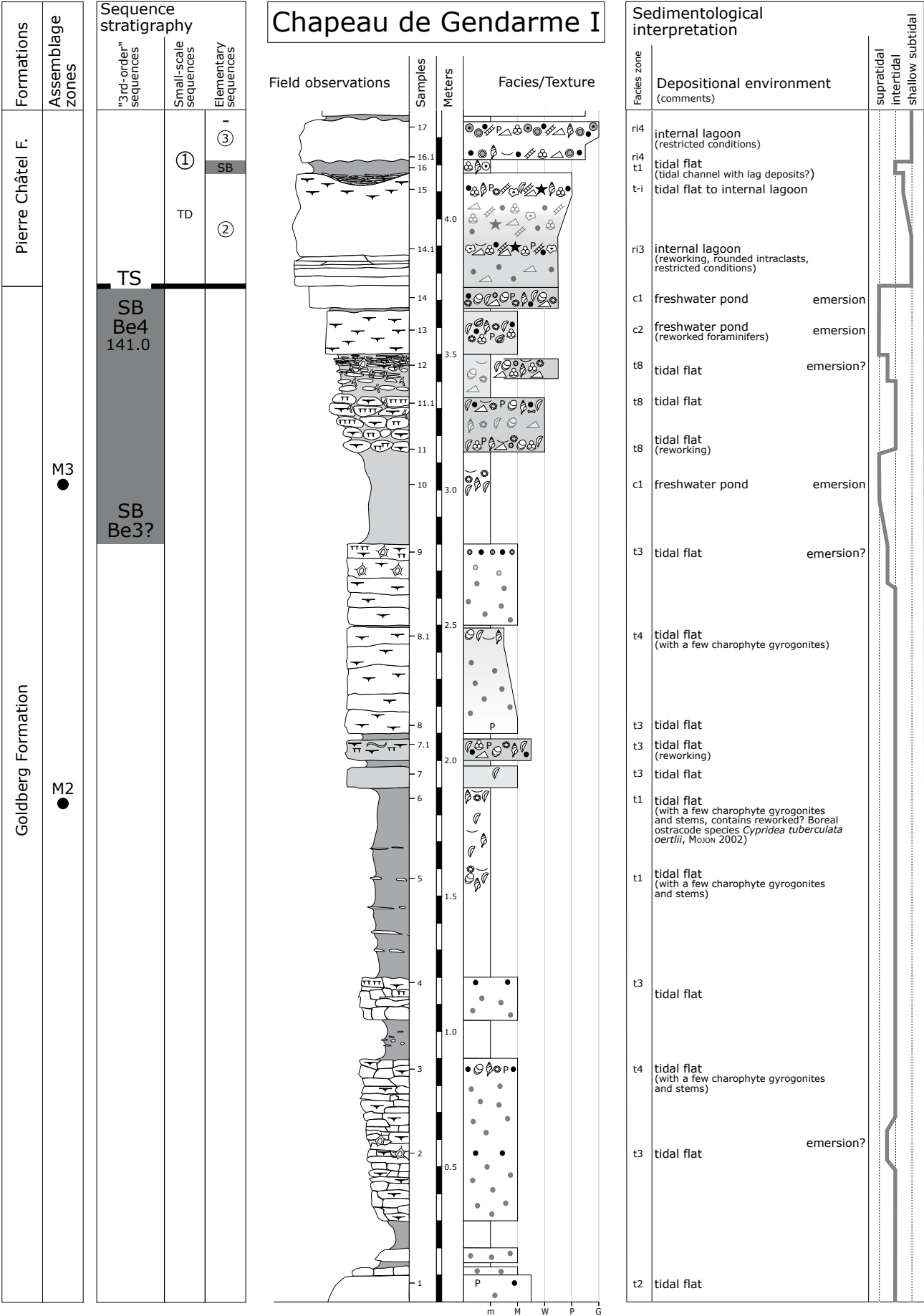


Fig. 4.17a - Chapeau de Gendarme section (part I).

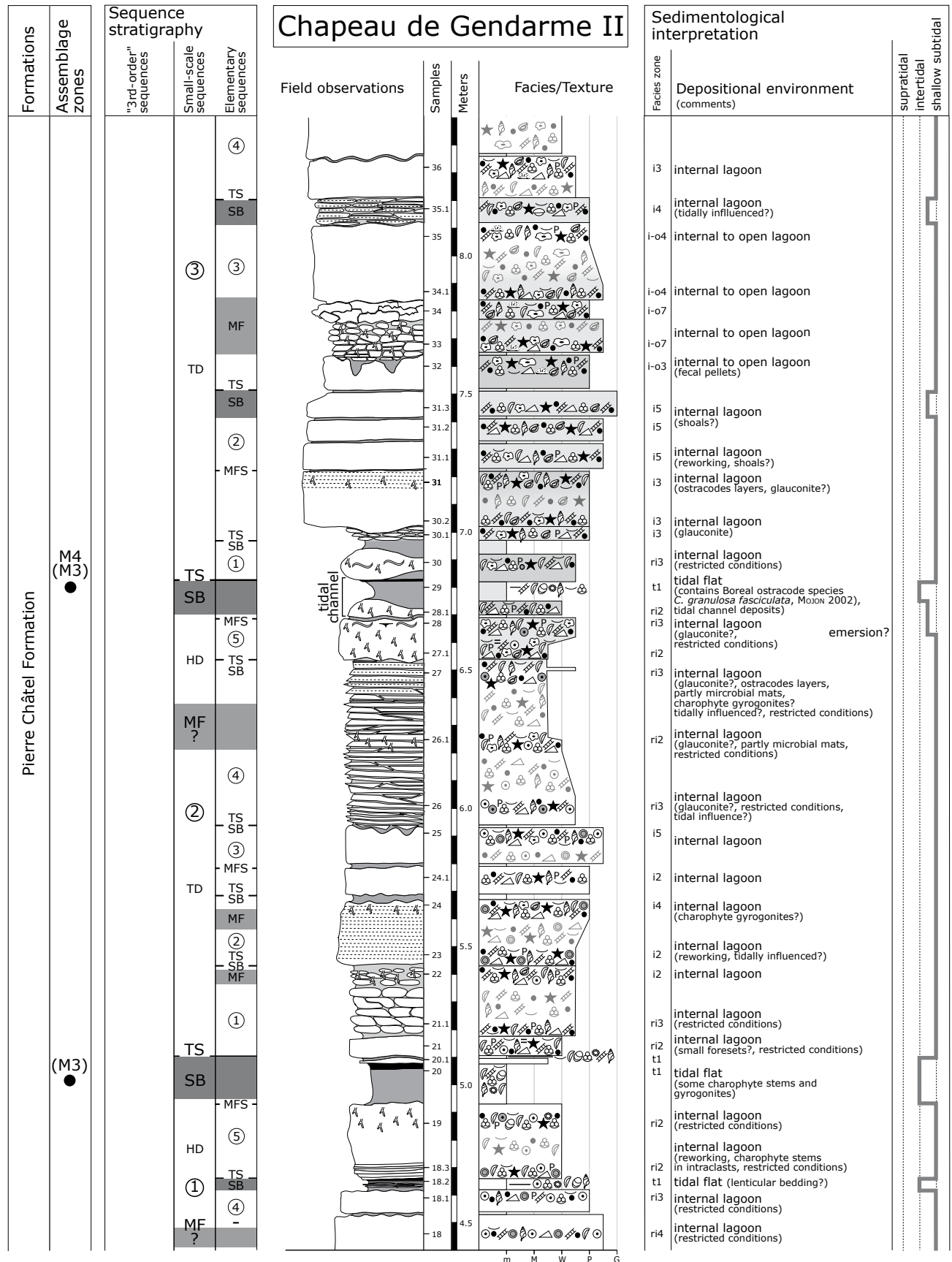


Fig. 4.17b - Chapeau de Gendarme section (part II).

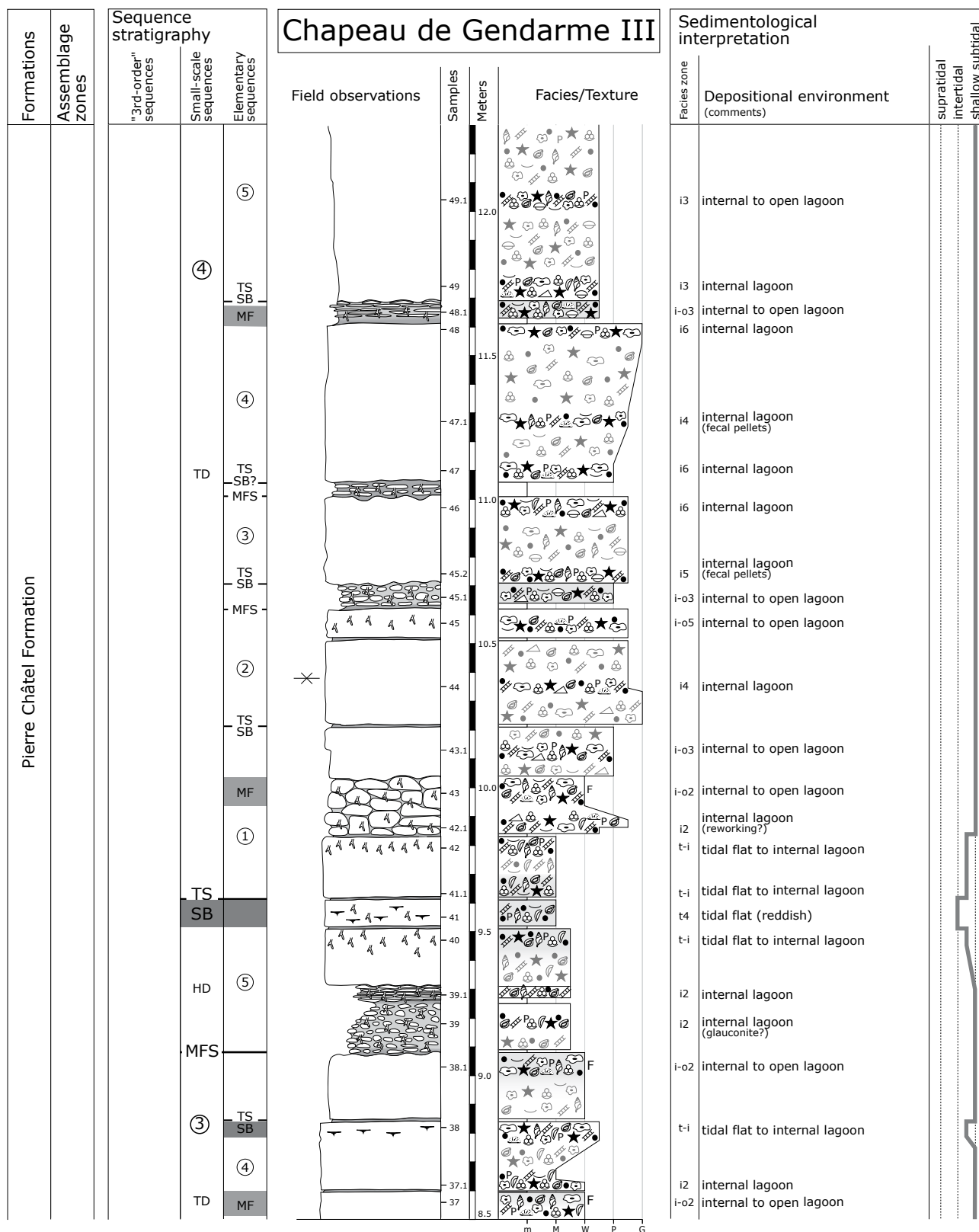
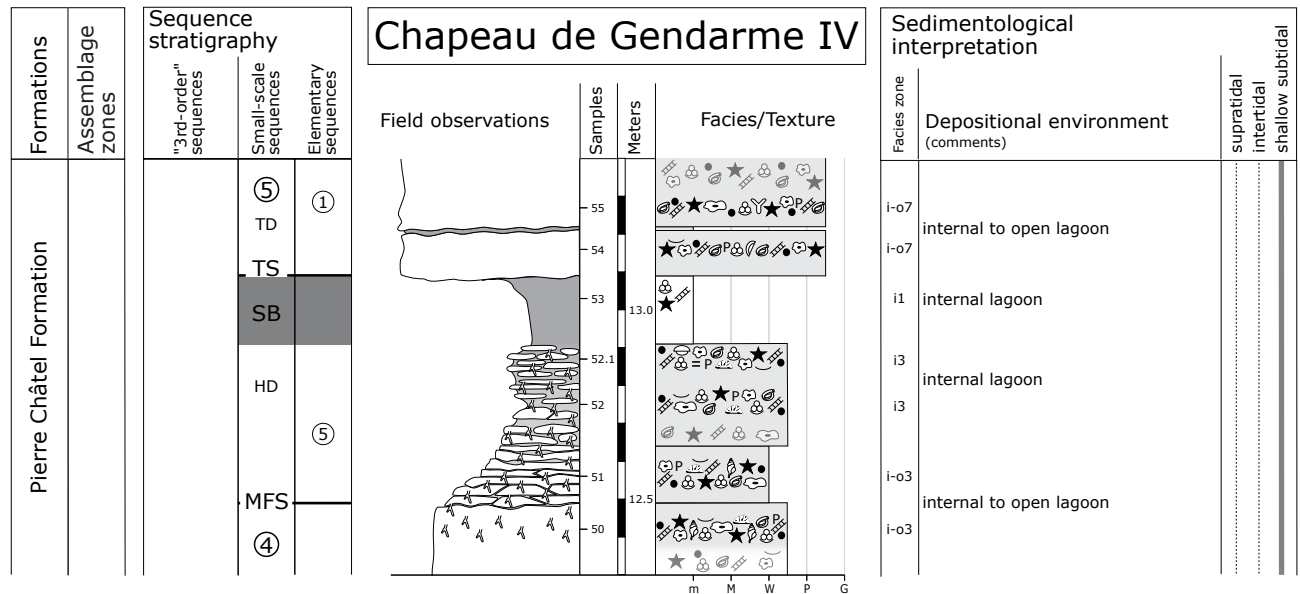


Fig. 4.17c - Chapeau de Gendarme section (part III).



**Fig. 4.17d** - Chapeau de Gendarme section (part IV).

lagoonal deposits.

A lowering of the relative sea level led to the deposition of the tidal flat deposits. It marks the sequence boundary of small-scale sequence 2. This small-scale sequence comprises five elementary sequences. A succession of internal-lagoonal sediments has been deposited during rising relative sea level. The transgressive deposits of this small-scale sequence consist of four elementary sequences (first to fourth elementary sequences). Progressive condensation at the top of the nodular interval is considered as maximum flooding of the first elementary sequence. Reworking at the base of the following massive, laminated bed is interpreted as sequence boundary and transgressive surface of the second elementary sequence. A stratigraphically overlying thin marl layer is considered as sequence boundary at the base of the third elementary sequence. The change to restricted conditions at the base of the thinly bedded interval is caused by a slight fall of the relative sea level. It marks the sequence boundary of the fourth elementary sequence. Bioturbation within this interval may be interpreted as maximum flooding of small-scale sequence 2. The transition from the thinly bedded interval to the bioturbated mud- wackestones is taken as sequence boundary of the fifth elementary sequence. The upper part of the fourth and the fifth elementary sequence build up the highstand deposits of small-scale sequence 2.

The tidal channel deposits mark the sequence boundary of small-scale sequence 3. It encompasses five elementary sequences. A rise of relative sea level is well marked by reworking processes (flat nodules

with intraclasts) at the base of the following massive bed. It indicates the transgressive surface of the first elementary sequence and of small-scale sequence 3. The discontinuity at the top of the bioturbated internal-lagoonal deposits represents the maximum-flooding surface of the first elementary sequence. The sequence boundary and the transgressive surface of the second elementary sequence are indicated by the increase of tidal influence during the deposition of the grainstone bed. The strongly bioturbated interval is interpreted as maximum flooding of the third elementary sequence. The undulated surface at its base is probably the result of bioturbation and/or omission on the lagoon bottom. A slight decrease of relative sea level is reflected by the increasing tidal influence (laminated interval). It is considered as sequence boundary, followed by the transgressive surface of the fourth elementary sequence. A decline of tidal influence points to a rise of relative sea level during the deposition of the following massive beds. The floatstone interval is interpreted as maximum flooding of this elementary sequence. The sequence boundary of the fifth elementary sequence is marked by an increasing tidal influence during a drop of relative sea level. The maximum-flooding surface of small-scale 3 and the fifth elementary sequence is well established at the base of the strongly bioturbated, nodular interval. The highstand deposits of small-scale sequence 3 display a rather reduced thickness.

A pronounced decrease of relative sea level is indicated by the tidal flat deposits. They mark the sequence boundary at the base of small-scale sequence 4. This small-scale sequence comprehends five elementary sequences. A rise of relative sea level



leads to an opening of the depositional environment (tidal flat to internal-lagoonal deposits) at the base of the first elementary sequence. The floatstone interval is considered as maximum flooding of this elementary sequence. The environmental change at the base of the massive bed composed of internal-lagoon sediments is taken as sequence boundary of the second elementary sequence. The discontinuity at the base of the nodular, bioturbated, internal- to open-lagoonal deposits is considered as maximum-flooding surface of the second elementary sequence. The following two massive beds, which are both capped by nodular intervals, represent each an elementary sequence (third and fourth elementary sequences). The discontinuities at the base of the nodular, bioturbated intervals between these beds are interpreted as maximum-flooding surfaces. The following massive bed has been deposited during rising relative sea level. The discontinuity at the top of this bed is interpreted as maximum-flooding surface of the fifth elementary sequence and small-scale sequence 4. Decreasing relative sea level led to a facies change and to the deposition of the muddy, bioturbated, internal-lagoonal sediments. These deposits represent the highstand deposits of this small-scale sequence.

The internal-lagoonal marls at the top of the section have been deposited during a fall of relative sea level. They are interpreted as sequence boundary zone of the following small-scale sequence 5.

#### 4.6.6 St. Claude

The St. Claude section was first described by MOUTY (1966). WAEHRY (1989) logged the section and

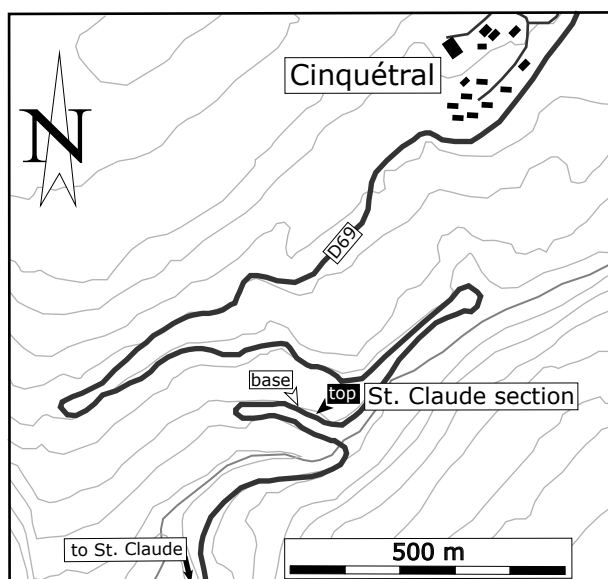


Fig. 4.18 - Location of the St. Claude section.

interpreted it in terms of sequence stratigraphy.

#### *Geographic, geologic and stratigraphic setting*

The section outcrops along the road D69 between the town of St. Claude and the village of Cinquétral (cf. Fig. 4.18). It is situated close to a dangerous curve in a succession of narrow serpentines (coordinates 872.280/2164.125 IGN map, 1/25000, 3327OT St-Claude).

The section has been dated by MOJON (2002) and ranges from the charophyte-ostracode assemblage zones M2 to M4. The beds are well accessible and not tectonically disturbed.

#### *Sedimentological interpretation* (Fig. 4.19a-c)

The Goldberg Formation mainly consists of marls and mudstones interpreted as tidal flat deposits. Charophyte-rich intervals are interpreted as tidal pond deposits (at 0.40 and at 2.20 meters). At the top of the Goldberg Formation, a small intraclast-rich pack- to grainstone is considered to reflect tidal channel deposits. The upper part of the Goldberg Formation was dated by MOJON (2002). It is in the range of the assemblage zones M2 to M3.

An environmental change to high-energy deposits (two massive beds of ooid- and intraclast-rich pack- to grainstones) marks a pronounced increase of accommodation during the transgression of the Pierre Châtel Formation (from 2.95 to 3.40 meters). A succession of tidal flat sediments caps the second high-energy bed. They indicate a gradual decrease of accommodation space. The top of this tidal flat succession has been dated by MOJON (2002). It lies in the assemblage zone M4.

The environmental change to a massive bed consisting of tidal flat to internal-lagoonal sediments reflects a deepening of the depositional system (at 3.75 to 3.85 meters). The following muddy, thinly-bedded, bioturbated interval has been deposited in a restricted, internal-lagoonal environment. It is capped by a massive internal-lagoonal bed. A succession of thinly-bedded, ooid-rich wacke- to packstones has been deposited in a restricted internal-lagoonal environment (from 4.10 to 4.60 meters). Bioturbation at the top of this thinly-bedded succession points to condensation and may be related to a slight deepening of the depositional system (at 4.60 meters). Circumgranular cracks at the top of a massive bed are interpreted as a pronounced tidal influence in a restricted, internal-lagoonal environment during a decrease of accommodation (at 4.80 meters).



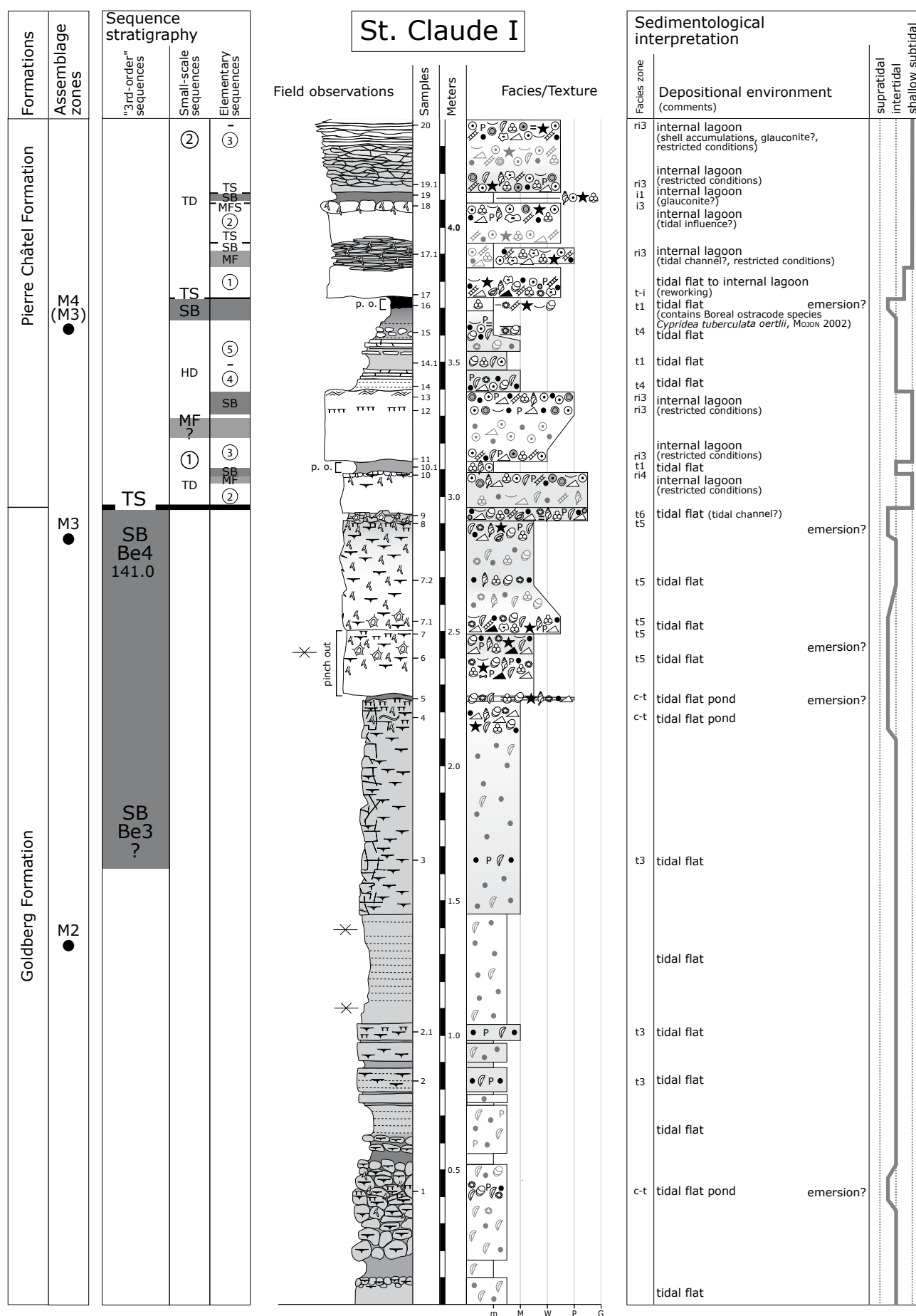


**Fig. 4.19a - St. Claude section (part I).**

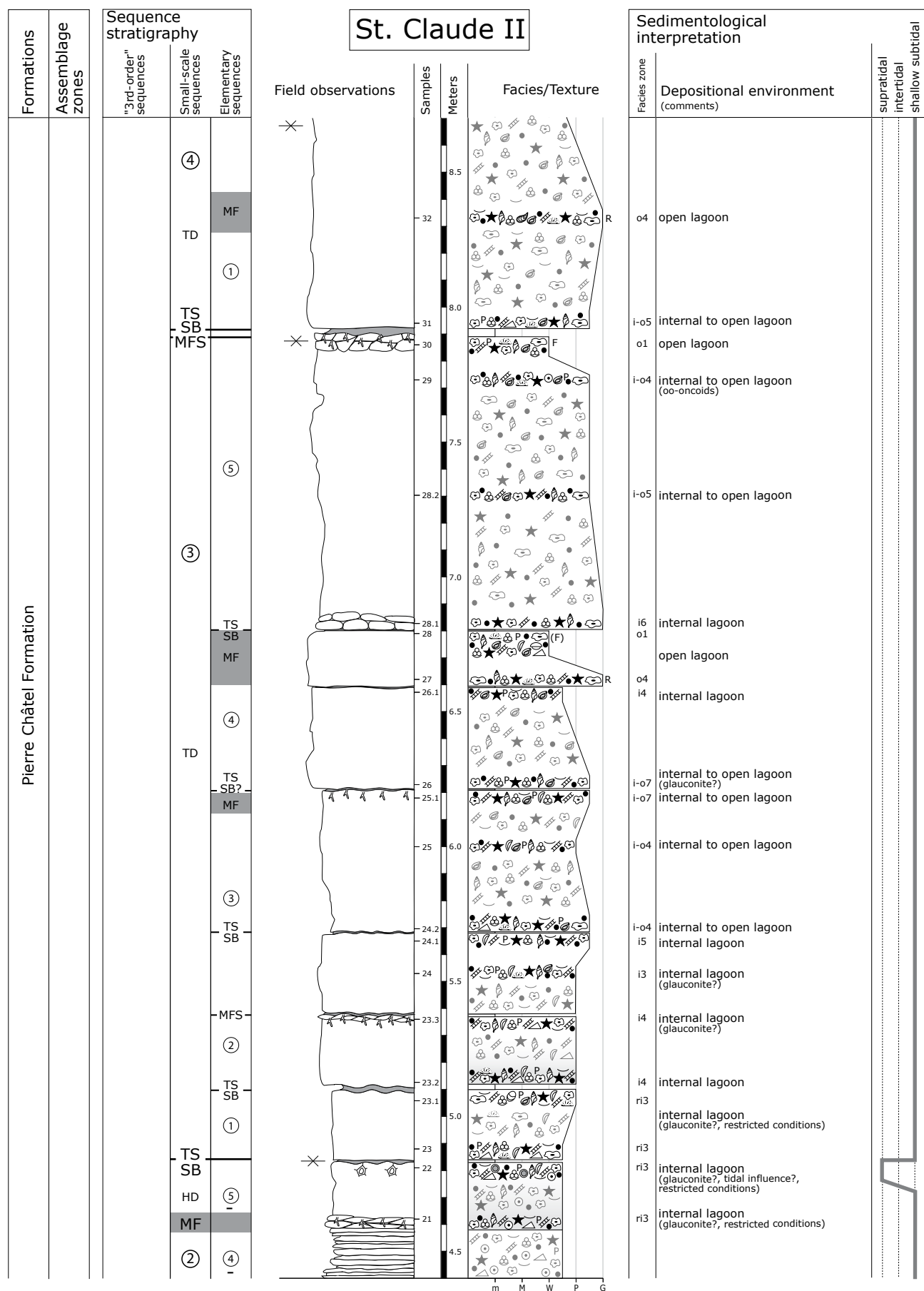


**Fig. 4.19b** - St. Claude section (part II).

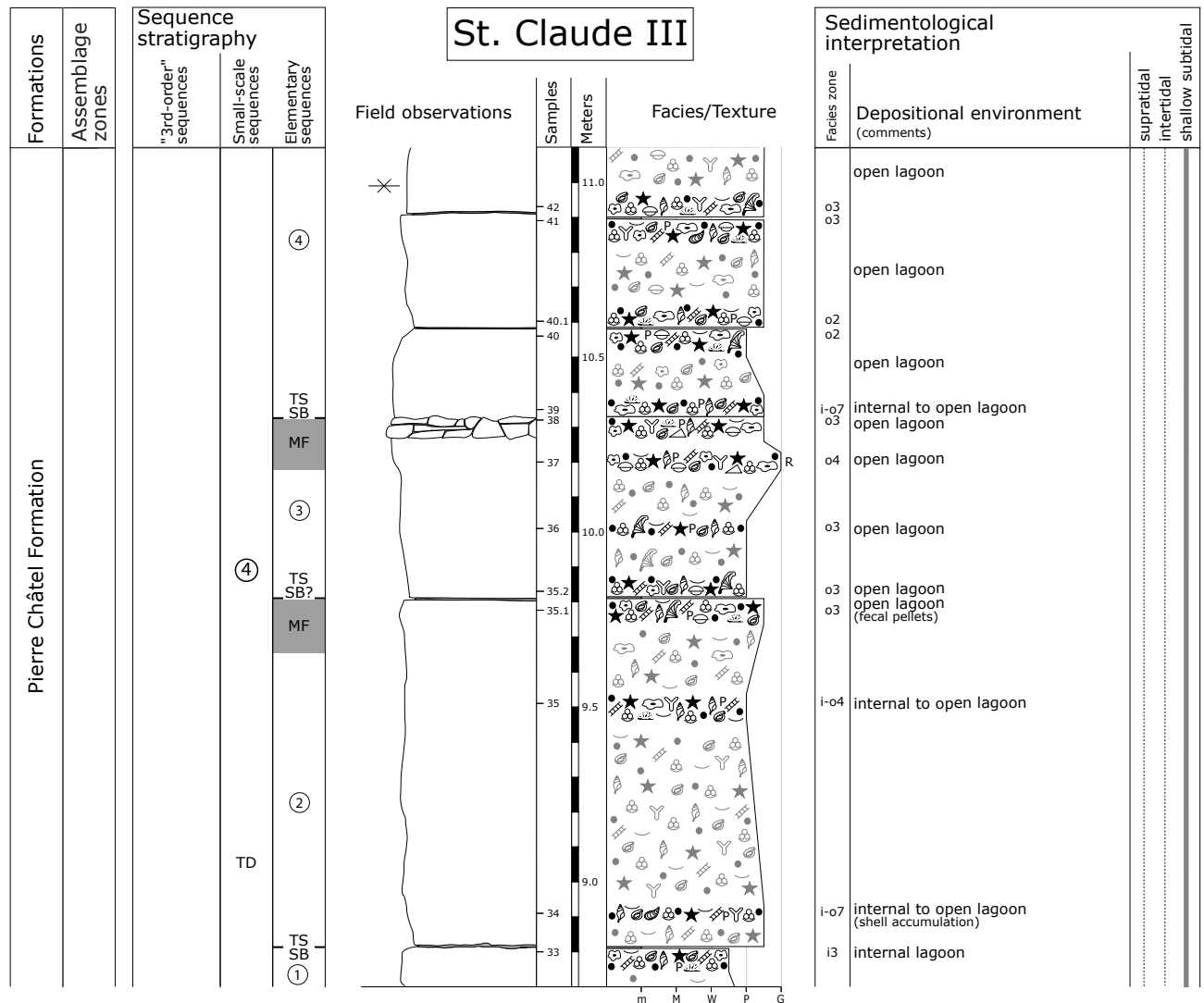


Fig. 4.19c - St. Claude section (part III).

The following bed has been deposited in an internal-lagoonal setting (from 5.10 to 5.65 meters). A slight opening of the depositional system is displayed by a succession of internal- to open-lagoonal deposits (from 5.70 to 6.80 meters). A nodular interval at the base of the following massive, thick bed consists of internal-lagoonal deposits displaying a slight decrease of accommodation space (at 6.85 meters). Within this thick bed, a gradual opening of the depositional system is indicated by the deposition of internal- to open-lagoonal sediments. The change to a strongly bioturbated floatstone at the top of this bed is interpreted as condensation interval in an open-lagoonal environment (at 7.95 meters).

The top of the section is characterized by massive, thick beds considered as a further opening of the depositional system (from 7.95 to 11.10 meters). The first beds represent internal- to open-lagoonal deposits

(from 7.95 to 9.50 meters). The deposition of internal-lagoonal sediments marks a pronounced decrease of accommodation space (at 8.80 meters). A gradual opening of the system is displayed by open-lagoonal deposits towards the top of the section (from 9.50 to 11.10 meters).

#### Sequence-stratigraphical interpretation (Fig. 4.19a-c)

Dating by charophyte-ostracode assemblages indicates that the top of the Goldberg Formation corresponds to the 3<sup>rd</sup>-order sequence boundary Be4 (according to HARDENBOL et al. 1998).

At least three elementary sequences form small-scale sequence 1. With the help of lateral correlation it is supposed that the first elementary sequence is missing due to non-deposition and/or erosion during

the transgression. The base of the first, ooid-rich, high-energy bed marks the transgression of the Pierre Châtel Formation over the Goldberg Formation. The two high-energy beds represent the transgressive deposits of small-scale sequence 1. It is suggested that each of them reflects an elementary sequence. The maximum flooding of this small-scale sequence has not been identified. The succession of tidal flat deposits terminates this small-scale sequence (highstand deposits). The interpretation of elementary sequences in the highstand deposits is not straightforward because diagnostic facies changes are lacking. However, based on lateral correlation, it is supposed that this interval comprehends two elementary sequences (fourth and fifth elementary sequences).

The top of the tidal flat succession is interpreted as sequence boundary of small-scale sequence 2. It comprises at least four elementary sequences. The transgressive surface is well defined by reworking and the change to internal-lagoonal deposits at the base of the first massive bed. Each of the following two massive beds is assumed to represent an elementary sequence (first and second elementary sequences). The thinly-bedded interval is thought to comprehend the third and the fourth elementary sequences. The nodular, strongly bioturbated interval at the top of this thinly-bedded succession is considered as maximum flooding of small-scale sequence 2. The highstand deposits are represented by the following massive bed (fifth elementary sequence).

The sequence boundary of small-scale sequence 3 is indicated by an irregular surface above an interval of circumgranular cracks. This small-scale sequence comprehends at least four elementary sequences. The bed succession is characterized by a general thickening-up trend, which reflects a gain of accommodation space during rising relative sea level (transgressive deposits). The identification of elementary sequences is uncertain in this succession. Hence, the sequence-stratigraphical interpretation on the elementary sequence scale is based on lateral correlation (cf. Chap. 6). The discontinuity at the top of the thick massive bed (nodular, bioturbated floatstone) is considered as maximum-flooding surface of small-scale sequence 3. The highstand deposits of this small-scale sequence are strongly reduced and represented by the marl interval above the maximum-flooding surface.

The sequence boundary and the transgressive surface of small-scale sequence 4 are situated at the base of the following massive bed. Three elementary sequences and parts of a fourth elementary sequence have been identified within the bed succession at the top of this section. They have been deposited during a

rising relative sea level reflected by an opening of the depositional system.

#### 4.6.7 Lavans

The Lavans section was first described by DÉTRAZ & MOJON (1989) and MOJON (1989). Besides a rough lithological log, the study of MOJON (2002) presents a detailed palaeontological investigation of this section.

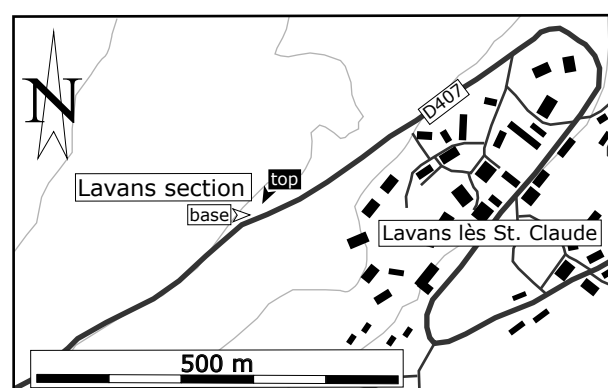


Fig. 4.20 - Location of the Lavans section.

#### *Geographic and stratigraphic setting*

The section outcrops along the road D470 about 400 meters away from the first crossroads at the western exit of the village of Lavans lès St. Claude (Fig. 4.20). The exposure of the outcrop is excellent because of a small cliff with subhorizontally-orientated beds (cf. Fig. 4.22). This orientation allows a lateral comparison of the beds (thickness variations) of over a lateral distance of 100 meters. The section has been logged at the end of the outcrop (up the road) where the beds are more easily accessible (coordinates 864.350/2159.600 IGN map, 1/25000, 3327OT St. Claude). Besides the lateral extent of the beds (Fig. 4.22), this section is characterized by a number of well-expressed bed surfaces and by the absence of major tectonic disturbances. The section is dated by MOJON (2002) and ranges from the charophyte-ostracode assemblage zones M2 to M4.

#### *Sedimentological interpretation* (Fig. 4.21a-c)

The top of the Goldberg Formation generally consists of tidal flat deposits. Partly, tidal flat pond sediments have been identified (at 0.10 and at 0.70

meters). An initial increasing of marine influence is indicated by the deposition of foraminifera, dasyclad algae, and echinoderms (from 1.70 to 2.10 meters). At the top of the Goldberg Formation a thin mud interval (at 2.10 meters) has been dated by MOJON (2002). It belongs to the biozone M4. Some new ostracode and gastropod species collected in this interval have been described and defined by MOJON (2002).

The deposition of a massive, ooid-rich pack- to grainstone interpreted as restricted, internal-lagoonal deposits marks the boundary between the Goldberg and the Pierre Châtel Formation. A mud- to wackestone interval overlies this bed. It is interpreted as freshwater pond deposits with seasonally brackish to hypersaline conditions (presence of charophyte stems together with evaporite pseudomorphs; at 2.30 meters). High-energy conditions prevailed during the deposition of the following massive, ooid-rich pack- to grainstone. It reflects a remarkable increase of accommodation space. A decrease of accommodation then caused the deposition of internal-lagoonal to tidal flat sediments. The nodular mud- to wackestone interval is interpreted as freshwater pond deposits (from 2.65 to 2.90 meters).

The following nodular bed contains internal-lagoonal sediments, which have been deposited during an opening of the depositional system. It is capped by a massive, ooid-rich pack- to grainstone within a restricted, internal-lagoonal setting. High-energy conditions of an internal-lagoonal environment dominate the following, nodular succession (from 3.35 to 3.65 meters). Reworking and the deposition of internal- to open-lagoonal sediments at the base of an interval with big nodules mark a further increase of accommodation (from 3.65 to 4.80 meters). No facies change can be observed within this nodular interval.

A succession of high-energy, internal-lagoonal deposits interpreted as fossil shoal deposits (low-angle cross-bedding structures; cf. Pl. 9/3) caps the nodular interval (from 4.80 to 5.85 meters). An opening of the depositional system is displayed by the floatstone interval at the top of the shoal succession. An environmental change to high-energy, internal- to open-lagoonal deposits at the base of a massive, thick bed displays a slight decrease of accommodation space (at 6.00 meters). A transition to open-lagoonal deposits within this thick bed is interpreted as a gradual opening of the depositional system.

The stratigraphically overlying marl interval of internal- to open-lagoonal composition indicates a loss of accommodation space (from 7.25 to 7.50 meters). A deepening of the depositional system is marked by a change to a nodular floatstone interval (from 7.50

to 7.70 meters). The further deepening trend of the depositional system is indicated by the succession of massive open-lagoonal deposits up to the top of the section. This trend is interrupted by a marl interval of internal- to open-lagoonal composition (from 8.95 to 9.15 meters). It probably reflects a slight decrease of accommodation space superimposed on a general opening trend of the depositional system.

#### *Sequence-stratigraphical interpretation* (Fig. 4.21a-c)

Charophyte-ostracode assemblages give evidence that the top of the Goldberg Formation corresponds to the 3<sup>rd</sup>-order sequence boundary Be4 (according to HARDENBOL et. al. 1998). The pinch out of the thin marl interval at the top of the Goldberg Formation probably points to a slight palaeorelief caused by exposure and/or erosion during the sequence boundary Be4.

Small-scale sequence 1 is composed of four elementary sequences. Based on the correlation with other sections, it is assumed that the first elementary sequence of this small-scale sequence is missing. The base of the ooid-rich pack- to grainstone is considered as boundary between the Goldberg and the Pierre Châtel Formation. A rise in relative sea level caused the deposition of the two massive ooid-rich beds. Each of them is interpreted as an elementary sequence (second and third one). Based on lateral correlation, it is assumed that the maximum flooding of this small-scale sequence lies in the second massive bed. A drop of relative sea level probably led to the deposition of tidal flat deposits represented by the following massive bed (fourth elementary sequence). The freshwater deposits reflect emersion during a pronounced fall of relative sea level and build up the fifth elementary sequence.

The sequence boundary of small-scale sequence 2 is set at the top of the emersive interval. A rise of relative sea level caused the deposition of internal-lagoonal deposits (nodular bed). This bed probably represents the first elementary sequence of this small-scale sequence. The sequence-stratigraphical interpretation of the following bed succession is not straightforward because characteristic facies changes are lacking. It is assumed that this small-scale sequence comprehends at least four elementary sequences. This assumption is based on lateral correlations (cf. Chap. 6).

It is supposed that during a rising relative sea level, shoal successions have been deposited. According to this assumption, the base of this shoal succession marks the transgressive surface of small-scale sequence 3. The sequence-stratigraphical interpretation of the shoal succession is not evident because they have

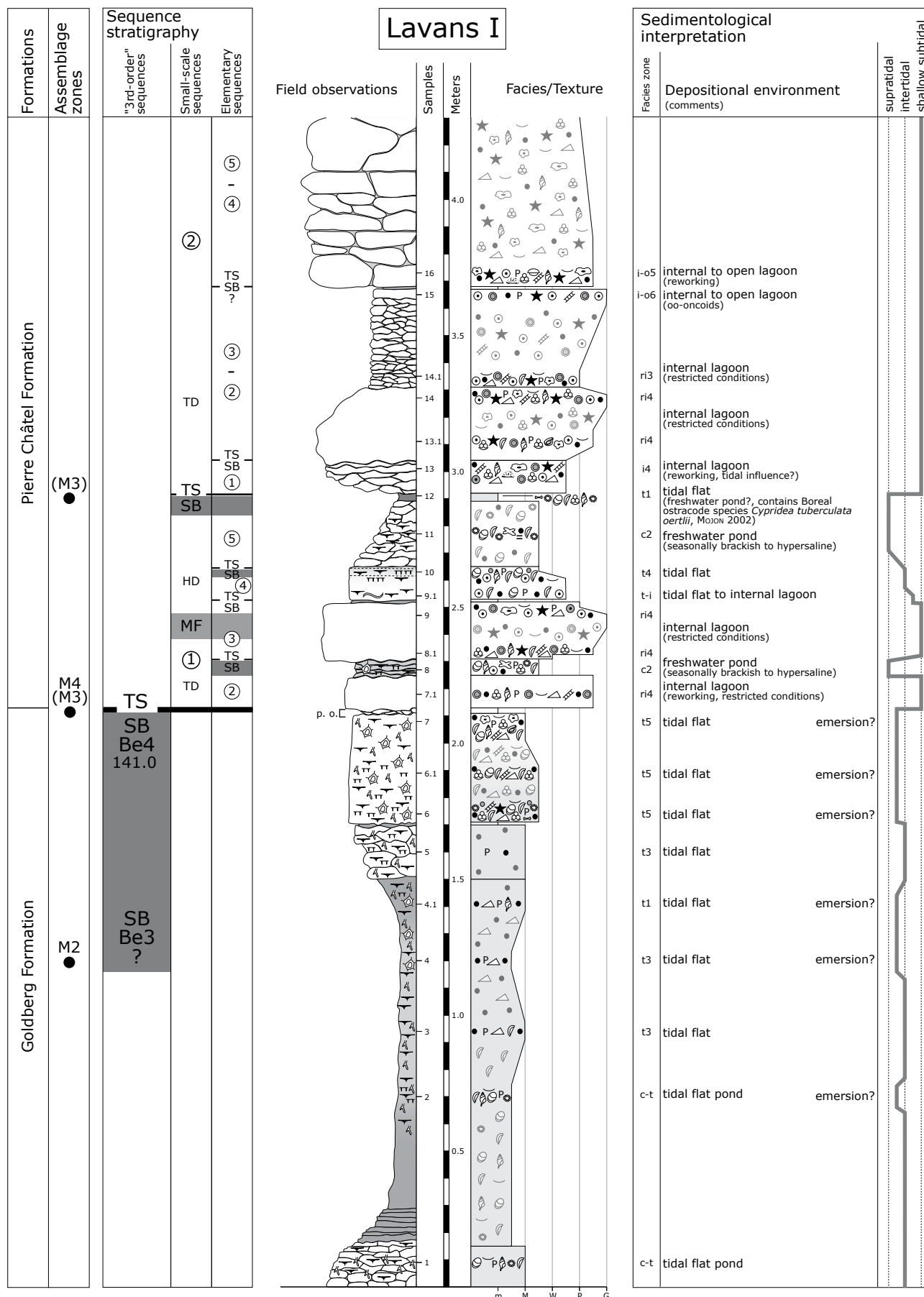
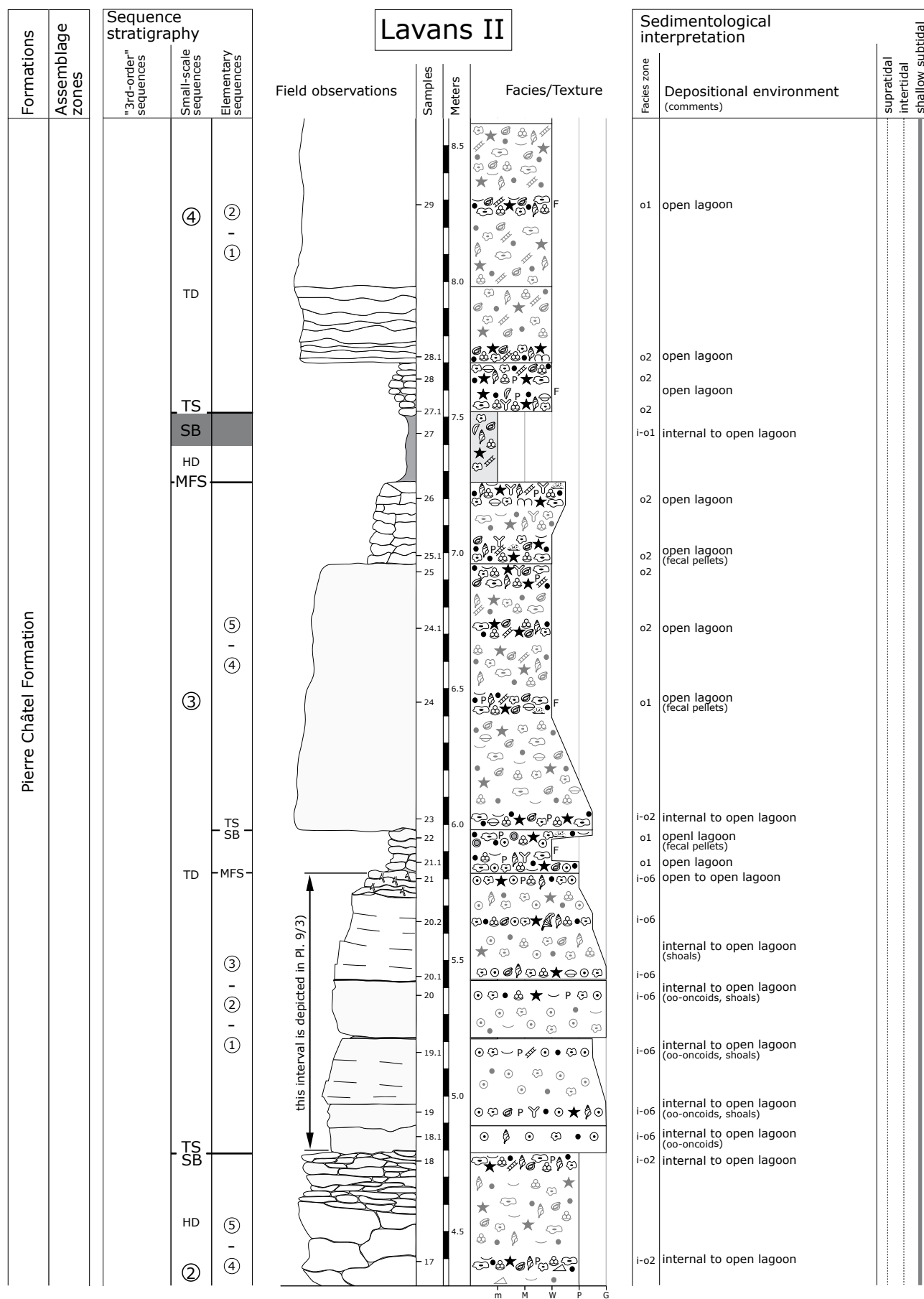


Fig. 4.21a - Lavans section (part I).



**Fig. 4.21b** - Lavans section (part II).

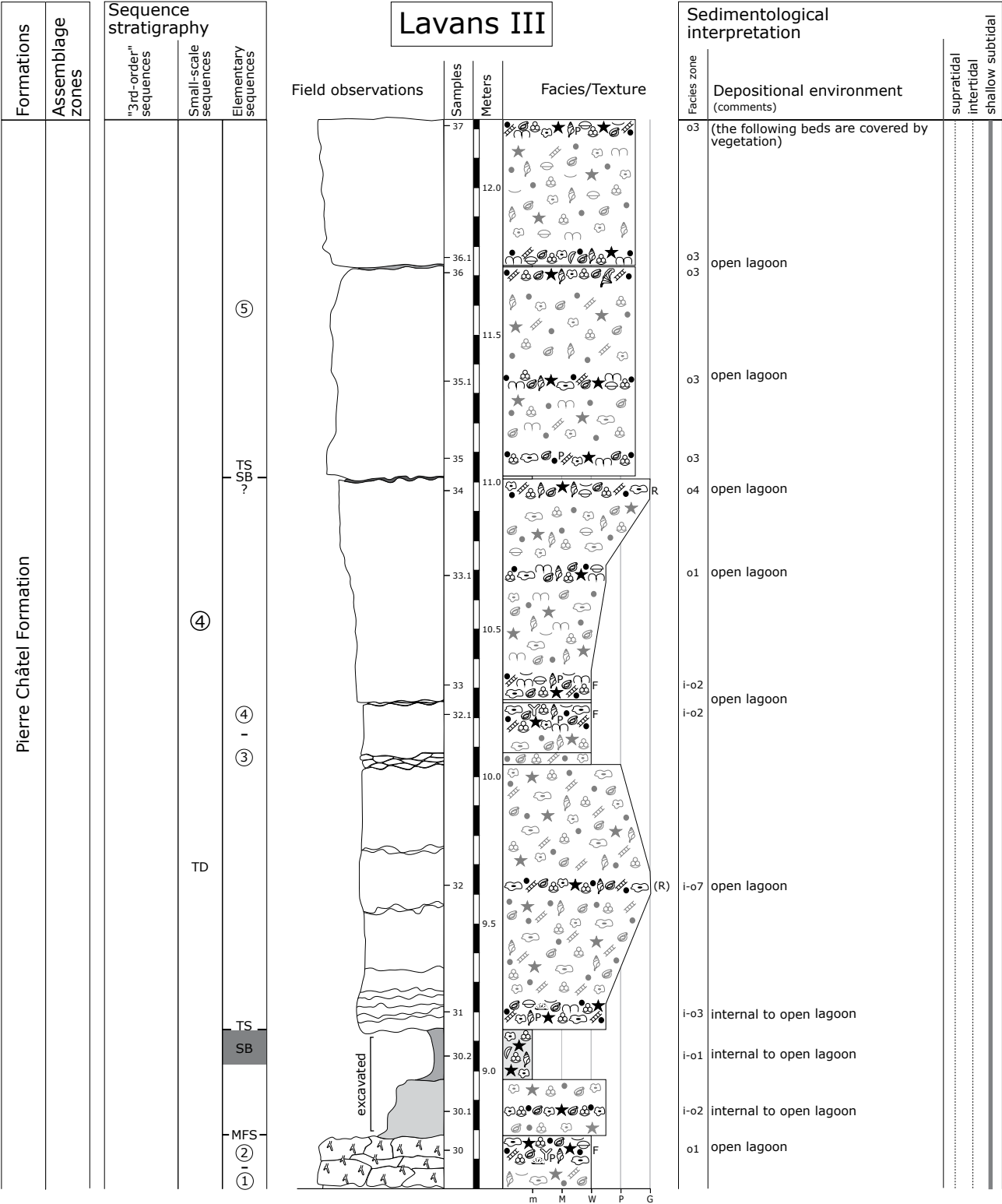


Fig. 4.21c - Lavans section (part III).

mainly been controlled by autocyclic processes. Considering lateral correlations, they contain up to three elementary sequences. The floatstone interval at the top of the shoal succession probably reflects condensation during rising relative sea level. The facies

change towards internal- to open-lagoonal deposits at the base of the massive, thick bed is considered as a slight decrease of relative sea level. It is interpreted as sequence boundary of the fourth (third?) elementary sequence. The discontinuity at the base of the marl



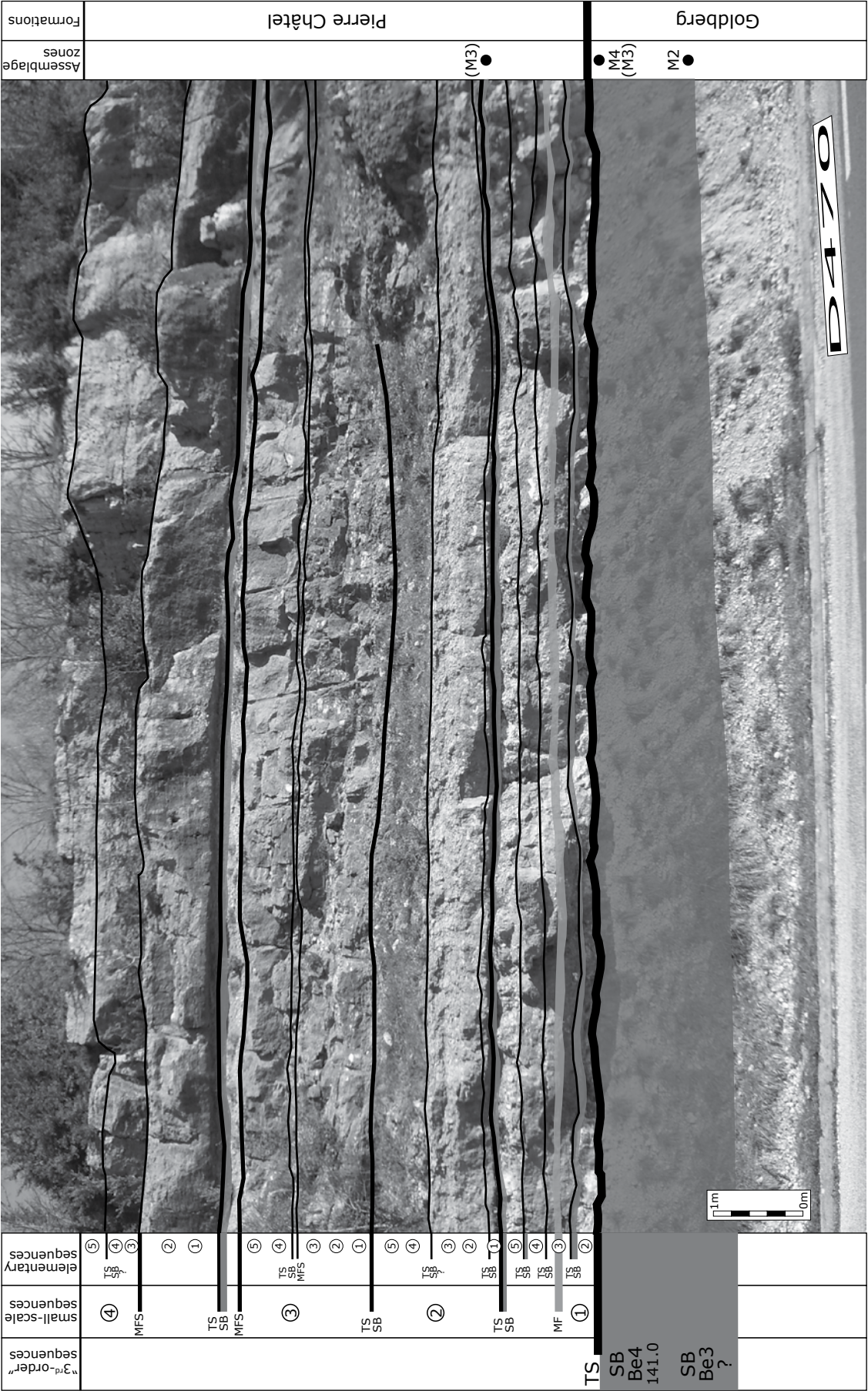


Fig. 4.22 - Outcrop of the Lavans section along the road D470 interpreted in terms of high-resolution sequence stratigraphy (3<sup>rd</sup>-order sequence stratigraphy according to HARDENBOI et al. 1998; assemblage zones according to MOIEN 2002).

interval is considered as maximum-flooding surface of small-scale sequence 3.

A decrease of relative sea level caused the deposition of the marl interval (internal- to open-lagoonal deposits). It is taken as sequence boundary at the base of small-scale sequence 4. Continuing opening and deepening of the depositional system up to the top of the section complicate the sequence-stratigraphical interpretation of this small-scale sequence. This is due to the absence of threshold effects, so that low-amplitude sea level fluctuations were not recorded. Fig. 4.22 shows the Lavans outcrop interpreted in terms of high-resolution sequence stratigraphy as discussed above.

#### 4.6.8 Thoirette

The Goldberg Formation of the Thoirette section was described and correlated with other Jura platform sections by STRASSER (1988). A first sequence-stratigraphical interpretation has been established by WAEHRY (1989).

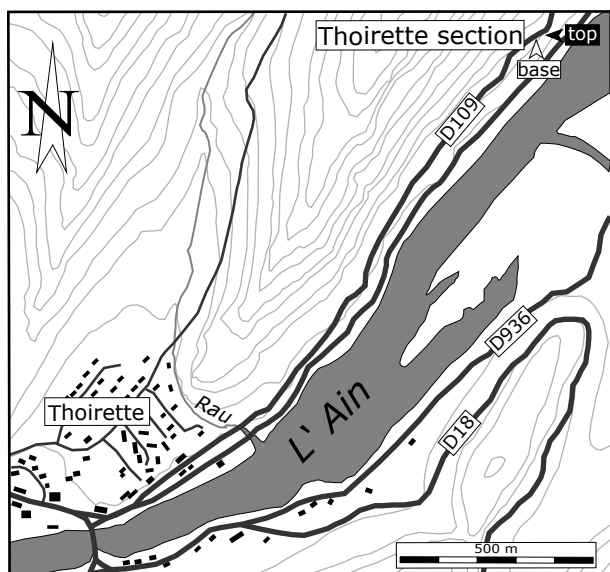


Fig. 4.23 - Location of the Thoirette section.

#### Geographic and stratigraphic setting

The section outcrops along the road D109 about 1100 meters from the river junction of the small tributary Rau and the river Ain on the east side of the village Thoirette (coordinates 847.650/2147.300, IGN map, 1/25000, 3228OT Oyonnaz, Fig. 4.23). The outcrop is situated along a dangerous road curve. Unfortunately, the Pierre Châtel Formation of the section is covered by a protection net, which complicates the field work.

The top of the Goldberg Formation has been dated by MOJON (2002). It lies in the charophyte-ostracode assemblages zone M1b to M2.

#### Sedimentological interpretation (Fig. 4.24a-b)

The top of the Goldberg Formation consists in general of tidal flat deposits. A discontinuity with a slightly undulating micro-relief is interpreted as a karst surface (at 1.90 meters). The nodular marl interval at the top of the Goldberg Formation has been dated by MOJON (2002) and lies in the assemblage zone M1b to M2. A karst surface at the base of the first massive bed points to an extended period of emersion (at 2.60 meters).

The karst surface is capped by tidal flat deposits, marking the boundary between the Goldberg and the Pierre Châtel Formation (at 2.60 meters). This facies change is related to a deepening of the depositional system. The top of this bed is characterized by a karst surface developed during emersion by a pronounced loss of accommodation space (at 3.05 meters).

Reworking and a facies change to internal-lagoonal sediments display a deepening of the depositional environment during the deposition of the following three massive beds. At the top of this bed succession, internal- to open-lagoonal sediments have been deposited (from 3.80 to 4.05 meters). They are interpreted to reflect a slight opening of the depositional system. A change to an open-lagoonal environment gives evidence for a further opening of the system (from 4.05 to 4.25 meters). The deposition of internal- to open-lagoonal facies is probably caused by a slight decrease of accommodation space (at 4.75 meters). A nodular, strongly bioturbated interval is capped by an oyster-rich hardground (at 5.80 meters). It points to condensation during a deepening of the depositional system.

The floatstone interval at the base of the following thick, massive bed is composed of internal- to open-lagoonal constituents pointing to a slight decrease of accommodation space. The deposition of the thick, massive bed at the top of the section occurred during a further deepening of the depositional environment (thickening-up). The following beds are covered by vegetation and have not been investigated.

#### Sequence-stratigraphical interpretation (Fig. 4.24a-b)

The dating by charophyte-ostracode assemblages of the nodular marl interval at the top of the Goldberg Formation indicates that it corresponds to the 3<sup>rd</sup>-order sequence boundary Be4 (according to HARDENBOL

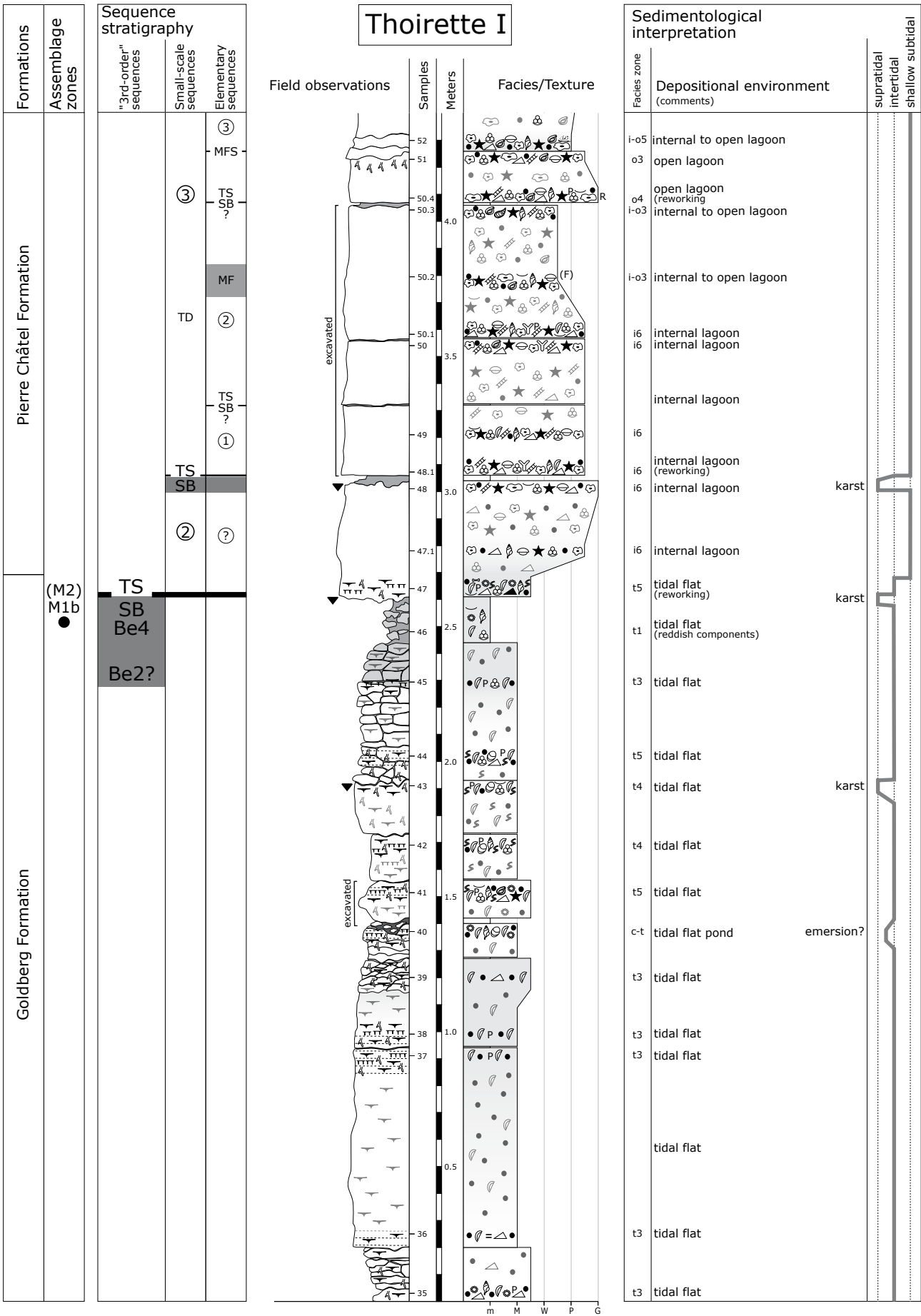
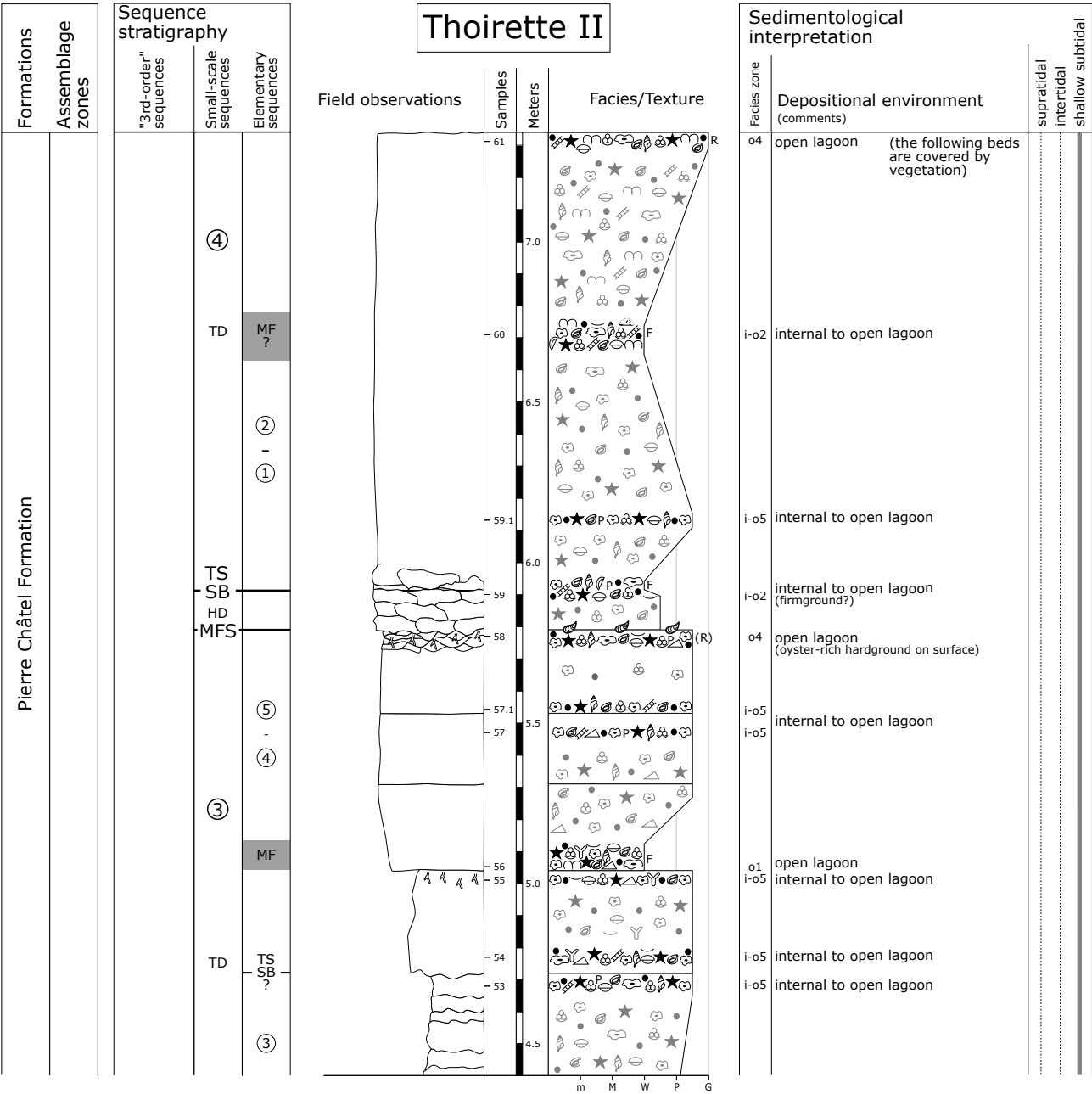


Fig. 4.24a - Thoirette section (part I).





**Fig. 4.24b** - Thoirette section (part II).

et al. 1998). Comparing the facies evolution and the stacking pattern of this section with other sections, it is assumed that the deposits of the Thoirette section correspond to the bed succession of small-scale sequences 2 to 4. Moreover, it is suggested that during the 3<sup>rd</sup>-order sequence boundary Be4, a remarkable palaeomorphology of the carbonate platform developed by erosion and karstification in the region of the Thoirette section (karst surface at the base of the first massive bed; cf. Chap. 9). Consequently, the first massive bed at the base of the Pierre Châtel Formation represents parts of small-scale sequence 2, which have been deposited during a rise of relative sea level. This

assumption is supported by the similarity of the facies evolution and the stacking pattern when compared with other sections (cf. Chap. 6).

The karst surface at the top of the first massive bed is considered as sequence boundary at the base of small-scale sequence 3. This sequence comprehends at least three elementary sequences. A rise in relative sea level is marked by reworked clasts and the deposition of internal-lagoonal sediments at the base of the following massive bed. By means of lateral correlation, it is supposed that the first massive beds at the base of this small-scale sequence comprise two elementary sequences. The sequence-stratigraphical

interpretation of the following bed succession up to the oyster-rich surface is not straightforward. By means of lateral correlation, it is supposed that this succession encloses three elementary sequences. The oyster-rich hardground is interpreted as maximum-flooding surface of small-scale sequence 3.

The sequence boundary and the transgression surface of small-scale sequence 4 are not well marked. It is assumed that the deposition of internal- to open-lagoonal sediments (floatstone interval) is caused by a slight decrease of relative sea level. The massive bed at the top of this section represents the lower part of the transgressive deposits of this small-scale sequence deposited during rising relative sea level.

#### 4.6.9 Poizat

The Goldberg Formation of the Poizat section has been described in different studies (e.g., DONZE 1953, AINARDI 1977, STRASSER & DAVAUD 1983).

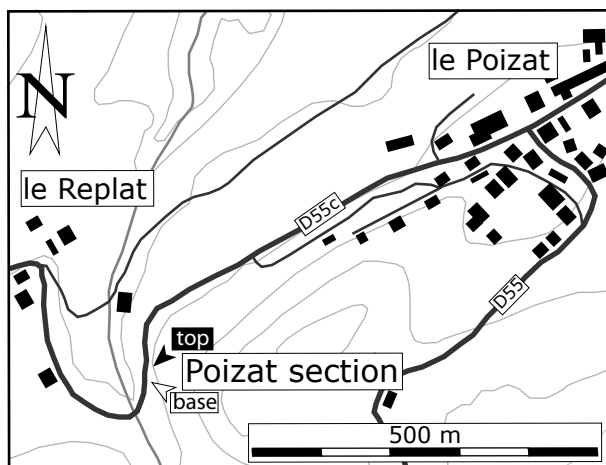


Fig. 4.25 - Location of the Poizat section.

#### *Geographic and stratigraphic setting*

The section outcrops along the road D55c between the small villages of Poizat and of le Replat (cf. Fig. 4.25). The outcrop lies on the eastern side of small valley about 50 meters from a small road bridge (coordinates 858.870/2132.320, IGN map, 1/25000, 32300T Nantua).

The section is partly covered by a protection net, which aggravates the fieldwork. Generally, the section is well exposed and not disturbed tectonically. The upper part of the Goldberg Formation has been dated by MOJON (2002) and lies within the charophyte-ostracode assemblage zones M2.

#### *Sedimentological interpretation* (Fig. 4.26a-c)

The upper part of the Goldberg Formation generally consists of tidal flat deposits. The first part of this section is dominated by marl intervals (from 0.10 to 1.45 meters). The top of the Goldberg Formation comprehends several beds of massive mud- to wackestones separated by thin marl layers. They are interpreted as tidal flat deposits. An interval within this bed succession (at 1.85 meters) has been dated by MOJON (2002). It lies in the assemblage zone M2.

The change to internal-lagoonal deposits at the base of the following massive beds marks the base of the Pierre Châtel Formation. The following bed succession equally consists of internal-lagoonal deposits. They have been deposited during a deepening of the depositional environment.

An interval of high-energy internal-lagoonal sediments displaying low-angle cross-bedding is supposed to have been deposited during a period of increasing accommodation space (from 3.70 to 3.85 meters). A slight opening of the depositional system is indicated by the accumulation of internal- to open-lagoonal sediments (from 3.95 to 4.25 meters). A nodular, bioturbated interval and a marl layer cap the internal- to open-lagoonal bed succession (at 4.30 meters). They point to a further opening of the depositional system and to condensation. The environmental transition from internal-lagoonal to tidally influenced deposits indicates a decrease of accommodation space (from 4.65 to 4.70 meters).

A thin, massive bed (4.70 to 4.80 meters) with microbial mats is supposed to indicate the relatively lowest accommodation space. Slight environmental changes from tidal flat to more internal-lagoonal conditions continue to occur up to the base of two thick beds (at 6.15 meters). An opening of the depositional system is displayed by the following two thick, massive beds consisting of internal-lagoonal deposits. Strong bioturbation has been observed at the top of the second massive bed (from 7.00 to 7.25 meters). This is interpreted as a period of condensation during an increase of accommodation space.

The following bed is characterized by low-angle cross-bedding indicating shoal deposits. They have been deposited during a deepening of the depositional system. The top of the section comprises two massive beds, which are mainly composed of internal- to open-lagoonal deposits.

#### *Sequence-stratigraphical interpretation* (Fig. 4.26a-c)

The dating by charophyte-ostracode assemblages

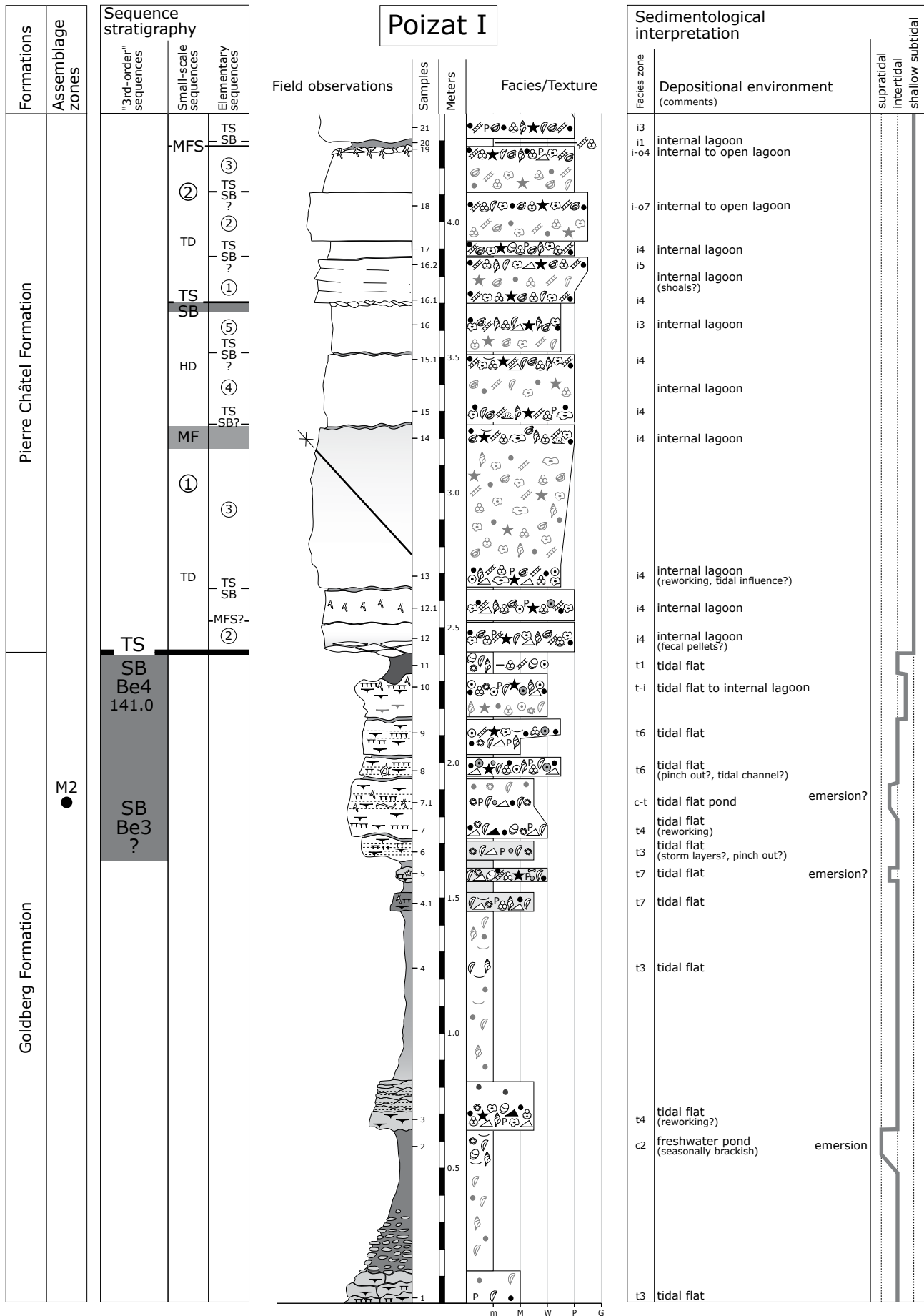


**Fig. 4.26a** - Poizat section (part I).

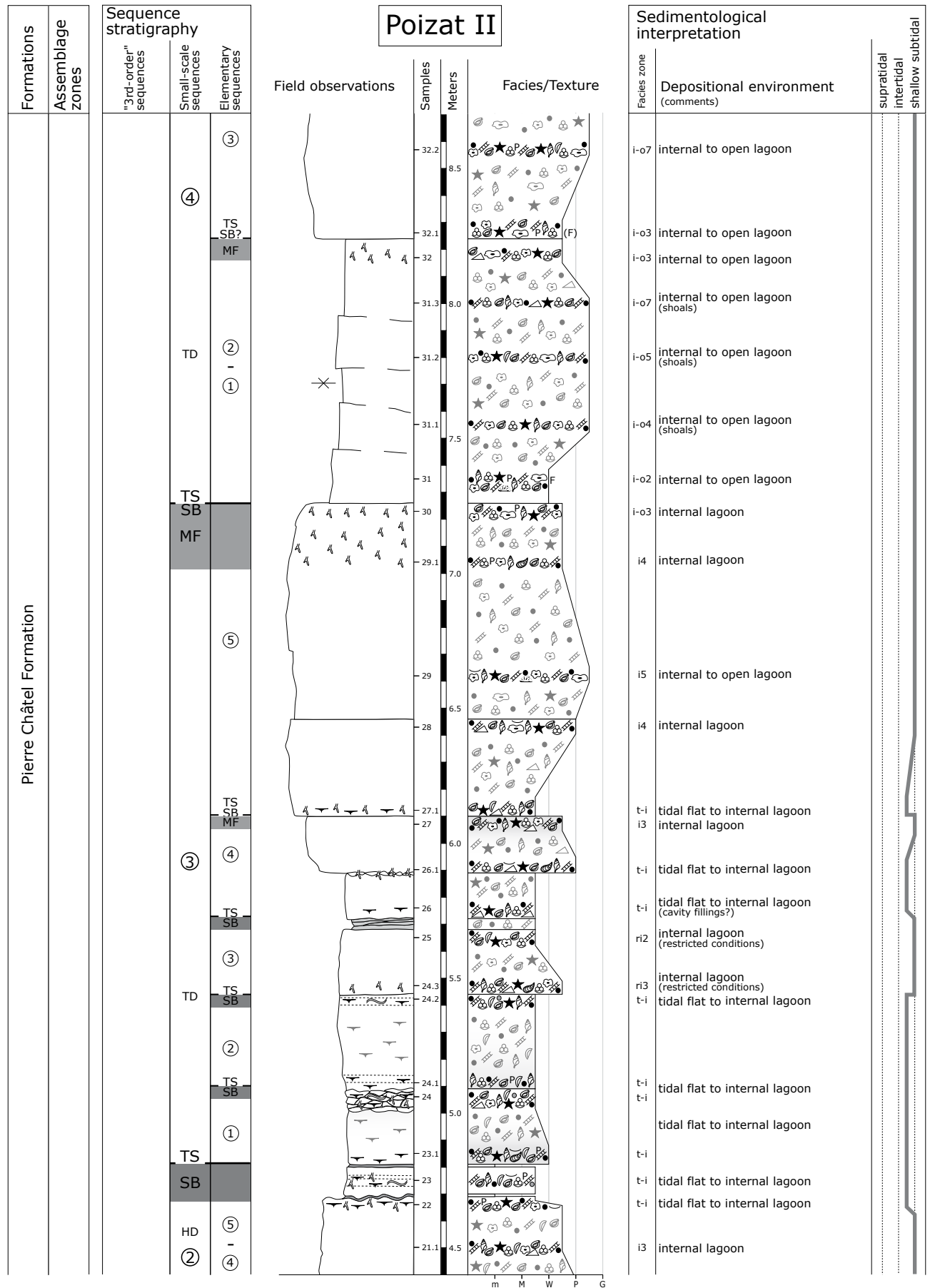


Fig. 4.26b - Poizat section (part II).

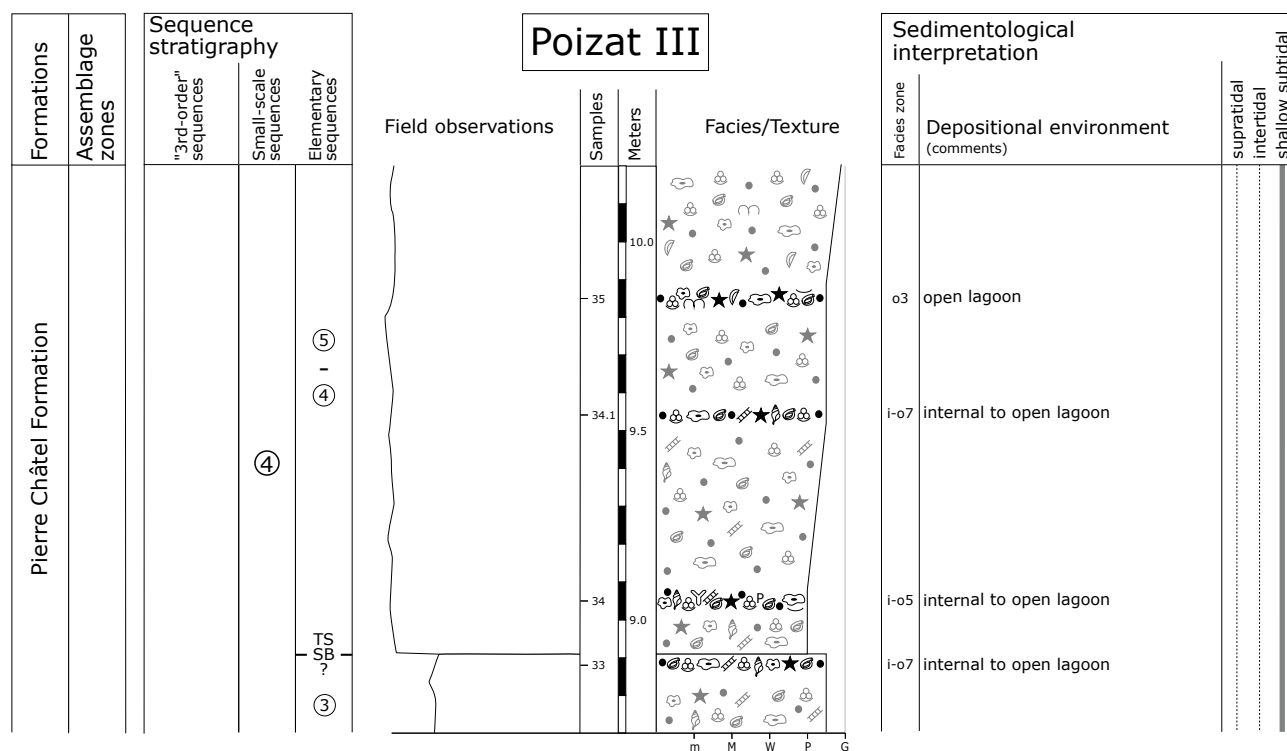


Fig. 4.26c - Poizat section (part III).

gives evidence that the top of the Goldberg Formation corresponds to the 3<sup>rd</sup>-order sequence boundary zone Be3 to Be4 (according to HARDENBOL et. al. 1998).

Based on lateral correlation, it is assumed that the first elementary sequence of small-scale sequence 1 is missing (cf. Chap. 6). The interpretation of elementary sequences within this small-scale sequence is not easy. It is supposed that it comprehends at least three elementary sequences.

The sequence boundary of small-scale sequence 2 is not expressed by a characteristic facies change. The corresponding transgressive surface is placed at the base of the cross-bedded interval, assuming that it marks an initial rise of relative sea level. By means of lateral correlation it is suggested that the transgressive deposits comprise at least two elementary sequences. The discontinuity at the base of the marl layer is considered as maximum-flooding surface of this small-scale sequence. A fall of relative sea level caused the environmental change from internal-lagoonal to tidally-influenced internal-lagoonal deposits. The highstand deposits of small-scale sequence 2 comprehend at least one elementary sequence.

The sequence boundary at the base of small-scale sequence 3 is set within the thin, massive bed with microbial mats. The following succession is characterized by relatively thin beds of tidal flat to internal-lagoonal deposits compared with the other

sections (cf. Chap. 6). This probably points to uplift of this platform location during rising relative sea level. As a consequence, the sequence boundaries on the elementary-sequence scale are generally well-expressed. At least three elementary sequences can be identified within this bed succession. A pronounced rise in relative sea level gives space for the deposition of the two massive beds and an environmental change to internal-lagoonal sediments. The two massive beds are interpreted as deposits of the fifth elementary sequence. The discontinuity at the top of the bioturbated interval is interpreted as maximum flooding of small-scale sequence 3. Highstand deposits are strongly reduced and/or absent.

The sequence boundary and the transgressive surface of small-scale sequence 4 are supposed to be amalgamated at the base of the shoal interval, which has been deposited during a rise of relative sea level. The top of the section is characterized by a further opening of the depositional system during rising relative sea level.

#### 4.6.10 Val de Fier

The Goldberg Formation of this section has been described in several studies (e.g., MOUTY 1966, STRASSER 1988, 1994). WAEHRY (1989) interpreted the top of the



Goldberg and the Pierre Châtel Formation in terms of sequence stratigraphy. A detailed palaeontological investigation of the Goldberg Formation has been published by MOJON (2002).

### *Geographic and stratigraphic setting*

The Val de Fier section is situated in the canyon of the Fier river (cf. Fig. 4.27). The road D14, which winds through this canyon, leads to the outcrop. Upriver, behind a small road tunnel, the first part of an active quarry (S.A.R.L. Caretti S.A.) can be seen on the left side of the road. Behind a sharp curve a second part of this quarry appears. The lower part of the section has been logged in the second part of the quarry. About 30 meters above the road behind the garage of the company, the Goldberg Formation and the first beds of the Pierre Châtel Formation outcrop (coordinates 872.925/2109.700, IGN map, 1/25000, 3331OT Rumilly-Seyssel). Parts of the Goldberg Formation are tectonically disturbed. The top of the section has been logged along the road curve between the two parts of the quarry (going downriver). The section has been dated by MOJON (2002) and ranges from the charophyte-ostracode assemblage zones M3 to M4.

### *Sedimentological interpretation* (Fig. 4.28a-c)

A succession of mud- to wacke-packstones interrupted by a marl interval characterizes the top of the Goldberg Formation. They generally consist of tidal flat deposits. Two small reverse faults cut the mudstone interval at the base of the section. The grayish-greenish marl interval at the top of the mudstones is interpreted as tidal flat deposits. It lies in the assemblage zone M3 (according to MOJON 2002). The top of the Goldberg Formation is marked by a light-brownish marl layer considered as tidal flat sediments. MOJON (2002) determined ostracodes from this level. It lies in the assemblage zone M4.

A slight opening of the depositional system is indicated by an environmental change to internal-lagoon deposits at the base of the first massive bed. It marks the boundary between the Goldberg and the Pierre Châtel Formation. The base of the Pierre Châtel Formation comprehends four relatively thin, massive beds composed of internal-lagoon sediments.

A reddish surface with desiccation cracks marks emersion during a shallowing at the top of the fourth massive bed (at 3.55 meters). The following bed

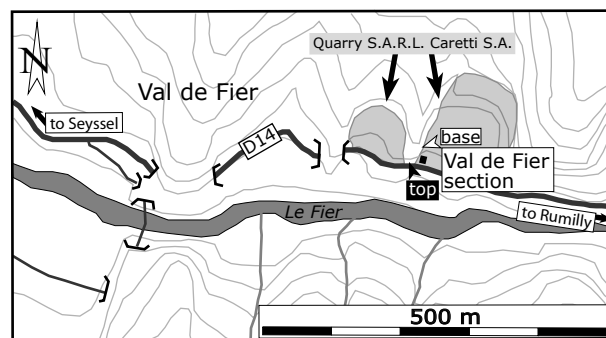


Fig. 4.27 - Location of the Val de Fier section.

succession is characterized by two thick, massive beds (from 3.55 to 7.90 meters). They have been deposited during a deepening of the depositional system. The transition to open-lagoonal deposits at the top of the second thick bed points to a slight deepening of the depositional environment. It is overlain by a nodular interval, which weathers back in the outcrop (from 7.90 to 8.45 meters). Two samples (taken at the base and top of this interval) indicate deposits of an internal- to open-lagoonal environment. The nodules probably point to bioturbation. The following bed succession is composed of internal- to open-lagoonal sedimentary rocks.

### *Sequence-stratigraphical interpretation* (Fig. 4.28a-c)

The dating by charophyte-ostracode assemblages gives evidence that the top of the Goldberg Formation corresponds to the 3<sup>rd</sup>-order sequence boundary Be4 (HARDENBOL et. al. 1998).

An initial rise of relative sea level is marked at the base of the four beds of the Pierre Châtel Formation. Based on lateral correlation, they are interpreted as deposits of small-scale sequence 2. A sequence-stratigraphical interpretation on the elementary sequence scale is not easy. It is assumed that this small-scale sequence comprehends up to three elementary sequences.

The sequence boundary at the base small-scale sequence 3 is marked by the reddish emersion interval. The following two thick, massive beds have been deposited during rising relative sea level. They are interpreted as the transgressive deposits of this small-scale sequence. The interpretation of elementary sequences is not straightforward because characteristic facies changes are missing. The maximum flooding of small-scale sequence 3 is marked by the deposition of open-lagoonal sediments at the top of the second massive bed.

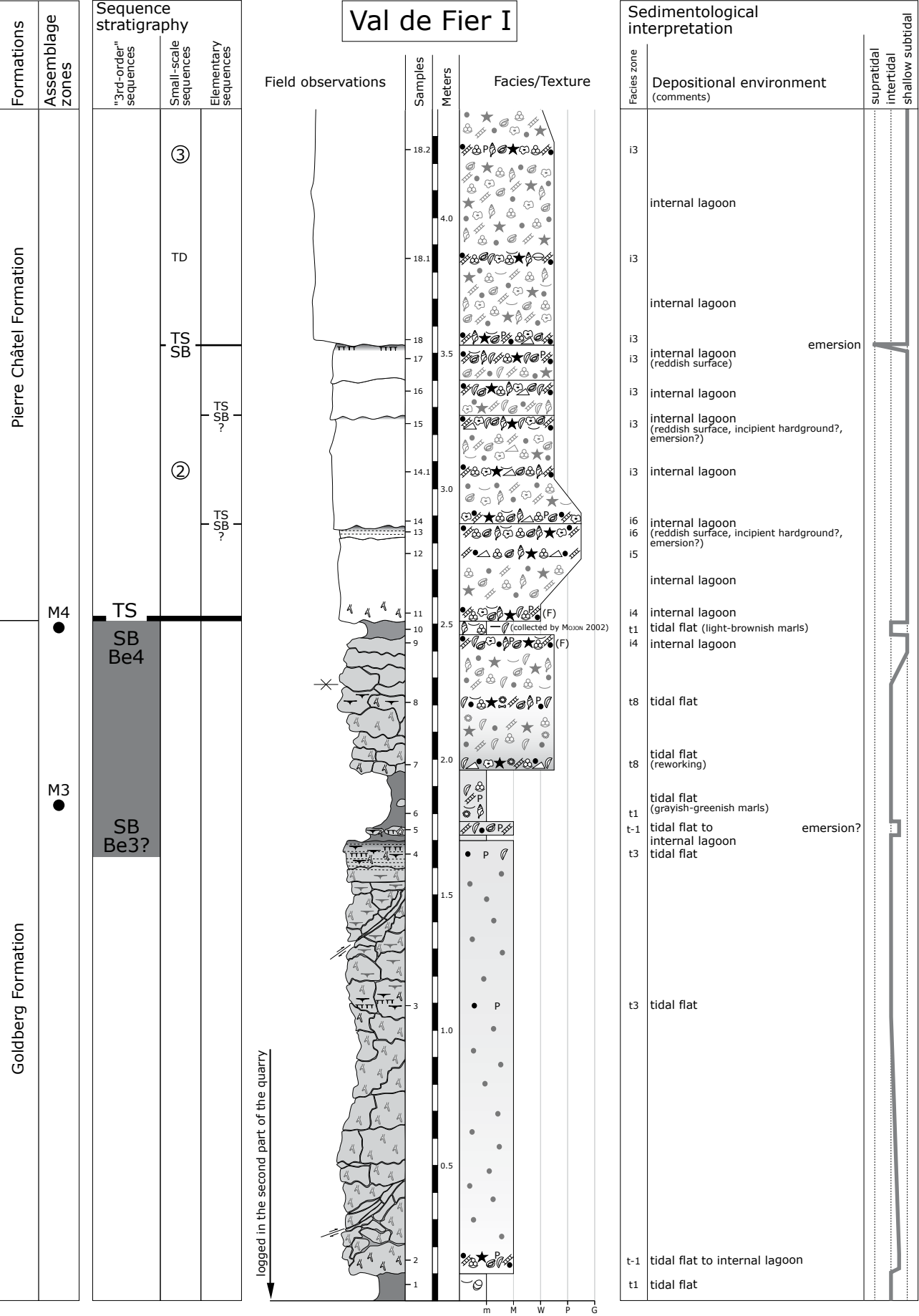
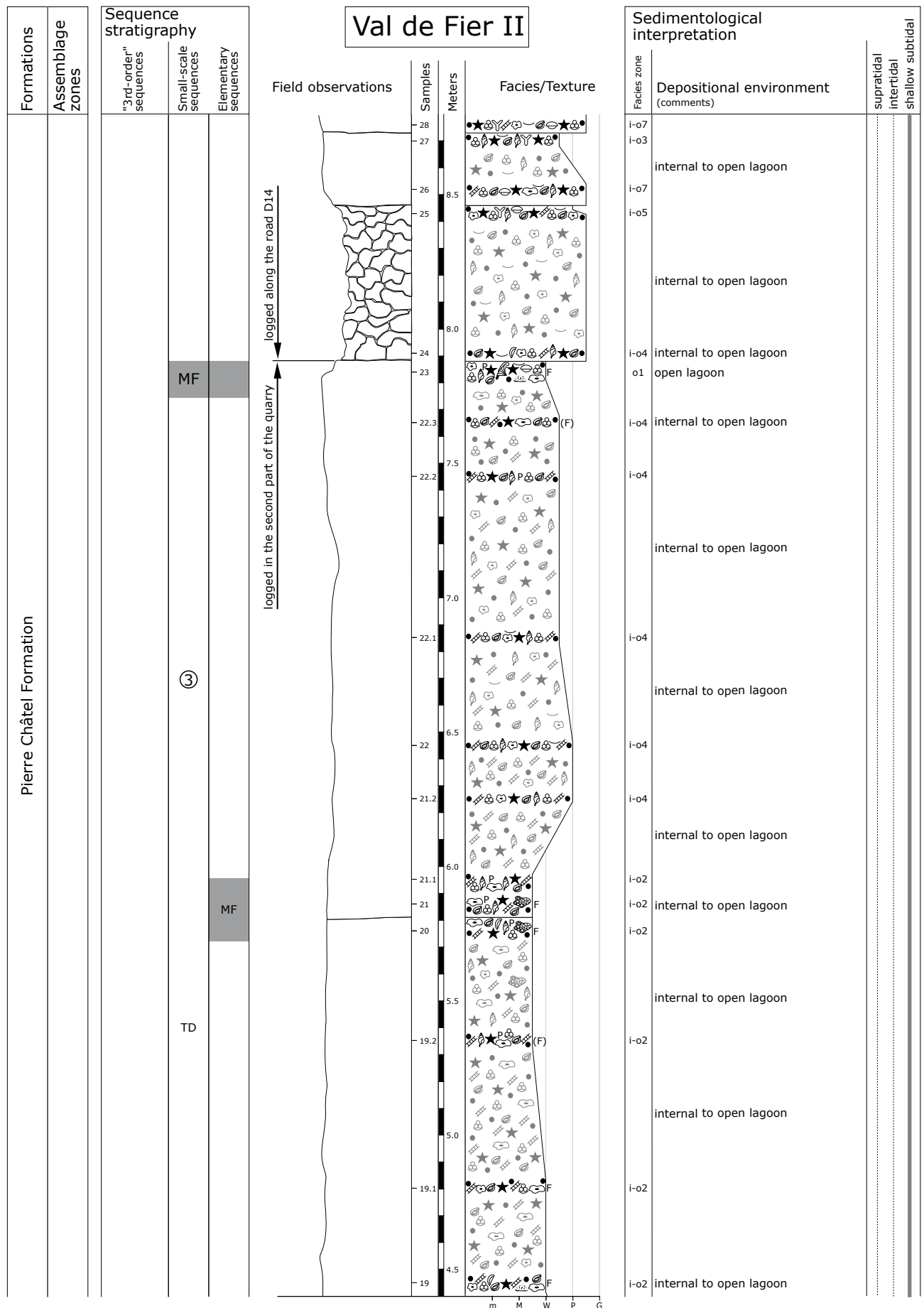


Fig. 4.28a - Val de Fier section (part I).



**Fig. 4.28b** - Val de Fier section (part II).

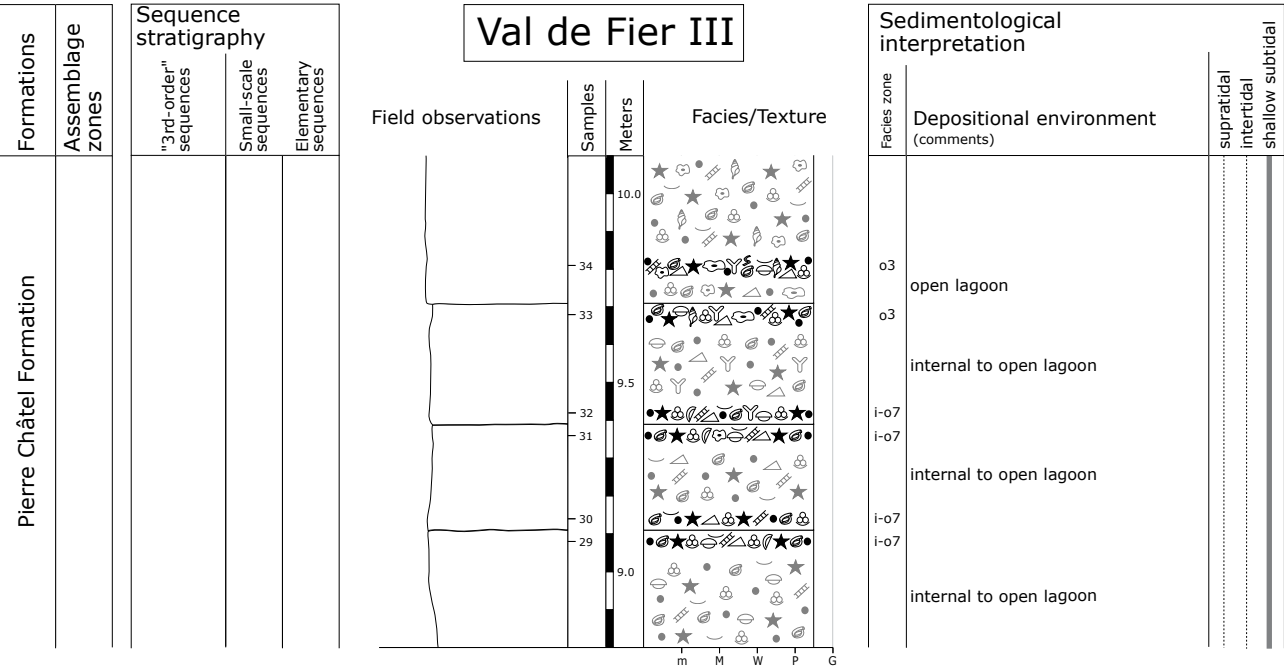


Fig. 4.28c - Val de Fier section (part III).

A sequence-stratigraphical interpretation of the following bed succession is hampered because of the absence of characteristic facies changes.

4.6.11 Yenne

The Goldberg Formation of this section is described and interpreted in terms of sequence stratigraphy in different studies (e.g.; WAEHRY 1989, STRASSER 1994). A detailed sequence-stratigraphical interpretation of the Late Tithonian to Middle Berriasian deposits of this section has been published by RAMEIL (2005). WAEHRY (1989) made a first sequence-stratigraphical interpretation of the Pierre Châtel Formation. A detailed palaeontological investigation of the Goldberg

Formation has been published by MOJON (2002).

*Geographic and stratigraphic setting*

The section is situated in a steep valley on the left side of the river Rhône (Pierre Châtel valley; cf. Fig. 4.29). It outcrops along the national road N504 about 50 meters away from a small road exit (car parking) on the right side in direction to the small town of Yenne (coordinates 865.470/2084.050, IGN map, 1/25000, 3232ET Belley). The section is well accessible because of the steep plunging of the beds along the road. The marly beds of the Goldberg Formation weather back beneath the massive cliffs of the Pierre Châtel Formation. The upper part of the Goldberg Formation is dated by MOJON (2002) and attributed to the charophyte-ostracode assemblage zone M1b.

*Sedimentological interpretation* (Fig. 4.30a-b)

The top of the Goldberg Formation consists of an alternation of marl and mudstone beds interpreted as tidal flat deposits. From the gray-brownish marl interval at 1.00 meters, small calcareous tubes have been collected. They resemble calcified roots of a palaeosol. The marls lie in the assemblage zone M1b (dated with charophytes by MOJON 2002). RAMEIL (2005) postulated that several small-scale sequences are missing at the top of the Goldberg Formation of this section. A bed succession of laminated mudstones with

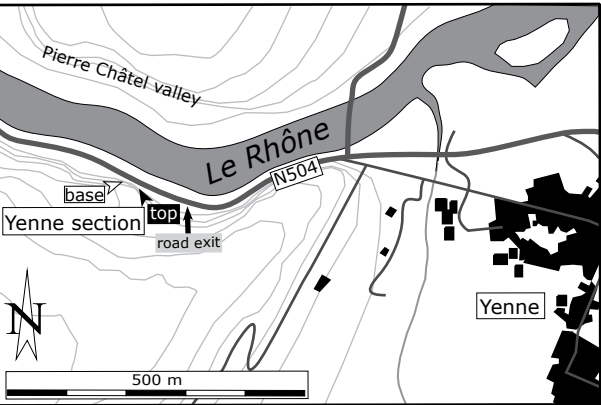
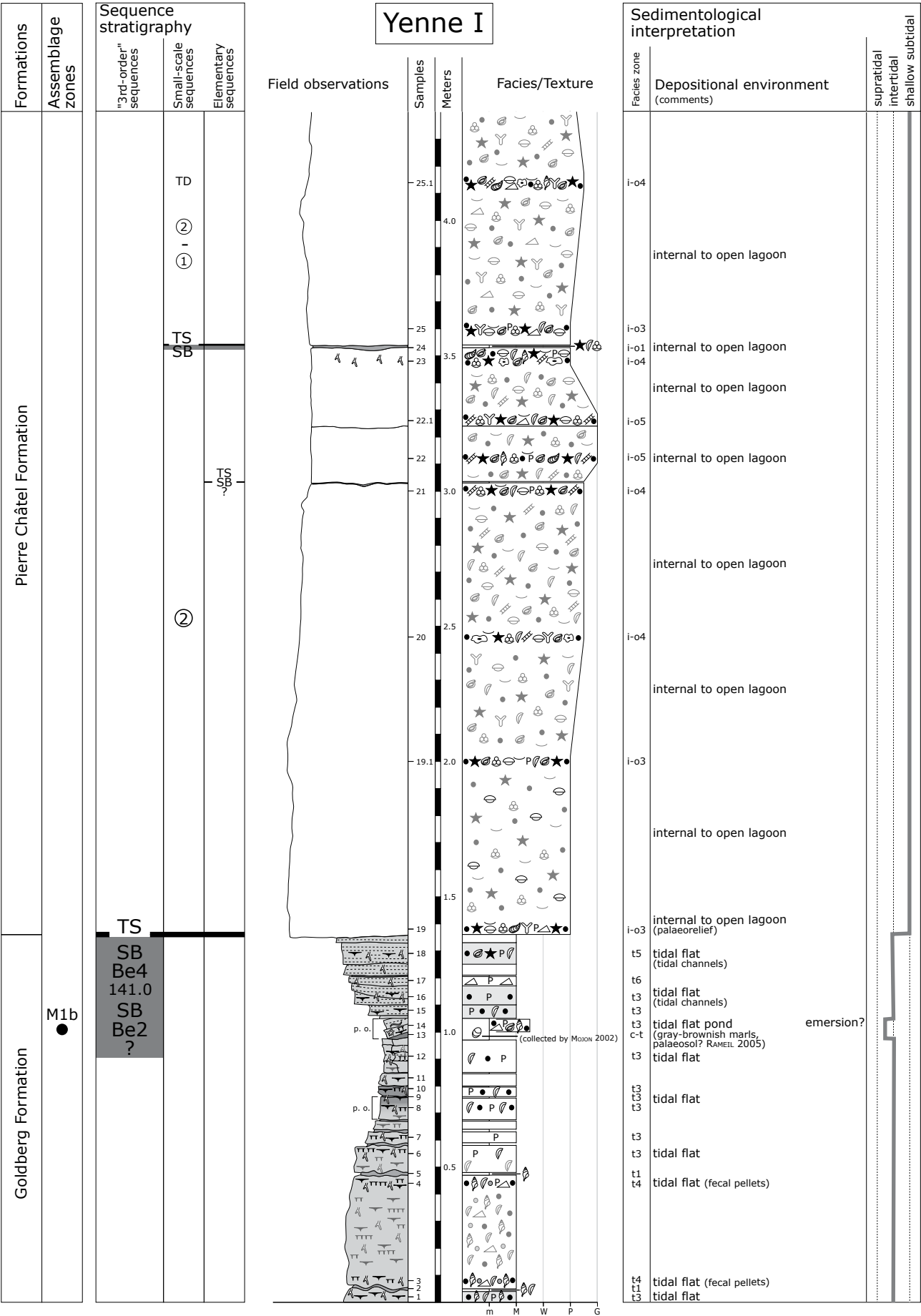


Fig. 4.29 - Location of the Yenne section (modified from RAMEIL 2005).



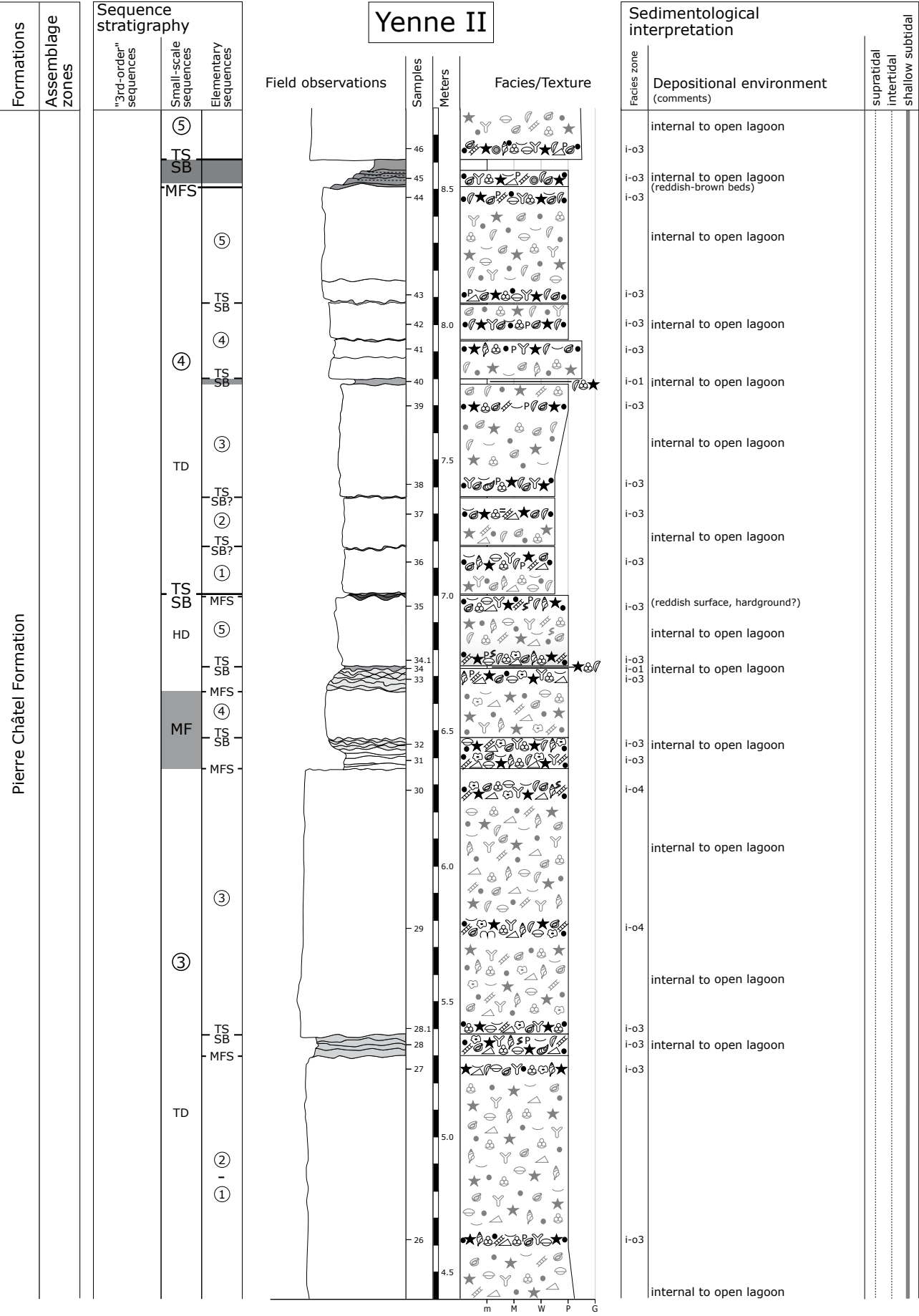


Fig. 4.30b - Yenne section (part II).

laterally varying thickness overlies the marl interval (from 1.05 to 1.35 meters). Sedimentary structures (e.g., oblique bed surfaces, lamination, and birdseyes) point to a succession of tidal channel deposits.

A striking environmental change to massive, internal- to open-lagoonal deposits marks the boundary between the Goldberg and the Pierre Châtel Formation. The first thick, massive bed of the Pierre Châtel Formation displays a slight lateral decrease of thickness (some decimeters) to the west (WAEHRY 1989, and pers. observation). This may indicate a palaeorelief. The relatively reduced thickness of the two beds above the first thick, massive bed probably points to a decreasing accommodation space (from 3.05 to 3.55 meters).

A thin marl layer is considered to reflect a further decrease of accommodation space. Two thick, massive beds follow above the thin marl interval and point to a rapid increase of accommodation space (from 3.55 to 6.35 meters). Between these two beds, a marly, wavy interval probably indicates a slight opening of the depositional environment (at 5.35 meters). Similar marly, wavy intervals occur at the top of the second thick bed and at the top of the following bed (at 6.40 and 6.70 meters). Each of them probably reflects a slight opening of the depositional system.

The top of the following bed is characterized by an irregular, reddish surface capped by a thin marl layer (at 7.00 meters). It is assumed that this interval has been deposited during decreasing accommodation space. The following bed succession consists of relatively thin beds separated by marl layers (from 7.00 to 8.65 meters). A slight opening of the depositional system is displayed at the top of the last massive bed of this succession (at 8.45 meters). This bed is capped by thin reddish-brown, laminated beds and a marl interval. The thin beds contain some superficial ooids, which probably indicate an increase of tidal influence during decreasing accommodation space. Parts of the Pierre Châtel Formation are affected by dedolomitization (RAMEIL 2005). This alteration complicates the facies interpretation of this section.

#### ***Sequence-stratigraphical interpretation*** (Fig. 4.30a-b)

The dating by charophytes gives evidence that

the gray-brownish marl interval possibly corresponds to the 3<sup>rd</sup>-order sequence boundary zone Be2 to Be4 (HARDENBOL et. al. 1998). The sequence-stratigraphical interpretation of the Pierre Châtel Formation is uncertain because of only subtle facies changes. As a consequence, the detailed sequence-stratigraphical interpretation is mainly based on the lateral correlation (cf. Chap. 6).

The base of the thick, massive bed marks the transgressive surface of small-scale sequence 2 and the base of the Pierre Châtel Formation. This interpretation implies that the first small-scale sequence has not been deposited and/or was eroded during the transgression. Elementary sequences have not been identified in this small-scale sequence.

The thin marl layer at the top of first massive bed is interpreted as sequence boundary at the base of small-scale sequence 3. The two thick beds have been deposited during rising relative sea level (transgressive deposits of this small-scale sequence). A slight increase of relative sea level is reflected by the deposition of the marly, wavy interval between the two thick beds. By means of lateral correlation, it probably corresponds to the maximum flooding of the third elementary sequence. A maximum-flooding surface has been identified within each of the following two marly, wavy intervals. They probably reflect slight rises of relative sea level on the elementary sequence scale (fourth and fifth elementary sequences). The interval between these two maximum-flooding surfaces is considered as a maximum-flooding zone of small-scale sequence 3.

A fall of the relative sea level led to the formation of the reddish surface and the thin marl layer. They are interpreted as sequence boundary of small-scale sequence 4. The following succession of relatively thin beds represents the transgressive deposits of this small-scale sequence. Each of the first three massive beds capped by thin marl layers, are interpreted as elementary sequences (first, second and third elementary sequences). Yet, the fourth and the fifth elementary sequences are probably composed of several thin beds. The discontinuity at the top of this bed succession is interpreted as maximum-flooding surface of small-scale sequence 4. The thin, reddish-brown beds and the marl interval indicate a falling relative sea level. This interval is interpreted as sequence boundary of small-scale sequence 5.

\*\*\*\*\*





## 5 - SECTIONS OF THE DORSET REGION

An extensive literature exists on studies of the Purbeckian deposits (*sensu anglico*). These publications mainly concentrate on sedimentological and palaeontological aspects of Purbeckian outcrops in southern England (Isle of Purbeck; e.g., ANDERSON & BAZLEY 1971, MORTER 1984, ANDERSON 1985, ENSOM 1985, CLEMENTS 1993, WESTHEAD & MATHER 1996, MILNER & BATTEN 2002).

The term Purbeckian has formerly been used to describe a geological time interval (Late Jurassic to Early Cretaceous; e.g., CASEY 1973). Nowadays, the time interval of the Purbeckian (Purbeck Limestone Group; see below) ranges from the Late Tithonian to the earliest Valanginian (e.g., ALLEN & WIMBLEDON 1991, JACQUIN *et al.* 1998). The term Purbeck has also been used to describe marginal-marine carbonate deposits, which outcrop along the English Channel coast on the Isle of Purbeck (e.g., BATTEN 2002) and in different mainly European locations corresponding more or less to the Purbeckian time interval (e.g., for the Goldberg Formation of the Jura platform; cf. Chap. 4).

Two sections have been logged and interpreted with high resolution in this study. The high-resolution interpretation is based on field observations and facies analyses (cf. Chap. 2). Notable lithological and palaeontological descriptions of the sections have been published by ENSOM (1985) and CLEMENTS (1993). This chapter concentrates on a high-resolution sequence-stratigraphical interpretation of the two sections. The same criteria have been applied for the selection of these two outcrops as for the Jura platform sections (cf. Chap. 4).

### 5.1 Previous work

In the 18<sup>th</sup> century, the Purbeck limestones south of Swanage have been quarried and mainly sold to London

as street pavements. The nomenclature of the beds derives from the quarry activities of those days. In 1826, Webster used the quarrymen's terms in a publication on the strata of Durlston Bay (ENSOM 2002a). Further investigations on the Durlston Bay outcrop have been made by FORBES (1850, 1851) and by AUSTEN (1952) (citations in ENSOM 2002a). Today's nomenclature is mainly based on publications of BRISTOW (1857, 1884) (in ENSOM 2002a). In 1857, a legendary excavation at Durlston Bay has been undertaken by Mr. S. H. Beckles who made a significant collection of mammal remains from the Purbeck Limestone Group. He systematically searched and investigated the Mammal Bed ("Mammal Pit" excavation; in SALISBURY 2002; Pl. 12/1). The mammal remains from the Durlston Bay then have been described by the eminent vertebrate palaeontologist Sir R. Owen. In 1871, he published the monograph "Fossil Mammalia of the Mesozoic Formations". An excellent historical overview on the Purbeck Limestone Group (mainly based on the Durlston Bay section) is given by WEST (2006). Moreover, other aspects concerning the Purbeck Limestone Group and an exhaustive bibliography are published on this homepage.

### 5.2 Geographic setting

The two sections are located on the English Channel coast of the Isle of Purbeck in Dorset (southern England; Fig. 5.1). Among other things, this coast is famous for its excellent Mesozoic outcrops (BRUNSDEN 2003). Since 2001, the Dorset and East Devon coast has been designated a World Heritage Site by the UNESCO (United Nations Educational, Scientific and Cultural Organization).

The Worbarrow Tout section is situated along the north-western part of the small peninsula Worbarrow

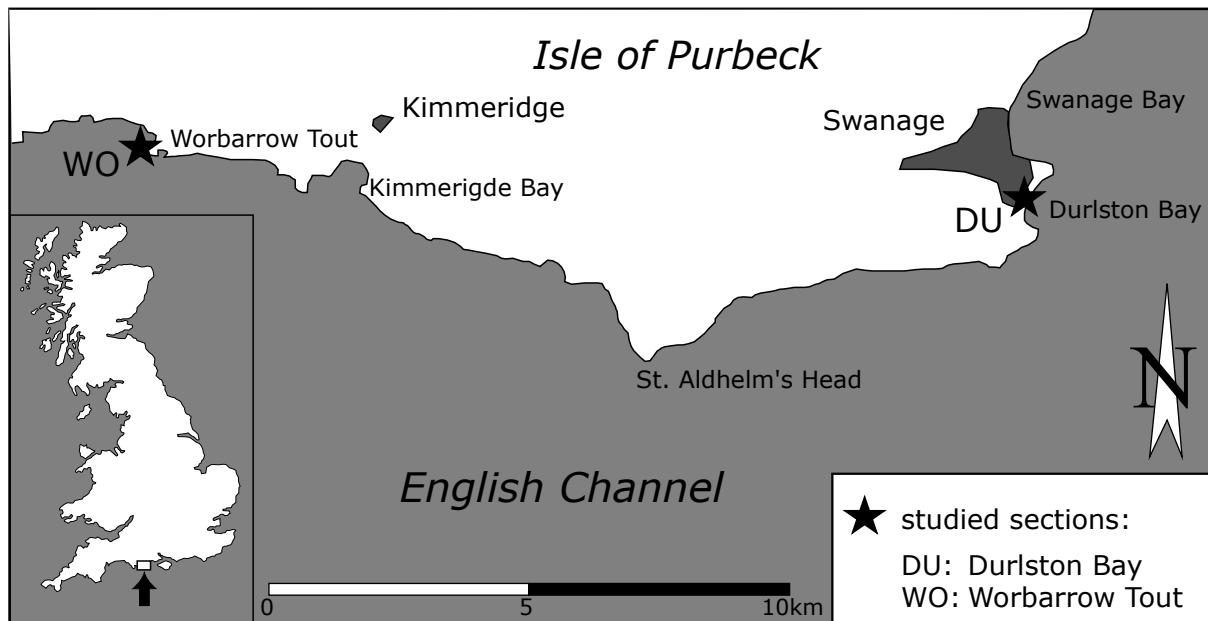


Fig. 5.1 - Location of the two sections studied in Dorset (Isle of Purbeck, southern England).

Tout. The Durlston Bay section outcrops along the coastal cliffs south-east of the seaside resort of Swanage.

### 5.3 Palaeogeography

The Dorset region is situated north of the Wessex

basin in the Channel sub-basin. During the Berriasian, the Wessex basin was in extension (e.g., RUFFELL 1995, UNDERHILL 2002; cf. Fig. 5.2). The extent of the Wessex basin is approximately coincident with its present limits, extending through eastern England, the English Channel, and into northern France (STONELEY 1982). During the Berriasian, it was bounded to the west by the Cornubian-Welsh Massif, to the north and east by the London-Brabant platform, and to the

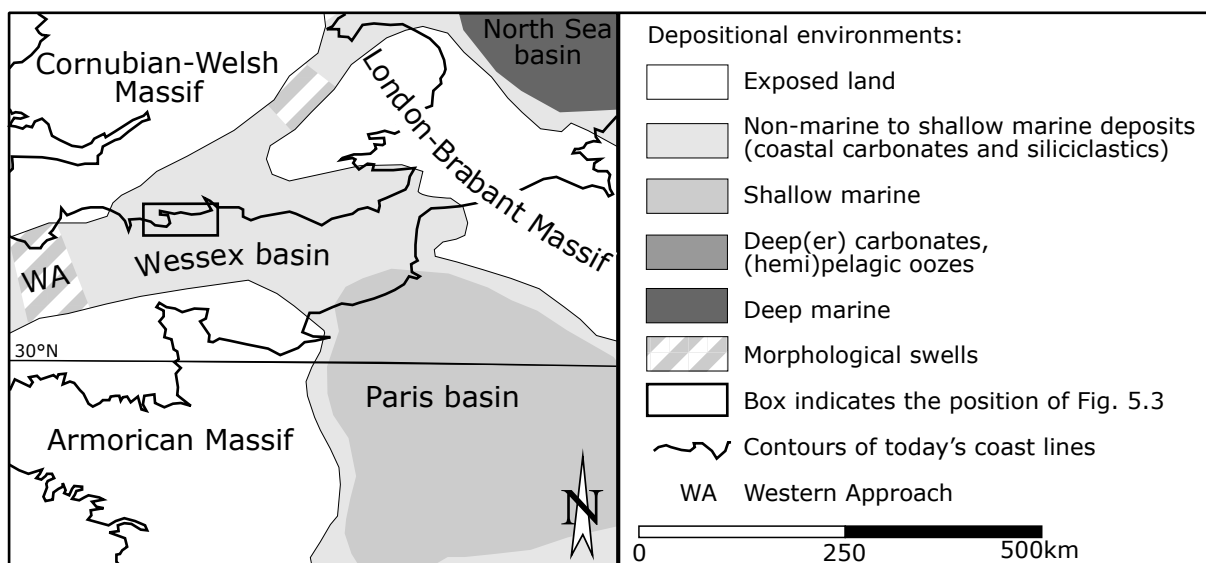
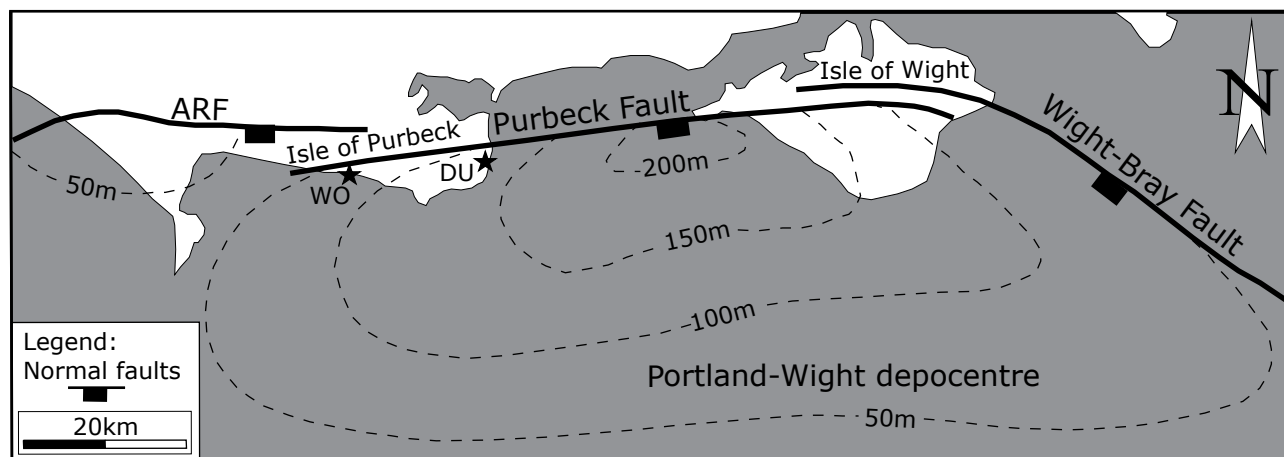


Fig. 5.2 - Palaeogeographic situation of the Wessex basin and its connections to the surrounding basins. The palaeogeographic map is based on THIERRY & BARRIER (2000; modified for the Berriasian from ALLEN 1963, RAWSON & RILEY 1982, KARNER et al. 1987, ZIEGLER 1988).



**Fig. 5.3** - Distribution and isopach map for the Purbeck Limestone Group in the Portland-Wight depocentre of the Channel sub basin south of the Purbeck Fault system. This fault system supposedly consists of a series of discontinuous fault segments. The thickness of the Purbeck Limestone Group derives from the integration of outcrop information with borehole data and isopach maps determined through seismic interpretation. The extent of the depocentre located west of the Isle of Wight is consistent with syn-sedimentary extensional fault activity along the Purbeck Fault. (ARF: Abbotsbury Ridgeway Fault, WO: Worbarrow Tout section, DU: Durlston Bay section; modified from UNDERHILL 2002).

south by the Armorican Massif. Marine connections of the Wessex basin to other marine basins during the Berriasian have been discussed controversially by the scientific community (e.g., ALLEN 1963, CASEY 1973, RAWSON & RILEY 1982, WIMBLETON & HUNT 1983, ALLEN & WIMBLETON 1991; cf. Chap. 8). Theoretically, marine connections have been postulated to the North Sea basin (between the London-Brabant Massif and the Cornubian-Welsh Massifs), to the Bay of Biscay rift (through the Western Approach between the Cornubian-Welsh and the Armorican Massif), and to the Paris basin (between the Armorican and the London-Brabant and Renish Massifs). It cannot be excluded that the Wessex basin was partly the northern branch of the Paris basin during the Berriasian termed Anglo-Paris basin in previous studies (e.g., DÖRHÖFER & NORRIS 1977b, WIMBLETON & HUNT 1983).

The Channel sub-basin is a late Palaeozoic to Tertiary extensional structure consisting of several E-W trending grabens and half-grabens, which rest on the Early Palaeozoic Variscan basement (KARNER et al. 1987, RUFFELL 1995). Horizontal tensional and vertical isostatic forces within the lithosphere controlled the evolution of these grabens and half-grabens during Permian to Early Cretaceous times (e.g., CHADWICK 1986). Four main depocentres within the Channel sub-basin, which are separated by intra-basinal highs, can be distinguished (KARNER et al. 1987, UNDERHILL & PATERSON 1998). The Durlston Bay and the Worbarrow Tout sections are located in the Portland-Wight depocentre (Fig. 5.3). This depocentre is limited to the

north by the Purbeck Fault system, which consists of a series of discontinuous, extensional fault segments and the Hampshire-Dieppe High (UNDERHILL 2002). Towards these faults, a thickening of the Late Jurassic to Early Cretaceous deposits has been observed (UNDERHILL 2002; Fig. 5.4). Moreover, the bed thickness in onshore locations increases in an easterly

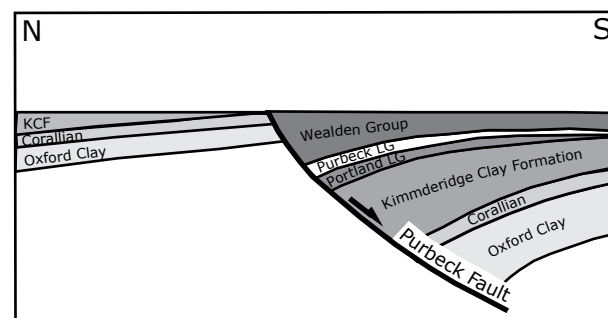


**Fig. 5.4** - Schematic N-S section depicting the Late Jurassic-Early Cretaceous syn-rift tectonics along the Purbeck Fault. LG: Limestone Group, KFC: Kimmeridge Clay Formation (only the lithologies from the Oxford Clay to the Wealden Group are illustrated). Modified from UNDERHILL (2002).

direction and reaches its maximum at Durlston Bay (e.g., WEST 1975, ENSOM 1985, CLEMENTS 1993; cf. Chap. 6). Offshore seismic mapping displays an elliptical pattern of subsidence south of the Purbeck Fault system during the deposition of the Purbeck Limestone Group (UNDERHILL 2002; Fig. 5.3).

## 5.4 Biostratigraphy

Biostratigraphical investigations have been carried out for the Durlston Bay section only. Dating is mainly based on ostracode and charophyte biozonations.

### *Ammonites*

Ammonites spanning the Jurassic-Cretaceous boundary have been found in Lincolnshire (Spilsby Sandstone), Norfolk (Sandringham Sands), and Yorkshire (Speeton Clay) of eastern England (e.g., CASEY 1973). Several Berriasian ammonite zones have been introduced and named for the first time by CASEY (1973). Among these, he defined the Runctoni zone of the Boreal ammonite zonation (Middle Berriasian; according to HARDENBOL et al. 1998). The ammonite-bearing sections in eastern England, however, are strongly condensed, marginal deposits. CASEY (1973; p. 196) states that “minor breaks characterize the contact of the Runctoni, Kochi and Icenii zones with superjacent strata”. CASEY (1973) related the Cinder Member to the Boreal Runctoni ammonite zone. HOEDEMAEKER (2002) presented a correlation scheme of several Berriasian sections in Tethyan and Boreal realms. He used the magnetostratigraphical interpretation of the Durlston Bay section established by OGG et al. (1991, 1994; see below) and correlated it with the magnetostratigraphy of the type-section in Berrias published by GALBRUN (1985) and GALBRUN et al. (1986) (cf. Chap. 6). Based on these publications, he correlated and dated the Durlston Bay section with Tethyan ammonite zones. However, the boundaries of the correlated ammonite zones are poorly constrained in the correlation scheme of HOEDEMAEKER (2002).

### *Charophytes*

The charophyte *Hemiglobator protoincrassatus* has been identified in two intervals at the transition of the Soft Cockle to the Marly Freshwater Member by FEIST et al. (1995). According to MOJON (2002), these intervals belong to the charophyte-ostracode assemblage zone M2 (cf. Tab. 4.3). The *Hemiglobator protoincrassatus* species found at base of Marly Freshwater Member (DB 75) already displays characteristics of the species *Hemiglobator maillardi* of assemblage zone M3 (MOJON 2002). The charophyte zonation established by FEIST et al. (1995) is mainly based on material deriving from boreholes of the Weald sub-basin. Partly, it corresponds to the assemblage zones published by

MOJON (2002). However, their boundaries are not well defined.

### *Ostracodes*

The stratigraphical value of ostracodes in the Dorset realm has been recognized for more than a century. “Edward Forbes in 1851 used them [ostracodes] to subdivide the Upper Jurassic Purbeck Beds of Dorset in southern England with possibly the oldest zonal scheme based on microfossils.” (KEEN 1993; p.41). In 1885, Jones published detailed lists of ostracodes from the Purbeck beds of Durlston Bay (KEEN 1993, HORNE 2002). Species and subspecies of the ostracode genus *Cypridea* have been used to create biozonations of continental deposits all over the world (citations in Chap. 2 and in KEEN 1993). The genus *Cypridea* is thought to have been able to adapt rapidly to fluctuating environmental conditions (r-selective strategist; KEEN 1993). Probably, it inhabited freshwater to brackish waters and was able to survive in temporary water bodies drying out seasonally (CARBONEL et al. 1988, HORNE 1995, 2002; cf. Tab. 2.1). Moreover, HORNE (2002; p. 60) stated that “it is fairly certain that Purbeck-Wealden cypridoideans were able to lay desiccation-resistant eggs, a strategy widely employed by non-marine cypridoideans today (...); such resting eggs also facilitate widespread dispersal by media such as wind and animals”. Moreover, limnocytherids and darwinulids, which generally produce no resting eggs for surviving arid phases (adult females brood their eggs in permanent water bodies; CARBONEL et al. 1988) also achieved regional distributions probably encapsulated as adults or juveniles in wet mud stuck to crocodiles or dinosaurs (ALLEN 1998).

Based on material deriving from boreholes of the Weald basin, ANDERSON & BAZLEY (1971) established an ostracode zonation. ANDERSON (1985) published posthumously a summary of all his work (between 1939 and 1985) and a revision of his ostracode zonation. HORNE (1995) reviewed previous schemes and revised the published ostracode zonations based on Anderson’s data. He used not only the ostracode species of *Cypridea* but also of *Theriosynoecum* (cf. Fig. 5.5)

ANDERSON & BAZLEY (1971) realized that the ostracode assemblages in Tithonian to Valanginian (Purbeckian to Wealden) strata are characterized by repeated alternations between fauna dominated by species of *Cypridea* (the C-phase) and those, in which the majority of individuals belongs to genera other than *Cypridea* (the S-phase). An alternation (cycle)

Ammonite subzones (HARDENBOL et al. 1998)	Ostracode biozonation (MOJON 2002)	Charophyte biozonation (MOJON 2002)	Assemblage zones (MOJON 2002)
<i>Paramimounum</i>	<i>Cypridea valdensis obliqua</i>	<i>Hemiglobator nurrensis</i>	M5
<i>Privasensis- Dalmasi</i>	<i>Cypridea granulosa fasciculata</i>	<i>Hemiglobator neocomensis</i>	M4
<i>Grandis- Subalpina</i>	<i>Cypridea granulosa fasciculata</i> <i>Cypridea granulosa granulosa</i> ( <i>Cypridea tuberculata oertlii</i> )	<i>Hemiglobator maillardi</i>	M3
<i>Grandis</i>	<i>Cypridea granulosa granulosa</i>	<i>Hemiglobator protoincrassatus</i>	M2?
<i>Jacobi- Grandis</i>	<i>Cypridea dunkeri carinata</i> <i>Cypridea tumescens praecursor</i> <i>Cypridea tumescens tumescens</i>	<i>Hemiglobator praecursor</i>	M1b

**Tab. 5.1** - Comparison of the ostracode biozonation, the charophyte biozonation, and the assemblage zones (charophyte-ostracode assemblages) according to MOJON (2002) with the Tethyan ammonite zonation according to HARDENBOL et al. (1998). The boundaries of the ostracode biozones are not well defined in MOJON (2002). Moreover, he used several ostracode species to delimit his ostracode biozones.

consisting of “an S-phase below and a C-phase above” has originally been defined as a “faunicycle” (ANDERSON & BAZLEY 1971; p. 30), although this definition has been watered down in later publications by Anderson (HORNE 1995). According to ANDERSON & BAZLEY (1971), the S-phases are believed to represent periods of higher salinity compared to the C-phases. This has been related to reduced rainfall during S-phases. Hence, they assumed that the alternations of ostracode assemblages through time were mainly controlled by changes in water salinity. The faunicycles have been used to refine and improve ostracode zonations and to

correlate deposits of outcrops and boreholes between different basins.

MOJON (2002) established an ostracode zonation, which is based on species of the genus *Cypridea* described from the Boreal realm (e.g., Paris basin; OERTLI 1963; Dorset realm; ANDERSON & BAZLEY, 1971). He combined this ostracode zonation with the charophyte zones of the Swiss and French Jura platform and established charophyte-ostracode assemblages (cf. Chap. 4; Tab. 5.1).

The Durlston Bay section has also been dated by MOJON (2002) (Fig. 5.5; Tab. 5.2). Transitional

Ostracode biozonation (MOJON 2002)	Charophyte biozonation (MOJON 2002)	Assemblage zones (MOJON 2002)	Studied members of the Durlston Bay section (CLEMENTS 1993)
<i>Cypridea granulosa fasciculata</i>		M4	Intermarine Member
			Cinder Member
<i>Cypridea granulosa fasciculata</i> - <i>Cypridea granulosa granulosa</i>	<i>Hemiglobator maillardi</i>	M3-M4	Cherty Freshwater Member
<i>Cypridea granulosa granulosa</i>	<i>Hemiglobator protoincrassatus</i>	M2	Marly Freshwater Member
<i>Cypridea aff. granulosa granulosa</i>		M2	Soft Cockle Member

**Tab. 5.2** – Comparison of the ostracode and the few charophyte species determined by MOJON (2002) from the Durlston Bay section with his assemblage zones and the members of Durlston Bay section according to CLEMENTS (1993).

forms of the ostracode species *Cypridea granulosa granulosa* and *Cypridea fasciculata fasciculata* have been described from the Cherty Freshwater Member by MOJON (2002) (Fig. 5.9b-c). Additionally, MOJON (2002) determined Boreal ostracodes in central Jura

platform samples (Tab. 5.3). He explains the occurrence of Boreal ostracodes on the central Jura platform with marine connections to the Boreal realm (Paris basin) during Berriasian times (cf. Chap. 9). Such connections mainly occurred during the assemblage zones M2 and

Boreal ostracodes found in central Jura platform sections	Assemblage zones	Sections where the ostracodes have been collected
<i>Cypridea granulosa fasciculata</i>	M4	Chapeau de Gendarme, Cornaux, Valangin*, Feurtilles*, Riedli*
<i>Cypridea tuberculata oertlii</i> (rare, endemic species)	M3	Lavans, St. Claude, Chapeau de Gendarme
<i>Cypridea granulosa granulosa</i> <i>Mantelliana cyrton</i>	M2	Riedli*, Maréchet*, Source de l'Ain*
<i>Cypridea binodosa</i> <i>Mantelliana cyrton</i>	M1b	Bonlieu*

**Tab. 5.3** - Boreal ostracode species found in different sections of the central Jura platform and their attribution to the assemblage zones according to MOJON (2002) (cf. Chap. 4). Sections marked with an asterix have not been investigated in this study.

M4 according to MOJON (2002). The co-occurrence of characteristic charophytes and ostracodes in samples of the Jura platform and of the Durlston Bay section supports Mojon's charophyte-ostracode assemblage zonation. This zonation is valid as a biostratigraphical tool at least for the intervals of the assemblage zones M2 and M4.

However, Anderson's "faunicycle" approach was criticized by HORNE (1995) who suggested that the cyclicity of cypridoidean and non-cypridoidean microfaunas may be linked with the permanence of water-bodies rather than changing salinity. The view that many Berriasian ostracodes in the Wessex basin inhabited ephemeral pools or lakes is supported by observations of great concentrations of their valves ("ostracodites"; cf. Pl. 10/6). It is not clear, however, whether such occurrences represent seasonally drying pools or occasional droughts affecting large lakes (ALLEN 1998).

Moreover, HORNE (2002; p. 54) stated that "ostracode faunas are undoubtedly facies-controlled and the extent to which their first and last occurrence (both within and between basins) are diachronous remains unclear". Furthermore, post-mortem transport evidenced by current-lineation, size sorting, and mixing have to be taken into account by dealing with ostracode valves (e.g., ALLEN 1998, HORNE 2002).

KEEN (1993; p. 62) writes that, "at the moment, the question of genotypic versus phenotypic variations [by species of the genus *Cypridea*] cannot be satisfactorily answered, although the majority of workers incline towards the former". A good compilation of Berriasian ostracode biostratigraphies and its limits is given in COLIN & LETHIERS (1988). They conclude that "(...), reliable biostratigraphy by means of ostracodes cannot be achieved without an adequate knowledge and understanding of their taxonomy, palaeoecology, phylogeny and palaeobiogeography". These conditions

are certainly fulfilled for parts of Mojon's charophyte-ostracode assemblages of the Berriasian interval used in this study.

### **Bivalves**

MORTER (1984) examined bivalves of the Purbeck Limestone Group from different boreholes of the Channel and the Weald sub-basins and grouped them into eight associations. According to this study, these associations indicate salinity events (transgression-regression sequences) within the Purbeck Limestone Group. MORTER (1984) related some major salinity events to ammonite zones published by CASEY (1973): The Cinder Beds (Member) event lies within the Runctoni ammonite zone and the Scallop event (Member) corresponds to the Icenii ammonite zone.

### **Palynology**

Microfloras have first been described from the Purbeck Limestone Group by Couper (1958) and Lantz (1958) (both in WIMBLEDON & HUNT 1983). DÖRHÖFER & NORRIS (1977a, b) presented a palynostratigraphy based on spore-pollen assemblages for the Berriasian of southern England. They correlated it with assemblages occurring in the Lower Saxony basin (NW Germany). HUNT (1987) used different sections of the Channel and the Weald sub-basins (e.g., Durlston Bay section) to analyse dinoflagellate cysts and acritarchs of the Purbeck Limestone Group. By means of cluster analysis, he established dinoflagellate cyst and acritarch assemblages and compared them with lithological, macro-, and microfaunal data. He related the variations in diversity and composition of these assemblages mainly to salinity changes. HOEDEMAEKER

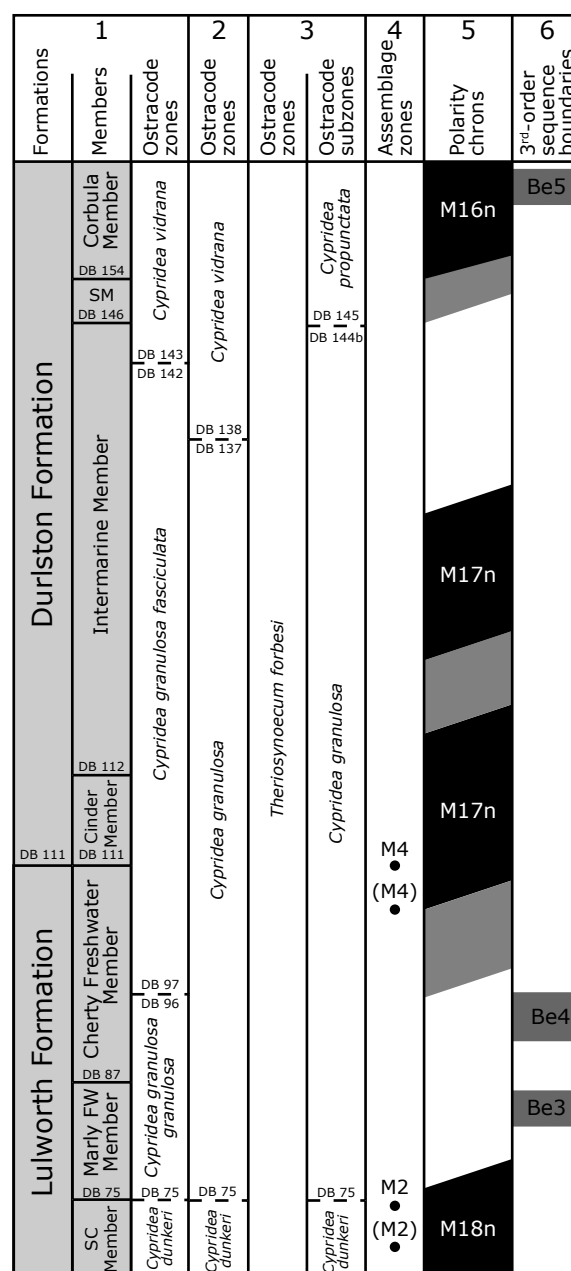
(2002), however, used Hunt's dinoflagellate cyst diversity for a sequence-stratigraphical interpretation of the Durlston Bay section. He considered diversity peaks of dinoflagellate cysts as maximum flooding and highstand deposits and low dinoflagellate cyst diversity as sequence boundaries. WIMBLEDON & HUNT (1983) discussed correlations of deposits from the Purbeck Limestone Group between sections of the Channel and Weald sub-basins. These correlations are based on palynology and ostracode biozonations. They conclude that "the latter [palynology] suggests that most of the Purbeck succession in the Weald post-dates much of that at Durlston Bay" (p. 277).

## 5.5 Magnetostratigraphy

OGG et al. (1991) published a magnetostratigraphy of the Durlston Bay section. According to this publication, the interval of the Durlston Bay section examined in this study ranges from polarity chron M18n (normal polarity) to M16n (Fig. 5.9a-g). The timing of the polarity chrons is based on the palynostratigraphic scheme of the Durlston Bay section published by WIMBLEDON & HUNT (1983). According to OGG et al. (1994), the top of the Soft Cockle Member is assigned to polarity chron M18n (Fig. 5.5). The Marly and Cherty Freshwater Member lie in the polarity chron M17r (r: reversed polarity). The Cinder Member and the lower part of the Intermarine Member match with the normal-polarity chron M17n. The upper part of the Intermarine Member belongs to the polarity chron M17r. The lower part of the polarity chron M16n can be related to the Scallop and the Corbula Member. Besides physical and technical inaccuracy of the magnetization measurements, lithological incompleteness (condensation and erosive intervals) have to be considered by interpreting and correlating the magnetostratigraphy of the Durlston Bay section with other sections (OGG et al. 1994).

## 5.6 Lithostratigraphy

Webster (1816) published a section through the Isle of Purbeck in which the term Purbeck Limestone has been marked (in ENSOM 2002a). The Purbeck Limestone Group was introduced by CLEMENTS (1993), although other authors have treated it as a formation (e.g., EL-SHAHAT & WEST 1983, ENSOM 1985). By tradition, the



- 1 Lithostratigraphy (formations and members) and ostracode zones (CLEMENTS 1993). (SC: Soft Cockle, FW: Freshwater, SM: Scallop Member)
- 2 Ostracode zones (ANDERSON 1985)
- 3 Ostracode zones and subzones (HORNE 1995)
- 4 Charophyte-ostracode assemblage zones (MOJON 2002)
- 5 Magnetostratigraphy (OGG et al. 1991) (black intervals: normal polarity, gray intervals: uncertain polarity)
- 6 Approximate 3<sup>rd</sup>-order sequence boundaries (HARDENBOL et al. 1998)

**Fig. 5.5** - Comparison of the lithostratigraphy of the Purbeck Limestone Group (Durlston Bay section) published by CLEMENTS (1993) with different ostracode zonations and the magnetostratigraphy of OGG et al. (1991). The positions of 3<sup>rd</sup>-order sequence boundaries are approximately indicated based on HARDENBOL et al. (1998).

Purbeck Limestone Group has been divided into the informal Lower, Middle, and Upper divisions based on ostracode zonations (e.g., ALLEN & WIMBLEDON 1991, CLEMENTS 1993). In this study, these informal divisions are not used.

CASEY (1973) introduced the terms “Lulworth Beds” for sedimentary rocks below the Cinder Member and “Durlston Beds” for strata above without indicating any particular lithostratigraphic significance (ENSOM 2002) (cf. Fig. 5.5). These terms have been used as formation names (e.g. CLEMENTS 1993). ENSOM (1985) named the members used in this study according to traditional lithostratigraphical subdivisions. WESTHEAD & MATHER (1996) presented a revised lithostratigraphic nomenclature. It is based on detailed logging of more central and westerly sections in Dorset. Their lithostratigraphy has been made with the aim to define mappable units. That is why they reduced the amount of members of the Purbeck Limestone Group proposed in earlier publications and regrouped them to five members. A historical overview of lithostratigraphic terms for the Purbeck Limestone Group is given in ENSOM (2002). In this study, the lithostratigraphical divisions are based on the publications of ENSOM (1985; Worbarrow Tout section) and of CLEMENTS (1993; Durlston Bay section). ENSOM (1985) and CLEMENTS (1993) gave numbers to most of the beds of these two sections (ENSOM 1985: abbreviation “WT” for Worbarrow Tout; CLEMENTS 1993: abbreviation “DB” for Durlston Bay).

## 5.7 Special features

The Purbeck Limestone Group of Dorset is well-known for its rich fossil content, which has been explored since the 19<sup>th</sup> century. The most famous fossil collector was Mary Anning (1799-1847) who discovered the first ichthyosaur in 1814, the first complete plesiosaur in 1824, and the first British flying reptile in 1828 (BRUNSEN 2003).

Mammal remains have mainly been described from the Mammal Bed and the Cherty Freshwater Member of the Durlston Bay section (e.g., KIELAN-JAWOROWSKA & ENSOM 1992, SIGOGNEAU-RUSSEL & KIELAN-JAWOROWSKA 2002). A list of vertebrate and invertebrate remains collected from the Durlston Bay and the Worbarrow Tout section is displayed in Fig. 5.6.

Sir Owen was the first to report ornithischian dinosaur remains from the Purbeck Limestone Group in 1861. Later, he described a complete jaw of an orni-

thischian dinosaur and classified it as an *Iguanodon hoggii*. These fossil remains probably derived from the Cherty Freshwater Member of the Durlston Bay section (NORMAN & BARRETT 2002). Additionally, a small jaw and teeth have been found by Sir Richard Owen who considered them as the remains of a small lizard (*Echinodon*). Nowadays, these remains are classified as *Echinodon beeklesii*, a small ornithischian dinosaur. The remains have probably been collected from the Marly and/or Cherty Freshwater Member of the Durlston Bay section (NORMAN & BARRETT 2002).

NORMAN & BARRETT (2002) proposed that the dinosaurs have been “passers by” in Dorset during the Berriasian. Moreover, they suggested that the environmental conditions (hot to very hot, semi-arid climate) were more conducive for smaller, more ecologically adaptable terrestrial vertebrates (e.g., lepidosaurs and mammals).

### *Dinosaur footprints*

In contrast to the relatively rare dinosaur remains, their footprints have been described from several surfaces of the Purbeck Limestone Group (e.g., DELAIR & SARJEANT 1985). Generally, they are preserved as tridactyl prints assigned either to ornithischian *Iguanodon* or to saurischian *Megalosaurus* (ENSOM 2002b). Several surfaces of dinosaur footprints have been identified in the Durlston Bay and the Worbarrow Tout section (e.g., ENSOM 1985, CLEMENTS 1993). A surface with several tridactyl footprints of the Worbarrow Tout section is displayed in Pl. 12/3. They have been assigned to “iguanodont tracks” by DELAIR & SARJEANT (1985) better described as tracks of an iguanodon-like animal according to LOCKLEY & HUNT (1995). Disturbed, partly nodular intervals, which are associated with dinosaur footprints may represent dinoturbation. Two intervals probably reflecting dinoturbation have been identified (one in each Dorset section).

### *Chert nodules*

Black, weathering-resistant chert nodules occur in several intervals of the Durlston Bay and the Worbarrow Tout section (e.g., ENSOM 1985, CLEMENTS 1993; Pl. 12/2). They are characteristic for the Cherty Freshwater Member. These nodules commonly contain freshwater organisms (charophytes, ostracodes, bivalves). The chert nodules have not been further investigated in this study.



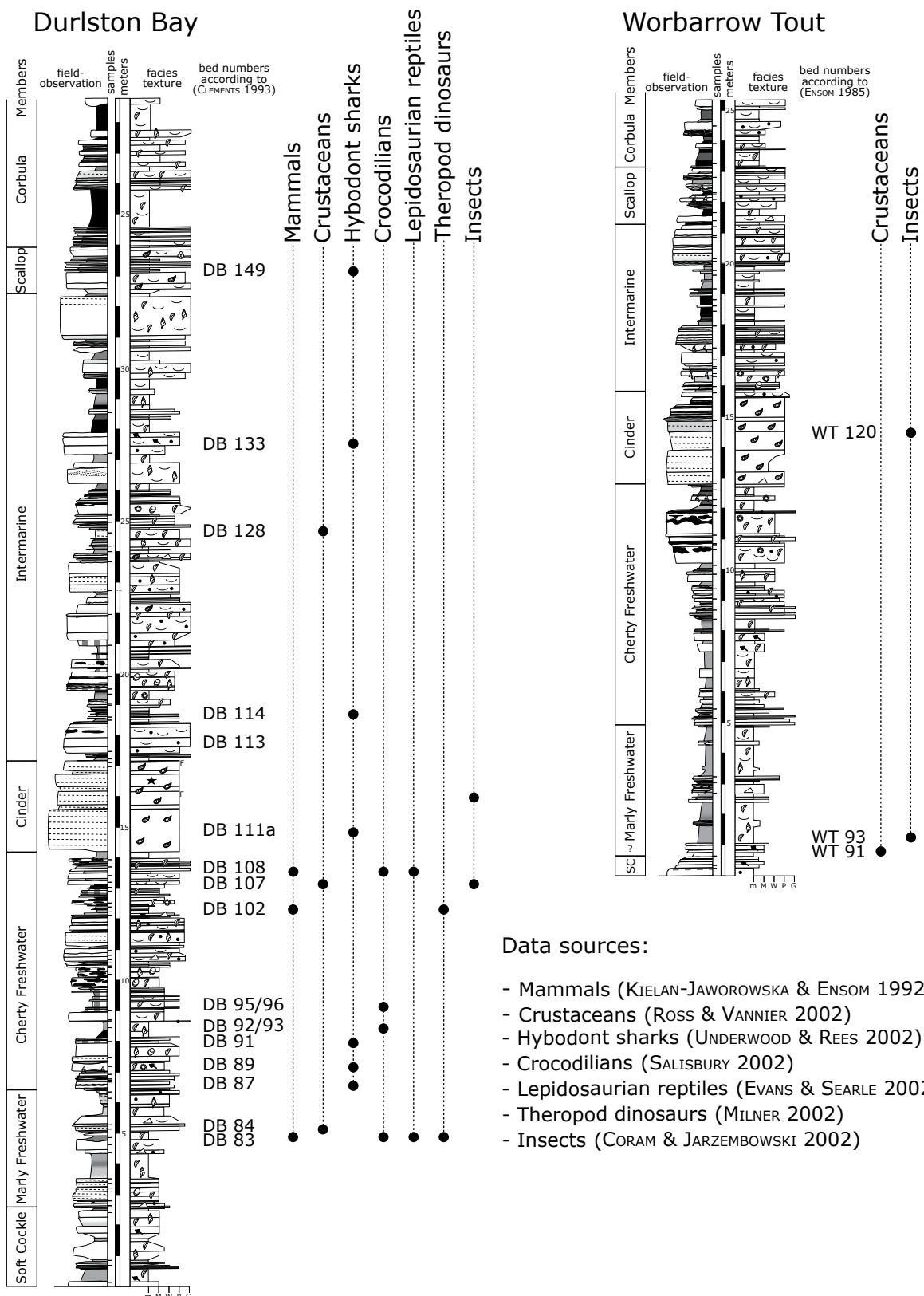


**Fig. 5.6** - Distribution of vertebrate and invertebrate remains described from the Durlston Bay and Worbarrow Tout sections as reported by different authors. The distribution shows fossils with a specific stratigraphic significance in the sections. Further descriptions and palaeontological significance of the listed fossil remains are given in the corresponding publications. (SC: Soft Cockle).

## 5.8 Description and interpretation of the sections

A detailed sedimentological description and interpretation is given as a graphical log for both Dorset sections. The sections are illustrated on a scale of 1:25. The same methods and procedure as for the Jura platform sections have been applied (cf. Chap. 4). Lateral correlation and best-fit solutions have been used in parts where sedimentological data are not sufficient to propose an unambiguous interpretation. For methods and procedure of correlation, the reader is referred to chapter 6.

The sections are presented in the following way (Fig. 5.7a):

- **Column ①** indicates lithostratigraphic units.
- **Column ②** shows the polarity zones published by OGG et al. (1991). The positions of the polarity zone boundaries are based on approximate measurements of the Durlston Bay log presented by OGG et al. (1991). Therefore, inaccuracy of measurement cannot be excluded. Uncertain polarity zone intervals are indicated in gray.
- **Column ③** outlines the ostracode biostratigraphy according to CLEMENTS (1993) and the charophyte-ostracode assemblage zones according to MOJON (2002). Brackets indicate reworked species of an earlier assemblage zone (according to MOJON 2002)
- **Column ④** displays the sequence-stratigraphical interpretation. Sequences (on all scales) are counted from SB/TS to SB/TS, even if they are only inferred. The “3<sup>rd</sup>-order” sequence-stratigraphical framework on the left side of this column is already displayed in this chapter to avoid repetitions. It is in agreement with the sequence-stratigraphical nomenclature of HARDENBOL et al. (1998).
- **Column ⑤** shows the logged section with the field observations (weathering profile) and sedimentary structures (left side), and the constituents and texture (right side) according to DUNHAM (1962) and EMBRY & KLOVAN (1971) (both in FLÜGEL 2004). The relative abundance of each constituent in a sample is indicated by the amount of symbols (cf. Fig. 5.7b; Chap. 2):
  - one symbol: present
  - two symbols: common
  - three symbols: abundant

- three symbols: abundant

- **Column ⑥** gives the interpretation of the depositional environments. On the right side, the facies of each sample is indicated (cf. Tab. 2.3). Additionally, the relative bathymetric trend between supratidal and shallow subtidal is illustrated.

In the Worbarrow Tout section, columns ② and ③ are not displayed (no magneto- and biostratigraphy). The position of the two sections is indicated on a map and by coordinates (Figs. 5.8 and 5.10). A legend for these figures is given in Fig. 4.7.

The Dorset sections mainly consist of supratidal to intertidal deposits (cf. Chap. 2). The fauna is dominated by ostracodes, bivalves, and gastropods. Locally, ostracodes and/or bivalves are dominant forming massive “ostracodites” and/or shell beds (cf. Chap. 2). Restricted lagoonal conditions (marginal-marine) prevailed during the deposition of the Cinder Member and of the Scallop Member (e.g., EL-SHAHAT & WEST 1983, CLEMENTS 1993, RADLEY 2002). Therefore, these subtle environmental changes make the sequence-stratigraphical interpretation of the Dorset sections rather delicate. Moreover, a lower number of samples have been investigated for the Dorset sections compared to the Jura sections (in average 2 samples per meter; cf. Annex 1).

### 5.8.1 Durlston Bay

The Durlston Bay section has been investigated since the 18<sup>th</sup> century (a good compilation is given in WEST 2006). The lithification and compaction history of shell beds in this section has been examined by EL-SHAHAT & WEST (1983). They conclude that shell beds displaying early cementation features have been deposited during supratidal phases and related these phases to mild uplift or halts of a slowly subsiding environment. CLEMENTS (1993) published an excellent bed-by-bed description and a detailed weathering profile of the Durlston Bay section. Additionally, he added numbers to most of the beds of this section (these numbers are displayed in the field observation column; the abbreviation “DB” means Durlston Bay). The lithostratigraphic divisions of this section (formations and members) are also based on CLEMENTS (1993). These numbers enable an easy orientation in later descriptions of the Durlston Bay section. The relative amounts of ostracode, gastropod, and bivalve species published by CLEMENTS (1993) have been integrated

①	②	③	④	⑤	⑥	a
Formations Members	Magnetostat. CLEMENTS (1993)	Bio-stratigraphy MOJON (2002)	Sequence stratigraphy "3rd-order" sequences Medium-scale sequences Small-scale sequences Elementary sequences	Section name	Sedimentological interpretation	
				Field observations Samples Meters Facies/Texture	Facies zone Depositional environment (comments)	supratidal intertidal shallow subtidal

<p><b>Field observations</b></p> <p><b>Sedimentary structures</b></p> <p>TT Desiccation cracks</p> <p>~ Polygonal mudcracks</p> <p>▼ Birdseyes</p> <p>⋈ Bioturbation</p> <p>~ Wave ripples</p> <p>~ Current ripples</p> <p>~ Lamination</p> <p>~ Low-angle cross-stratification</p> <p>~ Flaser bedding</p> <p>~ Lenticular bedding</p> <p>~ Wavy bedding</p> <p>~ Dinosaur footprints</p> <p>~ Dinoturbation</p> <p>~ Loading structures</p> <p>~ microbial mats</p> <p>~ palaeosol</p> <p><b>Lithology</b></p> <p>□ Limestones</p> <p>□ Marly</p> <p>□ Gray marls</p> <p>□ Dark-gray marls</p> <p>□ Brown-reddish marls</p> <p>□ Black marls</p> <p>□ Bituminous facies</p> <p>□ Cherts</p>	<p><b>Facies/Texture</b></p> <p>Facies (descriptive elements / components)</p> <div style="display: flex; justify-content: space-between;"> <div style="width: 45%;"> <p>● Peloids</p> <p>⊙ Ooids superficial</p> <p>△ Intraclasts</p> <p>○ Mud pebbles</p> <p>▲ Black pebbles</p> <p>= Organic matter</p> <p>☞ Plant debris</p> <p>☞ Bone fragments</p> <p>— Bivalves</p> <p>— Bivalves convex-up</p> <p>☞ Gastropods</p> <p>☞ Oysters</p> <p>★ Echinoderms</p> <p>⊙ Foraminifera</p> <p>☞ Charophyte oogonia</p> <p>☞ stems</p> </div> <div style="width: 45%;"> <p>☞ Ostracodes</p> <p><b>Non-calcareous components</b></p> <p>P Pyrite</p> <p>☞ Evaporite pseudomorphs</p> <p>□ Siliciclastics (present)</p> <p>□ Siliciclastics (common)</p> <p>□ calcareous sandstone to sandstone</p> <p><b>Texture</b></p> <p>m: Marls</p> <p>M: Mudstones</p> <p>W: Wackestones</p> <p>P: Packstones</p> <p>G: Grainstones</p> <p>F: Floatstones</p> </div> </div> <p><b>Abundance of constituents in a sample</b></p> <p>present (one symbol): ☞</p> <p>common (two symbols): ☞ ☞</p> <p>abundant (three symbols): ☞ ☞ ☞</p> <p>Black symbols: observed in thin section</p> <p>Gray symbols: observed by hand lens on outcrop or interpreted between samples</p>
---	--

<p><b>Sequence stratigraphy</b></p> <p>— SB — Sequence boundary</p> <p>— TS — Transgressive surface</p> <p>— MFS — Maximum-flooding surface</p>	<p>■ Sequence boundary interval</p> <p>■ Maximum flooding interval</p>
---	--

Fig. 5.7 - Legend for Dorset sections.

into the interpretation of this section. Especially the ostracodes have been used to estimate the salinity range of the depositional environments according to HORNE (2002; cf. Tab. 2.1). The lower part of this section (between DB 69-89) has also been investigated and

described by MOJON (2002). He used this interval as basis for a correlation with the Jura platform sections (Tethyan-Boreal correlation; cf. Chap. 6)

SCHNYDER (2003) utilized the distribution of dinoflagellates, foraminifera linings, and the algae

*Botryococcus* and *Celyphus rallus* to estimate marine and continental tendencies. ANDERSON (2004a) employed lithofacies analysis and palaeobiological data from the literature to explain the cyclic nature of the bed succession at Durlston Bay. He related the facies and palaeobiological changes of this section to allocyclic processes, which have been controlled by Milankovitch orbital forcing (cf. Chap. 7).

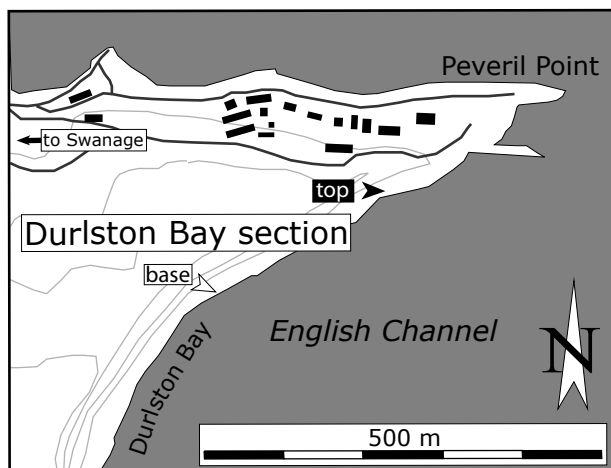


Fig. 5.8 - Location of the Durlston Bay section.

### Geographic and stratigraphic setting

The section outcrops along the cliffs at Durlston Bay southeast of the town of Swanage (coordinates 403.650/078.375, Ordnance Survey map, 1/25000, Explorer OL15, Purbeck & South Dorset; Fig. 5.8). The section has been logged from south to north along the cliffs. Different ostracode zonation have been published in the literature (e.g., ANDERSON 1985, CLEMENTS 1993, HORNE 1995; cf. Fig. 5.5). The biostratigraphical value of these ostracode zonation remains unclear (e.g., HORNE 2002). According to MOJON (2002), the part below the Cinder Member corresponds to the charophyte-ostracode assemblages zones M2 to M4. The magnetostratigraphy published by OGG et al. (1991, 1994) reveals that the studied interval of this section lies between the polarity chrons M18n and M16n.

### Sedimentological interpretation (Fig. 5.9a-g)

The bed at base of the section contains pseudomorphs after halite. Evaporite pseudomorphs are typical for deposits of the Hard Cockle and Soft Cockle Member. They are interpreted as sabkha-type sediments (e.g.,

WEST 1975, CLEMENTS 1993). The top of the Soft Cockle Member consists of tidal flat deposits commonly containing plant debris. Charophyte gyrogonites have been described by FEIST et al. (1995) from the thin marl layer at the boundary between the Soft Cockle and the Marly Freshwater Member (DB75a-b; at 2.50 meters). According to MOJON (2002), these marls lie in the charophyte-ostracode assemblage zone M2. The base of the Marly Freshwater Member consists of laminated, ostracode-rich mudstones, which are overlain by a thick marl interval (DB 76-81; from 2.50 to 4.35 meters). The top of these marls displays an erosive surface. It also marks the top of polarity chron M18n according to OGG et al. (1991).

The following two massive mud- to packstone beds are capped by the dark marly palaeosol of the Mammal Bed (DB 83; from 4.75 to 5.05 meters; cf. Pl. 12/1). It is well known for its rich mammal remains. Mud- to grainstone beds mainly containing bivalves, ostracodes, gastropods, and peloids characterize the following succession (DB 84-86; from 5.05 to 6.45 meters). Two laminated pack- to grainstone beds at the base of this succession contain intraclasts pointing to reworking processes possibly under tidal influence. Bituminous sediments considered as freshwater to brackish pond deposits as indicated by ostracodes and gastropods (CLEMENTS 1993) dominate the following bed (DB 86; from 6.30 to 6.40 meters; cf. Chap. 2). This organic-rich sediments may have been deposited in a shallow water body with reduced water-mass exchange. Anoxic bottom waters in this water body protected the organic-rich sediments from oxidation. Two erosive surfaces at the base and top of this bituminous interval are formed by reworking during the deposition of the overlying thin bivalve-rich packstones (storm layers?). The top of this bituminous interval marks the boundary between the Marly and the Cherty Freshwater Member. The following bed succession consists mainly of wacke- to packstones interpreted as tidal flat deposits (DB 87-89; from 6.45 to 7.35 meters). The beds at the base of this succession are rich in bivalve shells and intraclasts (partly black pebbles and plant debris) probably pointing to reworked and/or tidal channel deposits. An interval of beds with varying lateral thickness and an erosive base containing flaser and lenticular bedding is interpreted as tidal channel deposits (DB 88; from 6.75 to 6.95 meters). The thick, massive mud- to wackestone rich in ostracodes and charophyte stems (DB 89) have been deposited in a tidal flat pond because the ostracode assemblage of this interval does not indicate pure freshwater conditions (CLEMENTS 1993). The thin marl interval at the top of this bed points to an increase of clay minerals probably due to forced erosion in the

hinterland. The following thinly-bedded wacke- to packstones display a similar composition (ostracodes, gastropods, and charophyte gyrogonites and partly stems) as the beds below (DB 90; from 7.35 to 8.05 meters). They are also interpreted as tidal flat deposits. A bituminous interval caps this bed succession reflecting a change to more freshwater conditions and a lower hydrodynamic level (DB 91; from 7.95 to 8.05 meters). Two thin wacke- to packstone beds are considered as tidal flat deposits.

The following thick interval of grayish- to black marls represents intertidal to supratidal deposits (DB92-93; Fern Bed; from 8.15 to 8.65 meters). MOJON (2002) interpreted this interval as swamp deposits because of the occurrence of spores and debris of pteridophytes. It is assumed that this interval has probably been emerged recurrently. Bituminous mud- to packstone beds with intercalated thin shell layers (pack- and grainstones) characterize the following bed succession (DB 94-96; from 8.65 to 9.80 meters). They are interpreted as freshwater to brackish, quiet-water deposits of shallow ponds as indicated by the ostracodes and gastropods (CLEMENTS 1993). The thin shell layers probably mark pulses of increased tidal influence and/or storm deposits. Generally, it is assumed that this bituminous interval reflects strong condensation.

It is overlain by a thin marl layer (at 9.75 meters). Three massive mudstone beds with chert nodules characterize the following interval (DB 97; Flint Bed; from 9.80 to 10.45 meters). These beds contain gastropods, ostracodes and charophyte gyrogonites interpreted as tidal flat pond deposits. Each of them is capped by a thin marl layer. These chert beds lie at the base of a polarity chron with uncertain polarity direction (colored in gray; OGG et al. 1994). According to these authors, it possibly marks the base of the polarity chron M17n. Moreover, MOJON (2002) observed transitional forms of the ostracode species *Cypridea granulosa granulosa* and *Cypridea granulosa fasciculata* in this chert-rich interval. Tidal channels incise the top of the third bed with chert nodules (DB 98-100; from 10.45 to 10.65 meters).

A succession of massive shell beds (wacke- to grainstones) reflects an environmental change to more intertidal-shallow subtidal conditions with winnowing during high-energy phases ("shell beaches"; cf. Chap. 2; DB 101; from 10.65 to 12.05 meters). According to EL-SHAHAT & WEST (1983), these shell beds display an early meteoric cementation (uncompacted biosparrodites) indicating longer periods of subaerial exposure. A slightly undulated surface has been identified at 10.90 meters, probably pointing to an erosive discontinuity. Thin marl layers intercalated

between the shell beds suggest periods of lower energy. At the top of the massive shell beds (from 12.00 to 12.05 meters), a succession from flaser followed to lenticular beddings displays a shallowing trend, which terminates with the deposition of a thin marl layer (at 12.05 meters). At the base of the following marl interval (tidal flat deposit; DB 102; from 12.05 to 12.50 meters) several thin wacke- to packstone beds have been deposited containing intraclasts and plant debris, which points to reworking of a previously subaerial exposed surface (tidal channels?).

The marly layer is overlain by a massive wacke- to packstone bed with chert nodules and charophyte stems (DB 103). On its base, dinosaur footprints have been detected by CLEMENTS (1993). It is interpreted as tidal flat pond deposits. The following interval is characterized by a succession of thin mud- to wackestones, which mainly contains ostracodes (DB 104-106; from 12.65 to 13.15 meters). The upper part of this succession is bituminous (DB 105-106; from 12.80 to 13.15 meters). This part is interpreted as freshwater to brackish pond deposits (condensed interval). The base of the polarity chron M17n (with a good signal of the polarity direction) lies within the bituminous interval (OGG et al. 1991).

Pack- to grainstone beds ("shell beaches") build up the following bed succession (DB 107-109; from 13.15 to 14.00 meters). They are partly intercalated by thin marl intervals. According to EL-SHAHAT & WEST (1983), bed DB 108 displays early cementation in (uncompacted bed) indicating supratidal conditions (probably meteoric water conditions). The two beds at the top of this succession contain chert nodules (DB 109; from 13.85 to 14.00 meters).

The top of the second bed displays an erosive surface, which is overlain by a marl interval with centimeter-thick shell layers. Lenticular bedding and the occurrence of the oyster *Praeexogyra distorta* (according to CLEMENTS 1993) point to tidal influence (DB 110; from 14.00 to 14.25 meters). This interval has been dated by MOJON (2002). It lies in the charophyte-ostracode assemblage zone M4.

The deposition of the massive, oyster-rich beds of the Cinder Member (DB 111) indicates a remarkable environmental change to a restricted lagoon (euhaline, marine conditions; e.g., KELLY 1983, MORTER 1984, RADLEY 2002; cf. Pl. 13/2). The thickness of these beds (about 3 meters) points to an increase of accommodation during the deposition of the Cinder Member. Echinoderms of the species *Hemicidaris purbeckensis* have been described from the top of the Cinder Member (e.g., RADLEY 2002). The thin marl layer (at 15.60 meters) is interpreted to reflect an increase of clay-mineral input deriving from

the hinterland. It may indicate a slight decrease of accommodation during the deposition of the Cinder Member.

The Cinder Member is capped by a marl interval interpreted as tidal flat pond sediments. This interval marks the boundary to the Intermarine Member (DB 112; from 17.20 to 17.30 meters). Thin shell beds containing small oysters point to deposits of “shell beaches” (DB 112; from 17.30 to 17.40 meters). They are overlain by a marl interval, which is interpreted as tidal flat deposits. An increase of accommodation is marked by the following massive shell beds (“shell beaches”; DB 113; from 17.45 to 18.50 meters). At the top of these beds, a marl interval has been deposited. It is interpreted as tidal flat pond sediments. This marl interval is capped by thin shell beds considered as “shell beaches” (base of DB 114; from 18.55 to 18.75 meters). They are followed by an interval of thinly-bedded marls to mudstones containing plant debris. They reflect tidal flat sediments. This interval is overlain by thin shell beds (wackestones) containing some small oysters (DB 114; from 19.05 to 19.20 meters).

A thick marl interval caps this shell bed (DB 115; from 19.20 to 19.50 meters). Besides ostracodes and gastropods, it contains charophyte stems and gyrogonites pointing to freshwater pond deposits. It is assumed that this interval is strongly condensed due to recurrent emersion. Massive wacke- to packstone beds containing abundant charophyte gyrogonites point to tidal flat pond deposits (DB 116a-b; from 19.50 to 20.10 meters). Two bituminous intervals within these wacke- to packstones display slight environmental changes to more quiet-water freshwater conditions (at 19.55 and at 19.95 meters). From the surfaces of these intervals, dinosaur footprints have been described (CLEMENTS 1993). Bituminous marls have been deposited at the base of the following laminated wacke- to packstone interval (DB 117; from 20.10 to 20.20 meters). The ostracode assemblage (CLEMENTS 1993) indicates freshwater to brackish conditions in a shallow pond environment. The laminated wacke- to packstone is considered to represent tidal flat deposits (DB 118; from 20.20 to 20.50 meters).

The following thick bituminous interval reflects an environmental shift to freshwater (brackish) pond conditions (DB 119; 20.50 to 20.95 meters). It is intercalated with thin ostracode-rich layers. This interval is capped by massive wacke- to grainstone beds (DB 120-123; from 20.95 to 22.35 meters). The lower part of these beds is characterized by lenticular- and flaser-bedding structures, which point to tidal flat sediments (DB 120; from 21.00 to 21.40 meters). The upper part of these beds is dominated by bivalve shells

(some *Praeexogyra* oysters, CLEMENTS 1993; DB 122-123; from 21.95 to 22.35 meters). They are considered to reflect a change to more lagoonal and high-energy conditions (“shell beaches”).

The massive beds are overlain by marly wackestones interpreted as tidal flat deposits (DB 124a-b; from 22.30 to 22.65 meters). They contain some cross-bedded shell beds probably reflecting slight shifts to a more distal environmental position (“shell beaches”). A succession of massive bivalve-rich packstones follows the marly wackestones (DB 124c-125; from 22.65 to 23.70 meters). They are interpreted as “shell beach” deposits. According to EL-SHAHAT & WEST (1983), the shell beds of the interval DB 121-125 display an early meteoric cementation reflecting periods of subaerial exposure.

A bituminous interval at the top of the packstones is considered to represent freshwater to brackish pond deposits, as indicated by ostracodes and gastropods (CLEMENTS 1993; DB 125; from 23.70 to 23.75 meters). It is capped by two grainstone layers characterized by bedding surfaces covered with bivalve shells in convex-up positions (Pl. 13/1a; from 23.75 to 24.00 meters).

The second grainstone layer is overlain by a marl interval interpreted as tidal flat sediments (DB 126; from 24.00 to 24.20 meters). A succession of massive wacke- to grainstone beds cap the marl interval (DB 127-129b; from 24.20 to 25.80 meters). The first bed of this succession is rich in bivalve shells (“shell beaches” with some *Praeexogyra* and *Corbula* shells, CLEMENTS 1993; DB 127) and partly displays lenticular bedding structures. It is interpreted as tidal flat to shallow subtidal deposits. The following bed is characterized by fine lamination, which points to tidally-influenced deposits (DB 128; Pl. 11/2). Generally, it is assumed that the marl intervals between the massive beds reflect intertidal to supratidal sediments. Freshwater conditions are indicated by the occurrence of charophyte stems and gyrogonites at 25.60 meters (DB 129b). They reflect a supratidal environment (freshwater pond).

An erosive surface at the top of this bed succession reveals an important exposure interval (at 25.80 meters). The erosive surface is covered by dark gray to black marls intercalated by thin bivalve-rich layers (DB 130; from 25.80 to 26.30 meters). These marls mark the top of the polarity chron M17n according to OGG et al. (1991). Loading structures at the base of the following massive packstone suggest a relatively rapid sedimentation of sand-sized sediments on water-saturated marls (EL-SHAHAT & WEST 1983 and own observations; Under Rag, DB 131; from 26.30 to 26.95). This packstone is interpreted as shallow

lagoonal deposits (“shell beaches”). The following thinly-bedded mudstone interval represents tidal flat sediments (DB132; from 26.95 to 27.25 meters). It is covered by three massive mud- to packstone beds (Red Rag, DB 133; from 27.25 to 27.95 meters). The upper two beds contain different bivalve shells, bones, fecal pellets, and plant debris (CLEMENTS 1993). This mixture of continental and marine components probably reflects intertidal to shallow subtidal deposits. The following black marls (increase of organic matter content?) display a change to inter- and supratidal conditions (DB134; from 27.95 to 28.35 meters). A transition to dark gray marls with thin shell layers indicates more lagoonal conditions (DB135; from 28.35 to 28.55 meters). It is capped by two massive wacke- to packstone shell beds interpreted as intertidal to shallow subtidal sediments (DB 136; from 28.55 to 28.70 meters).

The following part of the section is poorly exposed. It has been drafted and interpreted according to the indications on the graphical log of CLEMENTS (1993). The massive wacke- to packstones are capped by a thick marl interval interpreted as tidal flat deposits (DB 137-138; from 28.70 to 29.70 meters). According to CLEMENTS (1993), the part between beds DB 133 and DB 144 is tectonically disturbed by faulting. Gyrogonite fragments have been reported from the marl layer DB 142 (CLEMENTS 1993), which points to supra- to intertidal conditions. The following succession consists of several massive shell beds (pack- to grainstones; DB 139-144b; from 29.70 to 32.40 meters). They are considered to represent intertidal to shallow subtidal deposits (“shell beaches”). The marl layers between the massive beds probably indicate intertidal to supratidal deposits. The massive Leaning Vein bed (DB 144a-b) shows early cementation features displaying periods of exposure (EL-SHAHAT & WEST 1983). It is capped by an interval of marls and mudstones interpreted as tidal flat deposits (DB 145-146; from 32.40 to 32.65 meters). This interval marks the base of a polarity chron with uncertain direction (OGG et al. 1991). It probably already corresponds to the chron M16n.

A marine incursion is indicated by the following massive shell beds of the Scallop Member (DB 147-153; from 32.65 to 34.00 meters). These beds contain mainly the bivalves *Praeexogyra*, *Chlamys*, and *Corbula* (which are considered as euhaline organisms; CLEMENTS 1993, RADLEY 2002) and are interpreted as shallow subtidal, lagoonal deposits. The foraminifer *Eoguttulina* has been described from the shell bed at 33.50 meters (CLEMENTS 1993, DB 150). A sandstone bed occurs from 33.70 to 33.90 meters (DB 152). The marl intervals between the shell beds probably reflect

inter- to supratidal sediments. The ostracodes and gastropods determined by CLEMENTS (1993) indicate freshwater to brackish conditions.

The *Corbula* Member does not contain any *Praeexogyra* and *Chlamys* any more (CLEMENTS 1993). The base of this member lies in the polarity chron M16n (OGG et al. 1991). The following thick marl interval (tidal flat deposits; DB 155; from 34.70 to 35.90 meters) is overlain by several massive shell beds (pack- to grainstones; DB 156-163; from 35.90 to 37.85 meters). The beds at the base of this interval have been described as calcareous sandstones (CLEMENTS 1993; DB 156-159; from 35.90 to 36.50 meters). A dark marl interval then is interpreted as tidal flat deposits (DB 164; from 37.85 to 38.50 meters).

### *Sequence-stratigraphical interpretation* (Fig. 5.9a-g)

Lateral correlation of the sections in Dorset has always been problematic and difficult (e.g., WESTHEAD & MATHER 1996). There are only a few marker-beds or members, which can be identified over tens of kilometers. Three of these marker intervals lie within the interval examined in this study: Mammal Bed, Cinder Member, and Scallop Member. They represent strata, which are thought to be more or less time-equivalent. It is assumed that the Mammal bed corresponds to the 3<sup>rd</sup>-order sequence boundary Be3 according to HARDENBOL et al. (1998). The Cinder Member is thought to represent a major transgressive interval lying in the 3<sup>rd</sup>-order sequence Be4. The maximum-flooding interval of this 3<sup>rd</sup>-order sequence corresponds to the Scallop Member. These interpretations are based on lateral correlation, biostratigraphy (MOJON, 2002), and magnetostratigraphy (OGG et al. 1991, 1994) (cf. Fig. 5.5; Chap. 6).

Six intervals between the Mammal Bed and the Scallop Member, which display periods of important condensation (relatively reduced thickness or absence of beds and elementary sequences) and/or emersion, have been identified. The interval from the Fern Bed (DB 92-93) to the top of the bituminous interval at 9.80 meters (DB 96) represents a period of restriction (freshwater pond to tidal flat deposits) related to a decrease of relative sea level. It is assumed that this interval corresponds to the 3<sup>rd</sup>-order sequence boundary Be4 according to HARDENBOL et al. (1998). This interpretation is supported on the one hand by the magnetostratigraphy (Be4 in M17r) and on the other hand by the biostratigraphy (Be4 between the charophyte-ostracode assemblage zones M2 and M4 according to MOJON 2002).

The tidal channel deposits (DB 98-100) are thought



**Fig. 5.9a** - Durlston Bay section (part I).





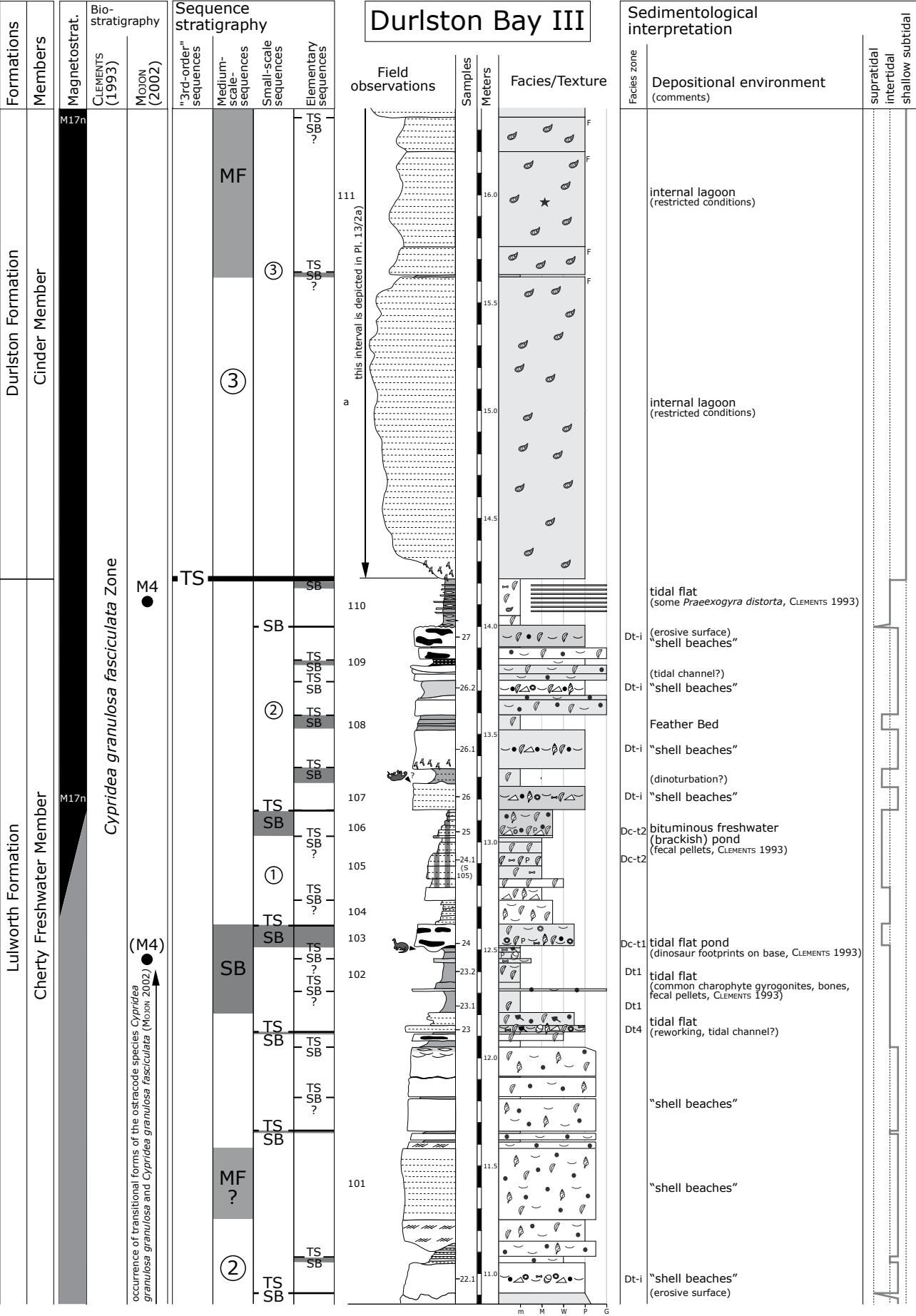


Fig. 5.9c - Durlston Bay section (part III).

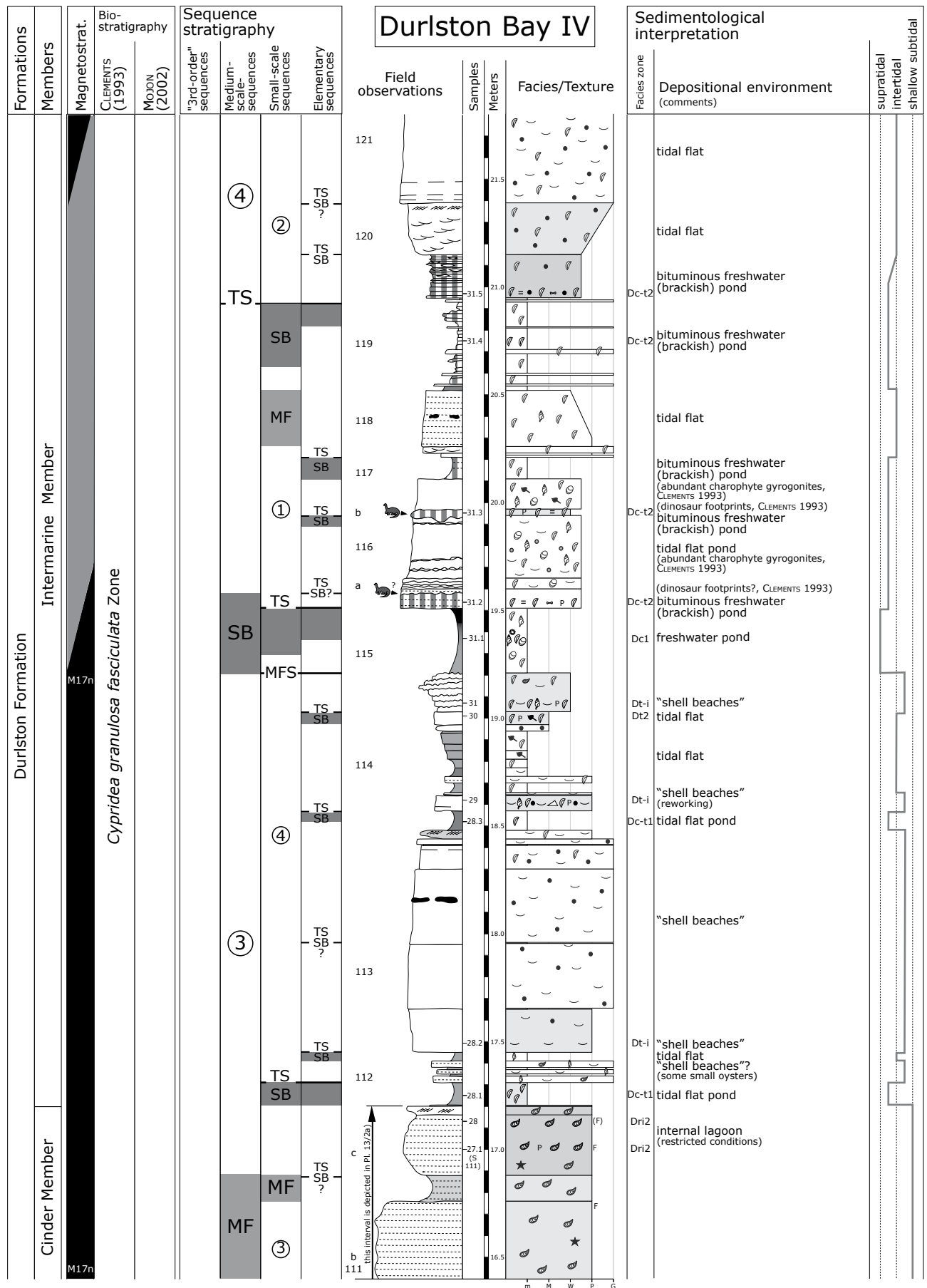


Fig. 5.9d - Durlston Bay section (part IV).

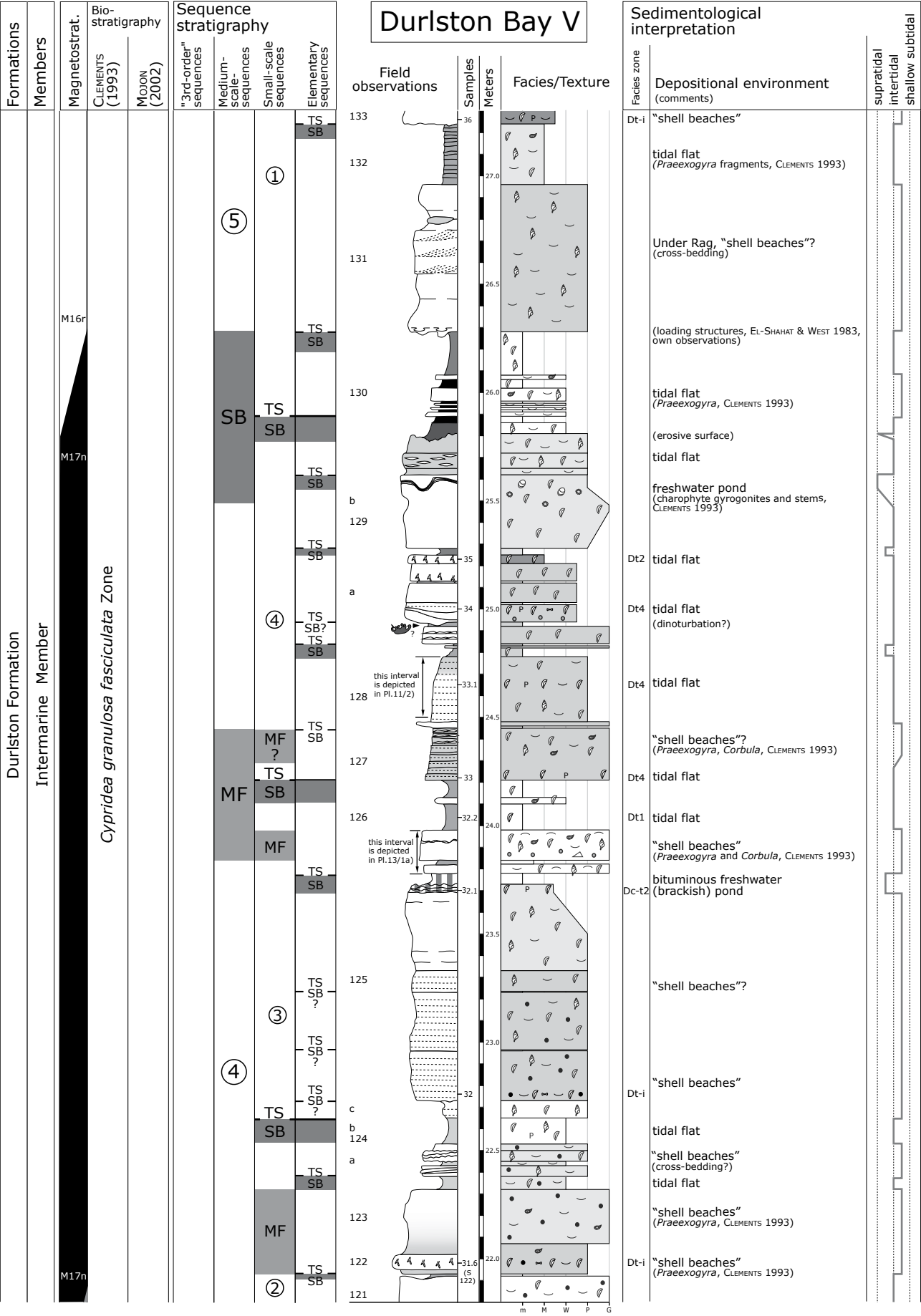


Fig. 5.9e - Durlston Bay section (part V).

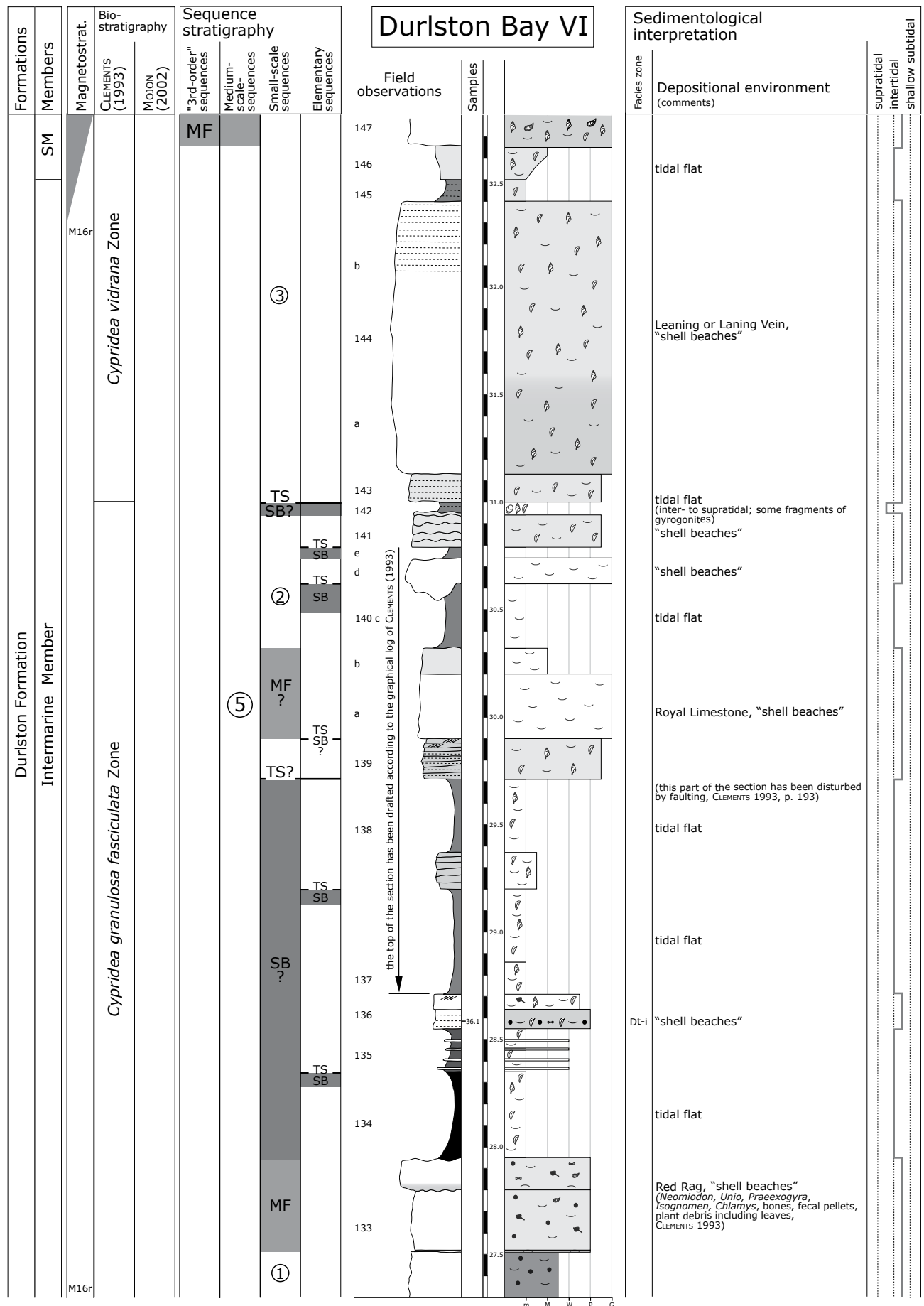
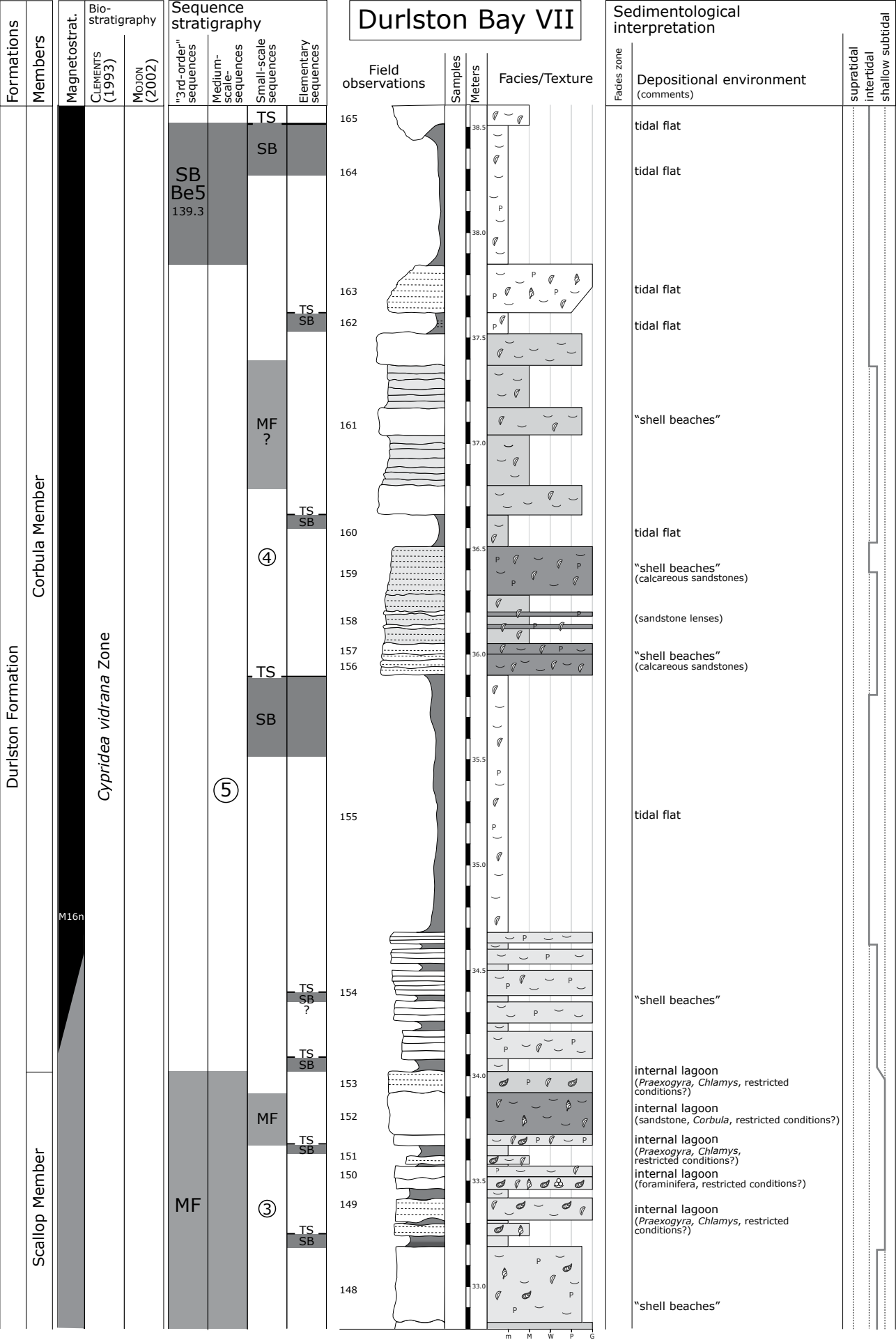


Fig. 5.9f - Durlston Bay section (part VI) (SM: Scallop Member).



m M W P G

to correspond to a second important condensation and emersion interval displayed by a relatively thin elementary sequence. The third significant fall of relative sea level is represented between the beds DB 102-103 (tidal pond to tidal flat deposits) where the identification of elementary sequences is not straightforward. The fourth interval displaying a major decrease of relative sea level is marked by the fresh-water deposits of DB 115. The interval between the beds DB 129b to 130 (tidal flat deposits) corresponds to a fifth interval of decreasing relative sea level. All these intervals are characterized by a reduced thickness and/or absence of beds and elementary sequences indicating low accommodation during falling sea level (medium-scale). It is assumed that these six intervals correspond to medium-scale sequence boundaries.

The tidal flat deposits at the top of the section (DB 164) are thought to represent the 3<sup>rd</sup>-order sequence boundary Be5 according to HARDENBOL et al. (1998). According to OGG et al. (1994), this interval lies in the polarity chron M16n. According to the chart of HARDENBOL et al. (1998), the 3<sup>rd</sup>-order sequence boundary Be5 is in the polarity chron M16n (cf. Fig. 1.2), which fits well into the sequence-stratigraphical correlation framework of the present study (cf. Chap. 6).

The thickness of the beds and elementary sequences between the Mammal Bed (DB 83) and the deposits below the Cinder Member (DB 111) is relatively reduced. Low accommodation potential leads to condensation (thin beds/elementary sequences) and/or non-deposition. The strong condensation in this part of the section is related to a lowstand situation on the long-term trend (3<sup>rd</sup>-order sequence). The sequence-stratigraphical interpretation is, therefore, complicated and uncertain. Some sequences are missing and/or not identifiable. Several sequence boundaries and transgressive surfaces of small-scale and elementary sequences are displayed in the graphical log. They are highly speculative and not further discussed.

A deepening and/or an opening trend of the system is displayed by the deposition of the Cinder Member and the following bed succession. Generally, the beds and the sequences (medium- and small-scale sequences) are thicker in this interval compared to the beds and sequences below the Cinder Member (thickening-up). However, the interpretation in terms of sequence-stratigraphy remains delicate because of weak facies changes and possibly autocyclic processes (especially on the scale of elementary sequences). Maximum floodings of small-scale and elementary sequences are usually not well expressed in these marginal-marine

deposits. Therefore, they are not illustrated in the graphical log.

The lateral correlation of this section with other sections (Jura platform) shows that small-scale sequences around the Cinder Member correspond to small-scale sequences described in the Jura platform section (Pierre Châtel Formation; cf. Chap. 6). Hence, the sequence-stratigraphical interpretation of this section concentrates on the four small-scale sequences around the Cinder Member. These four small-scale sequences build up a medium-scale sequence (DB 102-115). The sequence boundary of this medium-scale sequence corresponds to the tidal flat and pond deposits of the interval DB 102-103.

The sequence boundary of small-scale sequence 1 lies within the sequence boundary of this medium-scale sequence. It is represented by the massive tidal flat pond deposit of bed DB 103. This small-scale sequence is strongly condensed. It probably comprehends up to three elementary sequences. The upper part of the bituminous interval (DB 106) is assumed to correspond to the sequence boundary of small-scale sequence 2. It consists of five elementary sequences. The erosive surface at the top of the cherty bed DB 109 marks the sequence boundary of small-scale sequence 3. This sequence comprises the deposits of the Cinder Member. The marls at the base of the Cinder Member (DB 110) already contain oysters. They are considered to reflect an increasing marine influence during an initial rise of relative sea level (early transgressive deposits; cf. Chap. 3). It is assumed that this marl interval corresponds to the first elementary sequence of this small-scale sequence. The Cinder Member marks the beginning a major transgression. The base of the Cinder Member is considered as a transgressive surface on the 3<sup>rd</sup>-order sequence scale. It has been used to correlate sections of the Dorset region over long distances (e.g., WESTHEAD & MATHER 1996). For a long time, the boundary between the Jurassic and the Cretaceous systems have been set at the base of the Cinder Member (e.g., CASEY 1973). The identification of elementary sequences within the Cinder Member is not easy. A thin marl layer is considered as sequence boundary of an elementary sequence (at 15.65 meters). The maximum flooding of small-scale sequence 3 may correspond to the marly interval from 16.75 to 16.90 meters. The highstand deposits of this small-scale sequence contain more quartz grains, which may reflect an increase of erosion in the nearby hinterland during decreasing relative sea level. The tidal flat sediments at the base of bed DB 112 represent the sequence boundary of small-scale sequence 4. It comprehends at least four elementary sequences. Shell beds in the bed DB 112 mark transgressive deposits of the first elementary sequence. They are capped by a thin marl

interval, which is considered as sequence boundary of the following elementary sequence. The following massive shell beds (DB 113) probably comprehend two elementary sequences. However, a sequence boundary within these shell bed cannot be clearly identified. The tidal pond deposits at the top of the shell beds (base of bed DB 114) reflect a decrease of relative sea level. They mark the sequence boundary of the next elementary sequence. The following thin shell beds imply a slight rise in relative sea level and are interpreted as transgressive deposits of this elementary sequence. The tidal flat deposits at the top of bed DB 114 point to a decreasing relative sea level. They mark the sequence boundary of the last elementary sequence of this small-scale sequence. The transgressive deposits are represented by a massive shell bed (base of bed DB 115). It is capped by freshwater pond sediments (top of DB 115) indicating a remarkable fall of relative sea level. These deposits correspond to the sequence boundary of the following medium- and small-scale sequence.

The sequence-stratigraphical interpretation of the following part of this section has similarly been interpreted. Generally, it is assumed that the marly intervals represent intertidal and supratidal sediments corresponding to late highstand and possibly lowstand deposits. Massive shell beds (“shell beaches”) are considered to be more distal deposits (transition between tidal flat to restricted lagoonal sediments). Accordingly, they are interpreted as transgressive and possibly early highstand deposits reflecting rising relative sea level, and higher accommodation.

### 5.8.2 Worbarrow Tout

The earliest section from the Worbarrow Tout peninsula has been published by Bristow (1875; in ENSOM 1985). A detailed bed-by-bed description and a graphical log have been published by ENSOM (1985). He numbered the beds and intervals in his log. These numbers are indicated on the left side of the graphical log in this study (WT is used as an abbreviation for Worbarrow Tout). However, they do not correspond to the numbers displayed in the Durlston Bay section (ENSOM 1985).

#### *Geographic and stratigraphic setting*

This section outcrops along the northwestern cliffs of the small peninsula called Worbarrow Tout. This peninsula marks the southeastern end of Worbarrow Bay (Fig. 5.10). The section has been logged in

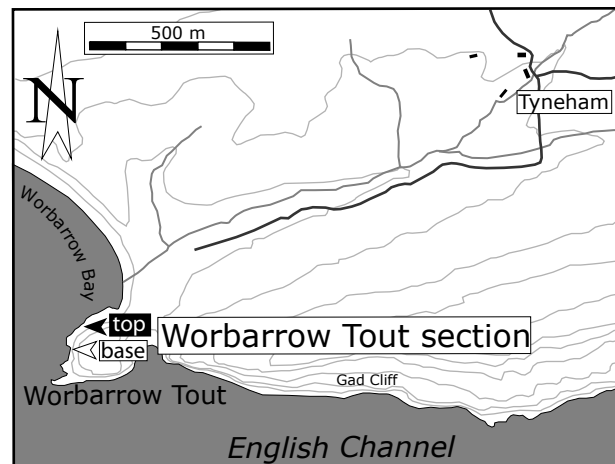


Fig. 5.10 - Location of the Worbarrow Tout section.

an approximately southwest to northeast direction (coordinates 386.900/079.650, Ordnance Survey map, 1/25000, Explorer OL15, Purbeck & South Dorset). The Worbarrow Tout section has never been dated. Lateral correlations is limited to lithological aspects (e.g., WESTHEAD & MATHER 1996). The litho-stratigraphic divisions (formations and members) derive from ENSOM (1985).

#### *Sedimentological and interpretation* (Fig. 5.11a-e)

The base of the studied interval of the Worbarrow section contains pseudomorphs after halite and is partly bituminous (Soft Cockle Member; WT 83-84; from 0.00 to 0.35 meters). It probably reflects seasonally hypersaline conditions in shallow tidal flat ponds. The following marl to wackestone beds contain plant debris and ostracodes. They represent tidal flat deposits (WT 85-89; from 0.35 to 1.05 meters). A thick interval of marls intercalated by massive mud- to wackestone beds (WT 90-99; from 1.05 to 4.95 meters) characterizes the Marly Freshwater Member (ENSOM 1985). At around 3.05 meters, a palaeosol containing bone fragments has been deposited. It is assumed that this palaeosol corresponds to the Mammal bed of the Durlston Bay section. A part of the marl-dominated interval pinches out laterally in an easterly direction (WT 90-96; from 1.05 to 4.25 meters).

Tidal flat deposits in the lower part of the Cherty Freshwater Member prevail up to a palaeosol interval (WT 100-104; from 4.95 to 8.40 meters). The palaeosol deposits are considered to reflect emersion and condensation (at about 8.35 meters). Ostracode-rich mud- to grainstones dominate the following bed succession (WT 105-111; from 8.40 to 10.25 meters). Partly, they are interrupted by marls. The entire



succession is thought to consist of tidal flat sediments. Two massive beds build up the following interval (WT 112-114; from 10.25 to 11.90 meters). The first massive bed is considered as shell bed ("shell beaches"; WT 112). At the top of this bed chert nodules are displayed. Dinosaur footprints have been observed at its surface (ENSOM 1985). A bed with a thick chert band containing birdseyes has been deposited at around 10.90 meters (WT 113; Pl. 12/2). Polygonal mudcracks are displayed at the surfaces of a thin mud- to wackestone bed (at 11.15 meters). The top of the second massive bed contains chert nodules, charophyte stems and pseudomorphs after halite (ENSOM 1985; WT 114). It is assumed that this interval represent freshwater to slightly brackish pond deposits. Seasonally, the conditions in the shallow pond were hypersaline. The top of this massive bed displays a slight relief considered as an erosive surface. This surface is capped by thin ostracode-rich layers deposited in a tidal flat environment (WT 115). At the top of these layers, polygonal mudcracks point to emersion (at 12.00 meters). The following succession is dominated by two marl intervals (tidal flat sediments), which are separated by a massive wackestone (WT 116-118; from 12.00 to 12.75 meters). These beds are assumed to be strongly condensed. The wackestone containing charophyte stems is interpreted as a tidal flat pond deposit (WT 117). At its base, dinosaur footprints have been discovered (ENSOM 1985). The surface of this bed is characterized by polygonal mudcracks. A thinly-bedded packstone rich in ostracodes overlies the second marl interval (WT 119; from 12.75 to 12.85 meters).

The Cinder Member caps this ostracode-rich packstone (WT 120a-b; from 12.85 to 15.05 meters). The beds of the Cinder Member are considered to represent reworked oyster banks in a restricted lagoonal environment. A change to beds containing bivalves and some small oysters is interpreted as an environmental shift to more coastal sediments ("shell beaches" to internal lagoonal deposits; WT 121; from 15.00 to 15.85 meters). Dinosaur footprints and polygonal mudcracks characterize the surface at the top of these beds (at 15.85 meters). The following bed succession comprehends thinly laminated marls and massive wacke- to packstones (WT 122-124; from 15.85 to 16.35 meters). A disturbed and partly nodular interval containing charophyte stems is interpreted as tidal pond deposits (WT 124). At its base, dinosaur footprints have been identified (ENSOM 1985). Probably, the disturbed, nodular interval reflects dinoturbation. Tidal flat deposits prevail up to a thin dark gray marl layer (WT 125-128; from 16.35 to 16.75 meters). The following bed succession is dominated by shell

beds representing "shell beaches" (WT 129-131; from 16.75 to 18.00 meters). An interval displaying lateral thickness variations is considered as tidal channel deposits (from 17.15 to 17.45 meters). Marls (partly dark gray to black) characterize the following interval (WT 132-142; from 18.00 to 20.00 meters). They are interpreted as tidal flat sediments. Massive shell-rich packstones interrupt this marl interval. It is overlain by massive pack- to grainstone beds (WT 143-145; from 20.00 to 21.30 meters). These beds mainly contain bivalve shells and ostracodes. They are assumed to represent deposits of "shell beaches". However, intervals in these beds with sedimentary structures like flaser and wavy bedding point to a more tidally-influenced depositional environment (tidal flat deposits; Pl. 11/3). The massive beds are capped by black laminated marls considered as tidal flat deposits (WT 146; from 21.30 to 21.40 meters). They mark the boundary between the Intermarine and the Scallop Member (ENSOM 1985). The following bed succession is characterized by an alternation of dark gray to black marls and massive wacke- to packstones (WT 147-153; from 21.40 to 23.25 meters). The marl intervals represent tidal flat deposits, whereas the massive beds are considered as "shell beaches". Scallop shells (*Chlamys*) are common in these beds (ENSOM 1985).

A change to two intervals of dark gray to black (partly reddish) marls marks the base of the Corbula Member (WT 154-156; from 23.25 to 24.25 meters). Evaporite pseudomorphs after gypsum have been identified at the top of these two marl intervals. The marls are interpreted as supratidal to intertidal deposits separated by an interval considered as tidal flat deposits (WT 155; from 23.85 to 23.95 meters). Shell beds cap the second marl interval (WT 157; from 24.25 to 24.70 meters). The top of the section consists of a thick marl interval interpreted as tidal flat deposits (WT 158-160; from 24.70 to 25.20 meters). At the top of this marl interval a shell bed has been deposited. It is slightly folded (WT 159). The interval at the top of the section pinches out laterally in an easterly direction (WT 154-160).

#### **Sequence-stratigraphical interpretation** (Fig. 5.11a-e)

The same criteria as in the Durlston Bay section have been used to interpret the Worbarrow Tout section in terms of sequence stratigraphy. At Worbarrow Tout, corresponding marker-beds (members and beds) are present (Mammal Bed, Cinder Member, and Scallop Member). These intervals can be correlated over long distances in the Dorset region. They are considered as more or less time-equivalent forming

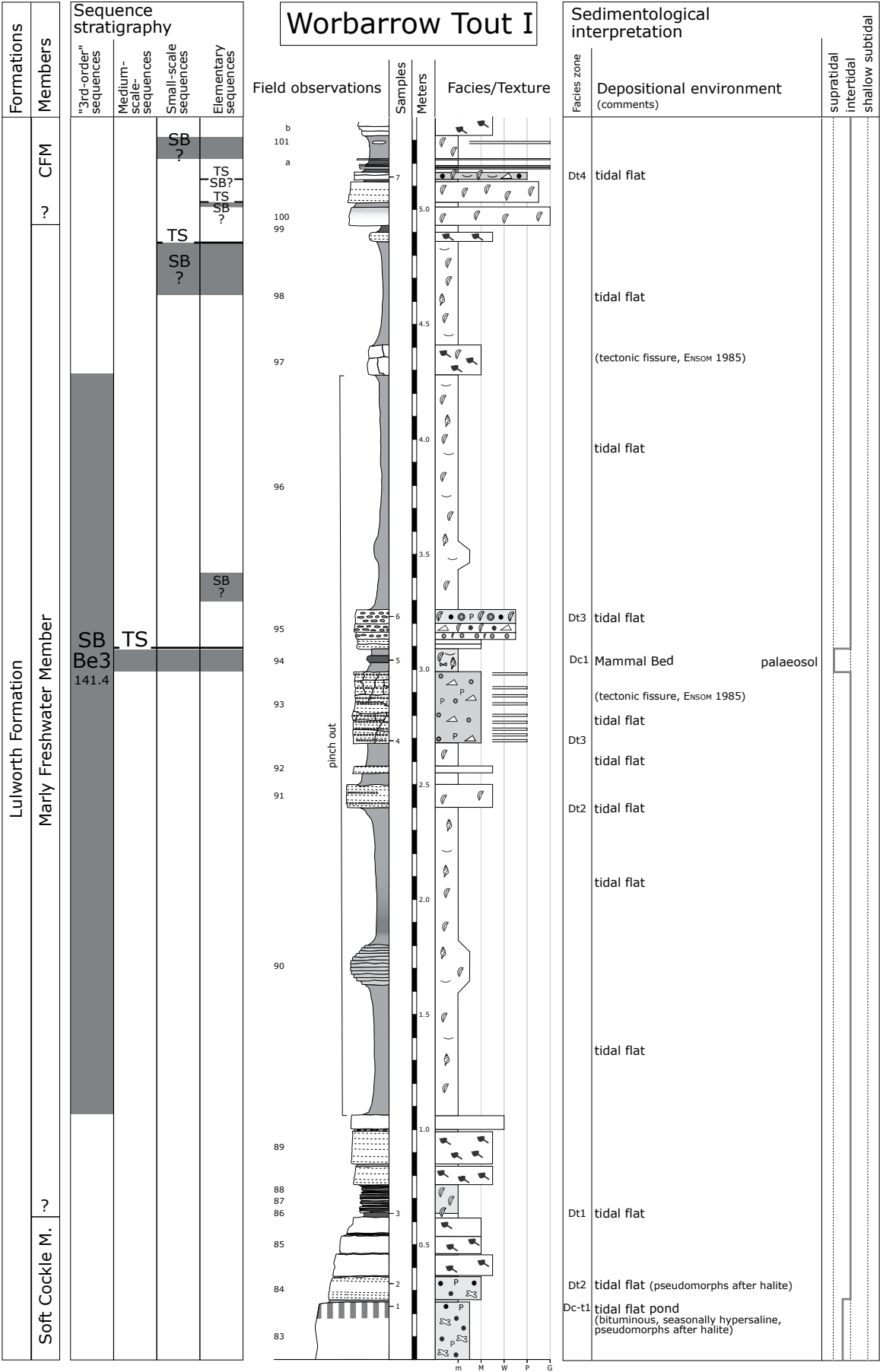
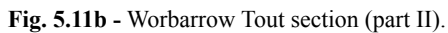
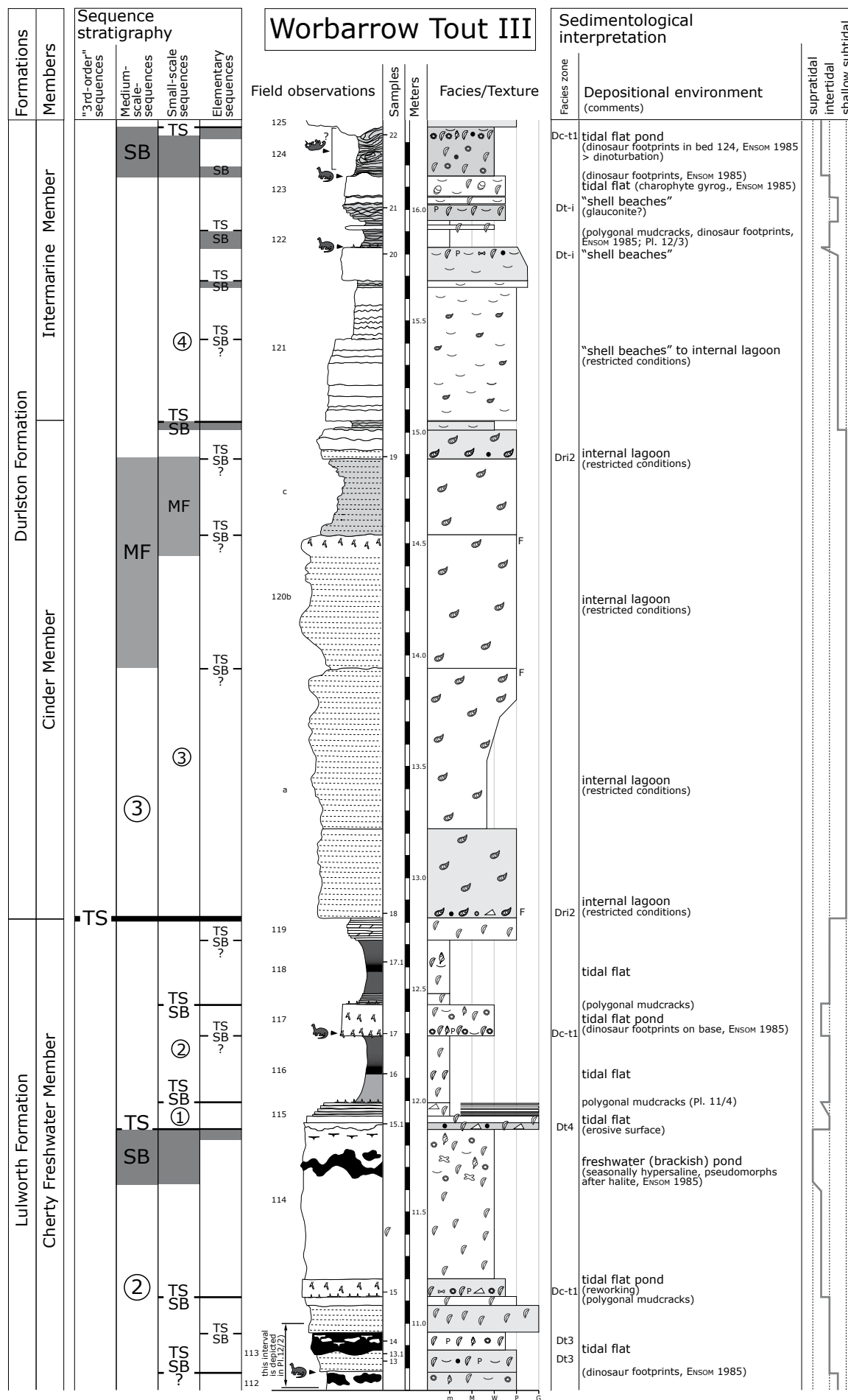


Fig. 5.11a - Worbarrow Tout section (part I) (CFM: Cherty Freshwater Member).



**Fig. 5.11b - Worbarrow Tout section (part II).**



**Fig. 5.11c** - Worbarrow Tout section (part III).

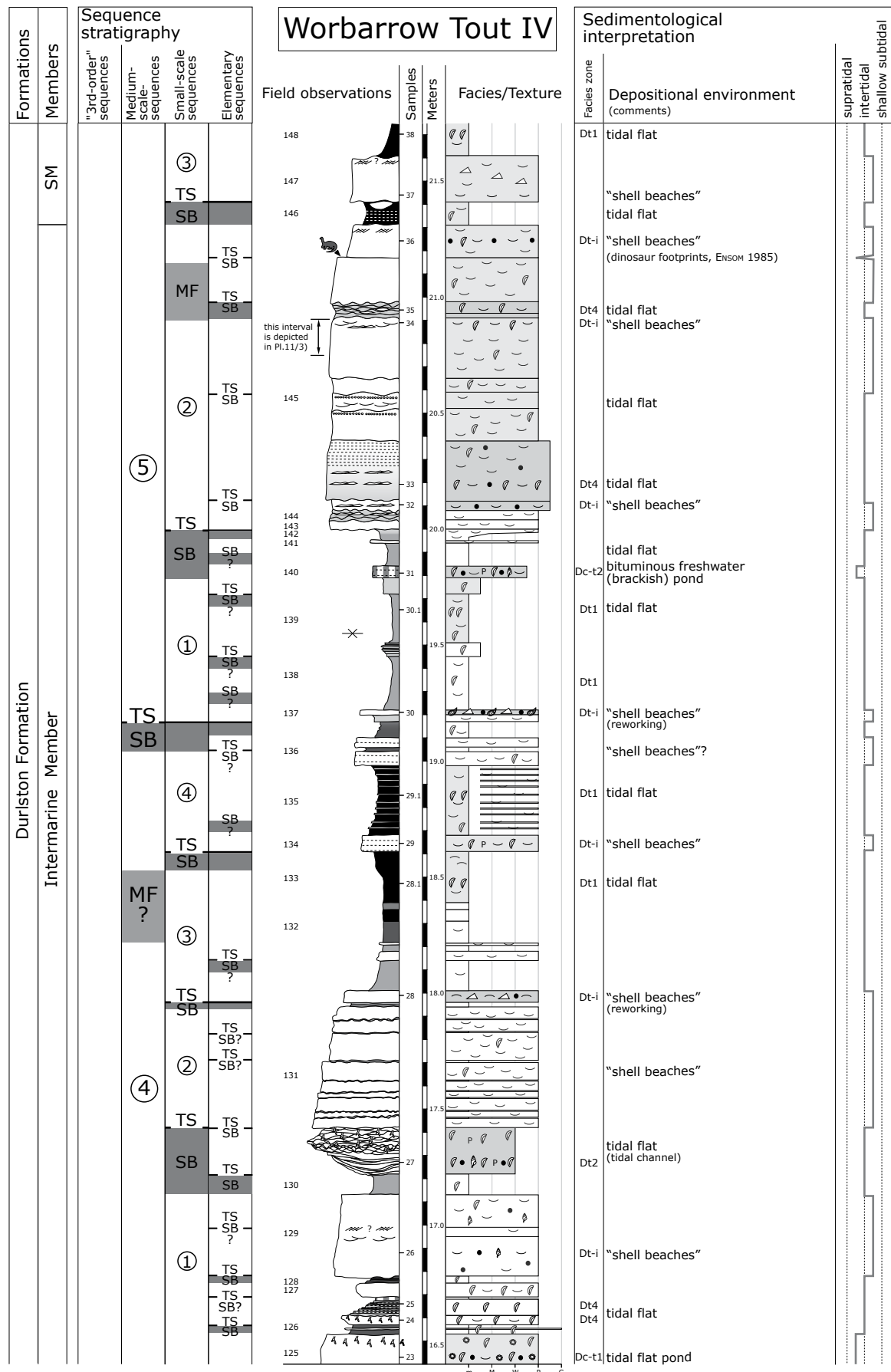


Fig. 5.11d - Worbarrow Tout section (part IV) (SM: Scallop Member).

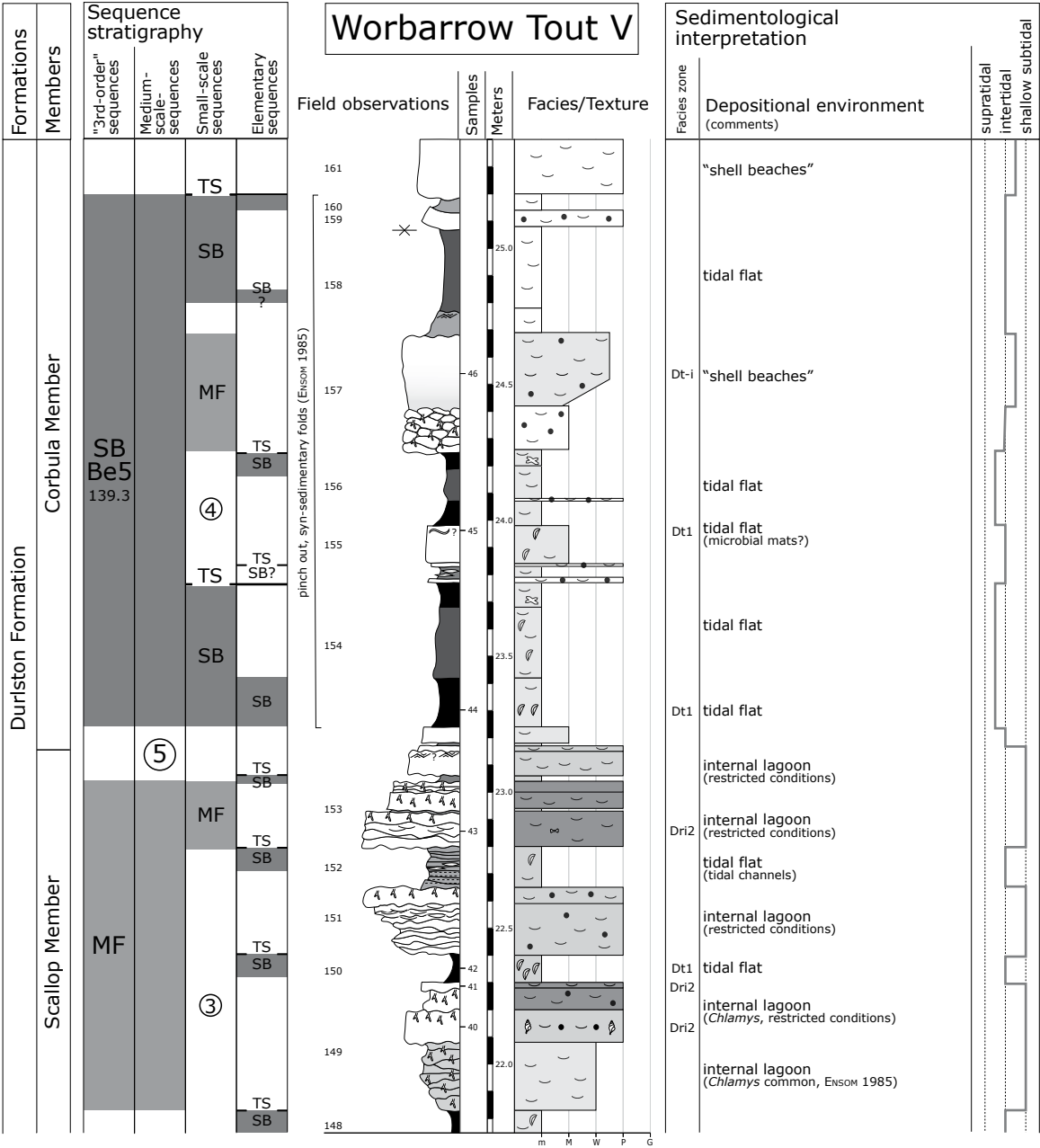
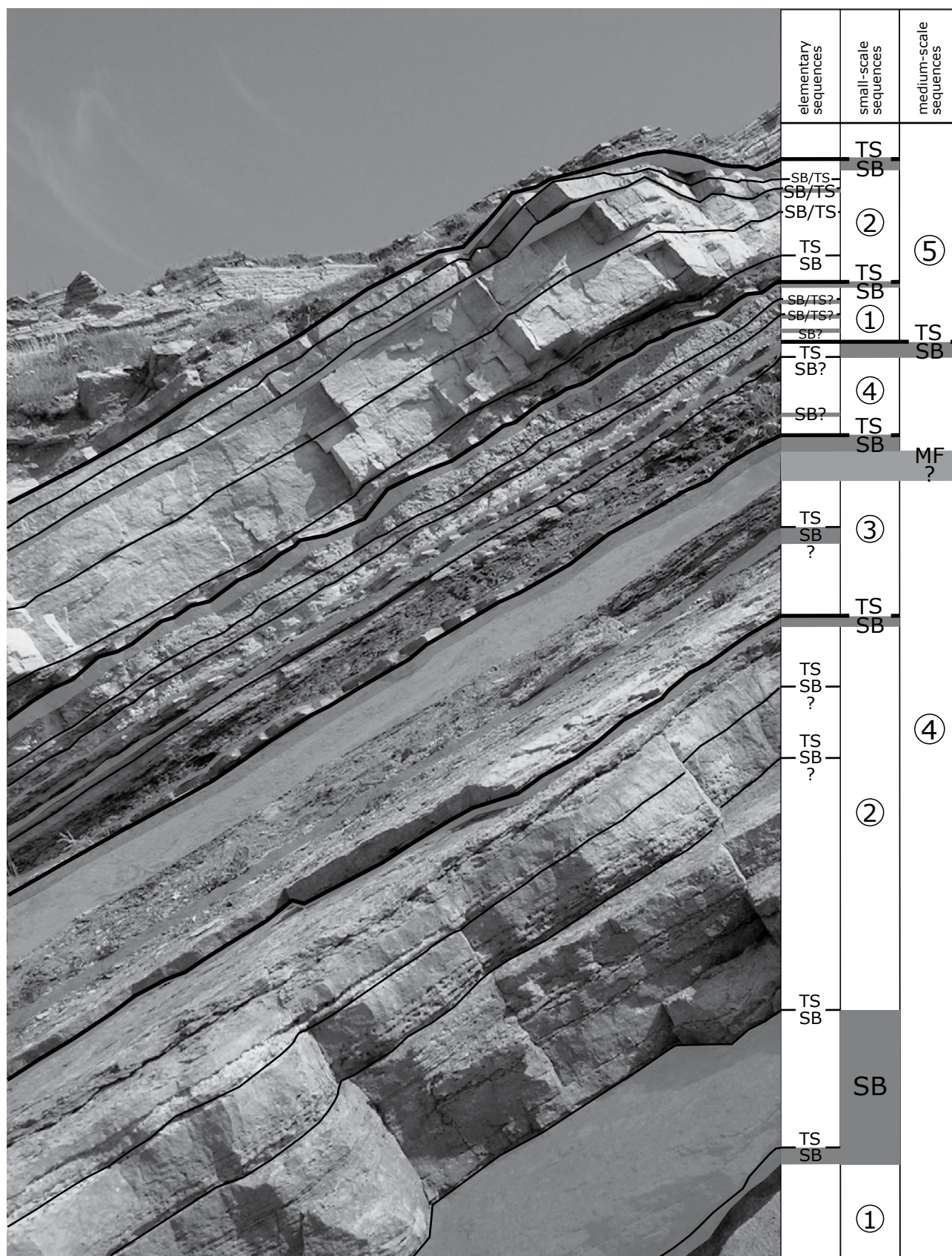


Fig. 5.11e - Worbarrow Tout section (part V).

a “lithostratigraphic correlation framework”. The Mammal Bed (WT 94) is assumed to correspond to the 3<sup>rd</sup>-order sequence boundary Be3 (HARDENBOL et al. 1998). The sequence boundary Be3 is thought to comprehend the entire interval which pinches out laterally (WT 90-96). This assumption implies that an important palaeorelief has been developed during the deposition of the beds around the top of the Soft Cockle and the base of the Marly Freshwater Member. As in Durlston Bay, the 3<sup>rd</sup>-order sequence boundary Be4 must lie between the Mammal Bed and the

Cinder Member. The best candidate for this sequence boundary is represented by the palaeosol interval (at about 8.35 meters). The interval between the 3<sup>rd</sup>-order sequence boundary Be4 and the erosive surface (at 11.90 meters) is characterized by a reduced thickness and/or absence of beds and elementary sequences probably due to condensation and non-deposition. Hence, the sequence-stratigraphical interpretation is not without difficulties and highly speculative. As a consequence, only a possible sequence-stratigraphical interpretation is presented in the graphical log.





**Fig. 5.12** - The Worbarrow Tout section interpreted in terms of high-resolution sequence stratigraphy. The outcrop image shows the upper part of the Intermarine Member (Durlston Bay Formation, WT 130-146).

Based on lateral correlation, it is thought that the interval between the erosive surface (at 11.90 meters) and the base of the Cinder Member comprehends at least two small-scale sequences (cf. Chap. 6). This implies that this interval is strongly condensed.

The base of the Cinder Member marks the beginning of a transgression on a long-term trend (3<sup>rd</sup>-order sequence scale). The entire Cinder Member encompasses one small-scale sequence. The interpretation of elementary sequences is delicate in the Cinder Member due to a lack of significant discontinuities. The sequence boundary of the following small-scale sequence is marked by the thin marly interval (at about 15.00 meters), which defines the boundary between the Cinder Member and the Intermarine Member. This small-scale interval comprehends at least four elementary sequences delimited by well-defined sequence boundaries. The nodular, “dinoturbated” interval is considered as a medium-scale sequence boundary. The following small-scale sequence contains at least three well-expressed elementary sequence boundaries (WT 125-129). The tidal channel interval (WT 130) represents the sequence boundary of the following small-scale sequence. The identification of elementary sequences in this small-scale sequence is not straightforward because it is solely composed of shell beds. The base of a thin shell bed containing reworked intraclasts and shells in convex-up position (at 18.00 meters) is considered as sequence boundary/transgressive surface of the following small-scale sequence (cf. Chap. 3). The sequence-stratigraphical interpretation of the marl interval (WT 132-142) is not straightforward because of reduced thickness and/or absence of beds and elementary sequences due to condensation and non-deposition. Moreover, facies changes are rather subtle, thus hampering a high-resolution sequence-stratigraphical interpretation. It is assumed that it encompassed two small-scale sequences. Additionally, based on lateral correlation, a medium-scale sequence boundary has been set at about 19.10 meters (cf. Chap. 6). A well-expressed small-scale sequence is represented by the massive beds of the following interval (WT 143-145). It comprises at least four elementary sequences delimited by well-defined sequence boundaries. The black laminated marls represent the sequence boundary of the following

small-scale sequence. This small-scale sequence mainly consists of the deposits of the Scallop Member. It contains five elementary sequences. Each of them is composed of a marl interval (sequence boundary) and a shell bed interval (transgressive and early highstand deposits). The Scallop Member is interpreted as maximum flooding on the long-term sequence scale (3<sup>rd</sup>-order sequence). The sequence boundary of the last small-scale sequence is set at the base of the dark gray to black marl interval (base of WT 154). This small-scale sequence comprehends the entire interval, which pinches out laterally. Elementary sequences are not well expressed, probably due to strong condensation. This interval is thought to represent the 3<sup>rd</sup>-order sequence boundary Be5 (according to HARDENBOL et al. 1998). The syn-sedimentary folding described by ENSOM (1985) is probably related to tectonic activity of the nearby Purbeck Fault system. It is assumed that these syn-depositional folds are of a local extent, only. Generally, the bed thicknesses of the Worbarrow Tout section are reduced compared to the beds of the Durlston Bay section. This confirms the lateral thickening of the strata (Purbeck Limestone Group) towards the east in the Dorset region (cf. Fig. 5.3). Fig. 5.12 shows the upper part of the Intermarine Member of this section (WT 130-146). It illustrates the high-resolution sequence-stratigraphical interpretation of this part of the Worbarrow Tout section.

The comparison of the faunicycles established by ANDERSON (1985) with the sequence-stratigraphical interpretation as proposed in this study is partly not in agreement. This may be explained by the fact that the definition of faunicycles is based on material deriving from different boreholes and outcrops of the Channel and Weald sub-basins. Additionally, faunicycles are mainly based on the relative occurrence of the ostracode genus *Cypridea*. HORNE (1995) stated that “(...) the zonation scheme [defined by reference to faunicycles] is supposedly based on ranges of species of the rapidly-evolving genus *Cypridea*, not on environmentally-controlled changes in assemblages” (p. 654). Moreover, he added that “at coarse resolution the zones and assemblages [of faunicycles] can be applied reasonably satisfactorily, but when high resolution is required the schemes simply do not come up to scratch” (p. 654).

\*\*\*\*\*



## 6 - CORRELATIONS

In a first step, intrabasinal correlations of the sections in the different regions are presented and explained. Different tools are used to correlate the sections: lithostratigraphy, biostratigraphy, magnetostratigraphy, and sequence stratigraphy. Each of these tools has a limited range of resolution (e.g., KAUFFMAN et al. 1991). The highest resolution is obtained by sequence-stratigraphical correlations on the scale of elementary sequences.

The correlation between the different depositional basins is discussed in a second step. One basinal section (Vocontian basin: Montclus section) is integrated in an interregional correlation scheme in order to obtain a better biostratigraphical control (ammonite and calpionellid biostratigraphy) for the sections of the Jura platform.

For the first time, a high-resolution sequence-stratigraphical correlation of the Tethyan (Jura platform and Vocontian basin) and the Boreal realm (Dorset region) of the Middle to Late Berriasian has been established in this study.

For the present study, no palinspastic reconstructions have been undertaken. The indicated distances between the sections are measured on today's geographical maps. For the Early Cretaceous world the distances would have to be stretched by a few kilometers between individual sections. Moreover, some lateral off-sets in the order of a few kilometers between sections cannot be excluded. However, the relative proximal-distal distribution of the sections is not affected.

### 6.1 Methods of correlation

#### 6.1.1 Biostratigraphy

Conventionally, biostratigraphy is the first method

to correlate sections over long distances by ascribing a specific biostratigraphical age to sedimentary successions. The first and last appearances of biomarkers are assumed to be synchronous on a regional scale, but taphonomic and ecological factors, and sampling bias, contribute to a certain degree of error. The Montclus section has been well dated by ammonites (LE HÉGARAT 1973, CLAVEL et al. 1986) and by calpionellids (JAN DU CHÊNE et al. 1993, PASQUIER 1995, HILLGÄRTNER 1999). Some ammonites have been found at the base of the Pierre Châtel Formation on the Jura platform (CLAVEL et al. 1986, WAEHRY 1989; see Chap. 4 for discussion).

The charophyte-ostracode assemblages published by MOJON (2002) are an excellent biostratigraphical tool to narrow down the time-resolution of the investigated sections of the Jura platform and the Dorset region. Although taphonomic and ecological problems have to be considered (cf. Chap. 4 and 5), these assemblages provide a time framework with a relatively high resolution.

The Vions Formation of the Jura platform has mainly been dated by benthic foraminifera (PASQUIER 1995, HILLGÄRTNER 1999). Benthic foraminifera are an important biostratigraphical tool for some sections, for which the dating by charophyte-ostracode assemblages has not been made (e.g., Marchairuz section; cf. Fig. 6.2).

#### 6.1.2 Magnetostratigraphy

Magnetostratigraphy is an additional tool for lateral correlation. Although inaccuracies of the magnetization measurements have to be considered, the magnetostratigraphy published for the Durlston Bay section by OGG et al. (1991, 1994) can be compared with the sequence- and chronostratigraphic chart of HARDENBOL et al. (1998). PASQUIER (1995) correlated

the Berriasian type-section at Berrias (Vocontian basin, France), where magnetostratigraphical investigations have been made by GALBRUN (1985) and GALBRUN et al. (1986), with the Montclus section presented in this study.

### 6.1.3 Lithofacies

Well-marked changes in lithofacies have always been used as criteria to define lithostratigraphic units and to correlate them laterally. Such changes are considered to reflect major environmental overturns on a local to regional scale. Large-scale changes in sedimentary architecture (prograding and retrograding of facies belts) may be rooted in external forcing, such as changeovers in plate-tectonic regime and/or substantial climate variations (RAMEIL 2005).

Depending on the resolution of the investigation, these overturns can have a more or less isochronous fingerprint traceable over large distances. However, small-scale diachronisms and lithological heterogeneities deriving from spatial and temporal variations of facies mosaics and/or lateral migration of facies belts are difficult to evaluate without applying other, facies-independent methods of correlation.

Major lithostratigraphic changes occur regularly on the Jura platform (HILLGÄRTNER 1999). An obvious one is the transgression of the Pierre-Châtel Formation on the Goldberg Formation (cf. Chap. 4). The base of this transgression has been used for regional correlations (e.g., MOUTY 1966). It is one of the targets of this study to have a closer look to this transgression with regard to its evolution in time and space (cf. Chap. 9).

In the Dorset region, the Cinder and Scallop Members have been used to correlate sections laterally (e.g., MORTER 1984). Especially the transgression of the Cinder Member has been correlated over long distances even between different sub-basins of southern England (Channel and Weald sub-basins; e.g., WESTHEAD & MATHER 1996).

### 6.1.4 Depositional sequences and diagnostic intervals or surfaces

The stacking pattern of depositional sequences can be used to identify large-scale trends in accommodation change (for definitions see chapter 3). Such trends are commonly of regional extent. However, the studied sections displayed in this chapter are not decompacted. Therefore, the comparison of thickness changes of laterally corresponding depositional sequences can

only be made qualitatively as a first approximation.

The investigated sedimentary record lies between two well-marked discontinuities, which are attributed to the 3<sup>rd</sup>-order sequence boundaries Be4 and Be5 according to HARDENBOL et al. (1998). Sequence boundaries at this scale can be dated with palaeontological and magnetostratigraphical methods. Accordingly, these sequence boundaries define chronostratigraphic correlation lines. The combination of sequence stratigraphy and cyclostratigraphy can further improve time resolution (cf. Chap. 7).

Between these major sequence boundaries, medium-scale sequences have been identified, which are generally well expressed by repetitions of diagnostic surfaces and/or intervals (sequence boundaries, transgressive surfaces, and maximum floodings). Medium-scale sequences build up a correlation framework, which has already been established by earlier studies for the Jura platform (PASQUIER 1995, HILLGÄRTNER 1999). For the Dorset region, a medium-scale sequence framework is provided in this study.

A medium-scale sequence at the base of a long-term transgressive trend has been chosen to investigate depositional sequences in more detail. It is assumed that during a long-term trend of sea level rise, the overall increase of accommodation results in a better record of smaller depositional sequences (cf. Chap. 3).

Small-scale sequences identified on the Jura platform are generally consistent with the ones interpreted in previous studies (PASQUIER 1995, PASQUIER & STRASSER 1997, HILLGÄRTNER 1999, STRASSER et al. 2004). However, in the Dorset region, the interpretation of small-scale sequences in the upper part of the Lulworth Formation is not straightforward, probably due to a relatively low increase of accommodation (long-term lowstand; cf. Chap. 5). During the long-term transgressive trend in the lower part of the Durlston Formation, the expression of small-scale sequences in the sedimentary record is better developed.

The identification of elementary sequences is not without difficulties in both regions. This is mainly due to the dominance of local factors on this scale of investigation. Moreover, the facies mosaics of shallow carbonate platforms with both lateral and vertical rapid facies variations reflect the dynamics and complexity of sedimentary systems where juxtaposed sub-environments evolved and shifted through space and time (SAMANKASSOU et al. 2003, WRIGHT & BURGESS 2005). Incompleteness of the sedimentary record also has to be taken into account (cf. Chap. 7). Local factors (e.g., platform morphology, differential subsidence, hydrodynamic

pattern, terrigenous input) modify the depositional record so that the expression of depositional sequences and discontinuity surfaces vary from section to section (e.g., SATTler et al. 2005). Long-distance correlations between different depositional basins, however, help to filter out local and regional effects (e.g., PITTET & STRASSER 1998b, STRASSER et al. 1999, SANDULLI & RASPINI 2004, SCHLAGER 2005). Furthermore, bio- and magnetostratigraphical resolution is lower than the time span represented by small-scale and elementary sequences investigated in this study (cf. Chap. 7). Accordingly, high-resolution correlation of depositional sequences can only result in a reasonable best-fit solution, which is consistent with the biostratigraphical framework (PASQUIER & STRASSER 1997). Several best-fit solutions of the investigated sections have been elaborated by the Fribourg working group over the last ten years (WAEHRY 1989, PASQUIER 1995, PASQUIER & STRASSER 1997, HILLGÄRTNER 1999, STRASSER et al. 2004). However, the higher sampling density and time resolution of this study as well as additional sections have led to reinterpretations of depositional sequences. Hence, a revised best-fit solution is here presented.

High-resolution correlations over long distances are usually based on diagnostic surfaces and/or intervals, which are assumed to be more or less isochronous (STRASSER et al. 2004, SATTler et al. 2005). The time resolution of investigation plays an important role when dealing with dia- and isochronous intervals and/or surfaces (e.g., KOWALEWSKI & BAMBACH 2002). The question has to be addressed, which surfaces and/or intervals have to be chosen for a satisfactory lateral correlation. Sequence boundaries may include hiatuses in marginal-marine environments because of erosion and/or non-deposition (cf. Fig. 6.1a). Depending on the time resolution of investigation (e.g., biostratigraphical resolution), a sequence-boundary interval may be isochronous, but its delimiting, physical surfaces cross time lines. Transgressive surfaces are generally not isochronous if there is a pre-existing morphological relief (Fig. 6.1b). Maximum-flooding intervals or surfaces have the best chance to homogenize a morphological relief in shallow-marine settings and, consequently, to be isochronous. Accordingly, they are considered to be ideal for correlation over long distances (e.g., EMBRY 2002, SANDULLI & RASPINI 2004; cf. Fig. 6.1c).

In order to simplify the representation of lateral correlations, medium-scale and small-scale sequences interpreted to be correlative are numbered homogeneously for all sections in each correlation chart, regardless of their numbers in preceding figures. The numbers refer to the best-fit solution established

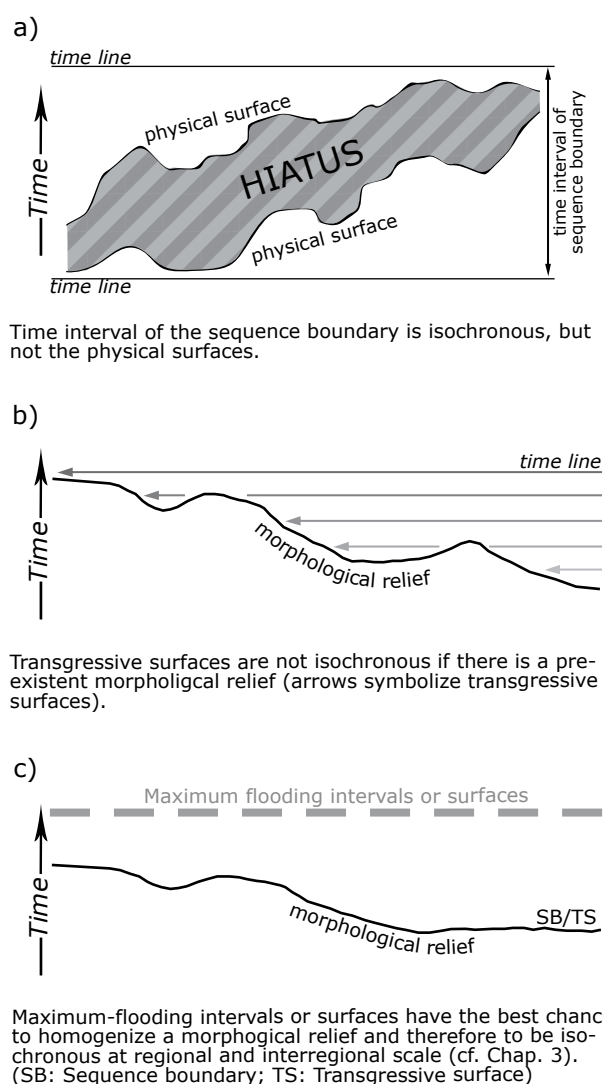


**Fig. 6.1** - Models illustrating diagnostic intervals or surfaces in time and space. a) Sequence boundaries; b) Transgressive surfaces; c) Maximum floodings.

in this study, which is based on the lateral correlation of all investigated sections (Fig. 6.13).

## 6.2 Correlation of the Jura platform sections

The correlation of the Jura platform sections is based on the studies of WAEHRY (1989), PASQUIER (1995), and HILLGÄRTNER (1999). Every section presented in this study has already been interpreted on a sequence-stratigraphical resolution of medium-scale and small-scale sequences between the 3<sup>rd</sup>-order sequence boundaries Be4 and Be5 (Middle to Late Berriasian according to HARDENBOL et al. 1998). This study takes advantage of this well-established

sequence-stratigraphical framework and zooms into a relatively small part (three small-scale sequences) of the interval between the sequence boundaries Be4 and Be5 (cf. Fig. 6.4).

### 6.2.1 Correlation of small-scale sequences

Three sections (Rusel, Marchairuz, and Chapeau de Gendarme) have been chosen to illustrate and discuss the sequence-stratigraphical correlation of small-scale sequences between the 3<sup>rd</sup>-order sequence boundaries Be4 and Be5 (Fig. 6.2).

#### *Biostratigraphy*

According to CLAVEL et al. (1986), the base of the Pierre Châtel Formation lies in the Privasensis ammonite subzone (cf. Figs. 4.4 and 6.3). The top of the Goldberg Formation and the base of the Pierre Châtel Formation have been dated by charophyte-ostracode assemblages (MOJON 2002; cf. Chap. 4). The top of the Goldberg Formation is in the range of assemblage zones M1b to M4. The base of the Pierre Châtel Formation lies in assemblage zone M4 and contains in some sections reworked species of assemblage zone M3 (cf. Chap. 4). According to the dating by charophyte-ostracode assemblages, the transition from the Goldberg Formation to the Pierre Châtel Formation lies in the range of the 3<sup>rd</sup>-order sequences boundaries Be2 to Be4 (Grandis to Privasensis ammonite subzones; cf. Fig. 4.4).

The top of the Pierre Châtel Formation and the base of the Vions Formation have been dated by benthic foraminifera (*Pseudotextulariella courtionensis* and *Pavlovecina allobrogensis*). According to PASQUIER (1995) and HILLGÄRTNER (1999), the transition between the Pierre Châtel and the Vions Formations coincides with the 3<sup>rd</sup>-order sequence boundary Be5 (Paramimounum ammonite subzone).

#### *Depositional sequences and diagnostic intervals or surfaces*

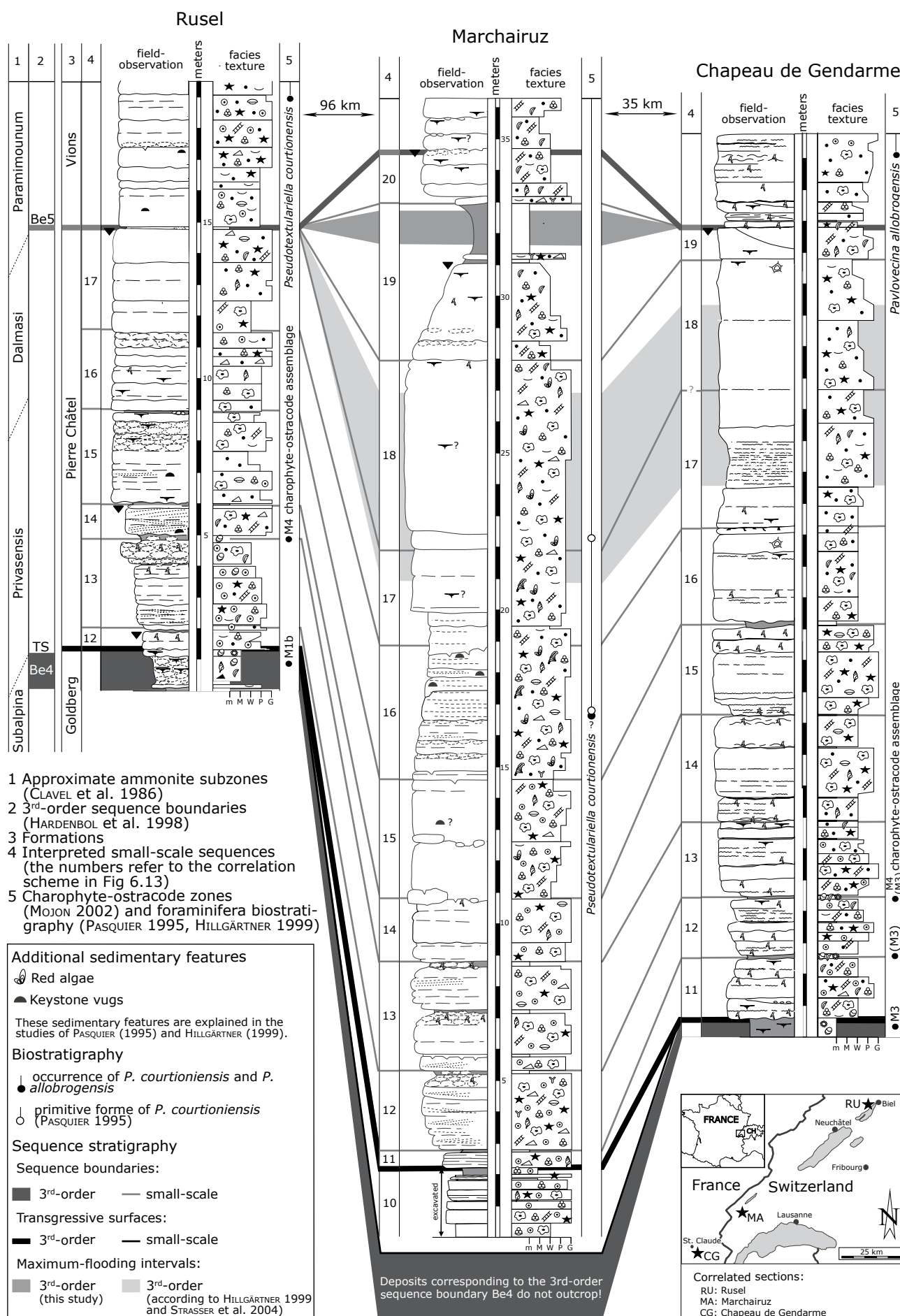
The transgression of the Pierre Châtel Formation onto the peritidal facies at the top of the Goldberg Formation has been considered as diachronous in previous studies (e.g., HÄFELI 1966, STEINHAUSER & CHAROLLAIS 1971, ARNAUD-VANNEAU & ARNAUD 1991). This interpretation resulted from the lateral facies heterogeneity at the base of the Pierre Châtel Formation. PASQUIER (1995) and STRASSER et al. (2004) postulated a step-wise transgression of the Pierre

Châtel Formation strongly depending on the pre-existing platform morphology.




The thick transgressive deposits (TD) are characterized by relatively restricted facies and repeated subaerial exposure in the platform interior (karstification; e.g., Rusel section), and open-lagoonal deposits in more distal platform positions (e.g., Marchairuz section). A transitional facies succession is indicated by the Chapeau de Gendarme section where relatively thin beds with restricted facies dominate at the base of the Pierre Châtel Formation, which gradually change to massive, open-lagoonal beds.

The large-scale maximum-flooding interval has been interpreted differently from the preceding studies, depending on a new sequence-stratigraphical interpretation and a new best-fit solution. Thick or condensed lagoonal deposits representing the relatively deepest facies have been interpreted as large-scale maximum-flooding intervals. PASQUIER (1995) and PASQUIER & STRASSER (1997) interpreted a perforated oyster-rich hardground at the top of the Rusel section (top of small-scale sequence 17) as large-scale maximum-flooding surface. A karst surface is superposed onto the hardground. Emersion at this surface is also indicated by stable isotopes (positive oxygen-isotope shift due to evaporation and negative carbon-isotope shift related to soil gas; cf. Chap. 8; PASQUIER 1995, PASQUIER & STRASSER 1997). This study gives preference to the interpretation of STRASSER et al. (2004) by assuming that the large-scale maximum flooding is not represented in the Rusel section. The large-scale maximum-flooding interval of the Marchairuz section follows the interpretation published by PASQUIER (1995) and PASQUIER & STRASSER (1997). It lies in a thick marl interval in small-scale sequence 19. Interpreting the relatively thickest beds as the large-scale maximum-flooding interval of the Chapeau de Gendarme section, HILLGÄRTNER (1999) and STRASSER et al. (2004) attributed it to small-scale sequences 17 to 18 (cf. Fig. 6.2). Following this interpretation, the corresponding maximum-flooding intervals of the Marchairuz and the Chapeau de Gendarme sections would be in the relatively thick beds of small-scale sequences 17 to 18. In this study, however, it is assumed that the large-scale maximum

**Fig. 6.2** – (facing page) Best-fit correlation of the large-scale depositional sequence between the 3<sup>rd</sup>-order sequence boundaries Be4 and Be5 (HARDENBOL et al. 1998) and the small-scale sequences of the Jura platform. The numbers of the small-scale sequences correspond to the ones of the correlation scheme in Fig. 6.13. Small-scale sequences 10 to 13 are displayed in detail in Figs. 6.4 and 6.5. For legend refer to Fig. 4.6.



Tethyan bio-, sequence- and magnetostratigraphy according to HARDENBOL et al. (1998)						Bio-, sequence-, and lithostratigraphic interpretations of the Jura platform and the Vocontian basin according to different authors											
Stages	Informal sub-stages	Zones	Subzones	3 <sup>rd</sup> -order sequence boundaries	Magneto-stratigraphy	Calpionellids	Zones	1	2	3	4	5	6	7	8	9	This study
BERRIASIAN	Late	BOISSIERI	Paramimounum	Be5	M16n	Calpionellopsis	D1	Vions			Be5	Be5	Be5	Be5	Vions	Be5	Be5
				139.3				?							M5		
	Middle	OCCITANICA	Dalmasi	Be4	M17n	Calpionella	C	Pierre Châtel			Be4	Be4	Be4	Be4	Pierre Châtel	Be4	Pierre Châtel
				141.0				?	Be4	Be4	Be4	Be4	Be4	Be4	M4	Be4	Be4
				Be3					Be3	Be3	Be3	Be3	Be3	Be3	?	Be3	Be3
				141.8													
	Early	JACOBI	Grandis	Be2?	M18n	Calpionella	B	Purbeckian									
				143.0													
BERRIASIAN	Early	JACOBI	Grandis	Be2?	M18n	Calpionella	B	Purbeckian									
				143.0													
	Middle	OCCITANICA	Dalmasi	Be4	M17n	Calpionella	C	Pierre Châtel			Be4	Be4	Be4	Be4	Pierre Châtel	Be4	Pierre Châtel
				141.0				?	Be4	Be4	Be4	Be4	Be4	Be4	M4	Be4	Be4
				Be3					Be3	Be3	Be3	Be3	Be3	Be3	?	Be3	Be3
				141.8													
	Late	BOISSIERI	Paramimounum	Be5	M16n	Calpionellopsis	D1	Vions			Be5	Be5	Be5	Be5	Vions	Be5	Be5
				139.3				?							M5		

 Diachronous limit of the sequence boundary  
 3<sup>rd</sup>-order sequence boundary  
 Isochronous limit of the sequence boundary

- 1 CLAVEL et al. (1986): Formations of Jura platform
- 2 JAN DU CHÊNE et al. (1993): Sequence-stratigraphical interpretation based on sections of the Vocontian basin
- 3 STEFFEN (1993): Sequence-stratigraphical interpretation based on sections of the Vocontian basin
- 4 PASQUIER (1995): Sequence-stratigraphical interpretation based on sections of the Jura platform and the Vocontian basin
- 5 PASQUIER & STRASSER (1997): Sequence-stratigraphical interpretation based on sections of the Jura platform and the Vocontian basin
- 6 HILLGÄRTNER (1999): Sequence-stratigraphical interpretation based on sections of the Jura platform and the Vocontian basin
- 7 HOEDEMAEKER (2002): Sequence-stratigraphical interpretation based on sections of the Jura platform. This sequence-stratigraphical interpretation mainly refers to the "French code" of ARNAUD-VANNEAU & ARNAUD (1991). ("BCU" means "Basinal Cretaceous Unconformity")
- 8 MOJON (2002): Charophyte-ostracode assemblages based on sections of the Jura platform
- 9 STRASSER et al. (2004): Sequence-stratigraphical interpretation based on sections of the Jura platform and the Vocontian basin

flooding of the Chapeau de Gendarme section has been truncated by the karst surface at the top of small-scale sequence 19 as in the Rusel section. Moreover, it better fits the lateral correlation of the sections in the Dorset region where the maximum-flooding interval lies within small-scale sequence 19 (Scallop Member; cf. Chap. 5)

Karst surfaces and/or palaeosols have been observed at the transition of the Pierre Châtel Formation to the Vions Formation and correlated throughout the Jura platform (PASQUIER 1995, PASQUIER & STRASSER 1997, HILLGÄRTNER 1999, STRASSER et al. 2004). They have been interpreted as 3<sup>rd</sup>-order sequence boundary Be5 (e.g., PASQUIER 1995, HILLGÄRTNER 1999). Accordingly, long-lasting exposure led to the erosion and/or condensation of small-scale sequences representing the large-scale highstand deposits. HILLGÄRTNER (1999) assumed that this widespread exposure was due to tectonic activity leading to uplift or strongly reduced subsidence during the deposition of the highstand sediments. As a consequence, the 3<sup>rd</sup>-order sequence between sequence boundaries Be4 and Be5 displays an extremely asymmetric stacking pattern reflected by thick transgressive and thin highstand deposits (cf. Fig. 6.2).

## 6.2.2 Correlation of elementary sequences

Four small-scale sequences at the base of the Pierre Châtel Formation have been chosen to investigate the sedimentary record in more detail (small-scale sequences 10 to 13; Fig. 6.4). Detailed sedimentological and sequence-stratigraphical interpretations of these intervals are given in Chap. 4 (small-scale sequences 0 to 4 in Chap. 4 correspond to small-scale sequences 10 to 14 in this chapter).

### *Biostratigraphy*

The range of the charophyte-ostracode assemblages at the top of the Goldberg Formation exhibits considerable differences between the sections (cf. Fig. 6.4). In three sections (Rusel, Thoirrette, and Yenne), this interval lies in the assemblage zone M1b, which corresponds to the Grandis ammonite subzone. STRASSER (1994) gave to consider that “it has to be

kept in mind that the top of the Goldberg formation commonly shows condensation due to non-deposition, reworking or erosion, so that dates furnished by fossils often cannot be attributed to a particular sequence” (p. 296).

Accordingly, a long-lasting hiatus has to be assumed at the top of the Goldberg Formation of these sections because the base of the Pierre Châtel Formation already lies in the assemblage zone M4 (Privasensis subzone). A relative decrease of the duration of this hiatus is suggested by the presence of assemblage zone M2 (Cornaux and Poizat), M3 (Chapeau de Gendarme and St. Claude), and M4 (Crozet, Lavans, and Val de Fier) at the top of the Goldberg Formation.

Several intervals in small-scale sequences 11 and 12 of different sections (Rusel, Cornaux, Chapeau de Gendarme, St. Claude, and Lavans) have been dated by charophyte-ostracode assemblages (MOJON 2002). They contain species of the assemblage zone M4 and/or reworked species of the assemblage zone M3. The last occurrence of a charophyte-ostracode assemblage zone in the investigated sections is situated at the sequence boundary of small-scale sequence 13 of the Rusel section.

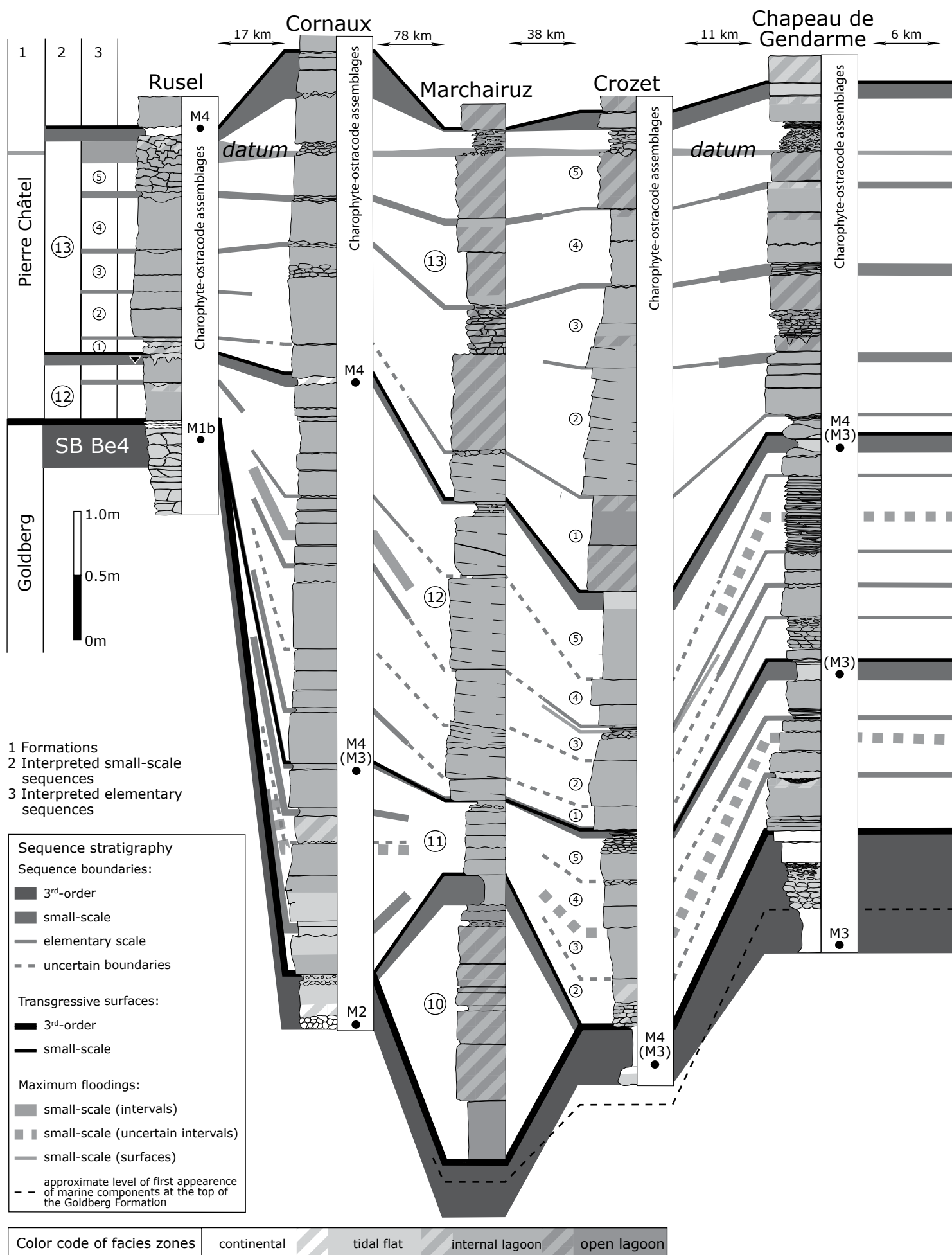
### *Depositional sequences and diagnostic intervals or surfaces*

The well-expressed maximum flooding (interval or surface) of small-scale sequence 13 of each section has been used as datum (Fig. 6.4). As a working hypothesis, it is assumed that these maximum floodings are more or less time-equivalent (cf. Fig. 6.1c). By counting small-scale and elementary sequences downwards from this datum, the large-scale transgression represented by the base of the Pierre Châtel Formation exhibits deviations of up to two small-scale sequences.

In several sections, however, marine components (mainly foraminifera) have been identified already at the top of the Goldberg Formation, below the large-scale transgressive surface. Pursuant to characteristic sedimentary structures (birdseyes and/or circumgranular cracks; cf. Chap. 4), these intervals have been interpreted as tidal flat deposits. This implies that repetitive marine ingressions (precursors of the Pierre Châtel transgression; STRASSER 1988) have been recorded at the top of the Goldberg Formation, prior

**Fig. 6.3** - (facing page) Figure displays the bio-, sequence-, and lithostratigraphic interpretations of the Jura platform and the Vocontian basin according to different studies. All limits are approximately indicated and adjusted to the sequence- and chronostratigraphic chart of HARDENBOL et al. (1998).







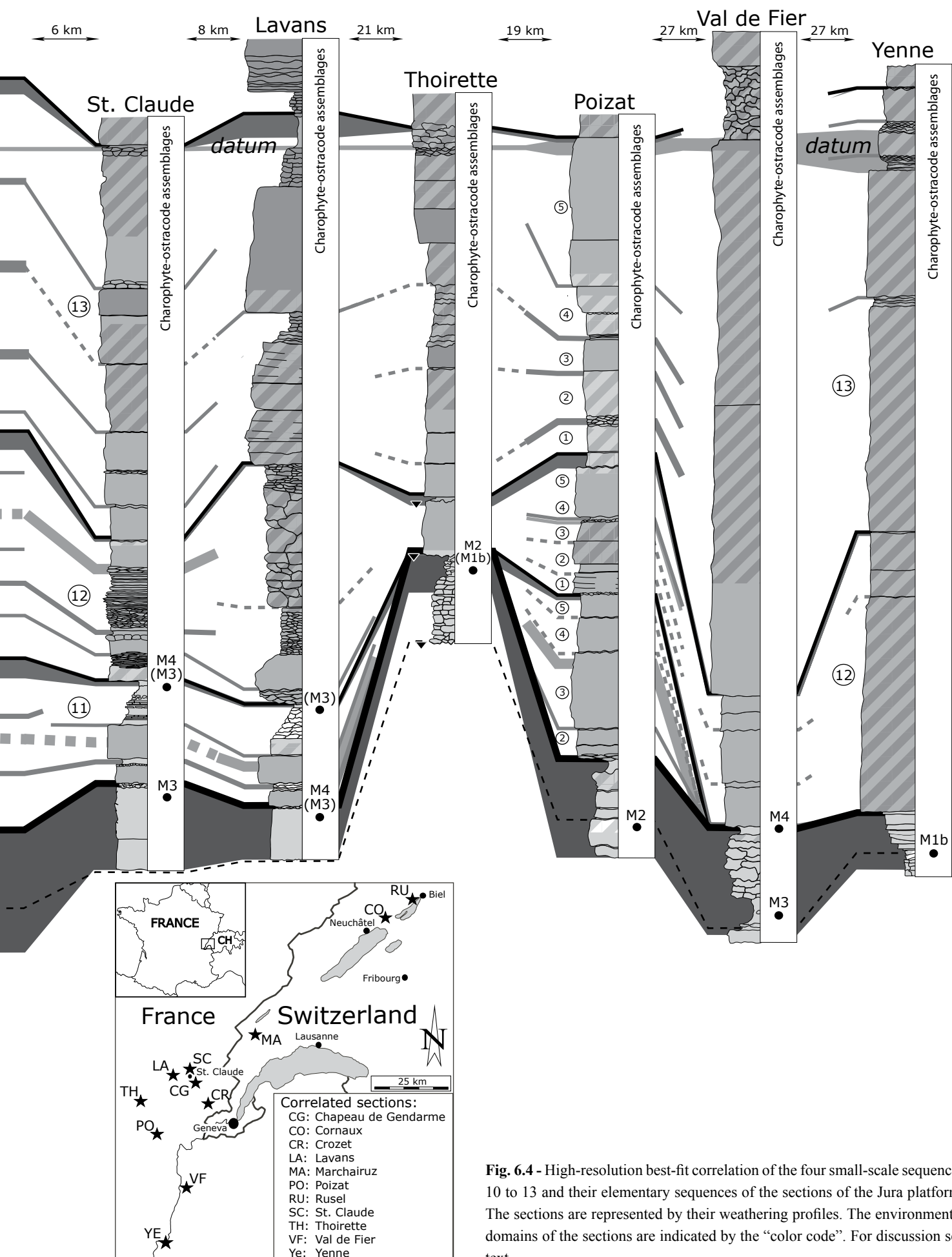


**Fig. 6.4** - High-resolution best-fit correlation of the four small-scale sequences 10 to 13 and their elementary sequences of the sections of the Jura platform. The sections are represented by their weathering profiles. The environmental domains of the sections are indicated by the “color code”. For discussion see text.

to the large-scale flooding of the platform. A black dotted line illustrates this first appearance of marine components in Fig. 6.4.

According to the sequence-stratigraphical interpretation, the large-scale transgression manifested itself at least two small-scale sequences earlier in Marchairuz than in Rusel or Thoirette. It has been postulated that the transgression started in the southwest of the Jura platform and continued to the northeast (e.g., WAEHRY 1989, PASQUIER 1995, HILLGÄRTNER 1999). The thickness of small-scale sequences generally decreases from southwest to northeast on the Jura platform suggesting higher accommodation potential in the southeast. Besides, the sediments of the sections on the southwestern Jura platform (Yenne and Val de Fier) are composed of relatively open-marine components compared with the sections in the northeast (Rusel and Cornaux).

A step-wise transgression encroaching the shallow carbonate platform in a southwest to northeast direction has been postulated by PASQUIER (1995) and STRASSER et al. (2004). STRASSER et al. (2004) published a description of the large-scale transgression on the scale of elementary sequences.

A morphological depression can be postulated in the region of the Marchairuz section. This section is composed of the relatively most marine components of all sections and displays relatively thick beds at the base of the Pierre Châtel Formation (cf. Figs. 6.2 and 6.4). Moreover, according to the sequence-stratigraphical interpretation, the large-scale transgression reaches the Marchairuz section at least one small-scale sequence before it is recorded in most of the other sections. The depression at Marchairuz may either represent a relatively deep bay and/or a broad, deep channel. MOJON (2002) postulated a shallow marine depression in the region of Marchairuz (central Jura graben), which connected the Tethys ocean with the Paris basin (cf. Chap. 9). This assumption is underlined by the identification of Boreal ostracodes on the Jura platform (cf. Chap 5; Tab. 5.3). This depression is probably related to tectonic lineaments.

The Jura platform was affected by block-faulting and differential subsidence during the Mesozoic (e.g., WILDI et al. 1989, LOUP 1992, ALLENBACH 2002). HILLGÄRTNER (1999) showed that the southern Jura platform was influenced by differential subsidence from Middle to Late Berriasian times. The Lavans section displays an extraordinary sedimentary succession, which can mainly be related to differential subsidence. At the base of the Pierre Châtel Formation, this section is characterized by peritidal and even supratidal deposits (small-scale sequence 11) implying a rather proximal position on the platform. An abrupt facies change then leads to internal- and/or open-lagoonal deposits in

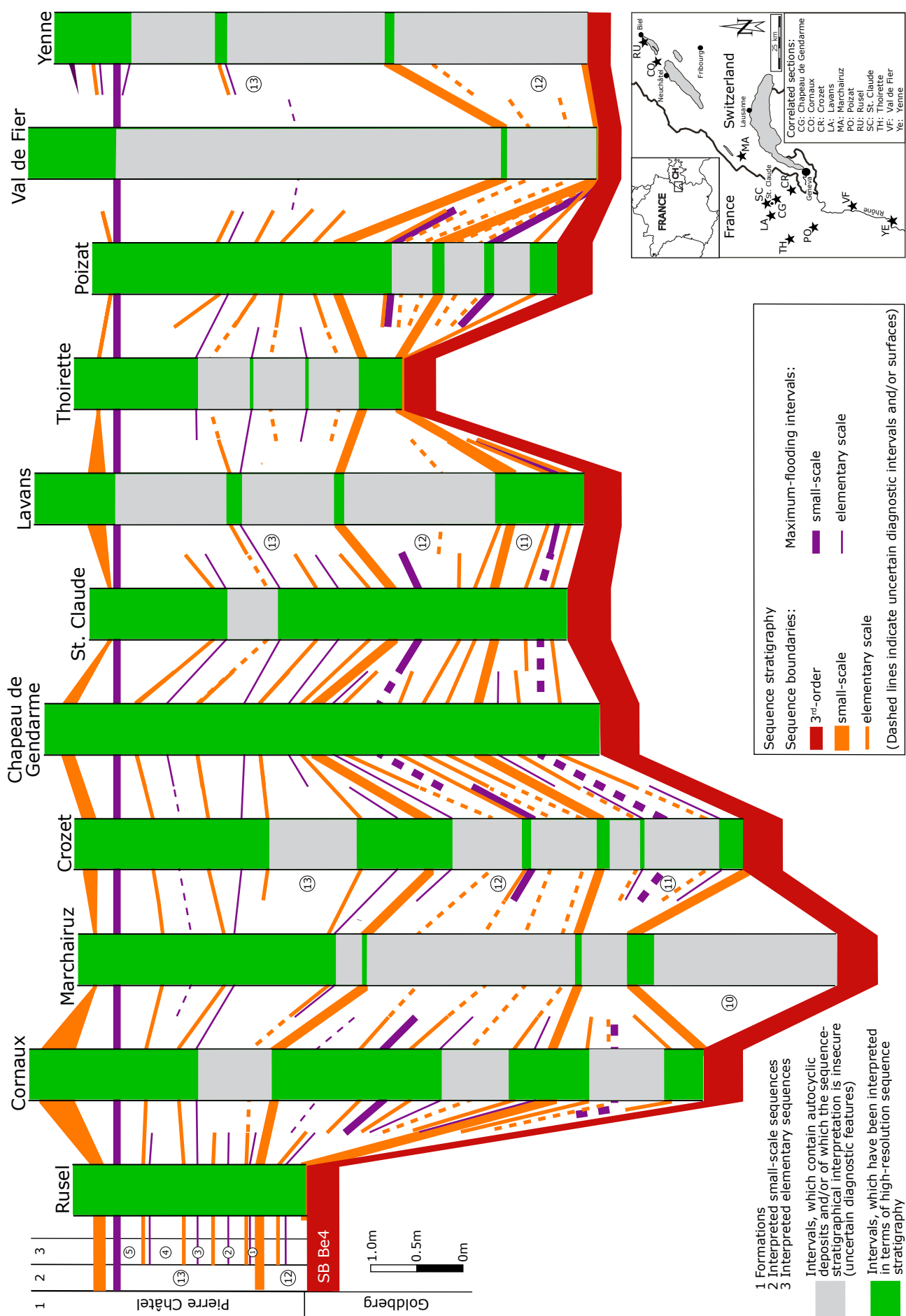
the following small-scale sequences. Moreover, this section is composed of the most open-marine facies (in the three investigated small-scale sequences) of all investigated sections. Such a drastic facies change can be related to a relatively strong differential subsidence probably caused by block-faulting. A similar facies succession is displayed by the Thoirette section. Several karst surfaces at the top of the Goldberg Formation and the base of the Pierre Châtel Formation (small-scale sequence 12) suggest that the Thoirette section has been located on a morphological high. According to the sequence-stratigraphical interpretation, small-scale sequence 11 is even missing in the Thoirette section. The abrupt facies change to internal- and/or open-lagoonal settings imply a rapidly increased subsidence during the following small-scale sequences. Increased subsidence can also be postulated for the Val de Fier section, in which small-scale sequence 13 is composed of only two thick beds. The absence of characteristic discontinuities and facies changes at this location (no threshold effects) may reflect the creation of a more or less constant accommodation space by high subsidence.

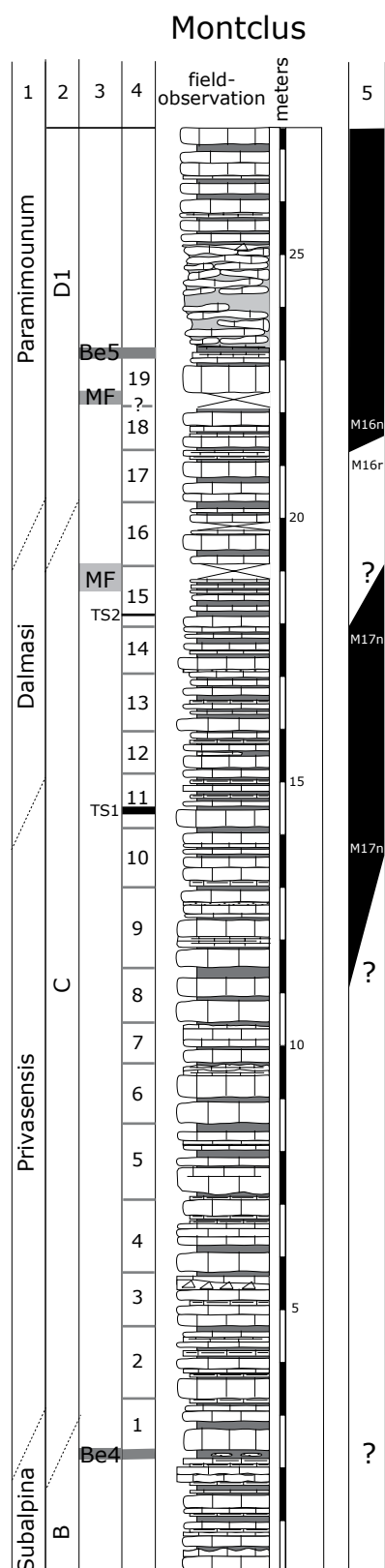
In contrast, small-scale sequence 12 of the Poizat section is composed of tidal flat to internal-lagoonal deposits, which does not correspond to the general facies evolution of the other sections. Accordingly, this interval cannot be explained by a gradual increase of accommodation space. It is thought that it has been controlled by a relative decrease of subsidence or even episodic uplift during the deposition of this interval.

The high-resolution investigation on the scale of elementary sequences proposed in this study enables the interpretation of the different factors influencing a shallow carbonate platform. However, on such a high-resolution, the interpretation of elementary sequences is not without difficulties (Fig. 6.4). This is mainly due to the interplay of allo- and autocyclic processes, which both are able to produce depositional sequences (cf. Chap. 3).

In the best case, the predominance of autocyclic processes can directly be deduced in the field. Migrating tidal channels or ooid shoals can be recognized based on their characteristic sedimentary structures and their limited lateral and vertical extension. The autocyclically controlled intervals displayed in Fig. 6.5 are mainly composed of shoal deposits. It appears that shoal intervals are more common at the base of the large-

**Fig. 6.5** – (facing page) Best-fit correlation of the four small-scale sequences 10 to 13 and their elementary sequences. Intervals, which contain autocyclic deposits and/or of which the sequence-stratigraphical interpretation is insecure are illustrated by gray intervals. For discussion refer to text.





- 1 Approximate ammonite subzones (Le Hégarat 1973)
- 2 Approximate calpionellid biostratigraphy based on Pasquier (1995) and Hillgärtner (1999)
- 3 3<sup>rd</sup>-order sequence boundaries based on Strasser et al. (2004)
- 4 Interpreted small-scale sequences based on Strasser et al. (2004)
- 5 Magnetostratigraphy published by Galbrun (1985) and Galbrun et al. (1986)  
The boundaries are approximately illustrated based on the correlation with the Berriasian type-section of Berrias established by Pasquier (1995)

scale transgression (small-scale sequences 11 to 12). This can be related to the generally higher depositional energy at the beginning of the transgression, and the deposition of low-energy, lagoonal deposits (mud-to packstones) once water depth has increased. Such depositional intervals cannot be interpreted directly in terms of high-resolution sequence stratigraphy (on the scale of elementary sequences)

Another problem has to be considered when interpreting and correlating sedimentary succession with high resolution. Depositional contrasts may not be recorded and/or are too subtle to be interpretable in shallow marine environments (e.g., Val de Fier and Yenne sections). This is mainly due to the absence of threshold effects, which lead to characteristic facies changes in subtidal environments ("missed beats" sensu Goldhammer et al. 1990; cf. Fig. 3.6b).

Nevertheless, in the four investigated small-scale sequences, a large part of the deposits can be interpreted in terms of high-resolution sequence stratigraphy (green intervals in Fig. 6.5). Besides the sequence boundaries, maximum floodings are important diagnostic features for detailed sequence-stratigraphical investigations. Some maximum-floodings intervals can be correlated over long distances (e.g., maximum flooding of elementary sequence 3 in small-scale sequence 13). Maximum floodings on the scale of elementary sequences are generally better expressed in small-scale sequences 12 and 13.

Accordingly, by correlating sequence boundaries and maximum floodings of elementary sequences, a high-resolution sequence-stratigraphical framework can be established. Intervals, which are composed of autocyclic deposits and/or of which sequence-stratigraphical investigations are uncertain can at least be constrained at the base and top by high-resolution sequence-stratigraphical correlations. Based on this sequence-stratigraphical correlation, a detailed illustration and discussion of the geodynamical evolution of the Jura platform during the Middle Berriasian transgression is presented in Chap. 9.

### 6.3 Basinal section (Vocontian basin)

A basinal section of the Vocontian basin (Montclus section; cf. Fig. 6.6), which is well-dated by

**Fig. 6.6** – (left side) Sequence-stratigraphical interpretation of the Montclus section. The small-scale sequences are indicated and numbered.

ammonites and calpionellids, has been chosen to correlate it with the sections of the Jura platform (cf. Fig. 6.8). This correlation enables an improvement of the biostratigraphical time control on the platform.

### 6.3.1 The Vocontian basin

The deposits of the Vocontian basin are nowadays situated in southeastern France (cf. Fig. 6.7). During the Berriasian, this basin was the southwestern continuation of the Ligurian Tethys. It was delimited to the north and west by the Helvetic shelf and the Jura platform and the landmass of the Massif Central (cf. Fig. 4.3). To the south, the Vocontian basin bordered the Provence platform. This basin has been filled with hemipelagic to pelagic sediments (carbonates and siliciclastics) and intermittent biodetrital influx from the surrounding platforms (e.g., STROHMENGER & STRASSER 1993).

The Berriasian type-section of Berrias was situated close to the western slope of the Vocontian basin (cf. Fig. 6.7). The sediments of the Montclus section have been deposited more in the centre of the Vocontian basin between two major, east-west oriented submarine canyons (Drôme and Méouge canyons; e.g., LE HÉGARAT 1973; cf. Fig. 6.7).

### 6.3.2 Hemipelagic to pelagic depositional systems of the Vocontian basin

The expression of environmental changes in basinal, hemipelagic to pelagic sections is completely different from those in platform environments. Environmental changes in basinal depositional settings are indicated by variations in palaeoecology (macro-, micro-, and nannofossils), different composition of organic matter, and/or changes of mineralogical and geochemical characteristics. These variations can be used for sequence-stratigraphical interpretations (e.g., JAN DU CHÊNE et al. 1993). Additionally, facies analyses and the geometric relationship of the strata (carbonate and marl beds) and variations of their stacking pattern in different basinal successions have been related to environmental changes associated with relative sea-level changes (e.g., STROHMENGER & STRASSER 1993; cf. Chap. 3). Different factors are thought to control the changes in stacking pattern in deep-marine depositional systems. The main factors are winnowing of fine-grained sediments by bottom currents, intensified export of platform material to more distal, basinal depositional settings (e.g., slumps and turbidites in basin floor fans, slope fans and lowstand

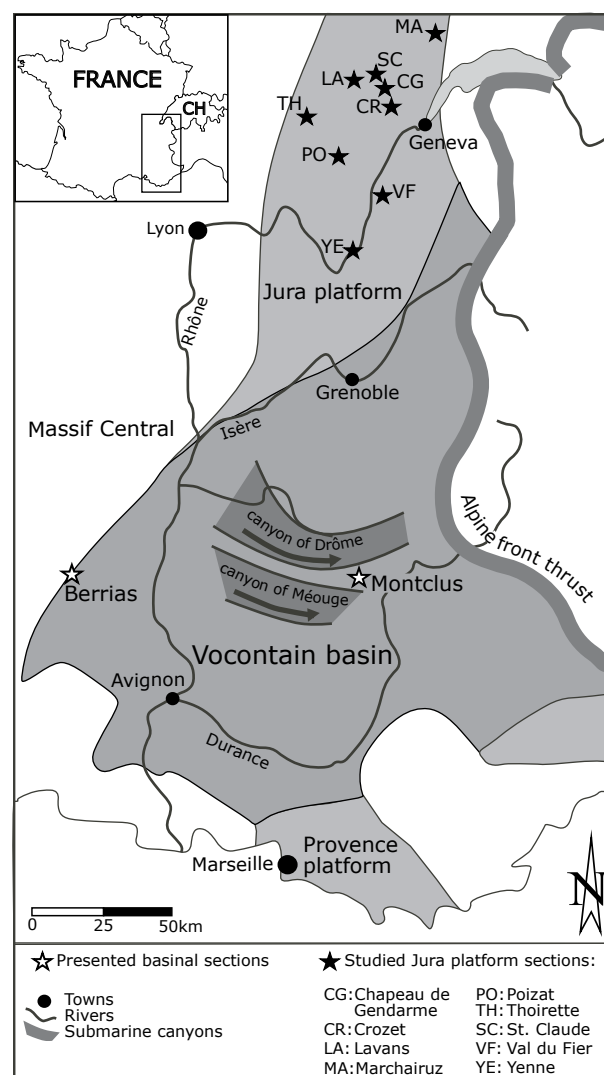


**Fig. 6.7** - Geographic location of the Montclus and the Berrias sections and palaeogeographic domains between the Jura and the Provence platform. The locations of some of the studied sections from the Jura platform are also indicated (modified from PASQUIER 1995)

prograding wedges, highstand shedding), fluctuations in the calcite compensation depth (CCD) and oxygen-minimum zones, and changes of climate and/or oceanic circulation patterns, which influence the planctonic productivity and the clay input and distribution (e.g., EINSELE & RICKEN 1991a, HILLGÄRTNER 1999).

The type-section of the Berriasian stage is located close the village of Berrias in southeastern France (Fig. 6.7). This section has been well investigated in terms of biostratigraphy (e.g., LE HÉGARAT & REMANE 1968, LE HÉGARAT 1973, 1980) and magnetostratigraphy (GALBRUN 1985, GALBRUN et al. 1986). Sedimentological investigations and sequence-stratigraphical interpretations of large-scale depositional sequences of this section have been

reported in previous studies (e.g., JAN DU CHÊNE et al. 1993, STROHMENGER & STRASSER 1993, STEFFEN 1993). PASQUIER (1995) and PASQUIER & STRASSER (1997) correlated 3<sup>rd</sup>-order sequence boundaries of the Berrias section with other sections of the Vocontian basin. Yet, the Berrias type-section is strongly condensed due to its position close to the basin and, therefore, sequence-stratigraphical interpretations are not straightforward (e.g., GORIN & STEFFEN 1991, JAN DU CHÊNE et al. 1993, STEFFEN 1993, STROHMENGER & STRASSER 1993, PASQUIER 1995, PASQUIER & STRASSER 1997).

### 6.3.3 Montclus section

The basinal section of Montclus has been chosen in order to analyze a more or less complete section (absence of major hiatuses) and to improve the biostratigraphical control of the investigated time interval (cf. Fig. 6.3). Sedimentological and sequence-stratigraphical interpretations are based on existing studies (PASQUIER 1995, PASQUIER & STRASSER 1997, HILLGÄRTNER 1999, STRASSER et al. 2004).

#### *Geographic and stratigraphic setting*

The Montclus section is located about 500 meters to the northeast of the village of Montclus next to the French departmental road (D499) towards Serres (coordinates 863.400/240.850, IGN map, 1/50000, Serres XXXII-39; cf. LE HÉGARAT 1973). A detailed map displaying the location of the Montclus section is given in HILLGÄRTNER (1999). The biostratigraphical dating is based on ammonites (Subalpina to Paramimounum subzones; LE HÉGARAT 1973) and calpionellids (zones B to D1; JAN DU CHÊNE et al. 1993, PASQUIER 1995, HILLGÄRTNER 1999).

#### *Sedimentological interpretation*

The entire sedimentary record is composed of a succession of hemipelagic to pelagic marls and limestones (cf. Fig. 6.6). The limestone beds contain mainly nannoplankton (e.g., COTILLON et al. 1980, STROHMENGER & STRASSER 1993). A succession of relatively thick, irregular, and locally channelled limestone beds form the base of this section (from 2.20 to 14.50 meters; STRASSER et al. 2004). The following interval is characterized by thinner and more homogeneous limestone-marl alternations (from 14.50 to 18.50 meters). A change to the relatively marliest

part of this section interval has been attributed to condensation (from 18.50 to 19.10 meters; STRASSER et al. 2004). It is followed by bed alternations displaying a thickening-up trend. The top of these bed alternations is capped by a particularly thick limestone bed (at 22.50 meters). This bed is overlain by a slumped interval (from 23.20 to 25.20 meters).

#### *Sequence-stratigraphical interpretation*

The sequence-stratigraphical interpretation displayed in Fig. 6.6 is based on the study of STRASSER et al. (2004). The sequence boundary Be4 (according to HARDENBOL et al. 1998) has been placed at the change of the sedimentation pattern from thinner to thicker beds at the limit between the Subalpina and Privasensis subzones (PASQUIER 1995, PASQUIER & STRASSER 1997, HILLGÄRTNER 1999, STRASSER et al. 2004).

The transition from relatively thick limestone beds to thinner and more homogeneous limestone-marl alternations has been interpreted as a first, large-scale transgressive surface (HILLGÄRTNER 1999, STRASSER et al. 2004). However, PASQUIER (1995) and PASQUIER & STRASSER (1997) placed a transgressive surface further up at around 18.10 meters. This diagnostic surface has been considered as a second transgressive pulse by HILLGÄRTNER (1999) and STRASSER et al. (2004). In this study, the first transgressive surface has been favored because it better fits the lateral correlation.

The relatively marliest part of the section, which is partly covered, has been interpreted as large-scale maximum flooding (PASQUIER 1995, HILLGÄRTNER 1999, STRASSER et al. 2004). PASQUIER & STRASSER (1997) considered the surface at around 21.20 meters as maximum-flooding surface and used it for lateral correlation. Moreover, they defined a maximum-flooding zone at the top of the large-scale sequence (from 18.50 to 21.60 meters). Considering lateral correlation, it is now assumed that the large-scale maximum flooding of this section is higher up, in the Paramimounum ammonite subzone. It is thought that it is located in the covered interval, which is capped by the thick limestone bed at 22.50 meters.

The 3<sup>rd</sup>-order sequence boundary Be5 (according to HARDENBOL et al. 1998) has been set below the slumped interval at 23.20 meters at the top of the thick limestones bed (PASQUIER 1995, HILLGÄRTNER 1999). PASQUIER & STRASSER (1997) placed this sequence boundary at the base of the thick limestone bed (at 22.50 meters). Later, STRASSER et al. (2004) considered the entire thick limestone bed as 3<sup>rd</sup>-order sequence-boundary interval Be5. The present study prefers

the first interpretation made by PASQUIER (1995) and HILLGÄRTNER (1999), which better matches the best-fit solution (cf. Figs. 6.8 and 6.13). The 3<sup>rd</sup>-order sequence boundaries Be4 and Be5 are well-developed and only slight discrepancies occur in the published interpretations. The large-scale transgressive surface is interpreted in agreement with previous studies. Yet, the interpretation of the large-scale maximum flooding is not straightforward. PASQUIER & STRASSER (1997) stated that “the maximum-flooding phase is more or less isochronous on the platform and in the basin, although the surface with the best-developed maximum-flooding features may be displaced by one or two small-scale composite sequences because of superimposed high-frequency sea-level fluctuations, and/or local variations in substrate morphology and sediment distribution” (p. 1071).

PASQUIER & STRASSER (1997) identified 20 small-scale sequences between the 3<sup>rd</sup>-order sequence boundaries Be4 and Be5 whereas HILLGÄRTNER (1999) interpreted 16 small-scale sequences. This difference arises from a changed interpretation of the elementary sequences and their stacking pattern within small-scale sequences (HILLGÄRTNER 1999). This study follows the interpretation of STRASSER et al. (2004), in which 19 small-scale sequences have been detected between the boundaries Be4 and Be5.

The bio- and sequence-stratigraphical correlation between the 3<sup>rd</sup>-order sequence boundaries Be4 and Be5 of the Berrias and the Montclus sections established by PASQUIER (1995) and PASQUIER & STRASSER (1997) enables to project the magnetostratigraphy of the Berrias section published by GALBRUN (1985) and GALBRUN et al. (1986) (cf. Fig. 6.6). The interval containing the 3<sup>rd</sup>-order sequence boundary Be4 has not been exactly determined because of a gap in the polarity sequence in the Berrias section (uncertain boundary between the polarity interval M18n and M17n; GALBRUN 1985). The upper part of polarity chron M17n occurs in the Dalmasi subzone (GALBRUN 1985). However, the sequence-stratigraphical interpretation of this part of the section (around the limit of the polarity chron M17n and M16r) is uncertain because it is composed of stacked lowstand deposits (STROHMENGER & STRASSER 1993; Strasser pers. comm.) Moreover, the dating by ammonites in this interval permits a certain play of interpretation (cf. LE HÉGARAT 1973). It is assumed that this limit lies in small-scale sequence 15 of the Montclus section (Dalmasi subzone). The corresponding, large-scale transgressive surface lies in the polarity chron M17n in small-scale sequence 11 (transition between Privasensis to Dalmasi subzones). The limit between the polarity chron M16r

and M16n is well constrained (Paramimounum subzone). It corresponds to small-scale sequence 18 in the Montclus section. Polarity chron M16n contains the large-scale maximum-flooding and the 3<sup>rd</sup>-order sequence boundary Be5.

### 6.3.4 Correlation of the Jura platform and the Vocontian basin sections

#### *Biostratigraphy*

The 3<sup>rd</sup>-order sequence boundary Be4 lies at the limit of the ammonite subzones Subalpina and Privasensis, which corresponds to the transition between the calpionellid zones B and C (cf. Fig. 6.8). The lateral correlation reveals that this interval comprises at least the charophyte-ostracode assemblage zones M3 and M4. The large-scale transgression occurs at the transition of the ammonite subzones Privasensis to Dalmasi and within calpionellid zone C, which corresponds to the charophyte-ostracode assemblage zone M4. The lower part of the Paramimounum ammonite subzone and the calpionellid zone D1 comprehend the large-scale maximum-flooding interval and the 3<sup>rd</sup>-order sequence boundary Be5.

#### *Depositional sequences and diagnostic intervals or surfaces*

A first depositional model has been proposed and illustrated by PASQUIER & STRASSER (1997) for the Berriasian, which has been modified by HILLGÄRTNER (1999). According to the latter model, relatively thin deposits are recorded on shallow platform environments during low sea level because of a generally reduced accommodation potential (frequent periods of non-deposition and/or erosion). Deposition in the basinal environments is mainly controlled by planktonic carbonate production creating relatively thick carbonate beds (e.g., PASQUIER & STRASSER 1997, HILLGÄRTNER 1999). As a consequence, the carbonate production shifts to the open-marine depositional setting of deep-marine basins. The predominantly planktonic origin of the carbonate is revealed by the content of nannoconids in the limestone beds (e.g., COTILLON et al. 1980, STROHMENGER & STRASSER, 1993). However, also export of carbonate mud from the platform to the basin has to be considered (PITTET et al. 1998a). During relative sea-level lowstand, fluvial systems had not the potential to cut down



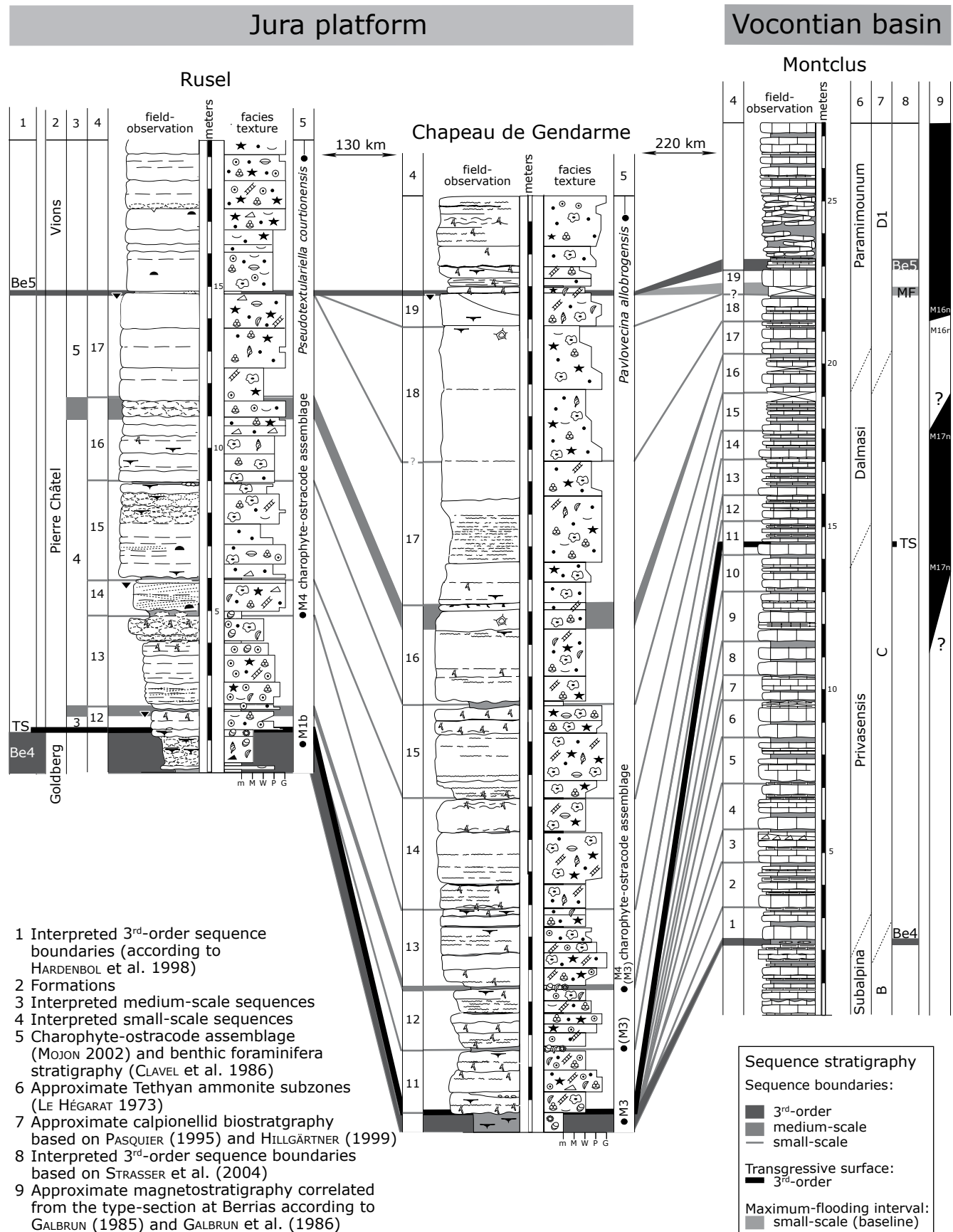


**Fig. 6.8** - Best-fit correlation of the large-scale depositional sequence between the 3<sup>rd</sup>-order sequence boundaries Be4 and Be5 (according to HARDENBOL et al. 1998) and their small-scale sequences of the Jura platform and the Vocontian basin. The numbers of small-scale sequences corresponds to the ones of the correlation scheme in Fig. 6.11. For the locations of the sections, please refer to Fig. 6.7.



into the shelf to create a by-pass situation for siliciclastics. Hence, siliciclastics are mainly concentrated in shallow lagoons on the platform (HILLGÄRTNER 1999; cf. Fig. 3.2a-b). In the basin, the first increase of clay content generally occurs during the sedimentation of transgressive deposits characterized by an increase of marl layers. This is mainly due to remobilization of clays formerly stored on the platform. Beds are thinner in the transgressive interval because carbonate production is concentrated on the platform. During maximum flooding, siliciclastic influx to platform areas and to the basin is commonly reduced due to retrogradation of their point sources (HILLGÄRTNER 1999). During accelerated sea-level rise, water depth on the platform increases too rapidly for the system to keep up, so that benthic carbonate production decreases. Partial give-up situations on shallow platforms enhance the creation of condensed intervals during maximum flooding (cf. Fig. 3.2d). At the same time, carbonate accumulation in the basin diminishes to a degree that marly sediments predominate because of decreasing planktonic carbonate production (e.g., PASQUIER & STRASSER 1997) and reduced carbonate export from the platform (PITTET et al. 1998a). During late highstand, decreasing bathymetry on the platform successively hinders the export of clays to basinal depositional settings, but increases highstand shedding of carbonate mud resulting in thin marl intervals and thick limestone beds (e.g., SCHLAGER et al. 1994).

## 6.4 Correlation of the Dorset sections

Lateral correlation schemes of sections in the Dorset area published in the literature (cf. Fig. 6.9) are mainly based on biostratigraphical and/or lithostratigraphical criteria (cf. Chap. 5). The magnetostratigraphy of the Durlston Bay published by OGG et al. (1991, 1994) furnished additional important stratigraphical information. However, a detailed sequence-stratigraphical correlation has not been published in the literature so far.

### 6.4.1 Correlation of large-scale sequences (3<sup>rd</sup>-order sequences)

In order to establish a sequence-stratigraphical framework comparable to those of the Jura platform and the Vocontian basin, the Dorset sections have been investigated on a larger scale from the 3<sup>rd</sup>-order sequence boundaries Be3 to Be5 (cf. Chap. 5). However, the focus has been set on the large-scale

depositional sequence between the 3<sup>rd</sup>-order sequence boundaries Be4 and Be5 (cf. Fig. 6.10).

### *Biostratigraphy*

The biostratigraphy for the marginal-marine deposits of the Berriasian in Dorset is mainly based on ostracodes (cf. Chap. 5). However, the biostratigraphical value of ostracodes has been questioned (e.g., HORNE 1995, 2002). A more satisfying biostratigraphical approach is given through the charophyte-ostracode assemblages established by MOJON (2002), which have been used for the Jura platform and the Dorset region (Durlston Bay section). According to this approach, the top of the Soft Cockle Member is in the assemblage zone M2, and the top of the Cherty Freshwater Member lies in the assemblage zone M4 (cf. Figs. 6.9 and 6.10). The large-scale transgression indicated at the base of the Cinder Member is situated in the assemblage zone M4.

### *Magnetostratigraphy*

The magnetostratigraphy established by OGG et al. (1991, 1994) for the Durlston Bay section reveals that the 3<sup>rd</sup>-order sequence boundary Be4 lies within polarity chron M17r (Runctoni ammonite subzone according to HARDENBOL et al. 1998). The large-scale transgression at the base of the Cinder Member is situated in the normal polarity chron M17n (Kochi ammonite subzone according to HARDENBOL et al. 1998). The 3<sup>rd</sup>-order maximum-flooding interval is at the transition between polarity chron M16r and M16n. The 3<sup>rd</sup>-order sequence boundary Be5 can unambiguously be attributed to the polarity chron M16n. According to the chronostratigraphic chart of GRADSTEIN et al. (2004), the interval between the 3<sup>rd</sup>-order sequence boundaries Be4 and Be5 lies in the Runctoni ammonite subzone.

OGG et al. (1991) stated that “the relatively long-duration chron M17r of Early Berriasian, a key component of the Tethyan “fingerprint” in matching polarity patterns, is not readily apparent in the Purbeck pattern; but its absence could be owing either to relative age span of the Purbeck Limestone [Purbeck Limestone Group], to the presence of a hiatus or to

**Fig. 6.9** – (following page) Bio-, sequence-, and lithostratigraphic interpretations of the Dorset region according to different studies. All limits are approximate and adjusted to the sequence- and chronostratigraphic chart of HARDENBOL et al. (1998).

BERRIASIAN													Boreal bio- and sequence-stratigraphy according to HARDENBOL et al. (1998)			Bio-, sequence-, and lithostratigraphic interpretations of the Dorset region according to different authors																																																																																																																																																																																																																																																																																																																																																																																																																																																																																
Early				Middle				Late					Stages	1			2			3			4		5			6		This study																																																																																																																																																																																																																																																																																																																																																																																																																																																																		
LAMPLUGH				RUNCTONI				KOCHI					Informal sub-stages	Members	Ostracode zones	Members	Ostracodes subzones	Members	Ostracode zones	Formations	Members	Members	Members	Marginal-marine	Members	Assemblage zones	Formations	Members	Marginal-marine																																																																																																																																																																																																																																																																																																																																																																																																																																																																			
Be2 143.5	Be3 141.8	Be4 141.0	Be5 139.3	~	~	~	~	~	~	~	~	~	~	~	~	~	~	~	~	~	~	~	~	~	~	~	~	~	~	~																																																																																																																																																																																																																																																																																																																																																																																																																																																																		
																															~	~	~	~	~	~	~	~	~	~	~	~	~	~	~	~	~	~	~	~	~	~	~	~	~	~	~	~	~	~	~	~	~	~	~	~	~	~	~	~	~	~	~	~	~	~	~	~	~	~	~	~	~	~	~	~	~	~	~	~	~	~	~	~	~	~	~	~	~	~	~	~	~	~	~	~	~	~	~	~	~	~	~	~	~	~	~	~	~	~	~	~	~	~	~	~	~	~	~	~	~	~	~	~	~	~	~	~	~	~	~	~	~	~	~	~	~	~	~	~	~	~	~	~	~	~	~	~	~	~	~	~	~	~	~	~	~	~	~	~	~	~	~	~	~	~	~	~	~	~	~	~	~	~	~	~	~	~	~	~	~	~	~	~	~	~	~	~	~	~	~	~	~	~	~	~	~	~	~	~	~	~	~	~	~	~	~	~	~	~	~	~	~	~	~	~	~	~	~	~	~	~	~	~	~	~	~	~	~	~	~	~	~	~	~	~	~	~	~	~	~	~	~	~	~	~	~	~	~	~	~	~	~	~	~	~	~	~	~	~	~	~	~	~	~	~	~	~	~	~	~	~	~	~	~	~	~	~	~	~	~	~	~	~	~	~	~	~	~	~	~	~	~	~	~	~	~	~	~	~	~	~	~	~	~	~	~	~	~	~	~	~	~	~	~	~	~	~	~	~	~	~	~	~	~	~	~	~	~	~	~	~	~	~	~	~	~	~	~	~	~	~	~	~	~	~	~	~	~	~	~	~	~	~	~	~	~	~	~	~	~	~	~	~	~	~	~	~	~	~	~	~	~	~	~	~	~	~	~	~	~	~	~	~	~	~	~	~	~	~	~	~	~	~	~	~	~	~	~	~	~	~	~	~	~	~	~	~	~	~	~	~	~	~	~	~	~	~	~	~	~	~	~	~	~	~	~	~	~	~	~	~	~	~	~	~	~	~	~	~	~	~	~	~	~	~	~	~	~	~	~	~	~	~	~	~	~	~	~	~	~	~	~	~	~	~	~	~	~	~



low sedimentation rates at that time” (p. 468). This observation is in agreement with the sequence-stratigraphical interpretation made in this study because the polarity chron M17r comprehends the interval of the two 3<sup>rd</sup>-order sequence boundaries Be3 to Be4 and parts of the large-scale lowstand deposits below the Cinder Member. It implies that non-deposition and condensation occurred during this polarity chron in the Dorset region.

#### ***Depositional sequences and diagnostic intervals or surfaces***

The investigated part of the Lulworth Formation of the Durlston Bay and the Worbarrow Tout sections exhibits sedimentological features (e.g., bituminous intervals, freshwater deposits, palaeosol intervals), that indicate recurrent episodes of emersion leading to reduced sediment accumulation, non-deposition and/or erosion. Accordingly, it is assumed that subsidence during the deposition of this part of the sections was relatively low. The top of the Lulworth Formation includes the 3<sup>rd</sup>-order sequence boundaries Be3 and Be4.

The base of the Cinder Member has been interpreted as a large-scale transgressive surface (small-scale sequence 11). It has been used to correlate different sections and boreholes of the Channel and Weald sub-basins (e.g., MORTER 1984, WESTHEAD & MATHER 1996). Different studies mention that the transgression of the Cinder Member may be diachronous (e.g., WIMBLEDON & HUNT 1983, NORRIS 1985).

A relative increase of the thickness of the depositional sequences is displayed above this large-scale transgressive surface (Durlston Formation). However, several intervals of the Intermarine Member are characterized by emersion features (cf. Chap. 5). It is assumed that halts and/or uplifts related to tectonic activity of the Purbeck Fault system overprinted the general transgressive trend during the deposition of the Intermarine Member. According to EL-SHAHAT & WEST (1983), the lithification and compaction history of shell beds at Durlston Bay can be related to such tectonic disturbances (cf. Chap. 5).

A relative opening of the depositional system is displayed by the Scallop Member (small-scale sequence 19). It has been interpreted as large-scale maximum-flooding interval in both investigated Dorset

sections. The large-scale correlation of the two Dorset sections is based on the Scallop Member, which has been considered to be more or less time-equivalent (datum; cf. Fig. 6.10).

The 3<sup>rd</sup>-order sequence boundary Be5 lies within the Corbula Member (small-scale sequence 20). At Worbarrow Tout, it is characterized by syn-sedimentary folds, which may be related to tectonic activity of the Purbeck Fault system (cf. Chap. 5).

The large-scale depositional sequence between sequence boundaries Be4 and Be5 is strongly asymmetric. According to the sequence-stratigraphical interpretation, the lowstand or early transgressive deposits comprehend at least 10 small-scale sequences, and the transgressive deposits are composed of about 8 small-scale sequences. The highstand deposits are strongly reduced and contain only one small-scale sequence.

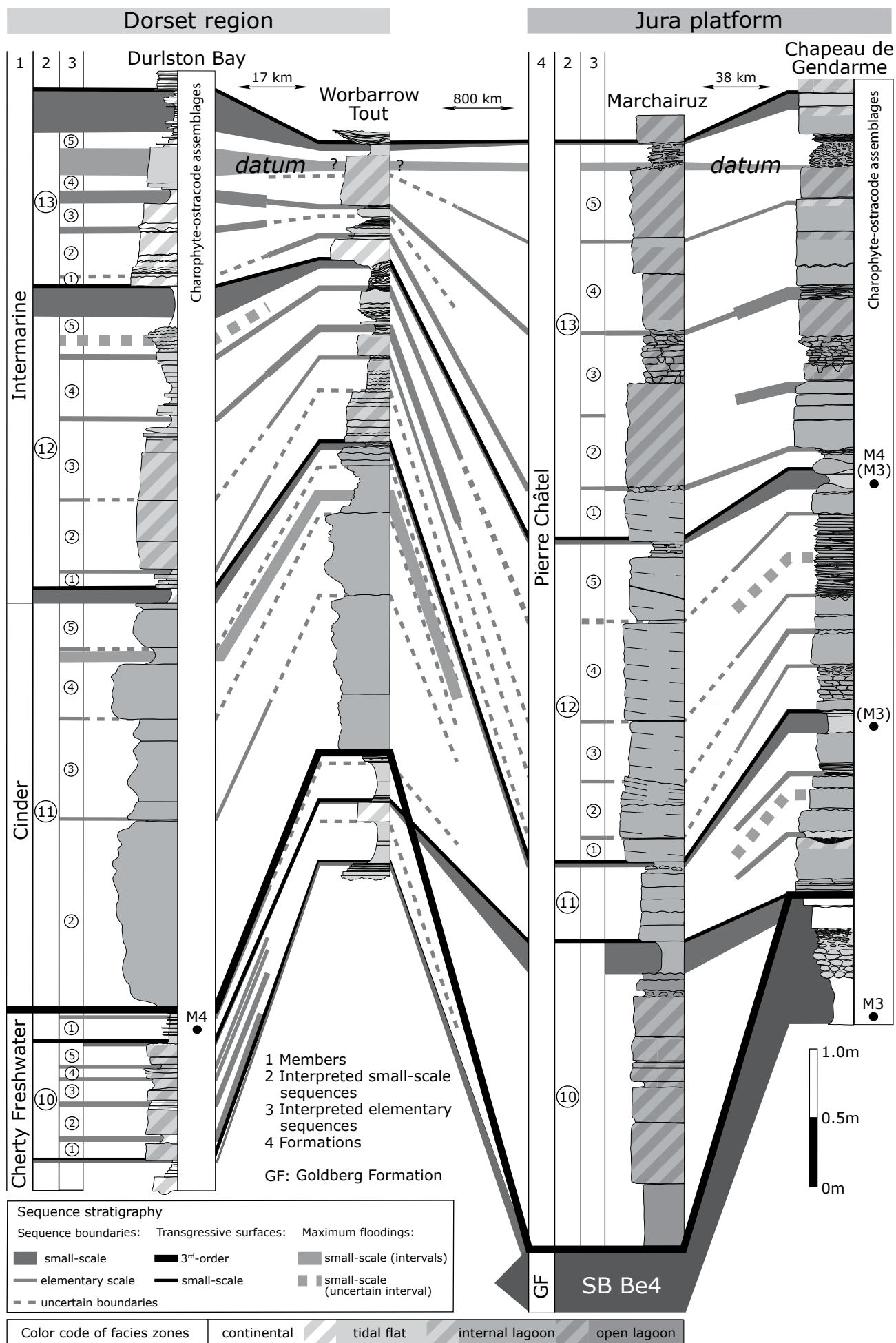
#### **6.4.2 Correlation of medium- and small-scale sequences**

##### ***Depositional sequences and diagnostic intervals or surfaces***

In both sections, 5 medium-scale sequences and 20 small-scale sequences have been interpreted between the 3<sup>rd</sup>-order sequence boundaries Be4 and Be5.

However, between the sequence boundary Be4 and large-scale transgressive surface at the base of the Cinder Member, the interpretation of depositional sequences is mostly not delicate because of the absence of facies contrasts. Small-scale sequences are commonly strongly reduced in thickness and/or not recorded at all in this interval. Medium-scale sequences are better represented in the sedimentary record and can be correlated between the two sections with relative ease. The large-scale transgressive deposits are characterized by relatively thick medium-scale and small-scale sequences. These depositional sequences are well-expressed by their sequence boundaries and transgressive surfaces and can easily be correlated. On the other hand, the interpretation of maximum-flooding intervals and surfaces is not straightforward (cf. Chap. 5). Generally, the small- and medium scale sequences of the Dorset section are thicker than the ones of the Worbarrow Tout section. This can be related to the fact that the depocentre lies offshore in the Channel sub-

**Fig. 6.11** – (facing page) High-resolution best-fit correlation of the four small-scale sequences 10 to 13 and their elementary sequences of the sections of the Dorset region and two selected sections of the Jura platform. The sections are represented by their weathering profiles. The environmental domains of the sections are indicated by the “color code”. Note the time-transgressive TS between the Dorset sections (e.g., Worbarrow Tout) and the Jura platform sections (e.g., Marchairuz). For discussion see text.



basin east of Durlston Bay (cf. Fig. 5.3).

### 6.4.3 Correlation of elementary sequences

A detailed correlation of small-scale sequences 10 to 13 and their elementary sequences of the Durlston Bay sections and two selected sections of the Jura platform are illustrated in Fig. 6.11. The elementary sequences in small-scale sequence 10 are only identifiable in the Durlston Bay section; at Worbarrow Tout, they are strongly reduced and/or not recorded.

Fig. 6.11 shows that the large-scale transgressive surface cuts the sequence boundary between the small-scale sequences 10 and 11, which connects the sections of Worbarrow Tout and Marchairuz. This implies that the large-scale transgressive surface is time-transgressive. A correlation of the elementary sequences in the Cinder Member is only partly possible. This is due to the lack of significant facies contrasts in the Cinder Member. However, the maximum-flooding interval of this small-scale sequence (in elementary sequence 4) is recorded in both Dorset sections.

Elementary sequences are better expressed in small-scale sequences 12 and 13. Accordingly, some of them can be correlated between the sections of the Dorset region and even to sections of the Jura platform. The sequence boundary between small-scale sequences 12 and 13 is well expressed in the Dorset sections as well as in the sections of the Jura platform. This sequence boundary is considered as a medium-scale sequence boundary, which is clearly recorded in both depositional regions (cf. Fig. 6.13).

With the help of a well-established bio- and sequence-stratigraphical best-fit framework, it is, therefore, possible to correlate even well-expressed elementary sequences over long distances (over 800 km) between different depositional regions. Different platform morphologies and differential subsidence strongly influence the expression of diagnostic interval or surfaces in different shallow-marine depositional basins and, hence, deviations of their interpretation are inevitable.

## 6.5 Correlation of all studied sections

Several authors have already proposed biostratigraphical correlations of Berriasian deposits between the Jura platform, the Vocontian basin, and the Dorset region (e.g., DÉTRAZ & MOJON 1989, ALLEN

& WIMBLEDON 1991, JAN DU CHÊNE et al. 1993, BLANC & MOJON 1996, MOJON 2002, HOEDEMAEKER 2002). The sequence-stratigraphical interpretation of the sections from the three depositional regions (Jura platform, Vocontian basin, and Dorset) presented here further enables the development of a correlation framework over long distances with a high resolution in a well-defined time window.

### 6.5.1 Biostratigraphy

#### *Ammonites*

The 3<sup>rd</sup>-order sequence boundary Be4 of the Jura platform and the Vocontian basin lies at the base of the Tethyan Privasensis subzones (e.g., CLAVEL et al. 1986, STEFFEN 1993, JAN DU CHÊNE et al. 1993, PASQUIER 1995, PASQUIER & STRASSER 1997, HILLGÄRTNER 1999, STRASSER et al. 2004; cf. Fig. 6.12). In Dorset, this sequence boundary lies within the Boreal Runcioni zone.

The large-scale transgression on the Jura platform and in the Vocontian basin began at the transition from the Privasensis to Dalmasi subzones (e.g., PASQUIER 1995, PASQUIER & STRASSER 1997, HILLGÄRTNER 1999, STRASSER et al. 2004). The base of the Cinder Member of Dorset has been attributed to the Runcioni ammonite zone (e.g., CASEY 1973, WIMBLEDON & HUNT 1983, MORTER 1984). ALLEN & WIMBLEDON (1991) correlate the large-scale transgression of the Cinder Member with the late Subalpina to Privasensis subzones. Consequently, within this biostratigraphical frame and based on high-resolution sequence stratigraphy, it is proposed that the base of the large-scale transgression (base of Pierre Châtel Formation and Cinder Member) lies in the Tethyan Privasensis to Dalmasi subzones, which correspond to the Boreal Kochi zone according to HARDENBOL et al. (1998).

The large-scale maximum-flooding interval of the Jura platform and the Vocontian basin shows the best biostratigraphical constraints according to PASQUIER & STRASSER (1997). They placed it in the lower part of Paramimounum subzone. Due to a different sequence-stratigraphical interpretation, however, HILLGÄRTNER (1999) and STRASSER et al. (2004) attributed the large-scale maximum-flooding interval to the upper part of the Dalmasi subzone. The maximum-flooding interval of the Dorset region (Scallop Member) has been placed by MORTER (1984) in the Icenii zone, which is certainly wrong. This ammonite zone must be much older according to the sequence- and chronostratigraphic

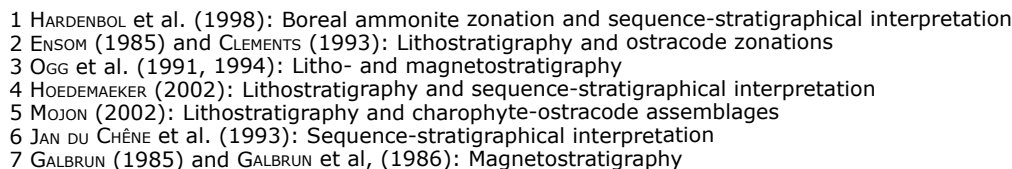


chart of HARDENBOL et al. (1998). The sequence-stratigraphical interpretation of the present study reveals that the maximum-flooding interval lies above the Kochi zone, in an interval, which has not been named in the chart of HARDENBOL et al. (1998) (this interval is indicated with a question mark in Figs. 6.10, 6.12, and 6.13).

Sequence boundary Be5 on the Jura platform and in the Vocontian basin has been set into the lower part of the Paramimounum subzone (e.g., PASQUIER

1995, PASQUIER & STRASSER 1997, HILLGÄRTNER 1999, STRASSER et al. 2004). MORTER (1984) roughly attributed the Corbula Member to the Boreal Stenomphalus ammonite zone. However, this correlation is questionable because this ammonite zone corresponds to the latest Berriasian according to HARDENBOL et al. (1998). According to the sequence-stratigraphical interpretation, the 3<sup>rd</sup>-order sequence boundary Be5 lies in the same undefined biostratigraphical interval as the large-scale maximum-flooding.



It is worth comparing the sequence-stratigraphical interpretation and ammonite biostratigraphy published by HOEDEMAEKER (2002) for the Jura platform and the Dorset region with the one established in this study (cf. Fig. 6.12). Such a comparison enables a critical view on the large-scale sequence-stratigraphical interpretation. However, it has to be stressed that the sequence-stratigraphical interpretation of HOEDEMAEKER (2002) is based on the so-called “French code”, which mainly refers to the study of ARNAUD-VANNEAU & ARNAUD (1991) and not to the chart of HARDENBOL et al. (1998).

The sequence-stratigraphical interpretation of the Jura platform published by HOEDEMAEKER (2002) is based on the studies of STRASSER (1988, 1994) focusing on the Goldberg Formation on the southern Jura platform (Salève section). Subsequent investigations of this section published by STRASSER & HILLGÄRTNER (1998) and HILLGÄRTNER (1999) have not been taken into account by HOEDEMAEKER (2002). The distribution of dinoflagellate cyst and acritarch associations of HUNT (1987) has been used by HOEDEMAEKER (2002) to interpret the Durlston Bay section in terms of sequence stratigraphy.

The large-scale sequence boundary Be3 is attributed to the Mammal bed of the Durlston Bay section and to the top of the Goldberg Formation, both lying in the lower part of the Subalpina subzone according to HOEDEMAEKER (2002). He named this boundary the “Basal Cretaceous unconformity” (BCU; cf. Fig. 6.12). It is one of the sequence boundaries, which “(...) were interpreted to represent rapid and extra deep sea-level falls, which are of much larger amplitude than those around most other sequence boundaries (HOEDEMAEKER 1995). These falls are attended by considerable extinctions of ammonite species followed by the appearance of many new species” (HOEDEMAEKER 2002; p. 239).

The upper part of the Marly Freshwater Member, the Cherty Freshwater Member, and the Cinder Member in Durlston Bay and the lower part of the Pierre Châtel Formation on the Jura platform are interpreted as highstand deposits lying in the Subalpina subzone. The Cinder Member and the lower part of the Pierre Châtel Formation correspond to the Runctoni ammonite zone (HOEDEMAEKER 2002).

The large-scale sequence boundary Be4 is placed on top of the Cinder Member of the Durlston Bay section and within the Pierre Châtel Formation on the Jura platform. This sequence boundary is located in the Subalpina subzone according to HOEDEMAEKER (2002). This sequence-stratigraphical interpretation cannot be

supported in the present study because neither at the top of the Cinder Member nor within the Pierre Châtel Formation a 3<sup>rd</sup>-order sequence boundary could be identified.

According to HOEDEMAEKER (2002), the lower part of the Intermarine Member and the upper part of the Pierre Châtel Formation represent large-scale highstand deposits corresponding to the Privasensis and the Dalmasi subzones. At the top of these intervals (top of the bed 133 according to CLEMENTS 1993; cf. Fig. 5.9f), another large-scale sequence boundary has been introduced by HOEDEMAEKER (2002), which has been called Be4'. This sequence boundary lies in the Dalmasi subzone.

The upper part of the Intermarine Member and the Scallop Member as well as the lower part of the Vions Formation have been interpreted as highstand deposits of the following large-scale sequence. HOEDEMAEKER (2002) attributed them to the Paramimounum subzone. The large-scale sequence boundary Be5 is situated just above the Scallop on top of the bed 153 (according to CLEMENTS 1993; cf. Fig. 5.9g).

The large-scale sequence stratigraphy of HOEDEMAEKER (2002) fits roughly the interpretation made in this study (e.g. Mammal Bed corresponding to large-scale sequence boundary Be3; top of Scallop Member in the range of the large-scale sequence boundary Be5). In detail, however, these two interpretations mismatch strongly. The differences in interpretation may be related to the fact that HOEDEMAEKER (2002) did not account for smaller depositional sequences (mainly medium-scale sequences) between his large-scale sequence boundaries.

### *Calpionellids*

The calpionellid biostratigraphy applied in this study is based on investigations of sections of the Vocontian basin (e.g., LE HÉGARAT & REMANE 1968, REMANE 1985, BLANC 1996). Additional investigations on calpionellids of the Montclus section have been made by PASQUIER (1995) and HILLGÄRTNER (1999). According to these studies, the 3<sup>rd</sup>-order sequence boundary Be4 is at the transition between the calpionellid zones B and C (cf. Figs. 6.6 and 6.8). The large-scale transgression starts in the upper part of zone C in the Montclus section, whereas in Berrias it is set in zone D1 (PASQUIER 1995, PASQUIER & STRASSER 1997). The large-scale maximum flooding and 3<sup>rd</sup>-order sequence boundary Be5 correspond both to zone D1 (e.g., PASQUIER 1995, PASQUIER & STRASSER 1997,



HILLGÄRTNER 1999).

### ***Charophyte-ostracode assemblages***

According to the dating made by MOJON (2002), 3<sup>rd</sup>-order sequence boundary Be4 of the Jura platform ranges from charophyte-ostracode assemblage M1b (Jacobi to Grandis subzones) to M4 (Subalpina to Dalmasi subzones; cf. Tab. 4.3, Figs. 6.12 and 6.13). It represents a major hiatus at the boundary between the Goldberg and Pierre Châtel formations. In the Dorset section, Be4 lies between the assemblage zones M2 and M4, which corresponds to the interval of the Tethyan ammonite subzones Grandis to Dalmasi. The beginning of the large-scale transgression on the Jura platform as well as in the Dorset region lies in the assemblage zone M4 (MOJON 2002). The large-scale maximum flooding and the 3<sup>rd</sup>-order sequence boundary Be5 have not been dated by charophyte-ostracode assemblages (MOJON 2002). However, according to MOJON (2002), the overlying Vions Formation corresponds to the assemblage zone M5.

### **6.5.2 Magnetostratigraphy**

The comparison of the magnetostratigraphical schemes published for the type-section of Berrias (Vocontian basin; GALBRUN 1985, GALBRUN et al. 1986) and for the Durlston Bay section (OGG et al. 1991, 1994) fits well with the large-scale sequence-stratigraphical interpretation of this study (cf. Figs. 6.12 and 6.13).

3<sup>rd</sup>-order sequence boundary Be4 lies in polarity chron M17r in the Durlston Bay section. This polarity chron has not adequately been detected in the Berrias section. The large-scale transgression occurred at the beginning of the polarity chron M17n in both regions. The lower part of polarity chron M16n comprehends the large-scale maximum-flooding interval as well as the 3<sup>rd</sup>-order sequence boundary Be5 in both regions.

### **6.5.3 Depositional sequences and diagnostic intervals (surfaces)**

The high-resolution sequence-stratigraphical interpretation enables for the first time a best-fit correlation on the scale of small-scale sequences and in the best case even on the scale of elementary sequences between the Tethyan (Jura platform and Vocontian basin) and

the Boreal (Dorset region) depositional realms of the Middle to Late Berriasian (cf. Figs. 6.11 and 6.13).

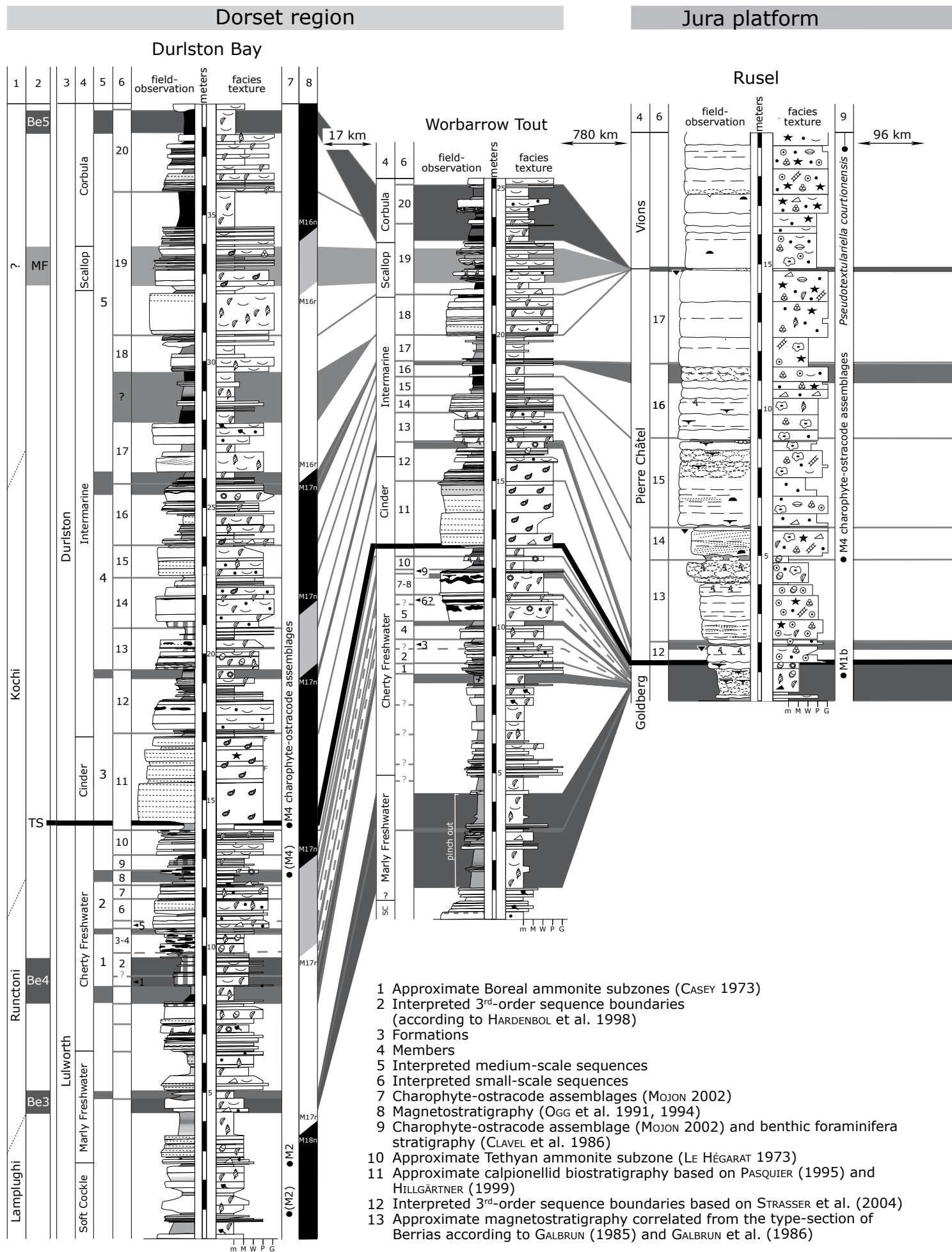
### ***Large-scale depositional sequence (3<sup>rd</sup>-order sequence)***

The 3<sup>rd</sup>-order sequence boundary Be4 is well-represented in all investigated sections and constrained by bio- and magnetostratigraphical schemes. The large-scale lowstand deposits are composed of at least 10 small-scale sequences in the Vocontian basin. In Dorset, the equivalent sequences are very thin. It cannot be excluded that some small-scale sequences have not been recorded. According to the dating by charophyte-ostracode assemblages, the large-scale lowstand deposits are not documented in the sedimentary record of the Jura platform sections. They have never been deposited or have partly been eroded during the large-scale transgression. Accordingly, the 3<sup>rd</sup>-order sequence boundary Be4 is thought to represent a major hiatus, which is directly overlain by the transgressive deposits of the Pierre Châtel Formation.

The large-scale transgressive surface lies within small-scale sequence 11, but its position differs on the scale of elementary sequences between the sections of the different regions (cf. Fig. 6.11). It is assumed that the Jura platform has been flooded in a step-wise manner by this large-scale transgression. The offset of the initial flooding (large-scale transgressive surface) is up to two small-scale sequences on the Jura platform.

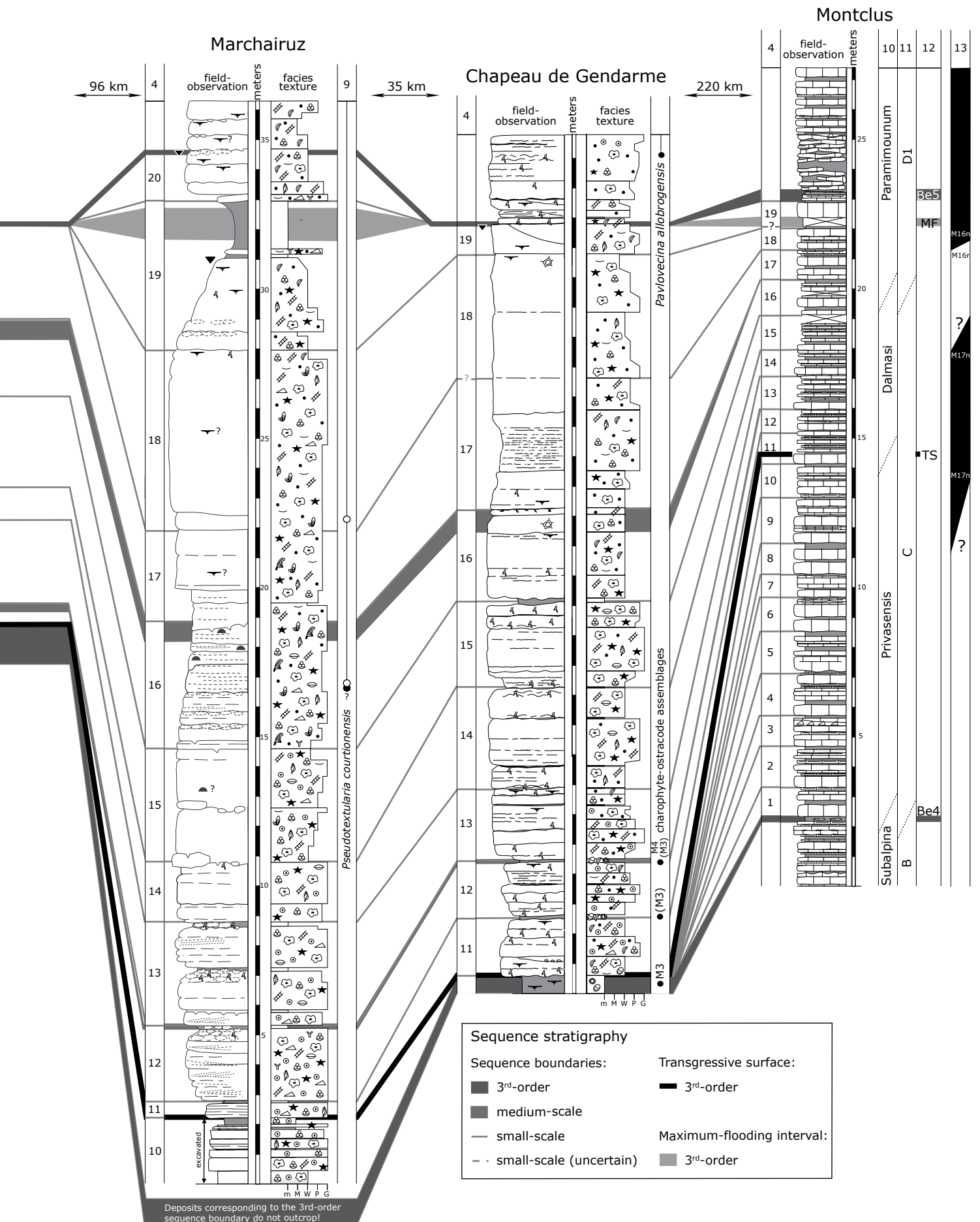
The large-scale maximum-flooding interval lies within small-scale sequence 19 in most of the sections. It is thought that in some sections of the Jura platform the large-scale maximum flooding is not recorded or was eroded during the formation of 3<sup>rd</sup>-order sequence boundary Be5. The identification of the maximum-flooding interval in the Montclus section is ambiguous and has been discussed controversially. In this study, it is assumed that it is in the range of small-scale sequences 18 to 19. This discrepancy can be related to different reactions of the sedimentary system in the basin and in shallow depositional environments to the same eustatic sea-level change, or to differential tectonic movements causing a shift of the time interval of fastest relative sea-level rise (STRASSER et al. 2004).

**Fig. 6.13** - (following pages) Best-fit correlation of the large-scale depositional sequences between 3<sup>rd</sup>-order sequence boundaries Be4 and Be5 according to HARDENBOL et al. (1998) and their small-scale sequences of all investigated regions.



## Jura platform

## Vocontian basin



The 3<sup>rd</sup>-order sequence boundary Be5 is well-expressed in all sections. It is suggested that in some sections of the Jura platform, this sequence boundary cannot only be explained by a decreasing relative sea level. Tectonic processes in combination with a falling relative sea level have been postulated to explain the formation of this 3<sup>rd</sup>-order sequence boundary (PASQUIER & STRASSER 1997, HILLGÄRTNER 1999).

### *Medium-scale sequences*

Five medium-scale sequences have been identified between 3<sup>rd</sup>-order sequence boundaries Be4 and Be5 in the Dorset sections. These sequences are better expressed in the large-scale transgressive deposits than in the lowstand deposits. A remarkable sequence boundary has been recorded at the transition between small-scale sequences 12 and 13 in the Dorset region (freshwater pond at Durlston Bay; cf. Fig. 5.9d and tidal flat pond with dinosaur footprints at Worbarrow Tout; cf. Fig. 5.11c), which has been interpreted as a medium-scale sequence boundary (limit between medium-scale sequences 3 to 4).

Generally, it has been stated that medium-scale sequences are poorly defined between the 3<sup>rd</sup>-order sequence boundaries Be4 and Be5 on the Jura platform (STRASSER & HILLGÄRTNER 1998, HILLGÄRTNER 1999, STRASSER et al. 2004). However, it is assumed that the particularly well-developed sequence boundary between small-scale sequences 12 and 13 on the Jura platform corresponds to the medium-scale sequence boundary identified in the Dorset sections; cf. Fig. 6.11). This sequence boundary is recorded on the Jura platform (cf. Fig. 6.4) as a karst surface (Rusel and Thoirette sections), supratidal to tidal flat deposits (Cornaux), tidal flat deposits (Crozet and Chapeau de Gendarme), tidal flat to internal-lagoonal deposits (St. Claude, Lavans, and Poizat sections), internal-lagoonal deposits (Marchairuz and Val de Fier sections), and internal- to open-lagoonal deposits (Yenne section). Accordingly, these facies generally display the relatively most restricted environments in this part of the sedimentary succession. Such striking facies changes may be related to a remarkable over-regional sea-level drop and/or to over-regional tectonic movements. This sequence boundary may correspond to boundary Be4', as introduced by HOEDEMAEKER (2002)

A similar observation can be made at the limit between small-scale sequences 16 to 17, which has been interpreted as medium-scale sequence boundary

(transition between medium-scale sequences 4 to 5). The corresponding interval of the Jura platform has not been investigated in this study. However, according to the interpretations of PASQUIER (1995), HILLGÄRTNER (1999), and STRASSER et al. (2004), it is possible to trace this medium-scale sequence boundary from the Dorset sections to at least some sections of the Jura platform. Medium-scale sequences are not well developed in the Vocontian basin and can be inferred only from platform-to-basin correlation (PASQUIER & STRASSER 1997, STRASSER et al. 2000).

### *Small-scale sequences*

The sequence boundaries and transgressive surfaces of small-scale sequences are commonly well-expressed in the investigated sections. However, the identification of maximum-flooding intervals or surfaces is more problematic. Nevertheless, during increasing accommodation, maximum-floodings commonly are better expressed in the sedimentary record. This is revealed by the maximum-flooding of small-scale sequence 13, which has been used as a base-line for the high-resolution correlation of the Jura platform sections.

Eighteen (Montclus section) to twenty small-scale sequences (Dorset and Marchairuz sections) have been identified between the 3<sup>rd</sup>-order sequence boundaries Be4 and Be5, which agrees with the sequence-stratigraphical interpretations made by PASQUIER & STRASSER (1997) and STRASSER et al. (2004) of sections from the Jura platform and the Vocontian basin.

### *Elementary sequences*

Some of the elementary sequences of small-scale sequences 10 to 13 can be traced between the Dorset region and the Jura platform. In the formation of sequences on this scale, intrinsic processes may overrule extrinsic controlling factors (e.g., relative sea-level changes). Intrinsic, autocyclic processes commonly produce sedimentary bodies of limited lateral and vertical extent (e.g., tidal channel or shoal intervals; cf. Chap. 3). Accordingly, autocyclic deposits are local phenomena, which are overprinted by facies changes caused by allocyclic processes acting at least on a regional scale (tectonic and/or sea-level changes). Nevertheless, autocyclic deposits can be delimited by high-resolution correlations (cf. Figs. 6.4 and 6.5). Long-distance correlations from one sedimentary basin

to another helps to filter out local and regional effects of platform morphology and differential subsidence. In the best case, best-fit correlations on the scale of elementary sequences give the opportunity to analyze the evolution of completely different depositional settings over long distances with a resolution of a few ten thousand years (cf. Chap. 7).

#### 6.5.4 Accommodation changes

The thickness of the interpreted sedimentary sequences reflects, as a first approximation, the changing accommodation space over time. However, it has to be kept in mind that bed thickness and accommodation generally do not have a linear relationship. This is due to facies-dependent differential compaction and because sediment not always fills up the available space (STRASSER et al. 1999). Assuming that the sequence boundaries of the depositional sequences are more or less time-equivalent, the lateral changes of accommodation across the three regions of investigation can be compared. The causes of these changes can be related to the combination of eustatic sea-level changes, tectonic movements, and the nature of the depositional regime (production and accumulation rates in carbonate-dominated systems).

##### *Morphological relief*

When analyzing marine transgressions, different factors must be considered. The position on the platform is a first important parameter controlling the sedimentary succession of a section. It can be assumed that in relatively distal positions on a platform transgression leads to rapid change from peritidal deposits to marine deposits. Such an environmental change is displayed in the sediments of the Thoirette, Poizat, Val de Fier, and Yenne sections (southwestern platform). The sedimentary succession in proximal positions is characterized by repeated facies changes from peritidal to subtidal and back to peritidal environments because accommodation generally is low (Rusel and Cornaux section; northwestern platform). The other sections display combinations between characteristics of typical distal and proximal settings. However, it is assumed that the platform margin was not linear but displayed promontories and bays (STRASSER et al. 2004), thus further complicating the facies distribution (cf. Chap. 9).

At the transition from the Goldberg to the Pierre

Châtel Formation, the Jura platform has been exposed for an extended period. During this exposure, an important platform morphology developed, which divided the platform into a complex pattern of highs and depressions. In some sections, antecedent platform morphologies have been observed on the outcrop scale (Rusel and Yenne sections; cf. Chap. 4). This is revealed by slight lateral variations in thicknesses of the depositional sequences at the top of the Goldberg Formation. Such a pre-existing morphology determines the geometry of the coast line and the distribution of depocentres on the platform during a transgression. The pre-existing relief also modifies the hydrodynamic setting (current and/or wave directions and intensity), the pattern of sediment production and deposition, and ecological conditions (e.g., water depth, salinity, turbidity, nutrient distribution) during the initial transgression. Generally, it can be concluded that “fluid dynamics drive sediment transport resulting in morphological change over time. Progressive modification of topography in turn alters boundary conditions for the fluid dynamics, which evolve to produce further changes in sediment-transport patterns and their depositional products (...). The essential properties of coastal morphodynamic processes are attributable to the feedback loop between topography and the fluid dynamics that drive sediment transport producing morphological change” (COWELL & THOM 1994; p. 33). However, it has to be kept in mind that, in carbonate-dominated depositional system, the source (carbonate factory) and distribution of sediments strongly depend on local conditions within the depositional environment itself.

##### *Differential subsidence and/or uplift*

The evolution of the Channel sub-basin can be related to tectonic activities along the Purbeck Fault system, which is located north of the Durlston Bay and Worbarrow Tout sections (e.g., UNDERHILL 2002). The location of the depocentre of the Channel sub-basin was more or less stable during the investigated time interval. Subsidence rate was generally low, and periods of halts or uplift cannot be excluded.

Several studies postulated that the lowstand deposits at the base of the large-scale transgression of the Jura platform (transition from the Goldberg formation to the Pierre Châtel Formation) are strongly reduced and/or absent due to non-deposition or erosion (STRASSER 1988, WAEHRY 1989, STRASSER 1994, PASQUIER 1995, PASQUIER & STRASSER 1997, STRASSER & HILLGÄRTNER

1998, HILLGÄRTNER 1999, STRASSER et al. 2004). This has been related to major tectonic activities at the time of 3<sup>rd</sup>-order sequence boundary Be4 (e.g., PASQUIER & STRASSER 1997, STRASSER & HILLGÄRTNER 1998, HILLGÄRTNER 1999, STRASSER et al. 2004).

The sequence-stratigraphical correlation across the Jura platform also suggests that in some sections (e.g., Rusel and Chapeau de Gendarme sections) the topmost depositional sequences are truncated by karst surfaces during the formation of sequence boundary Be5 (cf. Fig. 6.2). Other sections of the Jura platform (not investigated in this study) show a similar phenomenon (PASQUIER 1995, HILLGÄRTNER 1999). A fall of eustatic sea level alone cannot explain such exposure features. It has been assumed that tectonic activities (differential subsidence and block faulting) have to be considered at that time (e.g., PASQUIER 1995, HILLGÄRTNER 1999, STRASSER et al. 2004).

PASQUIER & STRASSER (1997) explained the asymmetry of the large-scale sequence between the 3<sup>rd</sup>-order sequence boundaries Be4 and Be5 by a general 2<sup>nd</sup>-order sea-level fall (HAQ et al. 1987, HARDENBOL et al. 1998). Such 2<sup>nd</sup>-order sequences are related to tectonic and tectono-eustatic changes (e.g., VAIL et al. 1977, RAWSON & RILEY 1982, VAIL et al. 1991, RUFFELL 1991). They correspond to the “T/R facies cycles” of JACQUIN et al. (1998) (cf. Fig. 1.2).

### *Sea-level fluctuations*

The fact that depositional sequences can be correlated over long distances between different depositional basins is a strong argument that other processes than tectonic activities must have been involved in producing changes in accommodation space. Also, the hierarchical stacking pattern observed in the studied sections implies that sedimentation was influenced by cyclic or periodic changes of controlling factors. It is assumed that high-frequency sea-level fluctuations were responsible for the repetitive stacking of depositional sequences on several scales observed in all studied sections. Other mechanisms, which lead global sea-level changes are discussed in Chapter 7.

### **6.5.5 Comparison with other depositional regions**

The high-resolution correlation of depositional sequences discussed in this chapter reveals that there must be a factor, which controls sedimentation on an interregional scale but with relatively small time

increments. Eustatic sea-level change certainly is an important controlling factor. However, the separation in a relative and an eustatic sea-level component is not feasible if regional subsidence is involved (e.g., BURTON et al. 1987, KENDALL et al. 1992, SOREGHAN & DICKINSON 1994, IMMENHAUSER 2005). Accordingly, it is likely that the interaction between various mechanisms are at least as important as each individual mechanism (HOUSE 1995). In order to estimate whether eustatic sea-level fluctuations have been recorded in the investigated sections, other depositional environments must be taken into account. GRÖTSCH et al. (1993) stated that “in order to distinguish between eustatic and tectonic causes it is of crucial importance that synchronism of sea-level events on a global scale in different tectonic regimes can be documented” (p. 197). Therefore, in addition to the correlation between the Jura and Dorset, other European studies, which describe a transgression during the Middle to Late Berriasian, have been chosen for comparison (cf. Fig. 6.14). A comparison on a finer time scale cannot be expected because high-resolution sequence-stratigraphical interpretations are not available in these studies.

### *Switzerland: Helvetic shelf*

The Helvetic shelf is the southern continuation of the Jura platform at the northern margin of the Tethys (cf. Figs. 4.3 and 6.14). This shelf was characterized by a complex pattern of different depocentres caused by extensional tectonics (e.g., FUNK 1985, WILDI et al. 1989, LOUP 1992). During the Berriasian, the calcareous-marly Öhrli Formation has been deposited in the northern part of the eastern Helvetic shelf. It passes laterally (to the south) into the marls of the Palfris Formation and other time-equivalent formations (e.g., ISCHI 1978, BURGER 1986). The lower part of these formations has mainly been dated by calpionellids, but the poor preservation of the species in the upper part makes a detailed biostratigraphical interpretation impossible (MOHR 1992a). The lower part of the Öhrli Formation (Unterer Öhrlikalk) has been attributed to the calpionellid zones C to D1 and is thought to have been deposited during the large-scale transgression investigated in this study (BURGER 1986, PASQUIER 1995, MOHR & FUNK 1995). MOHR (1992b), FUNK et al. (1993), and MOHR & FUNK (1995) established a sequence-stratigraphical interpretation for the eastern Helvetic shelf, which, however, differ from the one published by PASQUIER (1995) for the western Helvetic shelf. The differences are mainly

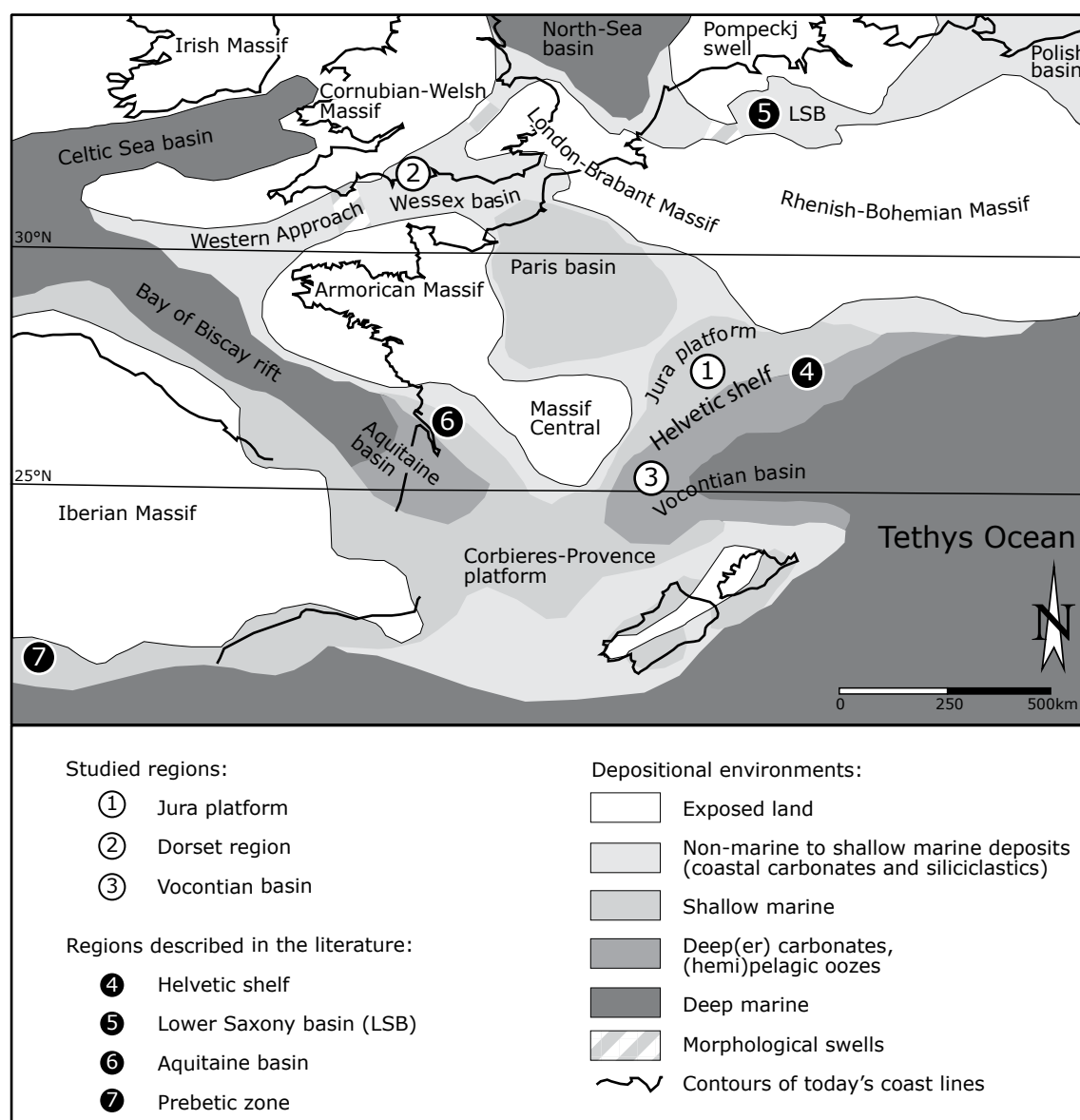


**Fig. 6.14** - Palaeogeographic location of studied sections and sections described in the literatures. The palaeogeographic map is based on THIERRY & BARRIER (2000; modified for the Berriasian from ALLEN 1963, RAWSON & RILEY 1982, CURNELLE & DUBOIS 1986, KARNER 1987, ZIEGLER 1988, ARNAUD 1988, MUTTERLOSE 1992, STRAUSS et al. 1993, GUILLOCHEAU et al. 2000, AURELL et al. 2003).

due to the uncertainties of the lithological limits and the low biostratigraphical resolution. According to PASQUIER (1995), the large-scale transgression between the sequence boundaries Be4 and Be5 is not well recorded on the Helvetic shelf.

#### ***Northern Germany: Lower Saxony basin***

Different Berriasian sections of the Lower Saxony basin have been well investigated by facies analysis (e.g., WIESNER 1983). The Lower Saxony basin is

the southernmost extension of the North Sea basin, which has been filled by shallow-marine and brackish to freshwater siliciclastics in the west, south and easternmost part of the basin during the Berriasian (e.g., WIESNER 1983, ELSTNER & MUTTERLOSE 1996, MUTTERLOSE & BORNEMANN 2000; cf. Fig. 6.14). Tectonic movements along northwest-southeast trending fault systems controlled the basin subsidence and the overall patterns of sedimentary thicknesses (MUTTERLOSE & BORNEMANN 2000).

Several studies correlated the brackish to hypersaline deposits of the Serpulit Member (top of the



Münder Formation) with the Cinder Member in Dorset, based on palynological events and ostracode assemblages (e.g., NORRIS 1969, ALLEN & WIMBLEDON 1991, STRAUSS et al. 1993). On the other hand, based on charophytes, FEIST & SCHUDACK (1991) and FEIST et al. (1995) correlated the overlying brackish to freshwater Wealden 1 Member of the Lower Saxony basin (base of the Bückeberg Formation) with the Cinder Member of Dorset. MOJON (2002) attributes the Wealden 1 Member to the charophyte-ostracode assemblage M4, which would correspond to the initial large-scale transgression at the base of the Cinder Member and the Pierre Châtel Formation. However, a marine fauna has been reported from deposits of the Wealden 4 Member, which is a stratigraphically younger interval of the Bückeberg Formation (e.g., STRAUSS et al. 1993, MUTTERLOSE & BORNEMANN 2000). It can be concluded that in the Lower Saxony basin no major transgression occurred during the deposition of the large-scale sequence investigated in this study.

#### ***Southwestern France: Aquitaine basin***

The section of Cherves-de-Cognac, which is situated at the northern margin of the Aquitaine basin (cf. Fig. 6.14), has been studied by facies analysis, palaeoecological investigations, and clay minerals by EL ALBANI et al. (2004). The upper interval of this section (U2) has been dated by ostracodes and charophytes by COLIN et al. (2004). Accordingly, at least part of this interval is time-equivalent with the Cinder Member in Dorset and the base of the Pierre-Châtel Formation on the Jura platform. EL ALBANI et al. (2004) interpreted the limestone-marl alternations and the faunal content as deposits belonging to an estuarine environment. Two transgressive trends from proximal (lagoon setting) to a relatively distal environment (shoreface setting) have been interpreted (EL ALBANI et al. 2004). These may correspond to pulses during the large-scale transgression investigated in this study.

#### ***Southern Spain: Prebetic zone***

A Berriasian section (part of the Sierra del Pozo Formation) of southern Spain (Prebetic zone; cf. Fig. 6.14), which is composed of subtidal to peritidal carbonate rocks, has been analyzed and interpreted in detail by JIMENEZ DE CISNERO & VERA (1993). The section encompasses the calpionellid zones B to D1 (JIMENEZ DE CISNERO & VERA 1993). The Prebetic zone was a passive margin situated adjacent to the Iberian continent (e.g., MARQUES et al. 1991). It has been assumed that the subsidence rate during the deposition of the Sierra del Pozo Formation was low (JIMENEZ DE CISNERO & VERA 1993). The same section has been reinterpreted by ANDERSON (2004b) who tentatively correlated the most open-marine and most carbonate-rich beds of this section with the Cinder Member of Dorset and the lower parts of Pierre Châtel Formation of the Jura platform. These beds are situated approximately in the middle of the section investigated by JIMENEZ DE CISNERO & VERA (1993) and ANDERSON (2004b), which implies that they lie in the calpionellid zone C.

A large-scale transgressive trend during Middle to Late Berriasian times is described in all location mentioned above except in the Lower Saxony basin. This may be related to differences in subsidence rates between these depositional basins. Moreover, detailed investigations in terms of sequence stratigraphy are needed in order to evaluate the influence of eustatic sea-level changes. It may be worth investigating the Sierra del Pozo and the Cherves-de-Cognac sections in more detail because charophytes and ostracodes have been described from these sections (JIMENEZ DE CISNERO & VERA 1993, COLIN et al. 2004, EL ALBANI et al. 2004). Possibly, these charophytes and ostracodes can be related to the charophyte-ostracode assemblage zones established by MOJON (2002) for the Jura platform and the Dorset region in order to obtain a good biostratigraphical time control.

\*\*\*\*\*



## 7 - CYCLOSTRATIGRAPHY

### 7.1 Introduction

Different mechanisms, which cause sea-level changes of regional and/or global extension have been proposed and discussed in the literature (e.g., DONOVAN & JONES 1979, DEWEY & PITMAN 1998, HALLAM 2001, IMMENHAUSER 2005). The construction of global sea-level curves for the Mesozoic implies that at least during certain time intervals sea-level fluctuations are comparable at different palaeogeographic localities (e.g., HAQ et al. 1987, SURLYK 1991, SAHAGIAN et al. 1996). The precision of such sea-level curves, of course, strongly depends on the biostratigraphical resolution and the parameters for backstripping.

#### 7.1.1 Sea-level changes

Fluctuations in global sea level (eustasy) result from changes in the volume of water in the ocean and/or the volume of ocean basins (e.g., DONOVAN & JONES 1979, PITMAN & GOLOVENKO 1983, JACOBS & SAHAGIAN 1993). The different processes have characteristic ranges of amplitudes and rates, which partly overlap each other (cf. Fig. 7.1).

##### *Changes of the water volume*

Water-volume changes are dominated by growth and decay of continental ice sheets, producing high-amplitude, rapid eustatic changes (up to 200 m by a rate of 20 m/ka; ka = thousand years). In addition, volume changes of alpine glaciers may contribute to slight eustatic sea-level changes (FAIRBRIDGE 1976). Sea-level changes are also caused by thermal expansion and retraction of the uppermost layer of ocean waters (GORNITZ et al. 1982), by thermally induced volume changes in deep-water circulation (SCHULZ & SCHÄFER-

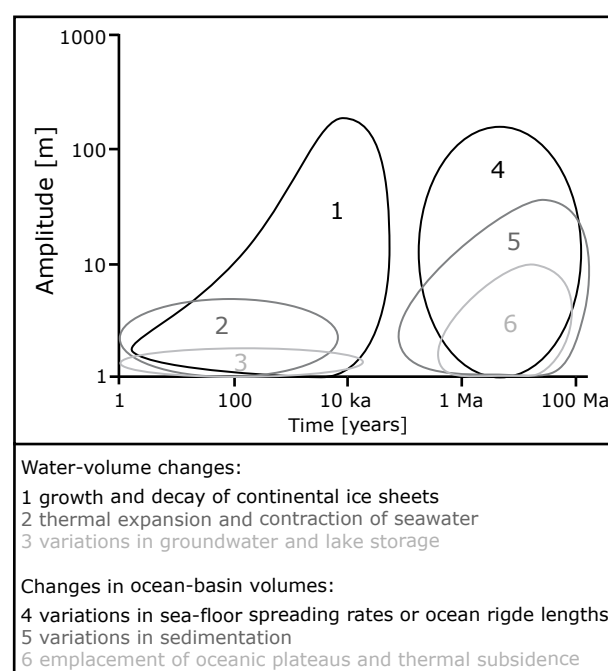


**Fig. 7.1** - Log-log diagram displaying timing and amplitudes of different geologic processes, which influence eustatic sea-level changes (modified from MILLER et al. 2005).

NETH 1997), by desiccation and inundation of marginal seas (e.g., HSÜ & WINTERER 1980, STRASSER 1988) and/or by water retention and release in lakes and aquifers (JACOBS & SAHAGIAN 1993). These processes lead to sea-level fluctuations at high rates (about 10 m/ka) and low amplitudes (about 5 to 10 m; MILLER et al. 2005). In any of these scenarios, climate plays an important role.

##### *Changes of the ocean basin volume*

Changes in ocean basin volume are dominated by slow variations in sea-floor spreading rates or ocean

ridge lengths (100 to 300 m amplitude at rates of 10 m/ma; ma = million years; DONOVAN & JONES 1979). Extreme changes in spreading rates may cause sea-level rises in the order of 10 m/ma, but it is difficult to explain rapid sea-level falls with changing spreading rates (e.g., IMMENHAUSER 2005). Variations in the deposition of land-derived sediments in the oceans lead to moderate amplitudes (< 60 m) with slow rates (10 m/ma; DONOVAN & JONES 1979).

Accordingly, the observed stacking pattern of the studied sections (changes in accommodation space) results from the combination of high-frequency sea-level fluctuations (caused mainly by climate changes) and differential subsidence. Changes in regional subsidence rate through time and differential subsidence due to local tectonic movements are important factors for the creation of accommodation space. However, these movements are either slow and continuous or abrupt and episodic. They cannot adequately explain the observed hierarchical stacking pattern of depositional sequences (STRASSER et al. 1999).

## 7.2 Orbital forcing

Since the glacial theory of the Swiss naturalist Louis Agassiz in the mid nineteenth century, it is known that during the Quaternary several recurrent intervals existed where phases of large ice sheets in the high and mid latitudes of the Earth (glacial period) are followed by phases of ice sheets with a reduced extension like the current one (interglacial period).

At the end of the 19<sup>th</sup> century, geologists interpreted pre-Cenozoic rhythmic sediment successions as the result of changes in orbital parameters (GILBERT 1985, BRADLEY 1929, WANLESS & SHEPARD 1936; for discussion see DE BOER & SMITH 1994b). In its basic form, the astronomical theories hold that variations of the Earth's orbit lead to changes in seasonal and geographic distribution of incoming solar radiation (insolation) at the top of the Earth's atmosphere.

In 1864, an astronomical theory for changes in orbital parameters has been published by the Scottish scientist James Croll. He combined geological field evidences with the astronomical advances of the French astronomer Le Verrier who calculated in 1843 that the Earth's eccentricity changes about every 100 ka owing to gravitational pull of the planets (e.g., CRONIN 1999, BERGER & LOUTRE 2004, FISCHER et al. 2004). Moreover, Croll also stated that the precession of the equinoxes have to be considered as a factor controlling changes in insolation.

The Serbian engineer and astrophysicist Milankovitch developed the theoretical basis explaining the orbital changes, which influence the Earth's insolation pattern in various seasons and latitudes (MILANKOVITCH 1941). He provided a mathematical description of insolation changes and their influence on climate, which mainly controlled the growth and decay of ice sheets in the Quaternary. This theory later became known as Milankovitch theory (SCHWARZACHER 1993).

SCHWARZACHER (1993) concluded that "its outstanding characteristic [planet system] is its stability, which is greater than in any other system that could have geological effects. It is also, thanks to its size, capable of generating cycles with periods, which are very much longer than any cycles we know of in the terrestrial environment. The stability, which of course is not absolute, permits us to treat the astronomical complex as a conservative system for considerable time spans". (p. 27).

### 7.2.1 Effects of orbital forcing

Insolation changes influence air temperature, growth and decay of ice sheets, atmospheric and oceanic circulation and rainfall pattern and evaporation as well as terrestrial and oceanic ecosystems. The interactions of the different climate-dependent systems of the Earth are controlled by complex feedback mechanisms on different spatial and temporal scales. These feedback mechanisms are only partially understood and are nowadays subject of intensive inter-disciplinary research.

#### *Quaternary*

Excellent chronostratigraphic control of the geological record in the Quaternary allowed to establish a direct link between orbitally controlled insolation changes and glaciation/deglaciation cycles (references in CRONIN 1999). An important study has been published by HAYS et al. (1976), which shows that by analyzing oxygen isotope ratios from planktonic foraminifera with mathematical methods (spectral analysis) the obtained frequencies match well with those predicted by the Milankovitch hypothesis. Since then, the conclusion that climatic change is forced by variations of orbital parameters had become inescapable at least for the Quaternary (SMITH 1989).

Because the physical laws of the solar system, which describe the gravitational effects of planetary bodies on the Earth's orbit, are well known, they can be calculated for the Quaternary (e.g., BERGER 1978,

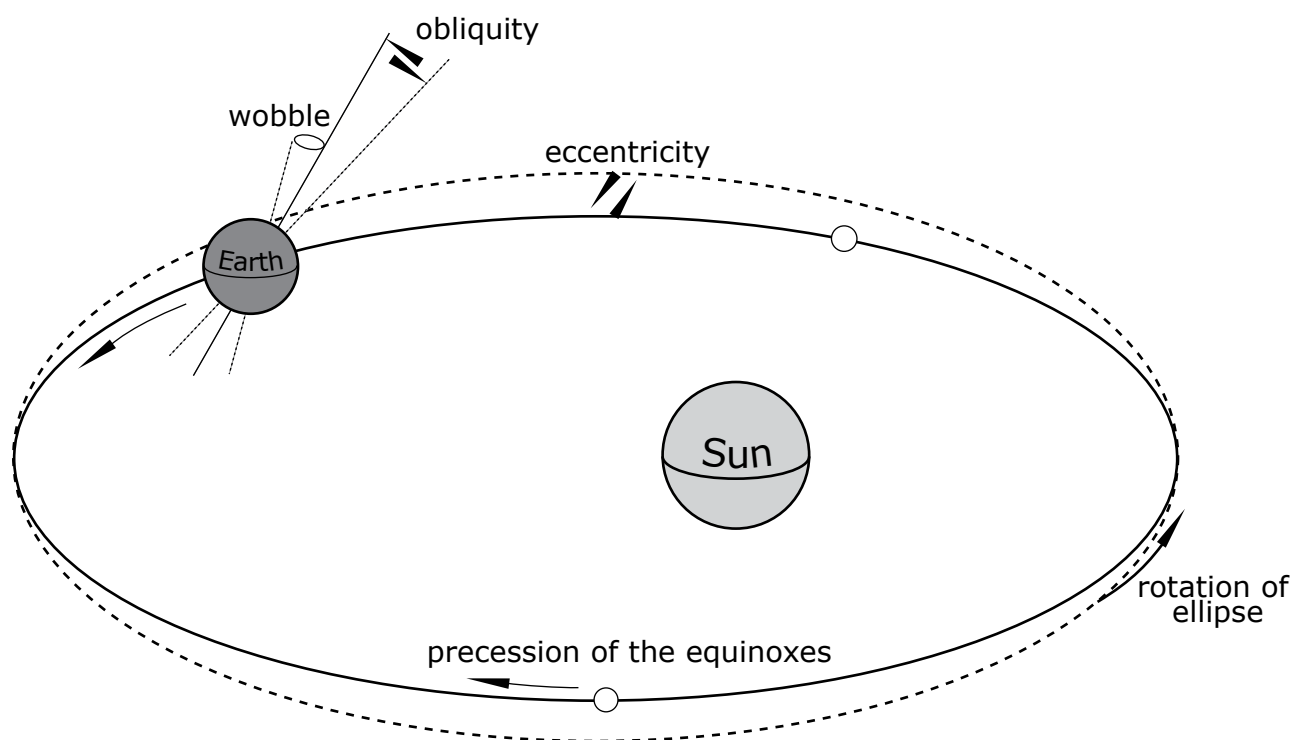


**Fig. 7.2** - Astronomical parameters that control insolation on Earth (precession, obliquity, and eccentricity (modified from STRASSER et al. 2007).

IMBRIE & IMBRIE 1980, IMBRIE et al 1992, IMBRIE et al. 1993) and the deeper geological past (BERGER et al. 1989a, b). The three important orbital parameters are the eccentricity, the obliquity, and the precession (e.g., SCHWARZACHER 2000, HINNOV 2000, BERGER & LOUTRE 2004).

The **eccentricity** is the measure of the degree of elongation or ellipticity of the Earth's orbit, which varies between nearly zero (circular orbit) and 0.06 (slightly elliptical) and has main periods of ~100 ka (short eccentricity cycles with present-day peak values of 94 ka and 128 ka) and ~400 ka (long eccentricity cycle; BERGER et al. 1989a, b, BERGER et al. 1992, SCHWARZACHER 2000, STRASSER et al. 2007; cf. Figs. 7.2 and 7.3). Eccentricity modulates the amplitude of the precession and the obliquity effects (e.g., IMBRIE & IMBRIE 1980, SCHWARZACHER 1993). It affects the total insolation of the Earth.

**Obliquity** describes the angle between the Earth's axis of rotation and the orbital plane and varies between 22 and 25° with a main period around 41 ka (present-day value; STRASSER et al. 2007 cf. Figs. 7.2 and 7.3). Its greatest effect is in high latitudes.

The **axial** or **astronomical precession** is the slow movement of the rotation axis around a circular path with one revolution relative to the stars completed every 26 ka. Due to the opposite movement of the eccentric orbit itself, the precession of the equinoxes

relative to the perihelion and aphelion – also called **climatic precession** – completes on full cycle with a main duration of about 21 ka (with present-day peak values at 19 and 23 ka; e.g., BERGER et al. 1989a, b, BERGER et al. 1992, SCHWARZACHER 2000, BERGER et al. 1989a; cf. Figs. 7.2 and 7.3). Precession affects the radiation intensity for each season mainly at low latitudes.

The quasi-periodic insolation changes are major factors influencing Earth's climate and producing

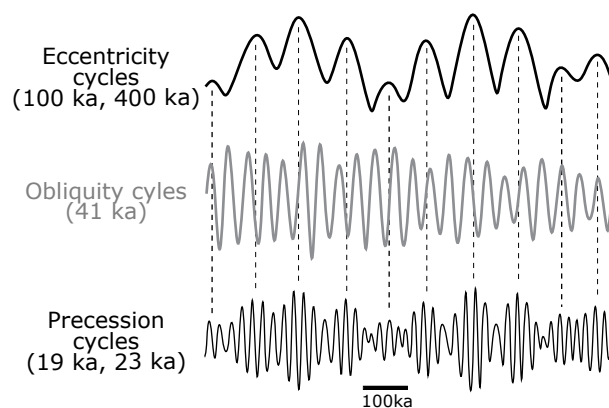


**Fig. 7.3** - Schematic insolation curves of the different orbital parameters. Note that the eccentricity acts as an amplitude modulator of the precession cycles (based on EINSELE & RICKEN 1991a).

cyclic environmental changes on the scales of tens to hundreds of thousands of years. Orbital insolation changes are also translated into sea-level fluctuations, which are then recorded as rhythmic sedimentary successions (e.g., BERGER & LOUTRE 2004).

### *Pre-Quaternary (Berriasian)*

Generally, the scientific community supports the opinion that the climate of the Berriasian was in a “greenhouse” mode, in which no major continental ice-sheets existed (READ 1995). Continental ice caps in high latitude were probably present in the Mesozoic, but their volumes were not sufficient to induce important glacio-eustatic changes (FRAKES et al. 1992, EYLES 1993, VALDES et al. 1995). Ephemeral continental ice-sheets probably existed at high latitudes during the Early Cretaceous (“cool mode”; FRAKES et al. 1992; cf. Chap. 8). Consequently, in “greenhouse” worlds eustatic sea-level changes were of low amplitudes (e.g., WRIGHT 1992, READ 1995, HALLAM 2001, STRASSER et al. 2004). Berriasian high-frequency sea-level changes were probably caused not only by glacioeustasy but also by thermal expansion of the ocean waters (STRASSER et al. 1999).

In the geological past, the periods of precession and obliquity were shorter because of the slowing of the Earth’s rotation (increase of the length of the day) and the increasing Earth-Moon distance (BERGER et al. 1989a, b). For the Berriasian (about 140 Ma according to HARDENBOL et al. 1998), the peaks of the precession signal are approximately at 18.5 ka and 22 ka and of the obliquity at about 38 ka and 49 ka (the values derive from Fig. 1 in BERGER et al. 1989a). The periodicities of the eccentricity are stable over time.

The calculation of the insolation fluctuations is made with the help of exceptionally computer-intensive numerical integrations of the solar system. However, calculated solutions begin to diverge when integrated over long periods (e.g., LASKAR et al. 1993). After approximately 30 Ma, the divergence becomes exponential indicating that parts of the solar system are chaotic and cannot be approximated by quasi-periodic solutions (SCHWARZACHER 2000). Therefore, no precise insolation curves can be calculated for the Berriasian.

## 7.3 Cyclostratigraphy

There are numerous high-resolution sedimentological investigations relating meter-scale rhythmic

successions to astronomically induced variations of insolation. The understanding of the relationship between orbital forcing and their sedimentary signatures in shallow- and deep-marine settings at different geological time intervals and localities has been a main domain of research in carbonate sedimentology during the last twenty years (e.g., FISCHER 1986, 1991, GROTZINGER 1986, GOLDHAMMER et al. 1987, 1990, 1993, READ & GOLDHAMMER 1988, D’ARGENIO et al. 1997, 1999, BUONOCUNTO et al. 1999, BOSENCE et al. 2000).

The term “cyclostratigraphy” was probably first introduced by FISCHER et al. (1988) at a meeting of the Global Sedimentary Geology Program (reference in STRASSER et al. 2007). According to the definition of HILGEN et al. (2004; p. 305) a sedimentary cycle is defined as “one succession of lithofacies that repeats itself many times in the sedimentary record and that is, or is inferred to be, causally linked to an oscillating system and, as a consequence, is (nearly) periodical and has a time significance. Different cycles can be described by their period, for example as a 100-ka cycle or, if this is not precisely known, as a cycle on the order of 100 ka.”

Cyclostratigraphic studies initially investigated limestone-marl alternations (called “cycles” in these concepts) of basinal settings (e.g., HOUSE 1985, FISCHER et al. 1990, BOND et al. 1993, SCHWARZACHER 1993, WEEDON 1993, COTILLON 1995). Later, rhythmic sedimentary successions have been investigated by spectral analysis of stacking patterns as well as geochemical and/or geophysical parameters (e.g., calcium carbonate content, colour intensity (gray level), magnetic susceptibility, x-ray fluorescence, elemental concentrations). The fluctuations of such parameters then have been related to climatic and (glacio-) eustatic cycles of periods in the range of 10 to 100 ka (e.g., GIRAUD et al. 1995a, b, WEEDON et al. 1999, PÁLIKE et al. 2001, D’ARGENIO et al. 2004b). Good examples, in which different cyclostratigraphic methods are used, have been published in DE BOER & SMITH (1994a), HOUSE & GALE (1995), and D’ARGENIO et al. (2004a).

Fischer-Plots are a classical method, which has been used to investigate accommodation changes of cyclic sedimentary successions on carbonate platforms (e.g., READ & GOLDHAMMER 1988, OSLEGER & READ 1991, GOLDHAMMER et al. 1987, 1990, 1993, MONTAÑEZ & OSLEGER 1993, BOSENCE et al. 2000, DALMASSO & FLOQUET 2001, HILLGÄRTNER & STRASSER 2003). Although their interpretation is controversial, Fischer-Plots can provide valuable clues for trends in accommodation changes (SADLER et al. 1993).

Cycle periodicities are commonly estimated by dividing the duration of the investigated interval between two chronostratigraphic tie-points by the number of identified sedimentary cycles and/or by time-series analysis (e.g., SCHWARZACHER 1993, SPRENGER & TEN KATE 1993, HUANG et al. 1993, D'ARGENIO et al. 1997, WEEDON et al. 1999). However, mathematical methods (e.g., time-series analysis) are only applicable to sedimentary systems that are well dated and composed of a relatively simple stratigraphic architecture (e.g., low facies variability, weak diagenetic alterations, regular shallowing-up trends to a well-defined bathymetric level, absence of significant hiatuses; e.g., COTILLON 1995, HILLGÄRTNER 1999, RAMEIL 2005). For complex, highly dynamic marginal-marine environments as investigated in this study, such a mathematical approach is not useful.

### 7.3.1 Cyclostratigraphic timeframe

Facies evolution, depositional surfaces, and the hierarchical stacking pattern of depositional sequences in the studied sections suggest that the sedimentary record was at least partly controlled by high-frequency, low amplitude sea-level fluctuations. As a working hypothesis, it is assumed that the investigated depositional settings were affected by orbitally controlled sea-level fluctuations, even if complex feedback mechanisms certainly distorted the primary insolation signal (STRASSER 1991). HOUSE (1995) describes these interactions as processes where “the orbital signal goes into a black box, out of which is extruded the stratigraphic record” (p. 533). The approach used in the Fribourg working group follows the concepts described in STRASSER et al. (1999).

#### *Timing*

The sequence-chronostratigraphic timeframe published by HARDENBOL et al. (1998) is used as a reference in this study. The studied interval lies between two radiometrically dated tie-points: the Tithonian-Berriasian boundary ( $144.2 \pm 2.6$  Ma; corresponds to 3<sup>rd</sup>-order sequence boundary Be1 according to HARDENBOL et al. 1998) and the Berriasian-Valanginian stage boundary ( $136.5 \pm 2.2$ ; corresponds to 3<sup>rd</sup>-order sequence boundary Va1 according to HARDENBOL et al. 1998). The error ranges of these radiometric dates are relatively large (more than 2 Ma) according to GRADSTEIN et al. (1995). All other dates in the Berriasian (e.g., biostratigraphical zones, polarity chrons, 3<sup>rd</sup>-order

sequences) in the chart of HARDENBOL et al. (1998) are interpolated between these two radiometrically dated anchor points (cf. Chap. 1).

According to HARDENBOL et al. (1998), the 3<sup>rd</sup>-order sequence boundaries Be4 and Be5 are dated at 141.0 Ma and at 139.3 Ma (cf. Fig. 1.2). The time comprised between these two sequence boundaries is, therefore, in the range of 1.7 million years.

In the Montclus section, which is assumed to be more or less complete between the 3<sup>rd</sup>-order sequence boundaries Be4 and Be5, 16 to 20 small-scale sequences have been identified (PASQUIER & STRASSER 1997, HILLGÄRTNER 1999). STRASSER et al. (2004) counted 19 small-scale sequences in this large-scale sequence of the Montclus section. This discrepancy depends on the interpretation if the thin beds of marly limestone intervals are considered as part of a couplet or as a separate couplet (= elementary sequence), and on excluding or including small-scale sequence 19 (cf. Chap. 6 and Fig 6.6).

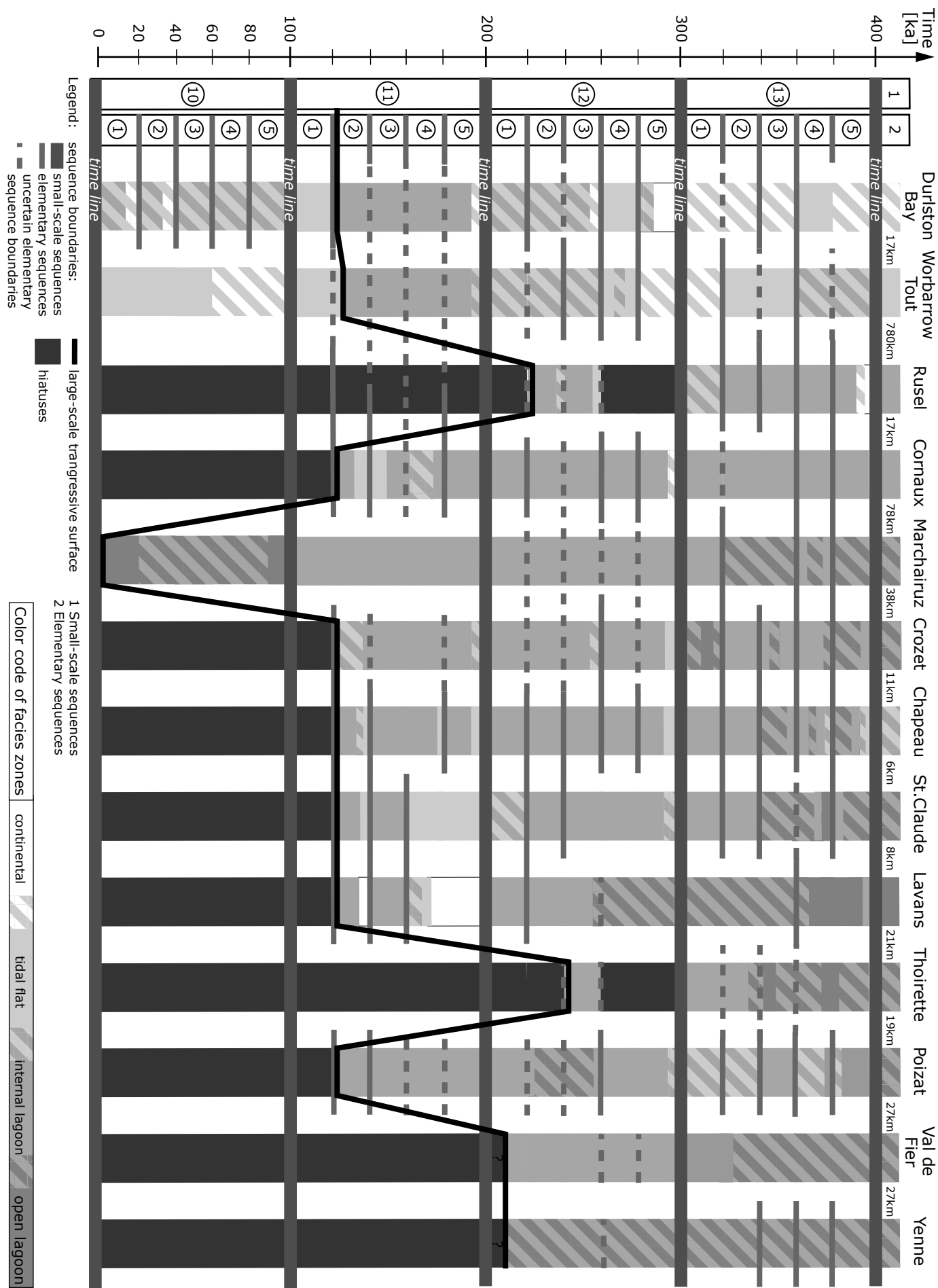
In the Dorset sections, 20 small-scale sequences between the 3<sup>rd</sup>-order sequence boundaries Be4 and Be5 have been identified (cf. Fig 6.10). Although the sequence-stratigraphical interpretations of small-scale sequences below the Cinder Member are uncertain where depositional sequences are strongly reduced, it is assumed that all small-scale sequences are recorded in the Durlston Bay and Worbarrow Tout sections.

Dividing the 1.7 million years of the investigated large-scale depositional sequence by 16 respectively 20 (numbers of small-scale sequences), the duration of a small-scale sequence is in the range of 85 ka to 106 ka. These numbers are close to the periodicity of the short orbital eccentricity cycle (100-ka cycle).

#### *Stacking pattern*

Different studies use the hierarchical stacking pattern of depositional sequences as a criterion for the influence of orbital forcing on deep and shallow-marine carbonates (e.g., GOLDHAMMER et al. 1990, OSLEGER & READ 1991, SCHWARZACHER 1993, SADLER 1994, LEHMANN et al. 1998, LEHRMANN & GOLDHAMMER 1999, RASPINI 2001). A consistent 4:1 relationship (bundling) between small- and medium-scale depositional sequences can be observed in the studied sections in Dorset (cf. Fig. 6.10). The same relationships have been detected in Jura platform sections of the Pierre Châtel and the Vions Formations (HILLGÄRTNER 1999, STRASSER et al. 2004).

Small-scale sequences comprehend 3 to 6 elementary sequences in the Middle to Late Berriasian of the



Jura platform (PASQUIER 1995, PASQUIER & STRASSER 1997, HILLGÄRTNER 1999, STRASSER et al. 2004). A similar bundling of depositional sequences has been reported from the Early Berriasian Goldberg Formation of the Jura platform by STRASSER (1988, 1994). In average, five elementary sequences build up one small-scale sequence in the marginal-marine deposits of the Dorset region and the Jura platform. Autocyclic deposits and/or missed beats exist in the sedimentary record of the investigated interval but they can be delimited by the sequence-stratigraphical correlation (cf. Chap. 6).

In the Berriasian of the Vocontian basin, the small-scale sequences show a comparable stacking pattern. It is thought that individual marl-limestone couplets correspond to the orbital precession signal (e.g., PASQUIER 1995, GIRAUD et al. 1995a, b, PASQUIER & STRASSER 1997, HILLGÄRTNER 1999, STRASSER et al. 2004).

### Timeframe

Several cyclostratigraphic studies in the Berriasian of the Jura Mountains have demonstrated that ...

- medium-scale (composite) sequences were formed by sea-level changes related to the long-eccentricity cycle (400ka).
- small-scale (composite) sequences are controlled by sea-level fluctuations related to the short-eccentricity cycle (100ka)
- elementary sequences were formed by sea level changes corresponding to the precession cycles (20 ka). (PASQUIER 1995, PASQUIER & STRASSER 1997, STRASSER & HILLGÄRTNER 1998, HILLGÄRTNER 1999, STRASSER et al. 2004).

Obliquity cycles have not been identified in the studied sections. This can be explained by the low latitudinal position of the study areas (cf. Fig. 1.5). However, other studies detected obliquity cycles also in regions situated at low latitudes during Early Cretaceous times (e.g., JIMENEZ DE CISNERO & VERA

1993, SPRENGER & TEN KATE 1993, GIRAUD et al. 1995a, SANDULLI & RASPINI 2004).



The time-space diagram (Fig. 7.4) illustrates the high-resolution correlation of the small-scale sequences 10 to 13 and their elementary sequences of the Dorset and the Jura platform sections around the large-scale transgression of the Middle Berriasian. The depositional sequences are delimited by their sequence boundaries. When assuming that each small- and elementary sequence represent an equal time increment (100-ka and 20-ka cycles), the sequence boundaries symbolize time lines. The facies successions between the time lines have approximately been interpolated according the facies analysis of the sections (cf. Chap 4 and 5). The time-space diagram, therefore, does neither account for different sedimentation rates, which are strongly facies-dependent, nor for non-deposition and/or erosion between two time lines

With the help of this diagram, the complex pattern of different facies (illustrated by their codes in Fig. 7.4) between the sections can be investigated along and between the time lines. The large-scale transgression is strongly diachronous with a time deviation of up to 220 ka between the Marchairuz and Rusel sections. According to the sequence-stratigraphical best-fit solution and the cyclostratigraphical assumption of this study, the large-scale transgression marked at the base of Cinder Member in the Dorset region and at the base of the Pierre Châtel Formation on the Jura platform starts in most sections (with the exception of four sections) at the base of the small-scale sequence 11 in the second elementary sequences. Over a distance of more than 780 km, the large-scale transgression occurred in eight sections in the same 20-ka cycles - a quite astonishing synchrony.

The sequence boundary between small-scale sequences 12 and 13 is well expressed in most of the sections by a relatively proximal facies and has been interpreted as a medium-scale sequence boundary (cf. Chap. 6). According to the cyclostratigraphic interpretation, emersion represented by continental deposits in Durlston Bay and by karst surfaces in Rusel and Thoirette lasted more than 20 ka at this sequence boundary. The assumption that the different scales of depositional sequences have been controlled by orbital forcing enables to propose a high-resolution time framework (SCHWARZACHER 2004). It can be used to monitor lateral and vertical facies changes in time over long distances between different depositional regions (STRASSER et al. 2004; cf. Chap. 9).

When combining sequence stratigraphy with cyclostratigraphy, it is also possible to estimate the time spans between sequence-stratigraphic surfaces (e.g., sequence boundaries), limits of biozones (ammonite

**Fig. 7.4** – (facing page) Time-space diagram illustrating the depositional environments indicated by the corresponding “color code” (see also Figs. 6.4 and 6.11) of small-scale sequences 10 to 13 and their elementary sequences of all the investigated sections of the Dorset region and the Jura platform. The sequence boundaries of the small-scale and the elementary sequences are considered as time lines delimiting the 100-ka and 20-ka orbital cycles.

SM Scallop Member  hiatuses  
CM Cinder Member  uncertain polarity chrons (according to OGG et al. 1991, 1994)

can be adjusted astrochronologically (cf. Fig. 7.6).

At Montclus (Vocontian basin), the Privasensis subzone exhibits a time span of 950 ka but only 400 ka are given in the chart. The duration of the Dalmasi subzone, however, is more or less consistent in both interpretations (deviation of about 100 ka). The 3<sup>rd</sup>-order maximum flooding in the chart of HARDENBOL et al. (1998) is at about 139.7 Ma. This assump-



Boreal chronostratigraphic chart of HARDENBOL et al. (1998)										Dorset region				Jura platform		Vocontian basin						Tethyan chronostratigraphic chart of HARDENBOL et al. (1998)					
Stage		Magneto- stratigraphy	Duration	Ammonite subzones	Duration	3 <sup>rd</sup> -order sequences	Duration	Magneto- stratigraphy	Duration	3 <sup>rd</sup> -order sequences	Duration	Bio- stratigraphy	3 <sup>rd</sup> -order sequences	Duration	Magneto- stratigraphy	Duration	Ammonite subzones	Duration	3 <sup>rd</sup> -order sequences	Duration	Ammonite subzones	Duration	3 <sup>rd</sup> -order sequences	Duration	Ammonite subzones	Duration	Stage
BERRIASIAN	Late	M16n		?		Be5	139.3	M16n		Be5	100ka	P. allobrogensis	1) ) MF	100ka	M16n		PARAMIMOUNUM		Be5		Be5		PARAMIMOUNUM		Be5		BERRIASIAN
		139.7	MF		139.7	M16r	200 - 300* ka	MF		M16r	300 - 400 ka		MF	139.7	400 ka	MF		139.3									
	Middle	M16r	700 ka	KOCHI	700 ka			1.30 Ma	M17n	700 - 800* ka	TS	800 - 900 ka	M4	TS	500 - 900 ka	?	M17n	DALMASI	500 ka	TS	700 - 800 ka	1.30 Ma	DALMASI	600 ka	DALMASI	600 ka	
		140.4																									
		M17n	500 ka																								140.7
		140.9																									
		M17r		RUNCTONI			Be4	141.0	M17r		Be4			hiatus	1.00 - 1.20 ma	?		PRIVA- SENSIS	950 ka	Be4	1.00 - 1.10 ma	Be4	141.0	PRIVA- SENSIS	400 ka		
																		SUB- ALPINA					SUB- ALPINA				

1) Hiatus at the 3<sup>rd</sup>-order sequence boundary Be5 on the Jura platform represents a time span of up to 300 ka (Rusel section).

\* When including intervals of uncertain polarity chrons (according to OGG et al. 1991, 1994) the chron M17n represents a time span in the range of 700 - 1400 ka and the chron M16r a range of 300 - 400 ka in the Durlston Bay section.

**Fig. 7.6** - Chronostratigraphy of the studied interval according to HARDENBOL et al. (1998), and comparison with the estimation of time spans (ammonites subzones and polarity chrons) based on cyclostratigraphic interpretation of the sections in Dorset, the Jura platform,

tion has been confirmed by the study of WORNARDT (1999). In the present study, the 3<sup>rd</sup>-order maximum flooding has been placed 100 ka below the 3<sup>rd</sup>-order sequence boundary Be5 (small-scale sequence 19, cf. 6.13). The discrepancy of up to 300 ka may be due to problems with attributing absolute ages to biozones, and/or to the fact that the best-developed expression of a diagnostic interval and/or surface in a sedimentary record does not necessarily occur at the same time in different palaeogeographic locations (JACQUIN & DE GRACIANSKY 1998, STRASSER et al. 2004).

Problems arise for the estimation of the duration of the polarity chrons. According to the interpretation of this study, the times span of the chron M17n is in the range of 700 to 800 ka at Durlston Bay (without uncertain polarity-chron intervals), whereas in the chart of HARDENBOL et al. (1998) it lasts 500 ka. The chron M16r has a duration in the range of 200 to 300 ka in the Durlston Bay section (without uncertain polarity-chron intervals). In the Montclus section, it is in the range of 300 to 400 ka. HARDENBOL et al. (1998) indicate a time span of 700 ka for the polarity chron M16r. The discrepancy between the Durlston Bay

section and the Montclus section can be related to the fact that the sequence-stratigraphical interpretation of the type-section of Berrias and hence, the correlation with the Montclus section are not without difficulties (STROHMENGER & STRASSER 1993, PASQUIER 1995, PASQUIER & STRASSER 1997; cf. Chap. 6). Moreover, the limits of the ammonite subzones in Berrias and in Montclus are generally not precisely defined. They offer a certain play of interpretation, which inevitably has an effect on the high-resolution sequence- and cyclostratigraphical best-fit resolution. An exception is displayed by the boundary between the Dalmasi and Paramimounum subzones, which is quite well delimited in the Berrias and Montclus sections (cf. LE HÉGARAT 1973).

### 7.3.2 Completeness of sedimentary record

Generally, sedimentation can be considered as a discontinuous process with unsteady accumulation rates (SADLER 1981, TIPPER 1983, SCHWARZACHER 1993, KOWALEWSKI & BAMBACH 2003). According to

SADLER (1981), sedimentary sequences “record the passage of geological times as an alternating set of sedimentary increments and gaps. The ratio of these two components is the completeness of a section” (p. 579). Therefore, completeness cannot be separated from the time scale of observation.

In shallow-marine deposits, parts of the geological record are lost in discontinuity surfaces during exposure by non-deposition and/or erosion (READ et al. 1986, STRASSER 1994, HILLGÄRTNER 1998, 1999, STRASSER et al. 1999, STRASSER & SAMANKASSOU 2003; cf. Fig. 3.9). Sedimentary successions of such environments thus only represent a fraction of the geological time (e.g., WRIGHT 1994, IMMENHAUSER & SCOTT 2002, BURGESS & WRIGHT 2003, MIALI & MIALI 2004). If sea level remains below the platform top during a long-term emersion and/or tectonic uplift, no signal can be recorded (HARDIE et al. 1986, GOLDHAMMER et al. 1990, STEINHAUFF & WALKER 1995). RAMEIL (2005) stated that “the crucial question is not if the sedimentary record is complete in general (it is not!), but if there are any longer-term hiatuses that produced missed beats” (p. 139). FOOS (1996) tried to separate long-term from short-term unconformities in shallow carbonate successions by analyzing diagenetic and sedimentological features. According to MARTÍN-CHIVELET & GIMÉNEZ (1992) and WRIGHT (1994), it is possible to roughly estimate the duration of a subaerial exposure by evaluating the maturity of palaeosols and/or karst surfaces. BUDD et al. (2002), however, question the direct relationship between macroscopic exposure features and their duration.

In order to estimate the duration of a hiatus, it is important to investigate several sections and to correlate them laterally (cf. Chap. 6). With the help of high-resolution sequence stratigraphy in combination with cyclostratigraphy, the duration of a hiatus can be estimated (e.g., RASPINI 2001, D’ARGENIO et al. 2004b). The Mammal Bed in Dorset has been interpreted as a palaeosol (cf. Chap. 5). It can be assumed that it comprehends a long time interval of exposure probably in the range of several ten thousand years. The palaeosol, which has been interpreted as 3<sup>rd</sup>-order sequence boundary Be4 at Worbarrow Tout may also represent a long-lasting unconformity (cf. Fig. 5.11b). Thick palaeosols, which are characterized by well-defined soil profiles, indicate long exposure times in the range of several 100 ka, whereas thin, unstructured (“incipient”) palaeosols reflect shorter exposure times (WRIGHT 1994).

Karst surfaces at Rusel and Thoirette (between small-scale sequence boundaries 12 and 13) were exposed during approximately 40 ka (cf. Fig. 7.4).

The time represented by the widespread karst surface at the boundary between the Pierre Châtel and the Vions formations (cf. Fig. 6.1) ranges from over 100 ka (Chapeau de Gendarme section) to more than 300 ka (Rusel section; cf. Fig. 7.6).

Different mathematical models have been published in the literature, which investigate the completeness of sedimentary successions (e.g., SADLER 1981, TIPPER 1983, PLOTNICK 1986, SADLER & STRAUSS 1990, SCHWARZACHER 1993, 1998, SCHLAGER et al. 1998, LEHRMANN & GOLDHAMMER 1999). Generally, they show that completeness and thickness of sedimentary successions are weakly positively correlated. Moreover, mathematical models reveal that depositional processes are not the primary control on the distribution of hiatuses at time scales longer than ten thousand years. At long time scales, the most influential factors depend less on the local depositional environment but on regional to over-regional factors (e.g., lithospheric subsidence, sea-level fluctuations, and/or climate changes; SADLER 1999). The best empirical estimates for rates of accumulation, subsidence, and sea-level fluctuations indicate that depositional sequences with a 10<sup>4</sup> to 10<sup>5</sup> years period (Milankovitch-frequency band) dominate the stratigraphic record of shallow marine carbonate environments (SADLER 1994). The stratigraphic record in greenhouse climates is commonly dominated by depositional sequences lasting about 20 ka. However, up to 50% of the time span of each depositional sequence is represented by hiatuses in shallow-marine deposits (SADLER 1994). IMMENHAUSER & SCOTT (2002) estimated that hiatuses capping depositional sequences of the Arabian platform in Oman may account for 30% to 70% of the cycle durations.

### 7.3.3 Precision of chronostratigraphic calibrations

Although the orbital control on sedimentary successions is widely accepted by the scientific community nowadays, there are some critical points, which have to be taken into account. Besides the theory that peritidal carbonate cycles are mainly produced by aperiodic processes (autocycles; e.g., DRUMMOND & WILKINSON 1993a, b, WILKINSON et al. 1996, 1997; cf. Chap. 3 and 6), the precision of chronostratigraphic calibrations of sedimentary records have been criticized as being insufficient to constrain the cycle duration (e.g., MIALI & MIALI 2004). They “suggest that attempts to develop a time scale [for pre-Quaternary strata] with an accuracy and precision in the 10<sup>4</sup>-year range by

calibrating it against conventional chronostratigraphic dates up to two orders of magnitude less precise represents a fundamentally flawed methodology” (p. 39).

GALE et al. (2002) specified the timing problem of shallow marine deposits by underlining that “the poor understanding of the relationship between sequence stratigraphy and cyclostratigraphy is partly the result of the nature of the sedimentary record. Relatively complete, well-dated successions that provide the clearest orbital signal were mostly deposited in deeper water environments and provide little evidence of sea-level change. In contrast, shallow-marine succession commonly show clear evidence of sea-level changes, but are usually incomplete and seldom show clear orbital cyclicity” (p. 291). According to SCHWARZACHER (1998), “sequence- and cyclostratigraphy are fundamentally different from biostratigraphy, because they are based on repetitive events. Such events miss the uniqueness of biological markers resulting from unidirectional evolution of life, but this disadvantage is often compensated for because repetitive events can lead to much higher resolution and completeness” (p. 2).

### 7.3.4 The long eccentricity cycle (400 ka): “A tuning fork”

Different studies identified the 400-ka eccentricity cycle in Mesozoic sedimentary successions (e.g., BUONOCUNTO et al. 1999, STRASSER et al. 2000, GALE et al. 2002, ANDERSON 2004b, D’ARGENIO et al. 2004b, MILLER et al. 2005). This orbital cycle is considered to be the most stable over prolonged intervals of time (HILGEN et al. 2004). When examining Late Jurassic and Early Cretaceous sedimentary successions, STRASSER et al. (2000) observed that lithologically well-developed sequence boundaries have been formed in tune with the 400-ka eccentricity cycles. In many cases, they match with the 3<sup>rd</sup>-order sequence boundaries of DE GRACIANSKY et al. (1998). STRASSER et al. (2000) stated that “long-term accommodation changes created by tectonic and tectono-eustatic mechanisms define the general frame for the development of depositional sequences, but the orbital insolation cycles give the “beat” for the making of beds and bedsets” (p. 309).

MATTHEWS & FROHLICH (2002) developed a mathematical model (PFM: Parametric Forward Model) in order to evaluate the physical limitations of possible continental ice-sheets in high latitudes from 65 to 190 Ma. In general, this model uses the extension of an ice-sheet area and the solar insolation at a specific

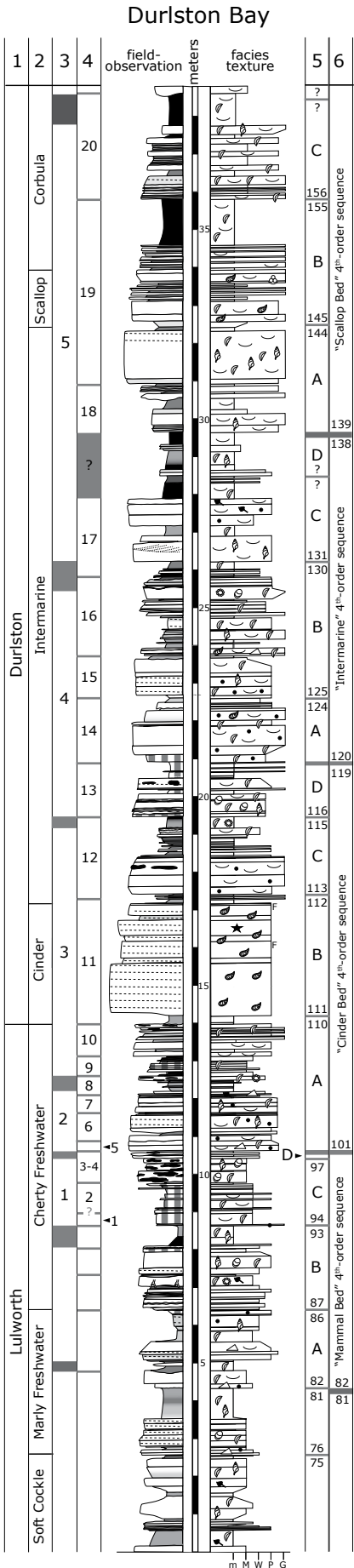
time (parameterization) and calculates the size of the ice sheet for the next time step. The changes in solar insolation thus lead to fluctuations in the extension of continental ice volumes and in the ocean water volume. The resulting fluctuations in global sea level are then recorded in the sedimentary successions (MATTHEWS & FROHLICH 2002, IMMENHAUSER & MATTHEWS 2004). The peaks interpreted as the 400-ka eccentricity cycles are well-expressed over the time span of calculation and have been considered as “a tuning fork” of the geologic time (MATTHEWS & FROHLICH 2002). Numerically-calculated 400-ka peaks of insolation curves may be used for approximately calibrating 400-ka cycles of “floating time scales” determined in orbitally controlled sedimentary successions of pre-Quaternary deposits.

### 7.3.5 Comparison with other Berriasian studies

Two studies relating Berriasian sedimentary successions to orbital forcing mechanisms are briefly discussed below. Although they used different parameters and methods to detect Milankovitch cycles in the sedimentary record, it is worth discussing the discrepancies between the different approaches and to search for possible explanations.

#### *Durlston Bay section*

A direct evaluation of two different cyclostratigraphic approaches can be undertaken by the comparison of the Durlston Bay section, which has also been investigated by ANDERSON (2004a). As a first impression, the positions of the sequence boundaries identified by ANDERSON (2004a) are identical with the ones interpreted in this study (cf. Fig. 7.7). However, interpretations in terms of sequence- and cyclostratigraphy are completely different. This is due to the differences in the applied methods. ANDERSON (2004a) considers limestone beds as the dominant facies at or near the bases of sequence or cycles at each scale (lowstand to transgressive deposits in this study). Shale beds are interpreted to be the prominent facies towards the tops of sequences or cycles (highstand deposits in this study). This sedimentological interpretation is quite the opposite of the one proposed in the present study (cf. Chap. 5). However, there is no simple rule for interpreting the complex architecture of marginal-marine deposits. Detailed facies analysis and sequence-stratigraphical investigations are



- 1 Formations
- 2 Members
- 3 This study: medium-scale sequences interpreted as 400-ka cycles
- 4 This study: small-scale sequences interpreted as 100-ka cycles
- 5 ANDERSON 2004a: 5<sup>th</sup>-order sequences interpreted as 100-ka cycles (numbers corresponds to the bed numbers of CLEMENTS 1993)
- 6 ANDERSON 2004a: 4<sup>th</sup>-order sequences interpreted as 400-ka cycles

**Fig. 7.7** - Comparison of two different sequence- and cyclostratigraphical interpretations of the Durlston Bay section of this study (on the left side) and of ANDERSON (2004a) (on the right side). For discussion refer to text.

essential for interpreting shallow-marine sedimentary succession.

Additionally, ANDERSON (2004a) takes the ostracode faunicycles of ANDERSON (1985) into account, which he relates to the 100-ka cycles (fifth-order sequences indicated by letters in Fig. 7.7). ANDERSON (2004a) also considers the transgressive events defined by MORTER (1984) based on molluscan associations (cf. Chap. 5), which he correlates with the first or second fifth-order sequence boundaries (small-scale sequences in this study) within fourth-order sequences (medium-scale sequences in this study).

According to ANDERSON (2004a), the fundamental process in producing a cyclic stratigraphic record is the precessional signal (ANDERSON & GOODWIN 1990). Moreover, he assumes that all sequence and cycle boundaries are caused by allocyclic processes of precessionally forced sea-level rises due to cessation of sedimentation when a critical rate of rise is attained (induction-deduction approach or “hermeneutic circle” according to MIALL & MIALL 2004). The degree of facies change that occurs at cycle boundaries is a function of the magnitude of sea-level rise and is the basis for bundling rock cycles (fifth-, fourth-, and third order sequences). Accordingly, the study of ANDERSON (2004a) is based on a strict assumption that solely allocyclic orbital-forcing mechanisms are able to produce hierarchically stacked rock sequences (or cycles). His approach is fundamentally different from the one applied in this study.

The present study is based on detailed facies analysis, which enables a detailed sequence-stratigraphical interpretation (cf. Chap. 3). Autocyclic processes are shown to coexist with allocyclic forcing mechanisms, following the statement of SMITH (1994) that “in many settings, the Milankovitch climatic signal that we know to exist is masked by the effects of other variables. In other settings it apparently comes through clearly, with all of its relative periodicities intact, and the other variables are reduced to a background role with only

minor influence on the structure of the resulting strata” (p. 536).

However, autocyclic deposits are generally of limited spatial and temporal extension in contrast to allocyclic intervals, which can be correlated over long distances (cf. Chap. 6). Accordingly, long-distance regional to interregional correlations are essential to distinguish between allocyclic and autocyclic signals in sedimentary records.

### ***Sierra del Pozo section***

The sedimentary record of Sierra del Pozo section in the Prebetic zone (cf. Chap. 6; for location refer to Fig. 6.14) has been related to orbital forcing by JIMENEZ DE CISNERO & VERA (1993) and ANDERSON (2004b). JIMENEZ DE CISNERO & VERA (1993) used Fischer-Plots and time-series analysis to estimate the duration of the shallowing-up sequence in the Sierra del Pozo section. The sequences are attributed to

precession and obliquity cycles, whereby the latter are dominant. ANDERSON (2004b) identified 20-ka, 100-ka, and 400-ka cycles in this section. His interpretation is based on the deductive assumption that the basic units in this section are precession cycles, which produce in combination with other Milankovitch cyclicities the hierarchical stacking pattern. The main differences in the interpretation of the stacking pattern and its relationship to orbital forcing mechanisms are due to the different facies interpretations by JIMENEZ DE CISNERO & VERA (1993) and ANDERSON (2004b). JIMENEZ DE CISNERO & VERA (1993) interpreted marly intervals as subtidal deposits, whereas ANDERSON (2004b) considered them mainly as supratidal sediments (mostly palaeosols). However, as shown in Chap. 3, the deposition of clay minerals in marls and shale intervals in marginal-marine environments and their interpretation in terms of sequence stratigraphy is not easy (cf. Fig. 3.2). In order to improve the environmental interpretation, detailed facies analysis of marls (e.g., by washing) are absolutely necessary.

\*\*\*\*\*



## 8 - PALAEOCLIMATE AND ENVIRONMENTAL CHANGE

### 8.1 Introduction

Until the 1980s, the Cretaceous palaeoclimate was considered to be warm and equal without any polar continental ice caps, a low equator-to-pole temperature gradient, and warm polar oceans (“greenhouse conditions”; e.g., HALLAM 1981, 1985). Later, this assumption has been questioned in several publications (e.g., KEMPER & SCHMITZ 1981, KEMPER 1983, FRAKES & FRANCIS 1988, SLOAN & BARRON 1990, MUTTERLOSE & KESSELS 2000, MILLER et al. 2005). These authors assessed the evidence for ice during this time of Earth history, although direct indications are sparse and commonly equivocal. In contrast, other studies (e.g., BENNETT & DOYLE 1996, MARKVICK & ROWLEY 1998) have found little evidence for ice and suggested that its presence is only based upon inference or wishful thinking.

Depositions of glacially derived sediments or minerals indicating cold water (e.g., tillites, dropstones, glendonites) have been reported from Mesozoic sediments at high palaeolatitudes (e.g., KEMPER & SCHMITZ 1981, FRAKES & FRANCIS 1988, FRANCIS & FRAKES 1993, FRAKES et al. 1995, ALLEY & FRAKES 2003). A marked increase of glacial tillites and dropstones has been observed at high latitudes during Tithonian to Early Berriasian times (FRAKES & FRANCIS 1990). However, glendonites have not been found in this time interval (e.g., KEMPER & SCHMITZ 1981, PRICE 1999). Although glaciogenic deposits are of paramount importance in palaeoclimate reconstructions, published accounts often lack essential details on the biostratigraphical and facies context, in which such materials occur (SELLWOOD & PRICE 1994, PRICE 1999).

An indirect approach to study Mesozoic climate has been through the application of computer simulations (e.g., GCM: General circulation model; e.g., BARRON

& WASHINGTON 1982, BARRON 1983, OGLESBY & PARK 1989, PARK & OGLESBY 1991, BARRON & MOORE 1994). Although such simulations strongly depend on specific boundary conditions at a defined time (e.g., palaeogeography, atmospheric CO<sub>2</sub>, ocean temperatures) and initial parameterization, several GCM studies simulated significant amounts of sea-ice during the Late Jurassic (Kimmeridgian to Tithonian; e.g., MOORE et al. 1992, VALDES et al. 1995). Moreover, climate models showed that the amount of solar energy available in mid and high latitudes during the winter was not sufficient to raise the land surface temperature above freezing. If the polar oceans were warm and the equator-to-pole temperature gradient low, atmospheric circulation would not have been strong enough to transport heat to continental interiors (COVEY & BARRON 1988, SLOAN & BARRON 1990). SELLWOOD & VALDES (1997) simulated the global cloud cover for Mesozoic times with the help of a GCM model. The simulation shows that high latitudes are warmer at low atmospheric pressure conditions, which further enhance the development of cloud covers. They concluded that the increased cloud cover may have caused the relative warm climate in the Mesozoic era at high palaeolatitudes.

Accumulation of ice at high latitudes, which waxed and waned in concert with the orbital cycles, probably caused meter-scale sea-level changes (PRICE et al. 1998, SELLWOOD et al. 1994, VALDES et al. 1995, VALDES & GLOVER 1999). Milankovitch-climate forcing may have caused extensive areas of permafrost and/or minor ice-sheets at high latitudes on the southern continents even in “greenhouse” periods (VALDES & GLOVER 1999, SELLWOOD et al. 2000). However, such relatively short-term cycles may not always be resolved from time series analysis of climate proxy data (e.g., VALDES et al. 1995, PRICE 1999).

In summary, the assumption that the Late Jurassic to Early Cretaceous climate was hot and uniform has

definitively to be abandoned because evidence of colder conditions in higher latitudes during certain periods are apparent. However, the temporal and spatial extensions of such phases and their consequences are still controversially discussed (e.g., SELLWOOD et al. 2000).

## 8.2 Palaeoclimate during the Berriasian

### 8.2.1 An overview

#### *Sedimentological indicators*

The marginal-marine deposits of the Late Tithonian to early Middle Berriasian in Dorset and on the Jura platform (cf. Chap. 5) contain evaporite pseudomorphs after gypsum and calcrete intervals, which indicate semi-arid conditions (e.g., STRASSER & DAVAUD 1982, PARRISH et al. 1982, DAVAUD et al. 1983, HALLAM 1984, FRANCIS 1984, WRIGHT 1994; cf. Fig. 8.1).

The increase of siliciclastics compared to carbonate deposits in the Dorset region and on the Jura platform, beginning in late Middle Berriasian times, gives a measure of the amount of continental run-off, which has been related to increased precipitation in the source area (HALLAM 1984, 1986; cf. Fig. 8.1). Tectonic uplift in the hinterland, however, may also contribute to increasing siliciclastic input into sedimentary basins. Hence, the siliciclastic-carbonate relationship alone is not sufficient for palaeoclimatic interpretations (RUFFELL & RAWSON 1994).

Coal deposits and the development of palaeosols in the Wealden facies of NW and Central Europe have been interpreted as a climate signal for more humid conditions from Late Berriasian times onwards (e.g., MEYER 1976, PELZER & WILDE 1987). Moreover, karst surfaces described from the Jura platform are generally related to more humid climates where precipitation is higher than evaporation. (e.g., WRIGHT 1988, 1994, SELLWOOD & PRICE 1994, D'ARGENIO & MINDSZENTY 1995, FOOS 1996).

#### *Floral and faunal indicators*

The climate conditions on land have been deduced from comparison with the thermal tolerances of present-day organisms and their fossil relatives (e.g., DOUGLAS & WILLIAMS 1982). Although this approach

is useful as a general guide, it must be carefully applied in palaeoclimate interpretations because the climatic tolerances of some ancient organisms and their adaptations to changing climate condition may have been different from those of their living relatives today (e.g., JEFFERSON 1982, KEMPER 1987, FRANCIS & FRAKES 1993).

During the Early Berriasian, the northern hemisphere was dominated by Cheirolepidiacean trees (xerophytic plants), an extinct family of conifers that produced *Classopollis* pollen (FRANCIS 1983, SLADEN & BATTEN 1984, NORRIS 1985, ALLEN & WIMBLEDON 1991, VAKHRAMEEV 1991, FRANCIS & FRAKES 1993, SCHNYDER 2003). Since pollen of this type have often been found in association with evaporitic sediments, their abundance has been related to arid conditions. During the Middle to Late Berriasian, moisture-loving ferns spread into lower latitudes whereas the dominance of conifers declined. This floral change has been interpreted as a climate signal for more humid conditions (e.g., PELZER & WILDE 1987, FRAKES et al. 1992). The relative increase of pteridophyte spores in Late Berriasian to Early Valanginian times indicates more humid conditions (e.g., PANTIĆ & BURGER 1981, SLADEN & BATTEN 1984, PELZER & WILDE 1987, ALLEN 1998).

The distribution of climate-sensitive reptiles, especially dinosaurs, has been used as a palaeoclimate indicator (e.g., AXELROD 1984, ALLEN 1998). The climate significance of dinosaur footprints and remains found at high latitudes (polar dinosaurs; e.g. RICH et al. 2002) has been discussed controversially, mainly due to the absence of modern descendants (RUFFELL & RAWSON 1994). Large dinosaurs may have migrated to warmer regions during cold seasons in polar regions (HAMMER & HICKERSON 1994) and smaller ones may have been well adapted to cold polar conditions. They probably hibernated at high latitudes (RICH et al. 1988).

#### *Clay-mineralogical and geochemical indicators*

Assemblages of clay minerals give further indications that a major climate change occurred during the Middle Berriasian. Palygorskite, commonly associated with evaporites, is a useful indicator of aridity (DECONINCK 1987). This clay mineral has been reported from Early Berriasian sediments in NW and Central Europe (e.g., DECONINCK 1987, HALLAM et al. 1991, SCHNYDER 2003; cf. Fig. 8.1). Kaolinite, which is formed in tropical to subtropical climates, has been taken as a unambiguous indicator for seasonally wet conditions (e.g., PERSOZ & REMANE 1976, COTILLON et



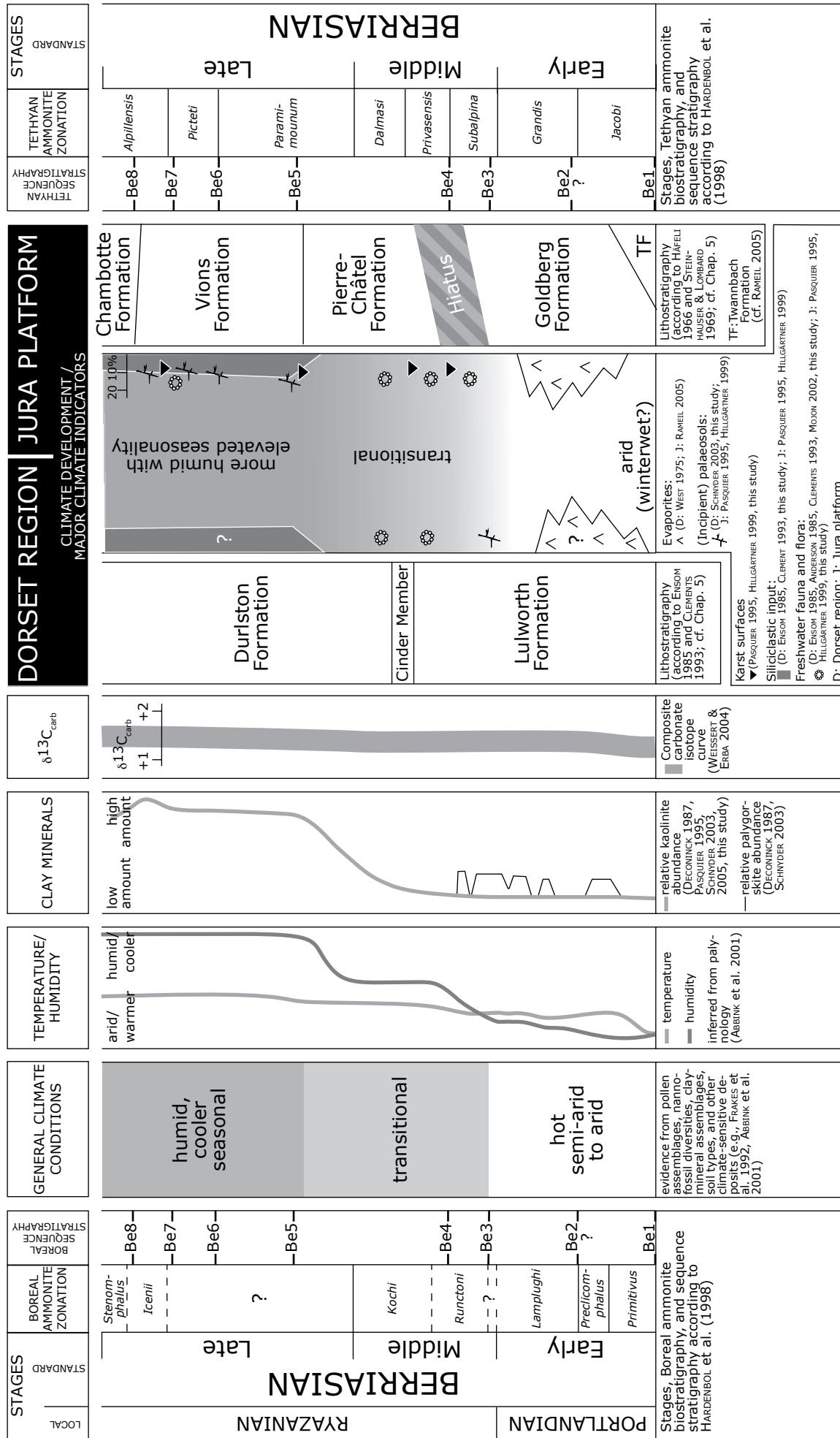


**Fig. 8.1** - General development of the climate in NW and Central Europe during the Berriasian based on different parameters (palynology, clay minerals, stable isotopes, and sedimentary features) published in the literature and on own observations in the Dorset region and on the Jura platform.

al. 1980, PERSOZ 1982, BURGER 1982, SLADEN 1983, SLADEN & BATTEN 1984, DECONINCK & DEBRABANT 1985, DECONINCK et al. 1985, HALLAM et al. 1991, ALLEN & WIMBLEDON 1991). A gradual increase of kaolinite during the Middle to Late Berriasian has been reported from different localities: e.g., Dorset (e.g., SLADEN 1983, SLADEN & BATTEN 1984, DECONINCK 1987, RASPLUS et al. 1987, SCHNYDER 2003, SCHNYDER et al. 2006), eastern Midlands (England; SLADEN 1983), Jura platform (DECONINCK & STRASSER 1987), Vocontian basin (southeastern France; DECONINCK & DEBARAVANT 1985, GEYER 1992, DECONINCK 1993), central Tunisia (SCHNYDER et al. 2005b), and Volga basin (southeastern Russia; RUFFELL et al. 2002). The increase of kaolinite has been interpreted as a climate signal for more humid conditions (cf. Fig. 8.1).

Stable isotopes used for palaeoclimate studies include carbon and oxygen (e.g., WEISSERT 1981, WEISSERT et al. 1985, WEISSERT & CHANNELL 1989, GRÖCKE et al. 2003, WEISSERT & ERBA 2004). High rates of preservation of organic carbon due to an increase of productivity of planktonic biota in ocean surface waters, anoxic conditions at the bottom of depositional basins, and/or elevated sedimentation rates with improved preservation of marine and terrestrial organic carbon usually result in a positive carbon isotope excursion (ARTHUR & SCHLANGER 1979, WEISSERT et al. 1985, WEISSERT & MOHR 1996). Carbon isotope excursions measured in hemipelagic and pelagic deposits reflect the partitioning of carbon between sinks of organic ( $C_{org}$ ) and carbonate carbon ( $C_{carb}$ ) by complex feedback mechanism, which act on different time scales (WEISSERT et al. 1998).

Composite carbon isotope curves derived from pelagic carbonates of the Southern Alps (Italy) show that Tithonian to Berriasian  $\delta^{13}C$  values are relatively low with only minor fluctuations ( $\delta^{13}C$  value of about +1.26 ‰; WEISSERT & CHANNELL 1989, WEISSERT & MOHR 1996, WEISSERT et al. 1998, WEISSERT & ERBA 2004; cf. Fig. 8.1).

Accumulation rates of organic matter dropped from Late Jurassic to the Early Berriasian (low  $C_{org}/C_{carb}$  burial rates). This change in the carbon budget has been related to low surface-water productivity of planktonic biota due to a decrease of nutrient supply from the land to the ocean. A decrease of nutrient supply caused by a reduction of continental run-off has been interpreted to reflect a climate change to drier conditions around the borders of the Tethys Ocean. During the Middle to Late Berriasian, the carbon system may have been changed as indicated by a slight increase of the  $\delta^{13}C$  value (cf. Fig. 8.1). It may reflect an acceleration of the hydrological cycle in a more humid climate (WEISSERT

& CHANNELL 1989).

Similar  $\delta^{13}C$  trends (not absolute values) of well-dated, pelagic Berriasian sediments has been measured in the Vocontian basin (EMMANUEL & RENARD 1993), in the Ionian basin (western Greece; SKOURTSIS-CORONEOU & SOLAKIUS 1999), in the Trapanese region (western Sicily; CECCA et al. 2001), and in the Gulf of Mexico (northeastern and central Mexico; ADATTE et al. 1996). Additionally, carbon isotope measurements on well-preserved belemnites and oysters also indicate comparable  $\delta^{13}C$  trends (e.g., PODLAHA et al. 1998, GRÖCKE et al. 2003, PRICE & MUTTERLOSE 2004). These studies relate carbon-isotope trends to the same palaeoceanographic and palaeoclimatic processes as described by WEISSERT & CHANNELL (1989).

### 8.3 Evidences from the study areas

40 samples (whole-rock) of three sections (Durlston Bay, Cornaux, and Chapeau de Gendarme) have been chosen to investigate geochemical changes (clay minerals and stable isotopes) with high resolution. For the analysis, obvious inhomogeneities (e.g., secondary calcite veins) in the samples were avoided. Marl and limestone samples have been prepared (crushed and pulverized) and analyzed in Dijon (clay minerals; Annex 2) and in Lausanne (stable isotopes; Annex 3).

#### 8.3.1 Clay minerals

##### *Introduction*

The formation of different clay minerals strongly depends on the weathering environment (SLADEN 1983). Clay-mineral formation results, either directly or indirectly, from the hydrolytic decomposition of primary aluminosilicates. The rates of these processes depend on the vertical water movement in soils, weathering profiles (saprolites) or parent rocks, which leads to leaching (wash out of cations and silica oxides by percolating waters). Leaching potential is controlled by the relationship between precipitation and evaporation (SINGER 1980). Therefore, climate (particularly seasonality, average annual temperature and precipitation) and non-climatic variables (topography, type of vegetation and organisms, parent rock composition, and length of time available for soil formation) contribute to the development of a specific weathering environment (e.g., SINGER 1980,

SLADEN 1983, CHAMLEY 1989, VELDE 1995). Because clay minerals are formed in soils or are eroded and transformed from parent rocks in the continental source area, they have to be transported to marine settings by water or wind. Erosion, reworking and transport may modify the composition of a clay assemblage, e.g., by mixing different horizons with different degrees of alteration (e.g., CURTIS 1990). The distribution of detrital clay minerals in marine sediments can thus be regarded as reflecting provenance, sediment sorting, and weathering processes on the adjacent continental areas.

High evaporation and relatively low annual precipitation in warm, semi-arid to temperate climates cause moisture in soil profiles to move upward, creating alkaline soils, which are rich in illite and smectite-illite mixed-layer minerals (SLADEN 1983, CHAMLEY 1989, CURTIS 1990). Limited time for soil development may additionally prevent intense chemical weathering in the source area. Under hot or cold arid conditions (desert or tundra), no soils develop. Hence, assemblages of clay minerals in such weathering environments reflect the composition of the underlying bedrock or of reworked, older soils (inherited association). Smectite and palygorskite are characteristic for soils with a shallow weathering profile in seasonal, semi-arid climates (Mediterranean climate). Palygorskite is an excellent marker for arid to semi-arid conditions (SINGER 1980). Fairly high evaporation in combination with high annual precipitation in warm humid to temperate climates leads to extensive leaching and to deep weathering profiles, creating kaolinite- and gibbsite-rich, acid soils (e.g., SINGER 1980, SLADEN 1983, WRIGHT 1994). The relationship between smectite formation in soils and climate is more debatable (e.g., SINGER 1984, HALLAM et al. 1991). The most favorable climatic conditions probably are those with strong seasonal contrasts. Although smectite is found today under different climatic conditions, its formation is generally related to climates, in which a pronounced dry season alternates with a shorter (or subordinate) wet season (SINGER 1984). Moreover, smectite may be entirely volcanogenic in origin, deriving directly from the weathering of lava and ash (bentonites; e.g., JEANS 2000). Accordingly, such deposits contain no climate signal.

## Methods

The clay-mineral associations have been determined by Prof. Deconinck and co-workers at the University of Dijon (France) using x-ray diffraction

(XRD) on oriented mounts. The used methods are described in the literature (e.g., BRINDLEY & BROWN 1980, HOLTZAPFFEL 1985, MOORE & REYNOLDS 1989; references in SCHNYDER et al. 2006).

Each sample was decarbonated using 0.2 N hydrochloric acid. The excess acid has been removed by successive washing with deionized water. The clay fraction ( $<2 \mu\text{m}$ ) has been separated by sedimentation and centrifugation using the analytical procedure of HOLTZAPFFEL (1985). Oriented pastes have then been prepared on glass slides. Three x-ray diagrams were made using a Philips diffractometer (PW 1730) with  $\text{CuK}\alpha$  radiation and Ni filter, after air-drying (untreated sample), saturation with ethylene-glycol, and heating at  $490^\circ\text{C}$  over two hours. The identification of clay minerals was made according to the position of the (001) series of basal reflections of the three x-rays diagrams. Semi-quantitative evaluations are based on the peak heights and surface areas summed to 100%, with a relative error of about 5% (HOLTZAPFFEL 1985).

## Jura platform

Clay mineral assemblages of the Goldberg Formation (cf. Chap. 4) are mainly composed of illite, smectite, and mixed layers. Chlorite, kaolinite, and palygorskite generally appear in very small quantities (HAFELI 1966, PERSOZ & REMANE 1976, PERSOZ 1982, DECONINCK 1987, DECONINCK & STRASSER 1987). The abundance of poorly crystallized smectites, the lack of significant chlorite, and the independence of clay mineralogy from lithology indicate that burial diagenesis did not (or only weakly) affect the clay mineral assemblages (DECONINCK & STRASSER 1987). A general trend from illite and detrital Al-Fe-smectite in the northwestern part of the Jura platform to authigenic illite in the southeast have been observed by DECONINCK & STRASSER (1987) and DECONINCK et al. (1988).

This pattern can be related to processes at surface temperature where smectite is transformed to illite by illitization in alkaline solutions during repeated wetting and drying in shallow ponds and lagoons in coastal settings (DECONINCK et al. 1988, DECONINCK et al. 2001). The supply of  $\text{K}^+$ -ions, which is necessary for this illitization process, may have been furnished by marine waters during ingressions into the marginal-marine environments (DECONINCK 1987, DECONINCK et al. 1988). Accordingly, it can be assumed that the original amount of smectite in these depositional settings was higher (DECONINCK 1987).

Kaolinite occurs in traces in the upper part of

small-scale sequence 13 in the Chapeau de Gendarme section (Pierre Châtel Formation; cf. Fig. 8.2). PASQUIER (1995) determined clay mineral assemblages in several sections of the Jura platform. In the Rusel section, the first appearance of kaolinite (8-10 %) occurs at the top of small-scale sequence 16 according to the sequence-stratigraphical interpretation of the present study (cf. Fig. 8.3; right side). At Marchairuz, however, kaolinite already appears at the base of the Pierre Châtel Formation (around 15-20 %; PASQUIER 1995) and slightly increases in small-scale sequence 16. The amount of kaolinite increases from small-scale sequence 16 upwards and remains relatively high during the Late Berriasian (PASQUIER 1995).

### *Southern England*

A general decrease of mixed-layer minerals combined with an increase of kaolinite at the transition of the Lulworth Formation to the Durlston Formation in southern England (cf. Chap. 5) has been interpreted as a change from seasonal arid to more humid climate conditions (SLADEN 1983, SLADEN & BATTEN 1984, ALLEN 1998). According to SCHNYDER et al. (2006), the clay minerals of the Durlston Bay section have not been affected by major burial diagenesis because the deposits have seen shallow burial of less than 1 km.

The lower part of the Lulworth Formation up to the Cherty Freshwater Member (at least DB 91) is characterized by a relatively high amount of mixed-layer minerals associated with traces of palygorskite and the absence of kaolinite (DECONINCK 1987, SCHNYDER 2003, SCHNYDER et al. 2006; SCHNYDER 2003 and SCHNYDER et al. 2006 used also the bed numbers of CLEMENTS 1993). Sporadic appearances of kaolinite (in traces) occur just above the Cinder Member (DB 112-114; SCHNYDER 2003, SCHNYDER et al. 2006). A subsequent increase of kaolinite and illite is displayed in the following beds of the Intermarine Member (DB 124b-130 base; less than 10 %). The proportion of kaolinite increases to 10-15 % (above DB 134) and reaches a value of 20-30% in the Late Berriasian to Early Valanginian deposits (SCHNYDER 2003, SCHNYDER et al. 2006). The increase of kaolinite, therefore, lies at the transition between small-scale sequences 16 and 17, according to the sequence-stratigraphical interpretation of the present study (cf. Fig. 8.3; right side). SCHNYDER et al. (2006) interpreted this clay-mineral succession as a step-wise change from semi-arid to semi-humid conditions (cf. Fig. 8.1). A transitional climate prevailed during the interval between the Marly Freshwater to the Intermarine Member (SCHNYDER 2003, SCHNYDER et al. 2006). The transitional climate system is also marked by highest

mixed-layer proportion. This may be related to the formation of authigenic Mg-rich smectite minerals in concentrated saline and/or alkaline solutions of coastal ponds or shallow lagoons caused by high evaporation rates (CHAMLEY 1989). Illitization of smectite by wetting and drying may also contribute to the high amount of mixed-layer clays (SCHNYDER et al. 2006).

### *Vocontian basin*

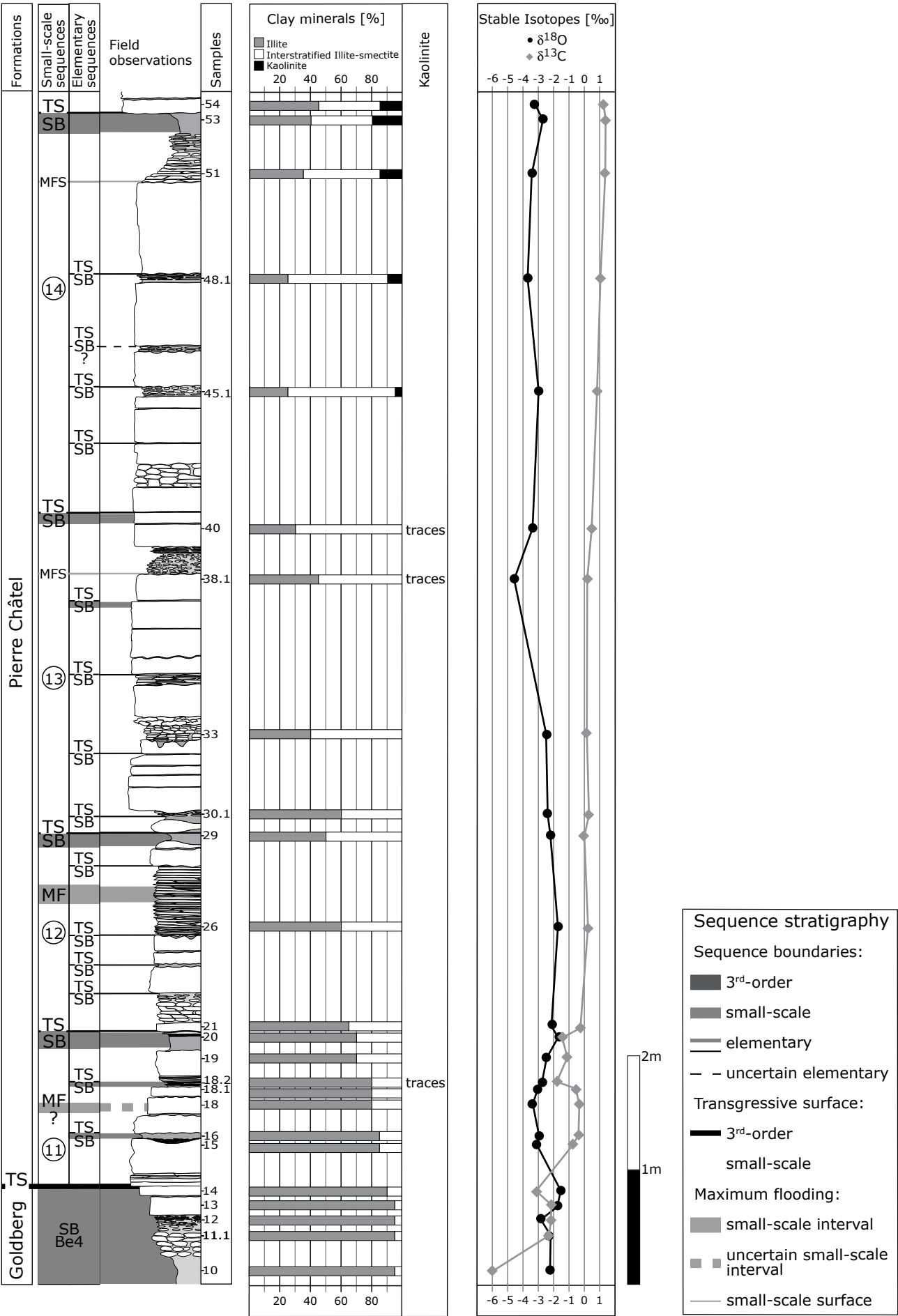
DECONINCK (1993) determined assemblages of clay minerals in the type-section of Berrias (cf. Chap. 6). The occurrence of kaolinite already begins in the Subalpina ammonite subzone below the 3<sup>rd</sup>-order sequence boundary Be4, according to the sequence-stratigraphical interpretation of PASQUIER (1995). A gradual increase of kaolinite occurs up to the large-scale maximum flooding in the Paramimounum ammonite subzone where a first peak of kaolinite has been measured (DECONINCK 1993). A second peak of kaolinite approximately corresponds to sequence boundary Be5 (Paramimounum ammonite subzone; PASQUIER 1995). DECONINCK (1993) related the increase of kaolinite in the transgressive deposits to more surficial erosion of kaolinite-rich soils during the large-scale sea-level rise. The distribution of clay minerals in shallow marine settings also strongly depends on hydrodynamic factors (differential settling processes; e.g., SINGER 1984, ADATTE & RUMLEY 1984, HALLAM 1986, DECONINCK & STRASSER 1987, CHAMLEY 1989). Kaolinite and illite is especially abundant on internal platform settings, which act as a trap for these minerals. Small-sized particles of smectite, however, are rather transported off-shore to open-marine settings far from their source area (DECONINCK et al. 1985, DECONINCK 1993).

GEYER (1992) observed a systematic decrease of kaolinite from relatively proximal to distal sections (relative to the platform margins) in the Vocontian basin during the Berriasian. Moreover, the diagenetic transformation of the clay minerals increases from west to east in the Vocontian basin due the increasing influence of the Alpine orogenesis (GEYER 1992).

### *High-resolution study*

A high-resolution investigation of clay minerals has been undertaken in small-scale sequence 11 in

**Fig. 8.2** – (facing page) Trends of clay mineral assemblages and stable isotopes ( $\delta^{18}\text{O}$  and  $\delta^{13}\text{C}$ ) in small-scale sequences 11 to 13 of the Chapeau de Gendarme section.



Dorset (Durlston Bay section) and on the Jura platform (Cornaux and Chapeau de Gendarme sections; Fig. 8.3). In the few measurements of the Durlston Bay section, the clay mineral assemblages remain more or less stable. The clay-mineral evolution in the sections of the Jura platform displays a similar pattern (high amounts of illite versus low amounts of interstratified illite-smectite). However, at the top of the Goldberg Formation, a remarkable amount of illite (Chapeau de Gendarme section) has been measured. This may reflect an increased rate of smectite illitization. This observation matches with the general increase of illite in a southeastern direction on the Jura platform.

However, the clay mineral assemblages do not reflect the high-frequency sea-level changes (elementary sequences) detected in this small-scale sequence. The early occurrence of a significant amount of kaolinite in the Marchairuz section may be related to the erosion of kaolinite during the initial transgression and/or to its palaeoposition in a morphological depression (cf. Chap. 6 and 9), in which kaolinite may have been trapped.

The arrival of clay in a depositional basin inevitably lags behind their formation on the continent and may occur a long time after a climate change (THIRY 2000). "Soil formation rates are slow and therefore the resolution of the palaeoclimatic record in marine clay may not be closer than 1 or 2 Ma" (THIRY 2000; p. 201).

### 8.3.2 Carbon and oxygen isotopes

#### *Introduction*

Carbon and oxygen stable isotopes in marginal-marine carbonates have been intensively studied (e.g., ALLEN & MATTHEWS 1982, PLATT 1989, GOLDSTEIN 1991, JOACHIMSKI 1991, 1994, JIMENEZ DE CISNEROS & VERA 1993, PATTERSON & WALTER 1994, RASSER & FENNINGER 2002, D'ARGENIO et al. 2004b). Most of these studies investigated stable isotopes in micrites from mud- to packstone samples ("modified whole rock" samples; PLUNKETT 1997), whereas in this study grainstones have also been measured (whole-rock samples; ALLEN & MATTHEWS 1982). Hence, the absolute values measured in this study may not be comparable to the ones given in the literature (post-depositional diagenetic overprints). However, the obtained trends can be compared.

Marine samples are characterized by relatively enriched  $\delta^{13}\text{C}$  values. Trends to progressively depleted  $\delta^{13}\text{C}$  values from open-marine to continental deposits

are mainly explained by salinity differences (marine versus meteoric water influences; e.g., JOACHIMSKI 1994). The most depleted  $\delta^{13}\text{C}$  values (lower than -4.5 ‰) have been measured in pedogenetically altered samples (e.g., JOACHIMSKI 1994). Such values are explained by equilibration with meteoric solutions, which are enriched in isotopically light soil gases (ALLEN & MATTHEWS 1982, LOHMANN 1988, JOACHIMSKI 1991, 1994). This is probably also a reason why carbon-isotope curves measured in samples of shallow-water settings are more "noisy" than in pelagic successions (D'ARGENIO et al. 2004b).

Oxygen isotope ratios show less facies dependence (JOACHIMSKI 1991, 1994). Relatively homogenous  $\delta^{18}\text{O}$  values are explained by diagenetic equilibration of the carbonates in an open, water-buffered oxygen system (ALLEN & MATTHEWS 1982). Depleted  $^{18}\text{O}$  in carbonates either results from an increase in temperature during burial diagenesis or reflect the interaction with isotopically depleted meteoric waters (LOHMANN 1988). Carbonates may also become enriched in  $^{18}\text{O}$  during subaerial exposure due to the removal of  $^{16}\text{O}$  by surface evaporation at the sediment-air interface (ALLEN & MATTHEWS 1982). Accordingly, relatively low  $\delta^{18}\text{O}$  values (meteoric diagenesis) or high  $\delta^{18}\text{O}$  values (evaporation) in a carbonate succession may point to exposure and are commonly related to sequence boundaries (e.g., PASQUIER 1995, HILLGÄRTNER 1999).

#### *Methods*

For the C and O isotope analysis, the same samples have been used as for the clay minerals. The measurements were carried out by L. Kocsis and Prof. T. Vennemann in the stable isotope laboratory of the University of Lausanne (Switzerland).

The isotopes were measured with a FINNIGAN DELTA PLUS XL mass spectrometer with an attached GASBENCH II and a PAL autosampler. Rock powders were reacted with 100 % phosphoric acid at 90° C. The produced  $\text{CO}_2$  was introduced into the GASBENCH II, which separates  $\text{CO}_2$  from water and other possible impurities. The treated gas was then sent in a "continuous flow" mode into the mass spectrometer. During the continuous flow, 10 measurements are made for each sample. The obtained raw results are regularly corrected in comparison with an internal standard (Carrara Marble: 2.05 ‰  $\delta^{13}\text{C}$  and -1.75 ‰  $\delta^{18}\text{O}$ ) between two samples. The internal standard is calibrated to the international standard NBS19 (1.95 ‰  $\delta^{13}\text{C}$  and -2.20 ‰  $\delta^{18}\text{O}$ ). The mean value of the 10 corrected raw results is calculated and represents the C and O isotope values for a given sample.



### High-resolution study

Carbon and oxygen isotopes of the Goldberg Formation on the Jura platform have well been investigated by JOACHIMSKI (1991, 1994). The peritidal to supratidal deposits of the upper part of the Goldberg Formation are strongly influenced by meteoric waters. The depleted  $\delta^{13}\text{C}$  value in sample 10 of the Chapeau de Gendarme section may be related to strong soil-gas influence (cf. Fig. 8.2). The shift to more positive  $\delta^{13}\text{C}$  values at the top of this section may be related to the increasing marine influence during the transgression. The  $\delta^{13}\text{C}$  values vary more strongly (from -6.00 to +1.20 ‰  $\delta^{13}\text{C}$ ) than the  $\delta^{18}\text{O}$  values (from -4.59 to -1.53 ‰  $\delta^{18}\text{O}$ ). This is a common phenomenon in peritidal to shallow subtidal deposits.

The negative covariance in small-scale sequence 11 in Dorset (Durlston Bay section) and on the Jura platform (Cornaux and Chapeau de Gendarme sections) may be explained by diagenetic alteration by meteoric waters (e.g., enriched in soil gas), temperature, and/or salinity variations (ALLEN & KEITH 1965, ALLEN & MATTHEWS 1982, JOACHIMSKI 1991, 1994; cf. Fig. 8.4). The sequence boundaries at the top and base of small-scale sequence 11 of the sections on the Jura platform are characterized by relatively low  $^{13}\text{C}$  values and relatively high  $\delta^{18}\text{O}$  values (increased influence of meteoric water and evaporation in late highstand to lowstand deposits). The top of the Goldberg Formation in the Cornaux section is characterized by strongly depleted  $\delta^{13}\text{C}$  values, which indicate alteration by pedogenesis. During the initial large-scale transgression, the  $\delta^{13}\text{C}$  values generally increase whereas the  $\delta^{18}\text{O}$  values slightly drop. These trends probably reflect the enhanced influence of marine waters in transgressive to early highstand deposits in small-scale sequence 11. Similar trends are suggested at the sequence boundaries on the scale of the elementary sequences (e.g., sequence boundaries between elementary sequences 4 and 5 in the Cornaux and Chapeau de Gendarme sections). Stable isotopes (mainly  $\delta^{13}\text{C}$  values), therefore, can be used for sequence-stratigraphical investigations even on the scale of elementary sequences.

### 8.3.3 Other sedimentological indications

#### Evaporites

Evaporites have been deposited on the Jura plat-

form during the Early Berriasian (e.g., CAROZZI 1948, MOJON & STRASSER 1987, STRASSER 1988, DÉTRAZ & MOJON 1989, RAMEIL 2005). A thick succession of sabkha deposits have been described from the central Jura platform (Dôle section; RAMEIL 2005; cf. Fig. 8.1). They are capped by a major collapse breccia, which indicates the former existence of massive evaporites between 3<sup>rd</sup>-order sequence boundaries Be2 and Be3 (RAMEIL 2005; cf. Fig. 8.1). Smaller collapse breccias have been found in the Lieu section (RAMEIL 2005). At least seasonally arid conditions are essential to form such evaporite deposits. Layers of windblown quartz silt found in these sabkha deposits also point to arid conditions in the hinterland (RAMEIL 2005).

Major collapse breccias (e.g., Cypris Freestones Member at Durlston Bay and Worbarrow Tout; ENSOM 1985, CLEMENTS 1993) and large gypsum masses (e.g., Soft Cockle Member at Durlston Bay and Worbarrow Tout; ENSOM 1985, CLEMENTS 1993) have been described in the lower part of the Lulworth Formation (Late Tithonian to Early Berriasian) at different locations in the Dorset region. These deposits represent supratidal to intertidal, hypersaline lagoons under a dry and semi-arid Mediterranean climate (WEST 1975).

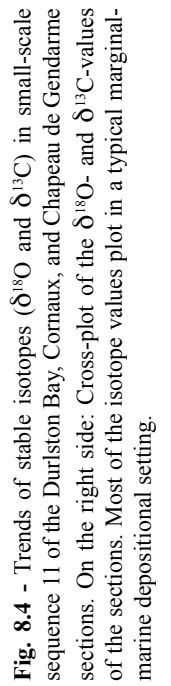
#### (Incipient) palaeosols

Incipient palaeosols and calcretes have been reported from the lower part of the Goldberg Formation on the southwestern Jura platform (Salève section; STRASSER & DAVAUD 1982; cf. Fig. 8.1). DAVAUD et al. (1983) related the occurrence of calcrete horizons on the southwestern border of the Jura platform to emergent areas (barrier-island system) during the Late Tithonian to Early Berriasian. Calcretes associated with desiccation features and evaporite pseudomorphs indicate hot, semi-arid climates, in which the evaporation rate is higher than precipitation (e.g., WRIGHT 1988, 1994, WRIGHT et al. 1988, 1995).

The gray-brownish marl interval in the Yenne section has been interpreted as a relatively well-developed palaeosol with root traces (RAMEIL 2005 and this study; cf. Chap. 4; Fig. 4.30a). According to the dating by MOJON (2002), it lies in the charophyte-ostracode assemblage M1b, indicating an Early Berriasian age (cf. Tab. 4.3).

The Mammal Bed in the Dorset section has been interpreted as a major palaeosol because of its bone and coal content (e.g., MOJON 2002, SCHNYDER 2003, ANDERSON 2004a; cf. Figs. 5.9a and 5.11a). Palaeosols indicate at least seasonally humid conditions that also





allowed for vegetation growth.

### ***Freshwater flora and fauna***

Freshwater flora and fauna (charophyte stems and oögonia, ostracodes, and bivalves; cf. Chap. 2) occur in different intervals of the Goldberg Formation on the Jura platform (e.g., MOJON & STRASSER 1987, STRASSER 1988, MOJON 2002; cf. Fig. 8.1). The amount of freshwater intervals increases significantly towards the top of the Goldberg Formation. Partly, they are associated with evaporite pseudomorphs, which indicates climate with alternating wet and dry periods (cf. Chap. 4). Freshwater intercalations occur up to the top of small-scale sequence 13 in the Pierre Châtel Formation on the Jura platform (Rusel section).

The Marly Freshwater Member in the Dorset sections contains some intervals with freshwater fauna and flora. A drastic increase of freshwater deposits occurs in the Cherty Freshwater Member (e.g., ANDERSON & BASZLEY 1971, MORTER 1984, ANDERSON 1985, HORNE 1995, 2002, MOJON 2002; cf. Chap. 5). In the Worbarrow Tout section, freshwater intervals of the Cherty Freshwater Member contain evaporite pseudomorphs (ENSOM 1985; cf. Fig. 5.11c), indicating dry periods, which punctuate the generally humid climate conditions. In other sections (e.g., Durlston Bay section), charophytes, evaporite pseudomorphs, and freshwater invertebrates occur in close association in the Cherty Freshwater Member (KIELAN-JAWOROWSKA & ENSOM 1992; cf. Fig. 5.6). They may reflect relatively rapid switches of the salinity conditions in this interval probably caused by a seasonal climate (ALLEN 1998). Several freshwater intervals also occur in the Intermarine Member. They are interpreted as lowstand deposits of medium-scale sequences (cf. Chap. 5 and 6).

### ***Karst surfaces***

At the top of the Goldberg Formation and the base of the Pierre Châtel Formation, karst surfaces have been observed in the Rusel and Thoirrette sections (cf. Chap. 4). Major karst surfaces have been reported at the transition from the Pierre Châtel Formation to the Vions Formation (3<sup>rd</sup>-order sequence boundary Be5; cf. PASQUIER 1995, HILLGÄRTNER 1999). They represent a time interval of up to 300 ka in Rusel (cf. Fig. 7.6). For the formation of these surfaces, rainy periods have to be postulated.

### ***Clastic input***

At the transition of the Pierre Châtel Formation to the Vions Formation, which corresponds to 3<sup>rd</sup>-order sequence boundary Be5, quartz input on the Jura platform increases considerably (PASQUIER 1995, HILLGÄRTNER 1999; cf. Fig. 8.1). High contents of quartz and rare associated minerals such as zircon, feldspar, pyroxene, and tourmaline begin to occur on the Jura platform at the base of the Vions Formation (HILLGÄRTNER 1999). The appearance of significant amounts of detrital quartz in the Vions Formation has been explained by fluvial input from emergent source areas to the northeast of the Jura platform (Rhenish-Bohemian Massif) and/or to the northwest (Armorican and/or Central Massif; STEINHAUSER & CHAROLLAIS 1971, BURGER 1982, 1986, BLANC 1996; cf. Fig. 6.14). HILLGÄRTNER (1999) observed a time-transgressive appearance of quartz from proximal to distal positions on the Jura platform at the base of the Vions Formation. He suggested that this diachronous quartz distribution is due to slow transport paths and/or inhomogeneous distribution on the platform. The increase of siliciclastics on the Jura platform may be related to an increase of erosion due to more precipitation in the hinterland (humid climate) and/or uplift of the source area. The remarkable increase of quartz at the transition of small-scale sequences 13 to 14 (corresponding to small-scale sequences 3 to 4 in Fig. 4.9a-b) in the Rusel section may be related to a nearby fluvial source and/or to a relatively proximal position of this section on the platform. The disappearance of significant amounts of quartz in the Rusel section until the return in the Vions Formation may be due to switching of deltas, probably caused by differential subsidence.

In Dorset, first peaks of significant amounts of siliciclastics have been observed in small-scale sequence 17 in the Durlston Bay section (cf. Fig. 5.9e-f) and in small-scale sequence 19 in the Worbarrow Tout section (cf. Fig. 5.11e). SLADEN (1983) assumed that the source area of the clay minerals in the Weald sub-basin, which has been separated by a morphological high from the Channel sub-basin, was situated to the north (London-Brabant Massif). For the Channel sub-basin (Dorset region; cf. Fig. 5.2), the source area of the siliciclastics probably was located to the northwest (Cornubian-Welsh Massif) and/or to the southwest (Armorican Massif; cf. Fig. 5.2). The deviation in the timing of siliciclastic input on the Jura platform and in the Dorset region is in the range of one small-scale sequence (100 ka). The timing of the first occurrence of

siliciclastics on the Jura platform cannot be adequately determined because of the hiatus at the transition from the Pierre Châtel Formation to the Vions Formation (karst surface at 3<sup>rd</sup>-order sequence boundary Be5; cf. Figs. 6.13 and 7.6). Probably, siliciclastics have already been deposited in significant amounts during the large-scale maximum-flooding interval (around small-scale sequence 19), as it has been observed in the Crêt de l'Anneau section of the Jura platform (PASQUIER 1995, HILLGÄRTNER 1999).

The rate of siliciclastic input depends on climate, lithology in the catchment area, relief, and distance between the source area and the depositional basin (LEEDER et al. 1998). The elevated amount of siliciclastics in Late Berriasian times has been interpreted as an indication of humid climate conditions (e.g., HALLAM et al. 1991, ALLEN 1998, HILLGÄRTNER 1999). The significant increase of siliciclastics in Dorset and on the Jura platform around 3<sup>rd</sup>-order sequence boundary Be5 can therefore be related to elevated erosion rates in the source area due to an increase of precipitation. In addition, low relative sea level at the sequence boundary may have facilitated the erosion and the transport towards these marginal-marine settings.

## 8.4 Long-term changes

### 8.4.1 Palaeotectonic evolution

At the transition of the Late Jurassic to Early Cretaceous, a major tectonic uplift phase caused by thermal doming controlled the long-term tectonic regime across Europe. This is documented by widespread erosional unconformities in northern Europe during the Berriasian (Volgian to Ryazanian; RAWSON & RILEY 1982, RUFFELL 1995). In terms of sequence stratigraphy, the Berriasian successions developed at the end of the 1<sup>st</sup>-order major regression that began in the Late Jurassic (Late Kimmeridgian), before the long term, 1<sup>st</sup>-order Early Cretaceous transgression (Late Berriasian; JACQUIN et al. 1998). A 2<sup>nd</sup>-order sequence (2<sup>nd</sup>-order cycle 10 according to JACQUIN et al. 1998) is superimposed on this 1<sup>st</sup>-order sequence. The investigated interval (Middle to Late Berriasian) lies between the boundaries of this 2<sup>nd</sup>-order sequence, i.e. between the transition of the Jurassic-Cretaceous boundary and the Late Cimmerian Unconformity of the Late Berriasian (e.g., ZIEGLER 1988, RUSCIADELLI 1999, GUILLOCHEAU et al. 2000). The Late Cimmerian

Unconformity has first been identified by seismic investigations in the North Sea basin. It marks a lithological break from organic-rich "hot" shales to "warm" shales with a reduced organic-matter content (e.g., RAWSON & RILEY 1982). The Jurassic-Cretaceous boundary is characterized by the deposition of continental to marginal-marine carbonates in different onshore settings in Europe (Purbeckian facies *sensu anglico*; around 3<sup>rd</sup>-order sequence boundaries Be1 to Be4). It includes the Goldberg Formation on the Jura platform and the upper parts of the Lulworth Formation in Dorset. The Late Cimmerian Unconformity lies within the Wealden facies (*sensu anglico*; around 3<sup>rd</sup>-order sequence boundary Be7), which consists mainly of continental to marginal-marine siliciclastics (e.g., DÉTRAZ et al. 1987, ALLEN & WIMBLEDON 1991, STRAUSS et al. 1993, HILLGÄRTNER 1999).

SLADEN (1983) and SLADEN & BATTEN (1984) related the increase of siliciclastics in the Wealden facies of the Weald sub-basin to enhanced weathering in the source area of the London-Brabant massif due to local uplift (increase of relief), in combination with a climate change to more humid conditions. However, the importance of tectonic uplift should not be overestimated because there is no significant increase of illite in the Lulworth and Durlston Bay sections. On the other hand, the kaolinite increase in the Late Berriasian is a widespread climate signal, which has been recorded in numerous sections in Europe (SCHNYDER et al. 2006).

The large-scale regression during the Late Tithonian to Late Berriasian observed in West Europe has been related to complex, large-scale plate tectonic movements (opening of the proto-North Atlantic and the Bay of Biscay; e.g., LEMOINE et al. 1986, JACQUIN et al. 1998, THIERRY & BARRIER 2000; Guillocheau, pers. comm.). The reconstruction of plate geometry and plate kinematics is not straightforward for the Berriasian and has been interpreted by different geodynamic models (e.g., ZIEGLER 1988, DORÉ 1991, WORTMANN et al. 2001, STAMPFLI et al. 2002, SCHETTINO & SCOTese 2002, GOLONKA 2004, CAVAZZA et al. 2004). Moreover, the timing and the expression of long-term sequences may differ between depositional basins because of the imprint of local tectonics (AURELL et al. 2003). Abrupt changes in subsidence rate and block faulting accentuated or attenuated the effects of sea-level changes in the sedimentary record. Differential uplift probably was responsible for the hiatus around 3<sup>rd</sup>-order sequence boundary Be4 on the Jura platform (e.g., STRASSER & HILLGÄRTNER 1998, HILLGÄRTNER 1999).

### 8.4.2 Palaeoceanographic evolution

The Central Atlantic-Western Tethys basin of the Early Cretaceous may have been similar to the modern Pacific Ocean, with a large marginal sea (HAY 1995). In comparison with the modern ocean, the term Tethyan refers to the region between the subtropical oceanic fronts whereas the terms Boreal and Austral indicate regions north and south of the subtropical oceanic fronts (for description of oceanic fronts refer to HAY 2002).

The Greenland-Norwegian Seaway probably was the deepest part of a transcontinental passage between the Laurentian Shield in the west and the Baltic Shield in east where significant exchange of Boreal and Tethyan water masses occurred between high-latitudes (Arctic basin) and low-latitudes (Central Atlantic and Tethys Ocean) during the Berriasian (cf. Fig. 8.5). This seaway has probably been bounded at both ends by relatively shallow morphological swells (MUTTERLOSE et al. 2003). During the Late Jurassic to Early Cretaceous, the southern end of the Greenland-Norwegian Seaway was connected to the Tethyan region across Central Europe via shallow epicontinental seaways (e.g., MUTTERLOSE & BORNEMANN 2002, MUTTERLOSE et al. 2003) following rift graben systems (e.g., ZIEGLER 1988). MUTTERLOSE et al. (2003) assumed that “with its curving path the passage from the Tethys to the Arctic was about 5000 km long” (p. 17). Other seaways probably connecting the Arctic basin with the Tethyan ocean have been postulated in East Europe (Carpathian seaway, Poland; e.g., MAREK & RACZYŃSKA 1973, MUTTERLOSE 1992 and the Pechorian seaway, Russia; BARABOSHKIN 2002, MUTTERLOSE et al. 2003). However, it has been controversially discussed whether these seaways connected high-latitudinal with low-latitudinal floral and faunal realms during the Berriasian (e.g., MUTTERLOSE 1992).

ADATTE et al. (1996) related the massive influx of Tethyan microfossils (calpionellids) and ammonites as well as changes in sedimentological and geochemical parameters (clay mineral assemblages and stable isotope values) of sections in northeastern and central Mexico to a global sea-level rise during the upper calpionellid zone B (Early Berriasian), which opened a seaway between the Central Atlantic and the Western Tethys ocean.

Moreover, BORNEMANN et al. (2003) assumed that around the Jurassic-Cretaceous boundary a marine connection between the Central Atlantic and the Pacific Ocean (Panama seaway) has been formed, which caused a circum-equatorial current system. This

current system may have transported warm Central Atlantic water westwards into the Pacific.

Information about ocean connections (e.g., presence/absence of suitable migration routes) and hydrologic parameters (e.g., temperature, salinity, and oxygen level) has mainly been obtained from faunal and floral distribution in palaeoceanographical reconstructions (e.g., MUTTERLOSE et al. 2003). The Late Tithonian to Late Valanginian is marked by a distinctive provincialism of different marine biota. The global fall in sea level (1<sup>st</sup>-order regression) at the Jurassic-Cretaceous boundary resulted in an almost complete separation of Boreal from Tethyan marine biota (e.g., RUFFELL & RAWSON 1994). Therefore, endemic biota are typical for this time interval, caused by the development of restricted, shallow epicontinental seas, which were separated by morphological swells (cf. Fig. 8.5).

The Berriasian palaeobiogeographic patterns are well documented by various groups of organisms, in particular by ammonites (e.g., CASEY 1973, MUTTERLOSE 1992, HOEDEMAEKER 1995, 2003, MELINTE 2002, BARABOSHKIN 1999, 2002, ZAKHAROV & ROGOV 2003, CECCA et al. 2005), belemnites (e.g., MUTTERLOSE et al. 1983, MUTTERLOSE 1992, PRICE et al. 2000), calcareous nannofossils (e.g., MUTTERLOSE 1992, STREET & BROWN 2000, MUTTERLOSE & KESSELS 2000, MELINTE 2002, RUFFELL et al. 2002, BORNEMANN et al. 2003), calpionellids (e.g., ADATTE et al. 1996, REMANE 1998), and ostracodes (e.g., SCHUDACK & SCHUDACK 1995, SCHUDACK 1996).

#### *Ammonites*

The Berriasian of NW Europe and Central Europe has been dominated by Boreal ammonite species (e.g., CASEY 1973, MUTTERLOSE 1992). Sections in the Russian and adjacent basins are dominated by Boreal ammonites with a high rate of endemism during the Early Berriasian. During the Middle to Late Berriasian (Late Occitanica to Late Boissieri ammonite zones), the successions in the Russian basin are characterized by an increasing amount of Tethyan ammonites relative to Boreal species (BARABOSHKIN 1999, 2002, ZAKHAROV & ROGOV 2003, CECCA et al. 2005). The Tethyan ammonites migrated from the Polish basin via the Belorussia seaway and from the Mangyshlak area via the Caspian seaway to the Russian basin (BARABOSHKIN 1999). Ammonite distributions are mainly controlled by their mode of life and the existence of warm or cool palaeocurrents (BARABOSHKIN 1999, ZAKHAROV

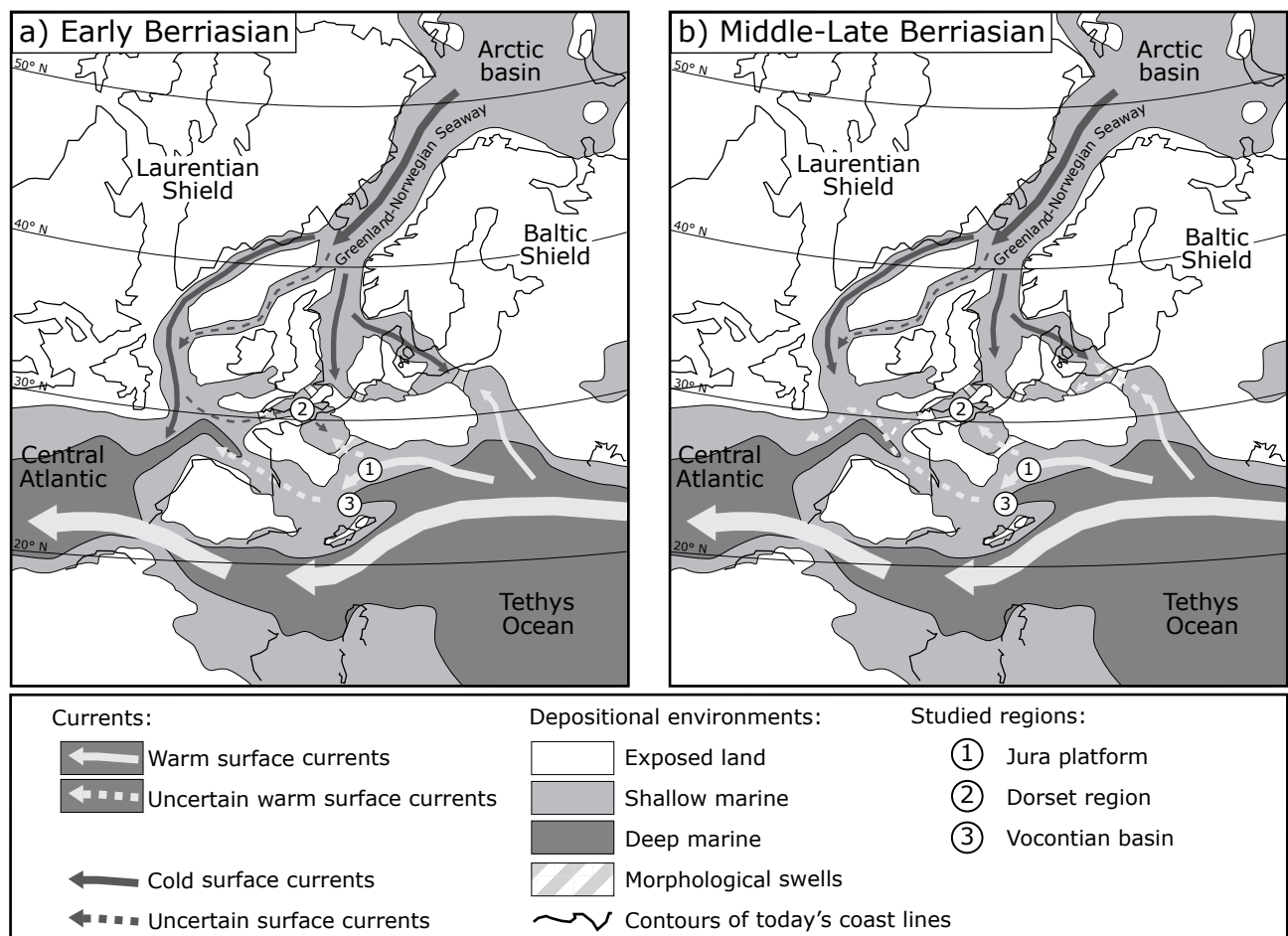


**Fig. 8.5** - Palaeogeographic and palaeoceanographic reconstructions for (a) Early Berriasian and (b) Middle-Late Berriasian (modified from ABBINK et al. 2001). With changing sea level and/or current patterns, the studied regions can be either under the influence of warm Tethyan currents or cold Boreal currents. The palaeogeographic map is based on THIERRY & BARRIER (2000; modified for the Berriasian from ALLEN 1963, RAWSON & RILEY 1982, CURNELLE & DUBOIS 1986, KARNER 1987, ZIEGLER 1988, ARNAUD 1988, MUTTERLOSE 1992, STRAUSS et al. 1993, GUILLOCHEAU et al. 2000, MUTTERLOSE & KESSELS 2000, AURELL et al. 2003).

& ROGOV 2003). HOEDEMAEKER (1995) analysed the diversity of ammonite species of the Early Cretaceous in South European sections. He observed major faunal turnovers between and partly within certain ammonite biozones. In the Berriasian, two major faunal turnovers have been identified by HOEDEMAEKER (1995, 2003), which correspond to 3<sup>rd</sup>-order sequence boundary Be3 (Basal Cretaceous Unconformity; cf. Chap. 6) and to 3<sup>rd</sup>-order sequence boundary Be7 (Late Cimmerian Unconformity). He related these turnovers to eustatic sea-level falls, which caused contractions of ammonite habitats. HOEDEMAEKER (1995) suggested that reductions of ammonite biotopes enhanced the selection pressure among them. Similar interpretations have been made by CECCA et al. (2005), based on changes in the distribution of taxonomic diversity for several Late Jurassic and Early Cretaceous intervals.

### *Calcareous nannofossils*

Dispersion of calcareous nannofossils is mainly caused by currents. The biogeography of living coccolithophores is controlled by abiotic factors such as nutrients, temperature, and surface currents (e.g., ROTH 1989, MUTTERLOSE 1992). The nannofossils assemblages of the Greenland-Norwegian Seaway and the Arctic basin indicate cool polar conditions for the Berriasian and Valanginian (MUTTERLOSE & KESSELS 2000). Boreal nannofloras have been found in NW Europe until Berriasian times, implying cold surface waters from high latitudes. Accordingly, no significant connections of the Boreal with the Tethyan realms are indicated by calcareous nannofossil assemblages during the Berriasian in NW Europe (MUTTERLOSE 1992, MUTTERLOSE & KESSELS 2000). Based on samp-

les from the Central Atlantic, BORNEMANN et al. (2003) assumed that relatively low atmospheric  $p\text{CO}_2$  during the Late Tithonian promoted the evolution of calcifying marine organisms (like calcareous nannofossils and calpionellids). Nannofossil carbonate accumulation rates increased during the Berriasian, which probably reflects a shift to higher carbonate productivity in open-marine settings. BORNEMANN et al. (2003) concluded that “the deep sea is thought to have become an important sink for  $\text{CaCO}_3$  from the latest Jurassic onwards” (p. 222).

### *Ostracodes*

Detailed analyses of spatial distributions of marine-brackish and non-marine ostracodes in NW and Central Europe during the Late Jurassic (Oxfordian) to the Early Cretaceous (Berriasian) have been published by SCHUDACK & SCHUDACK (1995). The marine-brackish ostracodes show a separation into three subprovinces in NW and Central Europe during the Berriasian, which reflects a high degree of endemism. However, the non-marine ostracodes are widespread in NW and Central Europe due to their optimal dispersal strategies (mainly the Cypridaceae; cf. Chap. 5). SCHUDACK (1999) analysed the benthonic, shallow-marine ostracode genus *Cytherelloidea*, which is used as an indicator for relatively warm water temperatures. A general shift of the northern boundary of occurrence of this thermophilic genus towards the south (French and Swiss Jura) during the Oxfordian to the Berriasian has been observed and interpreted as an increased influx of cold Boreal surface waters from the north into NW and Central Europe (SCHUDACK 1999).

In general, sea-level lowstands favor the development of endemism of marine organisms due to geographic isolations, whereas sea-level highstands allow increasing exchange and promote more cosmopolitan assemblages (e.g., HALLAM 1994, BRETT 1998, HOEDEMAEKER 1995, 2003, MUTTERLOSE et al. 2003). Because of the eustatic sea-level lowstand during the Late Tithonian to Early Berriasian, relatively deep marine connections between the Boreal and Tethyan faunal realms across the epicontinental seas in Europe were absent.

Moreover, the partial separation of the Tethyan and Boreal realms during sea-level lowstands in the Berriasian (Ryazanian) may have restricted ocean circulation (MUTTERLOSE & KESSELS 2000, MUTTERLOSE et al. 2003) and potentially enhanced discrete episodes

of ocean stratification. This promoted the deposition and preservation of organic carbon-rich sediments in terrestrial and/or shallow-marine settings in high-latitude areas (e.g., Lower Saxony Basin; WIESNER 1983; North Sea basin; RAWSON & RILEY 1982, ABBINK et al. 2001, Greenland-Norwegian Seaway; SMELRØR et al. 2001, SWIENTEK 2002, LIPINSKI et al. 2003, MUTTERLOSE et al. 2003, Barents Sea; LIPINSKI et al. 2003, LANGROCK et al. 2003).

MUTTERLOSE et al. (2003) assumed that the meteorite impact in the Barents Sea (Mjølner impact structure) may have changed the local palaeogeography and -oceanography by further deepening the passage from the Greenland-Norwegian Seaway to the Arctic basin, which enabled an increased water-mass exchange. The Mjølner meteorite impacted the Barents Sea close to the Volgian-Ryazanian boundary (DYPVIK et al. 1996, LANGROCK et al. 2003). DECONINCK et al. (2000) and SCHNYDER et al. (2005b) related an erosional conglomerate in Berriasian deposits of the Boulonnais (Grès des Oies Formation; northern France) to a tsunami event, which may have been triggered by an earthquake, a volcanic eruption, a giant submarine slide, or an impact of an extraterrestrial bolide. DECONINCK et al. (2000) consider the Cinder Member in Dorset as a possible time-equivalent, which would have been deposited because of the destruction of a morphological barrier by this tsunami event caused by the Mjølner impact. Uncertainties of the stratigraphic correlations and the absence of reliable biostratigraphical markers, however, limit this interpretation. Moreover, IRVINE et al. (2004) measured iridium concentrations of samples from the Grès des Oies Formation in Boulonnais and the Cinder Member in Dorset, which do not display elevated values. They conclude that there is no direct chemical evidence in these deposits for the Mjølner meteorite impact. SCHNYDER et al. (2005b) place the tsunami deposits at the Jurassic-Cretaceous boundary. They favor the assumption that these sediments are the result of an earthquake event mainly based on statistical arguments. It is worth noting that UNDERHILL (2002) relates the rapid death and unusual preservation of the Early Berriasian conifer forest on the Isle of Purbeck, which was covered by stromatolites (fossil forest; e.g., WEST 1975, FRANCIS 1983), to a rapid submergence caused by a co-seismic activity of the Purbeck Fault system (cf. Chap. 5). Because of the lack of precise dating, the relationship between the tsunami deposits in the Boulonnais region and the submerged fossil forest interval in the Dorset region remains speculative. It underlines, however, that the Purbeck Fault system probably caused earthquakes of

Time	Climate parameters	ALLEN (1998) southern England	ABBINK et al. (2001) southern North Sea
Middle-Late Berriasian	average annual temperature	> 10-25° C	25°C
	average annual precipitation	1250-1500 mm	~ 1750 mm
	climate	equable humid periods with low climatic variability; warm temperate climate	wet (sub)tropical
Early Berriasian	average annual temperature	> 10-25° C	27°C
	average annual precipitation	> 500 mm	< 40 mm
	climate	annual-seasonal with hot, dry summers and warm, wet winters; Mediterranean climate	arid, Mediterranean climate

**Tab. 8.1** – Different estimations of climate parameters and their palaeoclimatic interpretations for southern England (ALLEN 1998) and for the southern North Sea (ABBINK et al. 2001) for the Berriasian.

serious, regional consequences.

### 8.4.3 Palaeoclimatic evolution

From the Early Kimmeridgian to the Early Valanginian (between 155 to 135 Ma according to GRADSTEIN et al. 1995), Central Europe drifted approximately 5° northwards. Accordingly, the long-term climate change during the Middle Berriasian cannot be explained by this northward drift alone according to SCHNYDER (2003). He argues, that a similar long-term climate change has been described from the Russian platform, which did not drift northward. However, RUFFELL et al. (2002) mentioned a diachroneity of clay-mineral changes between sections of northern Europe and of the Russian platform during the Berriasian, which probably point to rather regional significance of changes in clay mineral assemblages. The northward drift of Central Europe, therefore, may partly explain the long-term climate change observed in Central and NW Europe during the Middle Berriasian.

ALLEN (1998) concluded that “the most fundamental change [in southern England] occurred during mid-Purbeck (mid-Berriasian), when the style of weathering altered (the “kaolinite”-event) and the prevalent winds may have switched from winter easterlies and summer westerlies to predominant westerlies” (p. 227). Moreover, he stated that the humid belt moved up from the south (Channel sub-basin) to the north (Weald sub-basin) during the deposition of the Intermarine Member. In general, it has been proposed that a change from a semi-arid Mediterranean to a semi-humid (temperate?) climate took place during the Middle Berriasian in

NW and Central Europe (ALLEN 1998, ABBINK et al. 2001, SCHNYDER 2003, SCHNYDER et al. 2006). The insect assemblages collected from the Lulworth and Durlston Formations (Durlston Bay and Worbarrow Tout sections) indicate a Mediterranean climate during the Berriasian in the Dorset region (CORAM & JARZEMBOWSKI 2002; cf. Fig. 5.6). A comparison of some climate parameters for southern England (ALLEN 1998) and the southern North Sea basin (ABBINK et al. 2001) and their palaeoclimatic interpretations are given in Tab. 8.1. Because both regions are located at approximately the same palaeolatitude (cf. Fig. 8.5), the differences in the estimations may be due to local climate-relevant factors (e.g., rain-shadow behind mountains, topography and extension of catchment areas).

A similar climate change is displayed in the sediments of the Jura platform (cf. Fig. 8.1). According to the sequence-stratigraphical correlation of this study, the increase of kaolinite is earlier on the Jura platform than in the Dorset region, which would underline the shift of humid conditions from south to north. It has been postulated that changing flow direction of relatively cold Boreal surface waters from the polar regions and warm, saline Tethyan bottom water through the Greenland-Norwegian Seaway to the south influenced the regional climate of at least NW and Central Europe during Early Kimmeridgian to Early Berriasian times (estuarine circulation model; e.g., SCHUDACK 1999, ABBINK et al. 2001, SWIENTEK 2002; cf. Fig. 8.5a). The cold Boreal surface waters in NW and Central Europe reduced atmospheric moisture transport from the sea to the continents (SCHUDACK 1999, ABBINK et al. 2001). This is explained by a decrease of evaporation over

cold surface waters and by the fact that cold air holds less atmospheric moisture.

The influx of cold surface currents into the European archipelago decreased during the Middle to Late Berriasian (ABBINK et al. 2001), probably due to the closing of parts of the Greenland-Norwegian seaway (DORÉ 1991). Consequently, the European epicontinental seas were partly flooded by warm Tethyan waters, which led to a climate shift with more humid conditions (ABBINK et al. 2001, MUTTERLOSE et al. 2003; cf. Fig. 8.5b).

The long-term climate change during the Berriasian in NW and Central Europe, therefore, is assumed to have primary been controlled by surface currents and their temperature. The dominance of Boreal cold or Tethyan warm surface waters may be related to the opening and closing of seaways due to tectonic movements. A key role in the climate evolution during the Berriasian plays the Greenland-Norwegian Seaway, which steered the exchange of cold Boreal and warm Tethyan water masses in NW and Central Europe. The climate in Europe, therefore, mainly depended on the one hand on the prevailing ocean current system (Boreal and/or Tethyan surface waters) and on the other hand on the proximity to the proto-North Atlantic (e.g., HALLAM 1986, HALLAM et al. 1991, RUFFELL & RAWSON 1994, ALLEN 1998).

An opposite climate trend has been reported from northeastern and central Mexico by ADATTE et al. (1996). The occurrence of kaolinite indicates warm, humid conditions during the Late Tithonian to Early Berriasian in this region. An increase of chlorite relative to kaolinite points to more cold and dry conditions in the source area during the Middle to Late Berriasian. Accordingly, the long-term climate change observed in the investigated areas is of regional extent and cannot be extrapolated on a global scale.

## 8.5 Short-term palaeoclimate and environmental changes

Short-term palaeoclimate and environmental changes in the Milankovitch-frequency band (cf. Chap. 7) were superimposed on the long-term trends described above. In marginal-marine environments (e.g., Dorset region and Jura platform), sea-level changes are the main mechanism controlling the formation of depositional sequences and environmental changes. The high-frequency, low-amplitude sea-level fluctuations were probably mainly caused by thermal expansion of the ocean water in tune with insolation

changes (READ 1995; cf. Chap. 7).

According to the cyclostratigraphic model of PERLMUTTER & MATTHEWS (1989, 1992), the boundaries of the atmospheric circulation cells (Hadley, Ferrel, and Polar cells) move equatorward during insolation minima and poleward during insolation maxima. Temperature and the positions of the atmospheric circulation cells control the latitudinal distribution of rainfall and evaporation.

Humid belts are located in atmospheric upwelling zones whereas dry to arid conditions prevail near atmospheric downwelling zones. Azonal parameters (e.g., land-sea distribution, topography), however, strongly modify the model of zonal atmospheric circulation cells (PERLMUTTER & MATTHEWS 1992). The investigated regions, which were located between the palaeolatitudes of about 25 to 35° N during the Berriasian (cf. Chap. 1), were affected by the zone of atmospheric downwelling between the Hadley and Ferrel cells. Applying this model, the investigated regions would have been located in the subhumid climate belt (humid the in Dorset region) during the insolation minima and in the dry climate belt during climate maximum (cf. Fig. 8.6).

As discussed in Chap. 3, clay minerals in marginal-marine settings are mainly deposited during falling relative sea level (lowstand deposits and sequence boundary intervals) or during rising relative sea level (transgressive deposits and maximum-flooding intervals). Clays in the marginal-marine settings may have been transported by rivers from the hinterland over long distances and/or they have been eroded and reworked from the nearby coastal area. In Dorset, marly intervals have generally been interpreted as late highstand to possibly lowstand deposits of elementary and small-scale sequences. This interpretation implies a clay input during falling relative sea level (cf. Chap. 5). It has been assumed that the source areas for clay minerals were located to the northwest (Cornubian-Welsh Massif) and/or to the southeast (Armorican Massif) of the Channel sub-basin, corresponding more or less to the same palaeolatitude as the Dorset region. According to the cyclostratigraphic model of PERLMUTTER & MATTHEWS (1989, 1992), subhumid to humid conditions prevailed during insolation minima at this palaeolatitude (cf. Fig. 8.6). This would support the interpretation that during falling relative sea level, which corresponds to time intervals of insolation minimum in the Milankovitch-frequency band, rather marly intervals have been deposited in the sections of the Dorset region.

Yet, the interpretation of clay mineral intervals in the sections on the Jura platform based on the



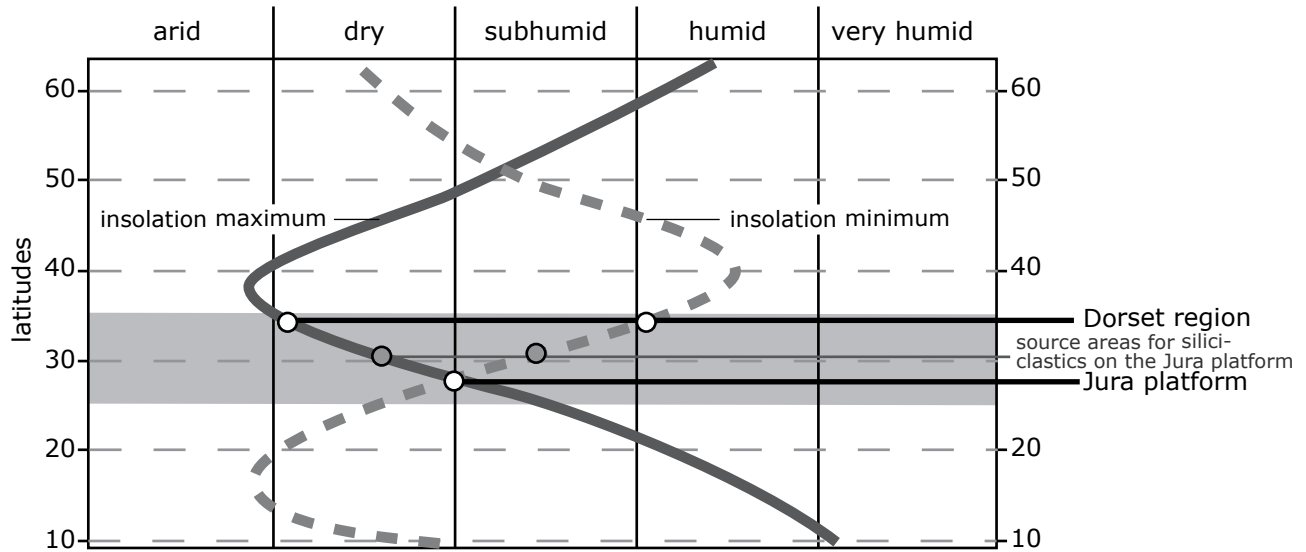


**Fig. 8.6** - Modified cyclostratigraphic model of PERLMUTTER & MATTHEWS (1989, 1992) applied to the Dorset region and Jura platform (palaeolatitudes in the range of 25° to 35° N). The Dorset region undergoes a succession of dry (insolation maxima) to humid conditions (insolation minima). The climate conditions on the Jura platform are dry during insolation maxima and subhumid during insolation minima. The source areas for siliciclastics on the Jura platform, however, was situated in a dry climate during insolation maxima and in a subhumid climate during insolation minima.

cyclostratigraphic model is not without difficulties. Marly intervals in these sections have been interpreted as sequence-boundary or maximum-flooding intervals of elementary and small-scale sequences. The Jura platform was situated at a palaeolatitude where dry to subhumid conditions prevailed during insolation minima and maxima according to the cyclostratigraphic model (cf. Fig. 8.6). During insolation minima (sequence-boundary intervals), the clay mineral content in the sections on the Jura platform was probably elevated as best indicated by the most proximal section of Rusel (cf. Fig. 4.9a-b). This may be explained by increased erosion of clay minerals in the source areas, which were located to the northeast (Rhenish-Bohemian Massif) and/or to the northwest (Armorican and/or Central Massif) of the Jura platform (cf. Fig. 4.3). Accordingly, during insolation minima, subhumid climate conditions prevailed in the source area north of the Jura platform, triggering the erosion of clay minerals, which then have been transported to the south by rivers and entered the Jura platform. Climate signals on the short term, therefore, may have been transferred from the north to the south. However, local factors in the source areas (e.g., slope, elevation, vegetation cover, rock types) and in the marginal-marine depositional settings (e.g., platform morphology, distance to river deltas, current patterns) may have complicated the distribution patterns.

PITTET & STRASSER (1998b) interpreted the input of

siliciclastics in Middle Oxfordian deposits of different palaeolatitudes at the scale of 100-ka cycles to changes in the extension of the Hadley and Ferrel cells due to orbital forcing. They assumed that tectonics have a major control on the availability of siliciclastics, whereas climatic conditions define at which moment they are transported to marine environments. A similar interpretation has been made by HUG (2003) based on Late Oxfordian deposits of the Jura platform.

The relative low  $\delta^{13}\text{C}$  values at the elementary sequence boundaries of small-scale sequence 11 (Fig. 8.4) probably point to pedogenetic alteration processes on the Jura platform. This implies that during sea-level lowstand (minimum insolation) coastal areas have at least partly been covered by vegetation, which indicates subhumid climate conditions.

ANDERSON & BAZLEY (1971) suggested that the ostracode faunicycles of the Dorset region (cf. Chap. 5) may reflect humid-dry climate cycles caused by Milankovitch-orbital forcing. Later, ANDERSON (2004a) used these faunicycles to interpret the Durlston Bay section in terms of cyclostratigraphy (see Chap. 7 for discussion). HORNE (2002) considers the dominance of C-phase ostracodes (cf. Chap. 5) as indicator for ephemeral water-bodies in a more arid climate whereas S-phase ostracodes imply in permanent water during humid climate conditions. However, he points out that temporary and permanent water bodies may exist close together and on a variety of time scales.

In deep-marine basins (e.g., Vocontian basin) humid-dry climate cycles may have influenced the continental runoff of clay minerals to the basin and/or controlled the periodic productivity changes of the calcareous plankton leading to the deposition of limestone-marl couplets (e.g., EINSELE & RICKEN 1991a, PASQUIER & STRASSER 1997; cf. Chap. 6).

The stacking pattern and chemical variations in Berriasian sediments of the Greenland-Norway Seaway have been interpreted to reflect orbital signals in the Milankovitch-frequency band (eccentricity, ob-

liquity, and precession cycles). Orbital forcing mainly controlled the fluctuations in the clastic influx to the Greenland-Norway Seaway and variations in carbonate and organic matter production (SWIENTEK 2002, LIPINSKI et al. 2003, MUTTERLOSE et al. 2003). SWENTIEK (2002) concluded that the obliquity modulated the marine anoxic conditions in the Greenland-Norway Seaway, whereas precession and eccentricity forced the terrestrial sediment and nutrient supply and the freshwater input to this seaway by changing the rainfall pattern in the source areas.

\*\*\*\*\*

## 9 - HISTORY OF A TRANSGRESSION

---

### 9.1 Introduction

As shown in the preceding chapters, the evolution of the Middle Berriasian transgression is complex in time and space. This chapter tries to illustrate the temporal and spatial evolution of the investigated palaeoenvironments (Dorset region, Jura platform, and Vocontian basin) by combining the sequence-stratigraphical (Chap. 6) with the cyclostratigraphical interpretations (Chap. 7). The long-term trends of the investigated regions between sequence-boundary intervals Be4 and Be5 will first be discussed and illustrated. The initial transgression will then be analysed in time steps of 100 ka and 20 ka. Actually, this chapter presents a translation of the time-space diagram (cf. Fig. 7.4) into palaeogeographic maps in a chronological order (cf. Figs. 9.3 and 9.4). This synthesis is based on the studied sections and on data derived from the literature (Helvetic shelf). It has to be kept in mind, however, that the palaeogeographic maps are strongly simplified and only hypothetical representations of the investigated Middle Berriasian environments. Nevertheless, they add in visualizing the dynamic evolution of the investigated regions.

### 9.2 Long-term evolution

The cross-sections shown in Fig. 9.2a-d illustrate the evolution of the Dorset region, the Jura platform, and the Vocontian basin in four time-intervals (Fig. 9.1). The orientation of the cross-sections is indicated on the palaeogeographic map in Fig. 9.1. They give an overview of the long-term interaction between tectonic (subsidence and/or uplift) and eustasy between the 3<sup>rd</sup>-order sequence-boundary intervals Be4 and Be5 (large-scale sequence).

#### 9.2.1 Long-term lowstand deposits (Fig. 9.2a)

During the long-term lowstand associated to sequence boundary Be4, mainly continental to intertidal deposits of the Cherty Freshwater Member (upper Lulworth Formation) have been deposited in the Dorset region (cf. Chap. 5). The “shell beaches”, which have been interpreted as intertidal to subtidal deposits, represent marine incursions. The tectonic evolution of the Channel sub-basin (Portland-Wight depocentre), where the investigated sections of the Dorset region are located, is mainly controlled by extensional tectonics along the Purbeck Fault system (KARNER et al. 1987, UNDERHILL 2002; cf. Figs. 5.3 and 5.4).

Lowstand deposits on the Jura platform are strongly reduced and/or absent due to erosion and non-deposition during the Early to Middle Berriasian. The top of the Goldberg Formation is characterized by continental to intertidal deposits (cf. Chap. 4). The proximity of marine environments, however, is displayed by the occurrence of marine components in some sections (cf. Fig. 6.4). The dating by charophyte-ostracode assemblages (MOJON 2002) reveals that the top of the Goldberg Formation represents different time intervals (M1b to M4; cf. Fig. 6.4). This is probably due to the development of an important platform morphology due to recurrent emersion intervals during the Early to Middle Berriasian, and to differential subsidence (block rotation combined with uplift; DÉTRAZ & STEINHAUSER 1988, STRASSER 1988, DÉTRAZ & MOJON 1989, PASQUIER 1995). These factors controlled the evolution of the complex pattern of morphological highs and depressions on the platform. A reef complex and shallow lagoons formed during the Late Tithonian to early Middle Berriasian on parts of the southern Jura platform, but emerged and were brecciated during sea-level lowstand in the Early to

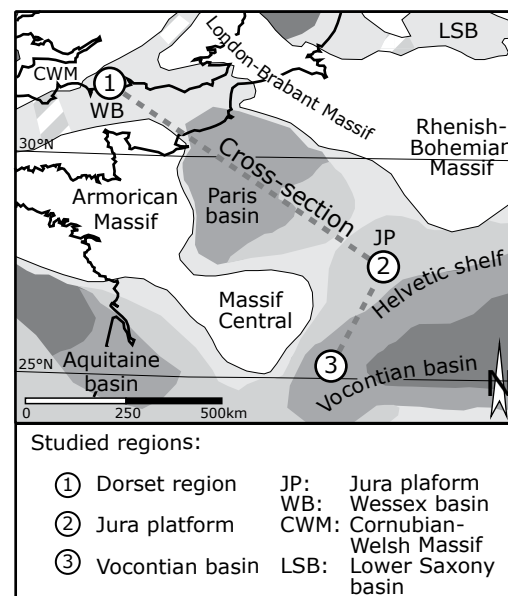
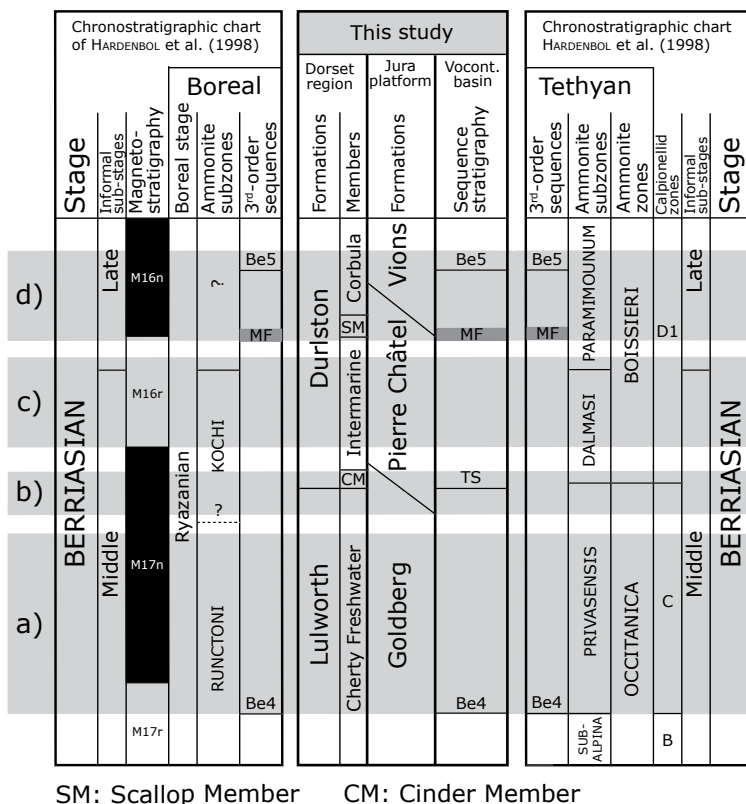


**Fig. 9.1** - Approximate timing and orientation of the cross-section intervals illustrated in Fig. 9.2a-d. For legend of the depositional environments refer to Fig. 6.14.

early Middle Berriasian times (reef of Echaillon; DÉTRAZ & STEINHAUSER 1988, DÉTRAZ & MOJON 1989). The growth of the reef complex during the Late Tithonian to Early Middle Berriasian formed a relatively steep slope (rim) at the transition from the southern Jura platform to the western Helvetic shelf (DÉTRAZ & STEINHAUSER 1988). The palaeofault of Isère delimited the southern extension of the Jura platform (ARNAUD 1988; cf. Fig. 4.3).

The lowstand deposits in the Vocontian basin (e.g., Montclus section) mainly consists of relatively thick limestone beds (STROHMENGER & STRASSER 1993, PASQUIER 1995, HILLGÄRTNER 1999; cf. Chap. 6). This has been explained by an increased planktonic carbonate productivity in the basin due to elevated nutrient input from the continents and import of carbonate mud from the surrounding exposed carbonate platforms during sea-level lowstand (e.g., PASQUIER & STRASSER 1997, HILLGÄRTNER 1999). In some sections, lowstand deposits are characterized by mass-flow deposits (STROHMENGER & STRASSER 1993, PASQUIER 1995, BLANC & MOJON 1996, HILLGÄRTNER 1999). Mass-flow deposits of the Vocontian basin have been related to slope instabilities during the sea-level lowstand (e.g., PASQUIER & STRASSER 1997, HILLGÄRTNER 1999).

During the Early to early Middle Berriasian (calpionellid zone B), mass-flow deposits have been described in sections of the western Helvetic shelf area (DÉTRAZ et al. 1987, DÉTRAZ & MOJON 1989). Moreover, symsedimentary tectonic movements (small-scale tilted

blocks) have been described from parts of the western Helvetic shelf during these times (Platé massif; DÉTRAZ & MOJON 1989). During the early Middle Berriasian (lower part of calpionellid zone C), the northern parts of the central and eastern Helvetic shelf (cf. Chap. 6) have been exposed and partly eroded, whereas in the southern parts clayey sediments were deposited (BURGER 1986, MOHR 1992b, FUNK et al. 1993, MOHR & FUNK 1995). MOHR & FUNK (1995) postulated that during the Berriasian, the eastern Helvetic shelf was a ramp-type platform without large reef complexes at the shelf margin.

## 9.2.2 Initial transgression (Fig. 9.2b)

The Middle Berriasian transgression in the Dorset region is marked by the deposition of the oyster banks (Cinder Member) in a shallow coastal bay or lagoon (cf. Chap. 5). Similar oyster-rich intervals have been described from the Weald sub-basin to the north. However, their stratigraphic positions have been discussed controversially (e.g., WIMBLEDON & HUNT 1983, MORTER 1984, NORRIS 1985, ALLEN & WIMBLEDON 1991, WESTHEAD & MATHER 1996). Probably, the rupture of a morphological barrier during the large-scale transgression led to the inflow of marine waters into parts of the Channel sub-basin and enabled the widespread colonization of oysters in mesohaline conditions (ALLEN 1998, RADLEY 2002).

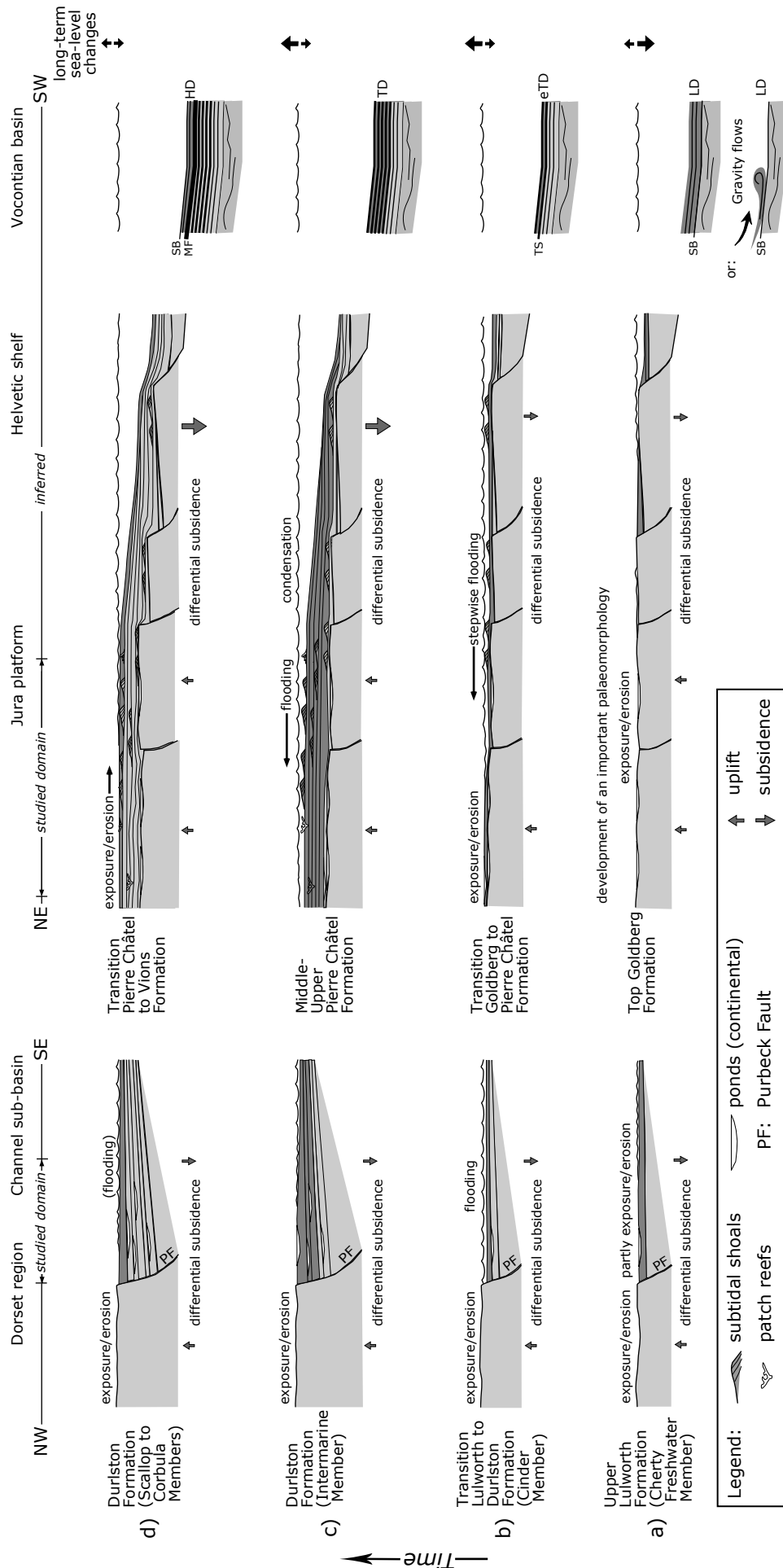


**Fig. 9.2** - Evolution of the Dorset region, Jura platform, and Vocontian basin between the 3<sup>rd</sup>-order sequence boundary intervals Be4 and Be5 (cf. Fig. 9.1). a) Long-term lowstand interval; b) Initial transgression; c) Long-term transgressive deposits; d) Long-term highstand deposits. Refer to text for discussion. The illustrations are not to scale.

High-resolution sequence- and cyclostratigraphic investigations reveal that the transgression flooded the Jura platform diachronously (WAEHRY 1989, PASQUIER 1995, HILLGÄRTNER 1999, STRASSER et al. 2004, this study; Figs. 9.3 and 9.4). The timing of the initial flooding at a given locality on the platform depends on its pre-existing morphology, which plays an important role by locally modifying accommodation and facies distribution.

In the Vocontian basin, the initial sea-level rise is indicated by the transition from relatively thick limestone beds to a succession of thinner and more homogeneous limestone-marl alternations (cf. Chap. 6). This has been related to an increase of the clay input to the basin due to enhanced remobilization of clays formerly stored on the nearby platforms (e.g., PASQUIER & STRASSER 1997, HILLGÄRTNER 1999, STRASSER et al. 2004).

During the early Middle Berriasian, the reef complex of the western Helvetic shelf was covered by bioclastic sands during the large-scale transgression (DÉTRAZ & MOJON 1989). Accordingly, the initial flooding of the emerged parts of the Helvetic shelf started during the early Middle Berriasian (Subalpina ammonite subzone; upper calpionellid zone B) and proceeded to the north onto the emerged Jura platform during the Middle Berriasian (Privasensis ammonite subzone; calpionellid zone C; DÉTRAZ & MOJON 1989).

### 9.2.3 Long-term transgressive deposits (Fig. 9.2c)

In the Dorset sections, the large-scale transgressive deposits are mainly composed of intertidal to subtidal sediments (Intermarine Member). They reflect a marginal-marine environment with slight lateral facies changes. This may be related to relatively low subsidence rates along the Purbeck Fault system. Such a depositional setting is rather sensitive to low-amplitude sea-level fluctuations as displayed by the recurrent emersion intervals (e.g., freshwater deposits at the sequence boundary between medium-scale sequences 3 to 4; cf. Fig. 6.10).

The transgressive deposits of the Jura platform display a general thickening-up trend, reflecting an important gain of accommodation space (cf. Fig. 6.2). The potential for carbonate production was elevated due to a combination of warm waters, low detrital input, and enhanced water circulation on the platform. Due to oligotrophic conditions, the growth potential of the Jura platform was relatively high and

patch reefs installed themselves in shallow-lagoonal environments (PASQUIER 1995, HILLGÄRTNER 1999). Bioclastic shoals protected the shallow lagoons from open-marine waters in the southern Jura platform (DÉTRAZ & MOJON 1989). The interaction of rising sea level in combination with differential subsidence created a complex pattern of lateral and vertical facies succession. Subsidence rates generally increased from proximal to distal position (from the Jura platform to the Helvetic shelf) due to extensional tectonics on the northern margin of the Tethys (e.g., FUNK 1985, ARNAUD 1988, WILDI et al. 1989, LOUP 1992, PASQUIER 1995). Accelerated differential subsidence and rising sea-level initiated the change from a flat-topped platform during the Early to Middle Berriasian to a distally steepened ramp during the late Middle to early Late Berriasian (Dalmasi to Paramimounum ammonite subzones; DÉTRAZ & STEINHAUSER 1988, HILLGÄRTNER 1999).

During the large-scale transgression, the clay content relative to the amount of carbonate increased in the Vocontian basin depending on the remobilization of clays on the surrounding platforms, on the current systems, and on the prevailing climate in the source areas. The planktonic productivity and the carbonate export from the platform decreased during rising sea level (cf. Chap. 6).

Bioclastic sediments progressively covered the hemipelagic limestone-marl alternations, which have been deposited on the distal parts of the western Helvetic shelf (DÉTRAZ & MOJON 1989). Shoal deposits prograded towards the south onto the western Helvetic shelf during the Middle Berriasian (DÉTRAZ & MOJON 1989, DÉTRAZ 1989, PASQUIER 1995). The margin of the southern Jura platform and the western Helvetic shelf evolved from a rimmed platform to a distally steepened ramp during Early Berriasian to Hauterivian times (ARNAUD-VANNEAU & ARNAUD 1991). The large-scale transgressive deposits of the northern parts of the central and eastern Helvetic shelf are also composed of massive platform carbonates representing mainly subtidal shoal sediments (Unterer Öhrlikalk; BURGER 1986, PASQUIER 1995, MOHR & FUNK 1995; cf. Chap. 6).

### 9.2.4 Long-term maximum-flooding and highstand deposits (Fig. 9.2d)

The Scallop Member, which indicates a marine incursion into the Channel sub-basin (MORTER 1984, ENSOM 2002, RADLEY 2002), has been interpreted to correspond to the large-scale maximum-flooding

interval of the Dorset sections (cf. Chap. 5; cf. Fig. 6.10). The large-scale highstand deposits of the Dorset sections are strongly reduced (lower part of the Corbula Member).

After the initial flooding of the flat-topped Jura platform and the start-up phase in platform growth during the large-scale transgression, high carbonate production progressively outpaced accommodation (shoaling-up trend) and forced the platform to prograde (HILLGÄRTNER 1998, 1999). Except for Marchairuz (cf. Fig. 6.2), the large-scale maximum-flooding interval is not preserved in the studied sections. It is assumed that a combination of sea-level fall, tectonic uplift, and/or reduced subsidence rates as well as the climate change to more humid conditions led to karstification, which marks the transition from the Pierre Châtel to the Vions Formation in several locations (PASQUIER 1995, PASQUIER & STRASSER 1997, HILLGÄRTNER 1999, STRASSER et al. 2004; cf. Fig. 6.2).

The identification of the large-scale maximum-flooding interval in the Montclus section is not easy (cf. Chap. 6). According to the sequence-stratigraphical interpretation of the present study, it lies below a relatively thick limestone bed, which corresponds to the large-scale highstand deposits (cf. Fig. 6.6).

During the large-scale highstand, subtidal sand bodies prograded from north to south on the Helvetic shelf during late Middle to early Late Berriasian times (upper calpionellid zone C to lower calpionellid zone D; DÉTRAZ & MOJON 1989, FUNK et al. 1993, MOHR & FUNK 1995, PASQUIER 1995).

### 9.3 Short-term evolution

Palaeogeographic maps, which show the long-term evolution during the Berriasian, have been designed for the Jura platform (e.g., STRASSER 1987, DÉTRAZ & MOJON 1989, WAEHRY 1989). They serve as a base for the series of maps constructed for the the Jura platform in the present study. Small-scale sequences 11 and 12 have been used to illustrate the evolution of the initial transgression in the Dorset region and on the Jura platform (Figs. 9.3 and 9.4). Five time-slices for each of these two small-scale sequences have been chosen. No palinspastic reconstruction has been made, i.e. the distances between the sections and their relative positions are not corrected. The proximal-distal distribution of the sections, however, is not affected and can be considered as representative. The palaeoenvironments between the investigated sections are interpolated according to the facies and sequence-

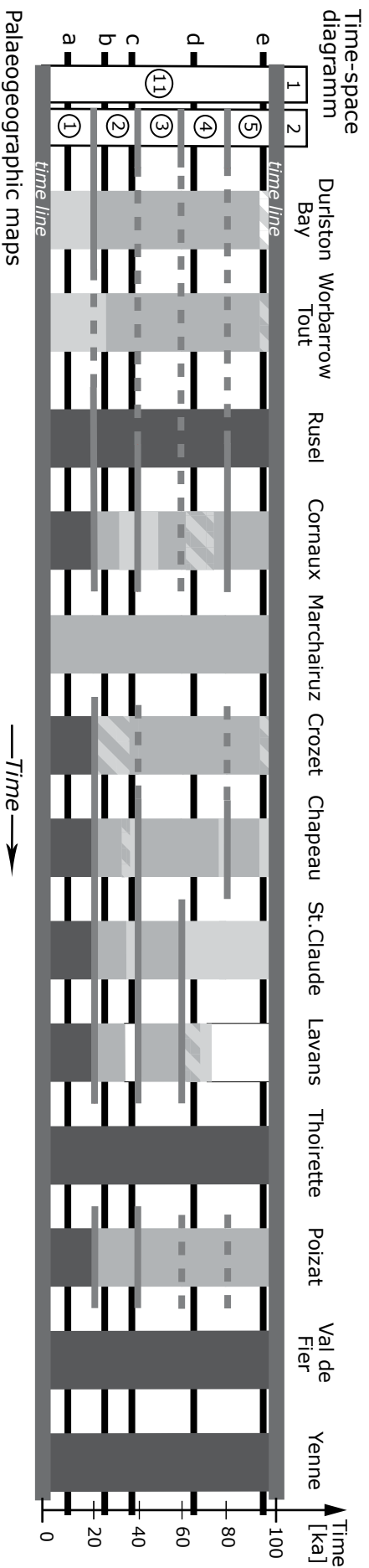
stratigraphical interpretations of the present study and data from the literature.

#### 9.3.1 High-resolution palaeogeographical evolution

##### *Dorset region*

The facies evolution in the Dorset region was controlled by the syndepositional movements along the large Purbeck Fault system (Abbotsbury-Ridgeway Fault, Purbeck Fault, and Wight-Bray Fault) north of the Portland-Wight depocentre (cf. Figs. 5.3 and 5.4). According to UNDERHILL (2002), the thickest part of Purbeck Limestone Group is located east of the Durlston Bay section (cf. Fig. 5.3). The lines of the isopachs in Fig. 5.3 have been considered as an indicator for the basin evolution and used for the detailed palaeoenvironmental reconstructions. It is assumed that a shallow lagoon covered most of the Portland-Wight depocentre. This lagoon was delimited to the north and east by the Purbeck Fault system, which marked the southern boundary of the partly emerged morphological high between the Channel and the Weald sub-basins (Hampshire-Dieppe high; UNDERHILL 2002). Low-relief land and shallow marine lagoons were adjacent in the west and south. The relative highest topographic elevations in the north were situated in the centre of the fault segments (footwall uplift) and decreased laterally forming low lying relay ramps between fault segments (UNDERHILL 2002). These relay ramps were potentially flooded during relative sea-level rise (Cinder Member; cf. Fig. 9.3b-d). It is assumed that shallow marine connections to lagoons in the south existed during rising sea level. Based on faunal relationships, it has been proposed that during the Berriasian, the Channel sub-basin was connected to the North Sea basin (e.g., CASEY 1973, RAWSON & RILEY 1982) and/or to the Paris basin (e.g., DÖRHÖFER & NORRIS 1977b, WIMBLEDON & HUNT 1983). Another marine connexion may have existed to the west via the Western Approach (cf. Figs. 5.2 and 8.5). Other studies assume that the Channel sub-basin was not connected to other marine basins at all (e.g., KELLY 1983, MORTER 1984). During relative sea-level falls (small-scale sequence-boundary intervals), the extension of the shallow lagoon may have significantly decreased and large areas were exposed (cf. Figs. 9.3e and 9.4j). Water-mass exchanges with other marine lagoons probably were reduced, leading to locally restricted conditions. The relay ramps were





Palaeogeographic maps

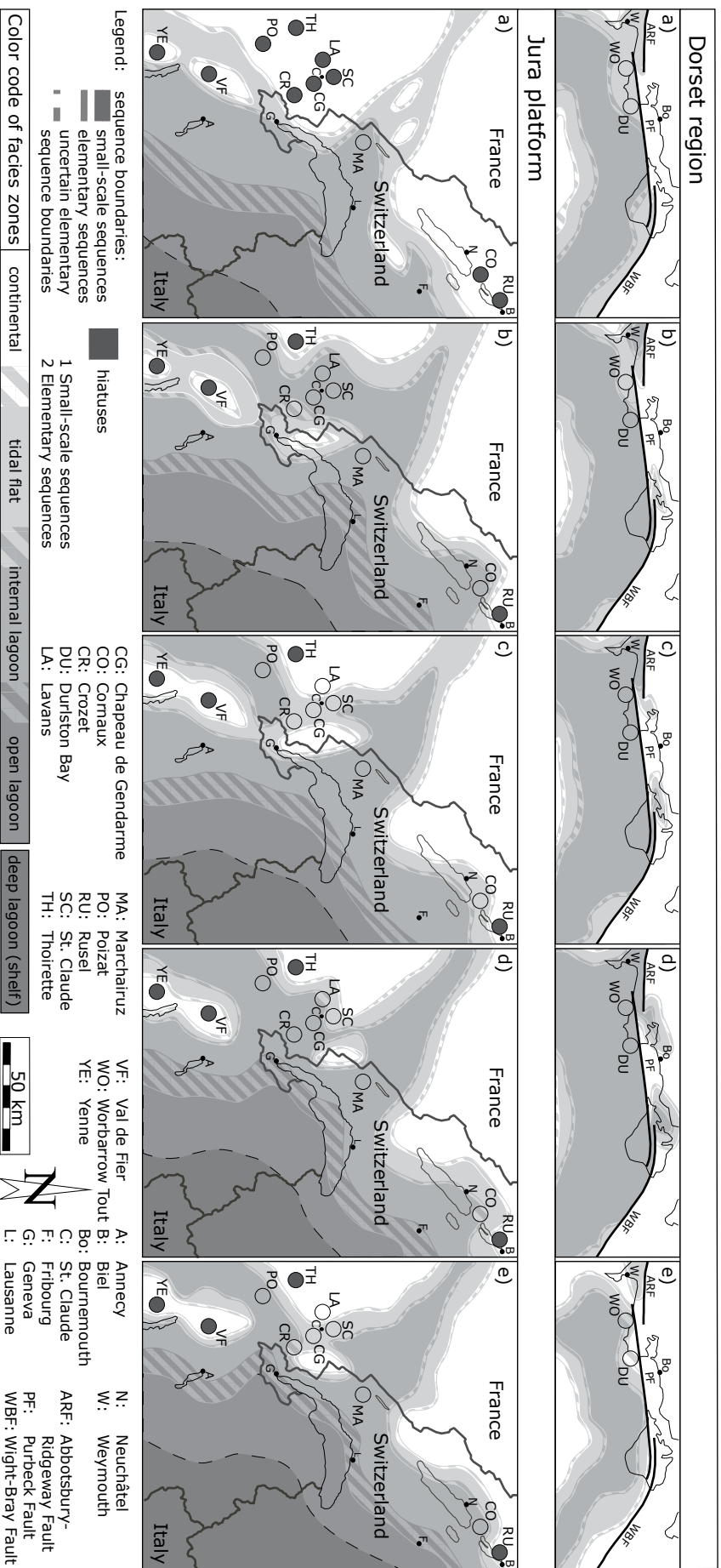
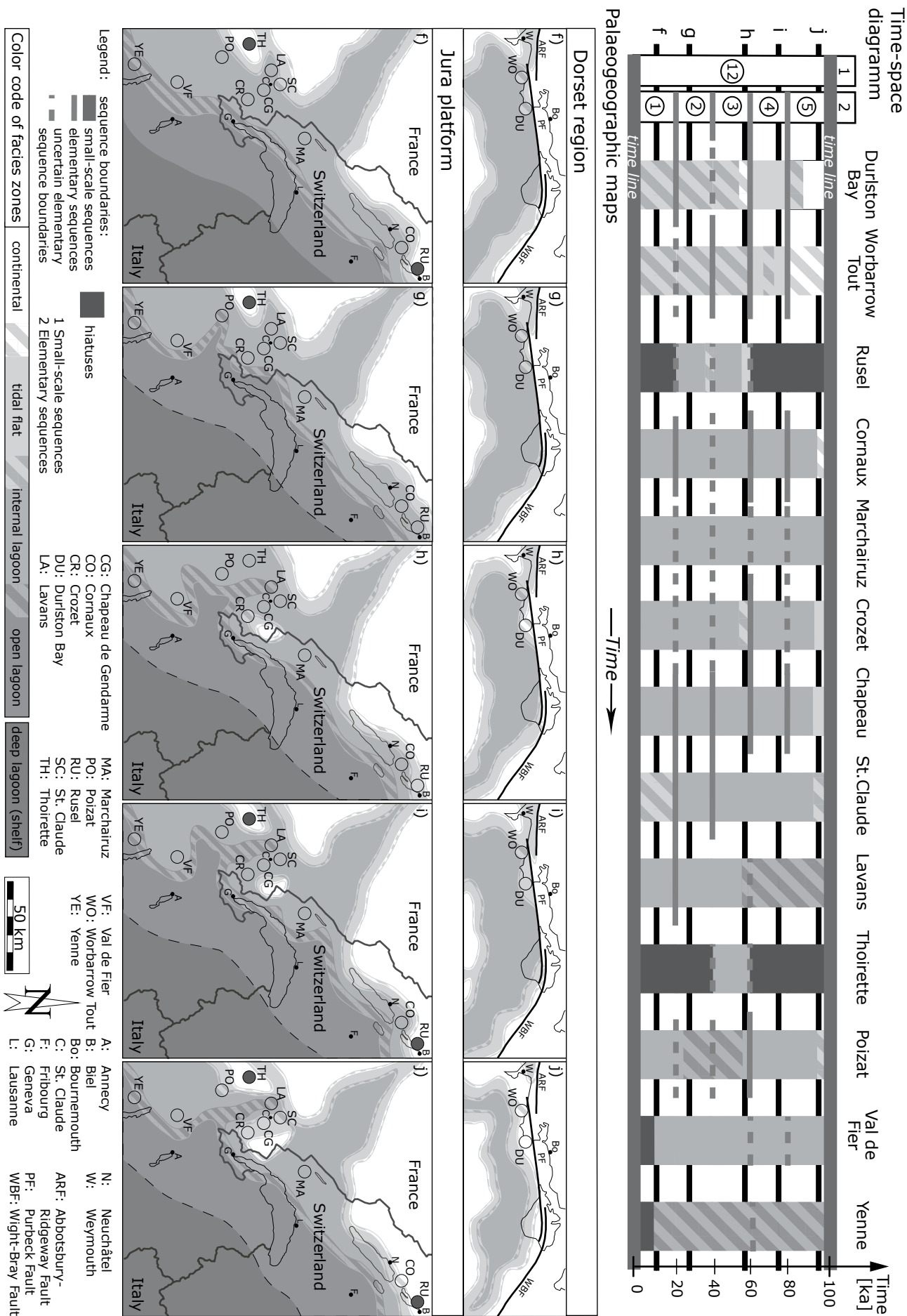


Fig. 9.3 - Figure illustrates five palaeogeographic maps (a-e) of the small-scale sequence 11. The interpolations between the sections are hypothetical. (Palaeogeographic maps without palinspastic reconstruction).





**Fig. 9.4** – Figure illustrates five palaeogeographical maps (f-j) of the small-scale sequence 12. The interpolations between the sections are hypothetical. (Palaeogeographic maps without palinspastic reconstruction).

emerged and served as passages for rivers bringing more freshwater from the Hampshire-Dieppe High in the north into the shallow lagoon. As a consequence, the water salinity in the lagoon probably decreased to brackish and stagnant conditions during relative sea-level lowstands. Such conditions may be reflected by the dark colored and partly bituminous deposits of the Intermarine Member (cf. Chap. 5). The change to more humid conditions during the deposition of the Intermarine Member (Late Middle to early Late Berriasian) enhanced furthermore the brackish conditions.

### *Jura platform*

The Jura platform and the northern parts of the Helvetic shelf have been flooded approximately from southwest to northeast (e.g., DÉTRAZ & STEINHAUSER 1988, WAEHRY 1989, PASQUIER 1995; cf. Chap. 6). The transgression encroached stepwise onto the emerged platforms at the transition of the Goldberg Formation to the Pierre Châtel Formation (PASQUIER 1995, STRASSER et al. 2004; cf. Fig. 9.3). The pre-existing platform morphology and differential subsidence were the main factors controlling the time of the initial flooding at a given location. According to the sequence-stratigraphical interpretation, emersion prevailed on the southwestern Jura platform (Yenne and Val de Fier sections) about 100 ka longer than in more northern locations (cf. Fig. 9.3). This interpretation may be explained by emerged morphological highs (islands), which were separated by a shallow-marine lagoon to the northwest (Poizat section; cf. Fig. 9.3b-e). The initial transgression in these elevated areas is marked by an abrupt facies change from supratidal to internal-to open-lagoonal sediments without any transitional environments (tidal flats). This points to a relatively distal position on the platform and/or to rapid tectonic subsidence. This study favors the interpretation that emerged morphological highs (islands) were present on the southwestern platform because of the abrupt facies change and the absence of detrital quartz in most of these sections (WAEHRY 1989).

A similar interpretation is made for the Thoirrette section. However, at this location, it is not clear whether the facies evolution represents a distal or a proximal position of the platform. It is supposed, that this section was first situated on the emerged mainland (Figs. 9.3a-e and 9.4f-g), then in an internal-lagoonal environment (initial transgression; Fig. 9.4h) and later on an island (Fig. 9.4i-j). An emerged morphological high (island) is also postulated east of the Crozet,

Chapeau de Gendarme, and St. Claude sections (cf. Fig. 9.3b-e). During the transgression in small-scale sequence 12, however, this morphological high was flooded (cf. Fig. 9.4f-g). An island in this area probably reappears during low relative sea levels (cf. Fig. 9.4h-f).

The Marchairuz section was located south of a shallow basin (morphological depression), which extended further north. This interpretation is mainly based on facies analysis, the thickness of the formation, and the distribution of detrital quartz in this area (STEINHAUSER & CHAROLLAIS 1971, PERSOZ & REMANE 1976, STRASSER 1987; cf. Chap. 6). Based on micropalaeontological arguments (cf. Chap. 5), MOJON (2002) postulated a marine connexion in this region between the Jura platform and the Paris basin (Central Jura graben). He assumed that tectonic movements along Variscan structures in the basement controlled the evolution of this graben system. LOUP (1992) stated that “the non-uniform subsidence patterns and driving mechanisms in the Jura-Plateau area [Plateau corresponds to the Molasse basin in Fig. 4.2] contrast with the homogenous character of the Helvetic sub-domains. This marked difference may express the major influence of late Variscan structures on the Mesozoic record in the Jura and Plateau, whereas basin development in the Helvetic realm is mainly controlled by extension on the North-Tethyan margin. For the Jura and Plateau sections, tectonic subsidence may be seen as an indirect consequence of extension, which reactivated ancient structures” (p. 567). The present study supports this interpretation because the initial transgression (open-lagoonal conditions) reaches the Marchairuz area already in small-scale sequence 10, which points to a morphological depression (cf. Figs. 6.4 and 7.4). Accordingly, an elongated shallow basin with a southeast to northwest orientation has been sketched in the area of the Marchairuz section. The existence of a marine connexion to the Paris basin during the deposition of small-scale sequences 11 and 12 is highly speculative. However, with increasing relative sea level and during the large-scale maximum flooding (around small-scale sequence 19; cf. Fig. 6.13), the Jura platform may have been connected with the Paris basin by a shallow marine channel. Such a seaway probably enabled the incursion of warm Tethyan water masses to the north during Middle to Late Berriasian times (cf. Fig. 8.5).

Increased differential subsidence may have caused the environmental change from internal to more open lagoonal conditions in the area of the Poizat section during the deposition of small-scale sequence 12 (cf. Fig. 9.4g). These subsidence movements may be

related to tectonic activities along the strike-slip zone of the Vuache fault (cf. Fig. 4.2). About 20 ka later, a similar abrupt environmental change from internal to open-lagoonal deposits occurred at the location of the Lavans section (Fig. 9.4h-g), which probably also indicates a relative increase of differential subsidence. As a hypothesis, this may be explained by a northward progradation of the tectonic activities along the Vuache fault (CHAROLLAIS et al. 1983).

The facies evolution of the Rusel section indicates that this section was located at the most proximal position on the platform compared with the other sections (e.g., freshwater interval at the sequence boundary between small-scale sequences 13 and 14; cf. Fig. 6.4). About 2 km to the northeast of the Rusel section in direction to the town of Biel (cf. Fig. 4.8), the Biel section has been investigated in several studies (MOJON & STRASSER 1987, BLANC & MOJON 1996, BLANC 1996, MOJON 2002). A breccia interval containing a tilted block with a volume of almost 3 m<sup>3</sup> has been described from the base of the Pierre Châtel Formation in this outcrop. MOJON & STRASSER (1987) postulated that this block has fallen down from a palaeocliff in Middle Berriasian times. BLANC & MOJON (1996) and BLANC (1996) related the breccia and the tilted block to collapse deposits, which filled a karst cave during the Middle to Late Berriasian (charophyte-ostracode assemblage M4). These interpretations indicate that during the Middle to Late Berriasian the palaeocoast was close to the section of Rusel and Biel at least during the Middle Berriasian.

### 9.3.2 Rates of palaeogeographic evolution

The proposed 20-ka framework allows to investigate environmental changes with high resolution. Although the reconstructions are hypothetical, palaeogeographic maps can be proposed, which integrate all the information on the lateral and vertical facies evolution of the sections. It can be shown that facies change rapidly in time and space in the order of a few thousand years. Facies may migrate over several tens of kilometers in a 20-ka cycle, strongly depending on the local accommodation space, energy conditions, platform morphology, and/or production and transport rates of the sediments. Morphological highs are adjacent to morphological depressions. Islands and shoals may protect lagoonal environments from strong current and wave activities. The dynamics of sand bodies strongly

depend on bottom morphology and on the prevailing water energy. Shoals mainly migrate as entire units in sudden bursts during storm events (e.g., BALL 1967, HINE 1977). During post-storm times, sandwaves migrate over the large-scale shoal bodies, building up vertically by accumulating sets of flood- and ebb-oriented cross-bedding separated by erosional or re-activations surfaces (cf. Chap. 2).

The superposition of long-term and short-term processes has to be considered when interpreting highly dynamic depositional system. Tectonic processes (uplift and/or subsidence) may change accommodation space locally and regionally by controlling the long-term evolution of the platform morphology. The short-term evolution of marginal-marine environments is strongly coupled to relative sea-level changes in the Milankovitch-frequency band. Low-amplitude sea-level fluctuations in shallow-marine settings are able to control the spatial dynamics of facies patterns. During relative sea-level rise, morphological barriers (e.g., coastal highs, shoals and/or islands) are flooded, which modifies the conditions in existing lagoons and/or creates new lagoonal environments. Moreover, water exchange on and off the shallow-lagoonal settings probably become more vigorous and the energy level within the lagoons may increase. Falling relative sea level leads to widespread emersion in low-relief coastal areas and on morphological highs. Such environmental changes modify also the physical and chemical conditions in marginal-marine settings (e.g., temperature, salinity, bathymetry, water energy, current patterns, oxygen concentration, alkalinity), which influence the in-situ carbonate productivity of the biota (e.g., TIPPER 1997, BRETT 1998, RANKEY 2004, WRIGHT & BURGESS 2005). Different threshold effects, therefore, control the evolution of marginal-marine carbonate environments in time and space in complex feedback mechanisms. Accordingly, the sensitivity of marginal-marine settings is related to both the rate of disturbances, such as sea-level fluctuations, and the rate of system response such as habitat migration (e.g., KENDALL & SCHLAGER 1981).

These processes can be observed today and are well recorded in Holocene and Pleistocene sediments. The high time-resolution obtained from cyclostratigraphical interpretations of ancient sedimentary records, enables a better comparison of sedimentary processes recorded in ancient and Pleistocene to Holocene deposits (e.g., STRASSER & SAMANKASSOU 2003, STRASSER et al. 2004).



## 10 - CONCLUSIONS AND OUTLOOK

Based on a well established bio- and sequence-stratigraphical framework, eleven sections on the Jura platform and one section of the Vocontian basin have been logged and interpreted in detail. This enabled a high-resolution sequence-stratigraphical correlation of these sections. Additionally, two sections of the Dorset region have been interpreted for the first time in terms of high-resolution sequence stratigraphy and integrated in the sequence-stratigraphical framework of the Jura platform and the Vocontian basin.

The main results of this study are:

- Marginal-marine carbonates in tropical to sub-tropical settings are ideal recorders of relative sea-level changes because they are extremely sensitive to environmental changes due to their rapid in-situ carbonate production (carbonate factory). Under optimal ecological conditions they can easily keep pace with relative sea-level rise. However, classification and interpretation of the highly variable facies mosaics in space and time in sedimentary successions are complex and, therefore, commonly oversimplified. In the high-resolution facies analysis of this study, transitional facies zones have been used in order to render the interpretation more realistic.
- Siliciclastics in carbonate-dominated environments are important because they enhance facies contrasts. However, their interpretation (mainly marl intervals) in terms of high-resolution sequence stratigraphy is commonly not straightforward and must be carefully investigated (SB or MF-intervals?). Moreover, siliciclastics in marginal-marine settings can be related to climate changes and/or tectonic activities in the hinterland.
- Detailed logging of the sections allows detecting the most significant facies changes and relating them to sea-level fluctuations on several scales (superimposition). Lateral pinch outs of beds must be considered when interpreting marginal-marine sediments in terms of high-resolution sequence stratigraphy. Sequence stratigraphy has the advantage that it deals with the vertical facies evolution of a sedimentary succession as a result of accommodation changes, which are thought to have been controlled by the combination of local autocyclic factors (shoal migration, differential subsidence) and allocyclic factors (eustatic sea-level changes, large-scale tectonics).
- Autocyclic intervals are common in highly dynamic depositional environments and may overrule allocyclic signals especially on the scale of elementary sequences. Accordingly, they have to be taken into account when interpreting sedimentary succession with high-resolution. Problematic intervals cannot be interpreted in terms of sequence-stratigraphy but they can at least be delimited at the top and base by sequence-stratigraphical correlations.
- In marginal-marine settings, transgressive deposits are ideal for investigating high-frequency sea-level changes because preservation potential increases with rising sea level (less hiatuses). The interval around an initial transgression is most interesting for high-resolution sequence-stratigraphical analysis because, on the long-term trend, it lies between late highstand to lowstand deposits, which are commonly affected by erosion and non-deposition (creating irregular topography) and late transgressive to maximum-flooding deposits, which commonly are dominated by more homogeneous subtidal sediments (absence of threshold effects).

- For high-resolution sequence-stratigraphical investigations, it is important that a well-constrained framework based on bio-, sequence-, and/or magnetostratigraphy is available. Starting with large-scale sequence interpretations, the resolution can be increased systematically. Sequence-stratigraphical investigation must be based on several correlated sections in order to obtain an adequate picture of the involved controlling factors (auto- versus allocyclic deposits).
- A best-fit correlation of all investigated sections between the 3<sup>rd</sup>-order sequence boundaries Be4 and Be5 has been worked out in the present study. It fits well into bio- and magnetostratigraphical frameworks published in the literature. The present study confirms the correlation of the base of the Pierre Châtel Formation with the base of the Durlston Formation (Cinder Member).
- The time interval between the 3<sup>rd</sup>-order sequence boundaries Be4 and Be5 and the stacking pattern reveals that the observed depositional sequences have been caused by sea-level fluctuations in the Milankovitch-frequency band. The asymmetry of the long-term sequence observed in all investigated sections is due to the superimposition of this 3<sup>rd</sup>-order sequence on a regressive trend on the 2<sup>nd</sup>-order scale. On the Jura platform, tectonic uplift additionally contributed to this asymmetry and caused widespread karstification at sequence boundary Be5.
- The medium-scale sequences detected on the Jura platform and in the Dorset region correspond to the long eccentricity cycles (400 ka). The long eccentricity cycles are the most stable cycles on the Milankovitch-frequency band and may be used as “tuning forks” for high-resolution sequence- and cyclostratigraphic investigations. In the Vocontian basin, the interpretation of medium-scale sequences is not easy. Hemipelagic depositional realms apparently are more sensitive to high-frequency sea-level fluctuations on the scale of elementary (precession cycles) and small-scale sequences (short eccentricity cycles).
- Small-scale sequences are well-expressed between the 3<sup>rd</sup>-order sequence boundaries Be4 and Be5 in all investigated regions. They have been correlated from the Vocontian basin over the Jura platform to the Dorset region. Accordingly, they serve as a framework for the interpretation and correlation of the elementary sequences. Small-scale sequences have been interpreted to correspond to the short eccentricity cycles with a period of 100 ka. These orbital cycles controlled the climate system and caused sea-level fluctuations, which were recorded by easily detectable facies changes.
- Elementary sequences are the smallest depositional units identified in the present study. They are related to the orbital precession cycles (20 ka). However, on this scale of investigation, autocyclic processes become important and may disturb allocyclic signals. Nevertheless, some elementary sequences can be correlated over long distances and between different depositional environments.
- Based on the high-resolution sequence- and cyclostratigraphic interpretation, it can be shown that the Middle Berriasian transgression on the Jura platform was not isochronous and differed between some sections by more than 200 ka. These differences are explained by the position of the sections on the platform, the pre-existing platform morphology (before the large-scale transgression), and differential subsidence. However, most of the sections on the Jura platform and in the Dorset region have been flooded in a narrow time range of a few thousand years (base of the second elementary sequence of small-scale sequence 11). In the Dorset region, the difference of the bed thicknesses can directly be related to the distance of a section to the Portland-Wight depocentre, which has been controlled by the activity of the Purbeck Fault system.
- Sequence- and cyclostratigraphical interpretations can be used to estimate the time ranges of bio- and/or magnetostratigraphical zones and thus improve existing time-scales (astrochronological tuning). In fact, the time ranges of some ammonite zones and polarity chrons tuned astrochronologically in the present study differ from the ones published by HARDENBOL et al. (1998).
- The analyses of clay minerals and stable isotopes ( $\delta^{13}\text{C}$ ,  $\delta^{18}\text{O}$ ) support the sequence-stratigraphical interpretation on the scale of elementary sequences. Especially the curves of the stable isotopes are in agreement with the interpretation of the elementary sequences and help to better understand the depositional processes (mainly exposure intervals). Slight changes in the clay mineral associations have also been measured on the level of elementary

sequences. Their interpretation, however, is more complex and may be related to changes in the delivery system (climate and/or tectonic signal), changes in the local current systems and water-energy levels, and geochemical alterations.

- The significant increase of kaolinite during late Middle Berriasian times observed by several authors (e.g., DECONINCK 1987, HALLAM et al. 1991, ALLEN 1998, SCHNYDER 2003) in Central and NW Europe can be confirmed. Besides local controlling factors (e.g., uplift in source area, distance to river deltas, coastal currents, water-energy), this kaolinite increase can be related to a long-term climate change from semi-arid (Mediterranean) to more humid conditions. According to the sequence- and cyclostratigraphic interpretation, the increase of kaolinite occurred earlier on the Jura platform than in the Dorset region. This long-term climate change may have been caused by a re-organisation of the circulation pattern of the oceanic surface waters in and between the European epicontinental seas in combination with the widening of the proto-North Atlantic. According to this model, warm Tethyan surface waters repelled Boreal cold surface waters to higher palaeolatitudes during late Middle Berriasian times.
- Short-term climate changes in the Milankovitch-frequency band are related to changes in the extension and latitudinal position of the atmospheric circulation cells (PERLMUTTER & MATTHEWS 1989, 1992). In this model, climate in Dorset would undergo a succession of dry (insolation maximum) to humid conditions (insolation minimum). On the Jura platform, the climate would not change much (the transition of dry to subhumid conditions). Rivers transported the climate signal from higher to lower palaeolatitudes by delivering siliciclastics (mainly clay minerals) to the Jura platform.
- The high-resolution sequence- and cyclostratigraphical interpretation and correlation enables the reconstruction of the palaeogeographic evolution with time steps of 20 ka and even less. It has been shown that facies changes strongly depend on threshold effects (e.g., rapid flooding of morphological highs). The evolution of the platform morphology in combination with sea-level fluctuations is the main factor controlling the water depth and water energy and thus the ecology of the carbonate-producing organisms and the distribution of the sediment. Differential tectonic movements

influenced the evolution of the platform morphology by creating and/or reducing accommodation space and by abruptly changing the position and geometry of depocentres.

The results of this thesis may serve as a starting point for further research:

As mentioned in Chap. 6, it would be interesting to correlate additional Middle Berriasian sections of other regions with the sections of the present study (e.g., the Sierra del Pozo and the Cherves-de-Cognac sections). However, the sections should be dated as precisely as possible in order to obtain a good time control. Once a sequence-stratigraphical correlation framework connecting several regions is established, it may be possible to estimate the changes in accommodation space by comparing decompacted thicknesses of depositional sequences on several scales (e.g., HILLGÄRTNER & STRASSER 2003, STRASSER et al. 2004). Furthermore, by filtering out local parameters (e.g., autocyclic processes, differential subsidence and/or uplift, facies-dependent accumulation rates), a sea-level curve may be reconstructed, which would be representative for all investigated sections (eustatic sea-level curve).

The combination of sequence- and cyclostratigraphy has an enormous potential to investigate marginal-marine carbonate systems with high resolution in time and space. It opens the possibility to quantify sedimentological processes (e.g., sediment accumulation rates, transportation rates) and ecological aspects of the past in comparison with the recent ones (e.g., STRASSER & SAMANKASSOU 2003, STRASSER et al. 2004). BOSSCHER & SCHLAGER (1993) stated that “cyclostratigraphy provides a measure of shorter time intervals, comparable to the late Quaternary. Cycles in the Milankovitch-frequency band provide equal durations for the sampling intervals and therefore an excellent basis for comparison of the obtained accumulation rates” (p. 346). Although ecological, chemical, physical, and climatic parameters changed through geologic time, the comparison between modern and ancient sediments and their depositional mechanisms is instructive.

The importance of additional factors, which control and determine boundary conditions for the biota and their productivity (e.g., temperature, nutrient availability, seawater chemistry, bathymetry; e.g., HALLOCK & SCHLAGER 1986, BRETT 1998, MUTTI & HALLOCK 2003) may be evaluated and compared for the specific marginal-marine settings of the Jura platform and the Dorset region. The long-term and

also the short-term climate changes influenced the trophic structure of the marginal-marine palaeocommunities by changes in the land-derived nutrient supply. Reworking of nutrients on the coastal plains (e.g., palaeosols) during the initial large-scale transgression may have led to mesotrophic to eutrophic conditions on the Jura platform stimulating the growth of opportunistic r-strategists (e.g., HOMEWOOD 1996, MASSE & MONTAGGIONI 2001). WRIGHT & BURGESS (2005) stated that “during the initial flooding of land areas in the early stages of major transgressions, the shallow waters may be especially prone to local effects and stratification, abnormal salinities and eutrophy, preventing the skeletal photoautotroph-dominated carbonate factory from fully developing” (p. 18).

Moreover, the distribution of dasycladaceans and benthic foraminifera in the Pierre Châtel Formation of the Jura platform and their relationship to other components may be of interest. These associations can be compared with other Berriasian sections described in the literature (e.g., ARNAUD-VANNEAU & DARSAC 1984, BUCUR & SĂSĂRAN 2005, SCHLAGINTWEIT et al. 2005, HUSINEC & SOKAČ 2006).

The distribution of ostracodes in the upper part of the Goldberg Formation may be compared to the

faunicycles described in the Dorset region (cf. Chap. 5). Such a comparison may allow to filter constrain the dominant factor (salinity and/or permanence of water bodies) controlling these ostracode associations. The shell accumulations observed in the Dorset sections (e.g., “shell beaches”, ostracodites) may be studied in detail and related to specific palaeoecological conditions.

Lateral and vertical facies changes on a decimetric to metric scale may be investigated and quantified in sections with a wide lateral extension (e.g., Rusel, Lavans, and Durlston Bay sections) and related to physical palaeoenvironmental parameters (e.g., energy-level, small-scale platform morphology, current directions, sediment sources and/or sinks, early diagenesis; e.g., DEMICCO & HARDIE 2002, SAMANKASSOU et al. 2003, WRIGHT & CHERNS 2004, WRIGHT & BURGESS 2005).

High-resolution sequence- and cyclostratigraphical investigations have a great potential for analyzing palaeoenvironments in time and space with the detail necessary to do justice to the complexity of these systems. This study may be helpful as a case example for the investigation of other coeval marginal-marine carbonate systems.

\*\*\*\*\*



## REFERENCES

- ABBINK, O., TARGARONA, J., BRINKHUIS, H. & VISSCHER, H. (2001) Late Jurassic to earliest Cretaceous palaeoclimatic evolution of the southern North Sea. *Global and Planetary Change* 30, 231-256.
- ADATTE, T. & RUMLEY, G. (1984) Microfaciès, minéralogie, stratigraphie et évolution de milieux de dépôts de la plate-forme berriasio-valanginienne des régions de Sainte-Croix (VD), Cressier et du Landeron (NE). *Bull. Soc. Neuch. Sci. Nat.* 107, 221-239.
- ADATTE, T., STINNESBECK, W., REMANE, J. & HUBBERTEN, H. (1996) Paleooceanographic changes at the Jurassic-Cretaceous boundary in the Western Tethys, northeastern Mexico. *Cretaceous Research* 17 (6), 671-689.
- AINARDI, R. (1977) Un paysage margino-littoral: Le "Purbeckien" du Jura méridional. *Bull. Soc. géol. France* 2, 257-264.
- ALLEN, J.R. & MATTHEWS, R.K. (1982) Isotope signatures associated with early meteoric diagenesis. *Sedimentology* 29, 797-817.
- ALLEN, P. (1963) L'âge du purbecko-wealdien d'Angleterre. *Colloque Crétacé inférieur* 34, 321-326.
- ALLEN, P. & KEITH, M.L. (1965) Carbon isotope ratios and palaeosalinities of Purbeck-Wealden carbonates. *Nature* 208, 1278-1280.
- ALLEN, P. & WIMBLEDON, W.A. (1991) Correlation of NW European Purbeck-Wealden (nonmarine Lower Cretaceous) as seen from the English type-areas. *Cretaceous Research* 12, 511-526.
- ALLEN, P. (1998) Purbeck-Wealden (early Cretaceous) climates. *Proceedings of the Geologist's Association* 109, 197-236.
- ALLENBACH, R.P. (2002) The ups and downs of "Tectonic Quiescence"- recognizing differential subsidence in the epicontinental sea of the Oxfordian in the Swiss Jura Mountains. *Sedimentary Geology* 150 (3-4), 323-342.
- ALLEY, N.F. & FRANKS, L.A. (2003) First known Cretaceous glaciation: Livingston Tillite Member of the Cadna-owie Formation, South Australia. *Australian Journal of Earth Sciences* 50, 139-144.
- ANDERSON, E.J. & GOODWIN, P.W. (1990) The significance of metre-scale allocycles in the quest for a fundamental stratigraphic unit. *J. Geol. Soc. London* 147, 507-518.
- ANDERSON, E.J. (2004a) Facies patterns that define orbitally forced third-, fourth-, and fifth-order sequences of sixth-order cycles and their relationship to ostracod faunicycles: The Purbeckian (Berriasian) of Dorset, England. In: D'ARGENIO, B., FISCHER, A.G., PREMOLI SILVA, I., WEISSERT, H. & FERRERI, V. (eds) *Cyclostratigraphy: Approaches and case histories*. *SEPM Spec. Publ.* 81, 245-260.
- ANDERSON, E.J. (2004b) The cyclic hierarchy of the "Purbeckian" Sierra del Pozo Section, Lower Cretaceous (Purbeckian), southern Spain. *Sedimentology* 51, 455-477.
- ANDERSON, F.W. & BAZLEY, R.A.B. (1971) The Purbeck Beds of the Weald (England). *Bull. Geol. Survey Great Britain* 34, 9-43.
- ANDERSON, F.W. (1985) Ostracod faunas in the Purbeck and Wealden of England. *J. Micropal.* 4 (22), 1-68.
- ANDREU, B., PEYBERNÈS, B. & CALVET, N. (1996) Ostracodes du passage Berriasien-Valanginien dans la vallée du Sègre, gorge d'Organya (zone sud-Pyrénéenne, Catalogne, Espagne). *Rev. Micropal.* 39 (3), 191-209.
- ARNAUD, H. (1988) Subsidence in certain domains of southeastern France during the Ligurian Tethys opening and spreading rates. *Bull. Soc. géol. France* 5, 725-732.
- ARNAUD-VANNEAU, A. & DARSAC, C. (1984) Caractères et évolution des peuplements de foraminifères benthiques dans les principaux biotopes de plates-formes carbonatées du Crétacé inférieur des Alpes du Nord (France). *Geobios Mém. spécial* 8, 19-23.
- ARNAUD-VANNEAU, A. & ARNAUD, H. (1991) Sédimentation et variations relatives du niveau de la mer sur les plates-formes carbonatées du Berriasien-Valanginien inférieur et du Barrémien dans les massifs subalpins septentrionaux et le Jura (Sud-Est de la France). *Bull. Soc. géol. France* 162 (3), 535-545.
- ARTHUR, M.A. & SCHLANGER, S.O. (1979) Cretaceous "Oceanic Anoxic Events" as causal factors in development of reef-reservoired giant oil fields. *AAPG Bull.* 63 (6), 870-885.

- AURELL, M., ROBLES, S., BÁDENAS, B., ROSALES, I., QUESADA, S., MELÉNDEZ, G. & GARCÍA-RAMOS, J.C. (2003) Transgressive-regressive cycles and Jurassic palaeogeography of northeast Iberia. *Sedimentary Geology* 162 (3-4), 239-271.
- AXELROD, D.I. (1984) An interpretation of Cretaceous and Tertiary biota in polar regions. *Palaeogeogr., Palaeoclim., Palaeoecol.* 45, 105-147.
- BALL, M.M. (1967) Carbonate sand bodies of Florida and the Bahamas. *J. Sed. Petro.* 37 (2), 556-591.
- BARABOSHKIN, E. (1999) Berriasian-Valanginian (Early Cretaceous) seaways of the Russian platform basin and the problem of Boreal/Tethyan correlation. *Geologica Carpathica* 50 (1), 5-20.
- BARABOSHKIN, E. (2002) Early Cretaceous seaways of the Russian platform and the problem of Boreal/Tethyan correlation. In: MICHALIK, J. (ed) *Tethyan/Boreal Cretaceous correlation*. 39-78 (Slovak Academy of Sciences).
- BARRON, E.J., HARRISON, C.G.A., SLOAN, J.L. & HAY, W.W. (1981) Paleogeography, 180 million years ago to the present. *Eclogae geol. Helv.* 74 (2), 443-470.
- BARRON, E.J. & WASHINGTON, W.M. (1982) Cretaceous climate: A comparison of atmospheric simulations with the geological record. *Palaeogeogr., Palaeoclim., Palaeoecol.* 40, 103-133.
- BARRON, E.J. (1983) A warm, equable Cretaceous: The nature of the problem. *Earth Sci. Rev.* 19, 305-338.
- BARRON, E.J. & MOORE, G.T. (1994) Climate model application in paleoenvironmental analysis. *SEPM Short Course* 33, 1-339.
- BATTEN, D.J. (2002) Palaeoenvironmental setting of the Purbeck Limestone Group of Dorset, southern England. In: MILNER, A.R. & BATTEN, D.J. (eds) *Life and environments in Purbeck times*. 13-20 (The Palaeontological Association London).
- BENNETT, M.R. & DOYLE, P. (1996) Global cooling inferred from dropstones in the Cretaceous: Fact or wishful thinking? *Terra Nova* 8, 182-185.
- BERGER, A. (1978) Long-term variations of caloric insolation resulting from the Earth's orbital elements. *Quaternary Research* 9, 139-167.
- BERGER, A., LOUTRE, M.F. & DEHANT, V. (1989a) Astronomical frequencies for pre-Quaternary paleoclimate studies. *Terra Nova* 1, 474-479.
- BERGER, A., LOUTRE, M.F. & DEHANT, V. (1989b) Influence of the changing lunar orbit on the astronomical frequencies of pre-Quaternary insolation patterns. *Paleoceanography* 4 (5), 555-564.
- BERGER, A., LOUTRE, M.F. & LASKAR, J. (1992) Stability of the astronomical frequencies over the Earth's history for paleoclimate studies. *Science* 255, 560-566.
- BERGER, A. & LOUTRE, M.F. (2004) Théorie astronomique des paléoclimats. *C. R. Geoscience* 336, 701-709.
- BLANC, E. (1996) Transect plate-forme- bassin dans les séries carbonatées du Berriasien supérieur et du Valanginien inférieur (domaines jurassien et nord-vocontien) *Chronostratigraphie et transferts des sédiments. Géologie Alpine Mém.* hs 25, PhD thesis, 312pp. (University of Grenoble).
- BLANC, E. & MOJON, P.-O. (1996) Un paléokarst du Crétacé basal (Berriasien moyen) dans le Jura suisse occidental (région de Bienne): Corrélations avec les domaines boréal et téthysien. *Cretaceous Research* 17, 403-418.
- BOND, G.C., DEVLIN, W.J., KOMINZ, M.A., BEAVAN, J. & McMANUS, J. (1993) Evidence of astronomical forcing of the Earth's climate in Cretaceous and Cambrian times. *Tectonophysics* 222, 295-315.
- BORNEMANN, A., ASCHWER, U. & MUTTERLOSE, J. (2003) The impact of calcareous nannofossils on the pelagic carbonate accumulation across the Jurassic-Cretaceous boundary. *Palaeogeogr., Palaeoclim., Palaeoecol.* 199 (3-4), 187-228.
- BOSENCE, D.W.J., WOOD, J.L., ROSE, E.P.F. & QING, H. (2000) Low- and high-frequency sea-level changes control peritidal carbonate cycles, facies and dolomitization in the Rock of Gibraltar (Early Jurassic, Iberian Peninsula). *J. Geol. Soc. London* 157, 66-74.
- BOSENCE, D.W.J. & WILSON, R.C.L. (2003) Carbonate depositional systems. In: COE, A.L. (ed) *The sedimentary record of sea-level changes*. 209-233 (The Open University).
- BOSSCHER, H. & SCHLAGER, W. (1993) Accumulation rates of carbonate platforms. *Journal of Geology* 101, 345-355.
- BRALOWER, T.J., LUDWIG, K.R., OBRADOVICH, J.D. & JONES, D.L. (1990) Berriasian (Early Cretaceous) radiometric ages from the Grindstone Creek Section, Sacramento Valley, California. *Earth and Planetary Science Letters* 98, 62-73.
- BRETT, C.E. (1998) Sequence stratigraphy, paleoecology, and evolution: Biotic clues and responses to sea-level fluctuations. *Palaaios* 13, 241-262.
- BRUNSDEN, D. (2003) The official guide to the Jurassic coast. Dorset and East Devon's World Heritage Coast. 64pp. (Coastal Publishing).
- BUCUR, I.I., KOCH, R., KIRMACI, Z.M. & KEMAL, T. (2004) Foraminifères du Jurassique supérieur et du Crétacé inférieur (Calcaire de Berdiga) de Kircaova (région de Kale-Gümüşhane, NE Turquie). *Rev. Paléobiologie* 23 (1), 209-225.
- BUCUR, I.I. & SĂSĂRAN, E. (2005) Relationship between algae and environment: An Early Cretaceous case study, Trascau Mountains, Romania. *Facies* 1, 1-13.
- BUDD, D.A., GASWIRTH, S.B. & OLIVER, W.L. (2002) Quantification of macroscopic subaerial exposure features in carbonate rocks. *J. Sed. Res.* 72, 917-928.
- BUONOCUNTO, F.P., D'ARGENIO, B., FERRERI, V. & SANDULLI, R. (1999) Orbital cyclostratigraphy and sequence stratigraphy of Upper Cretaceous platform carbonates at Monte Sant' Erasmo, southern Apennines, Italy. *Cretaceous Research* 20, 81-95.
- BURCHETTE, T.P., WRIGHT, V.P. & FAULKNER, T.J. (1990) Oolitic sandbody depositional models and geometries, Mississippian of southwest Britain: Implications for petroleum exploration

- in carbonate ramp settings. *Sedimentary Geology* 68, 87-115.
- BURGER, H. (1982) Tonmineralische und sedimentpetrographische Untersuchungen in der untersten Kreide des östlichen Helvetikums. *Schweiz. mineral. petrogr. Mitt.* 62, 369-414.
- BURGER, H. (1986) Fazielle Entwicklung und paläographische Rekonstruktion des helvetischen Schelfs während der untersten Kreide in der Zentral- und Ostschweiz. *Eclogae geol. Helv.* 79 (2), 561-615.
- BURGESS, P.M. & WRIGHT, V.P. (2003) Numerical forward modeling of carbonate platform dynamics: An evaluation of complexity and completeness in carbonate strata. *J. Sed. Res.* 73 (5), 637-652.
- BURNE, R.V., BAULD, J.R. & DE DECKKER, R. (1980) Saline lake charophytes and their geological significance. *J. Sed. Petro.* 50, 281-293.
- BURTON, R., KENDALL, C.G.S.C. & LERCHE, I. (1987) Out of our depth: On the impossibility of fathoming eustasy from the stratigraphic record. *Earth Sci. Rev.* 24, 237-277.
- CARBONEL, P., COLIN, J.-P., DANIELOPOL, D.L., LÖFFLER, H. & NEUSTRUEVA, I. (1988) Paleoecology of limnic ostracodes: A review of some major topics. *Palaeogeogr., Palaeoclim., Palaeoecol.* 62, 413-461.
- CAROZZI, A. (1948) Etude stratigraphique et micrographique du Purbeckien du Jura suisse. PhD thesis, 175pp. (University of Geneva, Suisse).
- CARTER, R.M. (1998) Two models: Global sea-level change and sequence stratigraphic architecture. *Sedimentary Geology* 122 (1-4), 23-36.
- CASEY, R. (1973) The ammonite succession at the Jurassic-Cretaceous boundary in eastern England. In: CASEY, R. & RAWSON, P.F. (eds) *The Boreal lower Cretaceous*. 193-266 (Seel House Press).
- CASTANIER, S., LE MÉTAYER-LEVREL, G. & PERTHUISOT, J.-P. (1999) Ca-carbonates precipitation and limestone genesis - the microbiogeologist point of view. *Sedimentary Geology* 126 (1-4), 9-23.
- CASTANIER, S., LE MÉTAYER-LEVREL, G. & PERTHUISOT, J.-P. (2000) Bacterial roles in the precipitation of carbonate minerals. In: RIDING, R.E. & AWRAMIK, S.M. (eds) *Microbial sediments*. 32-39 (Springer Verlag).
- CAVAZZA, W., ROURE, F., SPAKMAN, W., STAMPFLI, G.M. & ZIEGLER, P.A. (2004) *The TRANSMED Atlas: The Mediterranean region from crust to mantle*. 141pp. (Springer).
- CECCA, F., SAVARY, B., BARTOLINI, A., REMANE, J. & CORDEY, F. (2001) The Middle Jurassic-Lower Cretaceous Rosso Ammonitico succession of Monte Inici (Trapanese domain, western Sicily): Sedimentology, biostratigraphy and isotope stratigraphy. *Bull. Soc. géol. France* 172 (5), 647-660.
- CECCA, F., VRIELYNCK, B., LAVOYER, T. & GAGET, H. (2005) Changes in the ammonite taxonomical diversity gradient during the Late Jurassic-Early Cretaceous. *J. Biogeogr.* 32, 535-547.
- CHADWICK, R.A. (1986) Extension tectonics in the Wessex Basin, southern England. *J. Geol. Soc. London* 143, 465-488.
- CHAFETZ, H.S. (1986) Marine peloids: A product of bacterially induced precipitation of calcite. *J. Sed. Petro.* 56 (6), 812-817.
- CHAMLEY, H. (1989) *Clay sedimentology*. 622pp. (Springer).
- CHANNELL, J.E.T., BRALOWER, T.J. & GRANDESSO, P. (1987) Biostratigraphic correlation of Mesozoic polarity chrons CM1 to CM23 at Capriolo and Xausa (Southern Alps, Italy). *Earth and Planetary Science Letters* 85, 203-221.
- CHANNELL, J.E.T. & GRANDESSO, P. (1987) A revised correlation of Mesozoic polarity chrons and calpionellid zones. *Earth and Planetary Science Letters* 85, 222-240.
- CHANNELL, J.E.T., ERBA, E., NAKANISHI, M. & TAMAKI, K. (1995) Late Jurassic-Early Cretaceous time scales and oceanic magnetic anomaly block models. In: BERGGREN, W.A., KENT, D.V., AUBRY, M.-P. & HARDENBOL, J. (eds) *Geochronology, time scales, and global stratigraphic correlation*. SEPM Spec. Publ. 54, 51-63.
- CHAROLLAIS, J., CLAVEL, B., AMATO, E., ESCHER, A., BUSNARDO, R., STEINHAUSER, N., MACSOTAY, O. & DONZE, P. (1983) Etude préliminaire de la faille du Vuache (Jura méridional). *Bull. Soc. vaud. Sci. nat.* 76, 217-256.
- CHERCHI, A. & SCHROEDER, R. (2006) Remarks on the systematic position of *Lithocodium* Elliott, a problematic microorganism from the Mesozoic carbonate platforms of the Tethyan realm. *Facies* 52, 435-440.
- CLARI, P.A., DELA PIERRE, F. & MARTIRE, L. (1995) Discontinuities in carbonate successions: Identification, interpretation, and classification of some Italian examples. *Sedimentary Geology* 100, 97-121.
- CLAVEL, B., CHAROLLAIS, J., BUSNARDO, R. & LE HÉGARAT, G. (1986) Précision stratigraphique sur le Crétacé inférieur basal du Jura méridional. *Eclogae geol. Helv.* 79, 319-341.
- CLEMENTS, R.G. (1993) Type-section of the Purbeck Limestone Group, Durlston Bay, Swanage, Dorset. *Proceedings of the Dorset Natural History and Archeological Society* 114, 181-206.
- CLOETINGH, S. (1988) Intraplate stresses: A tectonic cause for third-order cycles in apparent sea level? In: WILGUS, C.E., HASTINGS, B.S., KENDALL, C.G.S.C., POSAMENTIER, H.W., ROSS, C.A. & VAN WAGONER, J.C. (eds) *Sea-level changes - an integrated approach*. SEPM Special Publ. 42, 19-29.
- CLOETINGH, S. (1991) Tectonics and sea-level changes: A controversy. In: MÜLLER, D.W., MCKENZIE, J.A. & WEISSERT, H. (eds) *Controversy in modern geology*. 249-277 (Academic Press Limited).
- CLOYD, K.C., DEMICCO, R.V. & SPENCER, R.J. (1990) Tidal channel, levee, and crevasse-splay deposits from a Cambrian tidal channel system: A new mechanism to produce shallowing-upward sequences. *J. Sed. Petro.* 60 (1), 73-83.
- COLLINSON, J.D. & THOMPSON, D.B. (1982) *Sedimentary*

- structures. 194pp. (George Allen & Unwin Ltd.).
- COLIN, J.-P. & LETHIERS, F. (1988) The importance of ostracods in biostratigraphic analysis. In: DE DEKKER, P. (ed) *Ostracoda in the Earth Sciences*. 27-45 (Elsevier).
- COLIN, J.-P., EL ALBANI, A., FÜRSICH, F.T., MARTÍN-CLOSAS, C., MAZIN, J.-M. & BILLON-BRUYAT, J.-P. (2004) Le gisement Purbeckien de vertébrés de Cherves-de-Cognac, Charente (SW France): Nouvelles données biostratigraphiques. *C. R. Palevol* 3 (1), 9-16.
- COLOMBIÉ, C. (2002) Sédimentologie, stratigraphie séquentielle et cyclostratigraphie du Kimméridgien du Jura suisse et Bassin vocontien (France): Relations plat-forme - bassin et facteurs déterminants. *GeoFocus* 4, 198pp.
- COLOMBIÉ, C. & STRASSER, A. (2003) Depositional sequences in the Kimmeridgian of the Vocontian Basin (France) controlled by carbonate export from shallow-water platforms. *Geobios* 36 (6), 675-683.
- COLOMBIÉ, C. & STRASSER, A. (2005) Facies, cycles, and controls on the evolution of a keep-up carbonate platform (Kimmeridgian, Swiss Jura). *Sedimentology* 52 (6), 1207-1227.
- COOPER, J.A.G. (1994) Lagoons and microtidal coasts. In: CARTER, R.W.G. & WOODROFFE, C.D. (eds) *Coastal evolution - Late Quaternary shoreline morphodynamics*. 219-265 (Cambridge University Press).
- COOPS, H. (2002) Ecology of charophytes: An introduction. *Aquatic Botany* 72 (3-4), 205-208.
- CORAM, R.A. & JARZEMBOWSKI, E.A. (2002) Diversity and ecology of fossil insects in the Dorset Purbeck succession, southern England. In: MILNER, A.R. & BATTEN, D.J. (eds) *Life and environments in Purbeck times*. 257-268 (The Palaeontological Association London).
- COTILLON, P., FERRY, S., GAILLARD, C., JAUTÉE, E., LATREILLE, G. & RIO, M. (1980) Fluctuation des paramètres du milieu marin dans le domaine vocontien (France Sud-Est) au Crétacé inférieur: Mise en évidence par l'étude des formations marno-calcaires alternantes. *Bull. Soc. géol. France* 5, 735-744.
- COTILLON, P. (1995) Constraints for using high-frequency sedimentary cycles in cyclostratigraphy. In: HOUSE, M.R. & GALE, A.S. (eds) *Orbital forcing timescales and cyclostratigraphy*. GSA Spec. Publ. 85, 133-141.
- COVEY, C. & BARRON, E.J. (1988) The role of ocean heat transport in climatic change. *Earth Sci. Rev.* 24, 429-445.
- COWELL, P.J. & THOM, B.G. (1994) Morphodynamics of coastal evolution. In: CARTER, R.W.G. & WOODROFFE, C.D. (eds) *Coastal evolution - Late Quaternary shoreline morphodynamics*. 33-86 (Cambridge University Press).
- CRONIN, T.M. (1999) *Principles of paleoclimatology*. 560pp. (Columbia University Press).
- CURNELLE, R. & DUBOIS, P. (1986) Evolution mésozoïque des grands bassins sédimentaires français: Bassins de Paris, d'Aquitaine et du Sud-Est. *Bull. Soc. géol. France* 4, 529-546.
- CURTIS, C.D. (1990) Aspects of climatic influence on the clay mineralogy and geochemistry of soils, palaeosols, and clastic sedimentary rocks. *J. Geol. Soc. London* 147, 351-357.
- DAHANAYAKE, K. (1977) Classification of oncoids from the Upper Jurassic carbonates of the French Jura. *Sedimentary Geology* 18, 337-353.
- DAHANAYAKE, K. (1983) Depositional environments of some Upper Jurassic oncoids. In: PERYT, T.M. (ed) *Coated Grains*. 377-385 (Springer).
- DALMASSO, H. & FLOQUET, M. (2001) Relation accommodation-production carbonatée dans le développement de séquences de dépôt élémentaires de plate-forme carbonatée: La série d'âge Tithonien-Berriasien de basse Provence occidentale. *Earth and Planetary Sciences* 333, 209-217.
- DARGA, R. & SCHLAGINTWEIT, F. (1991) Mikrofazies, Paläontologie und Stratigraphie der Lerchkogelkalke (Tithon-Berrias) des Dietrichshorns (Salzburger Land, Nördliche Kalkalpen). *Jb. Geol. B.-A.* 134 (2), 205-226.
- D'ARGENIO, B. & MINDSZENTY, A. (1995) Bauxites and related paleokarst: Tectonic and climatic event markers at regional unconformities. *Eclogae geol. Helv.* 88 (3), 453-499.
- D'ARGENIO, B., FERRERI, V., AMODIO, S. & PELOSI, N. (1997) Hierarchy of high-frequency orbital cycles in Cretaceous carbonate platform strata. *Sedimentary Geology* 113, 169-193.
- D'ARGENIO, B., FERRERI, V., RASPINI, A., AMODIO, S. & BUONOCUNTO, F.P. (1999) Cyclostratigraphy of a carbonate platform as a tool for high-precision correlation. *Tectonophysics* 315, 357-385.
- D'ARGENIO, B., FISCHER, A.G., PREMOLI SILVA, I., WEISSERT, H. & FERRERI, V. (2004a) Cyclostratigraphy: Approaches and case histories. *SEPM Spec. Publ.* 81, 311pp.
- D'ARGENIO, B., FERRERI, V., WEISSERT, H., AMODIO, S., BUONOCUNTO, F.P. & WISSLER, L. (2004b) A multidisciplinary approach to global correlation and geochronology, the Cretaceous shallow-water carbonates of southern Apennines, Italy. In: D'ARGENIO, B., FISCHER, A.G., PREMOLI SILVA, I., WEISSERT, H. & FERRERI, V. (eds) *SEPM Spec. Publ.* 81, 103-122.
- DA ROSA, A.A.S. & GARCIA, A.J.V. (2000) Palaeobiogeographic aspects of northeast Brazilian basins during the Berriasian before the break up of Gondwana. *Cretaceous Research* 21, 221-239.
- DARSAC, C. (1983) La plat-forme berriasio-valanginienne du Jura méridional aux massifs subalpins (Ain, Savoie). PhD thesis, 319pp. (University of Geneva, Switzerland).
- DAVAUD, E., STRASSER, A. & CHAROLLAIS, J. (1983) Présence d'horizons calcrétisés dans le Purbeckien du Jura méridional: Extension spatiale et conséquences paléogéographiques. *C. R. Acad. Sci.* 296, 575-578.
- DAVIES, P.J., BUBELA, B. & FERGUSON, J. (1978) The formation of ooids. *Sedimentology* 25, 703-730.
- DE BOER, P.L. & SMITH D., G. (1994a) Orbital forcing and cyclic

- sequences. IAS Spec. Publ. 19, 559pp.
- DE BOER, P.L. & SMITH, D.G. (1994b) Orbital forcing and cyclic sequences. In: DE BOER, P.L. & SMITH, D.G. (eds) Orbital forcing and cyclic sequences. IAS Spec. Publ. 19, 1-14.
- DECONINCK, J.-F., BEAUDOIN, B., CHAMLEY, H., JOSEPH, P. & RAOULT, J.-F. (1985) Contrôles tectonique, eustatique et climatique de la sédimentation argileuse du domaine subalpin français au Malm-Crétacé. *Rev. de Géol. Dynamique et de Géograph. Physique* 26 (5), 311-320.
- DECONINCK, J.-F. & DEBRABANT, P. (1985) Diagenèse des argiles dans le domaine subalpin: Rôles respectifs de la lithologie, de l'enfouissement et de la surcharge tectonique. *Rev. de Géol. Dynamique et de Géograph. Physique* 26 (5), 321-330.
- DECONINCK, J.-F. & STRASSER, A. (1987) Sedimentology, clay mineralogy, and depositional environment of Purbeckian green marls (Swiss and French Jura). *Eclogae geol. Helv.* 80 (3), 753-772.
- DECONINCK, J.-F. (1987) Minéraux argileux des faciès purbeckiens: Jura suisse et français, Dorset (Angleterre) et Boulonnais (France). *Ann. Soc. Géol. Nord*, 285-297.
- DECONINCK, J.-F., STRASSER, A. & DEBRABANT, P. (1988) Formation of illitic minerals at surface temperatures in Purbeckian sediments (Lower Berriasian, Swiss and French Jura). *Clay Minerals* 23, 91-103.
- DECONINCK, J.-F. (1993) Clay mineralogy of the Late Tithonian-Berriasian deep-sea carbonates of the Vocontian Trough (SE France): Relationships with sequence stratigraphy. *Bull. Centres Rech. Explor.-Prod. Elf Aquitaine* 17, 223-234.
- DECONINCK, J.-F., BAUDIN, F. & TRIBOVILLARD, N. (2000) The Purbeckian facies of the Boulonnais: A tsunami deposit hypothesis (Jurassic-Cretaceous boundary, northern France). *C. R. Acad. Sci.* 330, 527-532.
- DECONINCK, J.-F., GILLOT, P.-Y., STEINBERG, M. & STRASSER, A. (2001) Syn-depositional, low temperature illite formation at the Jurassic-Cretaceous boundary (Purbeckian) in the Jura Mountains (Switzerland and France): K/Ar and  $\delta^{18}\text{O}$  evidence. *Bull. Soc. géol. France* 173 (3), 343-348.
- DE GRACIANSKY, P.-C., HARDENBOL, J., JACQUIN, T. & VAIL, P.R. (1998) Mesozoic and Cenozoic sequence stratigraphy of European basins. *SEPM Spec. Publ.* 60, 786pp.
- DELAIR, J.B. & SARJEANT, W.A.S. (1985) History and bibliography of the study of fossil vertebrate footprints in the British Isles: Supplement 1973-1983. *Palaeogeogr., Palaeoclim., Palaeoecol.* 49, 123-160.
- DEMICO, R.V. (1983) Wavy and lenticular-bedded carbonate ribbon rocks of the Upper Cambrian Conococheague Limestone, Central Appalachians. *J. Sed. Petro* 53 (4), 1121-1132.
- DEMICO, R.V. & HARDIE, L.A. (1994) Sedimentary structures and early diagenetic features of shallow marine carbonate deposits. *SEPM Atlas Serie* 1, 256pp.
- DEMICO, R.V. & HARDIE, L.A. (2002) The "carbonate factory" revisited: A reexamination of sediment production functions used to model deposition on carbonate platforms. *J. Sed. Res* 72 (6), 849-857.
- DERCOURT, J. (1997) Géologie et géodynamique de la France. 318pp. (Dunod).
- DÉTRAZ, H., CHAROLLAIS, J. & REMANE, J. (1987) Le Jurassique supérieur-Valanginien des chaînes subalpines septentrionales (massifs des Bornes et de Platé, Haute-Savoie; Alpes occidentales): Analyse des résédimentations, architecture du bassin et influences des bordures. *Eclogae geol. Helv.* 80 (1), 69-108.
- DÉTRAZ, H. & STEINHAUSER, N. (1988) Le bassin delphino-helvétique et sa marge jurassienne sous contrôle tectonique entre le Kimméridgien et le Valanginien. *Eclogae geol. Helv.* 81 (1), 125-154.
- DÉTRAZ, H. (1989) Exemple de sédimentation sur une plate-forme externe bioclastique dominée par les marées: L'Autochtone de St.Maurice (Valais, Suisse) au Berriasian-Valangien. *Eclogae geol. Helv.* 82 (3), 795-815.
- DÉTRAZ, H. & MOJON, P.-O. (1989) Evolution paléogéographique de la marge jurassienne de la Téthys du Tithonique-Portlandien au Valangien: Corrélations biostratigraphique et séquentielle des faciès marins à continentaux. *Eclogae geol. Helv.* 82, 37-112.
- DEWEY, J.F. & PITMAN, W.C. (1998) Sea-level changes: Mechanisms, magnitudes and rates. In: PINDELL, J. L. & DRAKE, C. (eds) Paleogeographic evolution and non-glacial eustasy, northern South America. *SEPM Spec. Publ.* 58, 1-16.
- DIENI, I. & RADOIČIĆ, R. (1999) *Clypeina dragastani* sp. nov., *Salpingoporella granieri* sp. nov. and other dasycladalean algae from the Berriasian of Eastern Sardinia. *Acta Palaeont. Romaniae* 2, 105-123.
- DÖRHÖFER, G. & NORRIS, G. (1977a) Palynostratigraphische Beiträge zur Korrelierung jurassischer-kretazischer Grenzsichten in Deutschland und England. *N. Jb. Geol. Paläont. Abh.* 153 (1), 50-69.
- DÖRHÖFER, G. & NORRIS, G. (1977b) Discrimination and correlation of highest Jurassic and lowest Cretaceous terrestrial palynofloras in North-West Europe. *Palynology* 1, 79-93.
- DONOVAN, D.T. & JONES, E.J.W. (1979) Causes of world-wide changes in sea level. *J. Geol. Soc. London* 136, 187-192.
- DONZE, P. (1953) Sur des particularités remarquables de la microfaune dans certaines formations peu profondes jurassico-crétacées du Jura méridional: Une coupe du Purbeckien dans la région du Poizat. *C. R. S. Soc. Géol. France* 13.
- DORÉ, A.G. (1991) The structural foundation and evolution of Mesozoic seaways between Europe and the Arctic. *Palaeogeogr., Palaeoclim., Palaeoecol.* 87, 441-492.
- DOUGLAS, J.G. & WILLIAMS, G.E. (1982) Southern polar forests: The Early Cretaceous floras of Victoria and their palaeoclimatic significance. *Palaeogeogr., Palaeoclim., Palaeoecol.* 39, 171-185.
- DRAVIS, J.J. (1996) Rapidity of freshwater calcite cementation - implications for carbonate diagenesis and sequence strati-

- graphy. *Sedimentary Geology* 107, 1-10.
- DRUMMOND, C.N. & WILKINSON, B.H. (1993a) Carbonate cycle stacking patterns and hierarchies of orbitally forced eustatic sea level change. *J. Sed. Petro.* 63 (3), 369-377.
- DRUMMOND, C.N. & WILKINSON, B.H. (1993b) Aperiodic accumulation of cyclic peritidal carbonate. *Geology* 21, 1023-1026.
- DUPRAZ, C. (1999) Paléontologie, paléoécologie et évolution des faciès récifaux de l'Oxfordien Moyen-Supérieur (Jura suisse et français). *GeoFocus* 2, 200pp.
- DUPRAZ, C. & STRASSER, A. (1999) Microbialites and micro-encrusters in shallow coral bioherms (Middle to Late Oxfordian, Swiss Jura Mountains). *Facies* 40, 101-130.
- DYPRVİK, H., GUDLAUGSSON, S.T., TSICALAS, F., ATTREP, M., FERRELL, R.E., KRINSLEY, D.H., MØRK, A., FALÉIDE, J.I. & NAGY, J. (1996) Mjølner structure: An impact crater in the Barents Sea. *Geology* 24 (9), 779-782.
- EBLI, O. & SCHLAGINTWEIT, F. (1998) On some biostratigraphically important microfossils (benthic foraminifera, dasycladales) from subsurface Late Jurassic-Early Cretaceous shallow-water limestones of S-Germany. *Mitt. Bayer. Staatsslg. Paläont. hist. Geol.* 38, 9-23.
- EINSELE, G. & RICKEN, W. (1991a) Limestone-marl alternation - an overview. In: EINSELE, G., RICKEN, W. & SEILACHER, A. (eds) *Cycles and events in stratigraphy*. 24-47 (Springer).
- EINSELE, G. & RICKEN, W. (1991b) Introductory remarks. In: EINSELE, G., RICKEN, W. & SEILACHER, A. (eds) *Cycles and events in stratigraphy*. 611-616 (Springer).
- EL-SHAHAT, A. & WEST, I. (1983) Early and late lithification of aragonitic bivalve beds in the Purbeck Formation (Upper Jurassic-Lower Cretaceous) of southern England. *Sedimentary Geology* 35, 15-41.
- EL ALBANI, A., FÜRSICH, F.T., COLIN, J.-P., MEUNIER, M., HOCHULI, P., MARTÍN-CLOSAS, C., MAZIN, J.-M. & BILLON-BRUYAT, J.-P. (2004) Palaeoenvironmental reconstruction of the basal Cretaceous vertebrate bearing beds in the northern part of the Aquitaine Basin (SW France): Sedimentological and geochemical evidence. *Facies* 50, 195-215.
- EL ALBANI, A., MEUNIER, M. & FÜRSICH, F.T. (2005) Unusual occurrence of glauconite in a shallow lagoonal environment (Lower Cretaceous, northern Aquitaine Basin, SW France). *Terra Nova* 17, 537-544.
- ELSTNER, F. & MUTTERLOSE, J. (1996) The Lower Cretaceous (Berriasian and Valanginian) in NW Germany. *Cretaceous Research* 17, 119-133.
- EMBRY, A.F. (2002) Transgressive-Regressive (T-R) sequence stratigraphy. 22nd Annual Gulf Coast Section SEPM Foundation Bob F. Perkins Research Conference. 151-172.
- EMMANUEL, L. & RENARD, M. (1993) Carbonate geochemistry (Mn,  $\delta^{13}\text{C}$ ,  $\delta^{18}\text{O}$ ) of the Late Tithonian-Berriasian pelagic limestones of the Vocontian Trough (SE France). *Bull. Centres Rech. Explor.-Prod. Elf Aquitaine* 17, 205-221.
- ENSOM, P.C. (1985) An annotated section of the Purbeck Limestone Formation at Worbarrow Tout, Dorset. *Proceedings of the Dorset Natural History and Archeological Society* 106, 87-91.
- ENSOM, P. (2002a) The Purbeck Limestone Group of Dorset, southern England: A guide to lithostratigraphic terms. In: MILNER, A.R. & BATTEN, D.J. (eds) *Life and environments in Purbeck times*. 7-11 (The Palaeontological Association London).
- ENSOM, P. (2002b) Vertebrate trace fossils in the Purbeck Limestone Group of southern England. In: MILNER, A.R. & BATTEN, D.J. (eds) *Life and environments in Purbeck times*. 203-220 (The Palaeontological Association London).
- ESTEBAN, M. & KLAPPA, C.F. (1983) Subaerial exposure. In: SCHOLLE, P.A., BEBOUT, D.G. & MOORE, C.H. (eds) *Carbonate depositional environments*. AAPG Mem. 33, 1-54.
- EVANS, S.E. & SEARLE, B. (2002) Lepidosaurian reptiles from the Purbeck Limestone Group of Dorset, southern England. In: MILNER, A.R. & BATTEN, D.J. (eds) *Life and environments in Purbeck times*. 145-159 (The Palaeontological Association London).
- EYLES, N. (1993) Earth's glacial record and its tectonic setting. *Earth Sci. Rev.* 35 (1), 1-248.
- FAIRBRIDGE, R.W. (1976) Convergence of evidence on climatic change in ice ages. *Annals New York Academy of Science* 91, 542-579.
- FALCONNIER, A. (1931) Etude géologique de la région du col du Marchairuz. *Matér. Carte géol. Suisse (n.s.)* 27, 1-31.
- FEIST, M. & SCHUDACK, M.E. (1991) Correlation of charophyte assemblages from the nonmarine Jurassic-Cretaceous transitions of NW Germany. *Cretaceous Research* 12, 495-510.
- FEIST, M., LAKE, R.D. & WOOD, C.L. (1995) Charophyte biostratigraphy of the Purbeck and Wealden of southern England. *Palaeontology* 38 (2), 407-442.
- FISCHER, A.G. (1986) Climatic rhythms recorded in strata. *Ann. Rev. Earth Planet. Sci.* 14, 351-376.
- FISCHER, A.G., DE BOER, P.L. & PREMOLI SILVA, I. (1990) Cyclostratigraphy. In: GINSBURG, R.N. & BEAUDOIN, B. (eds) *Cretaceous resources, events and rhythms*. 139-172 (Kluwer).
- FISCHER, A.G. (1991) Orbital cyclicity in Mesozoic strata. In: EINSELE, G., RICKEN, W. & SEILACHER, A. (eds) 48-62 (Springer).
- FISCHER, A.G., D'ARGENIO, B., PREMOLI, S.I., WEISSERT, H. & FERRERI, V. (2004) Cyclostratigraphic approach to Earth's history: An introduction. *SEPM Spec. Publ.* 81, 5-13.
- FLESSA, K.W. (1998) Well-traveled cockles: Shell transport during the Holocene transgression of the southern North Sea. *Geology* 26 (2), 187-190.
- FLEXER, A., ROSENFELD, A., LIPSON-BENITAH, S. & HONIGSTEIN, A. (1986) Relative sea-level changes during the Cretaceous in Israel. *AAGP Bulletin* 70 (11), 1685-1699.
- FOOS, A. (1996) Comparison of subaerial exposure surfaces at major unconformities and capping shallowing-upward

- carbonate cycles. In: WITZKE, B.J., LUDVIGSON, G.A. & DAY, J. (eds) *Paleozoic sequence stratigraphy: Views from the North American Craton*. GSA Spec. Paper 306, 419-424.
- FLÜGEL, E. (1982) *Microfacies analysis of limestones*. 633pp. (Springer).
- FLÜGEL, E. (2004) *Microfacies of carbonate rocks: Analysis, interpretation and application*. 976pp. (Springer).
- FOLK, R.L. & CHAFETZ, H.S. (2000) Bacterially induced microscale and nanoscale carbonate precipitates. In: RIDING, R.E. & AWRAMIK, S.M. (eds) *Microbial sediments*. 40-49 (Springer).
- FRAKES, L.A. & FRANCIS, J.E. (1988) A guide to Phanerozoic cold polar climates from high-latitude ice-rafting in the Cretaceous. *Nature* 333, 457-549.
- FRAKES, L.A. & FRANCIS, J.E. (1990) Cretaceous palaeoclimates. In: GINSBURG, R.N. & BEAUDOIN, B. (eds) *Cretaceous resources, events and rhythms*. 273-287 (Kluwer).
- FRAKES, L.A., FRANCIS, J.E. & SYKTUS, J.I. (1992) *Climate modes of the Phanerozoic*. 1-270 (Cambridge University Press).
- FRAKES, L.A., ALLEY, N.F. & DEYNOUX, M. (1995) Early Cretaceous ice-rafting and climate zonation in Australia. *Int. Geol. Rev.* 37, 567-583.
- FRANCIS, J.E. (1983) The dominant conifer of the Jurassic Purbeck formation, England. *Palaeontology* 26 (2), 277-294.
- FRANCIS, J.E. (1984) The seasonal environment of the Purbeck (Upper Jurassic) fossil forests. *Palaeogeogr., Palaeoclim., Palaeoecol.* 48, 285-307.
- FRANCIS, J.E. & FRAKES, L.A. (1993) Cretaceous climates. In: WRIGHT, V.P. (ed) *Sedimentology Review/1*. 17-30 (Blackwell Scientific Publications).
- FRIEDMAN, G.M. (1998) Rapidity of marine carbonate cementation - implications for carbonate diagenesis and sequence stratigraphy: Perspective. *Sedimentary Geology* 119, 1-4.
- FÜRSICH, F.T. (1979) Genesis, environments, and ecology of Jurassic hardgrounds. *N. Jb. Geol. Paläont. Abh.* 158 (1), 1-63.
- FÜRSICH, F.T. (1993) Palaeoecology and evolution of Mesozoic salinity-controlled benthic macroinvertebrate associations. *Lethaia* 26, 327-346.
- FÜRSICH, F.T. & PANDEY, D.K. (2003) Sequence stratigraphic significance of sedimentary cycles and shell concentrations in the Upper Jurassic-Lower Cretaceous of Kachchh, western India. *Palaeogeogr., Palaeoclim., Palaeoecol.* 193, 285-309.
- FUNK, H. (1985) Mesozoische Subsidenzgeschichte im Helvetischen Schelf der Ostschweiz. *Eclogae geol. Helv.* 78 (2), 249-272.
- FUNK, H., FÖLLMI, K.B. & MOHR, H. (1993) Evolution of the Tithonian-Aptian carbonate platform along the Northern Tethyan margin, Eastern Helvetic Alps. In: SIMO, J.A.T., SCOTT, R.W. & MASSE, J.-P. (eds) *Cretaceous carbonate platforms*. AAPG Mem. 56, 387-407.
- FUNNELL, B.M. (1990) Global and European Cretaceous shorelines, stage by stage. In: GINSBURG, R.N. & BEAUDOIN, B. (eds) *Cretaceous resources, events and rhythms*. 221-272 (Kluwer).
- GALBRUN, B. (1985) Magnetostratigraphy of the Berriasian stratotype section (Berrias, France). *Earth and Planetary Science Letters* 74, 130-136.
- GALBRUN, B., RASPLUS, L. & LE HÉGARAT, G. (1986) Données nouvelles sur le stratotype du Berriasian: Corrélation entre magnétostratigraphie et biostratigraphie. *Bull. Soc. géol. France* 4, 575-584.
- GALE, A.S., HARDENBOL, J., HATHWAY, B., KENNEDY, W.J., YOUNG, J.R. & PHANSALKAR, V. (2002) Global correlation of Cenomanian (Upper Cretaceous) sequences: Evidence for Milankovitch control on sea level. *Geology* 30 (4), 291-294.
- GALLOWAY, W.E. (1989) Genetic stratigraphic sequences in basin analysis: I. Architecture and genesis of flooding-surface bounded depositional units. *AAPG. Bulletin* 73, 125-142.
- GEYER, M. (1992) Variations dans la composition de la fraction argileuse des calcaires tithoniques et berriasiens du domaine vocontien (SE France). *Eclogae geol. Helv.* 85 (2), 385-398.
- GIRAUD, F., BEAUFORT, L. & COTILLON, P. (1995a) Periodicities of carbonate cycles in the Valanginian of the Vocontian Trough: A strong obliquity control. In: HOUSE, M.R. & GALE, A.S. (eds) *Orbital forcing timescales and cyclostratigraphy*. GSA Spec. Publ. 89, 143-164.
- GIRAUD, F., BEAUFORT, L. & COTILLON, P. (1995b) Contrôle astronomique de la sédimentation carbonatée dans le Crétacé inférieur du Bassin vocontien (SE France). *Bull. Soc. géol. France* 4, 409-421.
- GISCHLER, E. & LOMANDO, A.J. (1999) Recent sedimentary facies of isolated carbonate platforms, Belize-Yucatan system, Central America. *J. Sed. Res.* 69 (3), 747-763.
- GOLDHAMMER, R.K., DUNN, P.A. & HARDIE, L.A. (1987) High frequency glacio-eustatic sea level oscillations with Milankovitch characteristics recorded in Middle Triassic platform carbonates in Northern Italy. *American Journal of Science* 287, 853-892.
- GOLDHAMMER, R.K., DUNN, P.A. & HARDIE, L.A. (1990) Depositional cycles, composite sea-level changes, cycle stacking patterns, and the hierarchy of stratigraphic forcing: Examples from Alpine Triassic platform carbonates. *GSA Bull.* 102, 535-562.
- GOLDHAMMER, R.K., LEHMANN, C. & DUNN, P.A. (1993) The origin of high-frequency platform carbonate cycles and third-order sequences (Lower Ordovician El Paso GP, West Texas): Constraints from outcrop data and stratigraphic modeling. *J. Sed. Res.* 63 (3), 318-359.
- GOLDSTEIN, R.H. (1991) Stable isotope signatures associated with palaeosols, Pennsylvanian Holder Formation, New Mexico. *Sedimentology* 38, 67-77.
- GOLONKA, J. (2004) Plate tectonic evolution of the southern margin of Eurasia in the Mesozoic and Cenozoic. *Tectonophysics* 381 (1-4), 235-273.
- GOODWIN, P.W. & ANDERSON, E.J. (1985) Punctuated ag-

- gradational cycles: A general hypothesis of episodic stratigraphical accumulation. *J. Geol.* 93 (5), 515-533.
- GORIN, E.G. & STEFFEN, D. (1991) Organic facies as a tool for recording eustatic variations in marine fine-grained carbonates - example of the Berriasian stratotype at Berrias (Ardèche, SE France). *Palaeogeogr., Palaeoclim., Palaeoecol.* 85, 303-320.
- GORNITZ, V., LEBEDEFF, S. & HANSEN, J. (1982) Global sea-level trend in the past century. *Science* 215, 1611-1614.
- GRADSTEIN, F.M., AGTERBERG, F.P., OGG, J.G., HARDENBOL, J., VAN VEEN, P., THIERRY, J. & HUANG, Z. (1995) A Triassic, Jurassic and Cretaceous time scale. *Geochronology time scales and global stratigraphic correlations*. SEPM Spec. Publ. 54, 95-126.
- GRADSTEIN, F.M., OGG, J.G. & G., S.A. (2004) A geologic time scale 2004. 589pp. (University Press Cambridge).
- GRANIER, B. & DELOFFRE, R. (1993) Inventaire critique des algues dasycladales fossiles II partie - les algues dasycladales du Jurassique et du Crétacé. *Rev. Paléobiologie* 12 (1), 19-65.
- GRÖCKE, D.R., PRICE, G.D., RUFFELL, A.H., MUTTERLOSE, J. & BARABOSHIN, E. (2003) Isotopic evidence for Late Jurassic-Early Cretaceous climate change. *Palaeogeogr., Palaeoclim., Palaeoecol.* 202, 97-118.
- GRÖTSCH, J., SCHROEDER, R., NOÉ, S. & FLÜGEL, E. (1993) Carbonate platforms as recorders of high-amplitude eustatic sea-level fluctuations: The late Albian *appenninica*-event. *Basin Research* 5, 197-212.
- GROTZINGER, J.P. (1986) Upward shallowing platform cycles: A response to 2.2 billion years of low-amplitude, high-frequency (Milankovitch band) sea level oscillations. *Paleoceanography* 1 (4), 403-416.
- GUILLOCHAU, F., ROBIN, C., ALLEMAND, P., BOURQUIN, S., BRAULT, N., DROMART, G., FRIEDENBERG, R., GARCIA, J.-P., GAULIER, J.-M., GAUMET, F., GROSDOY, B., HANOT, F., LE STRAT, P., METTRAUX, M., NALPAS, T., PRIJAC, C., RIGOLLET, C., SERRANO, O. & GRANDJEAN, G. (2000) Meso-Cenozoic geodynamic evolution of the Paris Basin: 3D stratigraphic constraints. *Geodynamica Acta* 13, 189-246.
- HÄFELI, C. (1966) Die Jura/Kreide-Grenzsichten im Bielerseegebiet (Kt. Bern). *Eclogae geol. Helv.* 59 (2), 565-695.
- HALLAM, A. (1981) Facies interpretation and the stratigraphic record. 291pp. (W. H. Freeman and Company).
- HALLAM, A. (1984) Continental humid and arid zones during the Jurassic and Cretaceous. *Palaeogeogr., Palaeoclim., Palaeoecol.* 47, 195-223.
- HALLAM, A. (1985) A review of Mesozoic climates. *J. Geol. Soc. London* 142, 433-445.
- HALLAM, A. (1986) Role of climate in affecting late Jurassic and early Cretaceous sedimentation in the North Atlantic. In: SUMMERHAYES, C.P. & SHACKLETON, N.J. (eds) *North Atlantic Palaeoceanography*. GSA. Spec. Publ. 21, 277-281.
- HALLAM, A., GROSE, J.A. & RUFFELL, A.H. (1991) Palaeoclimatic significance of changes in clay mineralogy across the Jurassic-Cretaceous boundary in England and France. *Palaeogeogr., Palaeoclim., Palaeoecol.* 81, 173-187.
- HALLAM, A. (1994) Jurassic climates as inferred from the sedimentary and fossil record. In: ALLEN, J.R.L., HOSKINS, B.J., SELLWOOD, B.W., SPICER, R.A. & VALDES, P.J. (eds) *Palaeoclimates and their modelling*. 79-88 (Chapman & Hall).
- HALLAM, A. (2001) A review of the broad pattern of Jurassic sea-level changes and their possible causes in the light of current knowledge. *Palaeogeogr., Palaeoclim., Palaeoecol.* 167 (1-2), 23-37.
- HALLOCK, P. & SCHLAGER, W. (1986) Nutrient excess and the demise of coral reefs and carbonate platforms. *Palaos* 1, 389-398.
- HAMMER, W.R. & HICKERSON, W.J. (1994) A crested theropod dinosaur from Antarctica. *Science* 264, 828-830.
- HANCOCK, P.L. & SKINNER, B.J. (2000) *The Oxford companion to the Earth*. 1174pp. (Oxford University Press).
- HAQ, B.U., HARDENBOL, J. & VAIL, P.R. (1987) Chronology of fluctuating sea levels since the Triassic (250 million years ago to present). *Science* 235, 1156-1167.
- HARDENBOL, J., THIERRY, J., FARLEY, M.B., JACQUIN, T., DE GRACIANSKY, P.-C. & VAIL, P.R. (1998) Mesozoic and Cenozoic sequence chronostratigraphic framework of European basins. In: DE GRACIANSKY, P.-C., HARDENBOL, J., JACQUIN, T. & VAIL, P.R. (eds) *Mesozoic and Cenozoic sequence stratigraphy of European Basins*. SEPM Spec. Publ. 60, 3-13.
- HARDIE, L.A., BOSELLINI, A. & GOLDDHAMMER, R.K. (1986) Repeated subaerial exposure of subtidal carbonate platforms, Triassic, northern Italy: Evidence for high-frequency sea-level oscillations on a 10<sup>4</sup>-year scale. *Paleoceanography* 1 (4), 447-457.
- HAY, W.W. (1995) Cretaceous paleoceanography. *Geologia Carpathica* 46 (5), 257-266.
- HAY, W.W. (2002) A new view of Cretaceous paleoceanography. In: MICHALIK, J. (ed) *Tethyan/Boreal Cretaceous correlation*. 11-37 (Slovak Academy of Sciences).
- HAYS, J.D., IMBRIE, J. & SHACKLETON, N.J. (1976) Variations in the Earth's orbit: Pacemaker of the ice ages. *Science* 194 (4270), 1121-1132.
- HILGEN, F., SCHWARZACHER, W. & STRASSER, A. (2004) Concept and definitions in cyclostratigraphy (second report of the cyclostratigraphy working group). In: D'ARGENIO, B., FISCHER, A. G., PREMOLI SILVA, I., WEISSERT H. & FERRERI, V. (eds) *Cyclostratigraphy: Approaches and case histories*. SEPM Spec. Publ. 81, 303-305.
- HILLGÄRTNER, H. (1998) Discontinuity surfaces on shallow-marine carbonate platform (Berriasian, Valanginian, France and Switzerland). *J. Sed. Res.* 68 (6), 1093-1108.
- HILLGÄRTNER, H. (1999) The evolution of the French Jura platform during the Late Berriasian to Early Valanginian: Controlling factors and timing. *GeoFocus* 1, 203pp.



- HILLGÄRTNER, H., DUPRAZ, C. & HUG, W. (2001) Microbially induced cementation of carbonate sands: Are micritic meniscus cements good indicators of vadose diagenesis? *Sedimentology* 48 (1), 117-131.
- HILLGÄRTNER, H. & STRASSER, A. (2003) Quantification of high-frequency sea-level fluctuations in shallow-water carbonates: An example from the Berriasian-Valanginian (French Jura). *Palaeogeogr., Palaeoclim., Palaeoecol.* 200 (1-4), 43-63.
- HINE, A.C. (1977) Lily Bank, Bahamas: History of an active oolite sand shoal. *J. Sed. Petro.* 47 (4), 1554-1582.
- HINNOV, F.A. (2000) New perspectives on orbitally forced stratigraphy. *Annu. Rev. Earth. Planet. Sci.* 28, 419-475.
- HOEDEMAEKER, P.J. & LEEREVELD, H. (1995) Ammonite evidence for long-term sea-level fluctuations between the 2nd and 3rd order in the lowest Cretaceous. *Cretaceous Research* 16, 231-241.
- HOEDEMAEKER, P.J. (2002) Correlating the uncorrelatables: A Tethyan-Boreal correlation of pre-Aptian Cretaceous strata. In: MICHALIK, J. (ed) *Tethyan/Boreal Cretaceous correlation*. 235-284 (Slovak Academy of Sciences).
- HOEDEMAEKER, P.J. & WALDEMAR HERNGREEN, G.F. (2003) Correlation of Tethyan and Boreal Berriasian-Barremian strata with emphasis on strata in the subsurface of the Netherlands. *Cretaceous Research* 24 (3), 253-275.
- HOMWOOD, P. (1996) The carbonate feedback system: Interaction between stratigraphic accommodation, ecological succession and the carbonate factory. *Bull. Soc. géol. France* 167 (6), 701-715.
- HORNE, D.J. (1995) A revised ostracod biostratigraphy for the Purbeck-Wealden of England. *Cretaceous Research* 16 (6), 639-663.
- HORNE, D.J. (2002) Ostracod biostratigraphy and palaeoecology of the Purbeck Limestone Group in southern England. In: MILNER, A.R. & BATTEN, D.J. (eds) *Life and environments in Purbeck times*. 53-70 (The Palaeontological Association London).
- HOUSE, M.R. (1985) A new approach to an absolute timescale from measurements of orbital cycles and sedimentary micro-rhythms. *Nature* 315, 721-725.
- HOUSE, M.R. & GALE, A.S. (1995) Orbital forcing timescales and cyclostratigraphy. *GSA Spec. Publ.* 85, 210pp.
- HOUSE, M.R. (1995) Orbital forcing timescales: An introduction. In: HOUSE, M.R. & GALE, A.S. (eds) *Orbital forcing timescales and cyclostratigraphy*. *GSA Spec. Publ.* 85. 1-18.
- HSÜ, K.J. & WINTERER, E.L. (1980) Discussion on causes of world-wide changes in sea level. *J. Geol. Soc. London* 137, 509-510.
- HUANG, Z., OGG, J.G. & GRADSTEIN, F.M. (1993) A quantitative study of Lower Cretaceous cyclic sequences from the Atlantic ocean and the Vocontian basin (SE France). *Paleoceanography* 8 (2), 275-291.
- HUBBARD, R.J. (1988) Age and significance of sequence boundaries on Jurassic and Early Cretaceous rifted continental margins. *AAPG Bull.* 72 (1), 49-72.
- HUDSON, D.J., CLEMENTS, R.G., RIDING, J.B., WAKEFIELD, M.I. & WALTON, W. (1995) Jurassic paleosalinities and brackish-water communities - a case study. *Palaios* 10, 392-407.
- HUG, W. (2003) Sequenzielle Faziesentwicklung der Karbonatplattform des Schweizer Jura im Späten Oxford und frühesten Kimmeridge. *GeoFocus* 7, 156pp.
- HUNT, C.O. (1987) Dinoflagellate cyst and acritarch assemblages in shallow-marine and marginal-marine carbonates: The Portland Sand, Portland Stone, and Purbeck Formations (Upper Jurassic/Lower Cretaceous) of southern England and northern France. In: HART, M.B. (ed) *Micropalaeontology of carbonate environments*. 208-225 (Ellis Horwood Ltd.).
- HUNT, D. & TUCKER, M.E. (1992) Stranded parasequences and the forced regressive wedge systems tract: Deposition during base-level fall. *Sedimentary Geology* 81, 1-9.
- HUNT, D. & TUCKER, M.E. (1995) Stranded parasequences and the forced regressive wedge systems tract: Deposition during base-level fall - reply. *Sedimentary Geology* 95 (1-2), 147-160.
- HUSINEC, A. & READ, J.F. (2006) Transgressive oversized radial ooid facies in the Late Jurassic Adriatic platform interior: Low-energy precipitates from highly supersaturated hypersaline waters. *GSA Bull.* 118 (5-6), 550-556.
- HUSINEC, A. & SOKAČ, B. (2006) Early Cretaceous benthic associations (foraminifera and calcareous algae) of a shallow tropical-water platform environment (Mljet Island, southern Croatia). *Cretaceous Research* 27, 418-441.
- IMBRIE, J. & IMBRIE, J.Z. (1980) Modeling the climatic response to orbital variations. *Science* 207, 943-953.
- IMBRIE, J., BOYLE, E.A., CLEMENS, S.C., DUFF, K.L., HOWARD, W.R., KUKLA, G., KUTZBACH, J., MARTINSON, D.G., MCINTYRE, A., MIX, A.C., MOLFINO, B., MORLEY, J.J., PETERSON, L.C., PISIAS, N.G., PRELL, W.L., RAYMO, M.E., SHACKLETON, N.J. & TOGGWEILER, J.R. (1992) On the structure and origin of major glaciation cycles: 1. Linear responses to Milankovitch forcing. *Paleoceanography* 7 (6), 701-738.
- IMBRIE, J., BERGER, A., BOYLE, E.A., CLEMENS, S.C., DUFFY, A., HOWARD, W.R., KUKLA, G., KUTZBACH, J., MARTINSON, D.G., MCINTYRE, A., MIX, A.C., MOLFINO, B., MORLEY, J.J., PETERSON, L.C., PISIAS, N.G., PRELL, W.L., RAYMO, M.E., SHACKLETON, N.J. & TOGGWEILER, J.R. (1993) On the structure and origin of major glaciation cycles: 2. The 100,000-year cycle. *Paleoceanography* 8 (6), 699-735.
- IMMENHAUSER, A., CREUSEN, A., ESTEBAN, M. & VONHOF, H.B. (2000) Recognition and interpretation of polygenic discontinuity surfaces in the Middle Cretaceous Shu'aiba, Nahr Umr, and Natih Formations of Northern Oman. *GeoArabia* 5, 299-323.
- IMMENHAUSER, A. & SCOTT, R.W. (2002) An estimate of Albian sea-level amplitudes and its implication for the duration of stratigraphic hiatuses. *Sedimentary Geology* 152, 19-28.
- IMMENHAUSER, A. & MATTHEWS, R.K. (2004) Albian sea-level

- cycles in Oman: The "Rosetta Stone" approach. *GeoArabia* 9, 11-46.
- IMMENHAUSER, A. (2005) High-rate sea-level change during the Mesozoic: New approaches to an old problem. *Sedimentary Geology* 175, 277-296.
- IRVINE, G.I., McDONALD, I., GALE, A.S. & REIMOLD, W.U. (2004) Platinum-group elements from the Purbeck Cinder Bed of England and Boulonnais of France: Implications for an impact event at the Jurassic-Cretaceous boundary. 66th Meeting of the Meteoritical Society, p. 97.
- ISCHI, H. (1978) Das Berriasien-Valanginien in der Wildhorn-Drusberg-Decke zwischen Thuner- und Vierwaldstättersee. PhD thesis, 142pp. (University of Bern, Switzerland).
- JACOBS, D.K. & SAHAGIAN, D.L. (1993) Climate-induced fluctuations in sea level during non-glacial times. *Nature* 361, 710-712.
- JACQUIN, T., DARDEAU, G., DURLET, C., DE GRACIANSKY, P.-C. & HANTZPERGUE, P. (1998) The North Sea cycle: An overview of 2<sup>nd</sup>-order transgressive/regressive facies cycles in Western Europe. In: DE GRACIANSKY, P.-C., HARDENBOL, J., JACQUIN, T. & VAIL, P. R. (eds) *Mesozoic and Cenozoic sequence stratigraphy of European Basins*. SEPM Spec. Publ. 60, 445-466.
- JACQUIN, T. & DE GRACIANSKY, P.-C. (1998) Transgressive/Regressive (second order) facies cycles: The effects of tectono-eustasy. In: DE GRACIANSKY, P.-C., HARDENBOL, J., JACQUIN, T. & VAIL, P.R. (eds) *Mesozoic and Cenozoic sequence stratigraphy of European basins*. SEPM Spec. Publ. 60, 31-42.
- JAN DU CHÈNE, R., BUSNARDO, R., CHAROLLAIS, J., CLAVEL, B., DECONINCK, J.-F., EMMANUEL, L., GARDIN, S., GORIN, G., MANIVIT, H., MONTEIL, E., RAYNAUD, J.-F., RENARD, M., STEFFEN, D., STEINHAUSER, N., STRASSER, A., STROHMENGER, C. & VAIL, P.R. (1993) Sequence-stratigraphic interpretation of Upper Tithonian-Berriasian reference sections in South-east France: A multidisciplinary approach. *Bull. Centres Rech. Explor.-Prod. Elf Aquitaine* 17, 151-183.
- JEANS, C.V., WRAY, D.S., MERRIMAN, R.J. & FISHER, M.J. (2000) Volcanogenic clays in Jurassic and Cretaceous strata of England and the North Sea Basin. *Clay Minerals* 35, 25-55.
- JEFFERSON, T.H. (1982) Fossil forest from the Lower Cretaceous of Alexander Island, Antarctica. *Palaeontology* 25 (4), 681-708.
- JIMENEZ DE CISNERO, C. & VERA, J.A. (1993) Milankovitch cyclicity in Purbeck peritidal limestones of the Prebetic (Berriasian, southern Spain). *Sedimentology* 40, 513-537.
- JOACHIMSKI, M.M. (1991) Stabile Isotope (C,O) und Geochemie der Purbeck-Mikrite in Abhängigkeit von Fazies und Diagenese (Berriasian/Schweizer und Französischer Jura, Süd-England). *Erlanger geologische Abhandlung* 119, 1-114.
- JOACHIMSKI, M.M. (1994) Subaerial exposure and deposition of shallowing upward sequences: Evidence from stable isotopes of Purbeckian peritidal carbonates (basal Cretaceous), Swiss and French Jura Mountains. *Sedimentology* 41, 805-824.
- JONES, B. & DESROCHERS, A. (1992) Shallow platform carbonates. In: WALKER, R.G. & JAMES, N.P. (eds) *Facies models, response to sea-level change*. *Geol. Assoc. Can.*, 277-301.
- KARNER, G.D., LAKE, S.D. & DEWEY, J.F. (1987) The thermal and mechanical development of the Wessex Basin, southern England. In: COWARD, M.P., DEWEY, J.F. & HANCOCK, P.L. (eds) *Continental extensional tectonics*. *Geol. Soc. Spec. Publ.* 28, 517-536.
- KAUFFMAN, E.G., ELDER, W.P. & SAGEMAN, B.B. (1991) High-resolution correlation: A new tool in chronostratigraphy. In: EINSELE, G., RICKEN, W. & SEILACHER, A. (eds) *Cycles and events in stratigraphy*. 795-819 (Springer).
- KEEN, M.C. (1993) Ostracods as palaeoenvironmental indicators: Examples from the Tertiary and Early Cretaceous. In: JENKINS, D.G. (ed) *Applied micropaleontology*. 41-67 (Kluwer Academic Publishers).
- KELLY, S.R.A. (1983) Boreal influence on English Ryazanian bivalves. *Zitteliana* 10, 285-292.
- KEMPER, E. & SCHMITZ, H.H. (1981) Glendonite - Indikatoren des polarmarinen Ablagerungsmilieus. *Geol. Rundsch.* 70 (2), 759-773.
- KEMPER, E. (1983) Über Kalt- und Warmzeiten der Unterkreide. *Zitteliana* 10, 359-369.
- KEMPER, E. (1987) Das Klima der Kreide-Zeit. *Geologisches Jahrbuch* 96, 5-185.
- KENDALL, G.S.C. & SCHLAGER, W. (1981) Carbonates and relative changes in sea level. *Marine Geology* 44, 181-212.
- KENDALL, C.G.S.C., MOORE, P. & WHITTLE, G. (1992) A challenge: Is it possible to determine eustasy and does it matter? In: DOTT, R.H.J. (ed) *Eustasy: The historical ups and downs of a major geological concept*. *GSA Mem.* 180, 93-107.
- KIDWELL, S.M. (1993) Taphonomic expressions of sedimentary hiatuses: Field observations on bioclastic concentrations and sequence anatomy in low, moderate and high subsidence settings. *Geol. Rundsch.* 82, 189-202.
- KIELAN-JAWOROWSKA, Z. & ENSOM, P. (1992) Multituberculate mammals from the Upper Jurassic Purbeck Limestone Formation of Southern England. *Palaeontology* 35 (1), 95-126.
- KINDLER, P., DAVAUD, E. & STRASSER, A. (1997) Tyrrhenian coastal deposits from Sardinia (Italy): A petrographic record of high sea levels and shifting climate belts during the last interglacial (isotopic substage 5e). *Palaeogeogr., Palaeoclim., Palaeoecol.* 133, 1-25.
- KOLLA, V., POSAMENTIER, H.W. & EICHENSEER, H. (1995) Stranded parasequences and the forced regressive wedge systems tract: Deposition during base-level fall - discussion. *Sedimentary Geology* 95, 139-145.
- KONDO, Y., ABBOTT, S.T., KITAMURA, A., J., K.P.J., NAISH, T.R., KAMATAKI, T. & S., S.G. (1998) The relationship between shellbed type and sequence architecture: Examples from Japan and New Zealand. *Sedimentary Geology* 122, 109-127.

- KOWALEWSKI, M. & BAMBACH, R.K. (2003) The limits of paleontological resolution. In: HARRIES, P.J. (ed) *Approaches in high-resolution stratigraphic paleontology*. 1-48. (Kluwer Academic Press).
- LANGROCK, U., STEIN, R., LIPINSKI, M. & BRUMSACK, H.-J. (2003) Paleoenvironment and sea-level change in the early Cretaceous Barents Sea - implications from near-shore marine sapropels. *Geo-Mar. Lett.* 23, 34-42.
- LASKAR, J., JOUTEL, F. & BOUDIN, F. (1993) Orbital, precessional, and insolation quantities for the Earth from -20Myr to +10Myr. *Astronomy and Astrophysics* 270, 522-533.
- LEEDER, M.R., HARRIS, T. & KIRKBY, M.J. (1998) Sediment supply and climate change: Implications for basin stratigraphy. *Basin Research* 10 (1), 7-18.
- LE HÉGARAT, G. & REMANE, J. (1968) Tithonique supérieur et Berriasien de l'Ardèche et de l'Hérault corrélation des ammonites et des calpionelles. *Geobios* 1, 7-69.
- LE HÉGARAT, G. (1973) Le Berriasien du Sud-Est de la France. *Doc. Lab. Géol. Fac. Sci. Lyon* 43, 576pp.
- LE HÉGARAT, G. (1980) Berriasien. *Mémoire du B. R. G. M.* 109, 96-105.
- LEHMANN, C., OSLEGER, D.A. & MONTAÑEZ, I.P. (1998) Controls on cyclostratigraphy of Lower Cretaceous carbonates and evaporites, Cupido and Coahuila platforms, Northeastern Mexico. *J. Sed. Res.* 68 (6), 1109-1130.
- LEHRMANN, D.J. & GOLDHAMMER, R.K. (1999) Secular variation in parasequence and facies stacking patterns of platform carbonates: A guide to application of stacking-pattern analysis in strata of diverse ages and settings. In: HARRIS, P.M., SALLER, A.H. & SIMO, J.A. (eds) *Advances in carbonate sequence stratigraphy: Application to reservoirs, outcrops and models*. SEPM Spec. Publ. 63, 187-225.
- LEMOINE, M., BAS, T., ARNAUD-VANNEAU, A., ARNAUD, H., GIDON, D., GIDON, M., BOURBON, M., DE GRACIANSKY, P.-C., RUDKIEWICZ, J.-L., MEGARD-GALLI, J. & TRICART, P. (1986) The continental margin of the Mesozoic Tethys in the Western Alps. *Marine and Petroleum Geology* 3, 179-199.
- LOCKLEY, M. & HUNT, A.P. (1995) *Dinosaurs tracks and other fossil footprints of the western United States*. 338pp. (Columbia University Press).
- LOHMANN, K.C. (1988) Geochemical patterns of meteoric diagenetic systems and their application to studies of paleo-karst. In: JAMES, N.P. & CHOQUETTE, P.W. (eds) *Paleokarst*. 58-80 (Springer).
- LOUP, B. (1992) Mesozoic subsidence and stretching models of the lithosphere in Switzerland (Jura, Swiss Plateau and Helvetic realm). *Eclogae geol. Helv.* 85 (3), 541-572.
- LIPINSKI, M., WARNING, B. & BRUMSACK, H.-J. (2003) Trace metal signatures of Jurassic/Cretaceous black shales from the Norwegian Shelf and the Barents Sea. *Palaeogeogr., Palaeoclim., Palaeoecol.* 190, 459-475.
- MAREK, S. & RACZYŃSKA, A. (1973) The stratigraphy and palaeogeography of the Lower Cretaceous deposits of the Polish Lowland area. In: CASEY, R. & RAWSON, P.F. (eds) *The Boreal lower Cretaceous*. (Seel House Press).
- MARKWICK, P.J. & ROWLEY, D.B. (1998) The geological evidence for Triassic to Pleistocene glaciations: Implications for eustasy. In: PINDELL, J.L. & DRAKE, C.L. (eds) *Paleogeographic evolution and non-glacial eustasy, northern South America*. SEPM Spec. Publ. 58, 17-43.
- MARQUES, B., OLÓRIZ, F. & RODRIGUEZ-TOVAR, F.J. (1991) Interactions between tectonics and eustasy during the Upper Jurassic and lowermost Cretaceous. Examples from the south of Iberia. *Bull. Soc. géol. France* 162 (6), 1109-1124.
- MARTÍN-CHIVELET, J. & GIMENEZ, R. (1992) Palaeosols in microtidal carbonate sequences, Sierra de Utiel Formation, Upper Cretaceous, SE Spain. *Sedimentary Geology* 81, 125-145.
- MARTÍN-CLOSAS, C. & SERRA-KIEL, J. (1991) Evolutionary patterns of Clavatoraceae (Charophyta) in the Mesogean Basins analysed according to environmental change during Malm and Lower Cretaceous. *Historical Biology* 5, 291-307.
- MASSE, J.-P., BUCUR, I.I., VIRGONE, A. & DALMASSO, H. (1999) Nouvelles espèces de dasycladales du Crétacé inférieur de Provence (S.E. France). *Rev. Micropal.* 42 (3), 231-243.
- MASSE, J.-P. & MONTAGGIONI, L.F. (2001) Growth history of shallow-water carbonates: Control of accommodation on ecological and depositional processes. *Int. J. Earth Sci.* 90, 452-469.
- MATTHEWS, R.K. & FROHLICH, C. (2002) Maximum-flooding surfaces and sequence boundaries: Comparisons between observations and orbital forcing in the Cretaceous and Jurassic (65-190). *GeoArabia* 7 (3), 503-538.
- MELINTE, M.C. (2002) Early Cretaceous Boreal immigrants in the Romanian Carpathians related to the biotic exchange between the Tethys and the Boreal realms. In: MICHALÍK, J. (ed) *Tethyan/Boreal Cretaceous correlation*. 79-93 (Slovak Academy of Sciences).
- MEYER, C.A. & THÜRING, B. (2003) The first iguanodontid dinosaur tracks from the Swiss Alps (Schrammenkalk Formation, Aptian). *Ichnos* 10, 221-228.
- MEYER, R. (1976) Continental sedimentation, soil genesis and marine transgression in the basal beds of the Cretaceous in the east of the Paris Basin. *Sedimentology* 23, 235-253.
- MIAL, A.D. (1986) Eustatic sea-level changes interpreted from seismic stratigraphy: A critique of the methodology with particular reference to the North Sea Jurassic record. *AAPG Bull.* 70 (2), 131-137.
- MIAL, A.D. (1991) Stratigraphic sequences and their chronostratigraphic correlation. *J. Sed. Petro.* 61 (4), 497-505.
- MIAL, A.D. & MIAL, C.E. (2001) Sequence stratigraphy as a scientific enterprise: The evolution and persistence of conflicting paradigms. *Earth Sci. Rev.* 54, 321-348.
- MIAL, A.D. & MIAL, C.E. (2004) Empiricism and model-building in stratigraphy: Around the hermeneutic circle in the pursuit of stratigraphic correlation. *Stratigraphy* 1 (1), 27-46.

- MICHALÍK, J. (2002) Foreword: How to recognize the "oceanos kingdom" of Cretaceous time? In: MICHALÍK, J. (ed) Tethyan/Boreal Cretaceous correlation. 1-10 (Slovak Academy of Sciences).
- MILANKOVITCH, M. (1941) Kanon der Erdbestrahlung und seine Anwendung auf das Eiszeitenproblem. Akad. Royal Serbe Spec. Publ. 132, Sect. Math. Nat. Sci. 33, 633pp.
- MILLER, K.G., KOMINZ, M.A., BROWNING, J.V., WRIGHT, J.D., MOUNTAIN, G.S., KATZ, M.E., SUGARMAN, P.J., CRAMER, B.S., CHRISTIE-BLICK, N. & PEKAR, S.F. (2005) The Phanerozoic record of global sea-level change. *Science* 310, 1293-1298.
- MILNER, A.R. & BATTEN, D.J. (2002) Life and environments in Purbeck times. *Special papers in palaeontology* 68, 268pp. (The Palaeontological Association London).
- MILNER, A.C. (2002) Theropod dinosaurs of the Purbeck Limestone Group, southern England. In: MILNER, A.R. & BATTEN, D.J. (eds) Life and environments in Purbeck times. 191-201 (The Palaeontological Association London).
- MITCHUM, R.M. & VAN WAGONER, J.C. (1991) High-frequency sequences and their stacking patterns: Sequence-stratigraphic evidence of high-frequency eustatic cycles. *Sedimentary Geology* 70, 131-160.
- MOHR, H. (1992a) Die Entwicklung der Calpionellen an der Jura-Kreide Grenze im Helvetikum der Ostschweiz. Rückschlüsse auf die Biostratigraphie und Sedimentationsgeschichte. *Eclogae geol. Helv.* 85 (1), 1-21.
- MOHR, H. (1992b) Der helvetische Schelf der Ostschweiz am Übergang vom späten Jura zur frühen Kreide. PhD thesis, 221pp. (ETH Zurich, Switzerland).
- MOHR, H. & FUNK, H. (1995) Die Entwicklung der helvetischen Karbonatplattform in der Ostschweiz (Tithonian-Berriasian): Eine sequenzstratigraphische Annäherung. *Eclogae geol. Helv.* 88 (2), 281-320.
- MOJON, P.-O. & STRASSER, A. (1987) Microfaciès, sédimentologie et micropaléontologie du Purbeckien de Bienne (Jura suisse occidental). *Eclogae geol. Helv.* 80 (1), 37-58.
- MOJON, P.-O. (1989) Polymorphisme écophénotypique et paléocologie des porocharacées (charophytes) du Crétacé basal (Bérriasien) du Jura franco-suisse. *Rev. Paléobiologie* 8 (2), 505-524.
- MOJON, P.-O. (2002) Les formations mésozoïques à charophytes (Jurassique moyen- Crétacé inférieur) de la marge téthysienne nord-occidentale (Sud-est de la France, Suisse occidentale, Nord-est de l'Espagne) Sédimentologie, micropaléontologie, biostratigraphie. PhD thesis, 386pp. (University of Grenoble, France).
- MOORE, G.T., HAYASHIDA, D.N., ROSS, C.A. & JACOBSON, S.R. (1992) Paleoclimate of the Kimmeridgian/Tithonian (Late Jurassic) world: I. Results using a general circulation model. *Palaeogeogr., Palaeoclim., Palaeoecol.* 93, 113-150.
- MORTER, A.A. (1984) Purbeck-Wealden Beds Mollusca and their relationship to ostracod biostratigraphy, stratigraphical correlation and palaeoecology in the Weald and adjacent areas. *Proceeding of the Geologists' Association* 95 (3), 217-234.
- MONTAÑEZ, I.P. & OSLEGER, D.A. (1993) Parasequence stacking patterns, third-order accommodation events, and sequence stratigraphy of Middle to Upper Cambrian platform carbonates, Bonanza King Formation, southern Great Basin. In: LOUCKS, R.G. & SARG, J.F. (eds) Carbonate Sequence Stratigraphy/Recent developments and applications. AAPG Mem. 57, 305-326.
- MOUTY, M. (1966) Le Néocomien dans le Jura méridional. PhD thesis, 256pp. (University of Geneva, Switzerland).
- M'RABET, A. (1984) Neocomian deltaic complex in Central Tunisia: A particular example of ancient sedimentation and basin evolution. *Sedimentary Geology* 40, 191-209.
- MUTTERLOSE, J., SCHMID, F. & SPAETH, C. (1983) Zur Paläobiogeographie von Belemniten der Unter-Kreide in NW-Europa. *Zitteliana* 10, 293-307.
- MUTTERLOSE, J. (1992) Migration and evolution pattern of floras and faunas in marine Early Cretaceous sediments of NW Europe. *Palaeogeogr., Palaeoclim., Palaeoecol.* 94, 261-282.
- MUTTERLOSE, J. & BORNEMANN, A. (2000) Distribution and facies patterns of Lower Cretaceous sediments in northern Germany: A review. *Cretaceous Research* 21, 733-759.
- MUTTERLOSE, J. & KESSELS, K. (2000) Early Cretaceous calcareous nannofossils from high latitudes: Implications for palaeobiogeography and palaeoclimate. *Palaeogeogr., Palaeoclim., Palaeoecol.* 160 (3-4), 347-372.
- MUTTERLOSE, J. & BORNEMANN, A. (2002) North Germany: The Early Cretaceous gateway between the Tethys and the Boreal realm. In: MICHALÍK, J. (ed) Tethyan/Boreal Cretaceous correlation. 213-234 (Slovak Academy of Sciences).
- MUTTERLOSE, J., BRUMSACK, H., FLÖGEL, S., HAY, W., KLEIN, C., LANGROCK, U., LIPINSKI, M., RICKEN, W., SÖDING, E., STEIN, R. & SWIENTEK, O. (2003) The Greenland-Norwegian Seaway: A key area for understanding Late Jurassic to Early Cretaceous paleoenvironments. *Paleoceanography* 18 (1), 1010-1035.
- MUTTI, M. & HALLOCK, P. (2003) Carbonate systems along nutrient and temperature gradients: Some sedimentological and geochemical constraints. *Int. J. Earth Sci.* 92, 465-475.
- NOE-NYGAARD, N., SURLYK, F. & PIASECKI, S. (1987) Bivalve mass mortality caused by toxic dinoflagellate blooms in a Berriasian-Valanginian lagoon, Bornholm, Denmark. *Palaaios* 2, 263-272.
- NORMAN, D.B. & BARRETT, P.M. (2002) Ornithischian dinosaurs from the Lower Cretaceous (Berriasian) of England. In: MILNER, A.R. & BATTEN, D.J. (eds) Life and environments in Purbeck times. 161-189 (The Palaeontological Association London).
- NORRIS, G. (1969) Miospores from the Purbeck Beds and marine Upper Jurassic of southern England. *Palaeontology* 12 (4), 574-620.
- NORRIS, G. (1985) Palynology and British Purbeck facies. *Geol. Mag.* 122 (2), 187-190.

- NOSE, M. (1995) Vergleichende Faziesanalyse und Palökologie korallenreicher Verflachungsabfolgen des iberischen Oberjura. PhD thesis, 237pp. (University of Stuttgart, Germany).
- OERTLI, H.J. (1963) Ostracodes du «Purbeckien» du bassin parisien. *Revue de l'institut français du pétrole* 18 (1), 5-38.
- OGG, J.G. & LOWRIE, W. (1986) Magnetostratigraphy of the Jurassic/Cretaceous boundary. *Geology* 14, 547-550.
- OGG, J.G., STEINER, M.B., COMPANY, M. & TAVERA, J.M. (1988) Magnetostratigraphy across the Berriasian-Valanginian stage boundary (Early Cretaceous), at Cehegin (Murcia Province, southern Spain). *Earth and Planetary Science Letters* 87, 205-215.
- OGG, J.G., HASENYAGER, R.W., WIMBLEDON, W.A., CHANNELL, J.E.T. & BRALLOWER, T.J. (1991) Magnetostratigraphy of the Jurassic-Cretaceous boundary interval-Tethyan and English faunal realms. *Cretaceous Research* 2, 455-482.
- OGG, J.G., HASENYAGER II, R.W. & WIMBLEDON, W.A. (1994) Jurassic-Cretaceous boundary: Portland-Purbeck magnetostratigraphy and possible correlation to the Tethyan faunal realm. *Geobios* 17, 519-527.
- OGLESBY, R.J. & PARK, J. (1989) The effect of precessional insolation changes on Cretaceous climate and cyclic sedimentation. *J. Geophys. Res.* 94 (D12), 14793-14816.
- OLIVET, J.-L. (1996) La cinématique de la plaque ibérique. *Bull. Centres Rech. Explor. Prod. Elf-Aquitaine* 20 (1), 131-195.
- OSLEGER, D. (1991) Subtidal carbonate cycles: Implications for allocyclic vs. autocyclic controls. *Geology* 19, 917-920.
- OSLEGER, D.A. & READ, J.F. (1991) Relation of eustasy to stacking patterns of meter-scale carbonate cycles, Late Cambrian, U.S.A. *J. Sed. Res.* 61 (7), 1225-1252.
- PÄLIKE, H., SHACKLETON, N.J. & ROHL, U. (2001) Astronomical forcing in Late Eocene marine sediments. *Earth and Planetary Science Letters* 193 (3-4), 589-602.
- PANTIĆ, N.K. & BURGER, H. (1981) Palynologische Untersuchungen in der untersten Kreide des östlichen Helvetikums. *Eclogae geol. Helv.* 74 (3), 661-672.
- PARK, J. & OGLESBY, R.J. (1991) Milankovitch rhythms in the Cretaceous: A GCM modelling study. *Palaeogeogr., Palaeoclim., Palaeoecol.* 90, 329-355.
- PARRISH, J.T., ZIEGLER, A.M. & SCOTese, C.R. (1982) Rain-fall patterns and the distribution of coals and evaporites in the Mesozoic and Cenozoic. *Palaeogeogr., Palaeoclim., Palaeoecol.* 40, 67-101.
- PASQUIER, J.-B. (1995) Sédimentologie, stratigraphie séquentielle et cyclostratigraphie de la marge nord-téthysienne au Berriasien en Suisse occidentale (Jura, Helvétique et Ultra-helvétique; comparaison avec les séries de bassin des domaines Vocontien et Subbrianconnais). PhD thesis, 274pp. (University of Fribourg, Switzerland).
- PASQUIER, J.-B. & STRASSER, A. (1997) Platform-to-basin correlation by high-resolution sequence stratigraphy and cyclo-stratigraphy (Berriasian, Switzerland and France). *Sedimentology* 44, 1071-1092.
- PATTERSON, W.P. & WALTER, L.M. (1994) Depletion of  $^{13}\text{C}$  in seawater  $\Sigma\text{CO}_2$  on modern carbonate platforms: Significance for the carbon isotopic record of carbonates. *Geology* 22, 885-888.
- PELZER, G. & WILDE, V. (1987) Klimatische Tendenzen während der Ablagerung der Wealden-Fazies in Nordwesteuropa. *Geologisches Jahrbuch* 96, 239-263.
- PERLMUTTER, M.A. & MATTHEWS, M.D. (1989) Global cyclostratigraphy - a model. In: CROSS, T.A. (ed) *Quantitative Dynamic Stratigraphy*. 233-260 (Prentice-Hall).
- PERLMUTTER, M.A. & MATTHEWS, M.D. (1992) Global cyclostratigraphy. *Encyclopedia of Earth System Science* 2, 379-393.
- PERSOZ, F. & REMANE, J. (1976) Minéralogie et géochimie des formations à la limite Jurassique-Crétacé dans le Jura et le Basin vocontien. *Eclogae geol. Helv.* 69 (1), 1-38.
- PERSOZ, F. (1982) Inventaire minéralogique, diagenèse des argiles et minéralostratigraphie des séries jurassiques et crétacées inférieures du Plateau suisse et de la bordure sud-est du Jura entre les lacs d'Annecy et de Constance. *Mat. Carte Géol. Suisse N.S.* 155, 52pp.
- PITMAN, W.C. & GOLOVCHENKO, I. (1983) The effect of sea-level change on the shelfedge and slope of passive margins. In: STANLEY, D.J. & MOORE, G.T. (eds) *The shelfbreak: Critical interface on continental margins*. SEPM Spec. Publ. 33, 41-58.
- PITTET, B. (1996) Contrôles climatiques, eustatiques et tectoniques sur des systèmes mixtes carbonates-siliciclastiques de plateforme: exemples de l'Oxfordien (Jura suisse, Normandie, Espagne). PhD thesis, 258pp. (University of Fribourg, Switzerland).
- PITTET, B. & GORIN, G. (1997) Distribution of sedimentary organic matter in a mixed carbonate-siliciclastic platform environment: Oxfordian of the Swiss Jura Mountains. *Sedimentology* 44 (5), 915-937.
- PITTET, B. & STRASSER, A. (1998a) Depositional sequences in deep-shelf environments formed through carbonate-mud import from the shallow platform (Late Oxfordian, German Swabian Alps and eastern Swiss Jura). *Eclogae geol. Helv.* 91, 149-169.
- PITTET, B. & STRASSER, A. (1998b) Long-distance correlations by sequence stratigraphy and cyclostratigraphy: Examples and implications (Oxfordian from the Swiss Jura, Spain, and Normandy). *Geol. Rundsch.* 86, 852-874.
- PITTET, B., STRASSER, A. & MATTIOLI, E. (2000) Depositional sequences in deep-shelf environments: A response to sea-level changes and shallow-platform carbonate productivity (Oxfordian, Germany and Spain). *J. Sed. Res.* 70 (2), 392-407.
- PLATT, N.H. (1989) Lacustrine carbonates and pedogenesis: Sedimentology and origin of palustrine deposits from the Early Cretaceous Rupelo Formation, W Cameros Basin, N Spain. *Sedimentology* 36, 665-684.

- PLOTNICK, R.E. (1986) A fractal model for the distribution of stratigraphic hiatuses. *J. of Geol.* 94, 885-890.
- PLUNKETT, J.M. (1997) Early diagenesis of shallow platform carbonates in the Oxfordian of the Swiss Jura Mountains. PhD Thesis. 155pp. (University of Fribourg, Switzerland).
- PODLAHA, O.G., MUTTERLOSE, J. & VEIZER, J. (1998) Preservation of  $\delta^{18}\text{O}$  and  $\delta^{13}\text{C}$  in belemnite rostra from the Jurassic/Early Cretaceous successions. *Am. J. Sci.* 298, 324-347.
- POSAMENTIER, H.W., JERVEY, M.T. & VAIL, P.R. (1988) Eustatic controls on clastic deposition I - conceptual framework. In: WILGUS, C.E., HASTINGS, B.S., KENDALL, C.G.S.C., POSAMENTIER, H.W., ROSS, C.A. & VAN WAGONER, J.C. (eds) *Sea-level changes - an integrated approach*. SEPM Spec. Publ. 42, 109-124.
- POSAMENTIER, H.W. & JAMES, D.P. (1993) An overview of sequence-stratigraphic concepts: Uses and abuses. In: POSAMENTIER, H. W., SUMMERHAYES, C. P., HAQ, B. U. & ALLEN, G. P. (eds) *IAS Spec. Publ.* 18, 3-18.
- PRATT, B.R. & JAMES, N.P. (1986) The St George Group (Lower Ordovician) of western Newfoundland: Tidal flat island model for carbonate sedimentation in shallow epeiric seas. *Sedimentology* 33, 313-343.
- PRATT, B.R. & JAMES, N.P. (1992) Peritidal carbonates. In: WALKER, R.G. & JAMES, N.P. (eds) *Facies models, response to sea-level change*. 303-322 (Geol. Assoc. Can.).
- PRICE, G.D., VALDES, P.J. & SELLWOOD, B.W. (1998) A comparison of GCM simulated Cretaceous "greenhouse" and "icehouse" climates: Implications for the sedimentary record. *Palaeogeogr., Palaeoclim., Palaeoecol.* 142, 123-138.
- PRICE, G.D. (1999) The evidence and implications of polar ice during the Mesozoic. *Earth Sci. Rev.* 48, 183-210.
- PRICE, G.D., RUFFELL, A.H., JONES, C.E., KALIN, R.M. & MUTTERLOSE, J. (2000) Isotopic evidence for temperature variation during the early Cretaceous (late Ryazanian-mid-Hauterivian). *J. Geol. Soc. London* 157, 335-343.
- PRICE, G.D. & MUTTERLOSE, J. (2004) Isotopic signals from Late Jurassic-Early Cretaceous (Volgian-Valanginian) sub-Arctic belemnites, Yatria River; Western Siberia. *J. Geol. Soc. London* 161, 959-968.
- RADLEY, J.D. (2002) Distribution and palaeoenvironmental significance of molluscs in the Late Jurassic-Early Cretaceous Purbeck Formation of Dorset, southern England: A review. In: MILNER, A.R. & BATTEN, D.J. (eds) *Life and environments in Purbeck times*. 41-51 (The Palaeontological Association London).
- RAMEIL, N., GÖTZ, A.E. & FEIST-BURKHARDT, S. (2000) High-resolution sequence interpretation of epeiric shelf carbonates by means of palynofacies analysis: An example from the Germanic Triassic (Lower Muschelkalk, Anisian) of East Thuringia, Germany. *Facies* 43, 123-144.
- RAMEIL, N. (2005) Carbonate sedimentology, sequence stratigraphy, and cyclostratigraphy of the Tithonian in the Swiss and French Jura mountains: a high-resolution record in sea level and climate. *GeoFocus* 13, 246pp.
- RANKEY, E.C. (2004) On the interpretation of shallow shelf carbonate facies and habitats: How much does water depth matter? *J. Sed. Res.* 74 (1), 2-6.
- RASPINI, A. (2001) Stacking pattern of cyclic carbonate platform strata: Lower Cretaceous of southern Appennines, Italy. *J. Geol. Soc. London* 158, 353-366.
- RASPLUS, L., FOURCADE, E., AMBROISE, D., ANDEOL, B., AZÉMA, J., BLANC, P., BUSNARDO, R., CLERC-RENAUD, T., DAMOTTE, R., DERCOURT, J., FOUCAULT, A., GALBRUN, B., GRANIER, B., LACHKAR, G., LE HÉGARAT, G., MAGNÉ, J., MANIVIT, H., MANGIN, A.-M., MASURE, E., MAZAUD, A., MICHAUD, F., MORAND, F., RENARD, M., SCHUBER, N. & TAUGOURDEAU, J. (1987) *Stratigraphie intégrée du sillon citrabinétique* (Sierra de Fontcalent, Province d'Alicante, Espagne). *Geobios* 20 (3), 337-387.
- RASSER, M.W. & FENNINGER, A. (2002) Palaeoenvironmental and diagenetic implications of  $\delta^{18}\text{O}$  and  $\delta^{13}\text{C}$  isotope ratios from the Upper Jurassic Plassen limestone (Northern Calcareous Alps, Austria). *Geobios* 35, 41-49.
- RAWSON, P.F. & RILEY, L.A. (1982) Latest Jurassic-Early Cretaceous events and the "Late Cimmerian Unconformity" in North Sea area. *AAPG Bull.* 66 (12), 2628-2648.
- READ, J.F., GROTZINGER, J.P., BOVA, J.A. & KOERSCHNER, W.F. (1986) Models for generation of carbonate cycles. *Geology* 14, 107-110.
- READ, J.F. & GOLDHAMMER, R.K. (1988) Use of Fischer plot to define third-order sea-level curves in Ordovician peritidal cyclic carbonates, Appalachians. *Geology* 16, 895-899.
- READ, J.F. (1995) Overview of carbonate platform sequences, cycle stratigraphy and reservoirs in greenhouse and ice-house worlds. In: READ, J. F., KERANS, C., WEBER, L. J., SARG, J. F. & WRIGHT, F. M. (eds) *Milankovitch sea-level changes, cycles, and reservoirs on carbonate platforms in greenhouse and ice-house worlds*. SEPM Short Course 35, 1-102.
- REINECK, H.-E. & WUNDERLICH, F. (1968) Classification and origin of flaser and lenticular bedding. *Sedimentology* 11, 99-104.
- REMANE, J. (1985) Calpionellids. In: BOLLI, H.M. & SAUNDERS, J.B. (eds) *Plankton stratigraphy*. 555-572 (Cambridge University Press).
- REMANE, J. (1991) The Jurassic-Cretaceous boundary: Problems of definition and procedure. *Cretaceous Research* 12, 447-453.
- REMANE, J. (1998) Les calpionelles: Possibilités biostratigraphiques et limitations paléobiogéographiques. *Bull. Soc. géol. France* 169 (6), 829-839.
- RICH, P.V., RICH, T. H., WAGSTAFF, B.E., McEwen Mason, J., DOUTHITT, C.B., GREGORY, R.T. & FELTON, E.A. (1988) Evidence for low temperatures and biologic diversity in Cretaceous high latitudes of Australia. *Science* 242, 1403-1406.
- RICH, T., H., VICKERS-RICH, P. & GANGLOFF, R.A. (2002) Polar

- dinosaurs. *Science* 295, 979-980.
- RICHTER, D.K. (1983) Calcareous Ooids: A Synopsis. In: PERYT, T.M. (ed) *Coated Grains*. 70-99 (Springer).
- RICKEN, W. & EDER, W. (1991) Diagenetic modification of calcareous beds - an overview. In: EINSELE, G., RICKEN, W. & SEILACHER, A. (eds) *Cycles and events in stratigraphy*. 430-449 (Springer).
- RIVELINE, J., BERGER, J.-P., FEIST, M., MARTÍN-CLOSAS, C., SCHUDACK, M.E. & SOULIÉ-MÄRSCHÉ, I. (1996) European Mesozoic-Cenozoic charophyte biozonation. *Bull. Soc. géol. France* 167 (3), 453-468.
- ROSS, A.J. & VANNIER, J. (2002) Crustacea (excluding ostracoda) and chelicerata of the Purbeck Limestone Group, southern England: A review. In: MILNER, A.R. & BATTEN, D.J. (eds) *Life and environments in Purbeck times*. 71-82 (The Palaeontological Association London).
- ROTH, P.H. (1989) Ocean circulation and calcareous nannoplankton evolution during the Jurassic and Cretaceous. *Palaeogeogr., Palaeoclim., Palaeoecol.* 74, 111-126.
- RUFFELL, A. (1991) Sea-level events during the Early Cretaceous in Western Europe. *Cretaceous Research* 12, 527-551.
- RUFFELL, A.H. & RAWSON, P.F. (1994) Palaeoclimate control on sequence stratigraphic patterns in the Late Jurassic to mid-Cretaceous, with a case study from Eastern England. *Palaeogeogr., Palaeoclim., Palaeoecol.* 110, 43-54.
- RUFFELL, A.H. (1995) Seismic stratigraphic analysis of non-marine Lower Cretaceous strata in the Wessex and North Celtic Sea basins. *Cretaceous Research* 16, 603-637.
- RUFFELL, A.H., PRICE, G.D., MUTTERLOSE, J., KESSELS, K., BARABOSHKIN, E. & GRÖCKE, D.R. (2002) Palaeoclimate indicators (clay minerals, calcareous nannofossils, stable isotopes) compared from two successions in the late Jurassic of the Volga Basin (SE Russia). *Geol. J.* 37, 17-33.
- RUSCIADELLI, G. (1999) Stratigraphie séquentielle et analyse de l'espace disponible du Jurassique supérieur et du Crétacé inférieur du bassin de Paris. *Atti Ticinensi di Scienze della Terra* 8, 3-83.
- SACHS, V.N., BASOV, V.A., ZAKHAROV, V.A., NALNJAIEVA, T.I. & SHULGINA, N.I. (1975) Jurassic-Cretaceous boundary, position of Berriasian in the Boreal realm and correlation with Tethys. *Colloque sur la limite Jurassique-Crétacé*. 137-141 (*Mémoires du B. R. G. M.*).
- SADLER, P.M. (1981) Sediment accumulation rates and the completeness of stratigraphic sections. *J. Geol.* 89, 569-584.
- SADLER, P.M. & STRAUSS, D.J. (1990) Estimation of completeness of stratigraphical sections using empirical data and theoretical models. *J. Geol. Soc. London* 147, 471-485.
- SADLER, P.M., OSLEGER, D.A. & MONTAÑEZ, I.P. (1993) On the labeling, length, and objective basis of Fischer plots. *J. Sed. Petro.* 63 (3), 360-368.
- SADLER, P.M. (1994) The expected duration of upward-shallowing peritidal carbonate cycles and their terminal hiatuses. *GSA Bull.* 106, 791-802.
- SADLER, P.M. (1999) The influence of hiatuses on sediment accumulation rates. *GeoResearch Forum* 5, 15-40.
- SAHAGIAN, D.L., PINOUS, O.V., OLFERIEV, A. & ZAKHAROV, V.A. (1996) Eustatic curve of Middle Jurassic-Cretaceous based on Russian platform and Siberian stratigraphy: Zonal resolution. *AAPG Bull.* 80 (9), 1433-1458.
- SALISBURY, S.W. (2002) Crocodilians from the Lower Cretaceous (Berriasian) Purbeck Limestone Group of Dorset, southern England. In: MILNER, A.R. & BATTEN, D.J. (eds) *Life and environments in Purbeck times*. 121-144 (The Palaeontological Association London).
- SALVINI-BONNARD, G., ZANINETTI, L. & CHAROLLAIS, J. (1984) Les foraminifères dans le Crétacé inférieur (Berriasien moyen-Valanginien inférieur) de la région de la Corraterie, Grand-Salève (Haute-Savoie, France): Inventaire préliminaire et remarques stratigraphiques. *Rev. Paléobiologie* 3 (2), 175-184.
- SAMANKASSOU, E., STRASSER, A., DI GIOIA, E., RAUBER, G. & DUPRAZ, C. (2003) High-resolution record of lateral facies variations on a shallow carbonate platform (Upper Oxfordian, Swiss Jura Mountains). *Eclogae geol. Helv.* 96, 425-440.
- SAMANKASSOU, E., TRESCH, J. & STRASSER, A. (2005) Origin of peloids in Early Cretaceous deposits, Dorset, South England. *Facies* 51, 275-284.
- SANDULLI, R. & RASPINI, A. (2004) Regional to global correlation of lower Cretaceous (Hauterivian-Barremian) shallow-water carbonates of the southern Apennines (Italy) and Dinarides (Montenegro), southern Tethyan Margin. *Sedimentary Geology* 165 (1-2), 117-153.
- SATTERLEY, A.K. (1996) The interpretation of cyclic successions of the Middle and Upper Triassic of the Northern and Southern Alps. *Earth Sci. Rev.* 40, 181-207.
- SATTLER, U., IMMENHAUSER, A., HILLGÄRTNER, H. & ESTEBAN, M. (2005) Characterization, lateral variability and lateral extent of discontinuity surfaces on a carbonate platform (Barremian to Lower Aptian, Oman). *Sedimentology* 52 (2), 339-361.
- SCHETTINO, A. & SCOTese, C. (2002) Global kinematic constraints to the tectonic history of the Mediterranean region and surrounding areas during the Jurassic and Cretaceous. In: ROSENBAUM, G. & LISTER, G.S. (eds) *Reconstruction of the evolution of the Alpine-Himalayan orogen*. *Journal of the Virtual Explorer* 8, 149-168.
- SCHINDLER, U. & CONRAD, M.A. (1994) The Lower Cretaceous Dasycladales from the northwestern Friuli platform and their distribution in chronostratigraphic and cyclostratigraphic units. *Rev. Paléobiologie* 13 (1), 59-96.
- SCHLAGER, W. (1981) The paradox of drowned reefs and carbonate platforms. *GSA Bull.* 92, 197-211.
- SCHLAGER, W. (1991) Depositional bias and environmental change - important factors in sequence stratigraphy. *Sedimentary Geology* 70, 109-130.
- SCHLAGER, W. (1993) Accommodation and supply - a dual control on stratigraphic sequences. *Sedimentary Geology* 86,

- 111-136.
- SCHLAGER, W., REIJMER, J.J.G. & DROXLER, A. (1994) Highstand shedding of carbonate platforms. *J. Sed. Res.* B64 (3), 270-281.
- SCHLAGER, W., MARSAL, D., VAN DER GEEST, P.A.G. & SPRENGER, A. (1998) Sedimentation rates, observation span, and the problem of spurious correlation. *Mathematical Geology* 30 (5), 547-556.
- SCHLAGER, W. (2005) Carbonate sedimentology and sequence stratigraphy. *SEPM concepts in sedimentology and paleontology* 8, 200pp.
- SCHLAGINTWEIT, F., GAWLICK, H.-J. & LEIN, R. (2005) Micropaleontology and biostratigraphy of the Plassen carbonate platform of the type locality (Upper Jurassic to Lower Cretaceous, Salzkammergut, Austria). *Journal of Alpine Geology* 47, 11-102.
- SCHMID, D.U. & LEINFELDER, R.R. (1996) The Jurassic *Lithocodium aggregatum-Troglotella incrustans* foraminiferal consortium. *Palaeontology* 39 (1), 21-52.
- SCHNYDER, J. (2003) Le passage Jurassique/Crétacé: Événements instantanés, variations climatiques enregistrées dans les faciès purbeckiens français (Boulonnais, Charentes) et anglais (Dorset). Comparaison avec le domain téthysien. PhD thesis, 380pp. (University of Lille, France).
- SCHNYDER, J., GORIN, G., SOUSSI, M., BAUDIN, F. & DECONINCK, J.-F. (2005a) Enregistrement de la variation climatique au passage Jurassique/Crétacé sur la marge sud de la Téthys: Minéralogie des argiles et palynofaciès de la coupe du Jebel Meloussi (Tunisie centrale, formation Sidi Kralif). *Bull. Soc. géol. France* 176 (2), 171-182.
- SCHNYDER, J., BAUDIN, F. & DECONINCK, J.-F. (2005b) A possible tsunami deposit around the Jurassic-Cretaceous boundary in the Boulonnais area (northern France). *Sedimentary Geology* 177, 209-227.
- SCHNYDER, J., RUFFELL, A., DECONINCK, J.-F. & BAUDIN, F. (2006) Conjunctive use of spectral gamma-ray logs and clay mineralogy in defining Late Jurassic-Early Cretaceous palaeoclimate change (Dorset, UK). *Palaeogeogr., Palaeoclim., Palaeoecol.* 229, 303-320.
- SCHUDACK, M.E. (1991) Eine Charophyten-Biozonierung für den Zeitraum Oberjura bis Berriasium in Westeuropa und ihr Vergleich mit Sequenzstratigraphie und eustatischer Meeresspiegelkurve. *Berl. Geowiss. Abh.* 134 (A), 311-332.
- SCHUDACK, M.E. (1993) Die Charophyten in Oberjura und Unterkreide Westeuropas: Mit einer phylogenetischen Analyse der Gesamtgruppe. *Berl. Geowiss. Abh.* 8 (E), 209pp.
- SCHUDACK, M.E. & SCHUDACK, U. (1995) Late Jurassic and Berriasian ostracod biostratigraphy in northwestern and central Europe. In: RIHA, J. (ed) *Ostracoda and Biostratigraphy*. 99-109 (Proc. 12<sup>th</sup> Int. Symp. on Ostracoda).
- SCHUDACK, M.E. (1996) Die Charophyten des Niedersächsischen Beckens (Oberjura-Berriasium): Lokazonierung, überregionale Korrelation und Palökologie. *N. Jb. Geol. Paläont. Abh.* 200 (1/2), 27-52.
- SCHUDACK, M.E. (1999) Ostracoda (marine/nonmarine) and palaeoclimate history in the Upper Jurassic of Central Europe and North America. *Marine Micropaleontology* 37 (3-4), 273-288.
- SCHULZ, M. & SCHÄFER-NETH, C. (1997) Translating Milankovitch climate forcing into eustatic fluctuations via thermal deep water expansion: A conceptual link. *Terra Nova* 9, 228-231.
- SCHWARZACHER, W. (1993) Cyclostratigraphy and the Milankovitch theory. 225pp. (Elsevier).
- SCHWARZACHER, W. (1998) Stratigraphic resolution, cycles and sequences. In: GRADSTEIN, F.M., SANDVIK, K.O. & MILTON, N.J. (eds) *Sequence stratigraphy - Concepts and applications*. NPF Spec. Publ. 8, 1-8.
- SCHWARZACHER, W. (2000) Repetitions and cycles in stratigraphy. *Earth Sci. Rev.* 50, 51-75.
- SCHWARZACHER, W. (2004) Obtaining timescales for cyclostratigraphic studies. In: D'ARGENIO, B., FISCHER, A. G. PREMOLI SILVA, I., WEISSERT H. & FERRERI, V. (eds) *Cyclostratigraphy: Approaches and case histories*. SEPM Spec. Publ. 81, 297-302.
- SELLWOOD, B.W. & PRICE, G.D. (1994) Sedimentary facies as indicators of Mesozoic palaeoclimate. In: ALLEN, J.R.L., HOSKINS, B.J., SELLWOOD, B.W., SPICER, R.A. & VALDES, P.J. (eds) *Palaeoclimates and their modelling*. 17-25 (Chapman & Hall).
- SELLWOOD, B.W. & VALDES, P.J. (1997) Geological evaluation of climate general circulation models and model implications for Mesozoic cloud cover. *Terra Nova* 9, 75-78.
- SELLWOOD, B.W., VALDES, P.J. & PRICE, G.D. (2000) Geological evaluation of multiple general circulation model simulations of Late Jurassic palaeoclimate. *Palaeogeogr., Palaeoclim., Palaeoecol.* 156 (1-2), 147-160.
- SEPTFONTAINE, M. (1981) Les foraminifères imperforés des milieux de plate-forme au Mésozoïque: Détermination pratique, interprétation phylogénétique et utilisation biostratigraphique. *Rev. Micropal.* 23 (3/4), 169-203.
- SHINN, E.A. (1983) Birdeyes, fenestrae, shrinkage pores, and loferites: A reevaluation. *J. Sed. Petro.* 53 (2), 0619-0628.
- SIGOGNEAU-RUSSELL, D. & KIELAN-JAWOROWSKA, Z. (2002) Mammals from the Purbeck Limestone Group of Dorset, southern England. In: MILNER, A.R. & BATTEN, D.J. (eds) *Life and environments in Purbeck times*. 241-255 (The Palaeontological Association London).
- SINGER, A. (1980) The palaeoclimatic interpretation of clay minerals in soils and weathering profiles. *Earth Sci. Rev.* 15, 303-326.
- SINGER, A. (1984) The paleoclimatic interpretation of clay minerals in sediments - a review. *Earth Sci. Rev.* 21, 251-293.
- SKOURTSIS-CORONEOU, V. & SOLAKIUS, N. (1999) Calpionellid zonation at the Jurassic/Cretaceous boundary within the Vigla Limestone Formation (Ionian Zone, western Greece) and carbon isotope analysis. *Cretaceous Research* 20, 583-595.
- SLADEN, C.P. (1983) Trends in Early Cretaceous clay mineralogy



- in NW Europe. *Zitteliana* 10, 349-357.
- SLADEN, C.P. & BATTEN, D.J. (1984) Source-area environments of Late Jurassic and Early Cretaceous sediments in southeast England. *Proceedings of the Geologist's Association* 95 (2), 149-163.
- SLOAN, L.C. & BARRON, E.J. (1990) "Equable" climates during Earth history? *Geology* 18, 489-492.
- SLOSS, L.L. (1963) Sequences in the cratonic interior of North America. *GSA Bull.* 74, 93-114.
- SMELROR, M., MORK, A., MORK, M.B.E., WEISS, H.M. & LOSETH, H. (2001) Middle Jurassic-Lower Cretaceous transgressive-regressive sequences and facies distribution off northern Nordland and Troms, Norway. In: MARTINSEN, O.J. & DREYER, T. (eds) *Sedimentary environments offshore Norway - Paleozoic to recent*. Norwegian Petroleum Soc. Spec. Publ. 10, 211-232.
- SMITH, A.G., SMITH, D.G. & FUNNELL, B.M. (1994) *Atlas of Mesozoic and Cenozoic coastlines*. 99pp. (Cambridge University Press).
- SMITH, D.G. (1989) Milankovitch cyclicity and the stratigraphic record - a review. *Terra Nova* 1, 402-404.
- SMITH, D.G. (1994) Cyclicity or chaos? Orbital forcing versus non-linear dynamics. In: DE BOER, P. L. & SMITH, D. G. (eds) *IAS Spec. Publ.* 19, 531-544.
- SOREGHAN, G.S. & DICKINSON, W.R. (1994) Generic types of stratigraphic cycles controlled by eustasy. *Geology* 22, 759-761.
- SPRENGER, A. & TEN KATE, W.G. (1993) Orbital forcing of calcutite-marl cycles in southeast Spain and an estimate for the duration of the Berriasian stage. *GSA Bull.* 105, 807-818.
- STAMPFLI, G.M., BOREL, G.D., MARCHANT, R. & MOSAR, J. (2002) Western Alps geological constraints on western Tethyan reconstructions. In: ROSENBAUM, G. & LISTER, G.S. (eds) *Reconstruction of the evolution of the Alpine-Himalayan orogen*. *Journal of the Virtual Explorer* 8, 77-106.
- STEFFEN, D. (1993) Influence des variations eustatiques sur la distribution de la matière organique dans les roches sédimentaires: Exemples des dépôts berriasiens des Bassins Vocontien, Ultrahelvétique et du Yorkshire. PhD thesis 106pp. (University of Geneva, Switzerland).
- STEFFEN, D. & GORIN, G. (1993) Palynofacies of the Upper Tithonian-Berriasian deep-sea carbonates in the Vocontian Trough (SE France). *Bull. Centres Rech. Explor.-Prod. Elf Aquitaine* 17, 235-247.
- STEINHAUFF, D.M. & WALKER, K.R. (1995) Recognizing exposure, drowning, and "missed beats": Platform-interior to platform-margin sequence stratigraphy of Middle Ordovician limestones, East Tennessee. *J. Sed. Res.* B65 (2), 183-207.
- STEINHAUSER, N. & LOMBARD, A. (1969) Définition de nouvelles unités lithostratigraphiques dans le Crétacé inférieur du Jura méridional (France). *C. R. Soc. Phys. Hist. nat. Genève* 4 (1), 100-113.
- STEINHAUSER, N. & CHAROLLAIS, J. (1971) Observations nouvelles et réflexions sur la stratigraphie du "Valanginien" de la région neuchâteloise et ses rapports avec le Jura méridional. *Geobios* 4 (1), 1-59.
- STONELEY, R. (1982) The structural development of the Wessex Basin. *J. Geol. Soc. London* 139, 543-554.
- STRASSER, A. & DAVAUD, E. (1982) Les croûtes calcaires (calcretes) du Purbeckien du Mont-Salève (Haute-Savoie, France). *Eclogae geol. Helv.* 75 (2), 287-301.
- STRASSER, A. & DAVAUD, E. (1983) Black pebbles of the Purbeckian (Swiss and French Jura): Lithology, geochemistry and origin. *Eclogae geol. Helv.* 76 (3), 551-580.
- STRASSER, A. (1984) Black-pebble occurrence and genesis in Holocene carbonate sediments (Florida Keys, Bahamas, and Tunisia). *J. Sed. Petro.* 54 (4), 1097-1109.
- STRASSER, A. (1986) Ooids in Purbeck limestones (lowermost Cretaceous) of the Swiss and French Jura. *Sedimentology* 33, 711-727.
- STRASSER, A. (1987) Detaillierte Sequenzstratigraphie und ihre Anwendung: Beispiel aus dem Purbeck des schweizerischen und französischen Jura. *Facies* 17, 237-244.
- STRASSER, A. (1988) Shallowing-upward sequences in Purbeckian peritidal carbonates (lowermost Cretaceous, Swiss and French Jura Mountains). *Sedimentology* 35, 369-383.
- STRASSER, A. (1991) Lagoonal-peritidal sequences in carbonate environments: Autocyclic and allocyclic processes. In: EINSELE, G., RICKEN, W. & SEILACHER, A. (eds) *Cycles and events in stratigraphy*. 709-721 (Springer).
- STRASSER, A. (1994) Milankovitch cyclicity and high-resolution sequence stratigraphy in lagoonal-peritidal carbonates (Upper Tithonian-Lower Berriasian, French Jura Mountains). In: DE BOER, P. L. & SMITH, D. G. *Orbital forcing and cyclic sequences*. *IAS Spec. Publ.* 19, 285-301.
- STRASSER, A. & HILLGÄRTNER, H. (1998) High-frequency sea-level fluctuations recorded on a shallow carbonate platform (Berriasian and Lower Valanginian of Mount Salève, French Jura). *Eclogae geol. Helv.* 91, 375-390.
- STRASSER, A., PITTET, B., HILLGÄRTNER, H. & PASQUIER, J.-B. (1999) Depositional sequences in shallow carbonate-dominated sedimentary systems: Concepts for high-resolution analysis. *Sedimentary Geology* 128, 201-221.
- STRASSER, A., HILLGÄRTNER, H., HUG, W. & PITTET, B. (2000) Third-order depositional sequences reflecting Milankovitch cyclicity. *Terra Nova* 12, 303-311.
- STRASSER, A. & SAMANKASSOU, E. (2003) Carbonate sedimentation rates today and in the past: Holocene of Florida Bay, Bahamas, and Bermuda vs. Upper Jurassic and Lower Cretaceous of the Jura Mountains (Switzerland and France). *Geologia Croatica* 56 (1), 1-18.
- STRASSER, A., HILLGÄRTNER, H. & PASQUIER, J.-B. (2004) Cyclostratigraphic timing of sedimentary processes: An example from the Berriasian of the Swiss and French Jura Mountains. In: D'ARGENIO, B., FISCHER, A.G., PREMOLI SILVA, I., WEISSERT, H. & FERRERI, V. (eds) *Cyclostratigraphy: Approaches and case histories*. *SEPM Spec. Publ.* 81, 135-151.

- STRASSER et al. (2007) Cyclostratigraphy – concepts, definitions, and applications. *Newsletters on Stratigraphy* (in press).
- STRAUSS, C., ELSTNER, F., JAN DU CHÊNE, R., MUTTERLOSE, J., REISER, H. & BRANDT, K.-H. (1993) New micro-paleontological and palynological evidence on the stratigraphic position of the “German Wealden” in NW-Germany. *Zitteliana* 20, 389-401.
- STREET, C. & BOWN, P.R. (2000) Palaeobiogeography of Early Cretaceous (Berriasian-Barremian) calcareous nannoplankton. *Marine Micropaleontology* 39 (1-4), 265-291.
- STROHMENGER, C. & STRASSER, A. (1993) Eustatic controls on the depositional evolution of Upper Tithonian and Berriasian deep-water carbonates (Vocontian Trough, SE France). *Bull. Centres Rech. Explor.-Prod. Elf Aquitaine* 17 (1), 183-203.
- SURLYK, F. (1991) Sequence stratigraphy of the Jurassic-Lowermost Cretaceous of East Greenland. *AAGP Bull.* 75 (9), 1468-1488.
- SWIENTEK, O. (2002) The Greenland Norwegian seaway: Climatic and cyclic evolution of Late Jurassic-Early Cretaceous sediments. PhD thesis, 119pp. (University of Köln, Germany)
- SWINCHATT, J.P. (1967) Formation of large-scale cross-bedding in a carbonate unit. *Sedimentology* 8, 93-120.
- THIERRY, J. & BARRIER, E. (2000) Early Tithonian (141 - 139Ma). In: DER COURT, J., GAETANI, M., VRIELYNCK, B., BARRIER, E., BIJU-DUVAL, B., BRUNET, M.F., CADET, J.-P., CRASQUIN, S. & SANDULESCU, M. (eds) *Peri-Tethys atlas*. 99-110 (CCGM/CGMW).
- THIRY, M. (2000) Palaeoclimatic interpretation of clay minerals in marine deposits: An outlook from the continental origin. *Earth Sci. Rev.* 49, 201-221.
- TIPPER, J.C. (1983) Rates of sedimentation, and stratigraphical completeness. *Nature* 302, 696-698.
- TIPPER, J.C. (1997) Modeling carbonate platform sedimentation - lag comes naturally. *Geology* 25, 495-498.
- TRUMPY, R. (1980) *Geology of Switzerland - a guide-book*. Part A: An outline of the geology of Switzerland, 7-24. (Wepf & Co.).
- TUCKER, M.E. (1993) Carbonate diagenesis and sequence stratigraphy. In: WRIGHT, V.P. (ed) *Sedimentology Review* 1, 51-72 (Blackwell Scientific Publ.).
- TUCKER, M.E. & WRIGHT, V.P. (1990) *Carbonate Sedimentology*. 482pp. (Blackwell).
- UNDERHILL, J.R. & PATERSON, S. (1998) Genesis of tectonic inversion structures: Seismic evidence of the development of key structures along the Purbeck-Isle of Wight Disturbance. *J. Geol. Soc. London* 155, 975-992.
- UNDERHILL, J.R. (2002) Evidence for structural controls on the deposition of the late Jurassic-early Cretaceous Purbeck Limestone Group, southern England. In: MILNER, A.R. & BATTEN, D.J. (eds) *Life and environments in Purbeck times*. 53-70 (The Palaeontological Association London).
- UNDERWOOD, C.J. & REES, J. (2002) Selachian faunas from the lowermost Cretaceous Purbeck Group of Dorset, southern England. In: MILNER, A.R. & BATTEN, D.J. (eds) *Life and environments in Purbeck times*. 83-101 (The Palaeontological Association London).
- VAIL, P.R., MITCHUM, R.M. & THOMPSON, D.B. (1977) Seismic stratigraphy and global changes of sea level, part 3: Relative changes of sea level from coastal onlap. In: PAYTON, C.E. (ed) *Seismic stratigraphy - applications to hydrocarbon exploration*. AAPG Mem. 26, 63-81.
- VAIL, P.R., AUDEMARD, F., BOWMAN, S.A., EISNER, P.N. & PEREZ-CRUZ, C. (1991) The stratigraphic signatures of tectonics, eustasy and sedimentology - an overview. In: EINSELE, G., RICKEN, W. & SEILACHER, A. (eds) *Cycles and events in stratigraphy*. 617-659 (Springer).
- VAKHRAMEEV, V.A. (1991) Jurassic and Cretaceous floras and climates of the Earth. 1-388 (Cambridge University Press).
- VALDES, P.J., SELLWOOD, B.W. & PRICE, G.D. (1995) Modelling Late Jurassic Milankovitch climate variations. In: HOUSE, M.R. & GALE, A.S. (eds) *Orbital Forcing Timescales and Cyclostratigraphy*. GSA Spec. Publ. 85, 115-132.
- VALDES, P.J. & GLOVER, R.W. (1999) Modelling the climate response to orbital forcing. In: SHACKLETON, N.J., MCCAVE, I.N. & WEEDON, G.P. (eds) *Astronomical (Milankovitch) calibration of the geological time-scale*. *Phil. Trans. R. Soc. London A* 357, 1873-1890.
- VAN HOUTEN, F.B. & PURUCKER, M.E. (1984) Glauconitic peloids and chamositic ooids – favourable factors, constraints, and problems. *Earth Sci. Rev.* 20, 211-243.
- VANSTONE, S.D. (1998) Late Dinantian palaeokarst of England and Wales: Implications for exposure surface development. *Sedimentology* 45 (1), 19-37.
- VAN WAGONER, J.C., MITCHUM, R.M., CAMPION, K.M. & RAHAMANIAN, V.D. (1990) Siliciclastic sequence stratigraphy in well logs, cores, and outcrops. *AAPG Methods in Exploration* 7, 55pp.
- VÉDRINE, S., STRASSER, A. & HUG, W. (2007) Oncoid growth and distribution controlled by sea-level fluctuations and climate (Late Oxfordian, Swiss Jura Mountains). *Facies*, (submitted).
- VELDE, B. (1995) Origin and mineralogy of clays. 334pp. (Springer).
- WAEHRY, A. (1989) Facies et séquences de dépôt dans la formation de Pierre-Châtel (Berriasien moyen, Jura méridional, France). Master thesis, 75pp. (University of Geneva, Switzerland).
- WARD, L.G. & ASHLEY, G.M. (1989) Introduction: Coastal lagoonal systems. *Marine Geology* 88, 181-185.
- WARREN, J. (2000) Dolomite: Occurrence, evolution and economically important associations. *Earth Sci. Rev.* 52, 1-81.
- WEEDON, G.P. (1993) The recognition and stratigraphic implications of orbital-forcing of climate and sedimentary cycles. In: WRIGHT, P. (ed) *Sedimentology Review* 1, 31-50.
- WEEDON, G.P., JENKINS, H.C., COE, A.L. & HESSELBO, S.P.

- (1999) Astronomical calibration of the Jurassic time-scale from cyclostratigraphy in British mudrock formations. *Phil. Trans. R. Soc. London. A* 357, 1787-1813.
- WEISSERT, H. (1981) Depositional processes in an ancient pelagic environment: The Lower Cretaceous Maiolica of the Southern Alps. *Eclogae geol. Helv.* 74 (2), 339-352.
- WEISSERT, H.J., MCKENZIE, J.A. & CHANNELL, J.E.T. (1985) Natural variations in the carbon cycle during the Early Cretaceous. *Geophysical Monograph* 32, 531-545.
- WEISSERT, H.J. & CHANNELL, J.E.T. (1989) Tethyan carbonate carbon isotope stratigraphy across the Jurassic-Cretaceous boundary: An indicator of decelerated global carbon cycling? *Paleoceanography* 4 (4), 483-494.
- WEISSERT, H. & MOHR, H. (1996) Late Jurassic climate and its impact on carbon cycling. *Palaeogeogr., Palaeoclim., Palaeoecol.* 122 (1-4), 27-43.
- WEISSERT, H., LINI, A., FÖLLMI, K.B. & KUHN, O. (1998) Correlation of Early Cretaceous carbon isotope stratigraphy and platform drowning events: A possible link? *Palaeogeogr., Palaeoclim., Palaeoecol.* 137 (3-4), 189-203.
- WEISSERT, H. & ERBA, E. (2004) Volcanism, CO<sub>2</sub>, and palaeoclimate: A Late Jurassic-Early Cretaceous carbon and oxygen isotope record. *J. Geol. Soc. London* 161, 1-8.
- WEST, I.M. (1975) Evaporites and associated sediments of the basal Purbeck Formation (Upper Jurassic) of Dorset. *Proc. Geol. Association* 86, 205-225.
- WEST, I.M. (2006) Geology of the Wessex Coast, southern England: <http://www.soton.ac.uk/~imw/index.htm>
- WESTPHAL, H., BÖHM, F. & BORNHOLDT, S. (2004a) Orbital frequencies in the carbonate sedimentary record: Distorted by diagenesis? *Facies* 50 (1), 3-11.
- WESTPHAL, H., MUNNECKE, A., PROSS, J. & HERRLE, J.O. (2004b) Multiproxy approach to understanding the origin of Cretaceous pelagic limestone-marl alternations (DSDP site 391, Blake-Bahama Basin). *Sedimentology* 51 (1), 109-126.
- WESTHEAD, R.K. & MATHER, A.E. (1996) An updated lithostratigraphy for the Purbeck Limestone Group in the Dorset type-area. *Proceeding of the Geologists' Association* 107, 117-128.
- WIESNER, M. (1983) Lithologische und geochemische Faziesuntersuchungen an bituminösen Sedimenten des Berrias im Raum Bentheim-Salzbergen (Emsland). PhD thesis 113pp. (University of Hamburg, Germany).
- WILDI, W., FUNK, H., LOUP, B., AMATO, E. & HUGGENBERGER, P. (1989) Mesozoic subsidence history of the European marginal shelves of the alpine Tethys (Helvetic realm, Swiss Plateau and Jura). *Eclogae geol. Helv.* 82/3, 817-840.
- WILKINSON, B.H., DIEDRICH, N.W. & DRUMMOND, C.N. (1996) Facies successions in peritidal carbonate sequences. *J. Sed. Res.* 66 (6), 1065-1078.
- WILKINSON, B.H., DRUMMOND, C.N., ROTHMAN, E.D. & DIEDRICH, N.W. (1997) Stratal order in peritidal carbonate sequences. *J. Sed. Res.* 67 (6), 1068-1082.
- WILSON, J.L. (1975) Carbonate facies in geologic history. 471pp. (Springer).
- WIMBLEDON, W.A. & HUNT, C.O. (1983) The Portland-Purbeck junction (Portlandian-Berriasian) in the Weald, and correlation of Latest Jurassic-Early Cretaceous rocks in southern England. *Geological Magazine* 120 (3), 267-280.
- WINTERER, E.L. (1991) The Tethyan Pacific during Late Jurassic and Cretaceous times. *Palaeogeogr., Palaeoclim., Palaeoecol.* 87, 253-265.
- WORNARDT, W.W.J. (1999) Revision of sequence boundaries and maximum-flooding surfaces: Jurassic to recent. Offshore Technology Conference Houston, 1-18.
- WORTMANN, U.G., WEISSERT, H., FUNK, H. & HAUCK, J. (2001) Alpine plate kinematics revisited: The Adria problem. *Tectonics* 20 (1), 134-147.
- WRIGHT, V.P. (1988) Paleokarsts and paleosols as indicators of paleoclimate and porosity evolution: A case study from the Carboniferous of South Wales. In: JAMES, N.P. & CHOQUETTE, P.W. (eds) *Paleokarst*. 329-341 (Springer).
- WRIGHT, V.P., PLATT, N.H. & WIMBLEDON, W.A. (1988) Biogenic laminar calcretes: Evidence of calcified root-mat horizons in paleosols. *Sedimentology* 35, 603-620.
- WRIGHT, V.P., PLATT, N.H., MARRIOTT, S.B. & BECK, V.H. (1995) A classification of rhizogenic (root-formed) calcretes with examples from the Upper Jurassic-Lower Cretaceous of Spain and Upper Cretaceous of southern France. *Sedimentary Geology* 100, 143-158.
- WRIGHT, V.P. (1992) Speculations on the control on cyclic peritidal carbonates: Ice-house versus greenhouse eustatic controls. *Sedimentary Geology* 76, 1-5.
- WRIGHT, V.P. (1994) Paleosols in shallow marine carbonate sequences. *Earth Sci. Rev.* 35, 367-395.
- WRIGHT, V.P. & CHERNS, L. (2004) Are there "black holes" in carbonate deposystems? *Geologica Acta* 2 (4), 285-290.
- WRIGHT, V.P. & BURGESS, P.M. (2005) The carbonate factory continuum, facies mosaics and microfacies: An appraisal of some of the key concepts underpinning carbonate sedimentology. *Facies* 51, 17-23.
- ZAKHAROV, V.A. & ROGOV, M.A. (2003) Boreal-Tethyan mollusk migrations at the Jurassic-Cretaceous boundary time and biogeographic ecotone position in the northern hemisphere. *Stratigraphy and Geological Correlation* 11 (2), 152-171.
- ZEISS, A. (1983) Zur Frage der Äquivalenz der Stufen Tithon/Berrias/Wolga/Portland in Eurasien und Amerika. Ein Beitrag zur Klärung der weltweiten Korrelation der Jura-/Kreide-Grenzschichten im marinen Bereich. *Zitteliana* 10, 427-438.
- ZIEGLER, P.A. (1988) Evolution of the Arctic-North Atlantic and the western Tethys. *AAPG Mem.* 43, 198pp.



## PLATES

---

## PLATE 1 - PELOIDS - OIDS - ONCOIDS

- 1 - Peloids and some radial ooids (1) in a pack- to grainstone. Transition Goldberg to Pierre Châtel Fm., facies ri3, sample Co10.1.
- 2a, b - (a) Radial ooids in a packstone (Pierre Châtel Fm.), facies ri3, sample Sc12; (b) Radial ooids in a grainstone (Pierre Châtel Fm.), facies i-o6, sample La15. Radial ooids have several laminae around their nucleus.
- 3 - Superficial ooids (arrows) in a wacke- to packstone (Goldberg Fm.), facies t7, sample Co7. They have one to two laminae around their nucleus
- 4 - Oo-oncoid in a pack- to grainstone (Pierre Châtel Fm.), facies ri4, sample Co13. The nucleus of these oncoids consists of an ooid. They display a transition from an ooid (concentric laminae) to an oncoid (irregular laminae). Oo-oncoids are commonly associated with radial ooids and small oncoids.
- 5 - Small oncoids (arrows) in a wacke- to packstone (Pierre Châtel Fm.), facies i-o3, sample Th50.3. They consist of micritic, irregular laminae around a nucleus.
- 6a, b - (a) *Bacinella*- oncoid in a wackestone (Pierre Châtel Fm.), facies i-o4, sample Cg51. These oncoids are characterized by meshworks of the cyanobacteria *Bacinella irregularis*; (b) Zoom of a *Bacinella irregularis* meshwork.

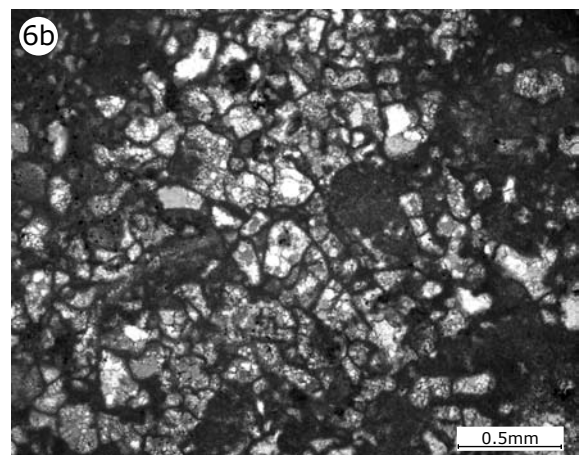
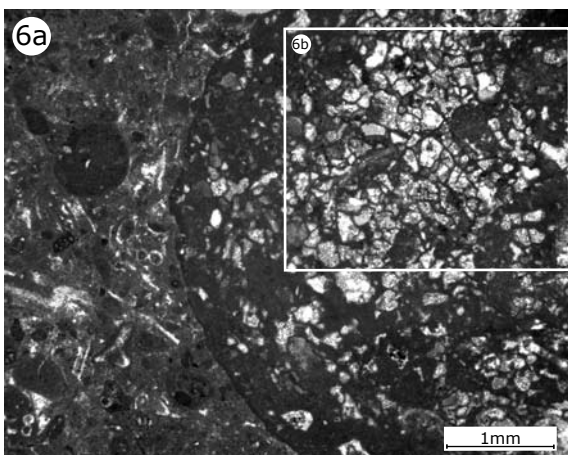
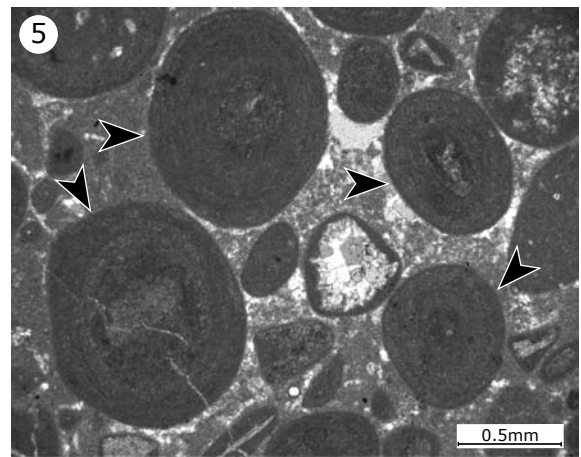
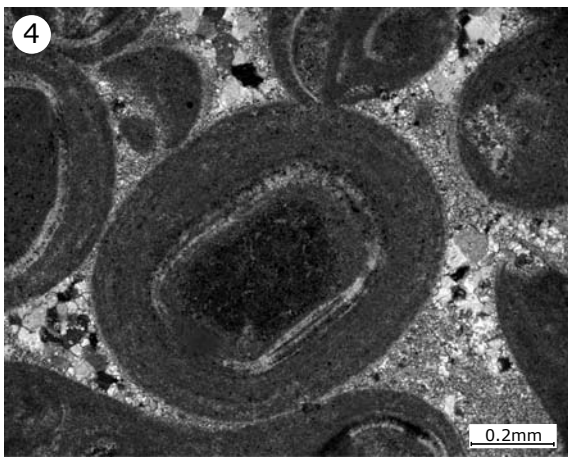
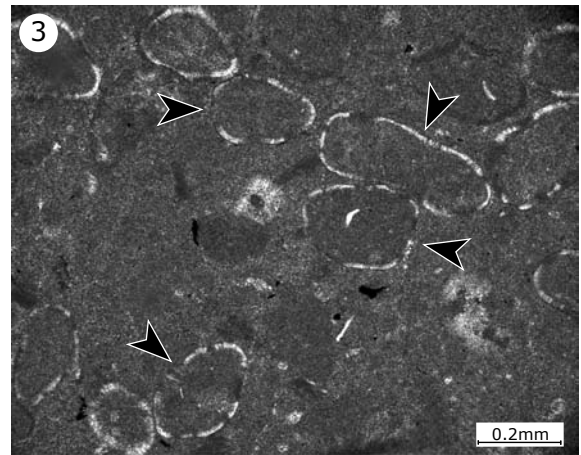
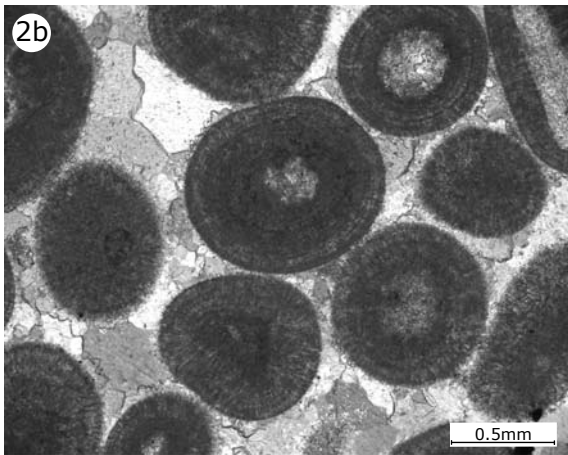
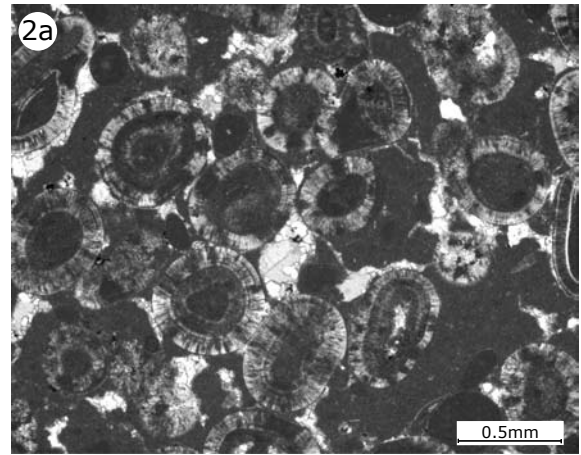
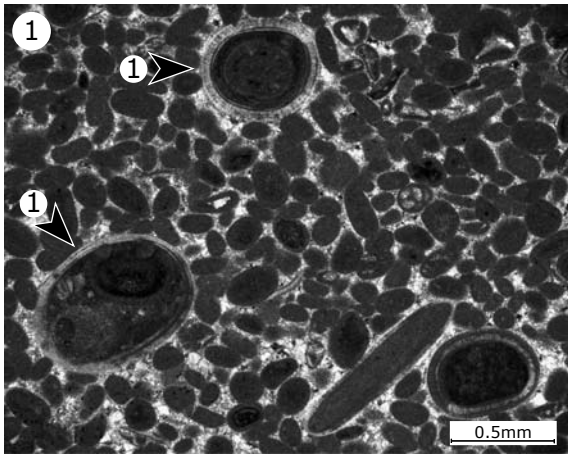


**PLATE 2 - FORAMINIFERA**

- 1a-c - Miliolid foraminifera, (a) *Quinqueloculina* sp. (?), lateral section, Pierre Châtel Fm., facies i-o4, sample Cr51; (b) *Istriloculina* sp. (?), lateral section, Pierre Châtel Fm., facies i-o3, sample La31; (c) large miliolid foraminifer, Pierre Châtel Fm., facies i-o2, sample La32.1.
- 2a, b - (a) Small cyclamminids (1) together with radial ooids (2) and ostracodes (3) in a wacke- to packstone (Pierre Châtel Fm.), facies ri3, sample Ru25; (b) Small cyclamminid (*Feurtillia* sp. ?), equatorial section, Pierre Châtel Fm., facies ri3, sample Co41.
- 3a-c - *Andersenolina alpina* (?) (ex *Trocholina alpina*), Pierre Châtel Fm., facies o1, (a) sample La29; (b) sample La30; (c) *Andersenolina elongata* (?) (ex *Trocholina elongata*), Pierre Châtel Fm., facies i4, sample Sc26.1.
- 4a, b - *Lenticulina* sp. (a) subequatorial (oblique) section, Pierre Châtel Fm., facies i-o5, sample La30.1; (b) axial section, Pierre Châtel Fm., facies ri2, sample Cg21.
- 5a, b - *Nautiloculina oolithica* (?) equatorial sections, Pierre Châtel Fm., (a) facies i6, sample Vf13; (b) facies i-o4, sample Cr40.
- 6a, b - *Redmondoides* sp. (?) (ex *Valvulina* sp.), (a) *Redmondoides* (1) occur together with radial ooids (2) in a pack- to grainstone (Pierre Châtel Fm.), facies ri3, sample La13.1; (b) *Redmondoides lugeoni* (?) (ex *Valvulina lugeoni*), axial section, Pierre Châtel Fm., facies i-o4, sample Cr28.1.
- 7 - *Mohlerina basiliensis* (?) (ex *Conicospirillina basiliensis*), axial section, Pierre Châtel Fm., facies i-o3, sample Ye32.
- 8 - Big cyclamminid, *Pseudocyclammina* sp. (?), subaxial section, Pierre Châtel Fm., facies i5, sample Cg31.2.
- 9 - Big cyclamminid, *Pseudocyclammina* sp. (?), equatorial section, Pierre Châtel Fm., facies i-o4, sample Co57.
- 10 - Big cyclamminids, *Anchispirocyclina* sp. (?) (arrow) in a packstone (Pierre Châtel Fm.), subaxial section, facies i4, sample Po14.



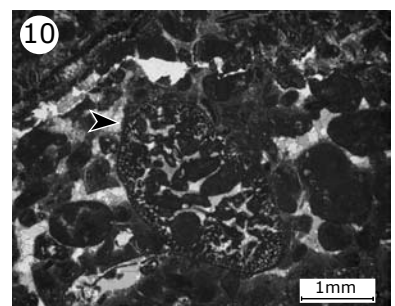
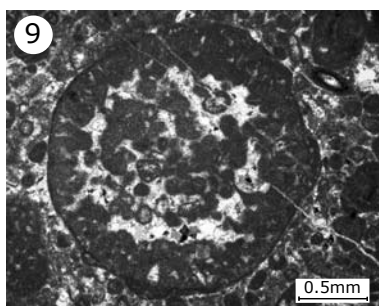
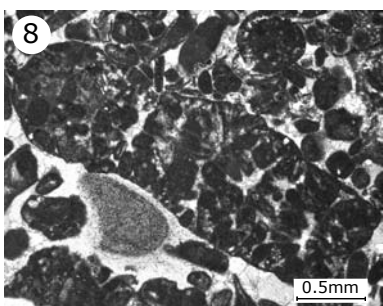
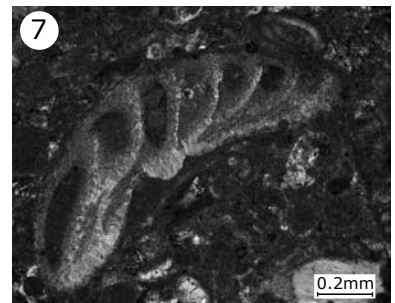
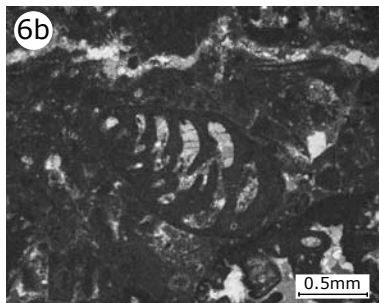
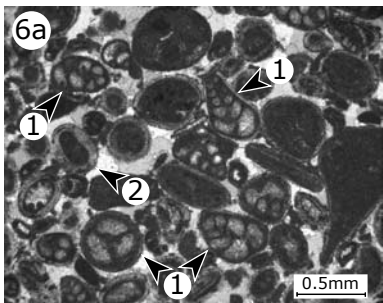
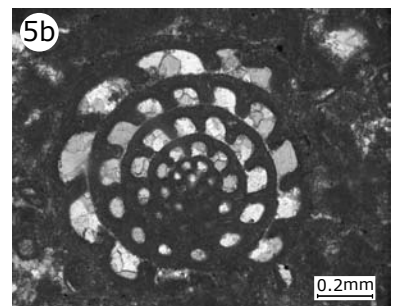
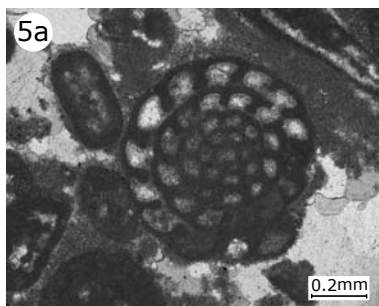
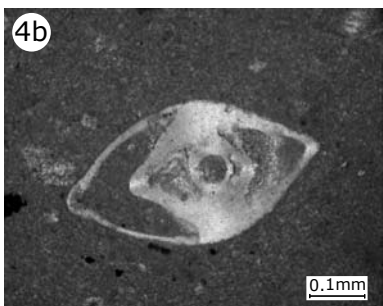
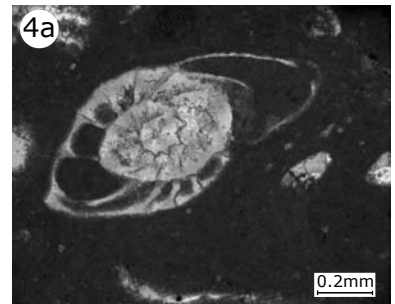
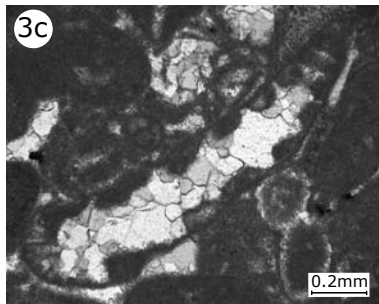
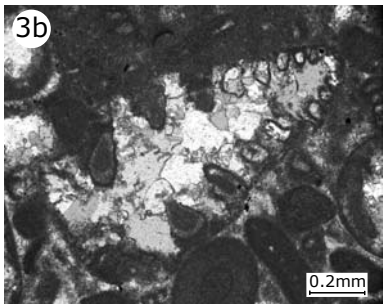
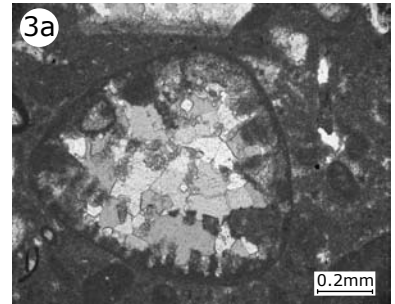
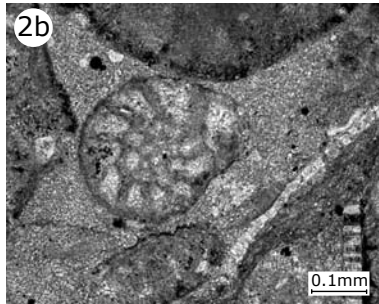
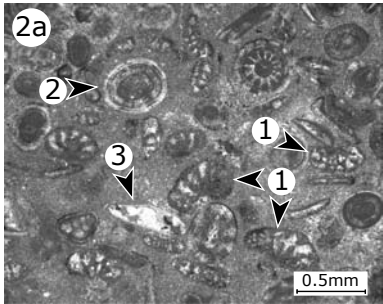
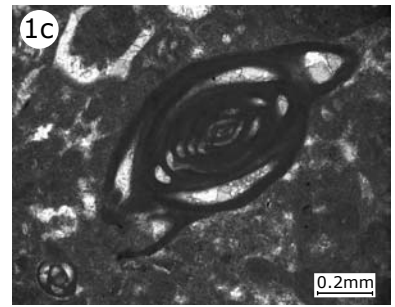
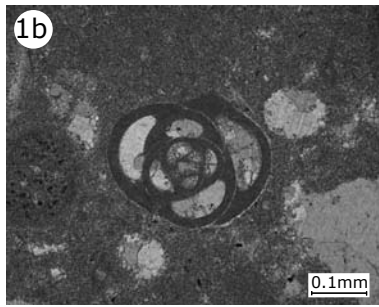
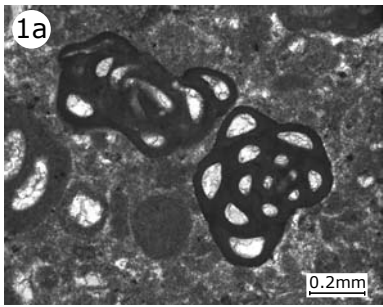


### PLATE 3 - DASYCLADACEANS

1a-c - *Clypeina sulcata*, Pierre Châtel Fm., (a) transversal- oblique sections, facies i2, sample Cg39.1; (b) oblique section, facies ri2, sample Cr27.2; (c) transversal- oblique section, facies i-o4, sample Cr21.1.

2a, b - *Clypeina* sp. (?), Pierre Châtel Fm., (a) facies ri2, sample Co44; (b) facies ri3, sample Ru29.

3 - *Terquemella* sp. (?), Pierre Châtel Fm., facies ri2, sample Co44.

4 - *Salpingporella annulata* (?), oblique section, Pierre Châtel Fm., facies i3, sample Cr16.1.

5 - *Clypeina estevezii* (?), oblique section, Pierre Châtel Fm., facies i-o4, sample Cr29.

6 - Fragments of *Clypeina? solkani* (?), transversal sections, Pierre Châtel Fm., facies i-o5, sample Ma8.1.

7 - Monospecific occurrence of *Clypeina sulcata*, Pierre Châtel Fm., facies ri2, sample Cr27.2. The monospecific accumulation of dasyclad algae probably points to a restricted lagoonal environment.

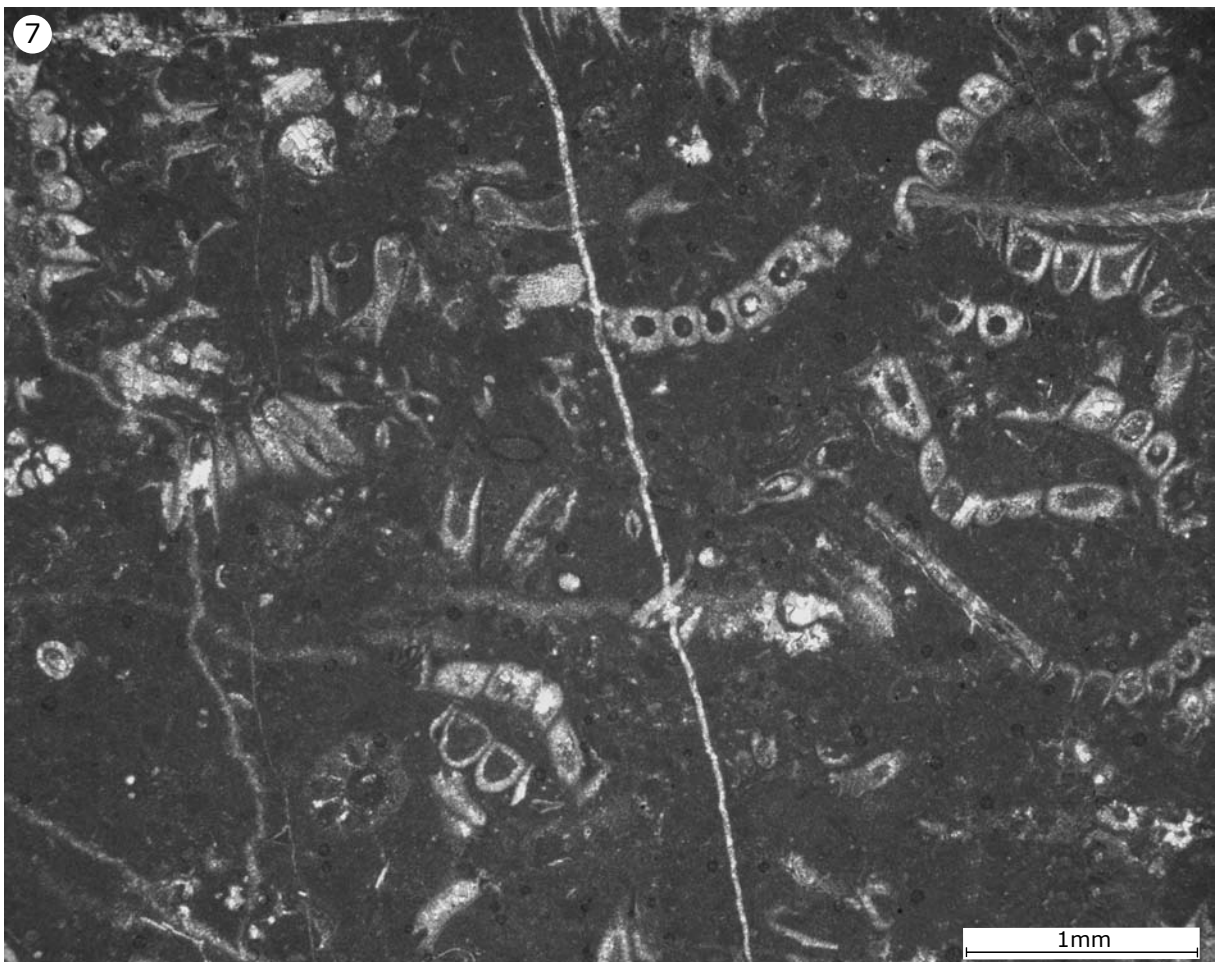
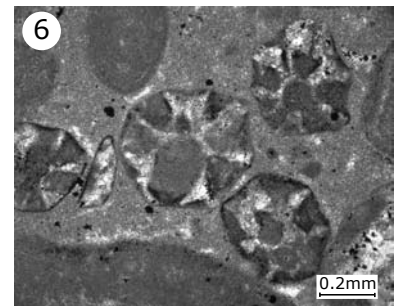
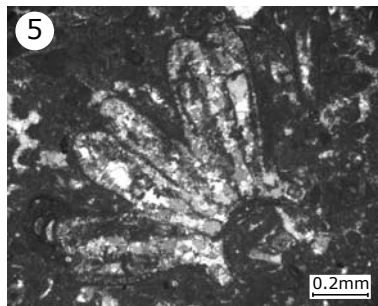
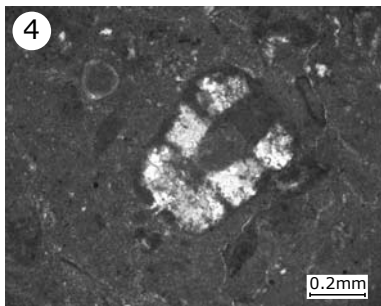
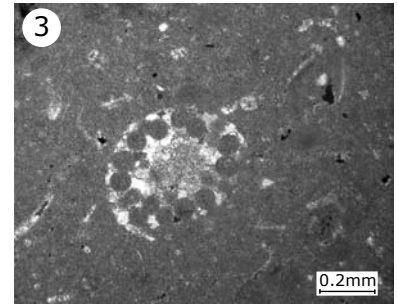
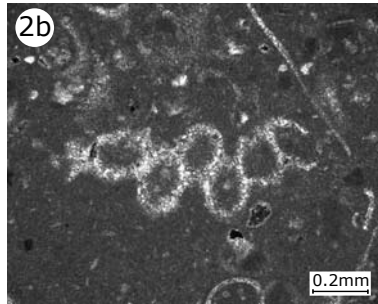
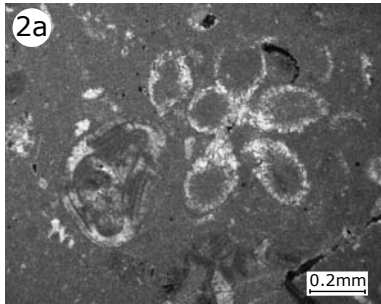
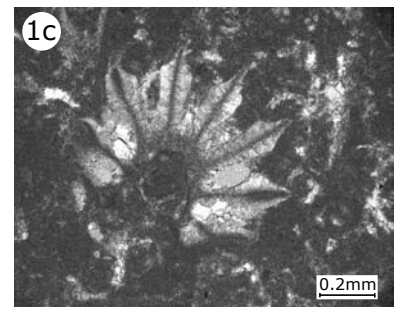
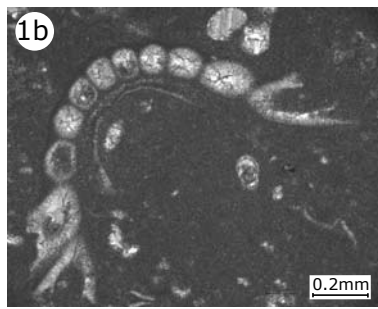
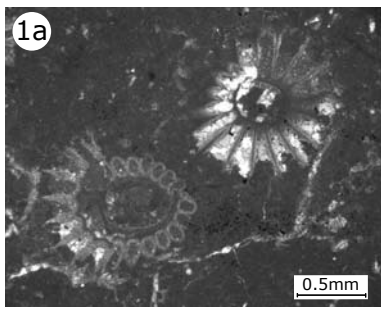


## **PLATE 4 - CHAROPHYTES – OSTRACODES - GASTROPODS**

1a-c - Charophyte stems, transversal sections; (a) Goldberg Fm., facies c2, sample Cr1; (b) Goldberg Fm., facies c-t, sample Th40; (c) Pierre Châtel Fm., facies c2, sample La11.

2a-h - Charophytes gyrogonites, axial sections, (a) gyrogonite (?), Pierre Châtel Fm., facies ri3, sample Cg24; (b) gyrogonite (?), Pierre Châtel Fm., facies ri3, sample Cg27; (c) Goldberg Fm, facies c-t, sample La2; (d, e) Pierre Châtel Fm., facies c2, sample La8, (d) gyrogonite (1) and stem (2), (e) gyrogonite (1) and radial ooid (2); (f) gyrogonites (1) and stem (2) in a wacke- to packstone (Goldberg Fm.), facies c2, sample Co9; (g, h) gyrogonites and stems (arrows) in a wackestone (Pierre Châtel Fm.), facies t4, sample Sc15.

3a-d - Ostracodes, (a) ostracodes with different sizes, Pierre Châtel Fm, facies i3, sample Cg31; (b) Goldberg Fm., facies t3, sample Th 35; (c) ostracode (1) and gyrogonite (2), Goldberg Fm., facies t4, sample Th42; (d) ostracode (1) and charophyte stem (2), Goldberg Fm., facies c1, sample Cg14.

4a-c - Gastropods, (a) Pierre Châtel Fm., facies i6, sample Ma6.05; (b) Goldberg Fm., facies t5, sample Th47; (c) Goldberg Fm., facies c2, sample Ru8.

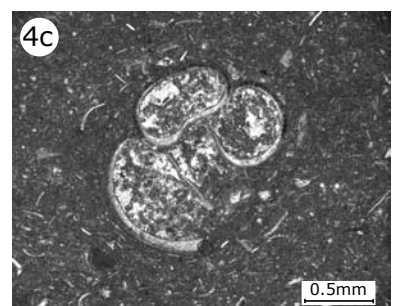
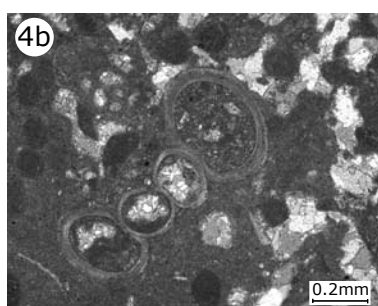
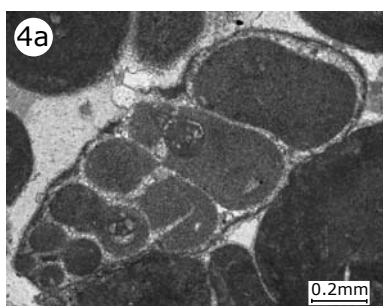
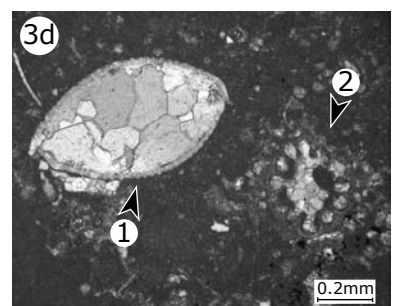
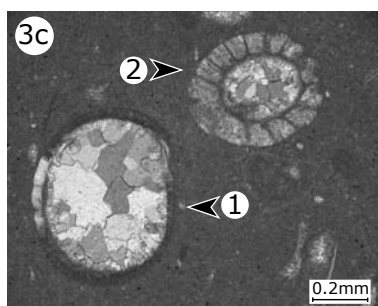
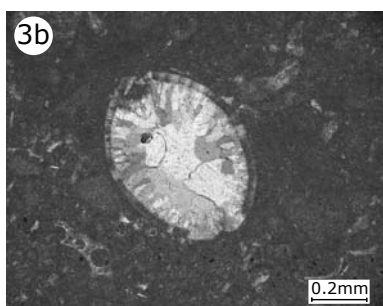
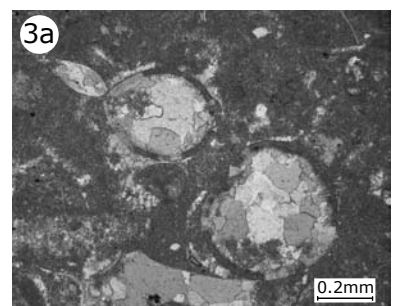
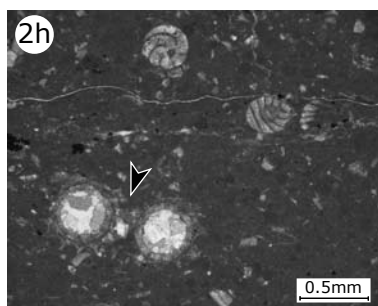
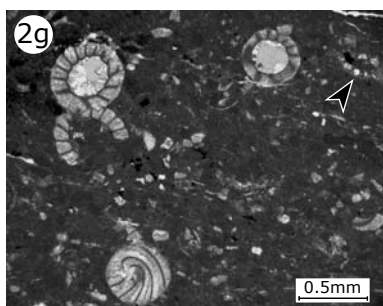
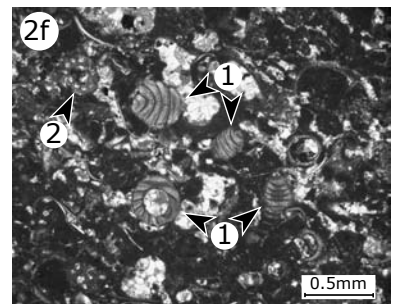
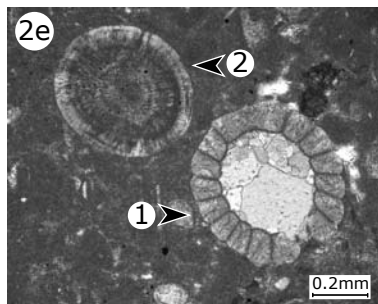
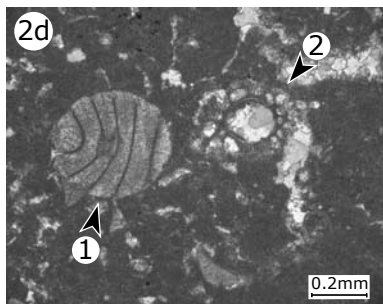
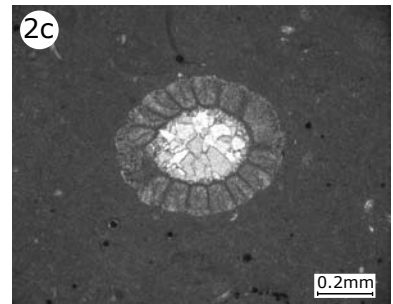
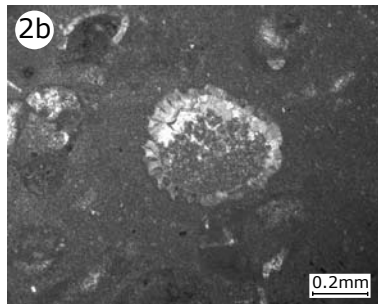
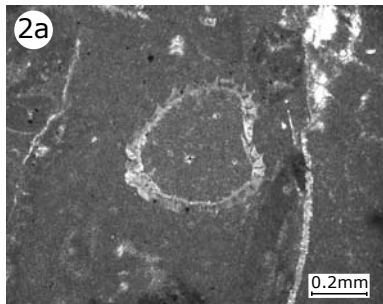
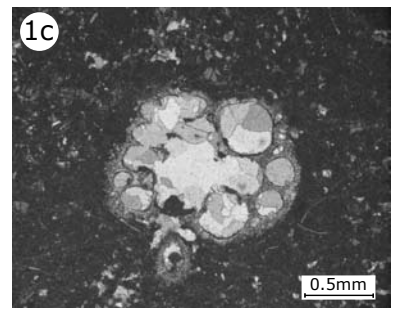
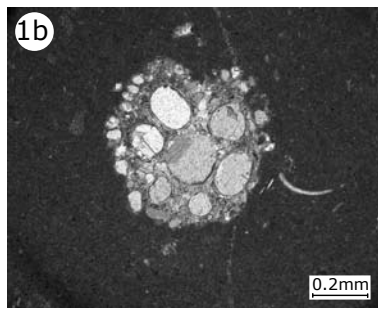
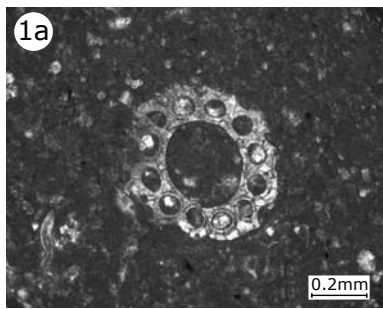


## **PLATE 5 - BRYOZOANS – SPONGES – CORALS – FECAL PELLETS – SERPULIDS**

- 1a, b - Bryozoans, (a) encrusting bryozoans (1) on a bivalve shell (2), Pierre Châtel Fm., facies o2, sample La25.1; (b) fragment of bryozoan (arrows) in a wacke- to packstone (Pierre Châtel Fm.), facies i-o3, sample Ye38.
- 2 - Part of a sponge (arrows), Pierre Châtel Fm., facies i-o3, sample La31.
- 3 - Part of a coral (arrows), Pierre Châtel Fm., facies o3, sample La36.
- 4 - Fecal pellet (*Favreina* sp. ?) (arrows), facies t4, sample Ye3.
- 5a-c - (a) Serpulids (arrows) in a wacke- to packstone (Goldberg Fm.), facies t7, sample Co7; (b) Serpulids (arrows) in a mudstone (Goldberg Fm.), facies t4, sample Th43; (c) Zoom of serpulids in 5b.



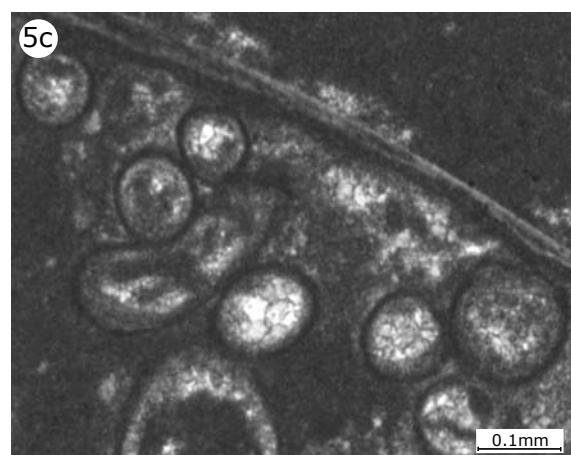
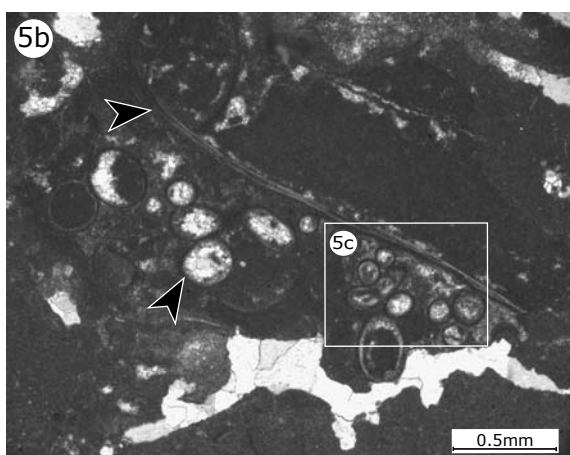
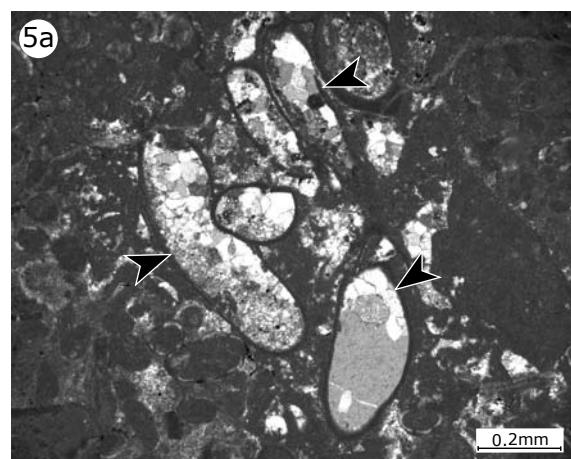
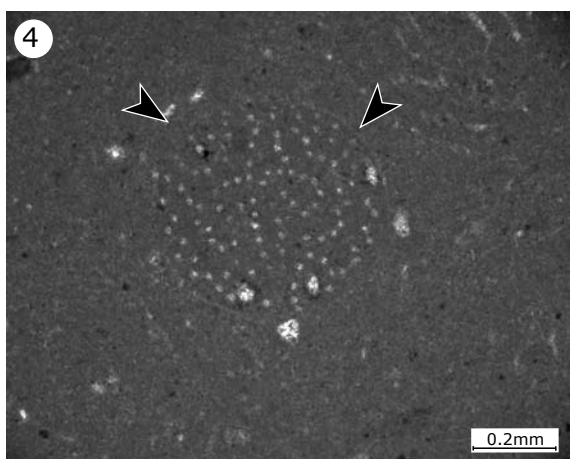
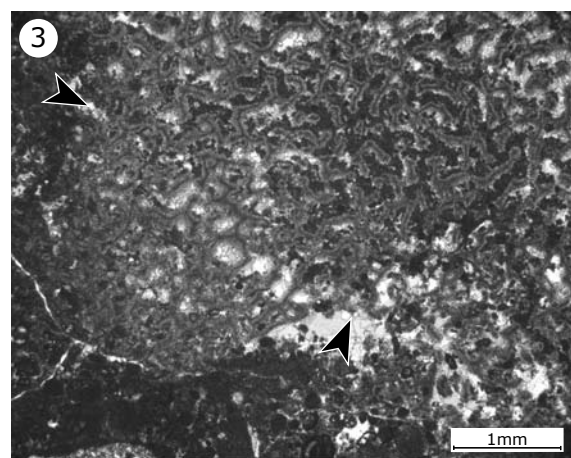
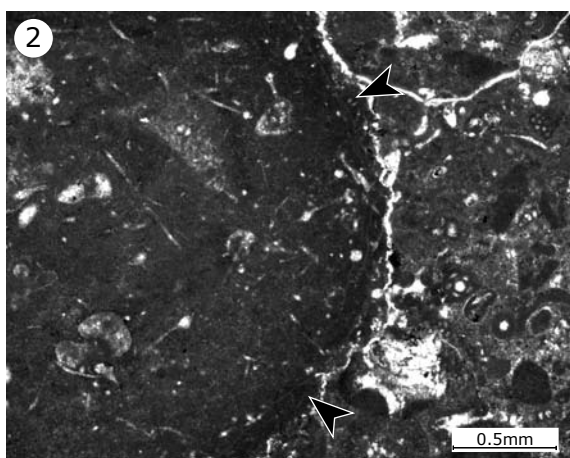
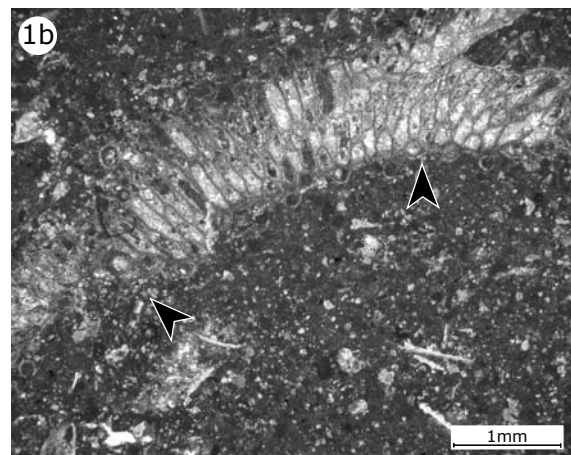
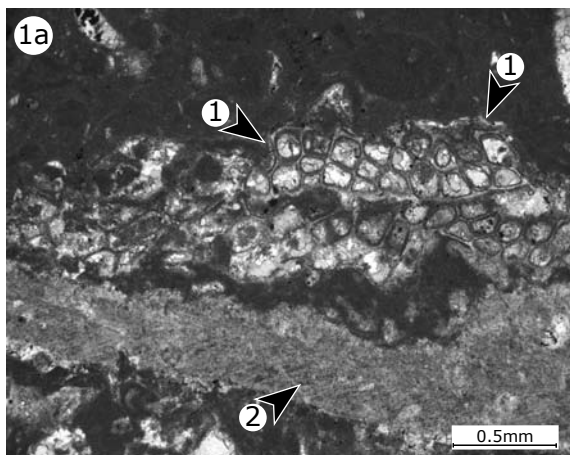


**PLATE 6 - CYANOBACTERIA – MICROPROBLEMATICA**

- 1a, b - Microproblematicum *Lithocodium aggregatum* in a rudstone (Pierre Châtel Fm.), facies o4, sample Sc32; (b) Zoom of *Lithocodium aggregatum*. This microproblematicum is commonly associated with the cyanobacteria *Bacinella irregularis* (cf. Chap. 2). SCHMID & LEINFELDER interpret *L. aggregatum* as foraminifer whereas it is also considered as a sponge (KOCH et al., 2002; in SCHLAGINTWEIT et al., 2005) or as colonies of calcified cyanobacteria (CHERCHI & SCHROEDER 2006). Generally, the occurrence of *Lithocodium aggregatum* is characteristic for open-lagoonal environments with normal salinity (e.g., SCHMID & LEINFELDER 1996, DUPRAZ 1999).
- 2a, b - Microproblematicum “*Thaumatoporella* sp.- ladders” in a rudstone (Pierre Châtel Fm.), facies o4, sample Th61; (b) Zoom of “*Thaumatoporella* sp.- ladders”. *Thaumatoporella* sp. occur in forms of thin, elongated “stripes” called “ladders” (translated from the German nomination “Leiter” of NOSE 1995, p. 125). They are commonly associated with *Bacinella*-oncoids in internal- to open-lagoonal environments.
- 3 - Cyanobacteria, (a) *Garwoodia* sp. (?) (arrows), Pierre Châtel Fm., facies i4, sample La13;
- 4 - Tubes (1) may represent different type of borings in a bivalve shell (2), Pierre Châtel Fm., facies o4, sample La34.
- 5a, b - (a) Strange borings (arrows) in a floatstone (Pierre Châtel Fm.), facies o1, sample La22; (b) Zoom of strange borings. These borings are post-depositional because they cut across grain boundaries (1). They have a diameter of about 0.05 mm and are partly limited by dark linings (2). Some borings display a segmented internal structure (3).



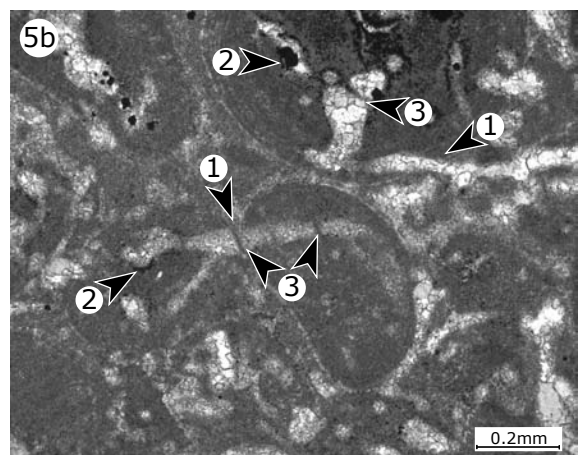
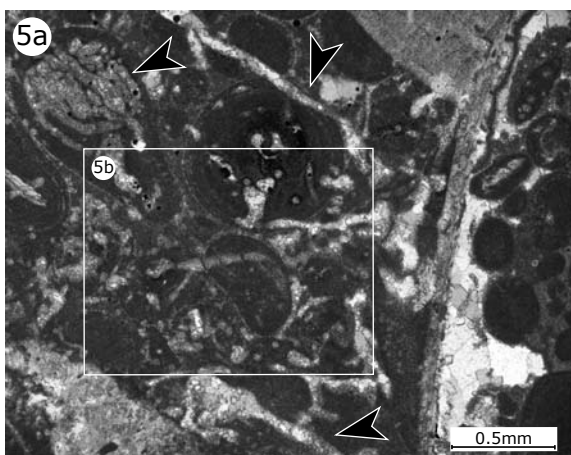
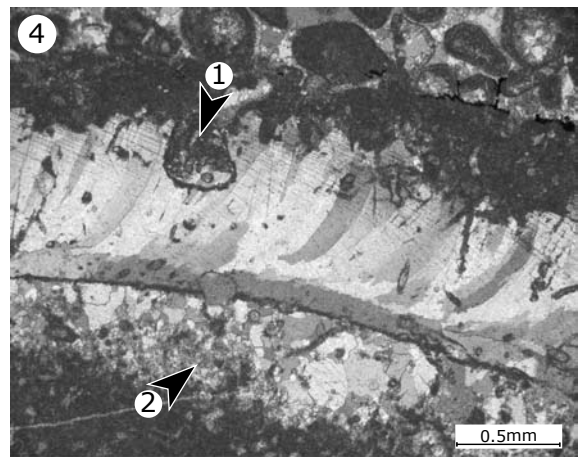
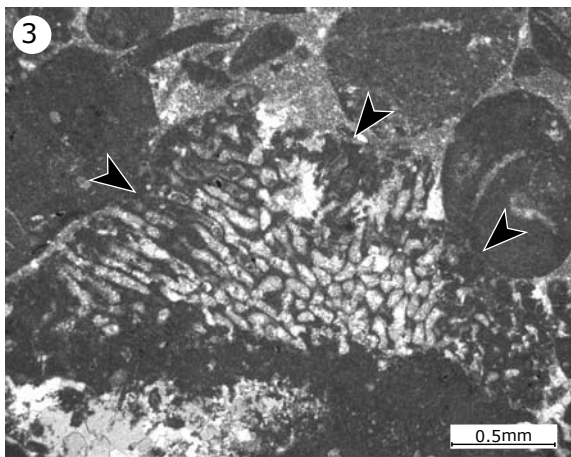
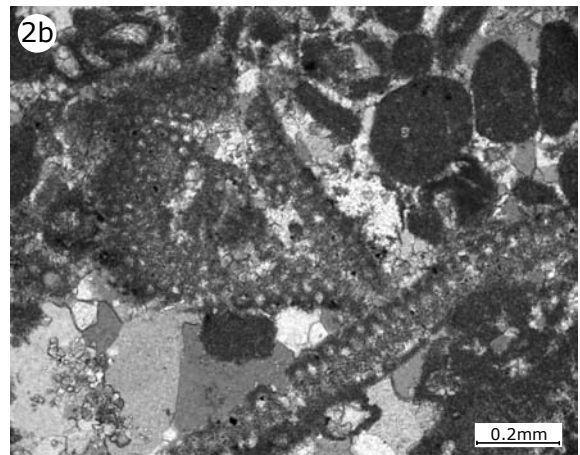
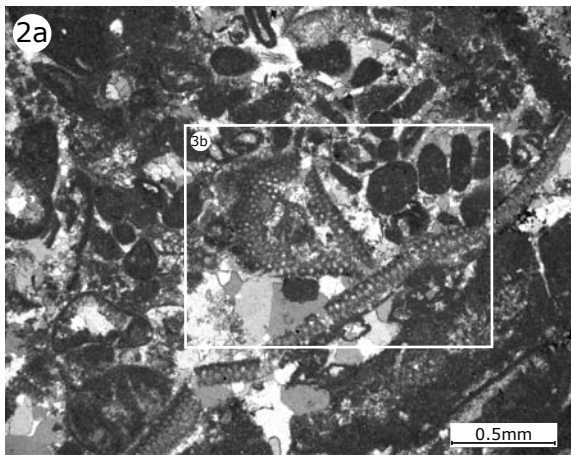
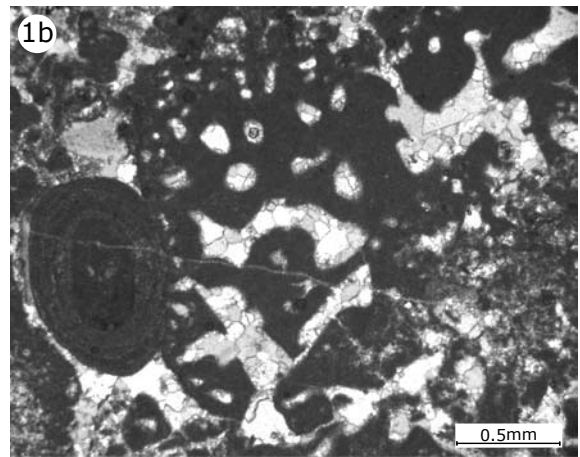
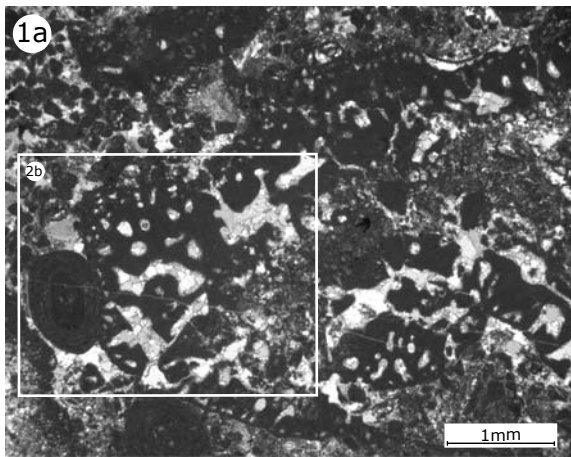


**PLATE 7 - CIRCUMGRANULAR CRACKS – DESICCATION CRACKS – BIRDSEYES –  
LAMINATION**

- 1- Circumgranular cracks around intraclasts in a pack- to grainstone (Goldberg Fm.), facies t6, sample Sc9.
- 2a, b - (a) Desiccation cracks in a mudstone (Goldberg Fm.), facies t3, sample Cg9; (b) desiccation cracks (1) and birdseyes (2) in a mudstone (Goldberg Fm.), facies t3, sample Cg4.
- 3a, b - Birdseyes in a mudstone (Goldberg Fm.), facies t3, sample Ye9; (b) birdseyes in a mudstone (Goldberg Fm.), facies c-t, sample Cg13.
- 4a, b - (a) Cavity filled with laminated micrite at the bottom (1) and a blocky cement at the top (2) (geopetal structure) in a mudstone (Goldberg Fm.), facies c-t, sample Th40; (b) cavities filled with blocky cement (1) and partly with vadose crystal silt (2) in a mudstone (Goldberg Fm.), facies t-i, sample Vf5. The occurrence of such cavities probably points to initial karstification processes (PLATT 1989).
- 5 - Alternations of ostracode-rich (1) and thinly laminated intervals (2) in a mud- to wackestones (Pierre Châtel Fm.), facies ri3, sample Cg27. The alternating lamination is interpreted as the influence of tidal currents in a restricted, internal lagoon.

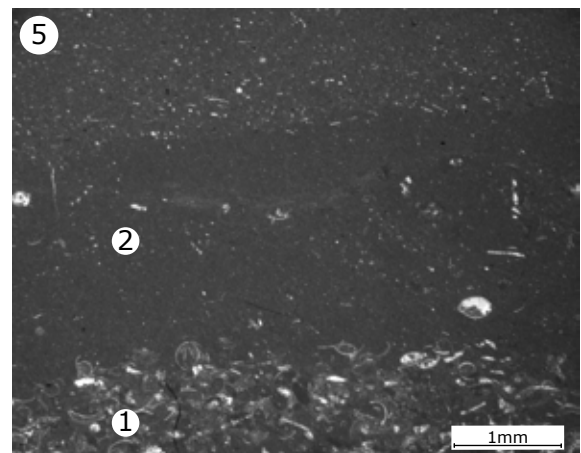
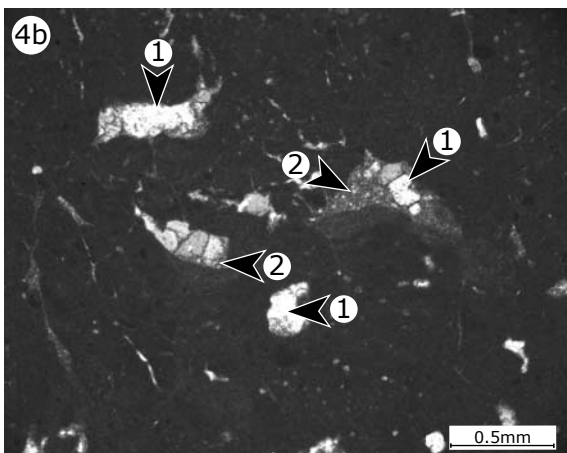
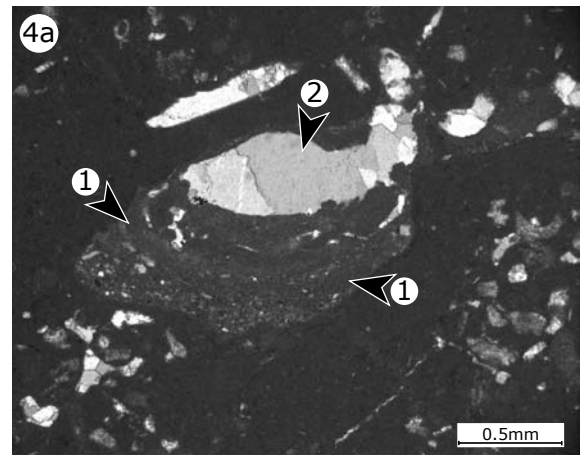
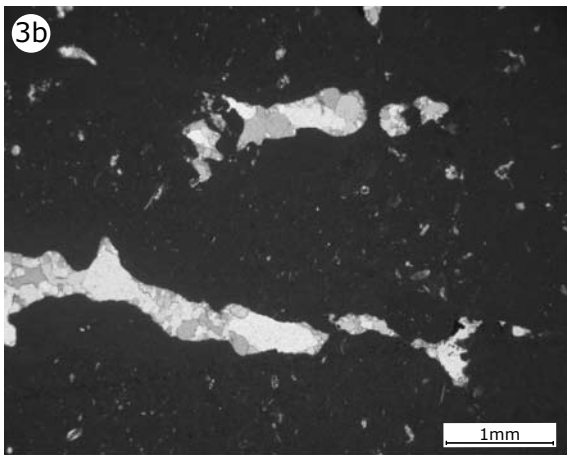
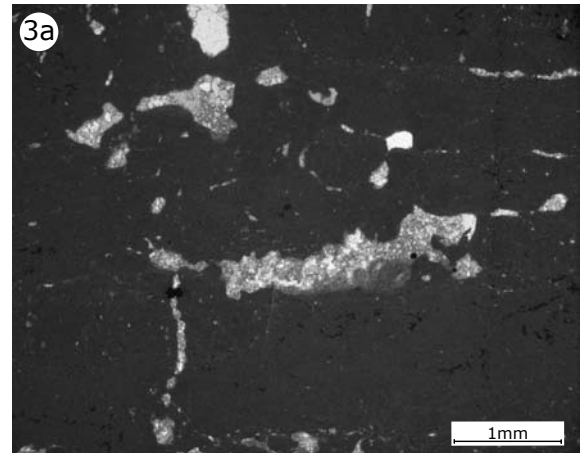
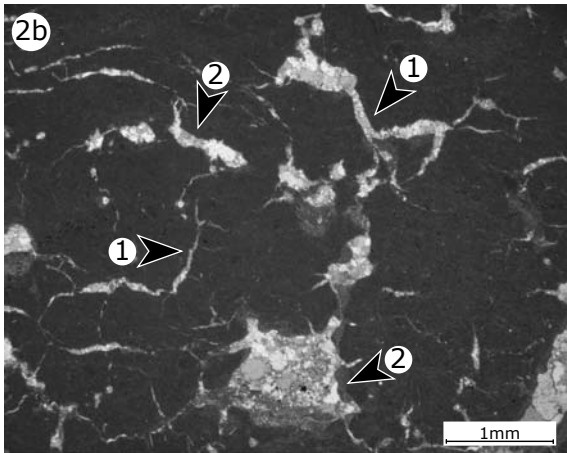
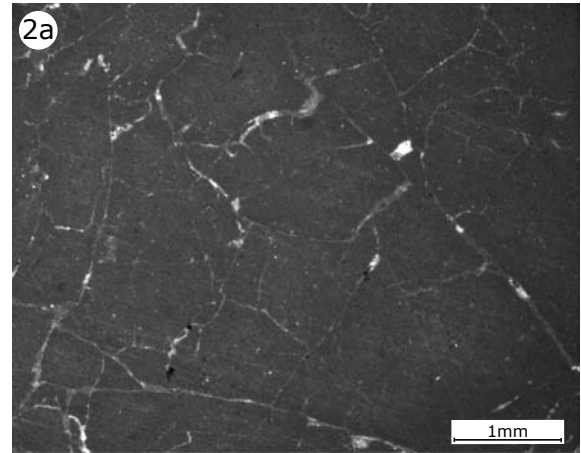
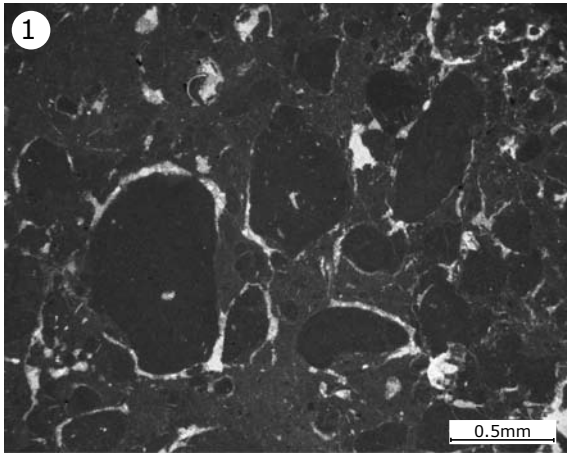


## **PLATE 8 - EVAPORITE PSEUDOMORPHS - MICROBIAL MATS -DISCONTINUITIES**

- 1a-c - (a) Gypsum pseudomorphs in a mudstone (Goldberg Fm.), facies c2, sample Co9; (b) Zoom of gypsum pseudomorphs; (c) gypsum pseudomorphs in a mudstone (Goldberg Fm.), facies t3, sample Co1.
- 2a, b - Microbial mats in a mud- to wackestones (Goldberg Fm.), facies t3, sample Ye14, thinly laminated microbial mats; (a) birdseyes (1) and sheet cracks (2); (b) birdseyes ? forming “diapir structures” (arrows).
- 3 - Hardground with encrusting oyster (arrow), Pierre Châtel Fm., Crozet section, surfaces at 10.05 m (cf. Chap. 4), coin of five Swiss Franc for scale.
- 4a, b - (a), (b) Different views on a microkarst surface displaying original karst morphology, Pierre Châtel Fm., Rusel section, interval around 2.25m (cf. Chap. 4), pen for scale.

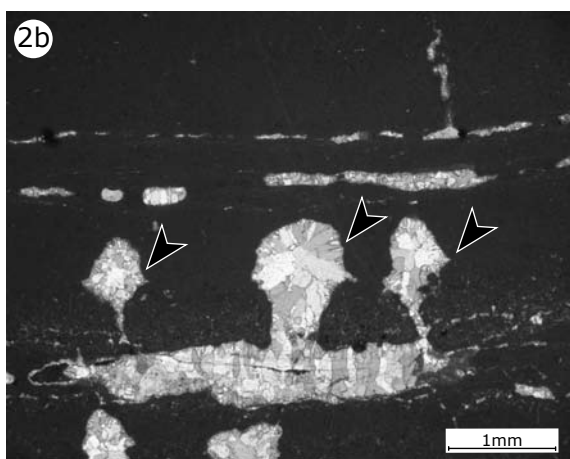
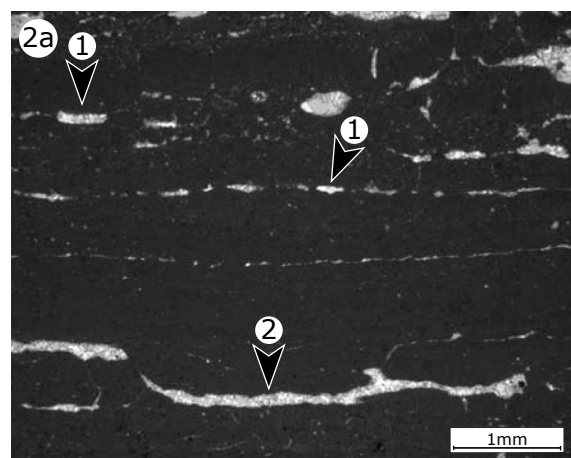
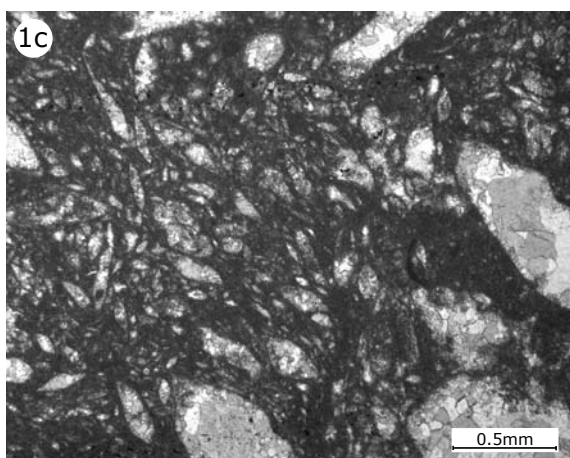
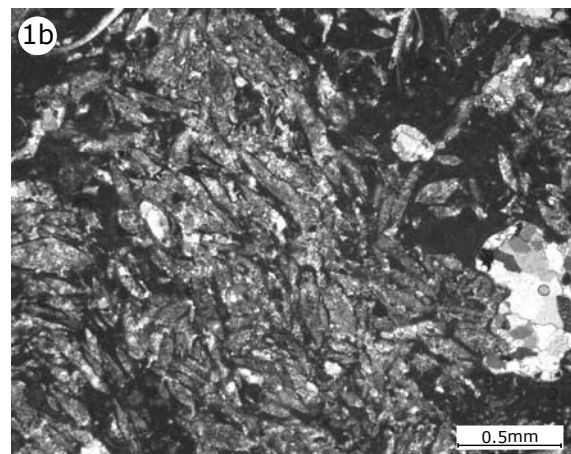
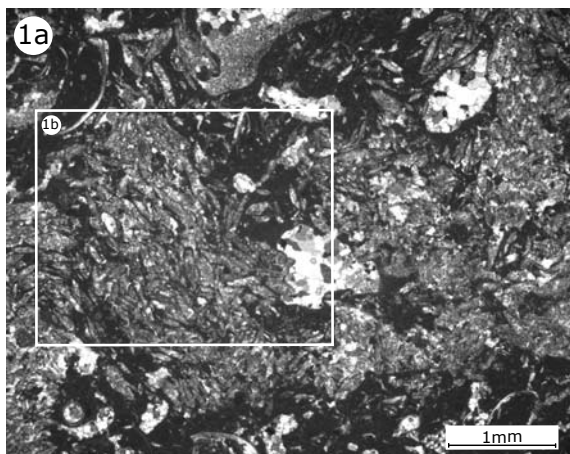


## PLATE 9 - SHOALS

Shoals are large-scale, cross-bedded sedimentary bedforms in the outcrops. They are characterized by foreset-beds with a low-angle tabular geometry. In the field, these bedforms have been analysed in two dimensions – the three-dimensional description of these bedforms is not possible. Generally, intervals of cross-bedded bedforms (white lines) are inclined to the “normal” beddings layers (black lines).

- 1 - Shoals of the Crozet section, Pierre Châtel Fm., interval from around 7.35 to 8.35 meters (cf. Chap. 4), hammer for scale.
- 2 - Shoals with reactivation surfaces (arrows) of the Marchairuz section, Pierre Châtel Fm., interval from around 3.85 to 5.05 meters (cf. Chap. 4), hammer for scale.
- 3 - Shoals of the Lavans section, Pierre Châtel Fm., interval from around 4.80 to 5.80 meters (cf. Chap. 4), uncle Hans for scale.



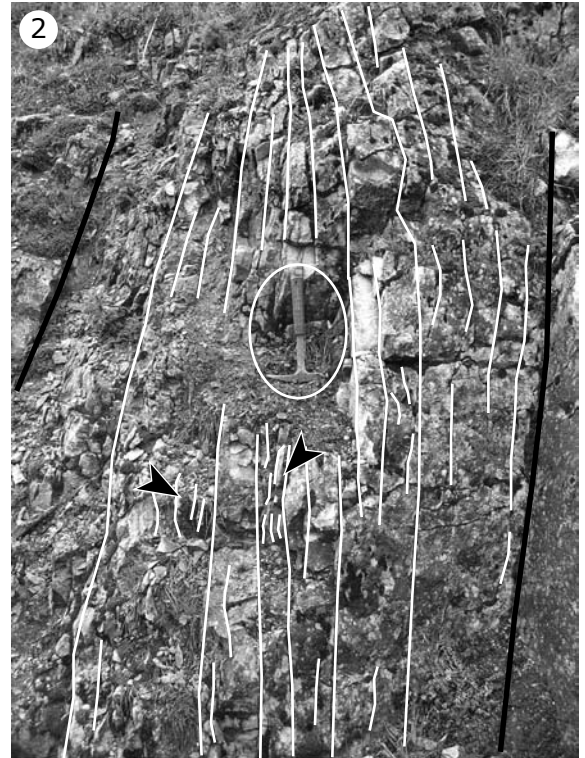


## PLATE 10 - BIVALVES - OSTRACODES

- 1 - (a, b) Bivalves (Neomiodontids) with well-preserved internal shell structures (arrows), Marly Freshwater Member, facies Dt-i, sample Du8. These densely packed shell accumulations have been interpreted as “shell beaches” of shallow lagoons. The good preservation of the aragonitic bivalve shells is probably due to the enclosing of the shell beds by impermeable clays isolating them from flowing meteoric water (EL-SHAHAT & WEST 1983).
- 2 - Oysters (*Praeexogyra distorta*) of the Cinder Member, facies ri2, sample Du28.
- 3 - Ostracodes (1) and charophyte stems (2) in a mud- to wackestone (Cherty Freshwater Member), facies Dc2, sample Du15.
- 4 - Silicification (1) of the pore space within a bivalve (2), Cherty Freshwater Member, facies Dt4, sample Du13.
- 5 - On the left side: Silicification (1) of the pore space within ostracodes (2); on the right side: cementation of the pore space within ostracodes by blocky calcite crystals (3), Cherty Freshwater Member, facies Dt4, sample Du13.
- 6 - Mass-concentration of ostracode shells in an ostracodite, Cherty Freshwater Member, facies Dt4, sample Du14. Such mass-concentrations probably point to “salinity crises” in shallow ephemeral ponds or lakes.



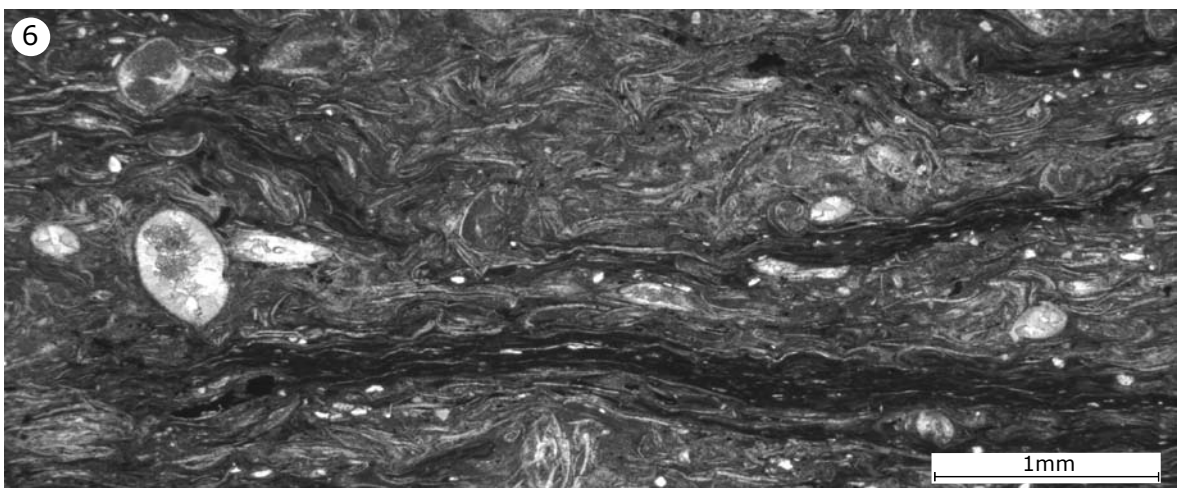
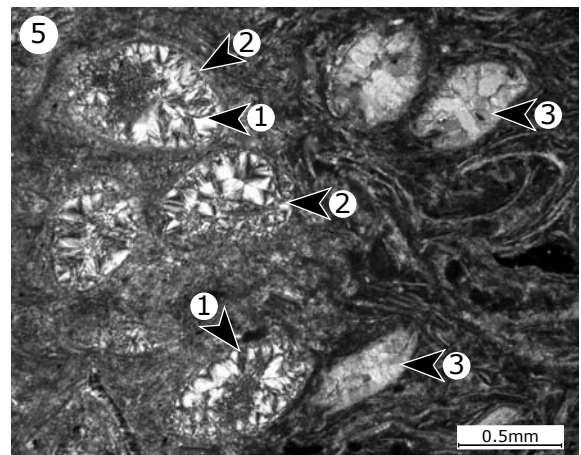
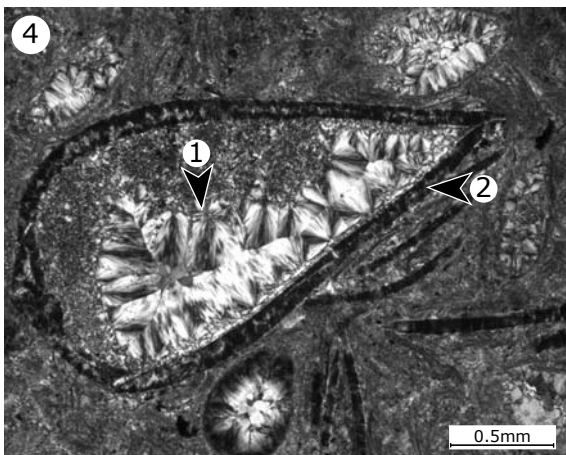
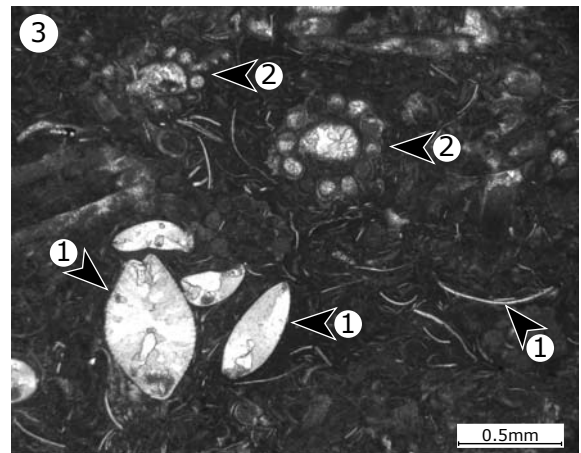
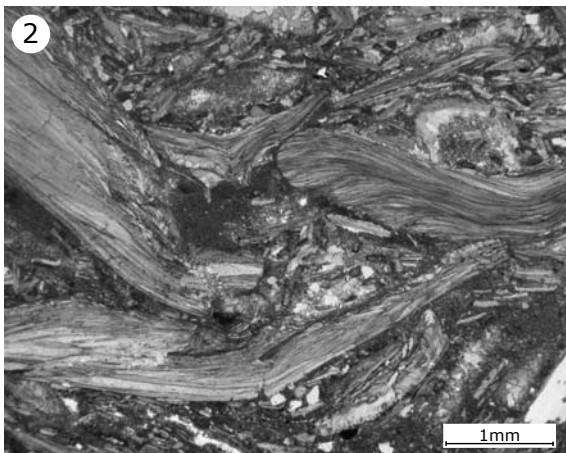
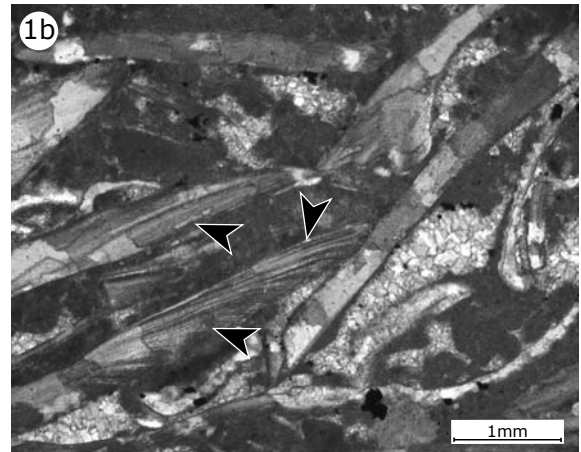
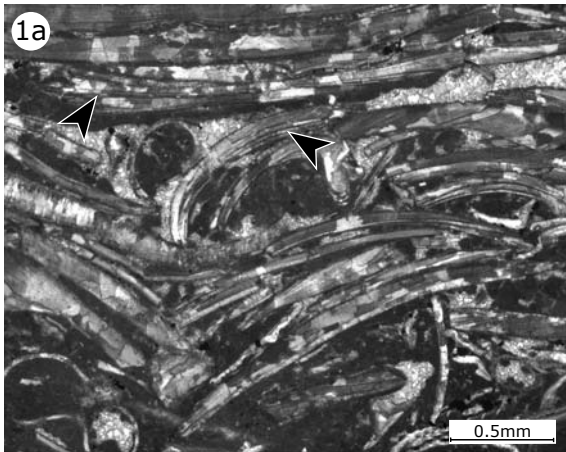


**PLATE 11 – BITUMINOUS DEPOSITS – LAMINATION – FLASER BEDDING –  
POLYGONAL MUDCRACKS**

- 1a-b - Dark, thinly laminated, bituminous mud- to wackestones with ostracode shells (arrows), (a) Marly Freshwater Member, facies Dc3, sample Du11.2; (b) Cherty Freshwater Member, facies Dc3, sample Du19.
- 2 - Fine lamination of a marly mud- to wackestone, Durlston Bay section, interval around 24.50 to 24.80 meters, scale bar 15 cm.
- 3a-b - (a) Flaser bedding in a massive packstone, Worbarrow Tout section, Intermarine Member, interval around 20.75 to 20.90 meters; (b) Detail of flaser bedding.
- 4 - Surface with polygonal mudcracks (arrows), Worbarrow Tout section, Cherty Freshwater Member, surface at 12.00 meters, scale bar 15 cm.

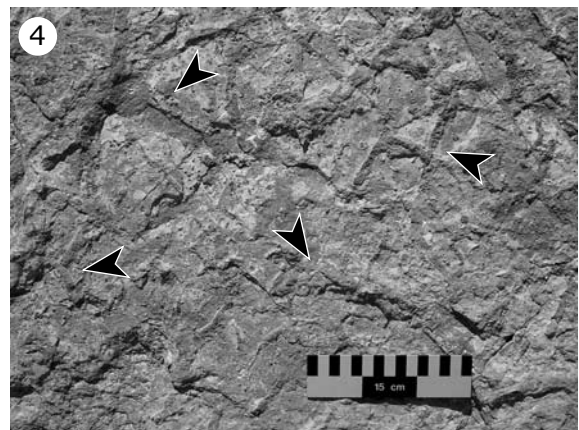
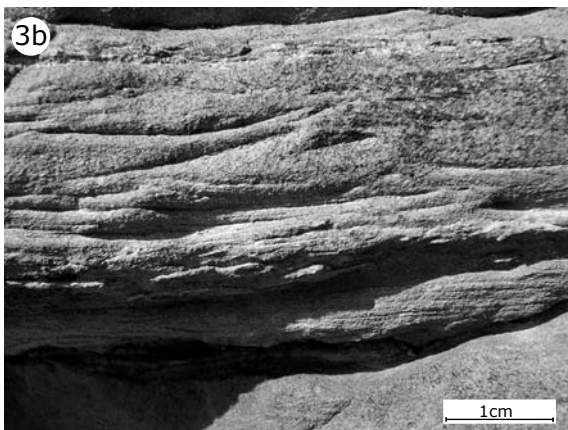
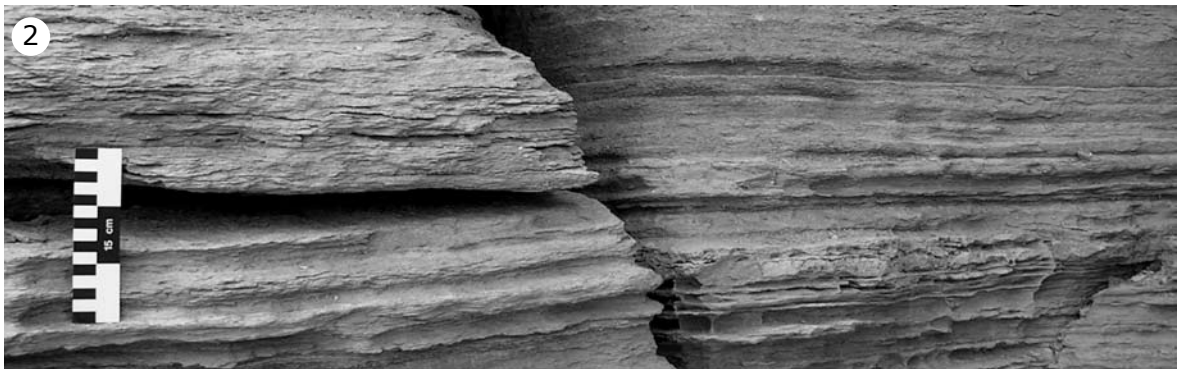
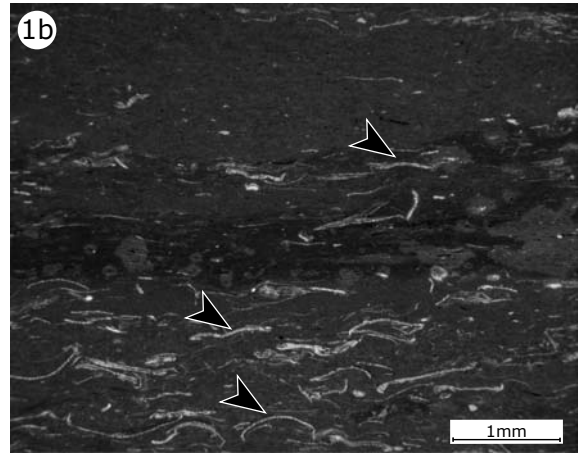
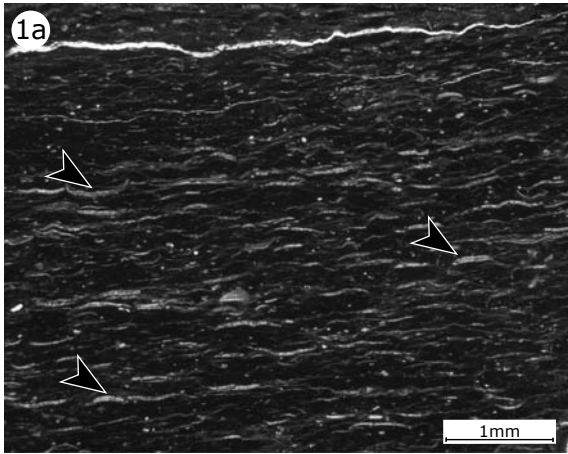


## PLATE 12 – MAMMAL BED – CHERT NODULES – DINOSAUR FOOTPRINTS

- 1 - Mammal Bed: Brownish marly palaeosol rich in mammalian teeth (e.g., KIELAN-JAWOROWSKA & ENSOM 1992). It is considered as a marker bed in this study and is interpreted as 3<sup>rd</sup>-order sequence boundary Be3 (according to HARDENBOL et al. 1998; cf. Chap. 6). Durlston Bay section (DB 83), Marly Freshwater Member, interval around 4.50 to 5.30 meters, hammer for scale.
- 2 - Black, irregular chert nodules within a massive ostracode- and bivalve-rich packstone. Example of a chert nodule containing bivalve shells (arrow). Worbarrow Tout section (WT 112), Cherty Freshwater Member, interval around 10.70 to 11.00 meters, scale bar 15 cm.
- 3 - Badly preserved tridactyl dinosaur footprints (negative epirelief; arrows) with blout toes as wide as long on a bed surface with desiccation cracks. This is typical for tracks of ornithischian dinosaurs like iguanodonts (e.g. MEYER & THÜRING 2003, Daniel Marty; pers. comm.). Worbarrow Tout section, Intermarine Member, surface at 15.85 meters (WT 122).

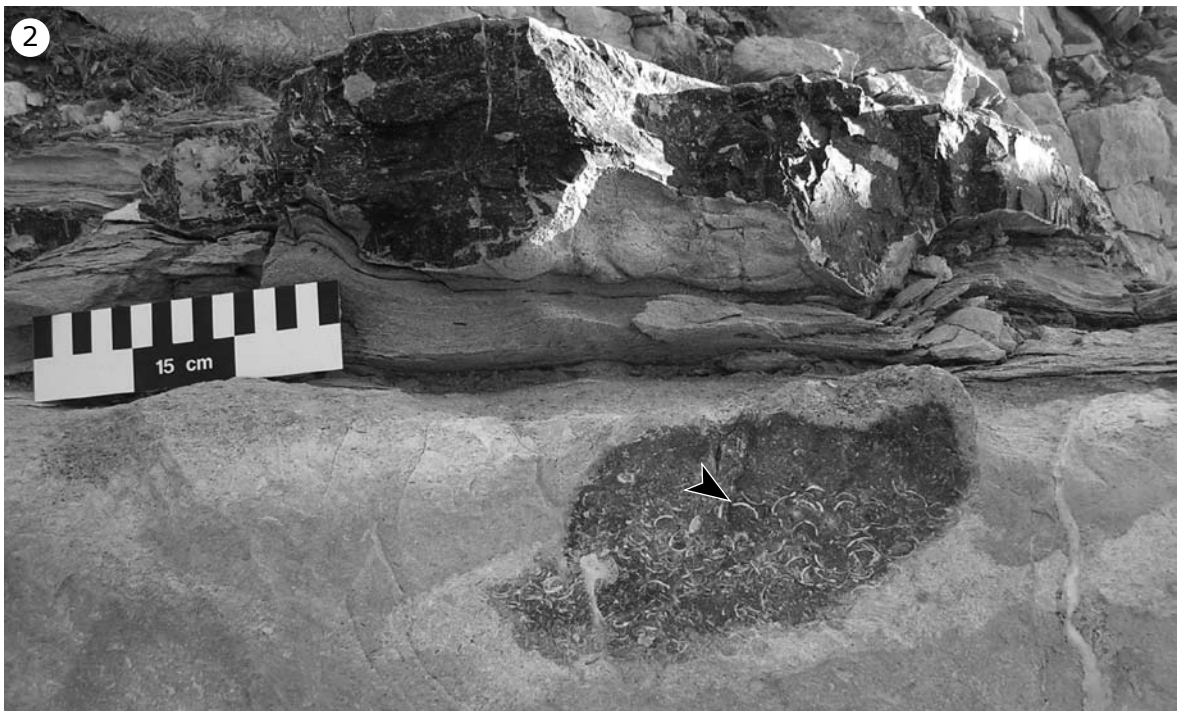
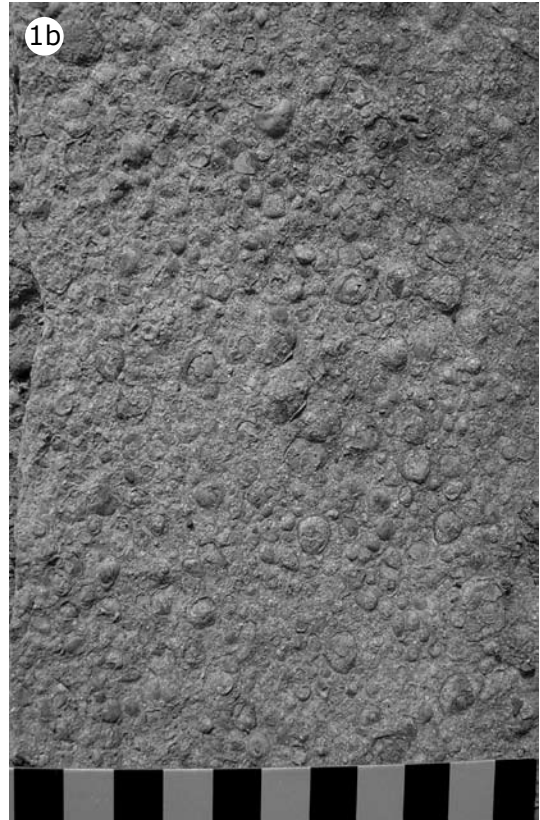
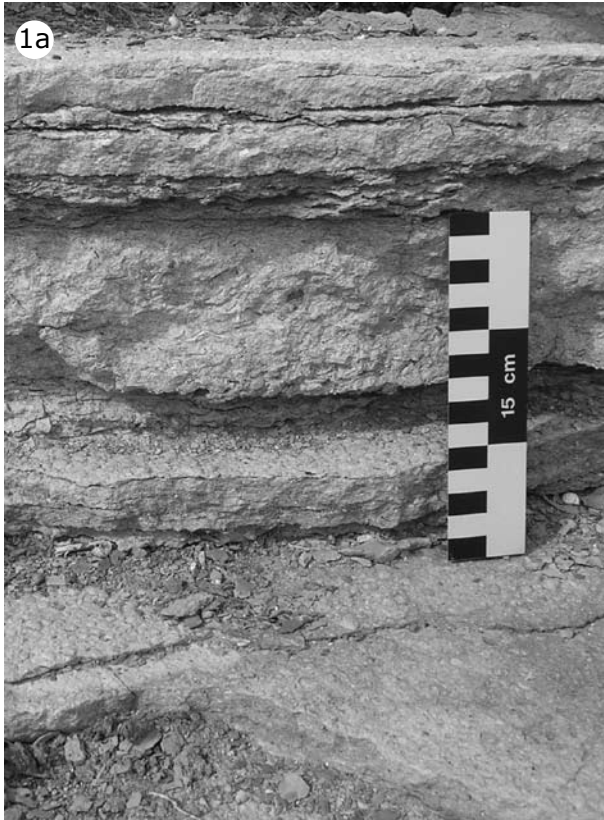


## PLATE 13 - SHELL BEDS

- 1a, b - a) Shell bed dominated by the bivalve *Neomodion*. Additionally, the bivalves *Praeexogyra* and *Corbula* have been identified in this shell bed (CLEMENTS 1993). Durlston Bay section (DB 126), Intermarine Member, interval around 23.70 to 24.00 meters, scale bar 15 cm. b) Surface of the shell bed mentioned above. It displays shell of the bivalve *Neomodion* in a convex-up orientation, which is generally interpreted as an indicator of winnowing in high-energy environments. One unit of the scale bar corresponds to 1cm.
- 2a, b - a) Cinder Member, consisting of densely stacked shells dominated by the oyster *Praeexogyra distorta*. It is generally considered to represent reworked oyster banks in a coastal bay indicating near-marine conditions (e.g., MORTER 1984, RADLEY 2002). Durlston Bay section (DB111), Cinder Member, interval around 14.25 to 17.20. b) Detail of a surface of the Cinder Member displaying shells of the oyster *Praeexogyra distorta*. One unit of the scale bar corresponds to 1cm.









# ANNEX

Sections	thin sections [number]	washed samples [number]	total samples [number]	height of sections [meter]	samples /meter (rounded)
Chapeau de Gendarme	76	6	82	13.40	6
Cornaux	71	7	78	13.50	6
Crozet	61	7	68	12.30	6
Lavans	56	3	59	12.25	5
Marchairuz	41	1	42	10.50	4
Poizat	51	5	56	10.20	6
Rusel	33	6	39	5.10	8
St. Claude	57	5	62	11.10	6
Thoirette	34	1	35	7.35	5
Val de Fier	41	3	44	10.10	4
Yenne	45	6	51	8.80	6
	Total: 566	Total: 50	Total: 616	Total: 114.50	Average: 5
Durlston Bay	59	11	70	28.70	2
Worbarrow Tout	41	14	55	25.40	2
	Total: 100	Total: 25	Total: 125	Total: 54.10	Average: 2
	Total: 666	Total: 75	Total: 741	Total: 168.60	Average: 4

**Annex 1** – Number of thin sections, numbers of washed samples, height, and samples per meter for each section. All materials concerning this study (thin sections, washed samples) are deposited at the Institute of Geology at the University of Fribourg in Switzerland.

Samples	Illite [%]	Illite-smectite [%]	Kaolinite [%]
Chapeau de Gendarme section			
CG 10	95	5	0
CG 11.1	95	5	0
CG 12	95	5	0
CG 13	95	5	0
CG 14	90	10	0
CG 15	85	15	0
CG 16	85	15	0
CG 18	80	20	0
CG 18.1	80	20	0
CG 18.2	80	20	traces
CG 19	70	30	0
CG 20	70	30	0
CG 21	65	35	0
CG 26	60	40	0
CG 29	50	50	0
CG 30.1	60	40	0
CG 33	40	60	0
CG 38.1	45	55	traces
CG 40	30	70	traces
CG 45.1	25	70	5
CG 48.1	25	65	10
CG 51	35	50	15
CG 53	40	40	20
CG 54	45	40	15
Cornaux section			
CO 9	30	70	0
CO 9.1	60	40	0
CO 10	60	40	0
CO 11	70	30	0
CO 11.1	75	25	0
CO 12	70	30	0
CO 12.1	65	35	0
CO 13	75	25	0
CO 14	70	30	0
CO 15	80	20	0
CO 15.1	80	20	0
CO 16	80	20	0
CO 17	80	20	0
Durlston Bay section			
DU 27	20	80	0
DU 28	15	85	traces
DU 28.1	20	80	traces

Annex 2 – Clay mineral data

Samples	$\delta^{13}\text{C}$ [‰ PDB]	$\delta^{18}\text{O}$ [‰ PDB]
Chapeau de Gendarme section		
CG 10	-6.00	-2.23
CG 11.1	-2.23	-2.19
CG 12	-2.18	-2.82
CG 13	-2.13	-1.79
CG 14	-3.14	-1.53
CG 15	-0.75	-3.08
CG 16	-0.42	-2.93
CG 18	-0.33	-3.36
CG 18.1	-0.54	-3.18
CG 18.2	-1.80	-2.75
CG 19	-1.11	-2.46
CG 20	-1.44	-1.85
CG 21	-0.26	-2.15
CG 26	0.19	-1.87
CG 29	-0.01	-2.22
CG 30.1	0.28	-2.40
CG 33	0.15	-2.65
CG 38.1	0.17	-4.59
CG 40	0.46	-3.40
CG 45.1	0.94	-3.01
CG 48.1	1.02	-3.87
CG 51	1.33	-3.47
CG 53	1.35	-2.74
CG 54	1.20	-3.27
Cornaux		
CO 9	-4.15	-3.32
CO 9.1	-4.48	-2.13
CO 10	-4.21	-2.54
CO 11	-1.57	-2.54
CO 11.1	-1.37	-2.91
CO 12	-0.93	-3.16
CO 12.1	-0.68	-2.84
CO 13	-0.50	-2.71
CO 14	-0.52	-1.84
CO 15	-0.47	-2.18
CO 15.1	-1.04	-2.11
CO 16	-0.47	-3.09
CO 17	-0.67	-1.39
Durlston Bay		
DU 27	0.20	-3.90
DU 28	0.22	-2.88
DU 28.1	-0.16	-2.34

Annex 3 – Stable isotope data

# CURRICULUM VITAE

---

I was born in Baar (canton of Zug, Switzerland), on the 15<sup>th</sup> of February 1975 to Adelrich and Elisabeth Tresch (born Peter). After obtaining the *Maturität Typus C* (natural sciences) from the *Kantonsschule of Zug* in 1996, I spent endless days in the *Rekrutenschule* (military training school).

In October 1996, I enrolled as a student in geology at the ETH in Zurich (Swiss Federal Institute of Technology Zurich). I received the diploma degree in geology (Swiss MSc equivalent) issued at the ETH in Zurich in May 2001. My diploma thesis entitled “*Dynamics of an Eocene mixed carbonate-siliciclastic coast (Hohgant region, Interlaken, Switzerland)*” (written in German) was carried out under the guidance of Prof. Helmut Weissert and Dr. Hanspeter Funk. After language-learning holidays in Saint Petersburg (Russia), I worked in several geological offices in Zurich.

In October 2002 I began to work on my doctoral thesis on carbonate sedimentology, sequence stratigraphy, and cyclostratigraphy at the Department of Geosciences (Geology - Palaeontology) of the University of Fribourg (Switzerland) under the direction of Prof. André Strasser. I occupied the position of a research and teaching assistant financed by the University of Fribourg.

Fribourg 12<sup>th</sup> December 2006